

DISSERTATION

STUDIES CONCERNING PLATINUM-CATALYZED 1,6-ENYNE CYCLOISOMERIZATIONS:

A UNIFIED SYNTHETIC APPROACH TO THE GELSEMIUM ALKALOIDS

Submitted by

Eric Thomas Newcomb

Department of Chemistry

In partial fulfillment of the requirements

For the Degree of Doctor of Philosophy

Colorado State University

Fort Collins, Colorado

Spring 2015

Doctoral Committee:

Advisor: Alan Kennan

Eric Ferreira

Amy Prieto

Brian McNaughton

Ramesh Akkina

Copyright by Eric Thomas Newcomb 2015

All Rights Reserved

ABSTRACT

STUDIES CONCERNING PLATINUM-CATALYZED 1,6-ENYNE CYCLOISOMERIZATIONS: A UNIFIED SYNTHETIC APPROACH TO THE GELSEMIUM ALKALOIDS

The development and application of transition metal-catalyzed enyne cyclization reactions is an ever growing and active area of research in modern organic synthesis. One prolific class of catalysts studied in this broad arena is that of pi-acidic metal complexes. Through further understanding of the fundamental processes of these alkynophilic metal catalysts, we are able to test new transformations in more complex settings.

Presented herein are our contributions to the understanding and further implementation of Pt-catalyzed alkyne activation chemistries. In particular, we have developed a chirality transfer protocol to synthesize highly enantioenriched *O*-tethered cyclopropane-containing compounds. The substrate scope for this process is broad, and the overall transformation is highly stereospecific. Additionally, we further refined a purported mechanistic pathway and extended this chemistry in a number of additional systems.

Furthermore, we explored the use of this cycloisomerization chemistry in our synthetic approach to the Gelsemium alkaloids. Specifically, the development of a Pt-catalyzed tandem cycloisomerization/[3,3]-sigmatropic rearrangement allowed us to build a motif shared among a large number of the alkaloids. Following successful implementation of this reaction, we then studied the use of additional late-stage cyclizations to synthesize gelesenicine. Our final two steps, a highly efficient hypervalent iodine-mediated cyclization followed by an iminyl radical cyclization, provided the natural product. Additionally, the synthesis was highly efficient—14 steps—without the use of protecting groups.

ACKNOWLEDGMENTS

My advisor, Eric Ferreira, has had the most influence on me as a scientist. Eric's great enthusiasm for science, both in the laboratory and the classroom, is inspiring. Learning from Eric first-hand was one of the most important things to my success here. He taught me how to think deeply about chemistry. Eric, you put your faith in me numerous times; I hope I didn't disappoint. Thank you for everything.

My graduate committee has been wonderfully supportive of me. I have the utmost respect and owe a great deal of gratitude to professors Alan Kennan, Brian McNaughton, Amy Prieto, and John Wood. Brian and Amy have been incredible; I always knew their doors were open to talk. Amy, I really don't know how you do it—scientist, mother, and business owner. The most amazing part is that you are successful in each of those things. Brian and John, your candid natures were always a welcome breath of fresh air to me. Alan, thanks for giving me a hard time. I needed it most of the time.

Before I arrived here in Colorado, I “learned how to learn”. My time at Kalamazoo College was transformative. Professors like Jeff Bartz, Greg Slough, Thomas Smith, and Jennifer Furchak took a person unprepared for college and helped me become the scientist I am today. I have since always tried to seek out good educators and mentors as they impact my life most. Thom, Scott, Leslie, Leah, Lauren, Liz, Lily (the name of every woman I knew in college started with an “L” apparently), Mithil, and Heather were the best friends I could have asked for in college. Thank you all for the parties, late night food runs, and being there for me when I needed it.

My first experience with synthetic chemistry came from some of the best chemists in the world, and I didn't even fully realize it at the time. To everyone at Bridge Organics, especially Ian Edmonds and Brad Hewitt, thank you for being patient with this over excited chemist-in-training.

I am incredibly fortunate to have worked with such a talented and hardworking group of people in the Ferreira Group. Sharing knowledge, laughs, and even some tears has made me a better person and scientist. To Paul Allegretti, Doug Rooke, Curtis Seizert, and Erin Stache: you are, hands down, the best chemists I have worked with. Paul, in many respects you are the most accomplished person in our lab;

please give yourself some credit. You have, above all else, shown me that it is possible to have a life outside of the lab and still get a huge amount of work done. Also, thanks for being my officemate for the past few months. I would have lost my marbles without you there with me. What to say about Doug Rooke? A person who, at the same time, has too many titles after his name AND enjoys lengthy discussions concerning gourmet hotdogs. Your passion for the work you do has always been inspiring. Curtis, it baffles me that we never came up with a nickname for you. In all seriousness, I couldn't imagine a better classmate than you. I knew that whenever I had a question about chemistry, you would not disregard it. For that, I am grateful. Erin, I still remember the day you told me you were leaving. I wasn't worried about you; I knew you would be fine. I thought if someone as intelligent, hardworking, and passionate as you wanted to leave, how could I ever make it? While those feelings eventually passed, my deep respect for you as a scientist has not.

The newer members of the Ferreira group have also left quite the impression on me. Suzie Stevenson, you are like the little sister I never had; I hope you don't take that the wrong way. You, like Paul, don't give yourself enough credit. Remember when you poured your ice-water bath in the garbage? I do, and it was awesome. Brian Knight (Oily Pete), there are a couple things I must be honest about. First, I will probably call you Oily Pete for the rest of my life. Secondly, and most importantly, I will always remember your first year in the lab and working next to you (the "dream team"). Tim Dreier, I am happy that you are enjoying your new lab AND am considering which bible e-newsletters to sign you up for. Enjoy! Tarik Ozumerzifon (I had to look up how to spell that just now), I really appreciate having you around the past few months. Without Paul and you around, I am sure that I would have lost it. I know it has been difficult for you in Colorado, but you are going to be just fine. Moreover, you are a smart guy that is a talented chemist. Francisco and Phil, I know you guys are working hard in Athens, GA. I cannot wait to see what kind of scientists you become.

I was extremely fortunate to have an excellent undergraduate student in my last two years, Blaine Pedersen. Whenever I thought I was pushing him too hard, he surprised me with a great result. Blaine, I know you will do great things at Yale. Now, get to work!

Various other people outside of the group have made my time here fun and intellectually stimulating. Classmates Paul, Garrett, Ae, Jacob, and Tim are all great people, and each has moved on to bigger and better things. Studying, stressing, and drinking with you all made those early years a blast. My classmates in the McNaughton group, Brett Blakeley and Sandra Deporter, always patiently answered my biology questions. Recently, the McNaughton Group has adopted me as an honorary member. It is a fairly one-sided membership: I steal forks, use refrigerator space, and go into the lab to vent. I truly appreciate all of those things. Nick Barczak, Todd Hyster, Kerem Ozboya (Oz), Kevin Oberg, Darrin Flannigan, Claire Filloux, Dan Shissler, Christina Klug, and Harit Vora are others that have been kind and gracious to me during my graduate studies.

Aaron Bedermann and Sarah Fredrick have become great friends and colleagues over the past five years; I am sure the relationships will continue for many years to come. Aaron, you have patiently listened to my rants and venting over gchat. I hope I have reciprocated this to some degree. You are going to great things at MIT and beyond. Sarah, you are a great scientist and individual. Thanks for the walks, the talks, and being a caring person in a place where that is undervalued.

Peter, Stephanie, Lindsay, and Ian Cox have become my family in Colorado, and I couldn't ask for a better extension. Thanks for all you have done for me over the past four years: the meals, the room to stay in, the conversation, and the support.

I want to give many thanks to my parents. Without both of them and my brother, I would not be the person that I am today. I inherited two traits from them that proved essential for success in graduate school—my mother's work ethic and my father's skeptical nature. My brother has also helped me in ways he probably isn't aware of. He has shown me that when someone is faced with adversity, the only thing to do is overcome.

Lindsay, over the past four years you have made me better. Your hardworking and independent nature is truly inspiring. Thank you for your patience, having faith in me, and never making me choose you or work. I hope you know would be an easy decision—you. I love you.

DEDICATION

For my family

TABLE OF CONTENTS

Abstract	ii
Acknowledgments	iii
Dedication	vi
Table of Contents	vii
List of Tables	xii
List of Figures	xiii
List of Schemes	xv
CHAPTER ONE: The Implementation of Transition Metal Catalysis in the Synthesis of Natural Products	1
1.1 Introduction: Examples of Transition Metal-Catalyzed Processes in Total Synthesis	1
1.2 The Synthetic Power of Pt-Catalyzed Alkyne Activation	3
CHAPTER ONE NOTES AND REFERENCES	5
CHAPTER TWO: Alkynophilic Metal Complexes in Organic Synthesis	6
2.1 Overview	6
2.2 Alkyne Activation in Total Synthesis	6
2.2.1 Au-Mediated Alkyne Activation in Total Synthesis.....	6
2.2.2 Pt-Mediated Alkyne Activation in Total Synthesis	9
2.2.3 Hg-Mediated Alkyne Activation in Total Synthesis.....	11
2.2.4 Alkyne Activation in Total Synthesis: Summary	12
2.3 Alkynophilicity	12
2.3.1 Characteristics of Alkynophilic Metal Complexes	13
2.3.2 Relativistic Effects	14

2.4 Conclusion	16
CHAPTER TWO NOTES AND REFERENCES	17
CHAPTER THREE: Cycloisomerization of Enynes as a Platform to Study Catalytic Reactivity	19
3.1 Overview	19
3.2 Cycloisomerization Reactions of Enynes	19
3.2.1 Introduction.....	19
3.2.2 Products and Pathways in the Cycloisomerization of 1,6-Enynes.....	20
3.3 1,6-Enyne Cycloisomerizations to Produce 3-Aza and 3-Oxabicyclo[4.1.0]heptenes	24
3.3.1 Racemic Examples and Mechanistic Proposals.....	24
3.3.2 Asymmetric Cases of 1,6-Enyne Cycloisomerizations to Produce 3-Aza and 3-Oxabicyclo[4.1.0]heptenes	26
3.4 Chirality Transfer Process to Produce Optically Enriched 3-Oxabicyclo[4.1.0]heptenes.....	28
3.4.1 Proposal	28
3.4.2 Substrate Synthesis	30
3.4.3 Initial Result and Optimization.....	30
3.4.4 Influence of Propargylic Substituent on Enantiospecificity	32
3.4.5 Tolerance and Limitations on Substitution.....	33
3.4.6 Stereochemical Confirmation and Model for Transfer of Stereochemical Information.....	35
3.4.6 <i>N</i> -Tethered Enyne Substrates.....	36
3.4.8 Reactions of Products	37
3.5 Additional Studies Concerning 1,6-Enyne Cycloisomerizations.....	38
3.5.1 Migration into Carbenoids Introduction	38
3.5.2 Proposal for Migration/Expansion in the Cycloisomerization of 1,6-Enynes	38
3.5.3 Results.....	39
3.5.4 Silicon Tether Strategies: Background	41

3.5.5 Proposal for Si-Tethering in 1,6-Enyne Cycloisomerization Reaction	41
3.5.6 Substrate Synthesis and Result on Si-Tethering Study.....	42
3.5.7 Tandem Process Background.....	43
3.5.8 Results and Potential Applications	44
3.6 Conclusion	45
3.7 Experimental Section	46
3.7.1 Materials and Methods.....	46
3.7.2 Enyne Cycloisomerizations	46
3.7.3 Optimization Studies.....	60
3.7.4 Additional Reactions.....	66
3.7.5 Substrate Syntheses.....	70
CHAPTER THREE NOTES AND REFERENCES	97
CHAPTER FOUR: Alkaloids Isolated From the Genus <i>Gelsemium</i>	102
4.1 Introduction	102
4.1.1 Overview.....	102
4.1.2 The Genus <i>Gelsemium</i>	102
4.2 The Six Structural Types of Alkaloids Isolated From the Genus <i>Gelsemium</i>	103
4.2.1 Alkaloids of the Yohimbane Type.....	104
4.2.2 Alkaloids of the Sarpagine Type	104
4.2.3 Alkaloids of the Koumine Type.....	105
4.2.4 Alkaloids of the Gelsemine Type	105
4.2.5 Alkaloids of the Humantenine Type.....	106
4.2.6 Alkaloids of the Gelsedine Type	106
4.3 Proposed Biosynthesis	107
4.3.1 Proposed Biogenesis of Sarpagine, Koumine, and Humantenine Type Alkaloids.....	107

4.3.2 Proposed Biogenesis of Gelsemine Type Alkaloids.....	109
4.3.3 Proposed Biogenesis of Gelsedine Type Alkaloids.....	109
4.4 Pharmacological Effects	110
4.4.1 Effects of Consuming Plants of the Genus <i>Gelsemium</i>	110
4.4.2 Biological Properties of the Gelsemium Alkaloids	111
4.5 Synthetic Approaches to the Gelsemium Alkaloids	112
4.5.1 Synthetic Approach to the Humantenine Type Alkaloids	112
4.5.2 Synthetic Approaches to the Gelsemine Type Alkaloids	114
4.5.3 Synthetic Approaches to the Gelsedine Type Alkaloids	116
4.6 Conclusion	122
CHAPTER FOUR NOTES AND REFERENCES.....	123
CHAPTER FIVE: Towards a Unified Synthesis of Gelsemium Alkaloids: The Total Synthesis of (±)-	
Gelsenicine	127
5.1 Overview	127
5.2 A Unified Synthetic Design of the Gelsemium Alkaloids.....	127
5.2.1 Structural Similarities in Alkaloids of the Gelsemine, Humantenine, and Gelsedine Types	128
5.2.2 Retrosynthetic Analysis and Proposed Route to Core Structure	128
5.3 First Generation Approach.....	131
5.3.1 Initial Synthetic Studies	131
5.3.2 Two Different Stereochemical Outcomes.....	133
5.4 Second Generation Approach	134
5.4.1 Revised Synthetic Strategy	134
5.4.2 Second Generation Synthetic Studies	135
5.4.3 Endgame Strategy	138
5.4.4 Second Generation Endgame Synthetic Studies.....	139

5.5 Third Generation Approach	140
5.5.1 Revised Endgame Synthetic Strategy	140
5.5.2 Successful Endgame Strategy: The Total Synthesis of (±)-Gelsenicine	141
5.6 Future Opportunities and Preliminary Results.....	142
5.6.1 Improving the Key Step Efficiency	142
5.6.2 Synthetic Analogs: Towards a Synthesis of 7- <i>Epi</i> -Gelsenicine	143
5.7 Conclusion	144
5.6 Experimental Section	146
5.6.1 Materials and Methods.....	146
5.6.2 Experimental Data Relevant to the Total Synthesis of Gelsenicine (187)	146
5.6.3 Experimental Data Relevant to the First Generation Approach	159
5.6.4 Additional Reactions.....	162
CHAPTER FIVE NOTES AND REFERENCES	167
APPENDIX ONE: Spectra Relevant to Chapter Three.....	169
APPENDIX TWO: Crystallographic Data Relevant to Compound 113k	251
APPENDIX THREE: Spectra Relevant to Chapter Five	257

LIST OF TABLES

CHAPTER THREE

Table 3.4.1. Optimization of Cycloisomerization Conditions	32
Table 3.4.2. Results of the Nature of the Stereocontrolling Group	33

LIST OF FIGURES

CHAPTER TWO

Figure 2.3.1. Three Characteristics of Alkyne Activation Catalysis and an Example of this Reactivity by Toste and Coworkers	14
Figure 2.3.2. Molecular Orbital Energies for Au, Hg, and, Pt Before and After Relativistic Considerations	15

CHAPTER THREE

Figure 3.4.1. Enantiospecific Cycloisomerization: Alkene Substitution Scope	33
Figure 3.4.2. Enantiospecific Cycloisomerization: Alkyne Substitution Scope	34
Figure 3.4.3. Unsuccessful Substrates in the Cycloisomerization	34
Figure 3.5.1. Ring Expansion Results with Ir- and Pt-Based Catalysts	40
Figure 3.5.2. Examples of Natural Products that Contain an Oxabicyclo[3.2.2]nonane Core	45

CHAPTER FOUR

Figure 4.2.1. The Six Gelsemium Alkaloid Structural Types	103
Figure 4.2.2. Alkaloids of the Yohimbane Type	104
Figure 4.2.3. Alkaloids of the Sarpagine Type	104
Figure 4.2.4. Alkaloids of the Koumine Type	105
Figure 4.2.5. Alkaloids of the Gelsemine Type	105
Figure 4.2.6. Alkaloids of the Humantenine Type	106
Figure 4.2.7. Alkaloids of the Gelsedine Type	106
Figure 4.4.1. Examples of Gelsemium Alkaloids that Exhibit Specific Biological Properties	111
Figure 4.4.2. Kitajima and Coworkers' Observation of Cytotoxicity for Gelsedine Type Alkaloids ..	112

CHAPTER FIVE

Figure 5.2.1. Oxabicyclo[3.2.2]nonane Structure Embedded in Gelsemine, Gelsedine, and Humantenine Type Alkaloids.....	128
Figure 5.2.2. General Retrosynthesis of Different Structural Types to Common Intermediate 282 ...	129
Figure 5.4.1. Initial Result and Optimization of Cycloisomerization on Dienyne (<i>E,E</i>)- 309	137
Figure 5.6.1. Advanced Intermediates 313 and 314 as Analogs.....	144

LIST OF SCHEMES

CHAPTER ONE

Scheme 1.1.1. Overman and Coworkers' Synthesis of Quadrigemine (1) and Psycholeine (2) Via Pd-Catalyzed Cross-Couplings.....	2
Scheme 1.1.2. Sequential Cyclobutane C–H Arylations in the Synthesis of Piperarborenine B (7) by Baran and Coworkers.....	3
Scheme 1.2.1. Pt-Catalyzed 1,6-Enyne Cycloisomerizations: Uses in Methods Development and Total Synthesis	4

CHAPTER TWO

Scheme 2.2.1. Late-Stage Au(I)-Catalyzed Alkyne Hydration in the Synthesis of Bryostatin 16 (14)....	7
Scheme 2.2.2. Two Similar Routes to (–)-Englerin A (17) and Mechanistic Pathway of the Key Steps.	8
Scheme 2.2.3. Fürstner's Pt-Catalyzed Carboalkoxylation in the Synthesis of Erypoegin H (25).....	9
Scheme 2.2.4. Pt-Catalyzed Cycloisomerization Reactions in Vanderwal and Coworkers' Synthesis of Echinopine B (32).....	11
Scheme 2.2.5. Deslongchamps and Coworkers' Synthesis of Hippuristanol (41).....	12

CHAPTER THREE

Scheme 3.1.1. Enantiospecific 1,6-Enyne Cycloisomerization and Extensions	19
Scheme 3.2.1. Variation in 1,6-Enyne Cycloisomerization Products	21
Scheme 3.2.2. Substrate Influence on Product Formation in Pt-Catalyzed Cycloisomerization of 1,6-Enynes.....	22
Scheme 3.2.3. Substrate Influence on Products Formed in Au-Catalyzed 1,6-Enyne Cycloisomerization	22

Scheme 3.2.4. Proposed Intermediates Leading to the Formation of Products with the General Structures of 73 and 76	23
Scheme 3.3.1. First Example of 3-Oxabicyclo[4.1.0]heptenes from 1,6-Enynes and Proposed Mechanism	24
Scheme 3.3.2. <i>N</i> -Tethered 1,6-Enyne Cycloisomerization with Alternative Mechanistic Proposal.....	25
Scheme 3.3.3. <i>N</i> - and <i>O</i> -Tethered 1,6-Enyne Cycloisomerization Catalyzed by PtCl ₂	25
Scheme 3.3.4. Alternative Mechanistic Proposal by Fürstner and Coworkers	26
Scheme 3.3.5. Example of Rh-Catalyzed Asymmetric 1,6-Enyne Cycloisomerization	27
Scheme 3.3.6. Example of Pt-Catalyzed Asymmetric 1,6-Enyne Cycloisomerization	27
Scheme 3.3.7. Examples of Au-Catalyzed Asymmetric 1,6-Enyne Cycloisomerizations.....	28
Scheme 3.4.1. Chirality Transfer Proposal with Enantioenriched Enyne Substrate	29
Scheme 3.4.2. Mechanistic Possibilities in Chirality Transfer Approach.....	20
Scheme 3.4.3. Synthesis of Enantioenriched 1,6-Enyne Substrate 108	30
Scheme 3.4.4. Initial Observation of Chirality Transfer with Catalytic PtCl ₂	31
Scheme 3.4.5. Confirmation of Absolute Stereochemistry in Cycloisomerization from Single Crystal X-Ray Structure of Aryl Bromide 113k	35
Scheme 3.4.6. Model for Stereochemical Transfer and Unfavorable Conformations	36
Scheme 3.4.7. <i>N</i> -Tethered 1,6-Enyne Cycloisomerization with Observed Chirality Transfer	36
Scheme 3.4.8. Previously Disclosed Reactions on <i>N</i> -Tethered Products	37
Scheme 3.4.9. Oxidative Cleavage to Produce Highly Enantioenriched Cyclopropane 125	37
Scheme 3.5.1. Example of 1,5-Enynes Undergoing Ring Expansion or C–H Insertion under Au-Catalysis.....	38
Scheme 3.5.2. Mechanistic-Based Proposal for Alkyl Migrations in the Cycloisomerization of 1,6-Enynes.....	39
Scheme 3.5.3. Initial Ring Expansion Result.....	39
Scheme 3.5.4. Silicon Tethering in [4+2] Cycloaddition and Post Cycloaddition Transformations.....	41

Scheme 3.5.5. Silicon Tethering Proposal in 1,6-Enyne Cycloisomerization	42
Scheme 3.5.6. Synthesis of Racemic Si-Tethered 1,6-Enyne Substrate 153	42
Scheme 3.5.7. Pt-Catalyzed Cycloisomerization Result on Si-Tethered Substrate 153	43
Scheme 3.5.8. 1,6-Enynes in Pt-Catalyzed Tandem Cycloisomerization/[3,3]-Sigmatropic Rearrangement	43
Scheme 3.5.9. Proposed Mechanistic Intermediates for Tandem Cycloisomerization/[3,3]-Sigmatropic Rearrangement with <i>N</i> - and <i>O</i> -Tethered 1,6-Enynes.....	44
Scheme 3.5.10. Chirality Transfer Observation in Pt-Catalyzed Tandem Process.....	44
 CHAPTER FOUR	
Scheme 4.3.1. Studies Concerning Early Biosynthetic Precursors to the Gelsemium Alkaloids	107
Scheme 4.3.2. Proposed Biogenesis of Sarpagine, Koumine, and Humantenine Type Alkaloids.....	108
Scheme 4.3.3. Proposed Biosynthetic Pathway to Gelsemine Type Alkaloids from (19 <i>Z</i>)- Anhydrovobasindiol (191)	109
Scheme 4.3.4. Proposed Biogenesis of Gelsedine Type Alkaloids from Rankinidine (199).....	110
Scheme 4.5.1. Sakai and Coworkers' Semisynthesis of Humantenirine (219) and 11- Methoxygelsemamide (201)	113
Scheme 4.5.2. A Racemic Synthesis of Gelsemine (196) by Fukuyama and Coworkers.....	114
Scheme 4.5.3. A Racemic Synthesis of Gelsemine (196) by Overman and Coworkers.....	115
Scheme 4.5.4. The Asymmetric Synthesis of Gelsemine (196) by Qin and Coworkers.....	116
Scheme 4.5.5. Sakai and Coworkers' Semisynthesis of Gelsedine Type Alkaloids.....	117
Scheme 4.5.6. Baldwin and Doll's Synthetic Approach to Gelsedine Type Alkaloids	118
Scheme 4.5.7. The Synthesis of (±)-7- <i>Epi</i> -20-Desethylgelsedine (253) by Kende and Coworkers.....	119
Scheme 4.5.8. The Synthesis of (+)-Gelsedine (202) by Hiemstra and Coworkers	120
Scheme 4.5.9. The Asymmetric Total Synthesis of Gelsemoxonine (162) by Fukuyama and Coworkers	121

Scheme 4.5.10. The Total Synthesis of Gelsemoxonine (162) by Carreira and Coworkers.....	122
 CHAPTER FIVE	
Scheme 5.1.1. Use of Tandem Cycloisomerization/[3,3]-Sigmatropic Rearrangement in the Total Synthesis of Gelsenicine	127
Scheme 5.2.1. Previously Observed Tandem Process and Proposed Implementation on Substrate 283	130
Scheme 5.2.2. Proposed Forward Route to Common Intermediate 282	130
Scheme 5.3.1. Synthesis of Dienynes (<i>E,E</i>)- 287 and (<i>E,Z</i>)- 287	131
Scheme 5.3.2. Cyclization Attempts on Dienynes (<i>E,E</i>)- 287 and (<i>E,Z</i>)- 287	132
Scheme 5.3.3. Observation of Methylene Cyclopropane 295	133
Scheme 5.3.4. Stereospecific and Stereoconvergent Processes	134
Scheme 5.4.1. Revised Synthetic Approach and the Structures of Gelsemamide (307) and 11- Methoxygelsemamide (201)	135
Scheme 5.4.2. Synthesis of Dienyne (<i>E,E</i>)- 309	135
Scheme 5.4.3. Cycloisomerization/[3,3]-Sigmatropic Rearrangement and Potential [1,5]-Homodienyl Pathway	138
Scheme 5.4.4. Allylic Oxidation: Synthesis of the Hypothesized Common Intermediate (306)	138
Scheme 5.4.5. Endgame Strategy to Gelsenicine (187)	139
Scheme 5.4.6. Synthetic Route to Pyrroline 313 and Failed Attempts to Access Amide 314	140
Scheme 5.5.1. Two Options for Finishing Gelsenicine (187)	140
Scheme 5.5.2. Successful Endgame to Gelsenicine (187)	141
Scheme 5.5.3. Divergent Conversion of Gelsenicine to Additional Alkaloids	142
Scheme 5.6.1. Current Route to Overcome [1,5]-Homodienyl Hydrogen Migration Byproduct	143
Scheme 5.6.2. Progress Towards 7- <i>Epi</i> -Gelsenicine (332)	144
Scheme 5.7.1 Total Synthesis of Gelsenicine (187)	145

CHAPTER ONE

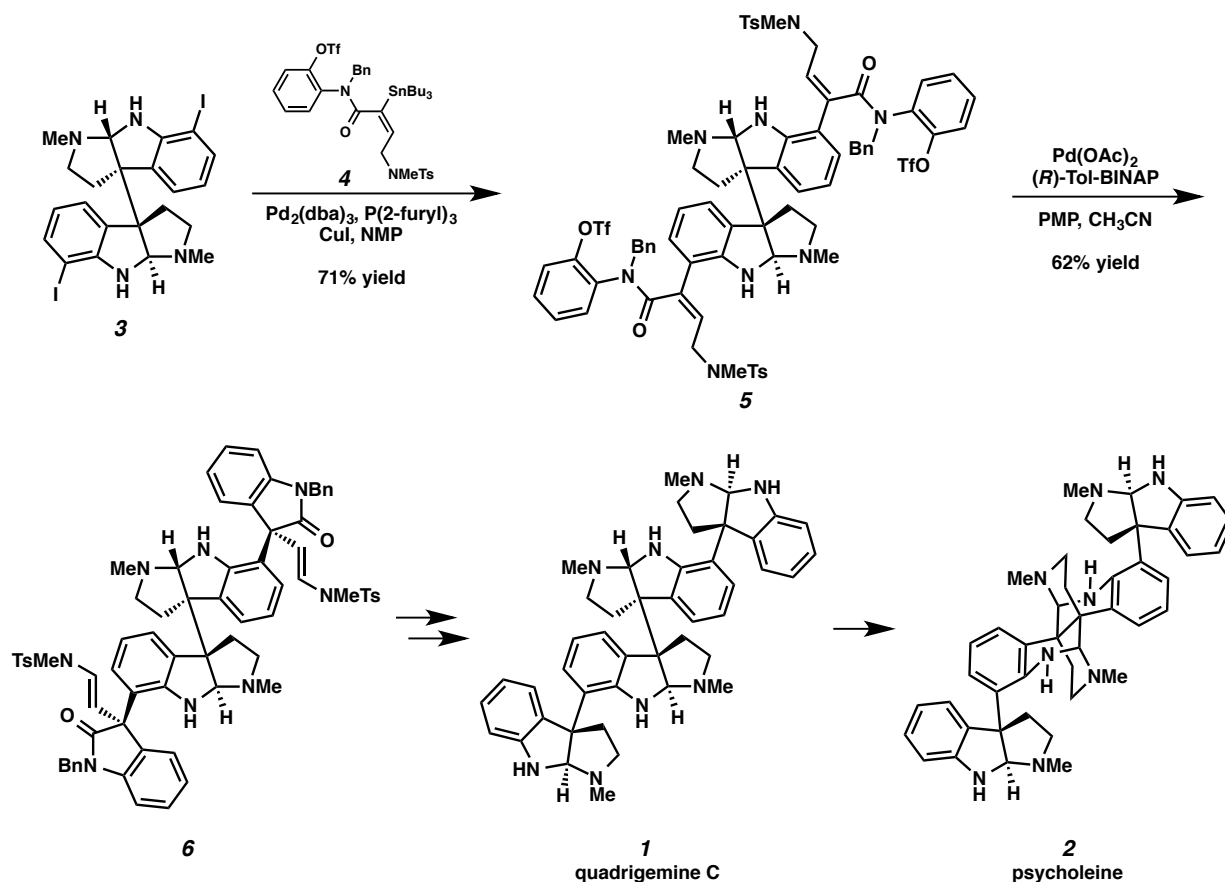
The Implementation of Transition Metal Catalysis in the Synthesis of Natural Products

1.1 Introduction: Examples of Transition Metal-Catalyzed Processes in Total Synthesis

Transition metal-catalyzed processes greatly impact our daily life; since the year 2000, three separate Nobel Prizes in Chemistry have focused on transition metal catalysis. These processes are applied in a number of arenas, including industrial gas manufacturing, macromolecule synthesis, drug manufacturing, and natural product synthesis. In fact, the synthesis of natural products commonly offers a “proving ground” of sorts for the use of these methods in complex settings.

While there are examples of synthetic methods born out of necessity, much more common is the discovery of a method and its future application. Moreover, testing synthetic methods in complex settings, such as in natural product synthesis or in biological systems, can further validate a technique. The two examples discussed below demonstrate the power of transition metal-mediated processes in the context of complex molecule synthesis.

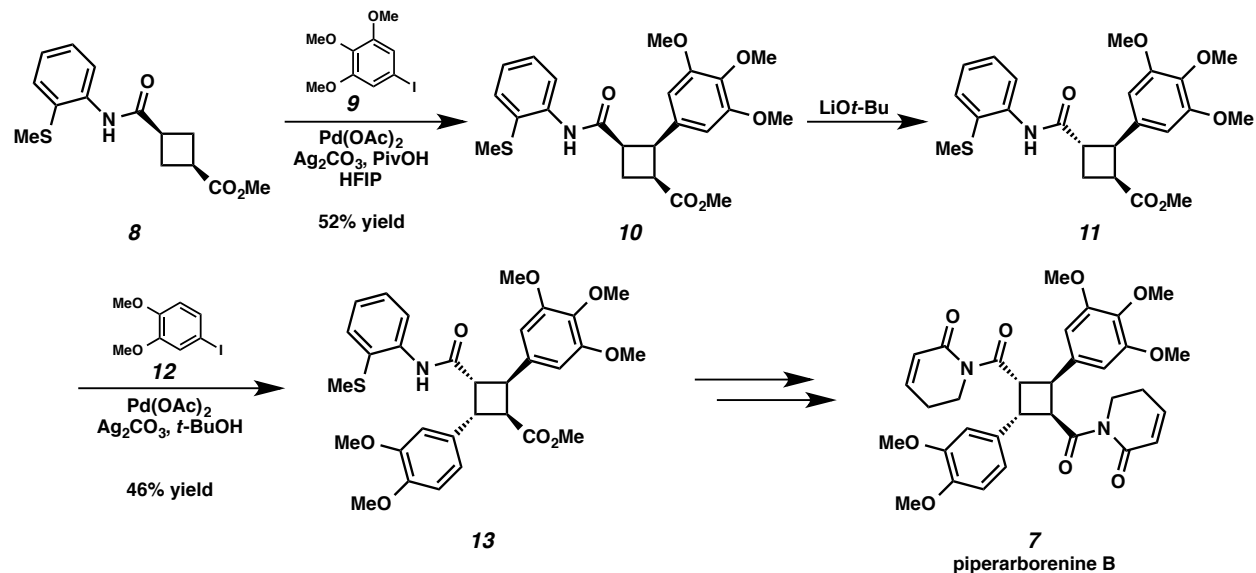
In 2002, Overman and coworkers disclosed the synthesis of quadrigemine C (**1**) and psycholeine (**2**), highlighting the power and efficiency of Pd-mediated cross-couplings (Scheme 1.1.1).¹ The researchers both leveraged earlier established chemistry and explored new methods. Specifically, a Pd-catalyzed Stille coupling of aryl iodide **3** with vinylstannane **4** provides compound **5** in 71% yield. Then, an enantioselective Heck cyclization affords bis oxindole **6** in 62% yield and 90% *ee*. In two steps they complete the total synthesis of quadrigemine C (**1**); furthermore, this natural product is converted to psycholeine (**2**) in a single step. The capability to form four C–C bonds in two steps (one step being enantioselective) is quite remarkable. Without the development of this chemistry, and its attempted use in a number of complex synthetic applications, we may never have come to appreciate its true potential.



Scheme 1.1.1. Overman and Coworkers' Synthesis of Quadrigemine (**1**) and Psycholeine (**2**) Via Pd-Catalyzed Cross-Couplings.

Baran and coworkers showcase Pd-catalyzed C–H activation chemistry in their 2011 synthesis of piperarborenine B (**7**, Scheme 1.1.2).² Previous approaches to these cyclobutane-containing natural products based on [2+2] photocyclizations were generally unselective. The Baran group envisioned utilizing sequential sp^3 C–H activation, based on work by Daugulis and coworkers.³ The first sp^3 C–H functionalization is completed on cyclobutane **8**, utilizing an unconventional 2-amidothioanisole directing group to provide arylated cyclobutane **10** in good yield. Following epimerization with lithium *tert*-butoxide to afford compound **11**, a second Pd-catalyzed C–H arylation with iodide **12** yields tetrasubstituted cyclobutane **13** and ultimately piperarborenine B (**7**). While transition metal-catalyzed

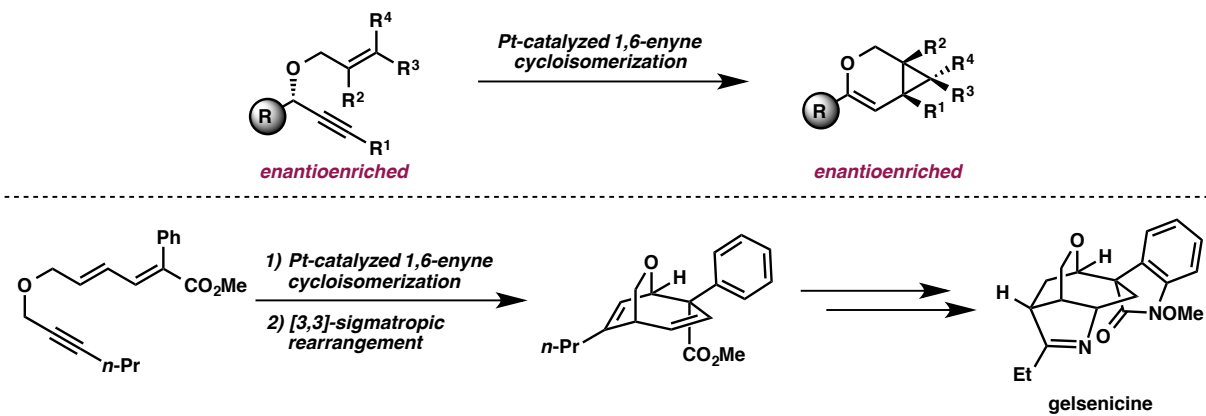
C–H activation chemistry remains a relatively young field, the exploration of its use in this example provides an arena for testing, validation, and innovation.



Scheme 1.1.2. Sequential Cyclobutane C–H Arylations in the Synthesis of Piperarborenine B (**7**) by Baran and Coworkers.

1.2 The Synthetic Power of Pt-Catalyzed Alkyne Activation

Herein we present our work regarding new Pt-catalyzed alkyne activation methods and applications of these methods in natural products synthesis. Specifically, we have developed a chirality transfer protocol to produce enantioenriched bicyclic compounds utilizing Pt-catalyzed 1,6-enyne cycloisomerization chemistry (Scheme 1.2.1).⁴ Following successful extensions of this chemistry to other methods, we are exploring its use in a unified strategy to access a number of natural products isolated from the genus *Gelsemium*. To date, these efforts have culminated in the first total synthesis of gelsenicine.



Scheme 1.2.1. Pt-Catalyzed 1,6-Enyne Cycloisomerizations: Uses in Methods Development and Total Synthesis.

CHAPTER ONE NOTES AND REFERENCES

¹ Lebsack, A. D.; Link, J. T.; Overman, L. E.; Stearns, B. A. *J. Am. Chem. Soc.* **2002**, *124*, 9008–9009.

² Gutekunst, W. R.; Baran, P. S. *J. Am. Chem. Soc.* **2011**, *133*, 19076–19079.

³ Zaitsev, V. G.; Shabashov, D.; Daugulis, O. *J. Am. Chem. Soc.* **2005**, *127*, 13154–13155.

⁴ Newcomb, E. T.; Ferreira, E. M. *Org. Lett.* **2013**, *15*, 1772–1775.

CHAPTER TWO

Alkynophilic Metal Complexes in Organic Synthesis

2.1 Overview

As outlined in Chapter 1, transition metal catalysts have allowed chemists to efficiently synthesize molecules of interest. Herein, the use of Ag-, Pt-, and Hg-catalyzed alkyne activation chemistry in the synthesis of complex molecules is stressed. The unique reactivity observed with the aforementioned metals is also explained.

2.2 Alkyne Activation in Total Synthesis

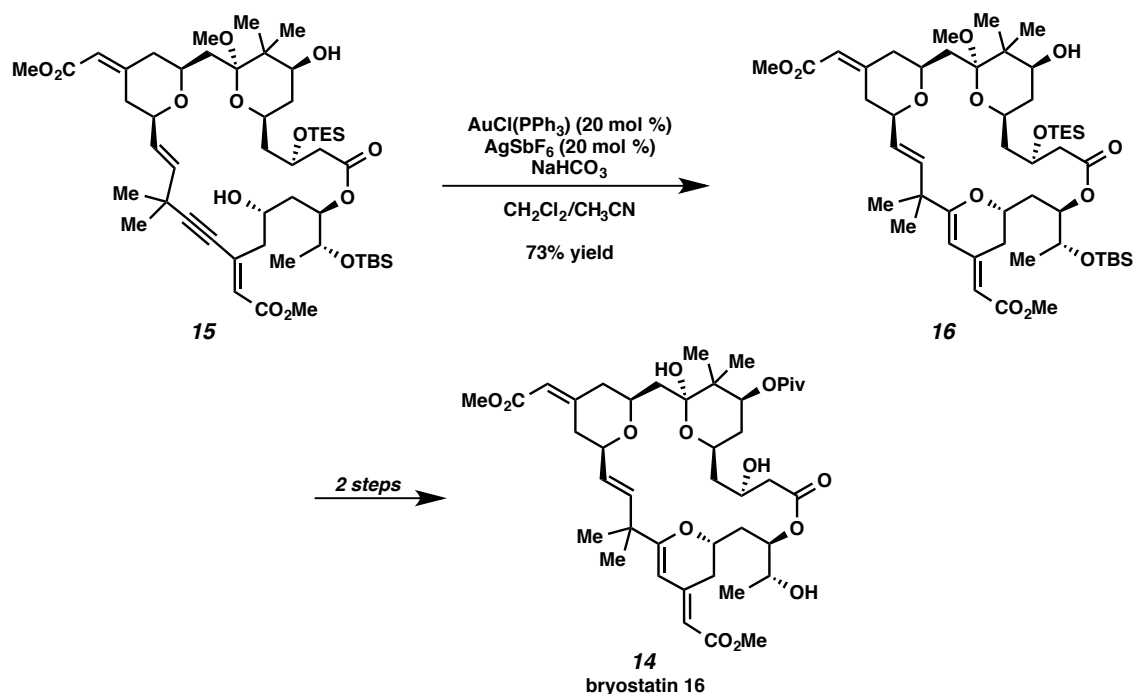
Alkyne activation has been utilized in a number of natural product syntheses. Commonly employed metal catalysts for these transformations include gold, platinum, and mercury. The examples highlighted herein with gold and platinum are not meant to be comprehensive yet are chosen to emphasize the selectivity, efficiency, and intriguing reactivity observed when this type of chemistry is used in complex settings. Purported mechanisms and/or intermediates are drawn when necessary because of the “molecular gymnastics” or cascade processes that can occur in a single reaction step.

2.2.1 Au-Mediated Alkyne Activation in Total Synthesis

Cationic Au(I) complexes are the most commonly employed catalysts for alkyne activation in natural product synthesis.¹ The popularity of these complexes is owed to their high stability and the predictable nature of the transformations they effect. Highlighted below are three examples that showcase the selectivity and interesting reactivity of Au-catalyzed alkyne activation in complex molecule synthesis.

Trost and Dong used a highly chemoselective Au-catalyzed alkyne hydration in their synthesis of bryostatin 16 (**14**, Scheme 2.2.1).² In the presence of an *in situ* generated cationic Au-complex, alkyne **15** provides dihydropyran-containing macrocycle **16** in 73% yield. It is notable that a hydration reaction of this nature can be performed selectively on such a highly functionalized substrate such as compound **15**.

Furthermore, the researchers found that the reaction selectively formed the *6-endo* cyclization product (**16**) and none of the product arising from *5-exo* cyclization.³

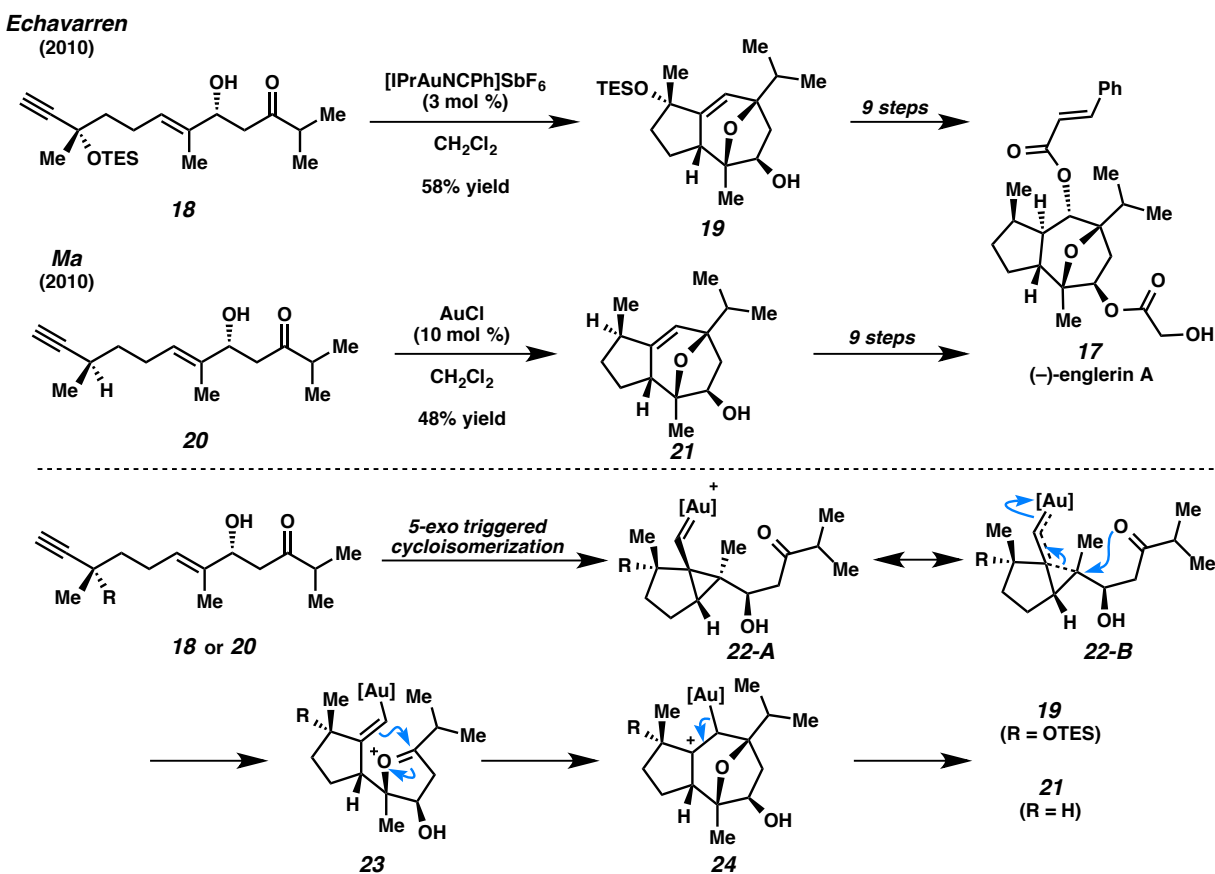


Scheme 2.2.1. Late-Stage Au(I)-Catalyzed Alkyne Hydration in the Synthesis of Bryostatin 16 (**14**).

In 2010, both the Echavarren and the Ma laboratories independently completed the synthesis of englerin A (**17**, Scheme 2.2.2).^{4,5} Both syntheses showcase the power of Au-catalyzed alkyne activation chemistry to access complex architectures from seemingly simple compounds. Echavarren and coworkers utilize enyne **18** (generated in eight steps from geraniol) in their key transformation. Subjecting enyne **18** to cationic gold catalysis provides ether **19** in 58% yield. Ether **19** is then converted to (–)-englerin A (**17**) in nine steps. Ma and coworkers rely on a remarkably similar approach in their synthesis of the natural product. Their key step precursor, enyne **20**, is made in five steps from (*R*)-citronellal. Exposing enyne **20** to catalytic AuCl provides ether **21** in 48% yield.⁶ Nine additional steps are necessary for the total synthesis of (–)-englerin A (**17**).

The proposed mechanism of this transformation demonstrates the complexity of these processes. Initially, the enyne undergoes a *5-exo* triggered cycloisomerization to ultimately arrive at the

Au-carbenoid (**22-A** \leftrightarrow **22-B**, Scheme 2.2.2). Attack of the carbonyl oxygen onto the quaternary carbon⁷ and C–C bond cleavage of the cyclopropane generates oxocarbenium **23**. After C–C bond formation via nucleophilic attack of the alkene and loss of the catalyst (through general intermediate **24**), ethers **19** and **21** are formed. The creative use of carbenoid intermediate **22-A/B** in an unconventional way allows for the core of these molecules to be made in short order and provides further understanding of the behavior of these intermediates in complex settings. While the ability to anticipate the favored reaction pathways observed with these two substrates (**18** and **20**) speaks to knowledge we have already gained concerning these transformations, the somewhat low yields indicate much is still to be learned about these catalysts and their application.

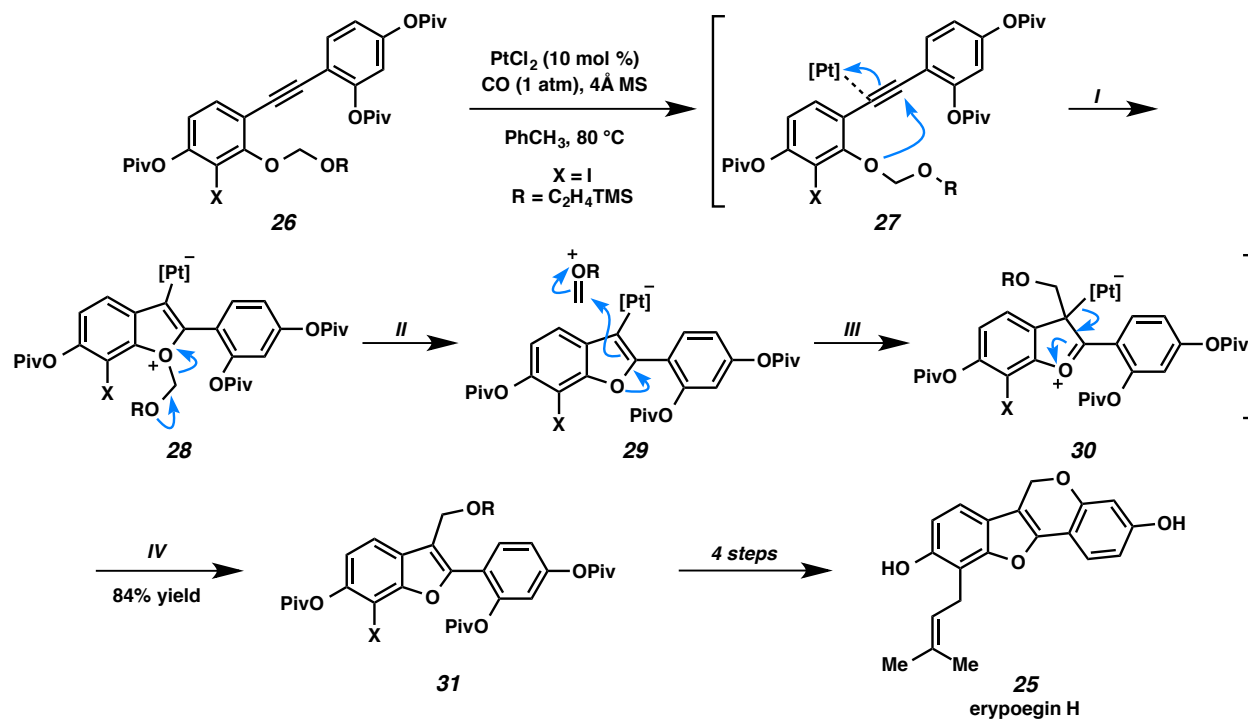


Scheme 2.2.2. Two Similar Routes to (–)-Englerin A (**17**) and Mechanistic Pathway of the Key Steps.

2.2.2 Pt-Mediated Alkyne Activation in Total Synthesis

Platinum has also been utilized as a catalyst in a number of alkyne activation steps in the context of total synthesis. While used less than its Au counterpart, it sometimes displays quite differential reactivity. The two examples below highlight the power of Pt-mediated alkyne activation and the fascinating mechanistic pathways that can occur with these catalysts.

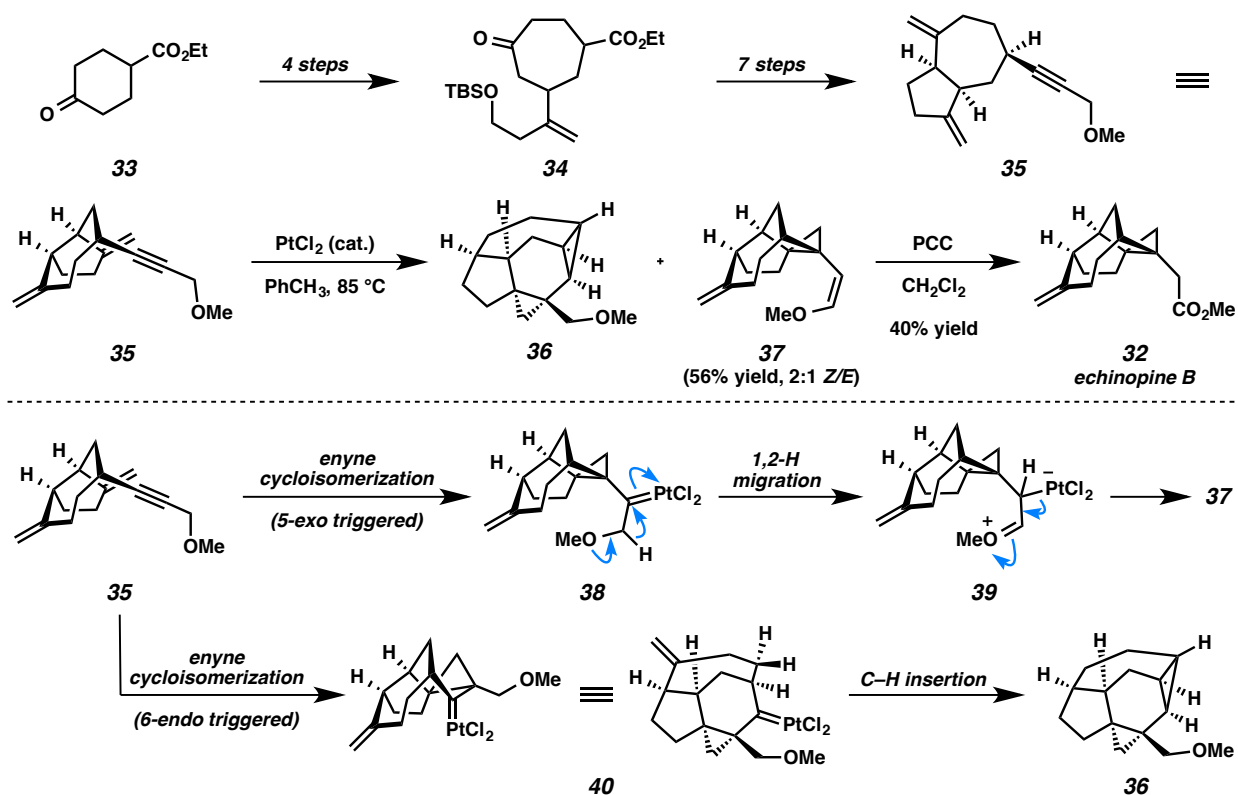
In 2007, Fürstner and coworkers reported the total synthesis of antibiotic erypoeigin H (**25**) and analogs (Scheme 2.2.3).⁸ Biaryl alkyne **26** is made in four steps using conventional chemistry; treatment of this alkyne (**26**) with catalytic PtCl₂ affords benzofuran intermediate **31** in 80% yield. This reaction is proposed to occur by initial intramolecular attack of the phenolic ether oxygen onto Pt-alkyne complex **27** (step I), followed by extrusion of the oxocarbenium (step II). Then, addition of vinyl platinate **29** into the oxocarbenium gives intermediate **30** (step III). Loss of PtCl₂ catalyst (step IV) generates benzofuran **31**. This intermediate is then converted to natural product erypoeigin H (**25**) in four steps. This single step allows for the formation of two bonds and the cleavage of one bond selectively. Additionally, the power of this reaction is showcased further in the synthesis of analogs of erypoeigin H.



Scheme 2.2.3. Fürstner's Pt-Catalyzed Carboalkoxylation in the Synthesis of Erypoeigin H (**25**).

Vanderwal and coworkers explored the use of Pt-catalyzed alkyne activation in the synthesis of echinopine B (**32**, Scheme 2.2.4).⁹ Cycloheptanone **34** is generated in four steps from cyclohexanone **33**. Elaboration of the cycloheptanone intermediate (**34**) to the cycloisomerization precursor (**35**) is completed in seven steps. Two products are observed when subjecting enyne **35** to catalytic PtCl₂: desired enol ether **37** and bicyclopropane-containing byproduct **36**. Their desired product (**37**) is converted to echinopine B (**32**) in 40% yield using the Corey-Suggs reagent.¹⁰

The authors offer mechanistic pathways to both products of the Pt-catalyzed cyclization. To generate the desired product (**37**), they propose an initial *5-exo* cyclization and subsequent formation of Pt-carbenoid **38**. This intermediate then undergoes a 1,2-hydrogen migration into the carbenoid to generate zwitterion **39**. Finally, enol ether **37** is formed after elimination of the metal catalyst. The authors believe bicyclopropane-containing byproduct (**36**) arises from a different pathway initiated by a *6-endo*-triggered cycloisomerization to provide endocyclic carbenoid **40**. This carbenoid then undergoes a C–H insertion to a β -hydrogen to ultimately form byproduct **36**. By exploring the use of this type of Pt-catalyzed cycloisomerization chemistry in the context of natural product synthesis, the authors discovered two competing pathways. These findings can ultimately lead to a deeper understanding of these processes and can inform future uses and limitations of such chemistry.

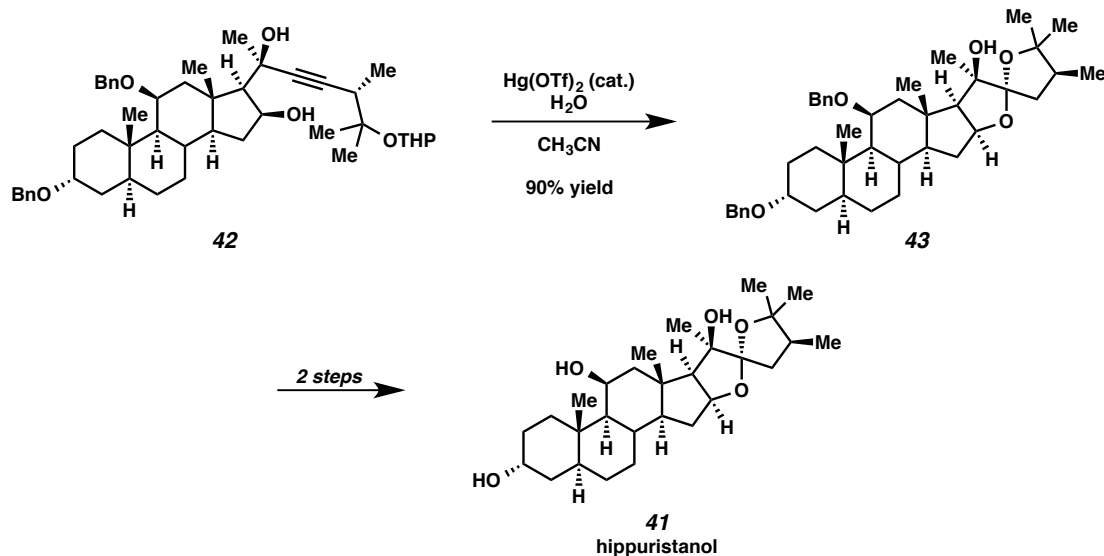


Scheme 2.2.4. Pt-Catalyzed Cycloisomerization Reactions in Vanderwal and Coworkers' Synthesis of Echinopine B (32).

2.2.3 Hg-Mediated Alkyne Activation in Total Synthesis

Stoichiometric mercury-promoted alkyne and alkene activation is well preceded. Mercury-catalyzed processes, however, are more commonly disclosed on alkyne-containing substrates than their alkene-containing counterparts. This stems from the fact that Hg-C(*sp*²) bonds resulting from Hg-alkyne activation are more labile compared to the alkene-derived Hg-C(*sp*³) bonds, which are quite kinetically stable. Thus, Hg-C(*sp*²) bonds are more advantageous in catalytic processes. In one recent example, Deslongchamps and coworkers disclosed the synthesis of antiproliferative agent hippuristanol (41, Scheme 2.2.5).¹¹ Key to their synthesis is a Hg-catalyzed cascade spiroketalization. In nine steps, they synthesize propargylic alcohol 42. Treatment of this alkyne (42) with catalytic Hg(OTf)₂ and water provides spiroketal 43 in 90% yield in 5 minutes; the authors state that the efficiency of this process is

owed to both the ability of the catalyst to activate the alkyne as well as the acidic nature of the reaction media. This intermediate (**43**) is then converted into their target natural product, hippuristanol (**41**), in two steps.



Scheme 2.2.5. Deslongchamps and Coworkers' Synthesis of Hippuristanol (**41**).

2.2.4 Alkyne Activation in Total Synthesis: Summary

Compared with many of the reactions catalyzed by transition metal complexes (e.g. Pd-mediated cross-couplings, olefin metathesis), catalytic alkyne activation chemistry is still a young field. Even so, it has been implemented numerous times in the synthesis of complex molecules. The selectivities, unique modes of reactivity, and simple reaction conditions in the example shown above are emblematic of this class of catalyst.

2.3 Alkynophilicity

Common to all of the examples described in the previous section, and the broad field of alkyne activation, is the concept of alkynophilicity. This term refers to the tendency of certain metals (Au, Pt, Hg, etc.) to activate alkynes towards nucleophilic addition due largely to the unique Lewis acidic nature of these metals towards C–C triple bonds. While metal-alkyne coordination is the strict definition of this

process—and the most common initial mechanistic step in these reactions—these metals display additional reactivity (i.e., pull/push reactivity) that renders them quite unlike any other Lewis acid.

2.3.1 Characteristics of Alkynophilic Metal Complexes

There are three related characteristics associated with Au-, Pt-, and Hg-mediated alkyne activation chemistry. The most fundamental of these is the Lewis acidic nature of certain metals to activate alkynes towards nucleophilic attack, i.e., pull-type reactivity (eq 1, Figure 2.3.1). Secondly, these alkyl metal complexes distinctive ability to stabilize adjacent positive charges (i.e., push-type reactivity, eq 2). Finally, as a result of their ability to stabilize charge efficiently, carbenoid-like reactivity is commonly observed in these transformations (eq 3). While all three of these traits are not always operative, Lewis acid-activation (eq 1) is necessary. If certain reaction factors are present, the remaining two characteristics can follow.

These traits are shown quite clearly in the Au(I)-catalyzed acetylenic Schmidt reaction, disclosed by Toste and coworkers in 2005 (**44** → **45**).¹² They propose initial activation of the alkyne for nucleophilic addition of the azide (pull-type reactivity) forming vinyl gold intermediate **47**. Loss of dinitrogen then occurs by formation of the Au-carbenoid (**48**) via push-type reactivity. A 1,2-alkyl migration into the metal-carbenoid generates carbocation **49**, and after elimination of the catalyst, provides intermediate **50**. This compound (**50**) undergoes isomerization to the isolated pyrrole (**45**).

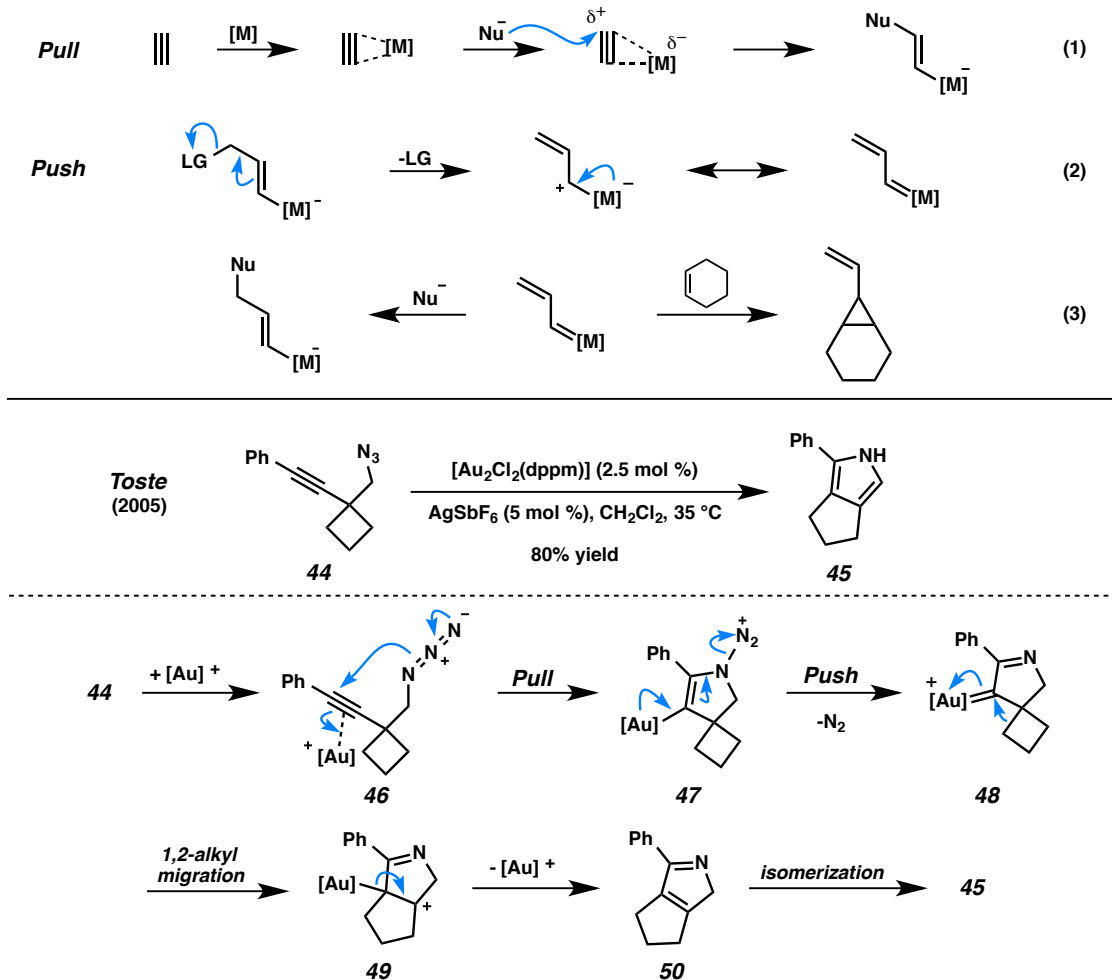


Figure 2.3.1. Three Characteristics of Alkyne Activation Catalysis and an Example of this Reactivity by Toste and Coworkers.

2.3.2 Relativistic Effects

The three characteristics briefly discussed above can largely be explained by relativistic properties.¹³ Therefore, a brief comment on the consequences of relativistic effects in these metal catalysts is necessary. As a result of special relativity, the mass of an entity (in this case, 6s electrons) approaches infinity as its speed approaches the speed of light. In heavier atoms ($Z > 70$), the radial velocity increases substantially, thus the mass of the electrons increases. Since the mass of the 6s electrons is inversely

proportional to the Bohr radius, contraction of the 6s orbitals result. This causes greater shielding of the 4f and 5d orbitals from the nucleus; thus, these orbitals expand.

In order from most to least, Au, Pt, and Hg are the transition metals most affected by relativistic effects.¹⁴ The superb Lewis acidity of Au(I), Hg(II), and Pt(II) can be explained by the relativistic contraction of the valence *s* and *p* orbitals (Figure 2.3.2). This equates to the lowest unoccupied molecular orbital (LUMO) being lower-lying in energy when compared to other transition metals of the same group. Additionally, the drastic relativistic energy stabilization of the 6s orbital makes these metals extremely “soft” Lewis acids, which further explains the specific/selective activation of very “soft” Lewis bases (i.e., alkenes and alkynes).

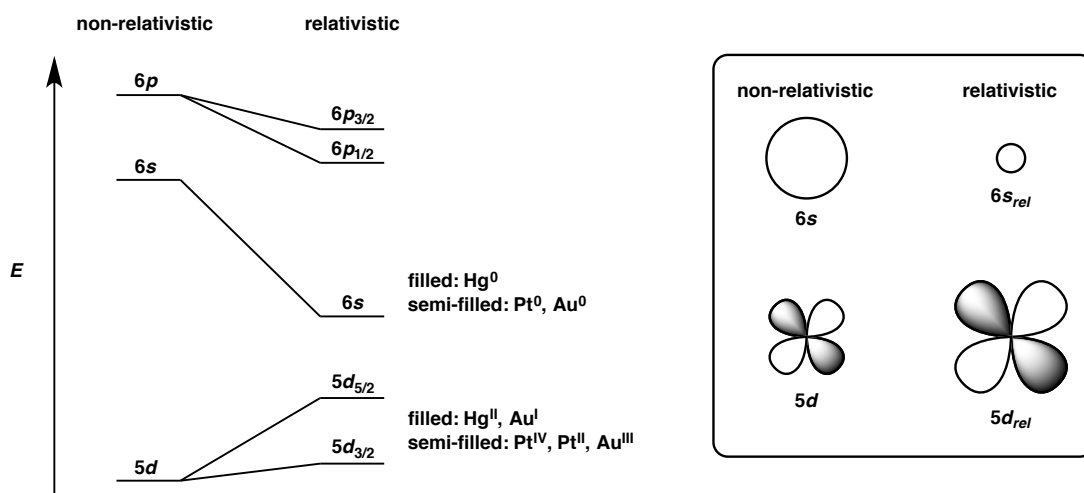


Figure 2.3.2. Molecular Orbital Energies for Au, Hg, and, Pt Before and After Relativistic Considerations.¹⁵

One intriguing aspect to the alkynophilic reactivity observed with these metals is the apparent selective activation of alkynes over alkenes. Although studies have shown the Au⁺-acetylene complex to be *ca.* 10 kcal mol⁻¹ higher in energy than the Au⁺-ethylene complex, this empirical discrimination is misguided.¹⁶ The selectivity arises from the nature of the metal complex LUMOs: the LUMO of the Au⁺-alkyne complex is most likely lower in energy than the LUMO of the Au⁺-alkene complex. This would

result in a more electrophilic Au⁺-alkyne complex and thus explain the observed alkynophilic nature of the metals.

The relativistic expansion of the *5d* orbitals is used to rationalize why these metals are able to stabilize adjacent positive charges so effectively (eq 2, Figure 2.3.1). The destabilization of the *5d* orbital (the highest occupied molecular orbital (HOMO) in these metals) raises the energy sufficiently to allow overlap with an empty *p* orbital (LUMO) on an adjacent carbon atom. This constructive overlap could give rise to the metal-stabilized cationic intermediates observed with Au, Pt, and Hg. It is unclear, however, whether the carbenoid-like reactivity observed in certain reactions with these metal catalysts occurs via a metal-carbenoid or simply a metal-stabilized carbocation. This argument arises from the ability, or lack thereof, for Au, Pt, and Hg to participate in appreciable backbonding. While the nature of the specific species are still argued, their unique carbenoid-like reactivity points to these metals not simply acting as Lewis acids.

2.4 Conclusion

Alkyne activation chemistry has been used successfully in a number of natural product syntheses. The examples shown above highlight some of the key features of this chemistry, including: highly selective hydrations or spiroketalizations, an efficient carboalkoxylation, and multiple C–C bond forming events in a single step. Additionally, the fundamental atomic properties of these metals (Au, Pt, and Hg), namely relativistic effects, explain much of their unique reactivity. Both the potential applications of alkyne activation chemistry in natural product synthesis, as well as the fundamental properties for reaction outcomes, have driven the work described in chapters three and five.

CHAPTER TWO NOTES AND REFERENCES

- ¹ Hashmi, A. S. K.; Rudolph, M. *Chem. Soc. Rev.* **2008**, *37*, 1766–1775.
- ² Trost, B. M.; Dong, G. *Nature* **2008**, *456*, 485–488.
- ³ This could be a result of the inherent electronics of the substrate or via catalyst control. The reason for the selectivity remains unclear.
- ⁴ Molawi, K.; Delpont, N.; Echavarren, A. M. *Angew. Chem., Int. Ed.* **2010**, *49*, 3517–3519.
- ⁵ Zhou, Q.; Chen, X.; Ma, D. *Angew. Chem., Int. Ed.* **2010**, *49*, 3513–3516.
- ⁶ When conditions resembling Echavarren's were employed on enyne **20** ([Au(PPh₃)Cl]/AgSbF₆) were employed, the product was obtained in 20% yield. See ref 5.
- ⁷ These general intermediates (**22-A** and **22-B**) are drawn as resonance contributors because of the unlikely nature of S_N2 chemistry on a fully substituted carbon to produce oxocarbenium **23**.
- ⁸ Fürstner, A.; Heilmann, E. K.; Davies, P. W. *Angew. Chem., Int. Ed.* **2007**, *46*, 4760–4763.
- ⁹ Michels, T. D.; Dowling, M. S.; Vanderwal, C. D. *Angew. Chem., Int. Ed.* **2012**, *51*, 7572–7576.
- ¹⁰ The synthesis of cycloisomerization product **37** constitutes a formal synthesis of echinopine B. See: Nicolaou, K. C.; Ding, H.; Richard, J.-A.; Chen, D. Y.-K. *J. Am. Chem. Soc.* **2010**, *132*, 3815–3818.
- ¹¹ (a) Ravindar, K.; Reddy, M. S.; Lindqvist, L.; Pelletier, J.; Deslongchamps, P. *Org. Lett.* **2010**, *12*, 4420–4423; (b) Somaiah, R.; Ravindar, K.; Cencic, R.; Pelletier, J.; Deslongchamps, P. *J. Med. Chem.* **2014**, *57*, 2511–2523.
- ¹² Gorin, D. J.; Davis, N. R.; Toste, F. D. *J. Am. Chem. Soc.* **2005**, *127*, 11260–11261.
- ¹³ (a) Gorin, D. J.; Toste, F. D. *Nature* **2007**, *446*, 395–403; (b) Leyva-Pérez, A.; Corma, A. *Angew. Chem., Int. Ed.* **2012**, *51*, 614–635; (c) Pitzer, K. S. *Acc. Chem. Res.* **1979**, *12*, 271–276; (d) Pyykko, P.; Desclaux, J. P. *Acc. Chem. Res.* **1979**, *12*, 276–281.
- ¹⁴ This does not include metals that are rarely used in catalysis.
- ¹⁵ This conceptual figure was reproduced from ref 13b.

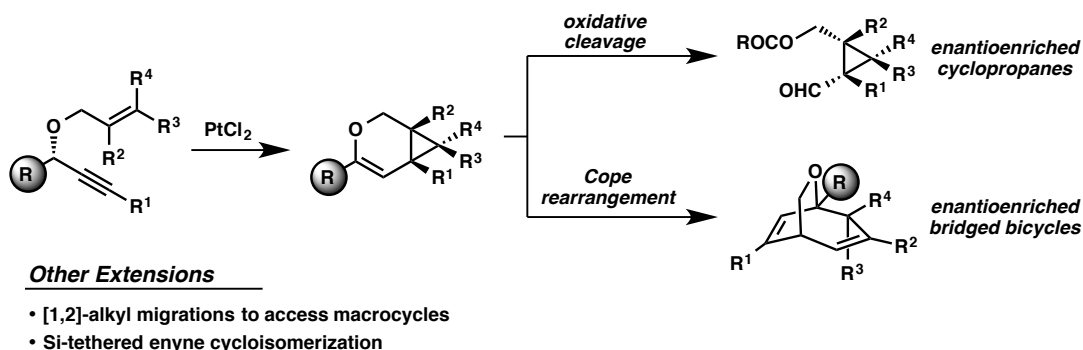
¹⁶ (a) Hertwig, R. H.; Koch, W.; Schröder, D.; Schwarz, H.; Hrušák, J.; Schwerdtfeger, P. *J. Phys. Chem.* **1996**, *100*, 12253–12260; (b) Nechaev, M. S.; Rayon, V. M.; Frenking, G. *J. Phys. Chem. A* **2004**, *108*, 3134–3142.

CHAPTER THREE

Cycloisomerization of Enynes as a Platform to Study Catalytic Reactivity

3.1 Overview

As detailed in Chapter Two, pi-acidic transition metals can be a powerful tool in the synthesis of complex molecules. Through our knowledge concerning the fundamental properties of alkyne activation catalysis, we can test and explore new reactivity in complex settings. Subsequently, our findings generate new understanding and thus fresh avenues of inquiry. Mechanistic questions surrounding the cycloisomerization of *N*- and *O*-tethered 1,6-enynes prompted us to explore current limitations in asymmetric catalysis. Namely, we developed a highly enantiospecific transformation for the synthesis of enantioenriched 3-oxabicyclo[4.1.0]heptenes. With the successful implementation of this idea, we have eliminated some possible mechanistic pathways for the cycloisomerization reaction. Also described are the expansion of this method by analysis and utilization of both proposed intermediates along the reaction pathway and products derived from cycloisomerization, respectively.



Scheme 3.1.1. Enantiospecific 1,6-Enyne Cycloisomerization and Extensions.

3.2 Cycloisomerization Reactions of Enynes

3.2.1 Introduction

Cycloisomerizations are a special class of ring-forming reactions. In a cycloisomerization reaction, no loss or gain of atoms occurs: the process is completely atom economical.¹ Well-known

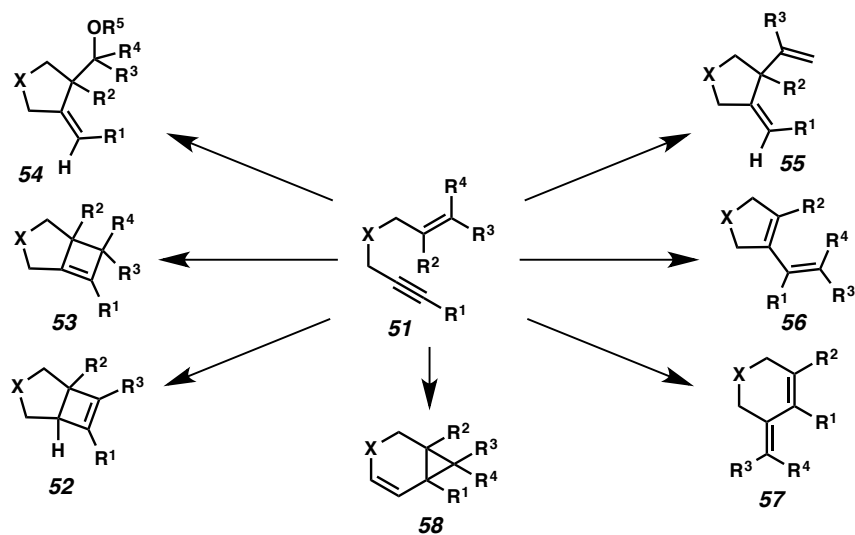
cycloisomerization reactions are the intramolecular Diels-Alder reaction (IMDA),² the intramolecular Michael addition,³ and the Conia-Ene reaction,⁴ among others. These transformations, however, are rarely classified as cycloisomerizations because of the prior discovery or importance of their respective intermolecular counterparts. Nonetheless, these reactions are prolific in complex molecule synthesis. Developing new types of cycloisomerization reactions will only lead to greater power and control in the field of molecule synthesis.

The use of transition metal complexes to catalyze organic transformations has led to a number of new cycloisomerization reactions. These new advances in cycloisomerization chemistry have also allowed chemists to discover a myriad of new reactivity in regards to both synthetic utility and mechanistic understanding.

3.2.2 Products and Pathways in the Cycloisomerization of 1,6-Enynes

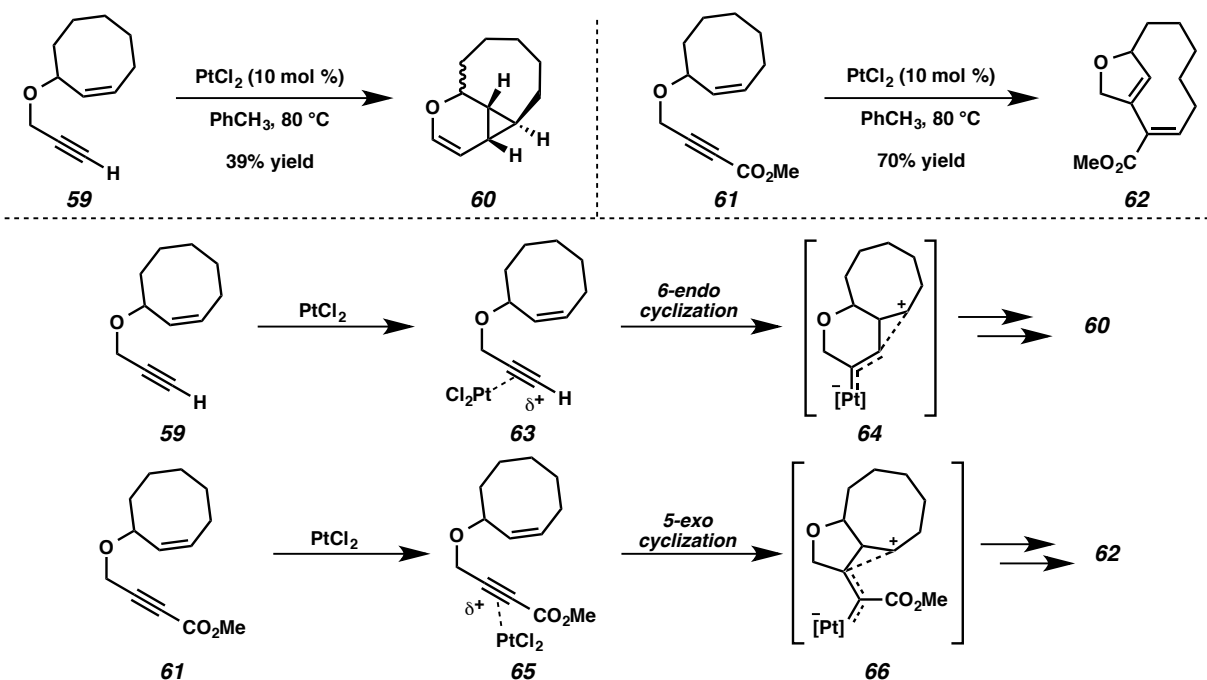
The cycloisomerization of enynes is a prolific reaction class in pi-acid catalysis. The reactions of 1,6-enynes, in particular, provide chemists with a unique platform for studying reactivity and mechanistic inquiry.⁵ Different substrate substitutions as well as catalyst choice yield disparate product formation. As a result, the underlying driving forces for various reaction pathways are probed, and a further understanding of pi-acid mediated alkyne activation is possible.

From a single general 1,6-enyne structure (**51**), a number of products can be realized (Scheme 3.2.1). These include cyclobutene-containing compounds (**52** and **53**), oxygenated products (**54**),⁶ numerous dienes (**55**, **56**, and **57**), and cyclopropane-containing bicycles (**58**). These motifs are produced via either an initial *5-exo* or *6-endo* cyclization of the alkene onto the activated alkyne. After this split in the mechanistic tree, various other branches can be made. Ether **54** and diene **55** are formed along the same *5-exo* cyclization pathway yet diverge in final steps, while bicycle **58** and diene **57** share a different common intermediate that is initiated by *6-endo* cyclization.



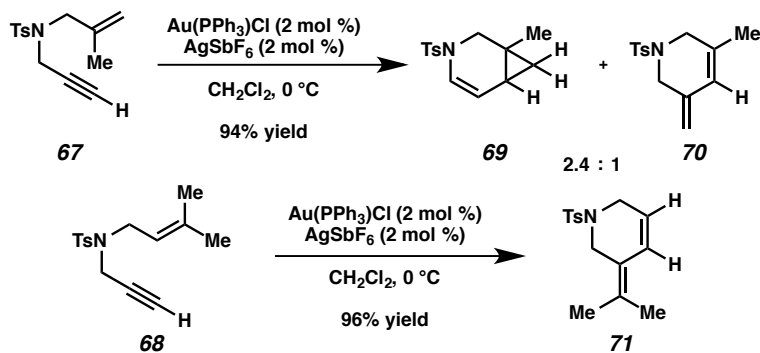
Scheme 3.2.1. Variation in 1,6-Enyne Cycloisomerization Products.

Many of these different reaction outcomes can be explained through the reaction pathways that are believed to be operative. Simple substrate variation can cause drastically distinctive outcomes. Under analogous reactions conditions (catalytic PtCl_2 in toluene at $80\text{ }^\circ\text{C}$), terminal alkyne **59** produces tricycle **60** in 39% yield,⁷ whereas the ester substituted alkyne (**61**) generates a formal enyne metathesis product (**62**, Scheme 3.2.2).⁸ These different outcomes are easily rationalized through the difference in electronic structure before nucleophile attack of the alkene. Following complexation of platinum chloride to each alkyne, either a *6-endo* or *5-exo* cyclization is favored. The *6-endo* cyclization is favored for the terminal alkyne substrate (**59**) to give transient zwitterion **64**. Conversely, *5-exo* cyclization is favored for ester-containing substrate **61** to provide a different transient zwitterion (**66**), as the electron-withdrawing group provides an initial electronic bias for metal coordination to the alkyne. Following cyclization, the respective products are formed via further rearrangements.



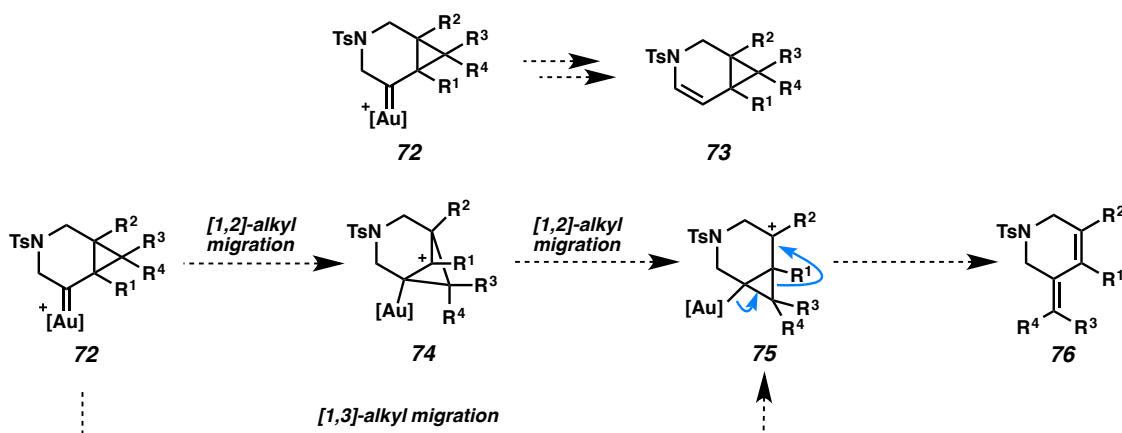
Scheme 3.2.2. Substrate Influence on Products Formed in Pt-Catalyzed Cycloisomerization of 1,6-Enynes.

Some results, however, are more difficult to rationalize from our current mechanistic understanding. One example is the cycloisomerization of enynes **67** and **68** to provide cyclopropane **69** and diene **70**, and diene **71**, respectively (Scheme 3.2.3).⁹ If, under Au-catalysis, certain substitution patterns are present, then dienes with the general structure of **70** are obtained as minor products. Alternatively, if enyne **68** is subjected to the same reaction conditions, then good conversions to diene **71** are observed.



Scheme 3.2.3. Substrate Influence on Products Formed in Au-Catalyzed 1,6-Enyne Cycloisomerization.

The product selectivities are difficult to explain via the purported intermediates and steps. Via intermediate **72**, cyclopropane-containing products (**73**) are formed from [1,2]-hydride migration and demetalation (Scheme 3.2.4). Conversely, either (a) two consecutive [1,2]-alkyl migrations or less likely (b) one [1,3]-alkyl migration, produces intermediate **75**. Following elimination, diene products (**76**) are obtained. If a species such as carbocation **75** is operative, then one could argue the steps to arrive at diene **70** should be lower in energy than those which provide compound **71** (Scheme 3.2.3), as the internal methyl group would stabilize a positive charge more effectively (R^2 , **75**). It may be that a simplistic picture of these reaction pathways is not sufficient and requires additional study to eliminate potential intermediates.



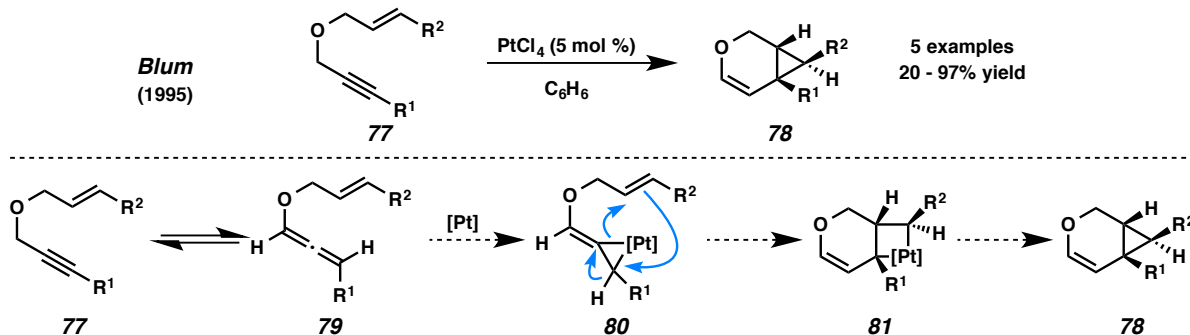
Scheme 3.2.4. Proposed Intermediates Leading to the Formation of Products with the General Structures of **73** and **76**.

The idea that a number of possible outcomes can arise from such a seemingly simple system is thought provoking. By attempting to understand these reaction outcomes in terms of mechanistic steps, we can inform future studies to discover new reactivity.

3.3 1,6-Enyne Cycloisomerizations to Produce 3-Aza and 3-Oxabicyclo[4.1.0]heptenes

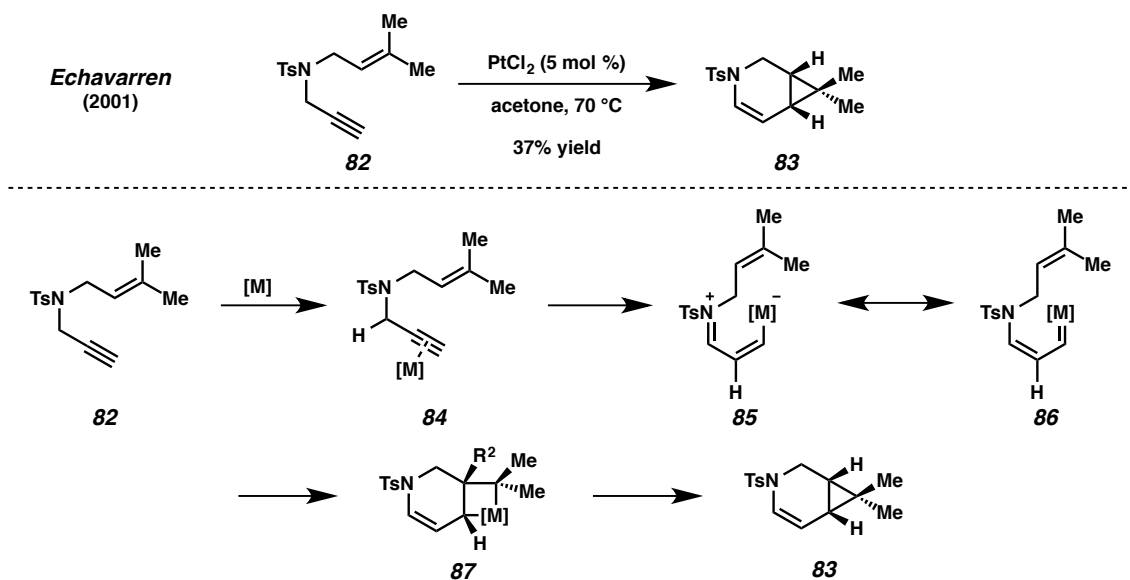
3.3.1 Racemic Examples and Mechanistic Proposals

In 1995, Blum and coworkers disclosed that under Pt(IV)-catalysis, *O*-tethered 1,6-enynes produce 3-oxabicyclo[4.1.0]heptenes (**77** → **78**, Scheme 3.3.1).^{10,11} Only five examples were reported, and most products were obtained in low yields. It was proposed that the reaction proceeds by isomerization of the alkyne of the substrate to the allene (**79**), followed by insertion of the Pt-catalyst. Migratory insertion provides metallocyclobutane **81**, and subsequent reductive elimination gives the bicyclic products observed. This discovery was made years before Au and Pt alkyne activation chemistry would explode into the thriving field it is today.



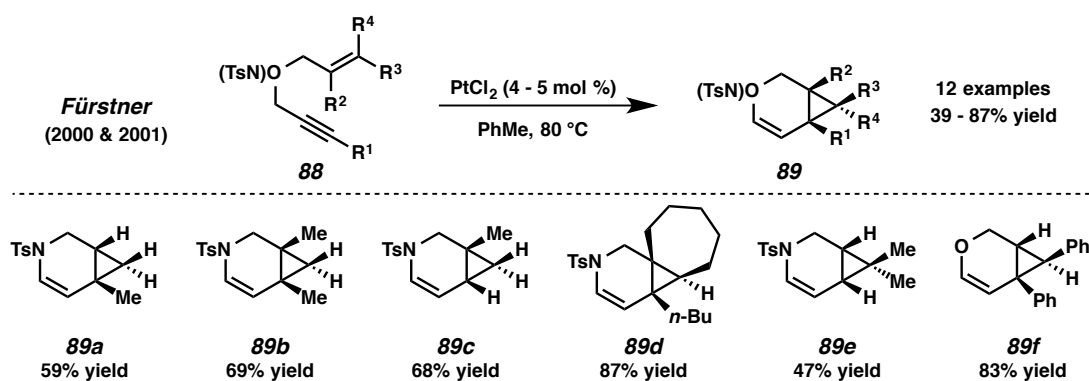
Scheme 3.3.1. First Example of 3-Oxabicyclo[4.1.0]heptenes from 1,6-Enynes and Proposed Mechanism.

In 2001, Echavarren and coworkers reported on the cyclizations of enynes by PtCl₂ (**82** → **83**, Scheme 3.3.2).⁹ While only two examples were described, their mechanistic picture was slightly different. They propose an initial 1,2-hydride migration to produce zwitterion **85**, which undergoes isomerization to carbenoid **86**. Following [2+2] cycloaddition, metallacyclobutane **87** is formed. Upon extrusion of the catalyst via reductive elimination, product **83** is formed.



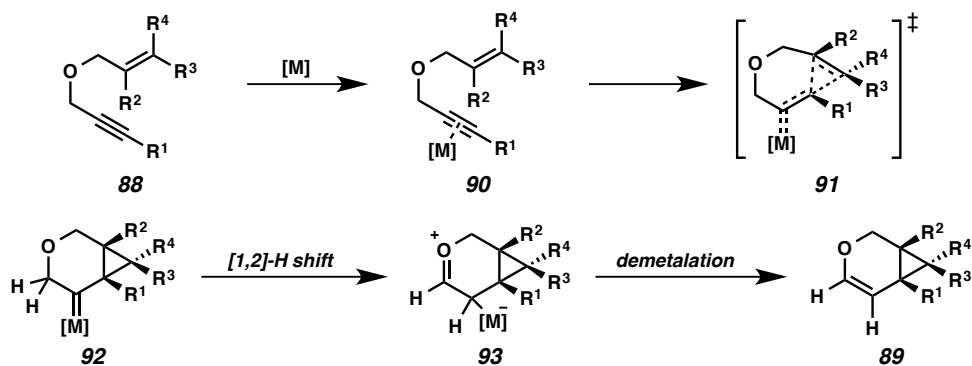
Scheme 3.3.2. *N*-Tethered 1,6-Enyne Cycloisomerization with Alternative Mechanistic Proposal.

Fürstner and coworkers found that with catalytic PtCl_2 at slightly elevated temperatures both *O*- and *N*-tethered 1,6-enynes undergo this type of cycloisomerization (**88** \rightarrow **89**, Scheme 3.3.3).⁸ From the representative products shown below, alkyl substitution is tolerated on the alkyne (**89a**, **89b**, **89d**) as well as aryl (**89f**). Furthermore, the researchers show that terminal alkynes are acceptable with *N*-tethered substrates only, an issue that has still yet to be overcome.



Scheme 3.3.3. *N*- and *O*-Tethered 1,6-Enyne Cycloisomerization Catalyzed by PtCl_2 .

Mechanistically, they propose initial activation of the alkyne by the metal in an η^2 manner (**88** \rightarrow **90**, Scheme 3.3.4). Cyclopropanation then occurs with concomitant carbenoid formation (through **91**) to produce intermediate **92**. A 1,2-hydride migration generates zwitterionic compound **93**. Finally, elimination of the metal produces bicycles with general structure **89**.



Scheme 3.3.4. Alternative Mechanistic Proposal by Fürstner and Coworkers.

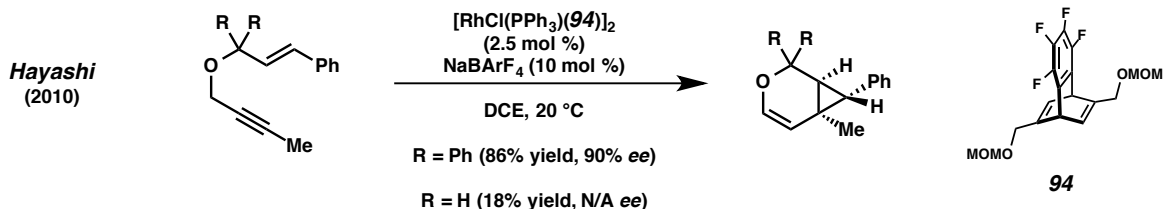
From these examples, it is apparent that there is some disagreement on the mechanistic steps and intermediates for this transformation. As additional transition metal complexes are competent in catalyzing this process,¹² there may in fact be distinct operable pathways for this overall transformation. Initial studies concerning the Au- and Pt-catalyzed reaction, however, could provide a more cohesive understanding of this overall transformation.

3.3.2 Asymmetric Cases of 1,6-Enyne Cycloisomerizations to Produce 3-Aza and 3-Oxabicyclo[4.1.0]heptenes

While the racemic version of this transformation is well explored, asymmetric variants employing chiral catalysts are hindered by several limitations. These limitations include narrow substrate scopes, cumbersome ligand syntheses, and the known instability of oxygen-tethered substrates under many reaction conditions.

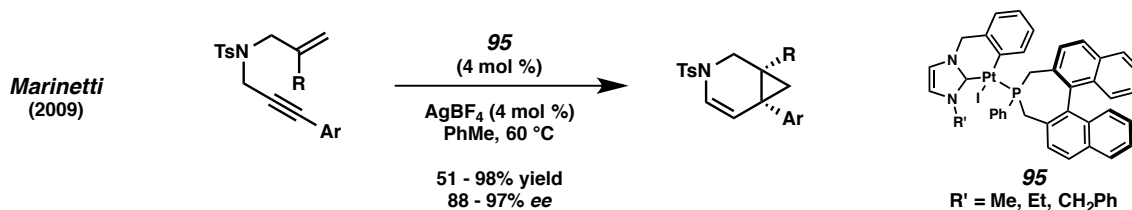
Hayashi and coworkers disclosed the use of a chiral diene (**94**)/Rh catalytic system to afford enantioenriched 3-oxa and 3-azabicyclo[4.1.0]heptenes (Scheme 3.3.5).¹³ Under the developed

conditions, *N*- and *O*-tethered enynes were explored as substrates. Two interesting observations can be made from the study. First, the reaction of *O*-tethered enynes necessitates geminal diphenyl substitution on the allylic carbon. When no such substitution is present, the yield falls from excellent (86%) to poor (18%). Secondly, only three *O*-tethered enynes were described in the study. Hayashi describes that the *O*-tethered substrates undergo polymerization while using a similar catalytic system.¹⁴



Scheme 3.3.5. Example of Rh-Catalyzed Asymmetric 1,6-Enyne Cycloisomerization.

Examples of Pt-catalyzed asymmetric alkyne activation are rare. Marinetti and coworkers have described the asymmetric cycloisomerization with a cyclometallated Pt(II) complex (**95**, Scheme 3.3.6).¹⁵ Variable yields and enantioselectivities are achieved on *N*-tethered 1,6-enyne substrates using this system. Notably, no discussion was made concerning *O*-tethered 1,6-enynes.

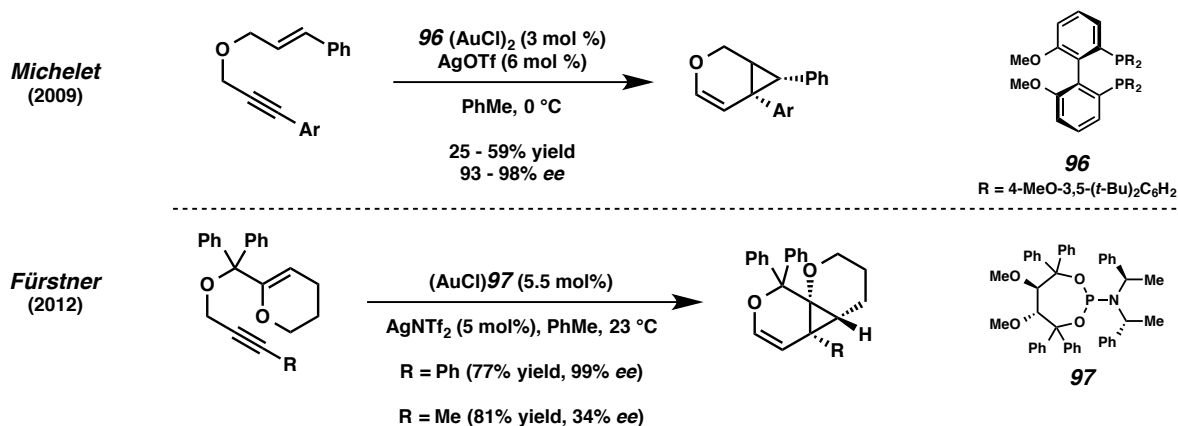


Scheme 3.3.6. Example of Pt-Catalyzed Asymmetric 1,6-Enyne Cycloisomerization.

Asymmetric Au-catalysis for the activation of alkynes has seen a number of great advances in the last decade. Michelet and coworkers have disclosed a Au(I)-catalytic system for the asymmetric cycloisomerization of *O*- and *N*-tethered 1,6-enynes (Scheme 3.3.7).¹⁶ This system makes use of a bis gold phosphine complex derived from biaryl bis phosphine **96**. Although enantioselectivities were

generally high (93-98%), yields suffered for *O*-tethered systems (25-59%). Additionally, aryl substitution was necessary on the alkyne.

Fürstner and coworkers have established the most general asymmetric method, utilizing chiral catalysts, to promote this cyclization (Scheme 3.3.7).¹⁷ By utilizing a TADDOL-derived phosphoramidite ligand (**97**) in conjunction with cationic Au, good yields and enantioselectivities are observed for both *O*- and *N*-tethered enynes. Just as in Hayashi's example, when *O*-tethered enynes are used, it is necessary to have allylic geminal disubstitution. Most importantly, when non-aryl alkynes are subject to the reaction conditions (e.g., CH₃), reduced stereoselection is observed (34% *ee*). It is proposed that there is a chiral pocket in which the aryl group can position, thus locking the alkyne complex in a single orientation. When a small aliphatic group is substituted, however, the ligand on the metal can rotate, decreasing the stereoselection. While these examples are not exhaustive,¹⁸ they effectively demonstrate the state of the art and limitations associated with rendering this reaction asymmetric.



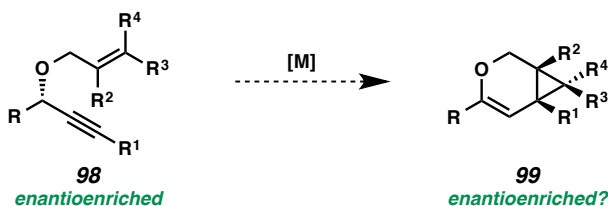
Scheme 3.3.7. Examples of Au-Catalyzed Asymmetric 1,6-Enyne Cyclizations.

3.4 Chirality Transfer Process to Produce Optically Enriched 3-Oxabicyclo[4.1.0]heptenes

3.4.1 Proposal

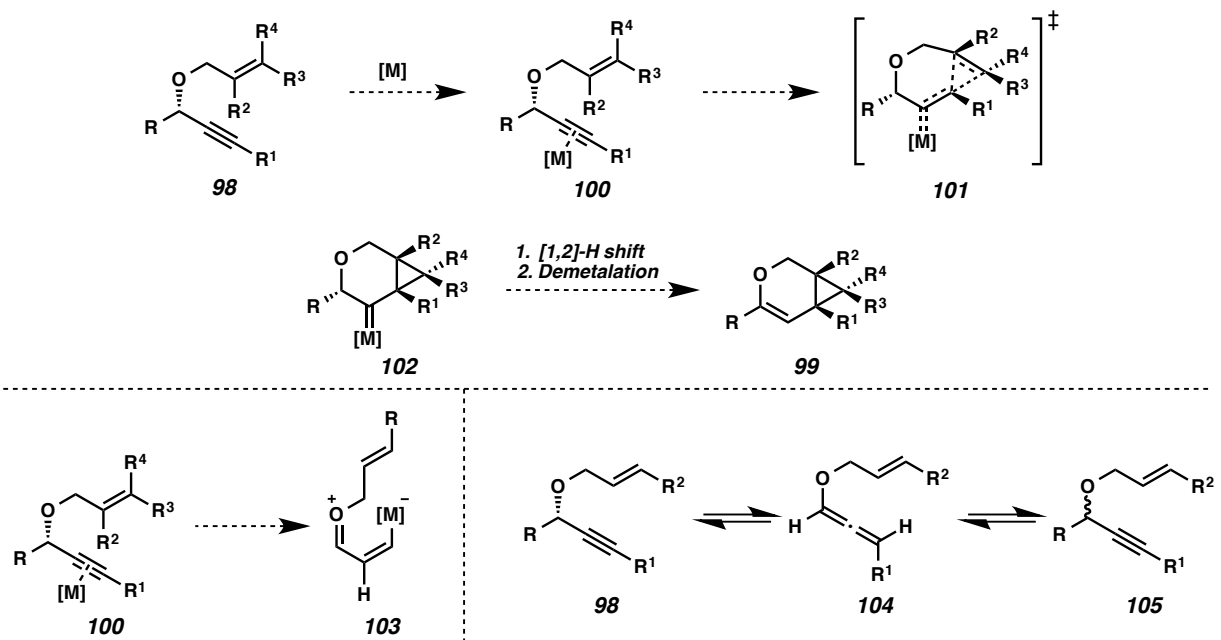
Given the difficulties associated with the synthesis of these enantioenriched bicyclic products using chiral catalysts, we envisioned that a chirality transfer-based approach could be more effective. Specifically, we were curious if an enantioenriched substrate with the general structure of **98** would

generate enantioenriched products (**99**, Scheme 3.4.1). For this idea to have merit when comparing it to previous asymmetric variants, the following must be satisfied: (1) the origin of chirality must be easily obtained, (2) the scope of the reaction should be general, and (3) the selectivities must be an improvement from previous approaches based on chiral catalysts.



Scheme 3.4.1. Chirality Transfer Proposal with Enantioenriched Enyne Substrate.

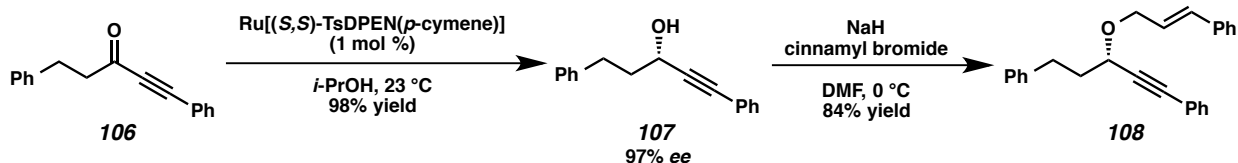
This strategy would utilize an R group, providing defined absolute stereochemistry at the propargylic carbon, to control the stereochemistry of cycloisomerization and leverage Fürstner and coworkers' proposed mechanism (Scheme 3.4.2). Since the stereochemical information of the propargylic carbon is lost in the subsequent 1,2-hydride migration step, the proposed transformation would be enantiospecific. That is, the absolute stereochemistry of enyne starting material **98** would relay in a traceless manner to the absolute stereochemistry of product **99**. Success of this proposal hinges on reaction mechanism: cyclopropane formation must occur *before* 1,2-hydride migration since propargylic stereochemistry is erased in this step. If one of the other proposed reaction mechanisms are operative, our proposal would have little chance of success. In Blum's proposed mechanism, reversible isomerization of propargyl ether to allenol (**98** \rightarrow **104** \rightarrow **105**) would most likely cause loss of stereochemical information. Additionally, because Echavarren's proposed mechanism occurs via an achiral intermediate (**103**), our idea would be unsuccessful.



Scheme 3.4.2. Mechanistic Possibilities in Chirality Transfer Approach.

3.4.2 Substrate Synthesis

One essential aspect to this study is generating the desired substrates easily and in high optical purity. After some optimization, the route exemplified in Scheme 3.4.3 fits both of those qualifications and allows for the rapid synthesis of many substrates with high *ee*. Enone **106** is asymmetrically reduced with Noyori's Ru-based transfer hydrogenation catalyst¹⁹ to the propargylic alcohol (**107**) in 98% yield and 97% *ee*. Williamson ether synthesis of the propargylic alcohol provides enyne **108** in good yield.

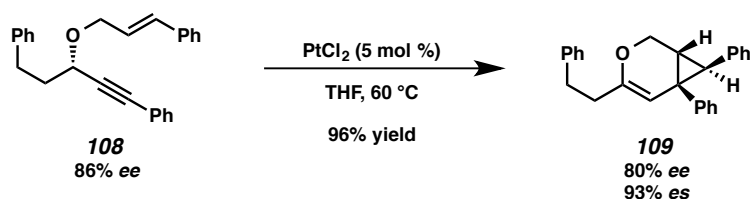


Scheme 3.4.3. Synthesis of Enantioenriched 1,6-Enyne Substrate **108**.

3.4.3 Initial Result and Optimization

As a promising lead, we observed chirality transfer with substrate **108** using 5 mol % $PtCl_2$ in THF at 60 °C, generating enantioenriched product **109** in 96% yield and 80% *ee* (Scheme 3.4.4).

Enantiospecificity (*es*) is used to determine the level of chirality transfer in our process.²⁰ Therefore in this initial finding, substrate **108** (86% *ee*) affording product **109** in (80% *ee*) indicates an *es* of 93%.



Scheme 3.4.4. Initial Observation of Chirality Transfer with Catalytic PtCl₂.

After this initial finding, the reaction conditions were optimized for the yield and *es* of bicycle **108** (Table 3.4.1). Au- and Ir-based catalysts give measurable chirality transfer and moderate yields (entries 1 and 2). The use of PtCl₄ in toluene (entry 3) provides good *es* yet disappointing yield, most likely caused by polymerization of the substrate. The highest yields are observed when using PtCl₂ as the catalyst. As seen in entry 4, PtCl₂ in toluene at elevated temperatures provides product **109** in 78% yield and 89% *es*. Running the reaction under an atmosphere of carbon dioxide does little to increase yield or chiral transfer (entry 6). Moreover, highly soluble Pt(II) catalysts [(C₂H₄)PtCl₂]₂ (entry 7) and Pt(PhCN)₂Cl₂ (entry 8) provide no improvement in yield. A slight increase in catalyst loading and temperature (7 mol %, 70 °C) provide the optimal conditions (entry 9), affording bicycle **109** in 90% yield and 90% *es*.²¹

Table 3.4.1. Optimization of Cycloisomerization Conditions.

entry	catalyst (mol %)	solvent, temp (°C)	t (h)	yield	ee (%)	es (%) ^a
1	(Ph ₃ P)AuNTf ₂ (5)	CH ₂ Cl ₂ , 23	0.5	52	84	87
2	[Ir(dbcot)Cl] ₂ (2.5) ^{b,c}	PhCH ₃ , 100	3	68	84	87
3	PtCl ₄ (5)	PhCH ₃ , 23	1	27	90	93
4	PtCl ₂ (5)	PhCH ₃ , 60	22	78	86	89
5	PtCl ₂ (5)	THF, 60	18	87	88	91
6	PtCl ₂ (5) ^b	THF, 60	14	86	86	89
7	[(C ₂ H ₄)PtCl ₂] ₂ (2.5)	THF, 23	28	84	86	89
8	Pt(PhCN) ₂ Cl ₂ (7)	THF, 60	48	64	87	90
9	PtCl ₂ (7)	THF, 70	18	90	87	90

^a Enantiospecificity (es) = [(ee_{product}) / (ee_{substrate})] x 100%. ^b Under 1 atm CO. ^c dbcot: dibenzo[*a,e*]cyclooctatetraene

3.4.4 Influence of Propargylic Substituent on Enantiospecificity

The nature of the propargylic substituent has influence on the degree of chirality transfer in the cycloisomerization (Table 3.4.2). When R is methyl or isobutyl the enantiospecificity is low, 82% and 80%, respectively. Both yield and *es* are found to be higher (93% and 94%, respectively) when R is hydrocinnamyl (**110c**, entry 3). Finally, when R is cyclohexyl (**110d**, entry 4) or isopropyl (**110e**, entry 5) the enantiospecificity is superb, providing products **111d** and **111e** in high levels of optical purity. Moving to a larger R group such as *tert*-butyl (**110f**, entry 6) leads to unidentifiable decomposition products. While both cyclohexyl and isopropyl substitution provide similar results, we explored scope and limitations on substrates with isopropyl substitution.²²

Table 3.4.2. Results of the Nature of the Stereocontrolling Group.

entry	R	ee (%)	product	yield ^a (%)	ee (%)	es (%)
1	Me (110a)	97	111a	90	80	82
2	<i>i</i> -Bu (110b)	97	111b	84	78	80
3	CH ₂ CH ₂ Ph (110c)	96	111c	93	90	94
4	Cy (110d)	99	111d	84	96	97
5	<i>i</i> -Pr (110e)	98	111e	80	97	99
6	<i>t</i> -Bu (110f)	96	–	<10	nd ^b	nd ^b

^a Isolated yield. ^b nd: Not determined.

3.4.5 Tolerance and Limitations on Substitution

Traceless chirality transfer is observed with diverse enyne substrates, which provide enantioenriched products in high yield and superb optical purity (Figure 3.4.1). Di- and tri-substituted alkenes are predictably tolerated under the reaction conditions and are obtained in excellent *ee*'s. It is noteworthy that products **111e** and **113d** arise from (*E*)- and (*Z*)-alkene substrates respectively. This indicates complete diastereoselectivity in regards to alkene geometry.

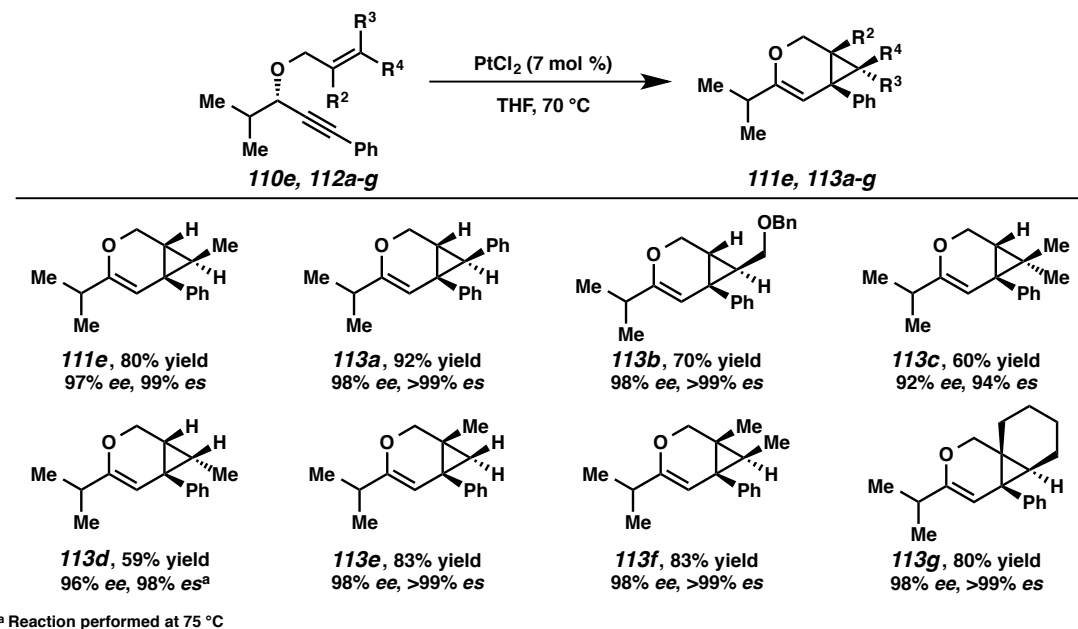


Figure 3.4.1. Enantiospecific Cycloisomerization: Alkene Substitution Scope.

Importantly, alkyne substitution does not affect the efficiency of our developed process. This has proven to be an issue in previous examples based on chiral catalysts.^{16,17} Methyl substitution affords bicycle **113h** in 68% yield and 93% *es* (Figure 3.4.2). Heteroaromatic substitution in the form of *N*-tosyl indole provides complex product **113i** in good yield and excellent transfer of chirality. Bicycle **113j** is obtained in exceptional optical purity and 86% yield, illustrating the stability of silyl ethers to the reaction conditions.

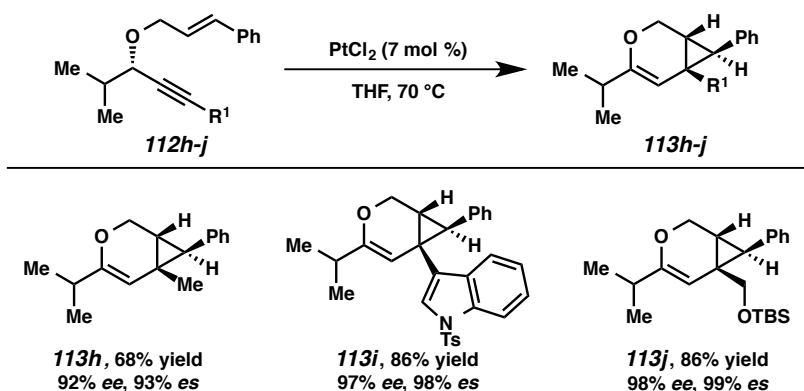


Figure 3.4.2. Enantiospecific Cycloisomerization: Alkyne Substitution Scope.

While the prior reactivity of ether **110f** has already been noted, other substrates are also not competent under the reaction conditions (Figure 3.4.3). Curiously, (*Z*)-alkene substrate **114** was completely unreactive under the reaction conditions. Fully substituted alkene substrate **115** is unreactive under normal reaction conditions and decomposes when heated to temperatures at or above 120 °C. Terminal alkyne **116** and allyl ether **117** were not tolerated under the reaction conditions.

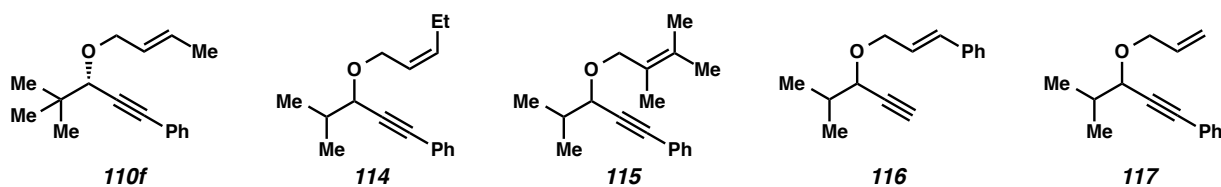
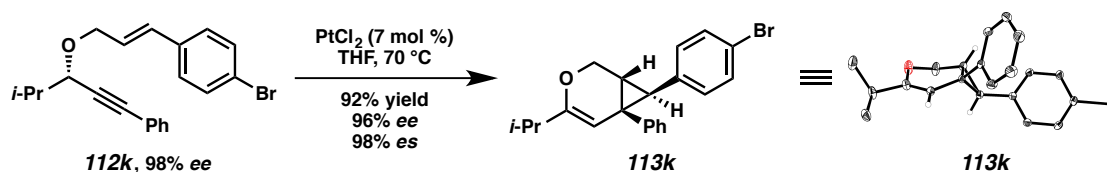


Figure 3.4.3. Unsuccessful Substrates in the Cycloisomerization.

This chirality transfer system tolerates various substitution patterns on both the alkene and alkyne moieties. Additionally, no geminal substitution is necessary for high yields and chiral induction. Such generality is not observed in similar enantioselective cycloisomerizations utilizing chiral catalysts.

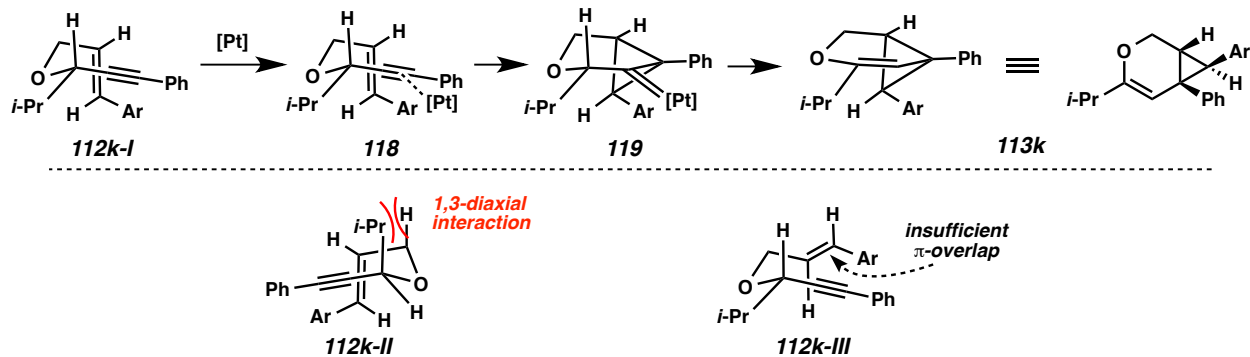
3.4.6 Stereochemical Confirmation and Model for Transfer of Stereochemical Information

During the investigation, we were curious how the stereochemistry of the substrate dictated the product chirality. Fortunately, the absolute stereochemistry of bromide **113k** could be determined by single crystal x-ray diffraction, and this informed our understanding of the stereochemistry of cycloisomerization (Scheme 3.4.5).



Scheme 3.4.5. Confirmation of Absolute Stereochemistry in Cycloisomerization from Single Crystal X-Ray Structure of Aryl Bromide **113k**.

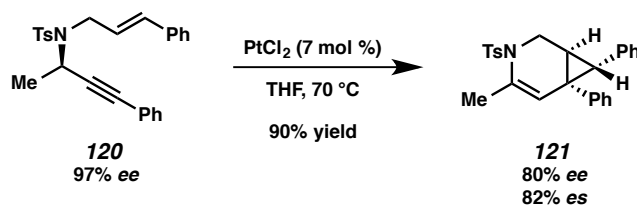
With information regarding the absolute stereochemical outcome of this process, we propose a model for the stereochemical transfer. The enyne is displayed in a chair conformation (**112k-I**, Scheme 3.4.6). In the proposed transition state, the bulky isopropyl group occupies the equatorial position, and the alkene orients to maximize orbital overlap (**118**). This type of orientation for attack agrees with previously published computational studies.²³ Carbenoid **119** is then formed in the cyclopropanation step. Finally, 1,2-hydride migration and demetalation provide product **113k**. Alternative possible orientations that provide product **113k** present issues. Conformation **112k-II** would contain a destabilizing 1,3-diaxial steric interaction. Additionally, conformation **112k-III** does not allow for the optimal overlap in the initial attack of the alkene.



Scheme 3.4.6. Model for Stereochemical Transfer and Unfavorable Conformations.

3.4.7 *N*-Tethered Enyne Substrates

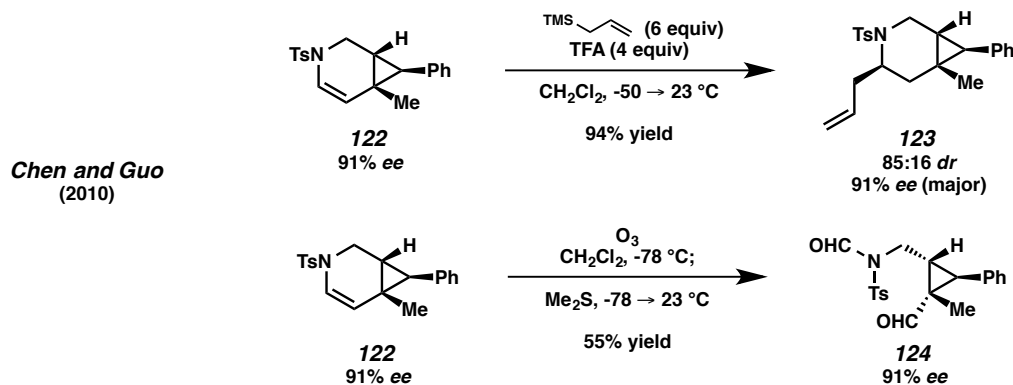
Even while many asymmetric examples have been disclosed for *N*-tethered 1,6-enynes, we were curious if these types of substrates would exhibit chirality transfer through our strategy. Indeed, substrate **120**, under the previously optimized conditions, does undergo the cycloisomerization to provide product **121** in 97% yield and 82% *es* (Scheme 3.4.7). This result is consistent with the Me-substituted *O*-tethered example discussed previously (Table 3.4.2, Entry 1).²⁴ As discussed earlier, the enantioselective examples based on chiral catalysts already provide rather general results for these products. That said, this finding still presents a number of questions: how is chirality transferred in this substrate, could this system be even more tolerant to substitution when compared to our ether substrates, and is this system entry into biologically relevant molecules? We expect this initial finding lays the groundwork for further investigations.



Scheme 3.4.7. *N*-Tethered 1,6-Enyne Cycloisomerization with Observed Chirality Transfer.

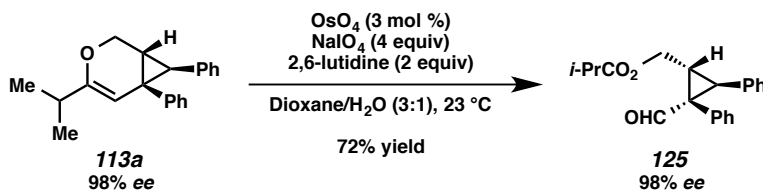
3.4.8 Reactions of Products

The oxidative cleavage and alkylation of 3-azabicyclo[4.1.0]heptenes has been described (Scheme 3.4.8).²⁵ Alkylation of *N*-tethered bicycle **122** with allylsilane and trifluoroacetic acid provides product **123** in good yield and diastereoselectivity. Additionally, ozonolysis of the same substrate (**122**) affords aldehyde **124** in moderate yield.



Scheme 3.4.8. Previously Disclosed Reactions on *N*-Tethered Products.

We were met with less successful results on the *O*-tethered products. Under typical ozonolysis conditions, unacceptable yields are obtained (<20% yield). Fortunately, oxidative cleavage with modified Johnson-Lemieux conditions²⁶ of bicyclic product **113a** provides highly substituted, highly enantioenriched cyclopropane **125** in 72% yield (Scheme 3.4.9). Importantly, cyclopropane **125** contains two differentiated functional group handles for further elaboration; moreover, this type of highly substituted enantioenriched cyclopropane would be difficult to access using alternative methods.

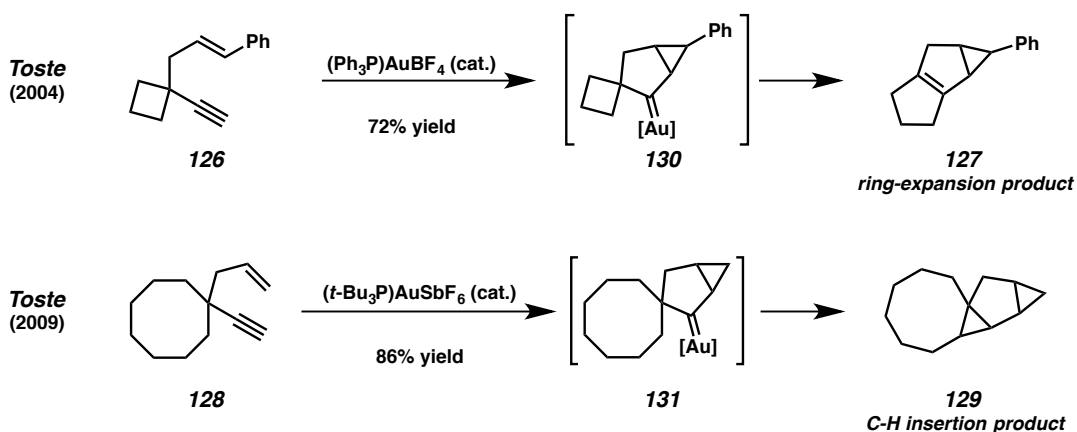


Scheme 3.4.9. Oxidative Cleavage to Produce Highly Enantioenriched Cyclopropane **125**.

3.5 Additional Studies Concerning 1,6-Enyne Cycloisomerizations

3.5.1 Migration into Carbenoids Introduction

The migration of alkyl groups into transition metal carbenoids can be a creative method to generate C–C bonds. While migrations into carbenes generated from the decomposition of diazo species have been widely explored,²⁷ migrations into Au and Pt carbenoids derived from alkynes are just beginning to be studied.²⁸ For example, Toste and coworkers disclosed this type of migration, as well a competing process, for 1,5-enynes under cationic Au-catalysis (Scheme 3.5.1).²⁹ When carbon-tethered 1,5-enyne **126** is subjected to cationic Au-catalysis, tricyclic **127** is produced. Conversely, enyne **128** undergoes Au-mediated cycloisomerization to ultimately produce bicyclopentane **129**. The ring expansion and C-H insertion processes are highly dependent on the size of the appended ring in the starting material and are proposed to occur via similar Au-carbenoid intermediates (**130** and **131**).

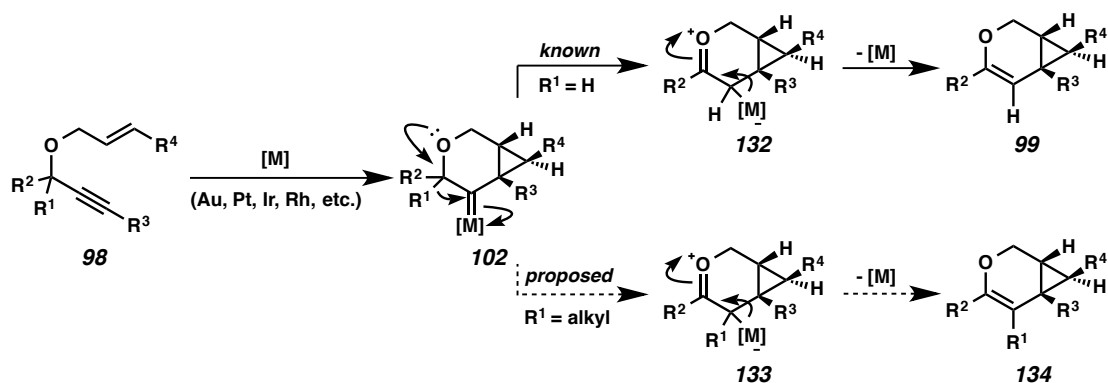


Scheme 3.5.1. Example of 1,5-Enynes Undergoing Ring Expansion or C–H Insertion under Au-Catalysis.

3.5.2 Proposal for Migration/Expansion in the Cycloisomerization of 1,6-Enynes

Driven still by mechanistic query, we considered proposed intermediate **102** and turned our attention to enyne substrates containing tetrasubstituted propargylic carbons (Scheme 3.5.2). The top reaction pathway (**98** \rightarrow **99**) is the process we leveraged in our chirality transfer exploration. After cycloisomerization, a [1,2]-hydride shift produces zwitterionic species **132** and ultimately product **99**. Substrates lacking propargylic hydrogens might instead undergo a [1,2]-alkyl migration into the Pt-

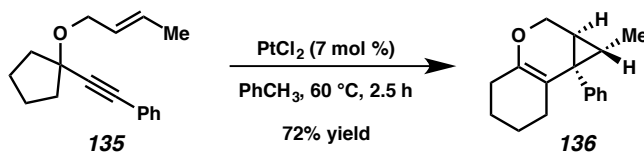
carbenoid (**102** → **133**). We thought this migration could be favored over a cyclopropane migration because of the added stabilization of the oxygen (oxocarbenium **133** as the major resonance contributor). A ring expansion, or in acyclic cases an alkyl shift, would provide access to highly substituted fused bicycles (**134**).



Scheme 3.5.2. Mechanistic-Based Proposal for Alkyl Migrations in the Cycloisomerization of 1,6-Enynes.

3.5.3 Results

The first substrate attempted, enyne **135**, did indeed provide proof of principle for the proposal. Subjecting enyne **135** to catalytic PtCl_2 in toluene at 60°C for 2.5 hours, fused tricycle **136** is isolated in 72% yield (Scheme 3.5.3). This product provides further evidence for the accepted mechanism, as isomerization to a highly strained allene is unlikely. Susan Stevenson took charge of this project and found new catalyst systems that provided excellent reactivity and generality.



Scheme 3.5.3. Initial Ring Expansion Result.

Treatment of substrates with catalytic $[\text{Ir}(\text{dbcot})\text{Cl}]_2$ or $[(\text{C}_2\text{H}_4)\text{PtCl}_2]_2$ under and atmosphere of CO provides tricyclic compounds in good yields.³⁰ Representative products are shown below in Figure 3.5.1. Various functionalities on the alkyne are tolerated under either reaction condition, as well as differential

substitution to the alkene. Highly functionalized products, such as pentasubstituted cyclopropane **138d** and indole **138h**, are isolated in moderate yields. Product **138i** is isolated in 80% yield and 49% yield under Pt and Ir catalysis, respectively. Cyclobutane-based substrate affords ring expansion bicycle **139** in 69% yield with catalytic PtCl₂ and an atmosphere of CO. This ring expansion methodology also provides access to large rings, which can be difficult to achieve by traditional cyclization methods. Macrocycles containing 8-, 9-, and 11-membered rings (**140**, **141**, and **142** respectively) were formed in moderate to good yields.

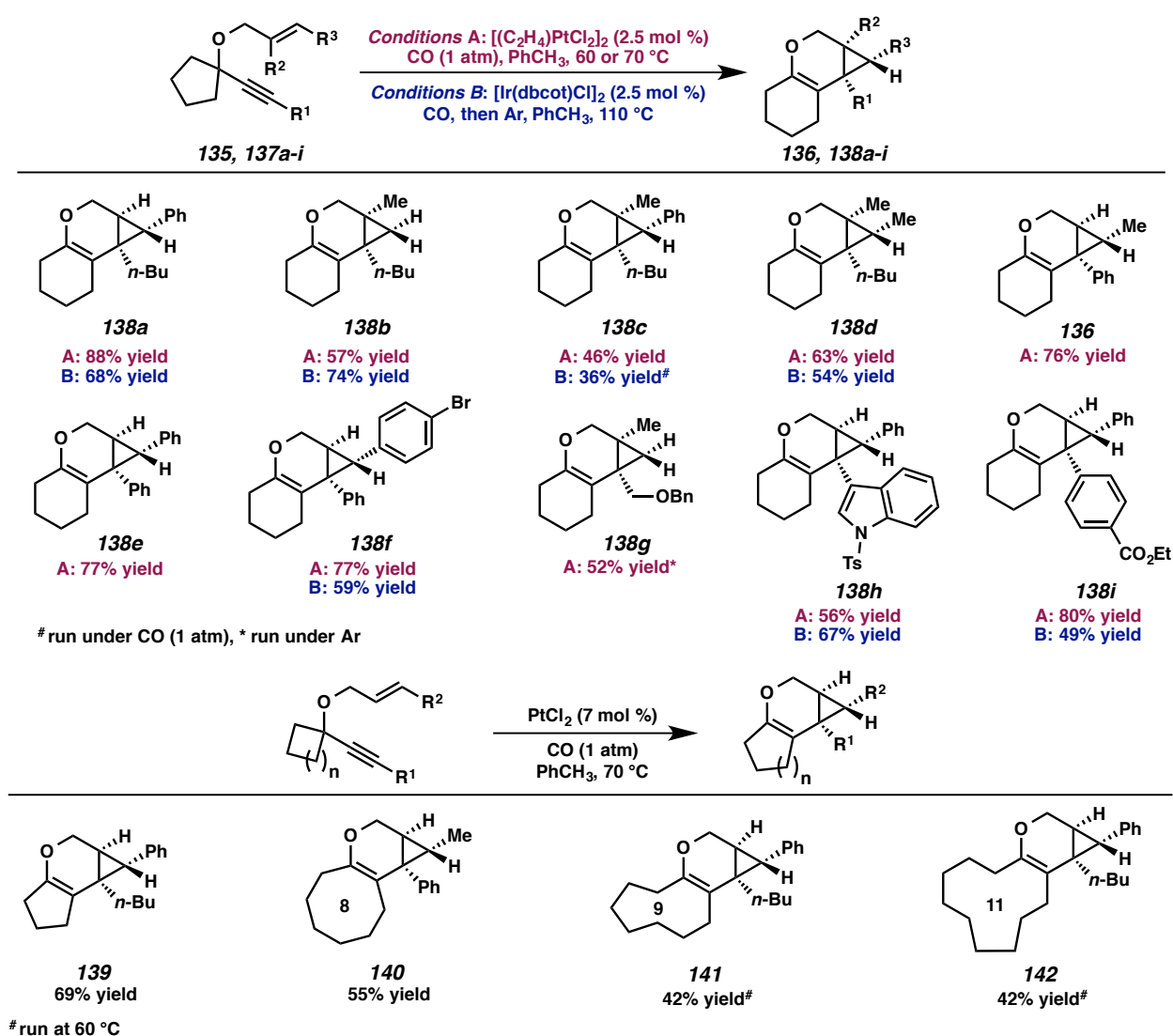
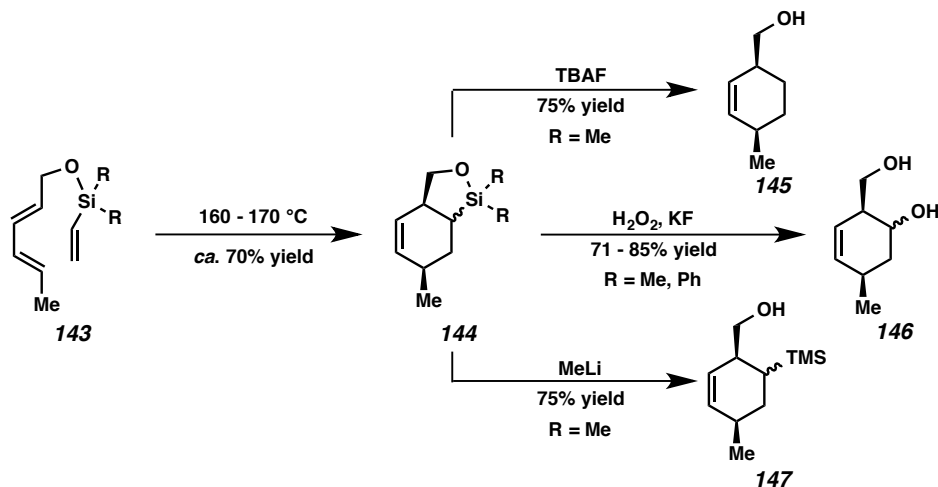


Figure 3.5.1. Ring Expansion Results with Ir- and Pt-Based Catalysts.

3.5.4 Silicon Tether Strategies: Background

Silyl-tethering is a common way to render unselective or poorly reactive intermolecular transformations intramolecular.³¹ It has been utilized in a number of C–C bond forming reactions. Silyl-tethering has been used extensively in Diels-Alder reactions. By rendering these cycloadditions intramolecular common limitations can be overcome. For example, vinyl siloxane-tethered diene **143** undergoes a thermal Diels-Alder reaction to afford fused bicycle **144** in good yields (Scheme 3.5.4).³² This type of [4+2] cycloaddition would be extremely difficult to achieve in an intermolecular reaction for electronic reasons; the dienophile is not sufficiently electron deficient. The product can then be desilylated with TBAF, providing a compound that would have hypothetically arisen from an untethered reaction between the dienyl alcohol and ethylene. Moreover, Tamao-Fleming oxidation provides diol **146**, or addition of methyl lithium affords trimethylsilyl product **147**. While silyl tethers have found many uses in complex molecule synthesis, their use has been explored minimally in alkyne activation chemistry.³³

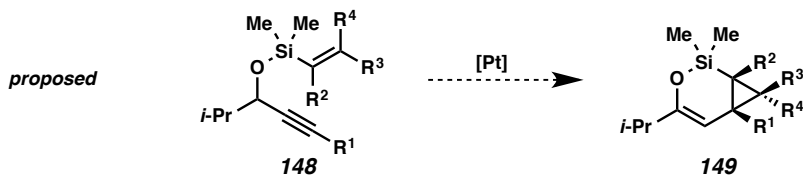


Scheme 3.5.4. Silicon Tethering in [4+2] Cycloaddition and Post Cycloaddition Transformations.

3.5.5 Proposal for Si-Tethering in 1,6-Enyne Cycloisomerization Reaction

As a result of the added utility Si-tethering can often achieve, we desire to explore its use in the cycloisomerization of 1,6-enynes. We propose that Si-tethered enynes with the general structure of **148** could provide products similar to bicyclic **149** (Scheme 3.5.5). This prospect does raise a few questions:

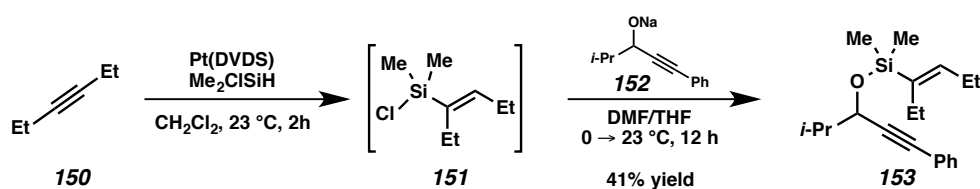
can we quickly access these substrates quickly and efficiently, will these substrates undergo our desired transformation, and can we use the Si-tether for post-cycloisomerization manipulations? Finally, if this transformation is successful, we aim to further extend this reactivity to our chirality transfer system.



Scheme 3.5.5. Silicon Tethering Proposal in 1,6-Enyne Cycloisomerization.

3.5.6 Substrate Synthesis and Result on Si-Tethering Study

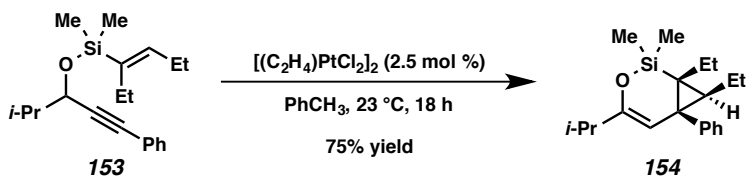
A number of approaches were explored to access the desired enyne substrates. While these structures were not trivial to synthesize, we found a suitable route to test reactivity (Scheme 3.5.6). In a two pot, single step procedure, hydrosilylation of 3-hexyne (**150**) with dimethylchlorosilane affords silyl chloride **151**, which is immediately used in the silylation of alkoxide **152**. This process is satisfactory for the synthesis of the described substrate (**153**, 41% yield); however, there is an inherent limitation. When a substrate bearing an unsymmetrical alkene is desired, a hydrosilylation requires either selectivity or separation power is necessary; the latter is extremely difficult on a labile silylchloride species.



Scheme 3.5.6. Synthesis of Racemic Si-Tethered 1,6-Enyne Substrate **153**.

On this single test case using unconventional cycloisomerization conditions (2.5 mol % Zeise's Dimer in toluene), the cycloisomerization of enyne **153** to bicycle **153** proceeds in 75% yield (Scheme 3.5.7). The racemic system was solely studied, as the potential of this transformation was stifled by the

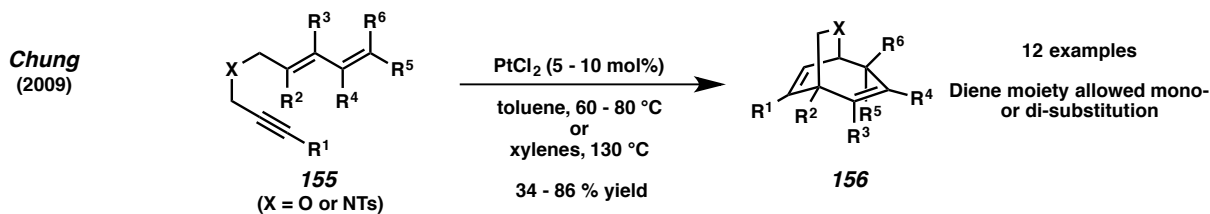
inability to easily access the desired substrates. Given recent work by Waston and coworkers concerning the silyl Heck reaction,³⁴ this challenge may be easily overcome in future investigations.



Scheme 3.5.7. Pt-Catalyzed Cycloisomerization Result on Si-Tethered Substrate **153**.

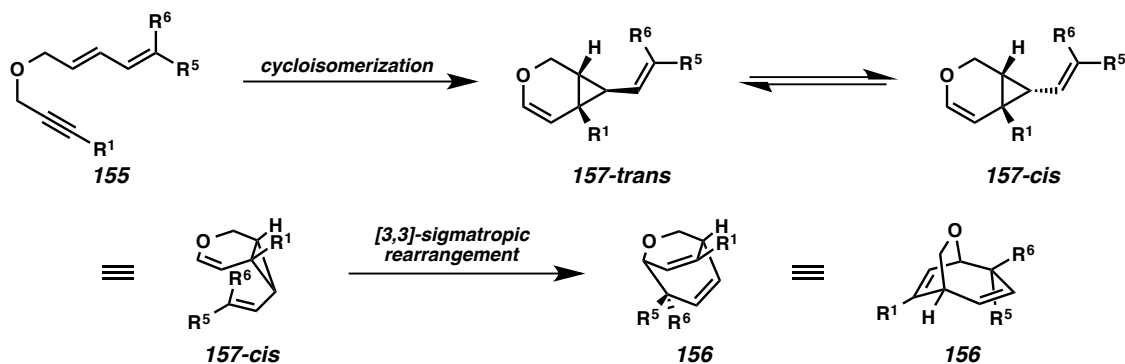
3.5.7 Tandem Process Background

As a result of our high substrate tolerance in the chirality transfer system, we considered further extension of this chemistry. We were particularly curious about exploring this method in a cascade reaction. A racemic tandem cycloisomerization/[3,3]-sigmatropic rearrangement of dienyne disclosed by Chung and coworkers in 2009 provided an ideal platform for expansion (Scheme 3.5.8).³⁵ In this reaction, dienyne substrates (**155**) undergo an initial Pt-catalyzed cycloisomerization followed by a divinyl cyclopropane rearrangement to provide bicyclic products (**156**).



Scheme 3.5.8. 1,6-Enynes in Pt-Catalyzed Tandem Cycloisomerization/[3,3]-Sigmatropic Rearrangement.

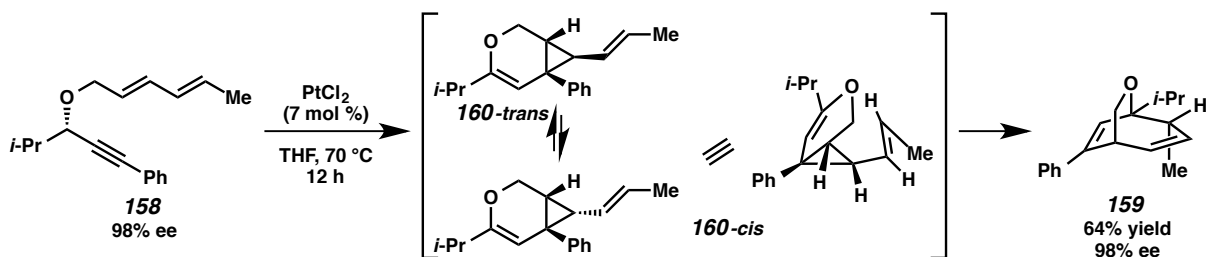
Extending the developed chirality transfer idea to this transformation would allow for the expedient access of these complex molecules in potentially high optical purity. A possible mechanistic pathway is shown below in Scheme 3.5.9 and is as follows: initial cycloisomerization gives the *trans*-cyclopropane intermediate (**157-trans**), which undergoes an epimerization to the *cis*-cyclopropane (**157-cis**), potentially via a diradical process.³⁶ The *cis*-divinylcyclopropane is then primed to undergo the [3,3]-rearrangement to afford product **156**.



Scheme 3.5.9. Proposed Mechanistic Intermediates for Tandem Cycloisomerization/[3,3]-Sigmatropic Rearrangement with *N*- and *O*-Tethered 1,6-Enynes.

3.5.8 Results and Potential Applications

We used our optimal R group and conditions in our initial study of chirality transfer for **158** (Scheme 3.5.10). The tandem cycloisomerization/[3,3]-sigmatropic rearrangement of dienyne **158** provides bicyclic compound **159** in 64% yield with complete transfer of chirality (98% *ee* → 98% *ee*). This result is quite remarkable in the fact that the chirality transfer is complete in the cycloisomerization step. Furthermore, the divinyl cyclopropane rearrangement is completely stereospecific; as this system needs to undergo the *trans* to *cis* isomerization (**160-*trans*** → **160-*cis***), it was unclear whether the geometry of the alkene would be stable under the conditions (i.e., provide a mixture of diastereomers). This aspect is further discussed in Chapter five.



Scheme 3.5.10. Chirality Transfer Observation in Pt-Catalyzed Tandem Process.

Proof of principle reactivity in the tandem cycloisomerization/[3,3]-sigmatropic rearrangement further bolsters the utility of chirality transfer process. The general structure of the products generated from this process is found in a number of natural products including kessane (**161**),³⁷ gelsemoxonine (**162**),³⁸ and ophiodilactone B (**163**, Figure 3.5.2).³⁹

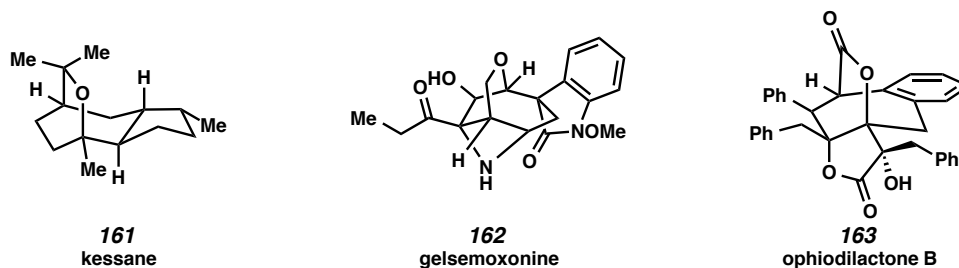


Figure 3.5.2. Examples of Natural Products that Contain an Oxabicyclo[3.2.2]nonane Core.

3.6 Conclusion

Several reactions were discovered and developed over the course of the studies described herein. It is critical to stress the utility of the chirality transfer process and the limitations it overcomes. The substrates are generated quickly and with high enantioselectivity. The system does not have strict substrate requirements (i.e., geminal allylic substitution or aryl substitution to the alkyne). Most importantly, the reaction conditions are simple: catalytic PtCl_2 in THF. During the investigation we determined the absolute stereochemistry of the products and developed a model for stereochemical transfer.

The C–C migration work highlights a fruitful extension based highly on our current understanding of the cycloisomerization reaction mechanism. The ring expansion products can be further elaborated to macrocyclic structures that are not easily obtained via previously established methods. The use of a siloxane-tethered enyne in the cycloisomerization provides intellectually stimulating questions in terms of utility and scope. Finally, the tandem cycloisomerization/[3,3]-rearrangement provides potential uses in complex molecule synthesis.

3.7 Experimental Section

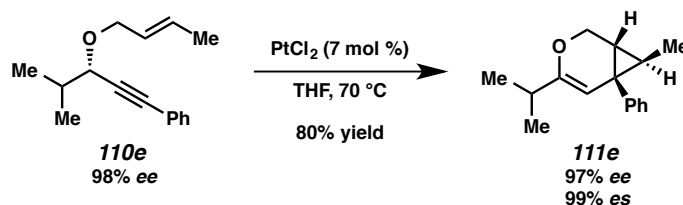
3.7.1 Materials and Methods

Reactions were performed under an argon atmosphere unless otherwise noted. Tetrahydrofuran, ether, dichloromethane, dimethylformamide, and toluene were purified by passing through activated alumina columns. All other solvents and reagents were used as received unless otherwise noted. Commercially available chemicals were purchased from Alfa Aesar (Ward Hill, MA), Sigma-Aldrich (St. Louis, MO), Oakwood Products (West Columbia, SC), Strem (Newburyport, MA), and TCI America (Portland, OR). Qualitative TLC analysis was performed on 250 mm thick, 60 Å, glass backed, F254 silica (Silicycle, Quebec City, Canada). Visualization was accomplished with UV light, exposure to iodine, exposure to *p*-anisaldehyde solution followed by heating, or exposure to KMnO₄ solution followed by heating. Flash chromatography was performed using Silicycle silica gel (230-400 mesh). ¹H NMR spectra were acquired on either a Varian Mercury 300 (at 300 MHz) or a Varian 400 MR (at 400 MHz) and are reported relative to SiMe₄ (δ 0.00). ¹³C NMR spectra were acquired on a Varian 400 MR (at 100 MHz) and are reported relative to SiMe₄ (δ 0.0). All IR spectra were obtained on NaCl plates (film) with a Bruker Tensor 27 and are reported in wavenumbers (ν). All optical rotations were obtained on a Rudolph Research Analytical Autopol III Polarimeter. High resolution mass spectrometry (HRMS) data were acquired by the Colorado State University Central Instrument Facility on an Agilent 6210 TOF LC/MS.

3.7.2 Enyne Cycloisomerizations

General procedure for the platinum catalyzed cycloisomerization of oxygen-tethered 1,6-enynes. To a solution of enyne in THF (0.030 M) under argon was added PtCl₂ (7 mol %). The resulting mixture was sealed and stirred at 70 °C. Upon completion, as determined by TLC, the reaction mixture was allowed to cool to ambient temperature. The mixture was then diluted with hexanes and passed through a small plug of alumina. The solvent was concentrated in vacuo and the crude residue was purified by flash chromatography.

General Notes: Without the addition of triethylamine to the flash chromatography eluent, decreased yields were observed. For ethereal enynes bearing a crotyl substituent (e.g., **110e**), the (*E*)-crotyl bromide that was used as the starting material precursor featured a small amount (~5%) of the corresponding (*Z*)-isomer. This isomer was carried through the enyne synthesis in forming the ether products, as well as the cycloisomerizations to form the bicycles. These isomers were generally inseparable from the major compound, and therefore small amounts are observed in the NMR spectra.



To a solution of enyne **110e** (25.0 mg, 0.109 mmol) in THF (3.63 mL, 0.030 M) under argon was added PtCl_2 (2.0 mg, 0.00763 mmol, 7.0 mol %). The resulting mixture was sealed, heated to 70 °C and stirred at that temperature for 40 h. Once cooled to ambient temperature, the mixture was diluted with hexanes and filtered through a small plug of alumina (0.5 x 2 cm, 4:1 hexanes/ Et_2O eluent). The solvent was removed by rotary evaporation and the resulting residue was purified by flash chromatography (99.5:0.5 hexanes/ Et_3N → 98.5:1:0.5 hexanes/ $\text{Et}_2\text{O}/\text{Et}_3\text{N}$ eluent), affording bicycle **111e** (19.9 mg, 80% yield).

Bicycle 111e:

Physical State: yellow oil.

R_f: 0.63 (9:1 hexanes/ Et_2O , KMnO_4).

IR (film): 2972, 2874, 1716, 1493 cm^{-1} .

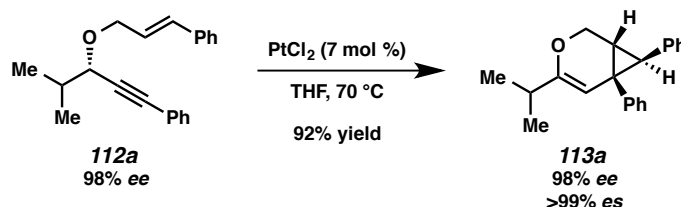
HRMS (ESI⁺): m/z calc. for $(\text{M} + \text{H})^+$ [$\text{C}_{16}\text{H}_{20}\text{O} + \text{H}$]⁺: 229.1587, found 229.1582.

¹H NMR (400 MHz, C_6D_6): δ 7.20-7.18 (comp m, 4H), 7.10 (dt, $J = 8.6, 4.3$ Hz, 1H), 5.19 (s, 1H), 4.17 (dd, $J = 10.3, 1.4$ Hz, 1H), 3.72 (dd, $J = 10.4, 2.0$ Hz, 1H), 2.27-2.19 (m, 1H), 1.49-1.43 (m, 1H), 1.26-1.20 (m, 1H), 1.07 (d, $J = 3.3$ Hz, 3H), 1.05 (d, $J = 3.3$ Hz, 3H).

¹³C NMR (100 MHz, CDCl_3): δ 156.3, 142.5, 129.8, 128.7, 126.5, 104.4, 62.9, 33.0, 30.1, 27.3, 26.1, 20.5, 20.4, 15.0.

Optical Rotation: $[\alpha]_D^{31} = +18.27$ ($c = 0.5$, CH_2Cl_2).

The *ee* was determined to be 97% by HPLC analysis (Daicel Chiralcel OJ-H, 1% 2-propanol in hexane, 1 mL/min, $\lambda = 230$ nm, major isomer 5.01 min, minor isomer 5.36 min).



To a solution of enyne **112a** (35.1 mg, 0.121 mmol) in THF (4.03 mL, 0.030 M) under argon was added PtCl_2 (2.3 mg, 0.00847 mmol). The resulting mixture was sealed, heated to 70 °C and stirred at that temperature for 20 h. Once cooled to ambient temperature, the mixture was diluted with hexanes and filtered through a small plug of alumina (0.5 x 2 cm, 4:1 hexanes/ Et_2O eluent). The solvent was removed by rotary evaporation and the resulting residue was purified by flash chromatography (99.5:0.5 hexanes/ $\text{Et}_3\text{N} \rightarrow 97.5:2:0.5$ hexanes/ $\text{Et}_2\text{O}/\text{Et}_3\text{N}$ eluent), affording bicycle **113a** (32.2 mg, 92% yield).

Bicycle **113a**:

Physical State: white solid.

R_f: 0.37 (9:1 hexanes/ Et_2O , KMnO_4).

IR (film): 2975, 1720, 1601, 1496 cm^{-1} .

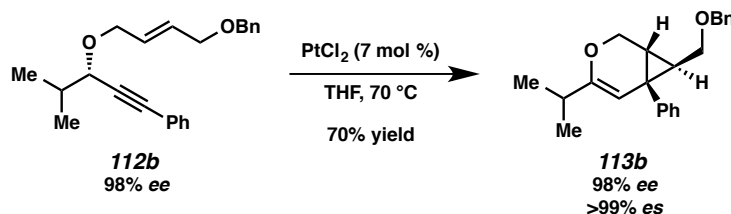
HRMS (DART+): m/z calc'd for $(\text{M} + \text{H})^+ [\text{C}_{21}\text{H}_{22}\text{O} + \text{H}]^+$: 291.1743, found 291.1742.

^1H NMR (400 MHz, C_6D_6): δ 7.07-6.84 (m, 8H), 6.70-6.67 (m, 2H), 5.24 (s, 1H), 4.23 (dd, $J = 10.4$, 1.3 Hz, 1H), 3.84-3.81 (m, 1H), 2.82 (d, $J = 5.8$ Hz, 1H), 2.31-2.22 (m, 1H), 2.06 (dt, $J = 5.8$, 0.9 Hz, 1H), 1.09 (d, $J = 6.9$ Hz, 3H), 1.07 (d, $J = 6.9$ Hz, 3H).

^{13}C NMR (100 MHz, C_6D_6): δ 157.0, 141.1, 138.5, 130.4, 128.5, 127.9, 126.6, 125.8, 104.3, 62.6, 36.9, 33.0, 32.4, 29.7, 20.4, 20.2.

Optical Rotation: $[\alpha]_D^{32} = +5.32$ ($c = 1.0$, CH_2Cl_2).

The *ee* was determined to be 98% by HPLC analysis (Chiralpak IC, hexane, 1.0 mL/min, $\lambda = 210$ nm, major isomer 8.82 min, minor isomer 8.47 min).



To a solution of enyne **112b** (68.0 mg, 0.203 mmol) in THF (6.78 mL, 0.030 M) under argon was added PtCl_2 (3.8 mg, 0.0142 mmol). The resulting mixture was sealed, heated to 70 °C and stirred at that temperature for 27 h. Once cooled to ambient temperature, the mixture was diluted with hexanes and filtered through a small plug of alumina (0.5 x 3 cm, 4:1 hexanes/ Et_2O eluent). The solvent was removed by rotary evaporation and the resulting residue was purified by flash chromatography (97.5:2:0.5 hexanes/ Et_2O / Et_3N eluent), affording bicycle **113b** (47.8 mg, 70% yield).

Bicycle **113b**:

Physical State: colorless oil.

R_f: 0.47 (9:1 hexanes/ Et_2O , KMnO_4).

IR (film): 2963, 2866, 1664, 1361 cm^{-1} .

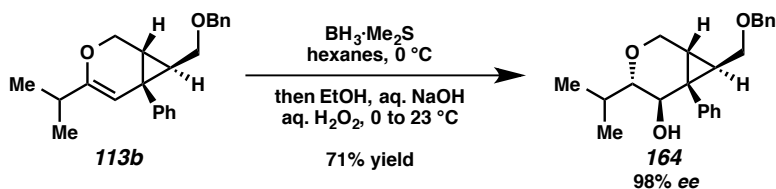
HRMS (DART+): *m/z* calc'd for $(\text{M} + \text{H})^+$ [$\text{C}_{23}\text{H}_{26}\text{O}_2 + \text{H}$] $^+$: 335.2011, found 335.2008.

¹H NMR (400 MHz, C_6D_6): δ 7.25-7.23 (m, 2H), 7.12-6.97 (comp m, 8H), 5.09 (s, 1H), 4.06 (dd, $J = 10.4, 1.4$ Hz, 1H), 4.03 (q, $J = 9.6$ Hz, 2H), 3.64 (dd, $J = 10.4, 2.0$ Hz, 1H), 3.01-2.90 (m, 2H), 2.12 (dtd, $J = 13.7, 6.8, 0.6$ Hz, 1H), 1.88 (dt, $J = 7.8, 5.8$ Hz, 1H), 1.35 (dd, $J = 5.1, 2.3$ Hz, 1H), 0.95 (d, $J = 4.0$ Hz, 3H), 0.93 (d, $J = 3.9$ Hz, 3H).

¹³C NMR (100 MHz, C_6D_6): δ 156.6, 142.1, 139.3, 129.9, 128.7, 128.5, 127.7, 127.5, 126.8, 103.9, 72.9, 70.5, 62.7, 32.9, 31.2, 27.4, 26.9, 20.4, 20.3.

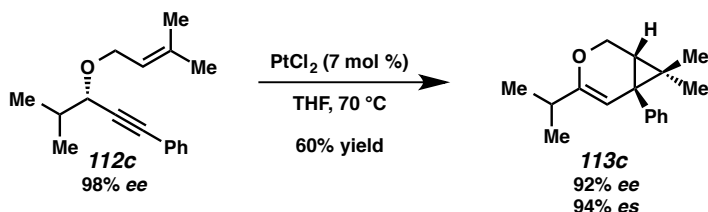
Optical Rotation: $[\alpha]_{\text{D}}^{33} = +64.26$ ($c = 1.0$, CH_2Cl_2).

The *ee* was determined to be 98% by hydroboration/oxidation and HPLC analysis:



To a solution of bicycle **113b** (10.0 mg, 0.030 mmol) in hexanes (300 μL) at 0 °C was added $\text{BH}_3 \cdot \text{Me}_2\text{S}$ (5.6 μL , 2.0 M in hexanes, 0.0105 mmol) dropwise. The resulting solution was stirred at ambient temperature for 3 h, cooled to 0 °C, and EtOH (38 μL) was added, followed by aq. NaOH (12 μL , 3 M), and aq. H₂O₂ (190 μL , 35%). The resulting mixture was allowed to warm to ambient temperature and stirred overnight. The mixture was extracted with CH₂Cl₂ (3 x 10 mL). The combined organic layers were washed with sat. aq. NaHCO₃ (5 mL), then brine (5 mL), and then dried over MgSO₄. The solvent was removed in vacuo and the resulting residue was purified by flash chromatography (9:1 \rightarrow 4:1 hexanes/Et₂O eluent), affording alcohol **164** (7.5 mg, 71% yield, *R_f*: 0.30 in 4:1 hexanes/Et₂O) as a colorless oil.

The *ee* was determined to be 98% by HPLC analysis (Daicel Chiralcel IA, 3% 2-propanol in hexane, 1 mL/min, λ = 210 nm, major isomer 7.96 min, minor isomer 9.08 min).



To a solution of enyne **112c** (30.1 mg, 0.124 mmol) in THF (4.13 mL, 0.030 M) under argon was added PtCl₂ (2.3 mg, 0.00868 mmol). The resulting mixture was sealed, heated to 70 °C and stirred at that temperature for 48 h. Once cooled to ambient temperature, the mixture was diluted with hexanes and filtered through a small plug of alumina (0.5 x 2 cm, 4:1 hexanes/Et₂O eluent). The solvent was removed by rotary evaporation and the resulting residue was purified by flash chromatography (99.5:0.5 hexanes/Et₃N \rightarrow 97.5:2:0.5 hexanes/Et₂O/Et₃N eluent), affording bicycle **113c** (18.1 mg, 60% yield).

Bicycle 113c:

Physical State: yellow oil.

R_f: 0.37 (9:1 hexanes/Et₂O, KMnO₄).

IR (film): 2966, 2870, 1666, 1492 cm⁻¹.

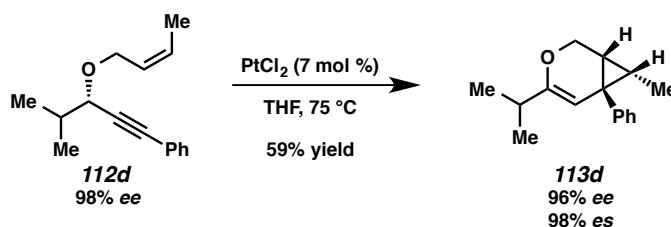
HRMS (DART+): *m/z* calc'd for (M + H)⁺ [C₁₇H₂₂O + H]⁺: 243.1743, found 243.1752.

¹H NMR (400 MHz, C₆D₆): δ 7.21-7.17 (comp m, 4H), 7.11-7.07 (m, 1H), 4.90 (s, 1H), 4.12 (dd, *J* = 11.3, 1.5 Hz, 1H), 4.05 (dd, *J* = 11.3, 4.1 Hz, 1H), 2.24 (dq, *J* = 13.7, 6.8 Hz, 1H), 1.26 (s, 3H), 1.13 (d, *J* = 4.2 Hz, 1H), 1.07 (d, *J* = 4.4 Hz, 3H), 1.05 (d, *J* = 4.4 Hz, 3H), 0.76 (s, 3H).

¹³C NMR (100 MHz, C₆D₆): δ 156.0, 144.5, 129.3, 128.7, 128.1, 127.9, 126.2, 98.8, 62.0, 33.3, 30.5, 29.4, 29.2, 25.3, 20.7, 20.6, 16.6.

Optical Rotation: [α]_D³⁰ = +208.09 (*c* = 0.5, CH₂Cl₂).

The *ee* was determined to be 92% by HPLC analysis (Daicel Chiralcel OJ-H, 1% 2-propanol in hexane, 1.0 mL/min, λ = 230 nm, major isomer 4.31 min, minor isomer 4.68 min).



To a solution of enyne **112d** (44.1 mg, 0.193 mmol) in THF (6.44 mL, 0.030 M) under argon was added PtCl₂ (3.6 mg, 0.0135 mmol). The resulting mixture was sealed, heated to 75 °C and stirred at that temperature for 36 h. Once cooled to ambient temperature, the mixture was diluted with hexanes and filtered through a small plug of alumina (0.5 x 2 cm, 9:1 hexanes/Et₂O eluent). The solvent was removed by rotary evaporation and the resulting residue was purified by flash chromatography (90:8:2:1 hexanes/CH₂Cl₂/Et₂O/Et₃N → 40:8:2:1 hexanes/CH₂Cl₂/Et₂O/Et₃N eluent), affording bicycle **113d** (25.9 mg, 59% yield).

Bicycle 113d:

Physical State: yellow oil.

R_f: 0.71 (15:4:1 hexanes/CH₂Cl₂/Et₂O, KMnO₄).

IR (film): 2963, 2871, 1668, 1492 cm⁻¹.

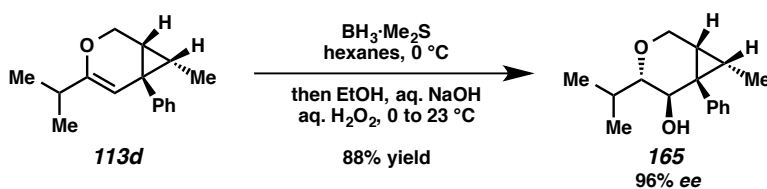
HRMS (DART+): *m/z* calc'd for (M + H)⁺ [C₁₆H₂₀O + H]⁺: 229.1592, found 229.1587.

¹H NMR (400 MHz, C₆D₆): δ 7.29-7.26 (m, 2H), 7.21-7.18 (m, 2H), 7.12-7.07 (m, 1H), 4.93 (s, 1H), 3.99-3.97 (m, 2H), 2.32-2.25 (m, 1H), 1.49-1.41 (m, 1H), 1.19 (dddd, *J* = 8.7, 3.4, 2.3, 1.0 Hz, 1H), 1.16 (d, *J* = 6.4 Hz, 3H), 1.10 (d, *J* = 4.4 Hz, 3H), 1.09 (d, *J* = 4.4 Hz, 3H).

¹³C NMR (100 MHz, C₆D₆): δ 157.6, 146.9, 128.7, 128.2, 127.9, 127.6, 126.1, 95.3, 61.9, 22.4, 26.5, 26.2, 24.7, 20.8, 8.7.

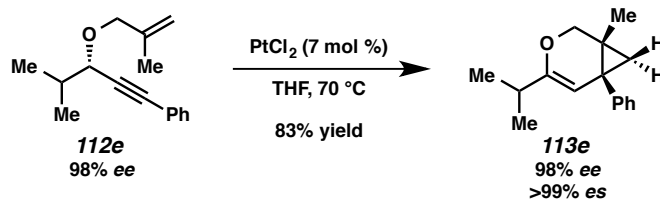
Optical Rotation: [α]_D³⁰ = +2.13 (*c* = 0.5, CH₂Cl₂).

The *ee* was determined to be 96% by hydroboration/oxidation and HPLC analysis:



To a solution of bicyclic **113d** (5.3 mg, 0.0232 mmol) in hexane (350 μL) at 0 °C was added BH₃•Me₂S (3.8 μL, 2.0 M in hexanes, 0.00690 mmol) dropwise. The resulting solution was stirred at ambient temperature for 3 h, cooled to 0 °C, and EtOH (40 μL) was added, followed by aq. NaOH (12 μL, 3 M), and aq. H₂O₂ (190 μL, 30%). The resulting mixture was allowed to warm to ambient temperature and stirred for 20 h. The mixture was extracted with CH₂Cl₂ (3 x 10 mL). The combined organic layers were washed with sat. aq. NaHCO₃ (5 mL), then brine (5 mL), and then dried over MgSO₄. The solvent was removed in vacuo and the resulting residue was purified by flash chromatography (9:1 hexanes/Et₂O eluent), affording alcohol **165** (5.0 mg, 88% yield, **R_f**: 0.30 in 9:1 hexanes/Et₂O) as a colorless solid.

The *ee* was determined to be 96% by HPLC analysis (Daicel Chiralcel IC, 0.5% 2-propanol in hexane, 1.2 mL/min, λ = 230 nm, major isomer 4.76 min, minor isomer 5.14 min).



To a solution of enyne **112e** (29.9 mg, 0.131 mmol) in THF (4.38 mL, 0.030 M) under argon was added PtCl_2 (2.4 mg, 0.00917 mmol). The resulting mixture was sealed, heated to 70 °C and stirred at that temperature for 26 h. Once cooled to ambient temperature, the mixture was diluted with hexanes and filtered through a small plug of alumina (0.5 x 2 cm, 4:1 hexanes/ Et_2O eluent). The solvent was removed by rotary evaporation and the resulting residue was purified by flash chromatography (99.5:0.5 hexanes/ Et_3N → 97.5:2:0.5 hexanes/ $\text{Et}_2\text{O}/\text{Et}_3\text{N}$ eluent), affording bicycle **113e** (25.0 mg, 83% yield).

Bicycle **113e**:

Physical State: colorless oil.

R_f: 0.42 (9:1 hexanes/ Et_2O , KMnO_4).

IR (film): 2964, 2870, 1666, 1446 cm^{-1} .

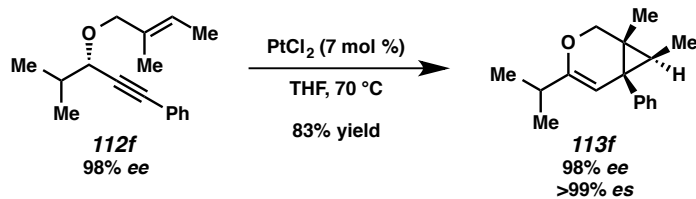
HRMS (DART+): m/z calc'd for $(\text{M} + \text{H})^+$ [$\text{C}_{16}\text{H}_{20}\text{O} + \text{H}$]⁺: 229.1592, found 229.1587.

¹H NMR (400 MHz, C_6D_6): δ 7.24-7.18 (m, 4H), 7.11-7.07 (m, 1H), 5.10 (s, 1H), 4.00 (d, $J = 10.3$ Hz, 1H), 3.45 (d, $J = 10.3$ Hz, 1H), 2.29-2.22 (m, 1H), 1.42 (d, $J = 4.4$ Hz, 1H), 1.15 (d, $J = 4.3$ Hz, 1H), 1.07 (d, $J = 6.9$ Hz, 3H), 1.05 (d, $J = 6.9$ Hz, 3H), 0.60 (s, 3H).

¹³C NMR (100 MHz, C_6D_6): δ 157.6, 143.0, 129.5, 128.4, 126.4, 103.7, 68.2, 32.7, 30.3, 28.0, 22.2, 20.6, 20.4, 16.6.

Optical Rotation: $[\alpha]_{\text{D}}^{32} = +55.32$ ($c = 0.1$, CH_2Cl_2).

The *ee* was determined to be 98% by HPLC analysis (Daicel Chiralcel OJ-H, 1% 2-propanol in hexane, 1.0 mL/min, $\lambda = 210$ nm, major isomer 4.51 min, minor isomer 4.20 min).



To a solution of enyne **112f** (30.1 mg, 0.124 mmol) in THF (4.13 mL, 0.030 M) under argon was added PtCl_2 (2.3 mg, 0.00868 mmol). The resulting mixture was sealed, heated to 70 °C and stirred at that temperature for 24 h. Once cooled to ambient temperature, the mixture was diluted with hexanes and filtered through a small plug of alumina (0.5 x 2 cm, 4:1 hexanes/ Et_2O eluent). The solvent was removed by rotary evaporation and the resulting residue was purified by flash chromatography (99.5:0.5 hexanes/ Et_3N → 97.5:2:0.5 hexanes/ $\text{Et}_2\text{O}/\text{Et}_3\text{N}$ eluent), affording bicycle **113f** (24.9 mg, 83% yield).

Bicycle **113f**:

Physical State: colorless oil.

R_f: 0.86 (9:1 hexanes/ Et_2O , KMnO_4).

IR (film): 2963, 2871, 1663, 1469, 1384 cm^{-1} .

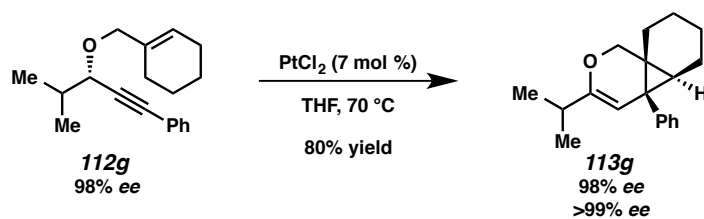
HRMS (DART+): m/z calc'd for $(\text{M} + \text{H})^+$ [$\text{C}_{17}\text{H}_{22}\text{O} + \text{H}$]⁺: 243.1743, found 243.1746.

¹H NMR (400 MHz, C_6D_6): δ 7.23-7.17 (comp m, 4H), 7.13-7.08 (m, 1H), 5.01 (s, 1H), 4.00 (d, $J = 10.2$ Hz, 1H), 3.56 (d, $J = 10.1$ Hz, 1H), 2.23 (dt, $J = 13.4, 6.7$ Hz, 1H), 1.69 (q, $J = 6.6$ Hz, 1H), 1.05 (d, $J = 3.4$ Hz, 3H), 1.04 (d, $J = 3.4$ Hz, 3H), 0.92 (d, $J = 6.6$ Hz, 3H), 0.76 (s, 3H).

¹³C NMR (100 MHz, C_6D_6): δ 156.1, 141.4, 131.4, 128.7, 126.5, 106.2, 69.0, 32.6, 31.2, 29.8, 26.3, 20.5, 20.4, 12.5, 11.6.

Optical Rotation: $[\alpha]_{\text{D}}^{32} = +351.49$ ($c = 0.25$, CH_2Cl_2).

The *ee* was determined to be 98% by HPLC analysis (Daicel Chiralcel OJ-H, 1% 2-propanol in hexane, 1.0 mL/min, $\lambda = 230$ nm, major isomer 4.30 min, minor isomer 3.96 min).



To a solution of enyne **112g** (31.7 mg, 0.188 mmol) in THF (3.93 mL, 0.030 M) under argon was added PtCl_2 (2.1 mg, 0.00782 mmol). The resulting mixture was sealed, heated to 70 °C and stirred at that temperature for 26 h. Once cooled to ambient temperature, the mixture was diluted with hexanes and filtered through a short plug of alumina (0.5 x 2 cm, 4:1 hexanes/ Et_2O eluent). The solvent was removed by rotary evaporation and the resulting residue was purified by flash chromatography (99.5:0.5 hexanes/ Et_3N → 97.5:2:0.5 hexanes/ Et_2O / Et_3N eluent), affording bicycle **113g** (24.0 mg, 80% yield).

Bicycle **113g**:

Physical State: colorless oil.

R_f: 0.33 (9:1 hexanes/ Et_2O , KMnO_4).

IR (film): 2936, 2869, 1664, 1602, 1447 cm^{-1} .

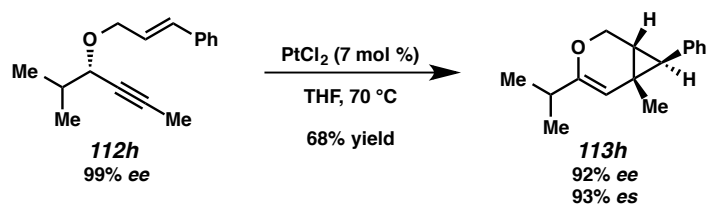
HRMS (DART+): m/z calc'd for $(\text{M} + \text{H})^+$ [$\text{C}_{19}\text{H}_{24}\text{O} + \text{H}$]⁺: 269.1900, found 269.1900.

¹H NMR (400 MHz, C_6D_6): δ 7.24-7.18 (comp m, 4H), 7.11-7.07 (m, 1H), 4.99 (s, 1H), 4.00 (d, $J = 10.2$ Hz, 1H), 3.64 (d, $J = 10.2$ Hz, 1H), 2.22 (dt, $J = 13.6, 6.8$ Hz, 1H), 1.76 (t, $J = 4.9$ Hz, 1H), 1.64 (ddd, $J = 14.2, 7.8, 5.0$ Hz, 1H), 1.27 (ddd, $J = 14.0, 7.6, 6.1$ Hz, 1H), 1.06 (d, $J = 1.9$ Hz, 3H), 1.04 (d, $J = 1.9$ Hz, 3H), 0.97-0.85 (m, 2H), 0.75-0.58 (m, 2H).

¹³C NMR (100 MHz, C_6D_6): δ 155.7, 142.3, 131.1, 128.8, 128.2, 127.9, 126.4, 106.6, 68.5, 32.63, 32.61, 30.5, 30.0, 29.0, 26.9, 23.1, 21.9, 21.6, 21.3, 20.5, 20.4.

Optical Rotation: $[\alpha]_{\text{D}}^{32} = +113.62$ ($c = 1.0$, CH_2Cl_2).

The *ee* was determined to be 98% by HPLC analysis (Daicel Chiralcel OJ-H, 100% hexane, 1.0 mL/min, $\lambda = 210$ nm, major isomer 4.78 min, minor isomer 12.69 min).



To a solution of enyne **112h** (6.5 mg, 0.0285 mmol) in THF (967 μL , 0.030 M) under argon was added PtCl_2 (0.5 mg, 0.00203 mmol). The resulting mixture was sealed, heated to 70 °C and stirred at that temperature for 17 h. Once cooled to ambient temperature, the mixture was diluted with hexanes and filtered through a small plug of alumina (0.5 x 2 cm, 9:1 hexanes/ Et_2O eluent). The solvent was removed by rotary evaporation and the resulting residue was purified by flash chromatography (97.5:2:0.5 hexanes/ Et_2O / Et_3N eluent), affording bicycle **113h** (4.4 mg, 68% yield).

Bicycle **113h**:

Physical State: colorless oil.

R_f: 0.42 (9:1 hexanes/ Et_2O , KMnO_4).

IR (film): 2974, 1715, 1602, 1498 cm^{-1} .

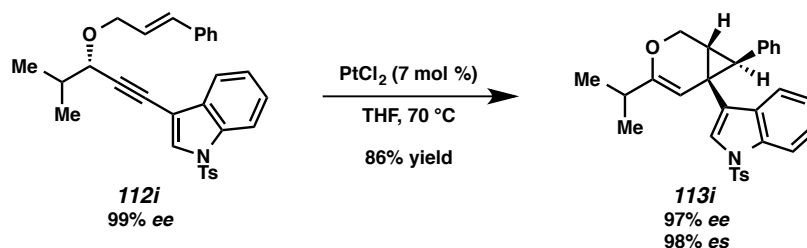
HRMS (DART+): *m/z* calc'd for $(\text{M} + \text{H})^+$ [$\text{C}_{16}\text{H}_{20}\text{O} + \text{H}$]⁺: 229.1587, found 229.1600.

¹H NMR (400 MHz, C_6D_6): δ 7.15-7.01 (comp m, 5H), 4.99 (s, 1H), 4.09 (dd, $J = 10.4, 0.8$ Hz, 1H), 3.68 (ddd, $J = 10.3, 2.2, 0.4$ Hz, 1H), 2.51 (d, $J = 5.7$ Hz, 1H), 2.31-2.24 (m, 1H), 1.36 (d, $J = 5.7$ Hz, 1H), 1.11 (t, $J = 6.9$ Hz, 6H), 0.92 (s, 3H).

¹³C NMR (100 MHz, C_6D_6): δ 157.5, 138.9, 129.1, 126.1, 103.8, 62.8, 35.1, 33.0, 28.5, 20.6, 20.3, 20.2, 18.4.

Optical Rotation: $[\alpha]_{\text{D}}^{33} = -8.40$ ($c = 0.076$, CH_2Cl_2).

The *ee* was determined to be 92% by HPLC analysis (Daicel Chiralcel IC, 0.1% 2-propanol in hexane, 1 mL/min, $\lambda = 254$ nm, major isomer 4.43 min, minor isomer 4.23 min).



To a solution of enyne **112i** (25.0 mg, 0.0517 mmol) in THF (1.73 mL, 0.030 M) under argon was added PtCl_2 (1.0 mg, 0.00364 mmol). The resulting mixture was sealed, heated to 70 °C and stirred at that temperature for 20 h. Once cooled to ambient temperature, the mixture was diluted with hexanes filtered through a small plug of alumina (0.5 x 2 cm, 1:1 hexanes/ Et_2O eluent). The solvent was removed by rotary evaporation and the resulting residue was purified by flash chromatography (4:1 hexanes/ Et_2O (0.5% Et_3N) eluent), affording bicycle **113i** (21.4 mg, 86% yield).

Bicycle **113i**:

Physical State: white semisolid.

R_f: 0.53 (1:1 hexanes/ Et_2O , KMnO_4).

IR (film): 2962, 1494, 1447, 1376 cm^{-1} .

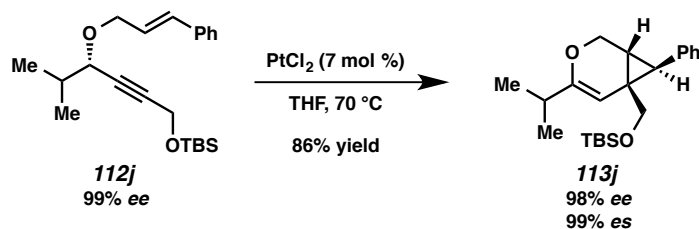
LRMS (ESI+): m/z calc'd for $(\text{M} + \text{H})^+$ [$\text{C}_{30}\text{H}_{29}\text{NO}_3\text{S} + \text{H}$] $^+$: 484.2, found 484.2.

^1H NMR (400 MHz, C_6D_6): δ 8.15-8.12 (m, 1H), 7.59-7.55 (m, 1H), 7.52-7.47 (m, 2H), 7.21-7.18 (s, 1H), 7.08-6.95 (comp m, 3H), 6.84-6.76 (comp m, 3H), 6.73-6.69 (m, 2H), 6.55-6.51 (m, 1H), 4.15 (dd, $J = 10.6, 1.3$ Hz, 1H), 3.80 (dd, $J = 10.5, 2.1$ Hz, 1H), 2.86 (d, $J = 6.0$ Hz, 1H), 2.25 (dt, $J = 13.5, 6.7$ Hz, 1H), 1.91 (d, $J = 5.9$ Hz, 1H), 1.72 (s, 3H), 1.08 (d, $J = 6.9$ Hz, 3H), 1.06 (d, $J = 6.8$ Hz, 3H).

^{13}C NMR (100 MHz, C_6D_6): δ 157.9, 144.2, 138.0, 136.3, 135.8, 131.6, 129.8, 128.4, 128.2, 128.1, 127.9, 127.0, 126.0, 125.6, 124.9, 123.2, 122.3, 120.8, 114.1, 102.6, 62.5, 36.2, 33.0, 28.8, 23.6, 21.1, 20.4, 20.2.

Optical Rotation: $[\alpha]_{\text{D}}^{32} = +14.89$ ($c = 0.5$, CH_2Cl_2).

The ee was determined to be 97% by HPLC analysis (Daicel Chiralcel OD-H, 10% 2-propanol in hexane, 1 mL/min, $\lambda = 254$ nm, major isomer 5.74 min, minor isomer 7.09 min).



To a solution of enyne **112j** (60.0 mg, 0.167 mmol) in THF (5.57 mL, 0.030 M) under argon was added PtCl_2 (3.2 mg, 0.0117 mmol). The resulting mixture was sealed, heated to 70 °C and stirred at that temperature for 29 h. Once cooled to ambient temperature, the mixture was diluted with hexanes and filtered through a small plug of alumina (0.5 x 3 cm, 9:1 hexanes/ Et_2O eluent). The solvent was removed by rotary evaporation and the resulting residue was purified by flash chromatography (99.5:0.5 hexanes/ Et_3N → 97.5:2:0.5 hexanes/ $\text{Et}_2\text{O}/\text{Et}_3\text{N}$ eluent), affording bicycle **113j** (51.6 mg, 86% yield).

Bicycle **113j**:

Physical State: colorless oil.

R_f: 0.50 (9:1 hexanes/ Et_2O , KMnO_4).

IR (film): 2956, 2858, 1729, 1471, 1255 cm^{-1} .

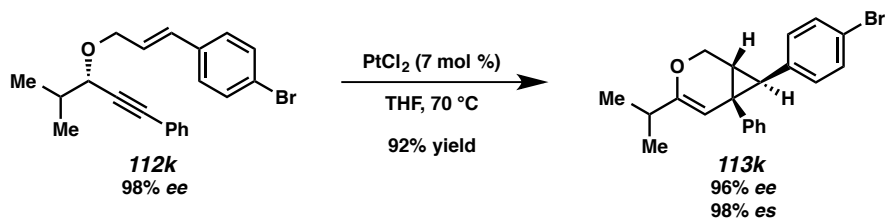
HRMS (DART+): *m/z* calc'd for $(\text{M} + \text{H})^+$ [$\text{C}_{22}\text{H}_{34}\text{O}_2\text{Si} + \text{H}$]⁺: 359.2406, found 359.2403.

¹H NMR (400 MHz, C_6D_6): δ 7.11 (d, *J* = 4.4 Hz, 4H), 7.06-7.02 (m, 1H), 5.51 (s, 1H), 4.12 (dd, *J* = 10.4, 1.2 Hz, 1H), 3.70 (dd, *J* = 10.4, 2.1 Hz, 1H), 3.54 (d, *J* = 10.4 Hz, 1H), 3.23 (d, *J* = 10.5 Hz, 1H), 2.67 (d, *J* = 5.8 Hz, 1H), 2.35-2.28 (m, 1H), 1.52 (dt, *J* = 5.8, 1.0 Hz, 1H), 1.13 (d, *J* = 5.5 Hz, 3H), 1.11 (d, *J* = 5.5 Hz, 3H), -0.09 (s, 3H), -0.16 (s, 3H).

¹³C NMR (100 MHz, C_6D_6): δ 158.0, 138.1, 129.5, 128.3, 126.4, 100.5, 64.5, 62.7, 34.9, 33.1, 26.7, 26.1, 25.5, 20.5, 20.3, 18.5, 5.4.

Optical Rotation: $[\alpha]_{\text{D}}^{31} = -90.21$ (*c* = 0.5, CH_2Cl_2).

The *ee* was determined to be 98% by HPLC analysis (Daicel Chiralcel IC, 100% hexane, 1.5 mL/min, λ = 230 nm, major isomer 4.68 min, minor isomer 4.45 min).



To a solution of enyne **112k** (110 mg, 0.298 mmol) in THF (9.93 mL, 0.030 M) under argon was added PtCl_2 (5.4 mg, 0.0201 mmol). The resulting mixture was sealed, heated to 70 °C and stirred at that temperature for 9 h. Once cooled to ambient temperature, the mixture was diluted with hexanes and filtered through a small plug of alumina (0.5 x 4.5 cm, 9:1 hexanes/ Et_2O eluent). The solvent was removed by rotary evaporation and the resulting residue was purified by flash chromatography (99.5:0.5 hexanes/ Et_3N → 97.5:2:0.5 hexanes/ $\text{Et}_2\text{O}/\text{Et}_3\text{N}$ eluent), affording bicycle **113k** (101 mg, 92% yield).

Bicycle **113k**:

Physical State: white solid.

R_f: 0.36 (9:1 hexanes/ Et_2O , KMnO_4).

IR (film): 3032, 2905, 1620, 1530, 1095 cm^{-1} .

HRMS (ESI+): m/z calc'd for $(\text{M} + \text{H})^+$ [$\text{C}_{21}\text{H}_{20}\text{BrO} + \text{H}$]⁺: 369.0849, found 369.0832.

¹H NMR (400 MHz, C_6D_6): δ 7.02-6.92 (comp m, 7H), 6.31-6.28 (m, 2H), 5.18 (s, 1H), 4.16 (dd, $J = 10.5, 1.3$ Hz, 1H), 3.77 (dd, $J = 10.4, 1.9$ Hz, 1H), 2.63 (d, $J = 5.8$ Hz, 1H), 2.30-2.20 (m, 1H), 1.88-1.85 (m, 1H), 1.07 (app. t, $J = 7.1$ Hz, 6H).

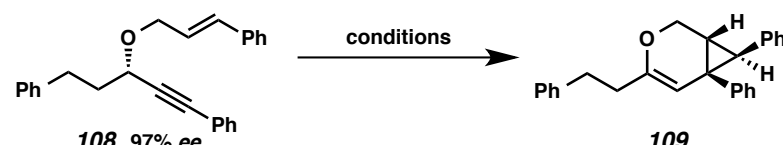
¹³C NMR (100 MHz, C_6D_6): δ 157.1, 140.5, 137.6, 131.0, 130.2, 129.6, 128.6, 126.8, 119.7, 104.0, 62.4, 36.1, 33.0, 32.5, 29.8, 20.4, 20.2.

Optical Rotation: $[\alpha]_{\text{D}}^{32} = -15.75$ ($c = 1.0$, CH_2Cl_2).

The *ee* was determined to be 98% by HPLC analysis (Daicel Chiralcel OJ-H, 0.5% 2-propanol in hexane, 1 mL/min, $\lambda = 254$ nm, major isomer 6.45 min, minor isomer 8.68 min).

3.7.3 Optimization Studies

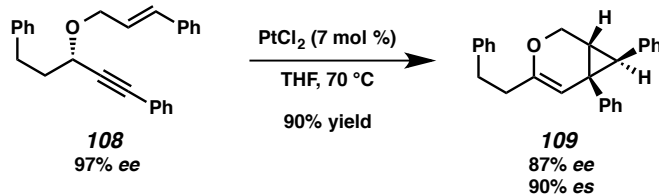
Catalyst Evaluation



entry	catalyst (mol %)	solvent, temp (°C)	t (h)	yield	ee (%)	es (%) ^a
1	(Ph ₃ P)AuNTf ₂ (5)	CH ₂ Cl ₂ , 23	0.5	52	84	87
2	[Ir(dbcot)Cl] ₂ (2.5) ^{b,c}	PhCH ₃ , 100	3	68	84	87
3	PtCl ₄ (5)	PhCH ₃ , 23	1	27	90	93
4	PtCl ₂ (5)	PhCH ₃ , 60	22	78	86	89
5	PtCl ₂ (5)	THF, 60	18	87	88	91
6	PtCl ₂ (5) ^b	THF, 60	14	86	86	89
7	[(C ₂ H ₄)PtCl ₂] ₂ (2.5)	THF, 23	28	84	86	89
8	Pt(PhCN) ₂ Cl ₂ (7)	THF, 60	48	64	87	90
9	PtCl ₂ (7)	THF, 70	18	90	87	90

^a Enantiospecificity (es) = [(ee_{product}) / (ee_{substrate})] x 100%. ^b Under 1 atm CO.
^c dbcot: dibenzo[a,e]cyclooctatetraene

General Procedure for Experiments in Table 3.4.1: To a solution of enyne **108** in the listed solvent under argon was added catalyst. The resulting mixture was sealed, heated to the prescribed temperature and stirred for the listed time. For entries 2 and 6, the solution was purged with a balloon of CO prior to heating. Once cooled to ambient temperature, the mixture was diluted with hexanes and filtered through a small plug of alumina (0.5 x 2 cm, 9:1 hexanes/Et₂O eluent). The solvent was removed by rotary evaporation and the resulting residue was purified by flash chromatography. The enantiomeric excess of bicycle **109** was analyzed by HPLC.



Entry 9. To a solution of enyne **108** (20.0 mg, 0.0567 mmol) in THF (1.90 mL, 0.030 M) under argon was added PtCl₂ (0.8 mg, 0.00285 mmol). The resulting mixture was sealed, heated to 70 °C and stirred at that temperature for 18 h. Once cooled to ambient temperature, the mixture was diluted with hexanes and

filtered through a small plug of alumina (0.5 x 2 cm, 9:1 hexanes/Et₂O eluent). The solvent was removed by rotary evaporation and the resulting residue was purified by flash chromatography (99.5:0.5 hexanes/Et₃N → 98.5:1:0.5 hexanes/Et₂O/Et₃N eluent), affording bicycle **109** (17.9 mg, 90% yield).

Bicycle 109:

Physical State: white solid.

R_f: 0.73 (9:1 hexanes/Et₂O, KMnO₄).

IR (film): 3061, 2923, 2863, 1665, 1497 cm⁻¹.

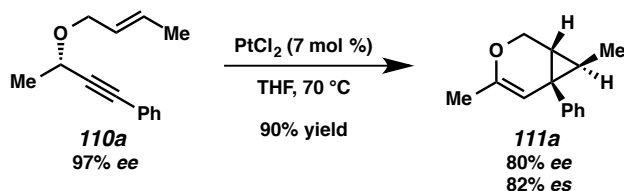
HRMS (ESI⁺): *m/z* calc'd for (M + H)⁺ [C₂₆H₂₄O + H]⁺: 353.1905, found 353.1891.

¹H NMR (400 MHz, C₆D₆): δ 7.18 (m, 2H), 7.11-6.85 (comp m, 11H), 6.72-6.70 (m, 2H), 5.10 (s, 1H), 4.20 (d, *J* = 10.5 Hz, 1H), 3.85 (dd, *J* = 10.5, 2.1 Hz, 1H), 2.87-2.73 (comp m, 3H), 2.32 (t, *J* = 7.8 Hz, 2H), 2.05 (d, *J* = 5.8 Hz, 1H).

¹³C NMR (100 MHz, C₆D₆): δ 150.9, 142.0, 140.8, 138.4, 130.3, 128.9, 128.6, 128.5, 128.00, 127.97, 126.6, 126.2, 125.8, 107.1, 62.5, 37.2, 36.6, 33.7, 32.4, 29.3.

Optical Rotation: [α]_D³⁰ = -0.43 (*c* = 1.0, CH₂Cl₂).

The *ee* was determined to be 87% by HPLC analysis (Daicel Chiralcel OD-H, 10% 2-propanol in hexane, 1 mL/min, λ = 210 nm, major isomer 6.04 min, minor isomer 12.23 min).



To a solution of enyne **110a** (10.0 mg, 0.0499 mmol) in THF (1.67 mL, 0.030 M) under argon was added PtCl₂ (0.9 mg, 0.00350 mmol). The resulting mixture was sealed, heated to 70 °C and stirred at that temperature for 12 h. Once cooled to ambient temperature, the mixture was diluted with hexanes and filtered through a small plug of alumina (0.5 x 2 cm, 9:1 hexanes/Et₂O eluent). The solvent was removed

by rotary evaporation and the resulting residue was purified by flash chromatography (99.5:0.5 hexanes/Et₃N → 98.5:1:0.5 hexanes/Et₂O/Et₃N eluent), affording bicycle **111a** (9.1 mg, 90% yield).

Bicycle 111a:

Physical State: yellow oil.

R_f: 0.59 (9:1 hexanes/Et₂O, KMnO₄).

IR (film): 2929, 1715, 1495, 1447 cm⁻¹.

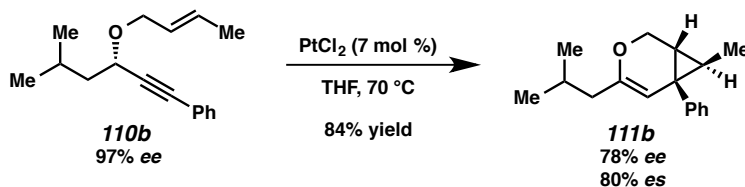
HRMS (ESI+): *m/z* calc'd for (M + H)⁺ [C₁₄H₁₆O + H]⁺: 201.1274, found 201.1273.

¹H NMR (400 MHz, C₆D₆): δ 7.25-7.07 (comp m, 5H), 5.09-5.05 (s, 1H), 4.12 (dd, *J* = 10.5, 1.1 Hz, 1H), 3.80 (dd, *J* = 10.5, 2.1 Hz, 1H), 1.67 (s, 3H), 1.43 (quintet, *J* = 6.0 Hz, 1H), 1.20-1.13 (comp m, 3H).

¹³C NMR (100 MHz, C₆D₆): δ 147.7, 142.3, 129.7, 128.7, 126.5, 106.7, 62.7, 29.4, 27.5, 26.5, 20.0, 15.0.

Optical Rotation: [α]_D³¹ = -31.92 (*c* = 0.1, CH₂Cl₂).

The *ee* was determined to be 80% by HPLC analysis (Daicel Chiralcel OJ-H, 5% 2-propanol in hexane, 1.0 mL/min, λ = 210 nm, major isomer 9.67 min, minor isomer 10.60 min).



To a solution of enyne **110b** (25.0 mg, 0.103 mmol) in THF (3.43 mL, 0.030 M) under argon was added PtCl₂ (1.9 mg, 0.00722 mmol). The resulting mixture was sealed, heated to 70 °C and stirred at that temperature for 24 h. Once cooled to ambient temperature, the mixture was diluted with hexanes and filtered through a small plug of alumina (0.5 x 2 cm, 4:1 hexanes/Et₂O eluent). The solvent was removed by rotary evaporation and the resulting residue was purified by flash chromatography (99.5:0.5 hexanes/Et₃N → 98.5:1:0.5 hexanes/Et₂O/Et₃N eluent), affording bicycle **111b** (21.1 mg, 84% yield).

Bicycle 111b:

Physical State: yellow oil.

R_f: 0.66 (9:1 hexanes/Et₂O, KMnO₄).

IR (film): 2960, 2872, 1727, 1495 cm⁻¹.

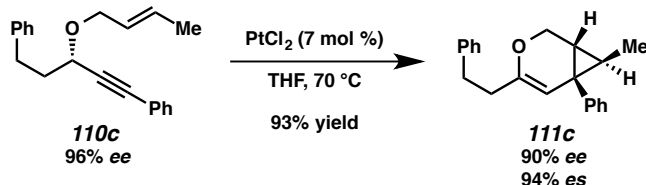
HRMS (ESI+): *m/z* calc'd for (M + H)⁺ [C₁₇H₂₂O + H]⁺: 243.1744, found 243.1746.

¹H NMR (400 MHz, C₆D₆): δ 7.22-7.18 (comp m, 4H), 7.13-7.07 (m, 1H), 5.15 (s, 1H), 4.14 (dd, *J* = 10.4, 1.3 Hz, 1H), 3.76 (dd, *J* = 10.3, 2.0 Hz, 1H), 2.03-1.82 (comp m, 4H), 1.48 (quintet, *J* = 6.0 Hz, 1H), 1.23-1.17 (comp m, 2H), 0.91 (d, *J* = 6.5 Hz, 3H), 0.88 (d, *J* = 6.5 Hz, 3H), 0.72 (d, *J* = 6.3 Hz, 3H).

¹³C NMR (100 MHz, C₆D₆): δ 150.5, 142.3, 129.7, 128.7, 126.5, 107.8, 62.7, 43.9, 29.9, 27.5, 26.42, 26.37, 22.7, 22.6, 15.0.

Optical Rotation: [α]_D³⁰ = -13.19 (*c* = 0.5, CH₂Cl₂).

The *ee* was determined to be 78% by HPLC analysis (Daicel Chiralcel OJ-H, 1% 2-propanol in hexane, 1 mL/min, λ = 210 nm, major isomer 4.91 min, minor isomer 6.01 min).



Bicycle 110c: To a solution of enyne **111c** (10.0 mg, 0.0344 mmol) in THF (1.15 mL, 0.030 M) under argon was added PtCl₂ (0.6 mg, 0.00238 mmol). The resulting mixture was sealed, heated to 70 °C and stirred at that temperature for 16 h. Once cooled to ambient temperature, the mixture was diluted with hexanes and filtered through a small plug of alumina (0.5 x 2 cm, 9:1 hexanes/Et₂O eluent). The solvent was removed by rotary evaporation and the resulting residue was purified by flash chromatography (99.5:0.5 hexanes/Et₃N → 98.5:1:0.5 hexanes/Et₂O/Et₃N eluent), affording bicycle **111c** (9.3 mg, 93% yield).

Bicycle 110c:

Physical State: white solid.

R_f: 0.53 (9:1 hexanes/Et₂O, KMnO₄).

IR (film): 2925, 2855, 1719, 1602 cm^{-1} .

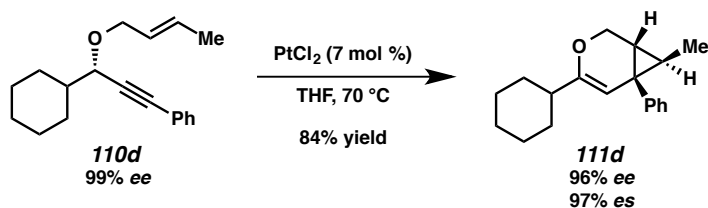
HRMS (ESI+): m/z calc'd for $(M + H)^+$ [$\text{C}_{21}\text{H}_{22}\text{O} + \text{H}$] $^+$: 291.1744, found 291.1735.

^1H NMR (400 MHz, C_6D_6): δ 7.18-6.98 (comp m, 10H), 5.06 (s, 1H), 4.11 (dd, $J = 10.4, 1.4$ Hz, 1H), 3.73 (dd, $J = 10.4, 2.2$ Hz, 1H), 2.76-2.71 (m, 2H), 2.28-2.23 (m, 2H), 1.39 (quintet, $J = 6.0$ Hz, 1H), 1.18-1.17 (m, 1H), 0.68 (d, $J = 6.3$ Hz, 3H).

^{13}C NMR (100 MHz, C_6D_6): δ 150.4, 142.1, 129.7, 128.8, 128.7, 128.6, 126.5, 126.2, 107.1, 62.8, 36.7, 33.9, 29.7, 27.4, 26.4, 15.0.

Optical Rotation: $[\alpha]_{\text{D}}^{31} = -8.51$ ($c = 0.1$, CH_2Cl_2).

The *ee* was determined to be 90% by HPLC analysis (Daicel Chiralcel OD-H, 3% 2-propanol in hexane, 1 mL/min, $\lambda = 210$ nm, major isomer 5.62 min, minor isomer 12.79 min).



To a solution of enyne **110d** (25.0 mg, 0.0932 mmol) in THF (3.10 mL, 0.030 M) under argon was added PtCl₂ (1.7 mg, 0.00652 mmol). The resulting mixture was sealed, heated to 70 °C and stirred at that temperature for 24 h. Once cooled to ambient temperature, the mixture was diluted with hexanes and filtered through a small plug of alumina (0.5 x 2 cm, 9:1 hexanes/Et₂O eluent). The solvent was removed by rotary evaporation and the resulting residue was purified by flash chromatography (99.5:0.5 hexanes/Et₃N → 98.5:1:0.5 hexanes/Et₂O/Et₃N eluent), affording bicycle **111d** (21.0 mg, 84% yield).

Bicycle 111d:

Physical State: colorless oil.

R_f: 0.85 (9:1 hexanes/Et₂O, KMnO₄).

IR (film): 2930, 2856, 1720, 1448 cm^{-1} .

HRMS (ESI+): m/z calc'd for $(M + H)^+$ [$\text{C}_{19}\text{H}_{24}\text{O} + \text{H}$] $^+$: 269.1900, found 269.1901.

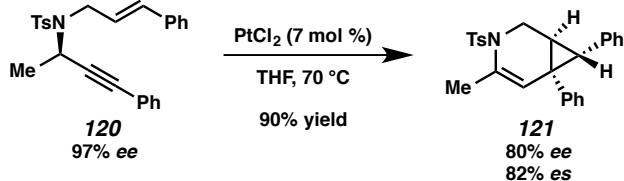
¹H NMR (400 MHz, C₆D₆): δ 7.23-7.19 (comp m, 4H), 7.14-7.09 (m, 1H), 5.17 (s, 1H), 4.18 (dd, *J* = 10.3, 1.4 Hz, 1H), 3.74 (dd, *J* = 10.3, 2.0 Hz, 1H), 1.99-1.83 (comp m, 4H), 1.70-1.62 (comp m, 2H), 1.59-1.53 (m, 1H), 1.49 (quintet, *J* = 6.0 Hz, 1H), 1.35-1.02 (comp m, 7H), 0.74 (d, *J* = 6.3 Hz, 3H).

¹³C NMR (100 MHz, C₆D₆): δ 155.8, 142.6, 129.8, 128.7, 126.5, 104.7, 99.1, 62.8, 42.8, 31.1, 30.9, 30.2, 27.3, 26.69, 26.67, 26.6, 26.1, 15.0.

Optical Rotation: $[\alpha]_D^{28} = +10.00$ (*c* = 1.0, CH₂Cl₂).

The *ee* was determined to be 96% by HPLC analysis (Daicel Chiralcel OJ-H, 1% 2-propanol in hexane, 1 mL/min, λ = 230 nm, major isomer 4.15 min, minor isomer 4.56 min).

3.7.4 Additional Reactions



To a solution of enyne **120** (50.0 mg, 0.120 mmol) in THF (4.61 mL, 0.030 M) under argon was added PtCl₂ (2.2 mg, 0.00840 mmol). The resulting mixture was sealed, heated to 70 °C and stirred at that temperature for 15 h. Once cooled to ambient temperature, the solvent was removed by rotary evaporation and the resulting residue was purified by flash chromatography (4:1 → 1:1 hexanes/EtOAc eluent), affording bicycle **121** (44.8 mg, 90% yield).

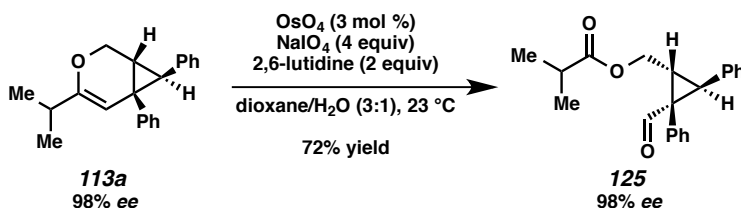
Bicycle **121**:

Physical State: white solid.

R_f: 0.62 (1:1 hexanes/EtOAc, KMnO₄).

¹H NMR (300 MHz, C₆D₆): δ 7.71 (d, *J* = 8.3 Hz, 2H), 7.08-6.72 (comp m, 10H), 6.40-6.38 (m, 2H), 5.42 (s, 1H), 4.44 (dd, *J* = 13.6, 2.4 Hz, 1H), 3.29 (dd, *J* = 13.6, 2.6 Hz, 1H), 2.16-2.10 (comp m, 4H), 1.97 (d, *J* = 5.7 Hz, 1H), 1.92 (s, 3H).

The *ee* was determined to be 80% by HPLC analysis (Daicel Chiralcel IC, 10% 2-propanol in hexane, 1 mL/min, λ = 210 nm, major isomer 17.97 min, minor isomer 14.04 min).



To a solution of bicycle **113a** (36.3 mg, 0.125 mmol) in dioxane (3.75 mL) at 23 °C was added OsO₄ (23.8 μL, 4% in H₂O, 0.00375 mmol) followed by 2,6-lutidine (29.0 μL, 0.250 mmol). To the resulting mixture was added a solution of NaIO₄ (106 mg, 0.500 mmol) in H₂O (1.25 mL). The resulting reaction

mixture was stirred vigorously for 48 h, at which time it was diluted with EtOAc (15 mL) and H₂O (10 mL). The layers were separated, and the aqueous phase was extracted with EtOAc (2 x 15 mL). The combined organic layers were washed with sat. aq. Na₂S₂O₃ (1 x 10 mL), then brine (1 x 10 mL), and dried over MgSO₄. The solvent was removed by rotary evaporation and the resulting residue was purified by flash chromatography (9:1 hexanes/EtOAc eluent), affording cyclopropane **125** (28.9 mg, 72% yield).

Cyclopropane **125**:

Physical State: colorless oil.

R_f: 0.53 (4:1 hexanes/EtOAc, anisaldehyde).

IR (film): 2969, 1733, 1704, 1191 cm⁻¹.

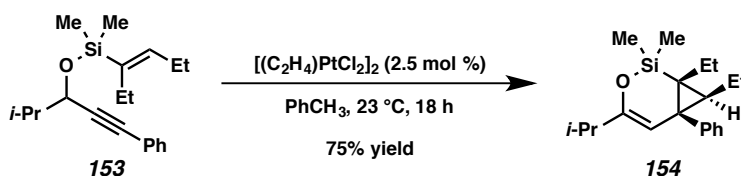
HRMS (ESI+): *m/z* calc'd for (M + Na)⁺ [C₂₁H₂₂O₃ + Na]⁺: 345.1467, found 345.1466.

¹H NMR (400 MHz, CDCl₃): δ 9.73 (s, 1H), 7.24-7.20 (comp m, 3H), 7.12-7.07 (comp m, 3H), 7.06-7.00 (m, 2H), 6.84-6.80 (m, 2H), 4.79 (dd, *J* = 11.9, 5.6 Hz, 1H), 4.29 (dd, *J* = 11.9, 9.7 Hz, 1H), 3.34 (d, *J* = 7.5 Hz, 1H), 2.93-2.87 (m, 1H), 2.60 (septet, *J* = 7.0 Hz, 1H), 1.21 (d, *J* = 3.6 Hz, 3H), 1.19 (d, *J* = 3.6 Hz, 3H).

¹³C NMR (100 MHz, CDCl₃): δ 199.3, 135.1, 134.6, 131.5, 128.7, 128.1, 128.0, 127.0, 61.3, 49.8, 38.2, 34.6, 34.1, 19.23, 19.16.

Optical Rotation: [α]_D²⁷ = -150.43 (*c* = 1.0 CH₂Cl₂).

The *ee* was determined to be 98% by HPLC analysis (Daicel Chiralcel OD-H, 15% 2-propanol in hexane, 1 mL/min, λ = 210 nm, major isomer 6.30 min, minor isomer 12.41 min).



To a solution of enyne **153** (40.0 mg, 0.127 mmol) in toluene (4.23 mL, 0.030 M) under argon was added Zeise's Dimer (1.87 mg, 0.00318 mmol). The resulting mixture was sealed and stirred at 23 °C for 18 h.

The mixture was then diluted with hexanes and passed through a small plug of alumina (0.5 x 2 cm, 9:1 hexanes/Et₂O eluent). The solvent was removed in vacuo and the resulting residue was purified by flash chromatography (3:1 hexanes/CH₂Cl₂ eluent with 0.5% Et₃N), affording bicycle **154** (30.0 mg, 75% yield).

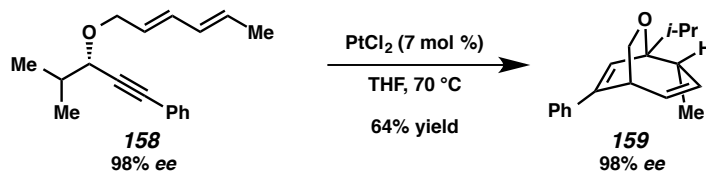
Siloxane 154:

Physical State: colorless oil.

R_f: 0.85 (3:1 hexanes/CH₂Cl₂, KMnO₄).

IR (film): 2964, 1656, 1461, 1305, 1252 cm⁻¹.

¹H NMR (400 MHz, C₆D₆): 7.30-7.27 (m, 2H), 7.22 (t, *J* = 7.6 Hz, 2H), 7.13-7.09 (m, 1H), 4.86 (s, 1H), 2.16 (dt, *J* = 13.6, 6.8 Hz, 1H), 1.74-1.64 (m, 1H), 1.57 (t, *J* = 6.6 Hz, 2H), 1.31-1.08 (m, 2H), 1.07-1.00 (comp m, 13H), 0.37 (s, 3H), 0.36 (s, 3H).



To a solution of enyne **158** (25.0 mg, 0.0980 mmol) in THF (3.28 mL, 0.030 M) under argon was added PtCl₂ (1.83 mg, 0.00688 mmol). The resulting mixture was sealed, heated to 70 °C and stirred at that temperature for 12 h. Once cooled to ambient temperature, the mixture was diluted with hexanes and passed through a small plug of alumina (0.5 x 2 cm, 4:1 hexanes/Et₂O eluent). The solvent was removed in vacuo and the resulting residue was purified by flash chromatography (97.5:2:0.5 hexanes/Et₂O/NEt₃ eluent), affording bicycle **159** (16.2 mg, 64% yield).

Bicycle 159:

Physical State: white solid.

R_f: 0.40 (9:1 hexanes/Et₂O, anisaldehyde).

IR (film): 2964, 1494, 1446, 1097, 949 cm⁻¹.

HRMS (ESI⁺): *m/z* calc'd for (M + H)⁺ [C₁₈H₂₂O + H]⁺: 255.1744, found 255.1743.

¹H NMR (400 MHz, C₆D₆): δ 7.29-7.26 (m, 2H), 7.19-7.17 (m, 2H), 7.13-7.09 (m, 1H), 5.92 (ddd, *J* = 10.8, 8.3, 2.4 Hz, 1H), 5.82 (d, *J* = 1.9 Hz, 1H), 5.31 (dd, *J* = 10.9, 3.8 Hz, 1H), 4.17 (dd, *J* = 8.1, 1.9 Hz, 1H), 3.64 (dd, *J* = 8.1, 1.9 Hz, 1H), 2.77-2.70 (m, 2H), 1.79 (dt, *J* = 13.4, 6.7 Hz, 1H), 1.13 (d, *J* = 4.7 Hz, 3H), 1.11 (d, *J* = 4.6 Hz, 3H), 0.75 (d, *J* = 7.4 Hz, 3H).

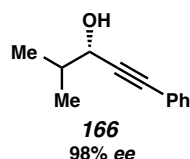
¹³C NMR (100 MHz, C₆D₆): δ 148.5, 139.0, 136.5, 127.6, 126.9, 126.8, 125.6, 79.9, 70.9, 42.3, 37.2, 34.9, 17.3, 15.6, 15.1.

Optical Rotation: $[\alpha]_D^{31} = -179.15$ (c = 1.0, CHCl₃).

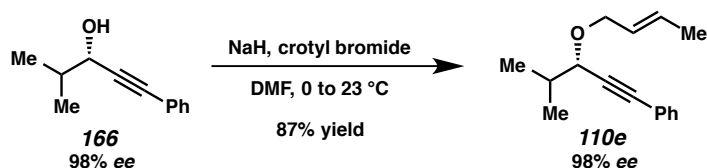
The *ee* was determined to be 98% by HPLC analysis (Diacel Chiralcel OJ-H, 1% 2-propanol in hexane, 1 mL/min, λ = 254 nm, major isomer 5.97 min, minor isomer 10.15 min).

3.7.5 Substrate Syntheses

General procedure for the synthesis of propargylic alcohols using the Noyori transfer hydrogenation: To a solution of an ynone in 2-propanol (0.1 M) under argon was added Ru[(*S,S*)-TsDPEN(*p*-cymene)] (.04-2 mol %). The resulting purple solution was stirred at ambient temperature until the reaction was complete (2-48 h). The solvent was removed in vacuo and the resulting residue was purified by flash chromatography, affording the enantioenriched propargylic alcohol.



Alcohol 166. Based on the general procedure, alcohol **166** was produced in >99% yield. All spectra matched those previously reported in the literature.⁴⁰ The *ee* was determined to be 98% by HPLC analysis (Daicel Chiralcel OD-H, 5% 2-propanol in hexane, 1 mL/min, $\lambda = 254$ nm, *S* isomer 12.18 min, *R* isomer 6.86 min). $[\alpha]_D^{32} = +2.98$ ($c = 1.0$, CHCl_3) (*S*) (Lit. $[\alpha]_D^{20} = +1.52$ ($c = 0.6$, CHCl_3) 47.4% *ee* (*S*)).



Enyne 110e. To a solution of alcohol **166** (90.6 mg, 0.520 mmol) in DMF (1.73 mL) at 0 °C under argon was added NaH (22.9 mg, 60% dispersion in mineral oil, 0.572 mmol) in one portion. The mixture was then allowed to warm to ambient temperature and stirred for 25 min. Crotyl bromide (53.6 μL , 0.520 mmol) was added and after 3 h, the reaction was quenched by slow addition of H_2O (3 mL). The mixture was extracted with hexanes (3 x 20 mL). The combined organic layers were washed sequentially with aq. LiCl (10% w/v, 5 mL), then brine (5 mL), and dried over MgSO_4 . The solvent was removed by rotary evaporation and the resulting residue was purified by flash chromatography (100% hexanes \rightarrow 9:1 hexanes/EtOAc eluent), affording enyne **110e** (103 mg, 87% yield).

Physical State: yellow oil.

R_f: 0.74 (4:1 hexanes/EtOAc, anisaldehyde).

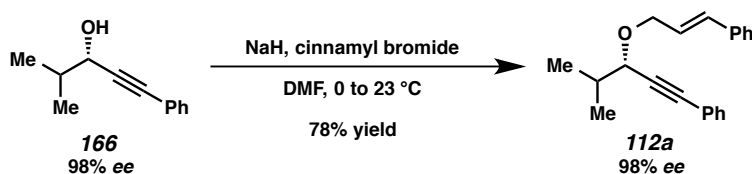
IR (film): 2963, 1490, 1444, 1350 cm⁻¹.

HRMS (ESI+): *m/z* calc'd for (M + H)⁺ [C₁₆H₂₀O + H]⁺: 229.1587, found 229.1583.

¹H NMR (400 MHz, CDCl₃): δ 7.47-7.42 (m, 2H), 7.33-7.29 (comp m, 3H), 5.82-5.72 (m, 1H), 5.67-5.57 (m, 1H), 4.28-4.23 (m, 1H), 4.06 (d, *J* = 5.8 Hz, 1H), 4.00-3.95 (m, 1H), 1.75-1.71 (m, 3H), 1.07 (d, *J* = 6.7 Hz, 3H), 1.04 (d, *J* = 6.8 Hz, 3H).

¹³C NMR (100 MHz, CDCl₃): δ 131.9, 129.8, 128.4, 128.3, 127.6, 123.2, 87.6, 86.4, 74.8, 69.8, 33.4, 19.0, 18.1.

Optical Rotation: [α]_D³¹ = -62.55 (*c* = 1.0, CH₂Cl₂).



Enyne 112a. To a solution of alcohol **166** (100 mg, 0.575 mmol) in DMF (1.91 mL) at 0 °C under argon was added NaH (27.6 mg, 60% dispersion in mineral oil, 0.896 mmol) in one portion. The mixture was then allowed to warm to ambient temperature and stirred for 20 min. Cinnamyl bromide (85.2 μL, 0.575 mmol) was added and after 3 h, the reaction was quenched by slow addition of H₂O (5 mL). The mixture was extracted with hexanes (3 x 20 mL). The combined organic layers were washed sequentially with aq. LiCl (10% w/v, 5 mL), then brine (5 mL), and dried over MgSO₄. The solvent was removed by rotary evaporation and the resulting residue was purified by flash chromatography (100% hexanes → 10:1 hexanes/EtOAc eluent), affording enyne **112a** (130 mg, 78% yield).

Physical State: colorless oil.

R_f: 0.55 (9:1 hexanes/EtOAc, anisaldehyde).

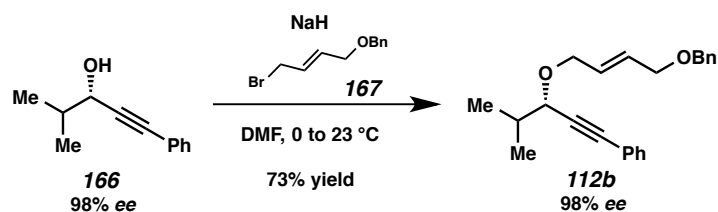
IR (film): 3062, 2966, 2874, 1723, 1491 cm⁻¹.

HRMS (APCI+): m/z calc'd for $(M + H)^+$ $[C_{21}H_{21}O + H]^+$: 291.1744, found 291.1752.

1H NMR (400 MHz, $CDCl_3$): δ 7.48-7.44 (m, 2H), 7.42-7.39 (m, 2H), 7.34-7.29 (comp m, 6H), 6.67 (d, $J = 15.9$ Hz, 1H), 6.34 (ddd, $J = 15.9, 6.7, 5.5$ Hz, 1H), 4.50 (ddd, $J = 12.7, 5.5, 1.6$ Hz, 1H), 4.23 (ddd, $J = 12.7, 6.7, 1.3$ Hz, 1H), 4.14 (d, $J = 5.8$ Hz, 1H), 2.06 (dq, $J = 12.8, 6.5$ Hz, 1H), 1.11 (d, $J = 6.7$ Hz, 3H), 1.07 (d, $J = 6.8$ Hz, 3H).

^{13}C NMR (100 MHz, $CDCl_3$): δ 137.0, 132.7, 131.9, 128.7, 128.40, 128.36, 127.8, 126.7, 126.2, 123.1, 87.4, 86.7, 75.1, 69.7, 33.5, 18.9, 18.2.

Optical Rotation: $[\alpha]_D^{32} = -85.75$ ($c = 1.0, CH_2Cl_2$).



Enyne 112b. To a solution of alcohol **166** (85.0 mg, 0.488 mmol) in DMF (1.63 mL) at 0 °C under argon was added NaH (23.4 mg, 60% dispersion in mineral oil, 0.585 mmol) in one portion. The mixture was then allowed to warm to ambient temperature and stirred for 20 min. Bromide **167**⁴¹ (118 mg, 0.488 mmol) was added and after 6 h, the reaction was quenched by slow addition of H_2O (3 mL). The mixture was extracted with hexanes (3 x 20 mL). The combined organic layers were washed sequentially with aq. LiCl (10% w/v, 5 mL), then brine (5 mL), and dried over $MgSO_4$. The solvent was removed by rotary evaporation and the resulting residue was purified by flash chromatography (100% hexanes \rightarrow 9:1 hexanes/EtOAc eluent), affording enyne **112b** (119 mg, 73% yield).

Physical State: colorless oil.

R_f : 0.47 (4:1 hexanes/EtOAc, anisaldehyde).

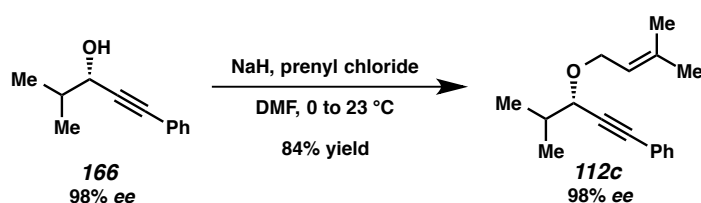
IR (film): 2962, 2853, 1490, 1454, 1102 cm^{-1} .

HRMS (APCI+): m/z calc'd for $(M + NH_4)^+$ $[C_{23}H_{26}O_2 + NH_4]^+$: 352.2277, found 352.2276.

¹H NMR (400 MHz, CDCl₆): δ 7.46-7.42 (m, 2H), 7.34 (d, *J* = 4.4 Hz, 4H), 7.32-7.28 (comp m, 4H), 5.91-5.88 (comp. m, 2H), 4.53 (s, 2H), 4.37-4.32 (m, 1H), 4.10-4.03 (comp m, 4H), 2.03 (dq, *J* = 12.8, 6.5 Hz, 1H), 1.08 (d, *J* = 6.7 Hz, 3H), 1.05 (d, *J* = 6.8 Hz, 3H).

¹³C NMR (100 MHz, CDCl₆): δ 131.9, 129.7, 129.5, 128.5, 128.39, 128.35, 127.9, 127.4, 87.4, 86.6, 75.2, 72.4, 70.4, 69.0, 33.4, 18.9, 18.1.

Optical Rotation: $[\alpha]_D^{34} = -83.62$ (*c* = 1.0, CH₂Cl₂).



Enyne 112c To a solution of alcohol **166** (90.1 mg, 0.517 mmol) in DMF (1.72 mL) at 0 °C under argon was added NaH (24.8 mg, 60% dispersion in mineral oil, 0.620 mmol) in one portion. The mixture was then allowed to warm to ambient temperature and stirred for 20 min. Prenyl chloride (58.3 μL, 0.517 mmol) was added and after 2.5 h, the reaction was quenched by slow addition of H₂O (5 mL). The mixture was extracted with hexanes (3 x 20 mL). The combined organic layers were washed sequentially with aq. LiCl (10% w/v, 5 mL), then brine (5 mL), and dried over MgSO₄. The solvent was removed by rotary evaporation and the resulting residue was purified by flash chromatography (100% hexanes → 50:1 hexanes/EtOAc eluent), affording enyne **112c** (105 mg, 84% yield).

Physical State: colorless oil.

R_f: 0.58 (9:1 hexanes/EtOAc, anisaldehyde).

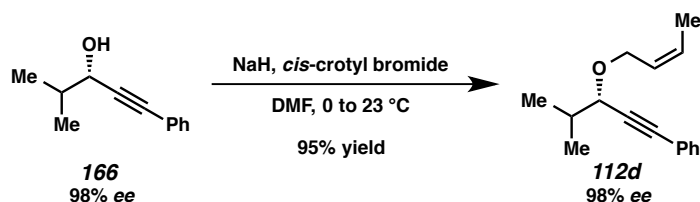
IR (film): 2965, 2930, 1723, 1490, 1444 cm⁻¹.

HRMS (DART+): *m/z* calc'd for (M + NH₄)⁺ [C₁₇H₂₂O + NH₄]⁺: 260.2014, found 260.2015.

¹H NMR (400 MHz, CDCl₆): δ 7.47-7.43 (m, 2H), 7.32-7.29 (comp m, 3H), 5.41-5.36 (m, 1H), 4.28 (dd, *J* = 11.5, 6.3 Hz, 1H), 4.07 (dd, *J* = 11.6, 7.6 Hz, 1H), 4.05 (d, *J* = 5.9 Hz, 1H), 2.02 (dq, *J* = 13.0, 6.6 Hz, 1H), 1.77 (s, 3H), 1.73 (s, 3H), 1.07 (d, *J* = 6.7 Hz, 3H), 1.05 (d, *J* = 6.8 Hz, 3H).

¹³C NMR (100 MHz, CDCl₆): δ 137.6, 131.9, 128.4, 128.3, 123.3, 121.1, 87.8, 86.3, 74.8, 65.5, 33.4, 26.0, 19.0, 18.3, 18.2.

Optical Rotation: $[\alpha]_D^{31} = -249.36$ ($c = 1.0$, CH₂Cl₂).



Enyne 112d. To a solution of alcohol **166** (100 mg, 0.574 mmol) in DMF (1.91 mL) at 0 °C under argon was added NaH (29.8 mg, 60% dispersion in mineral oil, 0.746 mmol) in one portion. The mixture was then allowed to warm to ambient temperature and stirred for 20 min. (*Z*)-Crotyl bromide⁴² (77.5 mg, 0.574 mmol) was added and after 3.5 h, the reaction was quenched by slow addition of H₂O (3 mL). The mixture was extracted with hexanes (3 x 20 mL). The combined organic layers were washed sequentially with aq. LiCl (10% w/v, 5 mL), then brine (5 mL), and dried over MgSO₄. The solvent was removed by rotary evaporation and the resulting residue was purified by flash chromatography (100% hexanes → 15:1 hexanes/EtOAc eluent), affording enyne **112d** (125 mg, 95% yield).

Physical State: colorless oil.

R_f: 0.56 (4:1 hexanes/EtOAc, anisaldehyde).

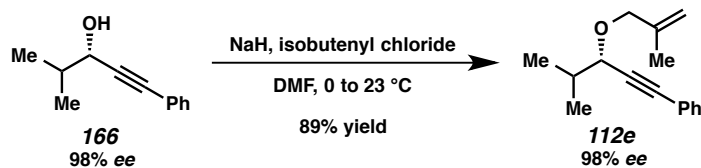
IR (film): 3023, 2969, 1659, 1490, 1071, 691 cm⁻¹.

HRMS (APCI+): m/z calc'd for (M + H)⁺ [C₁₆H₂₀O + H]⁺: 229.1592, found 229.1583.

¹H NMR (400 MHz, CDCl₆): δ 7.48-7.43 (m, 1H), 7.33-7.29 (comp m, 3H), 5.75-5.67 (m, 1H), 5.64-5.57 (m, 1H), 4.34 (dd, $J = 12.0, 5.8$ Hz, 1H), 4.19 (dd, $J = 11.9, 7.2$ Hz, 1H), 4.08 (d, $J = 5.9$ Hz, 1H), 2.02 (dq, $J = 13.2, 6.6$ Hz, 1H), 1.72 (d, $J = 6.8$ Hz, 3H), 1.08 (d, $J = 6.7$ Hz, 3H), 1.05 (d, $J = 6.8$ Hz, 3H).

¹³C NMR (100 MHz, CDCl₆): δ 131.9, 128.5, 128.4, 128.3, 126.9, 123.2, 87.7, 86.4, 74.86, 74.85, 64.3, 33.4, 18.9, 18.2, 13.4.

Optical Rotation: $[\alpha]_D^{30} = -182.55$ ($c = 1.0$, CH₂Cl₂).



Enyne 112e. To a solution of alcohol **166** (80.0 mg, 0.459 mmol) in DMF (1.53 mL) at 0 °C under argon was added NaH (22.0 mg, 60% dispersion in mineral oil, 0.551 mmol) in one portion. The mixture was then allowed to warm to ambient temperature and stirred for 20 min. Isobutenyl chloride (44.9 μL , 0.459 mmol) was added and after 2.5 h, the reaction was quenched by slow addition of H_2O (5 mL). The mixture was extracted with hexanes (3 x 20 mL). The combined organic layers were washed sequentially with aq. LiCl (10% w/v, 5 mL), then brine (5 mL), and dried over MgSO_4 . The solvent was removed by rotary evaporation and the resulting residue was purified by flash chromatography (100% hexanes \rightarrow 15:1 hexanes/EtOAc eluent), affording enyne **112e** (93.1 mg, 89% yield).

Physical State: colorless oil.

R_f: 0.83 (4:1 hexanes/EtOAc, anisaldehyde).

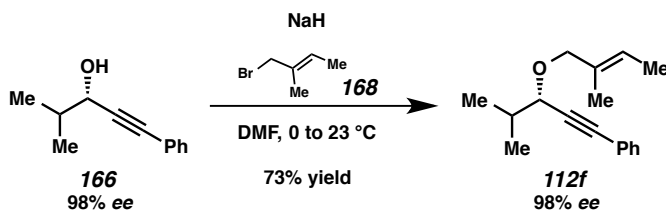
IR (film): 2963, 2872, 1598, 1490, 1071 cm^{-1} .

HRMS (ESI+): m/z calc'd for $(\text{M} + \text{NH}_4)^+ [\text{C}_{16}\text{H}_{20}\text{O} + \text{NH}_4]^+$: 246.1858, found 246.1859.

^1H NMR (400 MHz, CDCl_3): δ 7.47-7.43 (m, 2H), 7.33-7.29 (comp m, 3H), 5.04 (d, $J = 1.0$ Hz, 1H), 4.92 (d, $J = 0.7$ Hz, 1H), 4.20 (d, $J = 12.5$ Hz, 1H), 4.05 (d, $J = 5.9$ Hz, 1H), 3.98 (d, $J = 12.5$ Hz, 1H), 2.04 (dq, $J = 13.0, 6.6$ Hz, 1H), 1.78 (s, 3H), 1.09 (d, $J = 6.7$ Hz, 3H), 1.06 (d, $J = 6.8$ Hz, 3H).

^{13}C NMR (100 MHz, CDCl_3): δ 142.3, 131.9, 128.4, 128.3, 123.2, 112.5, 87.6, 86.4, 74.9, 72.9, 33.5, 19.8, 18.9, 18.3.

Optical Rotation: $[\alpha]_{\text{D}}^{32} = -116.81$ ($c = 1.0$, CH_2Cl_2).



Enyne 112f. To a solution of alcohol **166** (90.1 mg, 0.517 mmol) in DMF (1.72 mL) at 0 °C under argon was added NaH (24.8 mg, 60% dispersion in mineral oil, 0.628 mmol) in one portion. This mixture was then allowed to warm to ambient temperature and stirred for 20 min. Bromide **168**⁴³ (77.0 mg, 0.517 mmol) was added and after 2 h, the reaction was quenched by slow addition of H₂O (5 mL). The mixture was extracted with hexanes (3 x 20 mL). The combined organic layers were washed sequentially with aq. LiCl (10% w/v, 5 mL), then brine (5 mL), and dried over MgSO₄. The solvent was removed by rotary evaporation and the resulting residue was purified by flash chromatography (100% hexanes → 50:1 hexanes/EtOAc eluent), affording enyne **112f** (91.0 mg, 73% yield).

Physical State: yellow oil.

R_f: 0.59 (9:1 hexanes/EtOAc, anisaldehyde).

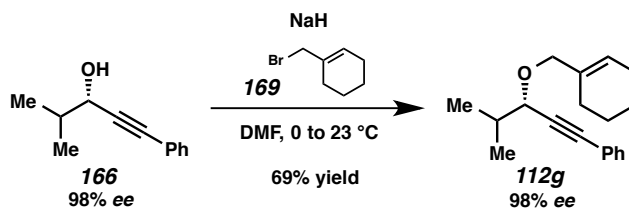
IR (film): 2963, 2925, 1723, 1490, 1383 cm⁻¹.

HRMS (DART+): *m/z* calc'd for (M + NH₄)⁺ [C₁₇H₂₂O + NH₄]⁺: 260.2014, found 260.2012.

¹H NMR (400 MHz, CDCl₆): δ 7.46-7.43 (m, 2H), 7.32-7.29 (comp m, 3H), 5.59-5.54 (m, 1H), 4.16 (d, *J* = 11.4 Hz, 1H), 3.99 (d, *J* = 6.0 Hz, 1H), 3.94 (d, *J* = 11.4 Hz, 1H), 2.02 (dq, *J* = 13.1, 6.6 Hz, 1H), 1.68 (s, 1H), 1.64 (dd, *J* = 6.7, 0.9 Hz, 1H), 1.08 (d, *J* = 6.7 Hz, 3H), 1.05 (d, *J* = 6.7 Hz, 3H).

¹³C NMR (100 MHz, CDCl₆): δ 132.9, 131.9, 128.4, 128.2, 123.3, 123.0, 87.8, 75.1, 74.4, 33.5, 18.9, 18.3, 13.9, 13.4.

Optical Rotation: [α]_D³² = -47.87 (*c* = 1.0, CH₂Cl₂).



Enyne 112g. To a solution of alcohol **166** (80.0 mg, 0.459 mmol) in DMF (1.53 mL) at 0 °C under argon was added NaH (22.0 mg, 60% dispersion in mineral oil, 0.551 mmol) in one portion. The mixture was then allowed to warm to ambient temperature and stirred for 20 min. Bromide **169**⁴⁴ (80.4 mg, 0.459 mmol) was added and after 12 h, the reaction was quenched by slow addition of H₂O (5 mL). The mixture was extracted with hexanes (3 x 20 mL). The combined organic layers were washed sequentially with aq. LiCl (10% w/v, 5 mL), then brine (5 mL), and dried over MgSO₄. The solvent was removed by rotary evaporation and the resulting residue was purified by flash chromatography (100% hexanes → 15:1 hexanes/EtOAc eluent), affording enyne **112g** (85.2 mg, 69% yield).

Physical State: yellow oil.

R_f: 0.60 (9:1 hexanes/EtOAc, anisaldehyde).

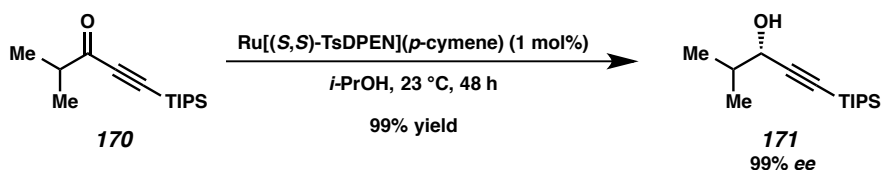
IR (film): 2928, 2837, 1668, 1490, 1445 cm⁻¹.

HRMS (ESI+): *m/z* calc'd for (M + NH₄)⁺ [C₁₉H₂₄O + NH₄]⁺: 286.2165, found 286.2163.

¹H NMR (400 MHz, C₆D₆): δ 7.45-7.42 (m, 2H), 6.99-6.95 (comp m, 3H), 5.78-5.76 (m, 1H), 4.30 (d, *J* = 11.4 Hz, 1H), 4.09 (d, *J* = 5.7 Hz, 1H), 4.00 (d, *J* = 11.4 Hz, 1H), 2.14-2.04 (m, 3H), 1.97-1.87 (m, 2H), 1.58-1.43 (m, 4H), 1.19 (d, *J* = 6.7 Hz, 3H), 1.13 (d, *J* = 6.8 Hz, 3H).

¹³C NMR (100 MHz, C₆D₆): δ 135.3, 132.1, 128.6, 128.2, 127.9, 125.0, 123.8, 88.6, 86.7, 74.7, 74.0, 34.0, 26.5, 25.4, 23.0, 22.9, 18.9, 18.5.

Optical Rotation: [α]_D³² = -145.32 (*c* = 1.0, CH₂Cl₂).



Alcohol 171. To a solution of ketone **170**⁴⁵ (1.00 g, 3.96 mmol) in 2-propanol (39.6 mL) under argon was added Ru[(*S,S*)-TsDPEN](*p*-cymene) (23.8 mg, 0.0396 mmol), and the resulting solution was stirred at ambient temperature for 48 h. The solvent was then removed by rotary evaporation, and the resulting residue was immediately purified by flash chromatography (9:1 hexanes/EtOAc eluent) to afford alcohol **171** (993 mg, 99% yield).

Physical State: colorless oil.

R_f: 0.42 (4:1 hexanes/EtOAc, anisaldehyde).

IR (film): 3356, 2960, 2170, 1464 cm⁻¹.

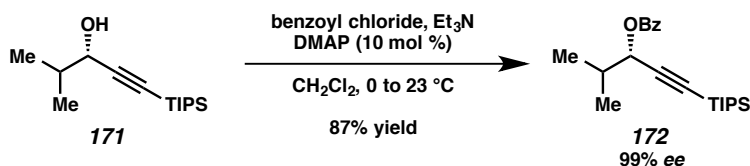
HRMS (DART+): *m/z* calc'd for (M + NH₄)⁺ [C₁₅H₃₀OSi + NH₄]⁺: 272.2404, found 272.2411.

¹H NMR (400 MHz, CDCl₃): δ 4.20 (d, *J* = 5.5 Hz, 1H), 1.89 (dtd, *J* = 13.5, 6.7, 5.5 Hz, 1H), 1.68 (br s, 1H), 1.09-1.06 (comp m, 17H), 1.03 (d, *J* = 6.7 Hz, 3H), 1.00 (d, *J* = 6.8 Hz, 3H).

¹³C NMR (100 MHz, CDCl₃): δ 107.5, 86.4, 85.6, 34.7, 18.8, 18.3, 17.4, 11.3.

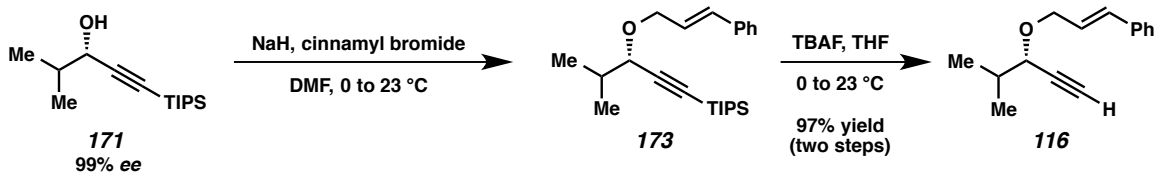
Optical Rotation: [α]_D³⁰ = -10.64 (*c* = 1.0, CH₂Cl₂).

The *ee* was determined 99% by conversion to the benzoate and HPLC analysis:



To a solution of alcohol **171** (10.0 mg, 0.0393 mmol), triethylamine (11.0 μL, 0.0786 mmol), and DMAP (0.48 mg, 0.00393 mmol) in CH₂Cl₂ (0.393 mL) at 0 °C was added benzoyl chloride (5.0 μL, 0.0432 mmol). The resulting solution was stirred at ambient temperature for 4.5 h. The solvent was then removed in vacuo and the resulting residue was purified by flash chromatography (9:1 hexanes/EtOAc eluent), affording benzoate **172** (12.2 mg, 87% yield, R_f = 0.65 in 4:1 hexanes/EtOAc eluent) as a colorless oil.

The *ee* of benzoate **172** was determined to be 99% by HPLC analysis (Daicel Chiralcel OD-H, 100% hexane, 1.3 mL/min, λ = 280 nm, *S* isomer 4.29 min, *R* isomer 4.08 min).



To a solution of alcohol **171** (150 mg, 0.589 mmol) and cinnamyl bromide (116 mg, 0.589 mmol) in DMF (1.96 mL) at 0 °C under argon was added NaH (30.6 mg, 60% dispersion in mineral oil, 0.766 mmol) in one portion. The mixture was then stirred at 0 °C for 20 min and ambient temperature for 4 h, at which time the reaction was quenched by slow addition of H₂O (5 mL). The mixture was extracted with hexanes (3 x 30 mL). The combined organic layers were washed sequentially with aq. LiCl (10% w/v, 5 mL), then brine (10 mL), and dried over MgSO₄. The solvent was removed by rotary evaporation to give crude ether **173**, which was used immediately in the next step.

To crude alkyne **173** in THF (0.736 mL) at 0 °C was added TBAF (2.65 mL, 1.0 M in THF, 2.65 mmol) dropwise over 5 min. The resulting solution was allowed to warm to ambient temperature and stirred for 15 min, at which time sat. aq. NaHCO₃ (5 mL) was added. The mixture was extracted with hexanes (3 x 20 mL). The combined organic layers were washed with brine (10 mL) and dried over MgSO₄. The solvent was removed by rotary evaporation, and the resulting residue was purified by flash chromatography (hexanes \rightarrow 9:1 hexanes/EtOAc eluent), affording alkyne **116** (122 mg, 97% yield).

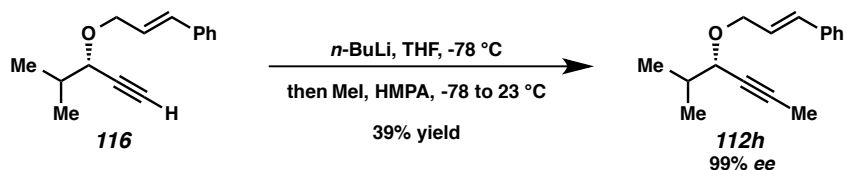
Alkyne **116**:

Physical State: colorless oil.

R_f: 0.46 (4:1 hexanes/EtOAc, anisaldehyde).

¹H NMR (400 MHz, CDCl₃): δ 7.43-7.38 (m, 2H), 7.35-7.30 (m, 2H), 7.26-7.22 (m, 1H), 6.64 (d, J = 15.9 Hz, 1H), 6.33-6.26 (m, 1H), 4.44 (ddd, J = 12.7, 5.4, 1.6 Hz, 1H), 4.15 (ddd, J = 12.7, 6.8, 1.3 Hz, 1H), 3.92 (dd, J = 5.8, 2.1 Hz, 1H), 2.44 (d, J = 2.1 Hz, 1H), 1.98 (dq, J = 13.0, 6.5 Hz, 1H), 1.05 (d, J = 6.7 Hz, 3H), 1.02 (d, J = 6.8 Hz, 3H).

¹³C NMR (100 MHz, CDCl₃): δ 136.9, 132.8, 128.7, 127.8, 126.7, 126.0, 81.9, 74.5, 74.3, 69.6, 33.1, 18.7, 17.9.



To terminal alkyne **116** (30.0 mg, 0.140 mmol) in THF (700 μL) at $-78\text{ }^\circ\text{C}$ was added *n*-BuLi (91.0 μL , 2.3 M in hexanes, 0.210 mmol). The reaction mixture was stirred at $-78\text{ }^\circ\text{C}$ for 1.5 h, then a solution of MeI (34.9 μL , 0.560 mmol) in HMPA (94.7 μL) was added. The mixture was allowed to warm to ambient temperature and stirred for 20 h, at which time it was quenched with H_2O (1 mL). The aqueous layer was extracted with hexanes (3 x 5 mL). The combined organic layers were washed with 10% aq. LiCl (2 mL), then brine (3 mL), and dried over MgSO_4 . The solvent was removed by rotary evaporation and the resulting residue was purified by flash chromatography (9:1 hexanes/EtOAc eluent), affording enyne **112h** (12.5 mg, 39% yield).

Enyne 112h:

Physical State: colorless oil.

R_f: 0.52 (4:1 hexanes/EtOAc, anisaldehyde).

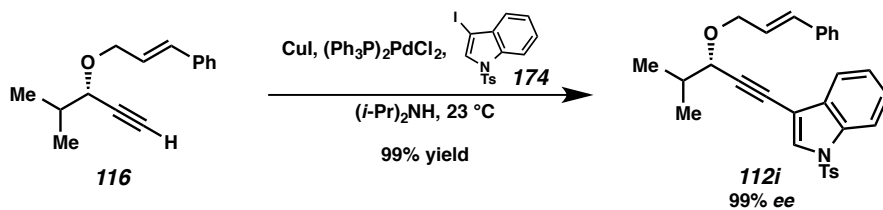
IR (film): 2961, 2922, 1496, 1072 cm^{-1} .

HRMS (DART+): *m/z* calc'd for $(\text{M} + \text{H})^+$ [$\text{C}_{16}\text{H}_{20}\text{O} + \text{H}$]⁺: 229.1587, found 229.1590.

¹H NMR (400 MHz, CDCl_3): δ 7.41-7.38 (m, 2H), 7.33-7.28 (m, 2H), 7.25-7.21 (m, 1H), 6.63 (d, *J* = 15.9 Hz, 1H), 6.30 (ddd, *J* = 15.9, 6.6, 5.5 Hz, 1H), 4.41 (ddd, *J* = 12.7, 5.4, 1.6 Hz, 1H), 4.12 (ddd, *J* = 12.7, 6.7, 1.3 Hz, 1H), 3.87 (dq, *J* = 5.8, 2.0 Hz, 1H), 1.97-1.90 (m, 1H), 1.89 (d, *J* = 2.1 Hz, 3H), 1.02 (d, *J* = 6.7 Hz, 3H), 0.99 (d, *J* = 6.8 Hz, 3H).

¹³C NMR (100 MHz, CDCl_3): δ 137.0, 132.4, 128.6, 127.7, 126.6, 126.4, 82.4, 74.8, 69.4, 33.3, 18.8, 18.0, 3.8.

Optical Rotation: $[\alpha]_{\text{D}}^{26} = -63.51$ (*c* = 2.0, CH_2Cl_2).



To a 2-dram vial under argon containing CuI (3.1 mg, 0.0163 mmol) and $(\text{Ph}_3\text{P})_2\text{PdCl}_2$ (5.7 mg, 0.00812 mmol) was added diisopropylamine (0.326 mL) followed by iodindole **174**⁴⁶ (84.2 mg, 0.212 mmol). This resulting mixture was stirred for 5 min, at which time a solution of ether **116** (35.0 mg, 0.162 mmol) in THF (0.200 mL) was added via syringe. The reaction mixture was stirred for 3 h then partitioned between ether (4 mL) and 1 M aq. HCl (5 mL). The aqueous layer was extracted with Et₂O (3 x 10 mL). The combined organic layers were washed with sat. aq. NaHCO₃ (5 mL), then brine (10 mL), and dried over MgSO₄. The solvent was removed by rotary evaporation and the resulting residue was purified by flash chromatography (9:1 hexanes/Et₂O eluent), affording enyne **112i** (78.3 mg, 99% yield).

Enyne **112i**:

Physical State: colorless oil.

R_f: 0.14 (9:1 hexanes/Et₂O, anisaldehyde).

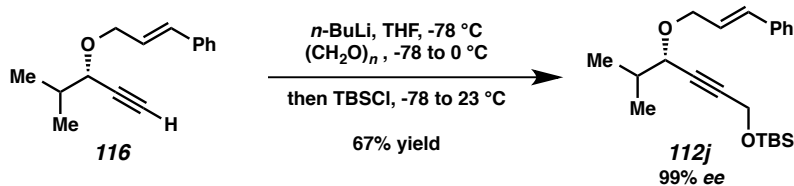
IR (film): 2962, 2871, 1494, 1376, 1189 cm⁻¹.

HRMS (DART+): m/z calc'd for $(\text{M} + \text{H})^+ [\text{C}_{30}\text{H}_{29}\text{NO}_3\text{S} + \text{H}]^+$: 484.1941, found 484.1942.

¹H NMR (400 MHz, CDCl₃): δ 7.99-7.96 (m, 1H), 7.80-7.77 (m, 2H), 7.74 (s, 1H), 7.63-7.61 (m, 1H), 7.42-7.28 (comp m, 5H), 7.25-7.22 (comp m, 4H), 6.68 (d, $J = 16.0$ Hz, 1H), 6.34 (ddd, $J = 15.9, 6.7, 5.5$ Hz, 1H), 4.51 (dd, $J = 12.7, 5.5$ Hz, 1H), 4.25 (dd, $J = 12.7, 6.7$ Hz, 1H), 4.19 (d, $J = 5.7$ Hz, 1H), 2.35 (s, 3H), 2.13-2.07 (m, 1H), 1.13 (d, $J = 6.7$ Hz, 3H), 1.10 (d, $J = 6.8$ Hz, 3H).

¹³C NMR (100 MHz, CDCl₃): δ 145.5, 136.9, 135.1, 134.3, 132.8, 131.1, 130.2, 129.1, 128.7, 127.8, 127.1, 126.7, 126.1, 125.6, 123.9, 120.6, 113.7, 105.0, 91.8, 75.2, 69.8, 33.4, 21.8, 18.9, 18.2.

Optical Rotation: $[\alpha]_{\text{D}}^{32} = -114.15$ ($c = 2.0$, CHCl₃).



To terminal alkyne **116** (120 mg, 0.560 mmol) in THF (1.12 mL) at $-78\text{ }^\circ\text{C}$ was added $n\text{-BuLi}$ (0.289 mL, 2.13 M in hexanes, 0.616 mmol) dropwise over 2 min. The resulting solution was allowed to warm to $0\text{ }^\circ\text{C}$ and stirred at that temperature for 30 min. The solution was then cooled back down to $-78\text{ }^\circ\text{C}$, and finely ground paraformaldehyde (18.7 mg, 0.616 mmol) was added in one portion. The solution was allowed to warm to ambient temperature and stirred for 5 h. The reaction mixture was cooled back to $0\text{ }^\circ\text{C}$ and TBSCl (127 mg, 0.840 mmol) was added. The resulting mixture was stirred at ambient temperature for 1 h and then quenched with sat. aq. NaHCO_3 (10 mL). The mixture was extracted with hexanes (3 x 20 mL). The combined organic layers were washed with brine (10 mL) and dried over MgSO_4 . The solvent was removed by rotary evaporation and the resulting residue was purified by flash chromatography (15:1 hexanes/EtOAc eluent), affording enyne **112j** (135 mg, 67% yield).

Enyne **112j**:

Physical State: colorless oil.

R_f: 0.83 (4:1 hexanes/EtOAc, anisaldehyde).

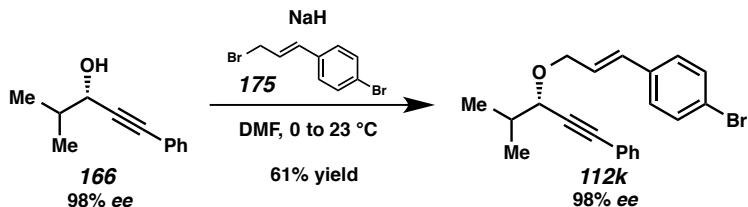
IR (film): 3028, 2959, 2858, 1728, 1495, 1255 cm^{-1} .

HRMS (DART+): m/z calc'd for $(\text{M} + \text{NH}_4)^+ [\text{C}_{22}\text{H}_{34}\text{O}_2\text{Si} + \text{NH}_4]^+$: 376.2672, found 376.2672.

¹H NMR (400 MHz, CDCl_3): δ 7.40-7.37 (m, 2H), 7.35-7.29 (m, 2H), 7.25-7.21 (m, 1H), 6.63 (d, $J = 15.9$ Hz, 1H), 6.28 (ddd, $J = 15.9, 6.7, 5.4$ Hz, 1H), 4.44-4.39 (comp m, 3H), 4.13 (ddd, $J = 12.6, 6.8, 1.3$ Hz, 1H), 3.94 (dt, $J = 5.8, 1.6$ Hz, 1H), 2.00-1.92 (m, 1H), 1.03 (d, $J = 6.7$ Hz, 3H), 1.00 (d, $J = 6.8$ Hz, 3H), 0.93-0.92 (m, 9H), 0.14 (s, 6H).

¹³C NMR (100 MHz, CDCl_3): δ 137.0, 132.7, 128.7, 127.8, 126.6, 126.2, 85.2, 82.8, 74.5, 69.5, 51.9, 33.3, 26.0, 18.8, 18.5, 18.1, 4.9.

Optical Rotation: $[\alpha]_D^{33} = -88.30$ ($c = 1.0, \text{CHCl}_3$).



To a solution of alcohol **166** (150 mg, 0.861 mmol) in DMF (2.87 mL) at 0 °C under argon was added NaH (41.2 mg, 60% dispersion in mineral oil, 1.03 mmol) in one portion. The mixture was then allowed to warm to ambient temperature and stirred for 20 min. Bromide **175**⁴⁷ (186 mg, 0.861 mmol) was added and after 1 h, the reaction was quenched by slow addition of H₂O (5 mL). The mixture was extracted with hexanes (3 x 30 mL). The combined organic layers were washed sequentially with aq. LiCl (10% w/v, 7 mL), then brine (7 mL), and dried over MgSO₄. The solvent was removed by rotary evaporation and the resulting residue was purified by flash chromatography (100% hexanes → 9:1 hexanes/EtOAc eluent), affording enyne **112k** (193 mg, 61% yield).

Enyne 112k:

Physical State: colorless oil.

R_f: 0.83 (4:1 hexanes/EtOAc, anisaldehyde).

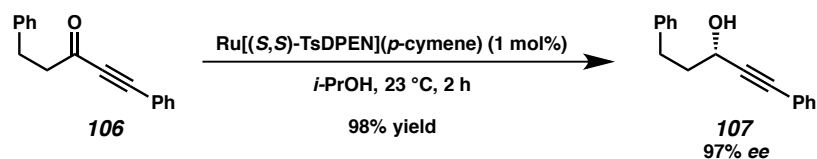
IR (film): 2964, 2869, 1659, 1491, 1075 cm⁻¹.

HRMS (DART+): *m/z* calc'd for (M + NH₄)⁺ [C₂₁H₂₁BrO + NH₄]⁺: 386.1120, found 386.1097.

¹H NMR (400 MHz, CDCl₃): δ 7.48-7.43 (m, 4H), 7.34-7.31 (m, 3H), 7.28-7.25 (m, 2H), 6.62 (d, *J* = 16.0 Hz, 1H), 6.34 (ddd, *J* = 15.9, 6.4, 5.4 Hz, 1H), 4.49 (ddd, *J* = 12.9, 5.4, 1.6 Hz, 1H), 4.21 (ddd, *J* = 12.9, 6.4, 1.4 Hz, 1H), 4.14 (d, *J* = 5.8 Hz, 1H), 2.14-2.02 (m, 1H), 1.12 (d, *J* = 6.7 Hz, 3H), 1.09 (d, *J* = 6.8 Hz, 3H).

¹³C NMR (100 MHz, CDCl₃): δ 135.9, 131.9, 131.8, 131.2, 128.4, 128.2, 127.2, 123.0, 121.5, 87.3, 86.8, 75.3, 69.5, 33.5, 18.9, 18.1.

Optical Rotation: [α]_D³² = -104.68 (*c* = 1.0, CH₂Cl₂).



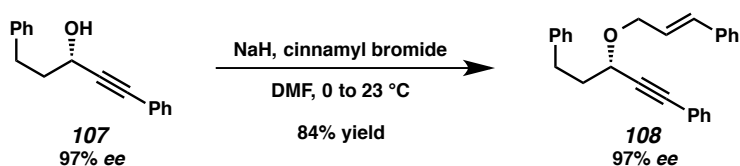
To a solution of ynone **106**⁴⁸ (80.0 mg, 0.341 mmol) in 2-propanol (3.41 mL) under argon was added $\text{Ru}[(S,S)\text{-TsDPEN}](p\text{-cymene})$ (2.1 mg, 0.00341 mmol). The resulting purple solution was stirred at ambient temperature for 2 h. The solvent was removed in vacuo and the resulting residue was purified by flash chromatography (9:1 hexanes/EtOAc eluent), affording alcohol **107** (79.3 mg, 98% yield).

Alcohol 107:

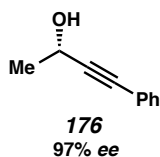
Physical State: colorless oil.

R_f: 0.38 (4:1 hexanes/EtOAc, anisaldehyde).

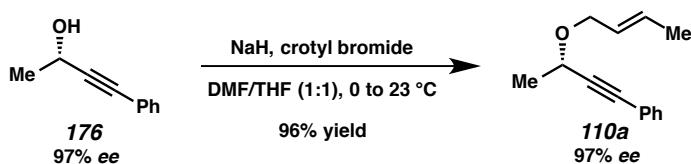
Note: All spectra matched those previously reported in the literature.⁴⁹ The *ee* was determined to be 97% by HPLC analysis (Daicel Chiralcel OD-H, 10% 2-propanol in hexane, 1 mL/min, $\lambda = 254$ nm, *S* isomer 25.13 min, *R* isomer 12.59 min). $[\alpha]_{\text{D}}^{26} = +37.45$ ($c = 0.5$, CHCl_3) (*S*) (Lit. $[\alpha]_{\text{D}}^{27} = +28.4$ ($c = 1.1$, CHCl_3) 49% *ee* (*S*)).



To a solution of alcohol **107** (400 mg, 1.69 mmol) in DMF (5.64 mL) at 0 °C under argon was added NaH (87.9 mg, 60% dispersion in mineral oil, 2.20 mmol) in one portion. The mixture was allowed to warm to ambient temperature and stirred for 20 min. Cinnamyl bromide (334 mg, 1.69 mmol) was added and after 1 h, the reaction was quenched by slow addition of H_2O (10 mL). The mixture was extracted with hexanes (3 x 50 mL). The combined organic layers were washed sequentially with aq. LiCl (10% w/v, 5 mL), then brine (5 mL), and dried over MgSO_4 . The solvent was removed by rotary evaporation and the resulting residue was purified by flash chromatography (9:1 hexanes/EtOAc eluent), affording enyne **108** (498 mg, 84% yield).

Enyne 108:**Physical State:** yellow oil.**R_f:** 0.77 (4:1 hexanes/EtOAc, anisaldehyde).**IR** (film): 3060, 2858, 1491, 1453, 1336 cm⁻¹.**HRMS** (APCI+): *m/z* calc'd for (M + H)⁺ [C₂₆H₂₄O + H]⁺: 353.1900, found 353.1903.**¹H NMR** (400 MHz, C₆D₆): δ 7.48-7.45 (m, 2H), 7.25-7.23 (m, 2H), 7.15-6.98 (comp m, 11H), 6.61 (d, *J* = 16.0 Hz, 1H), 6.32-6.24 (m, 1H), 4.50 (ddd, *J* = 12.7, 5.4, 1.6 Hz, 1H), 4.36-4.31 (m, 1H), 4.10 (ddd, *J* = 12.6, 6.5, 1.4 Hz, 1H), 2.91 (t, *J* = 7.7 Hz, 2H), 2.34-2.16 (m, 2H).**¹³C NMR** (100 MHz, C₆D₆): δ 141.9, 137.4, 132.6, 132.1, 129.0, 128.8, 128.7, 126.9, 126.6, 126.3, 123.5, 89.3, 86.6, 69.7, 68.8, 38.1, 32.0.**Optical Rotation:** [α]_D²⁶ = -43.62 (*c* = 1.0, CH₂Cl₂).

Based on the general procedure, alcohol **176** was produced in 88% yield. All spectra matched those previously reported in the literature.⁵⁰ The *ee* was determined to be 97% by HPLC analysis (Daicel Chiralcel OD-H, 20% 2-propanol in hexane, 1 mL/min, λ = 254 nm, *S* isomer 8.89 min, *R* isomer 5.03 min). [α]_D³¹ = -33.40 (*c* = 1.00, CHCl₃) (*S*) (Lit.⁵¹ [α]_D²⁰ = -33.0 (*c* = 0.94, CHCl₃) >99% *ee* (*S*)).



To a solution of alcohol **176** (70.0 mg, 0.479 mmol) in DMF (0.798 mL) and THF (0.798 mL) at 0 °C under argon was added NaH (21.1 mg, 60% dispersion in mineral oil, 0.527 mmol) in one portion. The mixture was allowed to warm to ambient temperature and stirred for 25 min. Crotyl bromide (49.4 μL,

0.479 mmol) was added and the resulting mixture was stirred for 2.5 h, at which point the reaction was quenched by slow addition of H₂O (4 mL). The volatile solvents were removed by rotary evaporation and the remaining mixture was extracted with Et₂O (3 x 20 mL). The combined organic layers were washed sequentially with aq. LiCl (10% w/v, 5 mL), then brine (5 mL), and dried over MgSO₄. The solvent was removed by rotary evaporation and the resulting residue was purified by flash chromatography (98:2 hexanes/Et₂O eluent), affording enyne **110a** (92.1 mg, 96% yield).

Enyne 110a:

Physical State: colorless oil.

R_f: 0.52 (9:1 hexanes/Et₂O, anisaldehyde).

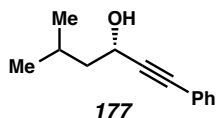
IR (film): 2986, 1490, 1443, 1099 cm⁻¹.

HRMS (ESI+): *m/z* calc'd for (M + H)⁺ [C₁₄H₁₆O + H]⁺: 201.1274, found 201.1266.

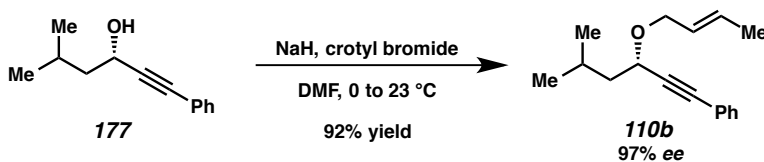
¹H NMR (400 MHz, CDCl₃): δ 7.46-7.41 (m, 2H), 7.33-7.28 (comp m, 3H), 5.84-5.73 (m, 1H), 5.69-5.57 (m, 1H), 4.42 (q, *J* = 6.6 Hz, 1H), 4.27-4.22 (m, 1H), 3.99-3.94 (m, 1H), 1.72 (d, *J* = 1.2 Hz, 3H), 1.53 (d, *J* = 6.6 Hz, 3H).

¹³C NMR (100 MHz, CDCl₃): δ 131.9, 130.3, 128.4, 127.4, 123.0, 89.4, 85.0, 69.6, 64.9, 22.4, 18.0.

Optical Rotation: [α]_D³¹ = -75.75 (*c* = 1.0, CH₂Cl₂).



Based on the general procedure, alcohol **177** was produced in 37% yield. All spectra matched those previously reported in the literature.⁵² The *ee* was determined to be 96% by HPLC analysis (Daicel Chiralcel OD-H, 5% 2-propanol in hexane, 1 mL/min, λ = 254 nm, *S* isomer 14.23 min, *R* isomer 6.98 min). [α]_D³¹ = -9.79 (*c* = 1.0, CHCl₃) (*S*) (Lit.⁵³ [α]_D²³ = +9.5 (*c* = 3.31, CHCl₃) 94% *ee* (*R*)).



To a solution of alcohol **177** (90.4 mg, 0.480 mmol) in DMF (1.60 mL) at 0 °C under argon was added NaH (21.1 mg, 60% dispersion in mineral oil, 0.528 mmol) in one portion. The mixture was then allowed to warm to ambient temperature and stirred for 30 min. Crotyl bromide (49.4 μ L, 0.480 mmol) was added and after 2 h, the reaction was quenched by slow addition of H₂O (3 mL). The mixture was extracted with hexanes (3 x 20 mL). The combined organic layers were washed sequentially with aq. LiCl (10% w/v, 5 mL), then brine (5 mL), and dried over MgSO₄. The solvent was removed by rotary evaporation and the resulting residue was purified by flash chromatography (100% hexanes \rightarrow 15:1 hexanes/EtOAc eluent), affording enyne **110b** (107 mg, 92% yield).

Enyne 110b:

Physical State: yellow oil.

R_f: 0.34 (15:1 hexanes/EtOAc, anisaldehyde).

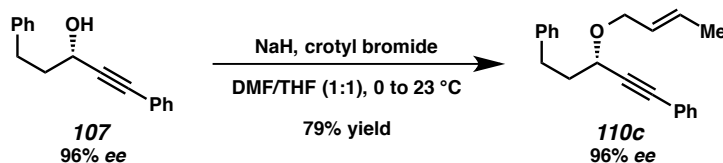
IR (film): 2957, 2869, 1490, 1467 cm⁻¹.

HRMS (ESI⁺): *m/z* calc'd for (M + H)⁺ [C₁₇H₂₂O + H]⁺: 243.1744, found 243.1730.

¹H NMR (400 MHz, C₆D₆): δ 7.48-7.42 (m, 2H), 7.01-6.94 (comp m, 3H), 5.71-5.63 (m, 2H), 4.45-4.39 (comp m, 2H), 4.05-4.01 (m, 1H), 2.09 (app. septet, *J* = 6.8 Hz, 1H), 1.95 (ddd, *J* = 13.6, 7.7, 6.6 Hz, 1H), 1.77 (ddd, *J* = 13.5, 7.3, 6.2 Hz, 1H), 1.53 (d, *J* = 4.7 Hz, 3H), 0.92 (d, *J* = 1.8 Hz, 3H), 0.90 (d, *J* = 1.8 Hz, 3H).

¹³C NMR (100 MHz, C₆D₆): δ 132.1, 128.9, 128.6, 128.4, 89.9, 86.0, 69.7, 45.4, 25.3, 23.0, 22.6, 17.8.

Optical Rotation: $[\alpha]_D^{31} = -69.36$ (*c* = 1.0, CH₂Cl₂).



(Note: This alcohol **107**, at 96% *ee*, was generated in a separate transfer hydrogenation from the aforementioned one at 97% *ee*.) To a solution of alcohol **107** (35.0 mg, 0.148 mmol) in DMF (0.350 mL) and THF (0.350 mL) at 0 °C under argon was added NaH (6.5 mg, 60% dispersion in mineral oil, 0.163

mmol) in one portion. The mixture was allowed to warm to ambient temperature and stirred for 20 min. Crotyl bromide (15.3 μ L, 0.148 mmol) was added and after 4 h, the reaction was quenched by slow addition of H₂O (4 mL). The volatile solvents were then removed by rotary evaporation and the remaining mixture was extracted with Et₂O (3 x 20 mL). The combined organic layers were washed sequentially with aq. LiCl (10% w/v, 5 mL), then brine (5 mL), and dried over MgSO₄. The solvent was removed by rotary evaporation and the resulting residue was purified by flash chromatography (9:1 hexanes/EtOAc eluent), affording enyne **110c** (33.9 mg, 79% yield).

Enyne 110c:

Physical State: yellow oil.

R_f: 0.73 (4:1 hexanes/EtOAc, anisaldehyde).

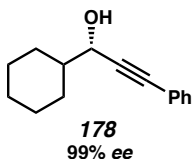
IR (film): 2930, 2857, 1491, 1454, 1335 cm⁻¹.

HRMS (ESI+): *m/z* calc'd for (M + H)⁺ [C₂₁H₂₂O + H]⁺: 291.1744, found 291.1741.

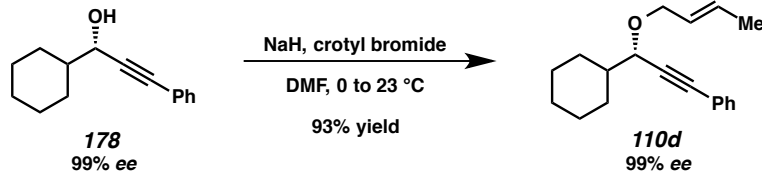
¹H NMR (400 MHz, CDCl₃): δ 7.45 (m, *J* = 1.6 Hz, 2H), 7.34-7.18 (comp m, 8H), 5.86-5.73 (m, 1H), 5.72-5.56 (m, 1H), 4.31-4.24 (comp m, 2H), 3.96 (dd, *J* = 11.5, 6.8 Hz, 1H), 2.86 (t, *J* = 7.8 Hz, 2H), 2.23-2.04 (m, 2H), 1.73 (d, *J* = 6.3 Hz, 3H).

¹³C NMR (100 MHz, CDCl₃): δ 141.7, 131.89, 131.87, 130.2, 128.7, 128.5, 128.43, 128.41, 127.4, 126.0, 123.0, 88.4, 86.1, 69.7, 68.3, 37.50, 37.45, 31.73, 31.70, 18.0.

Optical Rotation: $[\alpha]_D^{31} = -17.23$ (*c* = 1.0, CH₂Cl₂).



Based on the general procedure, alcohol **178** was produced in 73% yield. All spectra matched those previously reported in the literature.⁵⁴ The *ee* was determined to be 98% by HPLC analysis (Daicel Chiralcel OD-H, 15% 2-propanol in hexane, 1 mL/min, λ = 254 nm, *S* isomer 12.18 min, *R* isomer 6.86 min). $[\alpha]_D^{32} = +8.72$ (*c* = 1.0, CHCl₃) (*S*) (Lit. $[\alpha]_D^{25} = +11.7$ (*c* = 0.63, CHCl₃) 79% *ee* (*S*)).



To a solution of alcohol **178** (90.1 mg, 0.420 mmol) in DMF (1.40 mL) at 0 °C under argon was added NaH (18.5 mg, 60% dispersion in mineral oil, 0.462 mmol) in one portion. The mixture was then allowed to warm to ambient temperature and stirred for 20 min. Crotyl bromide (43.3 μL , 0.420 mmol) was added and after 3 h, the reaction was quenched by slow addition of H_2O (3 mL). The mixture was extracted with hexanes (3 x 20 mL). The combined organic layers were washed sequentially with aq. LiCl (10% w/v, 5 mL), then brine (5 mL), and dried over MgSO_4 . The solvent was removed by rotary evaporation and the resulting residue was purified by flash chromatography (hexanes \rightarrow 9:1 hexanes/EtOAc eluent), affording enyne **110d** (105 mg, 93% yield).

Enyne 110d:

Physical State: yellow oil.

R_f: 0.77 (4:1 hexanes/EtOAc, anisaldehyde).

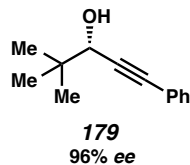
IR (film): 2927, 2854, 1490, 1330 cm^{-1} .

HRMS (ESI⁺): m/z calc'd for $(\text{M} + \text{H})^+$ [$\text{C}_{19}\text{H}_{24}\text{O} + \text{H}$]⁺: 269.1900, found 269.1903.

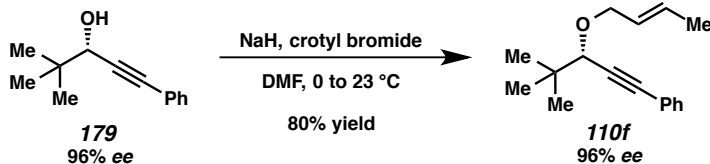
¹H NMR (400 MHz, CDCl_3): δ 7.47-7.42 (m, 2H), 7.33-7.29 (comp m, 3H), 5.82-5.71 (m, 1H), 5.65-5.57 (m, 1H), 4.28-4.22 (m, 1H), 4.06 (d, $J = 6.2$ Hz, 1H), 3.98-3.93 (m, 1H), 1.95-1.88 (m, 2H), 1.78-1.64 (comp m, 8H), 1.33-1.09 (comp m, 7H).

¹³C NMR (100 MHz, CDCl_3): δ 131.9, 129.9, 128.4, 127.6, 123.2, 87.9, 74.1, 69.8, 43.0, 29.4, 28.7, 26.6, 26.2, 26.1, 18.0.

Optical Rotation: $[\alpha]_{\text{D}}^{31} = -25.53$ ($c = 0.5$, CH_2Cl_2).



Based on the general procedure, alcohol **179** was produced in 76% yield. All spectra matched those previously reported in the literature.⁵⁵ The *ee* was determined to be 96% by HPLC analysis (Daicel Chiralcel OD-H, 3% 2-propanol in hexane, 1 mL/min, $\lambda = 254$ nm, *S* isomer 8.17 min, *R* isomer 6.60 min). $[\alpha]_D^{32} = +1.06$ ($c = 1.0$, CHCl_3) (*S*) (Lit.⁵⁶ $[\alpha]_D^{25} = +2.4$ ($c = 4.0$, CHCl_3) 94% *ee* (*S*)).



To a solution of alcohol **179** (90.0 mg, 0.478 mmol) in DMF (1.59 mL) at 0 °C under argon was added NaH (21.0 mg, 60% dispersion in mineral oil, 0.526 mmol) in one portion. The mixture was then allowed to warm to ambient temperature and stirred for 20 min. Crotyl bromide (49.3 μL , 0.478 mmol) was added and after 4.5 h, H_2O (3 mL) was added dropwise. The mixture was extracted with hexanes (3 x 20 mL). The combined organic layers were washed sequentially with aq. LiCl (10% w/v, 5 mL), then brine (5 mL), and dried over MgSO_4 . The solvent was removed in vacuo and the resulting residue was purified by flash chromatography (100% hexanes \rightarrow 15:1 H/Et₂O eluent), affording enyne **110f** (92.7 mg, 80% yield).

Enyne 110f:

Physical State: yellow oil.

R_f: 0.62 (9:1 hexanes/Et₂O, anisaldehyde).

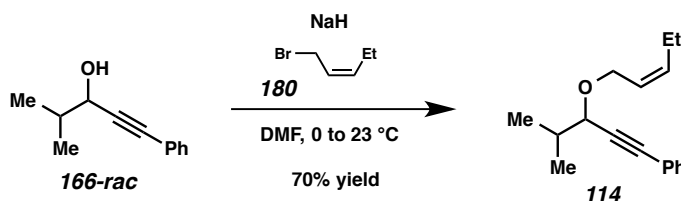
IR (film): 2969, 2871, 1724, 1489, 1284 cm^{-1} .

HRMS (ESI+): m/z calc'd for $(\text{M} + \text{H})^+$ [$\text{C}_{17}\text{H}_{22}\text{O} + \text{H}$]⁺: 243.1744, found 243.1736.

¹H NMR (400 MHz, CDCl₃): δ 7.47-7.42 (m, 2H), 7.32-7.28 (comp m, 3H), 5.83-5.72 (m, 1H), 5.64-5.55 (m, 1H), 4.31-4.24 (m, 1H), 3.99-3.93 (m, 1H), 3.87 (s, 1H), 1.74-1.70 (m, 3H), 1.07-1.04 (m, 9H).

¹³C NMR (100 MHz, CDCl₃): δ 131.9, 129.4, 128.4, 128.2, 127.8, 123.3, 87.9, 86.3, 78.0, 70.3, 35.9, 26.1, 18.0.

Optical Rotation: $[\alpha]_D^{32} = -37.23$ ($c = 1.0$, CH₂Cl₂).



To a solution of alcohol **166-rac** (150 mg, 0.870 mmol) in DMF (3.00 mL) at 0 °C under argon was added NaH (42.0 mg, 60% dispersion in mineral oil, 1.04 mmol) in one portion. The mixture was then allowed to warm to ambient temperature and stirred for 20 min. Bromide **180** (130 mg, 0.870 mmol) was added and after 2 h, H₂O (3 mL) was added dropwise. The mixture was extracted with hexanes (3 x 20 mL). The combined organic layers were washed sequentially with aq. LiCl (10% w/v, 5 mL), then brine (5 mL), and dried over MgSO₄. The solvent was removed in vacuo and the resulting residue was purified by flash chromatography (100% hexanes → 15:1 H/EtOAc eluent), affording enyne **114** (148 mg, 70% yield).

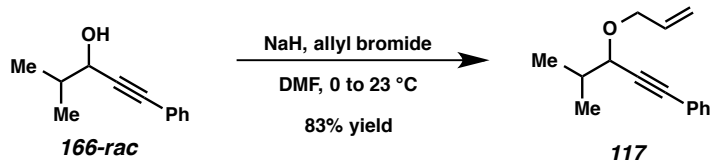
Enyne 114:

Physical State: colorless oil.

R_f: 0.72 (4:1 hexanes/EtOAc, anisaldehyde).

HRMS (ESI+): m/z calc'd for (M + H)⁺ [C₁₇H₂₂O + H]⁺: 243.1743, found 243.1736.

¹H NMR (300 MHz, CDCl₃): δ 7.48-7.45 (m, 2H), 7.35-7.29 (comp m, 3H), 5.69-5.51 (m, 2H), 4.36-4.30 (m, 1H), 4.19 (dd, $J = 12.0, 7.1$ Hz, 1H), 4.09 (d, $J = 5.9$ Hz, 1H), 2.22-2.11 (m, 2H), 2.02 (dt, $J = 12.7, 6.7$ Hz, 1H), 1.11-0.97 (comp m, 6H).

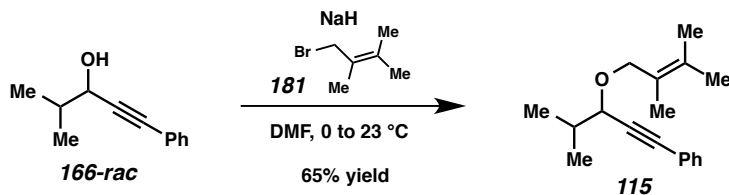


To a solution of alcohol **166-rac** (500 mg, 2.87 mmol) in DMF (9.50 mL) at 0 °C under argon, was added NaH (126 mg, 60% dispersion in mineral oil, 3.16 mmol) in one portion. The mixture was then allowed to warm to ambient temperature and stirred for 20 min. Allyl bromide (248 μL , 2.87 mmol) was added and after 2 h, H₂O (8 mL) was added dropwise. The mixture was extracted hexanes (3 x 30 mL). The combined organic layers were washed sequentially with aq. LiCl (10% w/v, 10 mL), then brine (10 mL), and dried over MgSO₄. The solvent was removed in vacuo and the resulting residue was purified by flash chromatography (hexanes \rightarrow 15:1 hexanes/EtOAc eluent), affording enyne **117** (508 mg, 83% yield).

Enyne 117:

Physical State: colorless oil.

R_f: 0.62 (9:1 hexanes/EtOAc, KMnO₄).



To a solution of alcohol **166-rac** (80.1 mg, 0.459 mmol) in DMF (1.53 mL) at 0 °C under argon, was added NaH (22.0 mg, 60% dispersion in mineral oil, 0.551 mmol) in one portion. The mixture was then allowed to warm to ambient temperature and stirred for 20 min. Bromide **181**⁵⁷ (74.8 mg, 0.459 mmol) was added and after 3 h, H₂O (5 mL) was added dropwise. The mixture was extracted hexanes (3 x 20 mL). The combined organic layers were washed with aq. LiCl (10% w/v, 5 mL), then brine (5 mL), and dried over MgSO₄. The solvent was removed in vacuo and the resulting residue was purified by flash chromatography (hexanes \rightarrow 15:1 hexanes/Et₂O eluent), affording enyne **115** (77.0 mg, 65% yield).

Enyne 115:

Physical State: colorless oil.

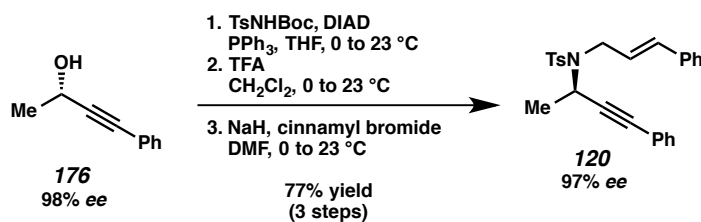
R_f: 0.63 (9:1 hexanes/Et₂O, anisaldehyde).

IR (film): 2961, 2926, 2872, 1490, 1065 cm⁻¹.

HRMS (APCI+): *m/z* calc'd for (M + H)⁺ [C₁₈H₂₄O + H]⁺: 257.1905, found 257.1898.

¹H NMR (400 MHz, CDCl₃): δ 7.47-7.42 (m, 2H), 7.32-7.29 (comp m, 3H), 4.19 (s, 2H), 3.95 (d, *J* = 6.3 Hz, 1H), 2.01 (dq, *J* = 13.2, 6.6 Hz, 1H), 1.80 (d, *J* = 1.2 Hz, 3H), 1.74 (t, *J* = 1.1 Hz, 3H), 1.71 (s, 3H), 1.08 (d, *J* = 6.7 Hz, 3H), 1.05 (d, *J* = 6.7 Hz, 3H).

¹³C NMR (100 MHz, CDCl₃): δ 131.8, 130.6, 128.4, 128.2, 124.9, 123.4, 88.3, 86.0, 74.3, 69.6, 33.5, 21.1, 20.4, 19.0, 18.5, 17.0.



To a solution of propargylic alcohol **176** (201 mg, 1.37 mmol), TsNHBoc (410 mg, 1.51 mmol), and triphenylphosphine (395 mg, 1.51 mmol) in THF (9.13 mL) at 0 °C was added diisopropyl azodicarboxylate (299 μL, 1.51 mmol) as a solution in THF (*ca.* 1.0 mL) dropwise over 30 min. The resulting mixture was stirred at 0 °C for 6 h, at which time the ice water bath was removed. After stirring for an additional 13 h at ambient temperature, the volatile materials were removed. The resulting residue was purified by flash chromatography (4:1 hexanes/EtOAc eluent), affording the Boc-protected amine intermediate (503 mg, 92% yield). **R_f:** 0.23 (4:1 hexanes/EtOAc, anisaldehyde/UV).

To the Boc-protected amine product (498 mg, 1.25 mmol) in CH₂Cl₂ (12.5 mL) at 0 °C was added trifluoroacetic acid (430 μL, 5.62 mmol), dropwise over 5 min. The ice water bath was removed and the resulting solution was stirred at ambient temperature for 4 h, at which time the volatile materials were removed. The resulting residue was azeotroped with toluene (4 x 10 mL) and immediately used crude. **R_f:** 0.57 (2.5% MeOH in chloroform, anisaldehyde/UV).

resulting residue was purified by flash chromatography (hexanes → 15:1 hexanes/Et₂O eluent), affording enyne **153** (675 mg, 41% yield).

Enyne 153:

Physical State: colorless oil.

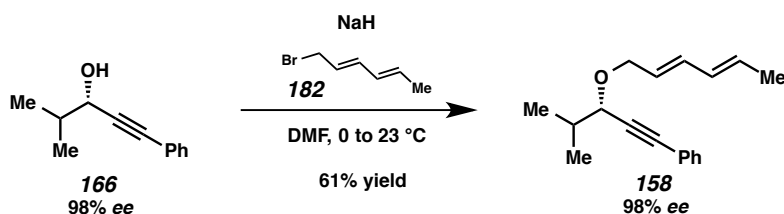
R_f: 0.69 (4:1 hexanes/EtOAc, anisaldehyde).

IR (film): 2963, 2873, 1613, 1251, 1069 cm⁻¹.

HRMS (APCI+): *m/z* calc'd for (M + H)⁺ [C₂₀H₃₀OSi + H]⁺: 315.2139, found 315.2138.

¹H NMR (400 MHz, C₆D₆): δ 7.15-7.13 (m, 2H), 7.04-7.00 (comp m, 3H), 5.62 (t, *J* = 6.8 Hz, 1H), 4.05 (d, *J* = 5.8 Hz, 1H), 1.98-1.83 (comp m, 4H), 1.64 (tq, *J* = 6.6, 6.4 Hz, 1H), 0.78-0.69 (comp m, 13H), 0.00 (d, *J* = 2.2 Hz, 6H).

¹³C NMR (100 MHz, C₆D₆): δ 195.0, 191.2, 182.6, 179.2, 179.0, 174.4, 141.1, 135.8, 119.7, 86.4, 73.1, 72.5, 69.5, 68.9, 65.9, 65.1, 49.9, 49.6.



To a solution of alcohol **166** (90.1 mg, 0.574 mmol) in DMF (1.72 mL) at 0 °C under argon was added NaH (24.8 mg, 60% dispersion in mineral oil, 0.620 mmol) in one portion. The mixture was then allowed to warm to ambient temperature and stirred for 20 min. Sorbyl bromide **182**⁵⁸ (91.6 mg, 0.569 mmol) was added and after 2 h, H₂O (5 mL) was added dropwise. The mixture was extracted with hexanes (3 x 20 mL). The combined organic layers were washed sequentially with aq. LiCl (10% w/v, 5 mL), then brine (5 mL), and dried over MgSO₄. The solvent was removed in vacuo and the resulting residue was purified by flash chromatography (hexanes → 9:1 hexanes/EtOAc eluent), affording dienyne **158** (106 mg, 81% yield).

Dienyne 158:

Physical State: colorless oil.

R_f: 0.75 (4:1 hexanes/EtOAc, anisaldehyde).

IR (film): 2962, 2872, 1662, 1490, 1384, 1098 cm⁻¹.

HRMS (ESI+): *m/z* calc'd for (M + H)⁺ [C₁₈H₂₂O + H]⁺: 255.1744, found 255.1742.

¹H NMR (400 MHz, CDCl₃): δ 7.48-7.43 (m, 2H), 7.33-7.29 (comp m, 3H), 6.27 (dd, *J* = 15.1, 10.5 Hz, 1H), 6.08 (ddd, *J* = 15.1, 10.5, 1.5 Hz, 1H), 5.75-5.63 (comp m, 2H), 4.34 (dd, *J* = 12.5, 5.6 Hz, 1H), 4.08 (d, *J* = 5.6 Hz, 1H), 4.04 (d, *J* = 6.6 Hz, 1H), 2.02 (qt, *J* = 6.6, 6.4 Hz, 1H), 1.76 (dd, *J* = 6.7, 0.6 Hz, 1H), 1.06 (app. dd, *J* = 11.7, 6.7 Hz, 1H).

¹³C NMR (100 MHz, CDCl₃): δ 194.9, 133.6, 131.9, 131.0, 130.1, 128.4, 128.3, 126.8, 123.2, 87.5, 86.5, 74.7, 69.4, 33.4, 18.9, 18.3, 18.1.

Optical Rotation: [α]_D³¹ = -140.64 (*c* = 1.0, CHCl₃).

CHAPTER THREE NOTES AND REFERENCES

¹ (a) Trost, B. M. *Acc. Chem. Res.* **2002**, *35*, 695–705; (b) Trost, B. M. *Angew. Chem., Int. Ed. Engl.* **1995**, *34*, 259–281.

² Ciganek, E. *Org. React.* **1984**, *32*, 1–374.

³ Little, R. D.; Masjedizadeh, M. R.; Wallquist, O.; McLoughlin, J. I. *Org. React.* **1995**, *47*, 315–552.

⁴ Conia, J. M.; Le Perchec, P. *Synthesis* **1975**, 1–19.

⁵ Zhang, L.; Sun, J.; Kozmin, S. A. *Adv. Synth. Catal.* **2006**, *348*, 2271–2296.

⁶ While this product is not a cycloisomerization product strictly speaking, it does share many mechanistic attributes with the other reactions discussed.

⁷ The authors note “the lower yield is partly due to losses during workup caused by the lability of the product which is formed as two diastereoisomers...”

⁸ (a) Fürstner, A.; Szillat, H.; Stelzer, F. *J. Am. Chem. Soc.* **2000**, *122*, 6785–6786; (b) Fürstner, A.; Stelzer, F.; Szillat, H. *J. Am. Chem. Soc.* **2001**, *123*, 11863–11869.

⁹ Méndez, M.; Muñoz, M. P.; Nevado, C.; Cárdenas, D. J.; Echavarren, A. M. *J. Am. Chem. Soc.* **2001**, *123*, 10511–10520.

¹⁰ Blum, J.; Beer-Kraft, H.; Badrieh, Y. *J. Org. Chem.* **1995**, *60*, 5567–5569.

¹¹ Murai also reported the formation of these products as a byproduct in 1996. See: Chatani, N.; Furukawa, N.; Sakurai, H.; Murai, S. *Organometallics* **1996**, *15*, 901–903.

¹² Ota, K.; Lee, S. I.; Tang, J.-M.; Takachi, M.; Nakai, H.; Morimoto, T.; Sakurai, H.; Kataoka, K.; Chatani, N. *J. Am. Chem. Soc.* **2009**, *131*, 15203–15211.

¹³ Nishimura, T.; Kawamoto, T.; Nagaosa, M.; Kumamoto, H.; Hayashi, T. *Angew. Chem., Int. Ed.* **2010**, *49*, 1638–1641.

¹⁴ Nishimura, T.; Maeda, Y.; Hayashi, T. *Org. Lett.* **2011**, *13*, 3674–3677.

¹⁵ (a) Brissy, D.; Skander, M.; Jullien, H.; Retailleau, P.; Marinetti, A. *Org. Lett.* **2009**, *11*, 2137–2139; (b) Jullien, H.; Brissy, D.; Sylvain, R.; Retailleau, P.; Naubron, J.-V.; Gladiali, S.; Marinetti, A. *Adv. Synth. Catal.* **2011**, *353*, 1109–1124.

¹⁶ (a) Chao, C.-M.; Beltrami, D.; Toullec, P. Y.; Michelet, V. *Chem. Commun.* **2009**, 6988–6990; (b) Pradal, A.; Chao, C.-M.; Toullec, P. Y.; Michelet, V. *Beilstein J. Org. Chem.* **2011**, *7*, 1021–1029.

¹⁷ Teller, H.; Corbet, M.; Mantilli, L.; Gopakumar, G.; Goddard, R.; Thiel, W.; Fürstner, A. *J. Am. Chem. Soc.* **2012**, *134*, 15331–15342.

¹⁸ (a) Shibata, T.; Kobayashi, Y.; Maekawa, S.; Toshida, N.; Takagi, K. *Tetrahedron* **2005**, *61*, 9018–9024; (b) Barbazanges, M.; Augé, M.; Moussa, J.; Amouri, H.; Aubert, C.; Desmarests, C.; Fensterbank, L.; Gandon, V.; Malacria, M.; Ollivier, C. *Chem. Eur. J.* **2011**, *17*, 13789–13794; (c) Deschamps, N. M.; Elitzin, V. I.; Liu, B.; Mitchell, M. B.; Sharp, M. J.; Tabet, E. A. *J. Org. Chem.* **2011**, *76*, 712–715.

¹⁹ (a) Haack, K.-J.; Hashiguchi, S.; Fujii, A.; Ikariya, T.; Noyori, R. *Angew. Chem., Int. Ed.* **1997**, *36*, 285–288; (b) Matsumura, K.; Hashiguchi, S.; Ikariya, T.; Noyori, R. *J. Am. Chem. Soc.* **1997**, *119*, 8738–8739.

²⁰ Enantiospecificity ($es = \frac{ee_{product}}{ee_{reactant}} * 100\%$) is a straightforward method for determining the conservation of stereochemistry in the transformation. See: (a) Denmark, S. E.; Burk, M. T.; Hoover, A. *J. Am. Chem. Soc.* **2010**, *132*, 1232–1233; (b) Greene, M. A.; Yonova, I. M.; Williams, F. J.; Jarvo, E. *Org. Lett.* **2012**, *14*, 4293–4296.

²¹ Further increases to temperature and/or catalyst loading had deleterious effects on yield and *es*.

²² While we chose to continue this study with R = isopropyl, others may find other groups suitable for utilizing this method in other synthetic applications.

²³ Soriano, E.; Ballesteros, P.; Marco-Contelles, J. *J. Org. Chem.* **2004**, *69*, 8018–8023.

²⁴ The stereochemistry drawn is derived from the *O*-tethered substrates and was not confirmed in this single *N*-tethered case.

- ²⁵ Chen, Z.; Zhang, Y.-X.; Wang, Y.-H.; Zhu, L.-L.; Liu, H.; Li, X.-X.; Guo, L. *Org. Lett.* **2010**, *12*, 3468–3471.
- ²⁶ Yu, W.; Mei, Y.; Kang, Y.; Hua, Z.; Jin, Z. *Org. Lett.* **2004**, *6*, 3217–3219.
- ²⁷ M. P. Doyle, M. A. McKervey and T. Ye, *Modern Catalytic Methods for Organic Synthesis with Diazo Compounds*, Wiley-Interscience, New York, 1998.
- ²⁸ (a) Shiroodi, R. K.; Gevorgyan, V. *Chem. Soc. Rev.* **2013**, *42*, 4991–5001; (b) Crone, B.; Kirsch, S. F. *Chem. Eur. J.* **2008**, *14*, 3514–3522; (c) Garayalde, D.; Nevado, C. *Beilstein J. Org. Chem.* **2011**, *7*, 767–780.
- ²⁹ (a) Luzung, M. R.; Markham, J. P.; Toste, F. D. *J. Am. Chem. Soc.* **2004**, *126*, 10858–10859; (b) Horino, Y.; Yamamoto, T.; Ueda, K.; Kuroda, S.; Toste, F. D. *J. Am. Chem. Soc.* **2009**, *131*, 2809–2811.
- ³⁰ Stevenson, S. M.; Newcomb, E. T.; Ferreira, E. M. *Chem. Commun.* **2014**, *50*, 5239–5241.
- ³¹ (a) Gauthier, D. R.; Zandi, K. S.; Shea, K. J. *Tetrahedron* **1998**, *54*, 2289–2338; (b) Bracegirdle, S.; Anderson, E. A. *Chem. Soc. Rev.* **2010**, *39*, 4114–4129.
- ³² (a) Stork, G.; Chan, T. Y.; Breault, G. A. *J. Am. Chem. Soc.* **1992**, *114*, 7578–7579; (b) Sieburth, S. M.; Fensterbank, L. *J. Org. Chem.* **1992**, *57*, 5279–5281.
- ³³ (a) Park, S.; Lee, D. *J. Am. Chem. Soc.* **2006**, *128*, 10664–10665; (b) Horino, Y.; Luzung, M. R.; Toste, F. D. *J. Am. Chem. Soc.* **2006**, *128*, 11364–11365.
- ³⁴ Martin, S. E. S.; Watson, D. A. *J. Am. Chem. Soc.* **2013**, *135*, 13330–13333.
- ³⁵ (a) Kim, S. Y.; Park, Y.; Chung, Y. K. *Angew. Chem., Int. Ed.* **2009**, *49*, 415–418; (b) Kim, S. Y.; Park, Y.; Son, S.; Chung, Y. K. *Adv. Synth. Catal.* **2012**, *354*, 179–186; (c) Chung, Y. K.; Chang, K.-M.; Kim, J. H. *J. Inorg. Organomet. Polym.* **2014**, *24*, 15–32;
- ³⁶ Hudlicky, T.; Fan, R.; Reed, J. W.; Gadamasetti, K. G. *Org. React.* **1992**, *41*, 1–133.
- ³⁷ (a) Hikino, H.; Hikino, Y.; Takeshita, Y.; Shirata, K.; Takemoto, T. *Chem. Pharm. Bull.* **1967**, *15*, 321–324; (b) Papageorgiou, V. P.; Ochir, G.; Motl, O.; Argyriadou, N.; Dunkel, H. *J. Nat. Prod.* **1985**, *48*,

851–853; (c) Zalkow, L. H.; Baxter, J. T.; McClure, R. J., Jr.; Gordon, M. M. *J. Nat. Prod.* **1986**, *43*, 598–608.

³⁸ Initial isolation: Lin, L.-Z.; Cordell, G. A.; Ni, C.-Z.; Clardy, J. *Phytochemistry* **1991**, *30*, 1311–1315.
Structural revision: Kitajima, M.; Kogure, N.; Yamaguchi, K.; Takayama, H.; Aimi, N. *Org. Lett.* **2003**, *5*, 2075–2078.

³⁹ Ueoka, R.; Fujita, T.; Matsunaga, S. *J. Org. Chem.* **2009**, *74*, 4396–4399.

⁴⁰ Fang, T.; Du, D.-M.; Lu, S.-F.; Xu, J. *Org. Lett.* **2005**, *7*, 2081–2085.

⁴¹ Kottirsch, G.; Koch, G.; Feifel, R.; Neumann, U. *J. Med. Chem.* **2002**, *45*, 2289–2293.

⁴² Haynes, R. K.; Katsifis, A. G. *Aust. J. Chem.* **1989**, *42*, 1455–1471.

⁴³ Lorenz, M.; Kalesse, M. *Org. Lett.* **2008**, *10*, 4371–4374.

⁴⁴ Pagès, L.; Llebaria, A.; Camps, F.; Motins, E.; Miravittles, C.; Moretó, J. M. *J. Am. Chem. Soc.* **1992**, *114*, 10449–10461.

⁴⁵ Helal, C. J.; Magriotis, P. A.; Corey, E. J. *J. Am. Chem. Soc.* **1996**, *118*, 10938–10939.

⁴⁶ Witulski, B.; Buschmann, N.; Bergsträßer, U. *Tetrahedron* **2000**, *56*, 8473–8480.

⁴⁷ Hammond, M. L.; Zambias, R. A.; Chang, M. N.; Jensen, N. P.; McDonald, J.; Thompson, K.; Boulton, D. A.; Kopka, I. E.; Hand, K. M.; Opas, E. E.; Luell, S.; Bach, T.; Davies, P.; MacIntyre, D. E.; Bonney, R. J.; Humes, J. L. *J. Med. Chem.* **1990**, *33*, 908–918.

⁴⁸ Yamaguchi, M.; Shibato, K.; Fujiwara, S.; Hirao, I. *Synthesis* **1986**, 421–422.

⁴⁹ Wu, P.-Y.; Wu, H.-L.; Shen, Y.-Y.; Uang, B.-J. *Tetrahedron: Asymmetry* **2009**, *20*, 1837–1841.

⁵⁰ Morris, D. J.; Hayes, A. M.; Wills, M. *J. Org. Chem.* **2006**, *71*, 7035–7044.

⁵¹ Zhang, X.; Lu, Z.; Fu, C.; Ma, S. *Org. Biomol. Chem.* **2009**, *7*, 3258–3263.

⁵² Pathak, K.; Bhatt, A. P.; Abdi, S. H. R.; Kureshy, R. I.; Khan, N. H.; Ahmad, I.; Jasra, R. V. *Chirality* **2007**, *18*, 82–88.

⁵³ Takita, R.; Yakura, K.; Ohshima, T.; Shibasaki, M. *J. Am. Chem. Soc.* **2005**, *127*, 13760–13761.

- ⁵⁴ Zhong, J.-C.; Hou, S.-C.; Bian, Q.-H.; Yin, M.-M.; Na, R.-S.; Zheng, B.; Li, Z.-Y.; Liu, S.-Z.; Wang, M. *Chem. Eur. J.* **2009**, *15*, 3069–3071.
- ⁵⁵ Tanaka, K.; Shoji, T. *Org. Lett.* **2005**, *7*, 3561–3563.
- ⁵⁶ Frantz, D. E.; Fässler, R.; Carreira, E. M. *J. Am. Chem. Soc.* **2000**, *122*, 1806–1807.
- ⁵⁷ Clennan, E. L.; Chen, X. *J. Am. Chem. Soc.* **1989**, *111*, 5787–5792.
- ⁵⁸ Ziegler, F. E.; Petersen, A. K. *J. Org. Chem.* **1994**, *59*, 2707–2714.

CHAPTER FOUR

Alkaloids Isolated From the Genus *Gelsemium*



*Gelsemium sempervirens*¹

4.1 Introduction

4.1.1 Overview

The purpose of this chapter is to provide a synopsis of the many alkaloids produced by plants in the genus *Gelsemium*. A number of aspects regarding these natural products are discussed. Emphasis is placed on the structural classification system, biosynthesis, and biological properties of these molecules. Additionally, synthetic approaches to these natural products are highlighted.

4.1.2 The Genus *Gelsemium*

Gelsemium is a genus of flowering plants belonging to the family Gelsemiaceae.² *Gelsemium sempervirens*, *Gelsemium elegans*, and *Gelsemium rankinii* are the three species that comprise the genus. *Gelsemium sempervirens* and *G. rankinii* are native to southeastern United States, while *G. elegans* is

found in Southern Asian and Oceania countries. All three of the flowering shrubs are poisonous, a consequence of the large number of cytotoxic alkaloids found in the plants. Though the toxic effects of these plants are well documented, they have been used in traditional Chinese medicine for the treatment of numerous ailments; strangely enough, these medicinal properties are also attributed to these alkaloids. Herein, we describe much of the phytochemistry concerning the alkaloids isolated from the genus *Gelsemium*. Additionally, studies related to the synthesis of some of the natural products are highlighted.

4.2 The Six Structural Types of Alkaloids Isolated From the Genus *Gelsemium*

The number of alkaloids isolated and characterized from *Gelsemium* totals more than 120 distinct natural products.³ These compounds have been largely classified into six types based on structural characteristics: Yohimbane, Sarpagine, Koumine, Gelsemine, Gelsedine, and Humantenine (Figure 4.2.1).⁴ The numbering system is fully shown on gelsevirine (**186**).

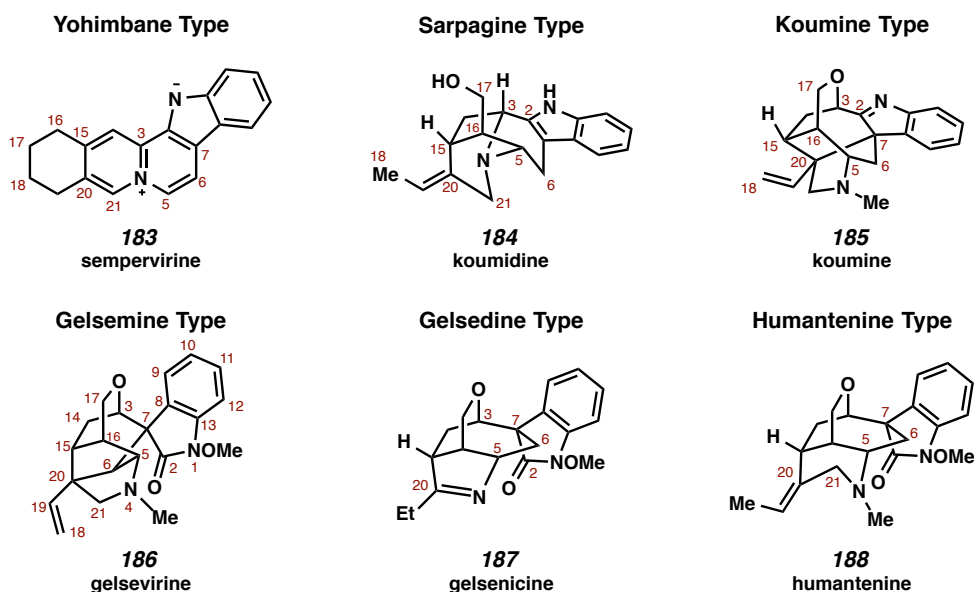


Figure 4.2.1. The Six Gelsemium Alkaloid Structural Types.

4.2.1 Alkaloids of the Yohimbane Type

The Yohimbane type comprises the fewest natural products; thus far, only three have been isolated, all from *G. sempervirens*. This structural type is the least complex of the alkaloids within this family and includes sempervirine (**183**),⁵ sempervilam (**189**),⁶ and ourouparine (**190**, Figure 4.2.2).⁷ The Yohimbane structural features include C17–C18, C2–C3, and C3–N4 bonds. Additionally, the pentacyclic structure is unique to this structural class.

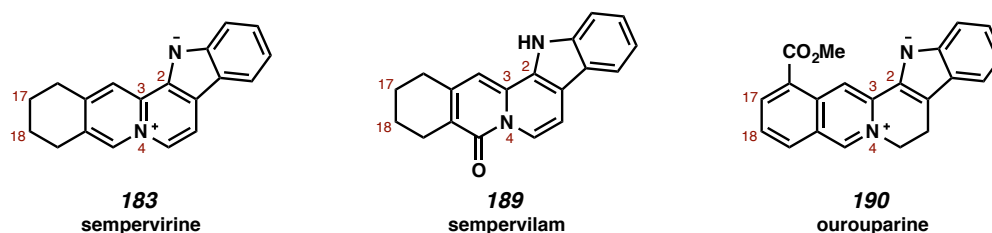


Figure 4.2.2. Alkaloids of the Yohimbane Type.

4.2.2 Alkaloids of the Sarpagine Type

Indole alkaloids of the type Sarpagine are more complex than those found in the Yohimbane type. Natural products koumidine (**184**),⁸ (19*Z*)-anhydrovobasindiol (**191**),⁹ dehydrokoumidine (**192**),¹⁰ and 19-*Z*-16-*epi*-voacarpine (**193**)⁶ are examples of the sarpagine type (Figure 4.2.3). Common traits among these alkaloids are the N4–C21, N4–C5, C5–C16, and C2–C3 bonds. Additionally, the majority of Sarpagine type alkaloids contain C3–N4 connectivity, (19*Z*)-anhydrovobasindiol (**191**) notwithstanding. These compounds are further differentiated from the Yohimbane type by lack of a C17–C18 bond, a characteristic seen in the remaining structural types.

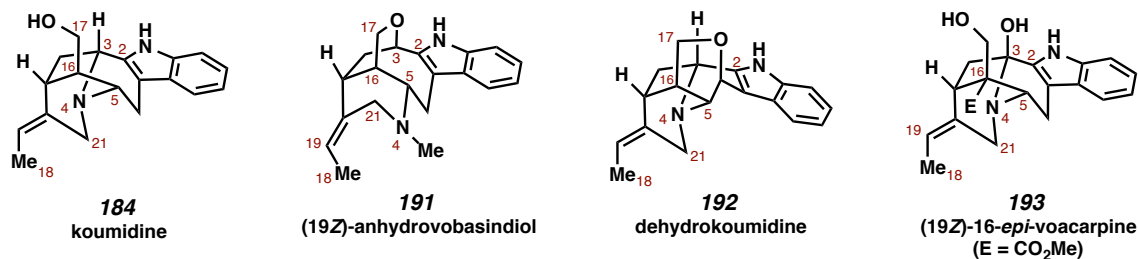


Figure 4.2.3. Alkaloids of the Sarpagine Type.

4.2.3 Alkaloids of the Koumine Type

Alkaloids of the Koumine variety are the most complex of the non-oxindole types. Over 20 Koumine type natural products have been isolated to date. Koumine (**185**),¹¹ 21-oxokoumine (**194**),¹² and (19*R*)-kouminol (**195**)¹³ fall under this classification (Figure 4.2.4). Alkaloids within this type share bonds C2–C3, N4–C5, N4–C21, and C5–C16. A C7–C20 bond is the most defining characteristic of the Koumine type natural products.

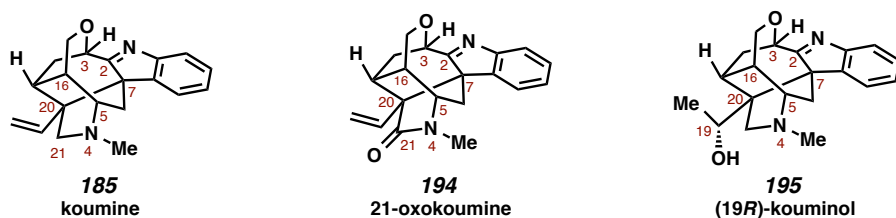


Figure 4.2.4. Alkaloids of the Koumine Type.

4.2.4 Alkaloids of the Gelsemine Type

The natural products gelsevirine (**186**),⁸ gelsemine (**196**),¹⁴ (4*R*)-gelsevirine-*N*⁴-oxide (**197**),¹⁵ and 21-oxogelsemine (**198**)¹⁶ exemplify this structural class (Figure 4.2.5). These natural products lack the C2–C3 bond connectivity and contain a C3–C7 bond connection, providing the distinctive spirooxindole motif. The characteristic is common among the Geselmine, Humantenine, and Gelsedine type alkaloids. Alkaloids of this type are further classified by N4–C21, N4–C5, and most distinctively C6–C20 bonds.

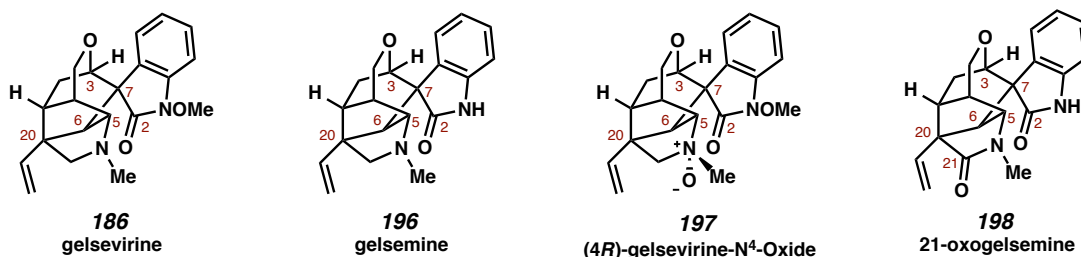


Figure 4.2.5. Alkaloids of the Gelsemine Type.

4.2.5 Alkaloids of the Humantenine Type

Alkaloids of this type are classified by N4–C21, N4–C5, and C3–C7 bond connections. Lack of the C6–C20 bond is what differentiates this type from the Gelsemine type. The majority of humantenine type alkaloids contain spirooxindole structures, as seen in humantenine (**188**),¹⁷ rankinidine (**199**),¹⁸ and gelgamine B¹⁹ (**200**, Figure 4.2.6). Only recently were alkaloids with a degraded oxindole motif, such as 11-methoxygelsemamide (**201**),²⁰ isolated.

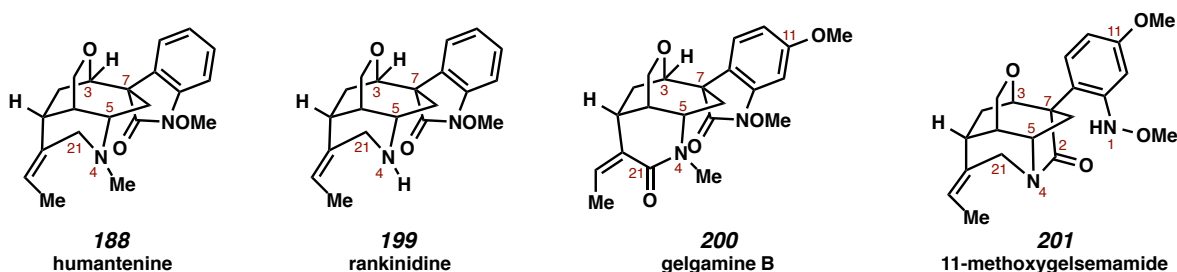


Figure 4.2.6. Alkaloids of the Humantenine Type.

4.2.6 Alkaloids of the Gelsedine Type

Gelsedine type natural products gelsenicine (**187**),⁹ gelsedine (**202**),²¹ 14-acetoxygelsenicine (**203**),²¹ and gelsemoxonine (**162**)²² are shown below in Figure 4.2.7. These are similar in structure to Humantenine type natural products by the presence of N4–C20, N4–C5, and C3–C7 bonds. Moreover, the distinguishing feature of Gelsedine type alkaloids is the lack of C21.

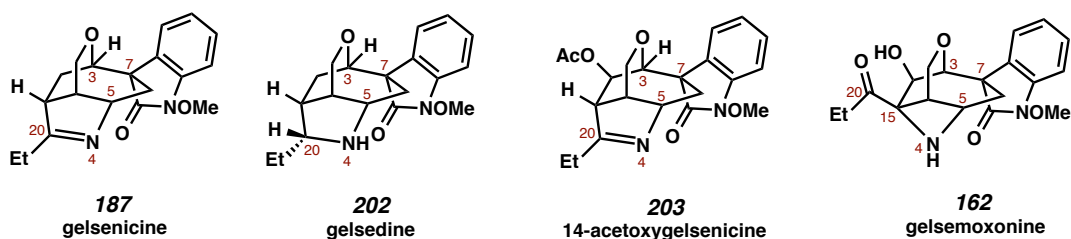


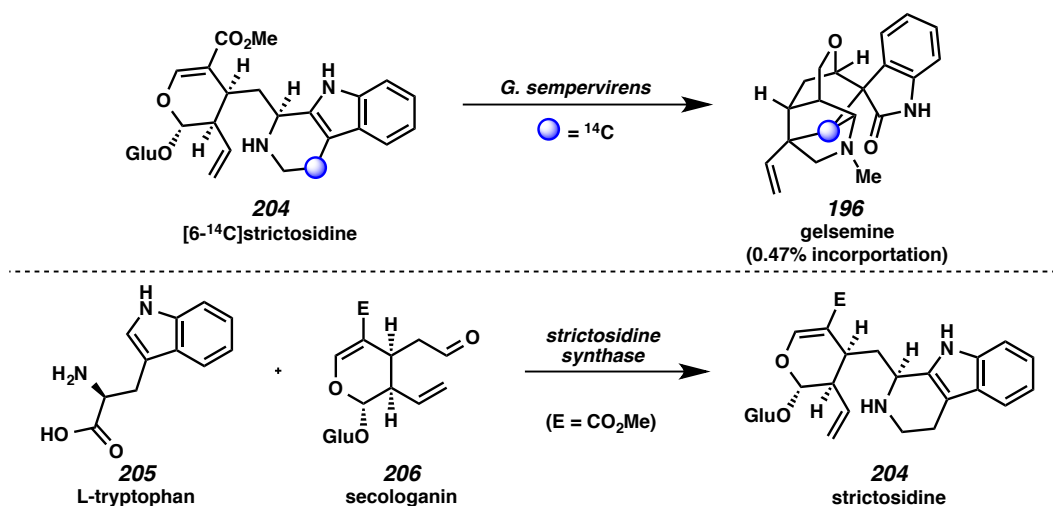
Figure 4.2.7. Alkaloids of the Gelsedine Type.

4.3 Proposed Biosynthesis

Little is known about the enzymatic processes responsible for the production of the Gelsemium alkaloids. Chemical methods have been used to further support or eliminate hypothetical pathways. These studies have resulted in refined, yet unproven biosynthetic pathways. Furthermore, the isolation of previously proposed intermediates has provided more evidence to a suggested pathway; conversely, the discovery of some alkaloids has completely shifted long held proposals.

4.3.1 Proposed Biogenesis of Sarpagine, Koumine, and Humantenine Type Alkaloids

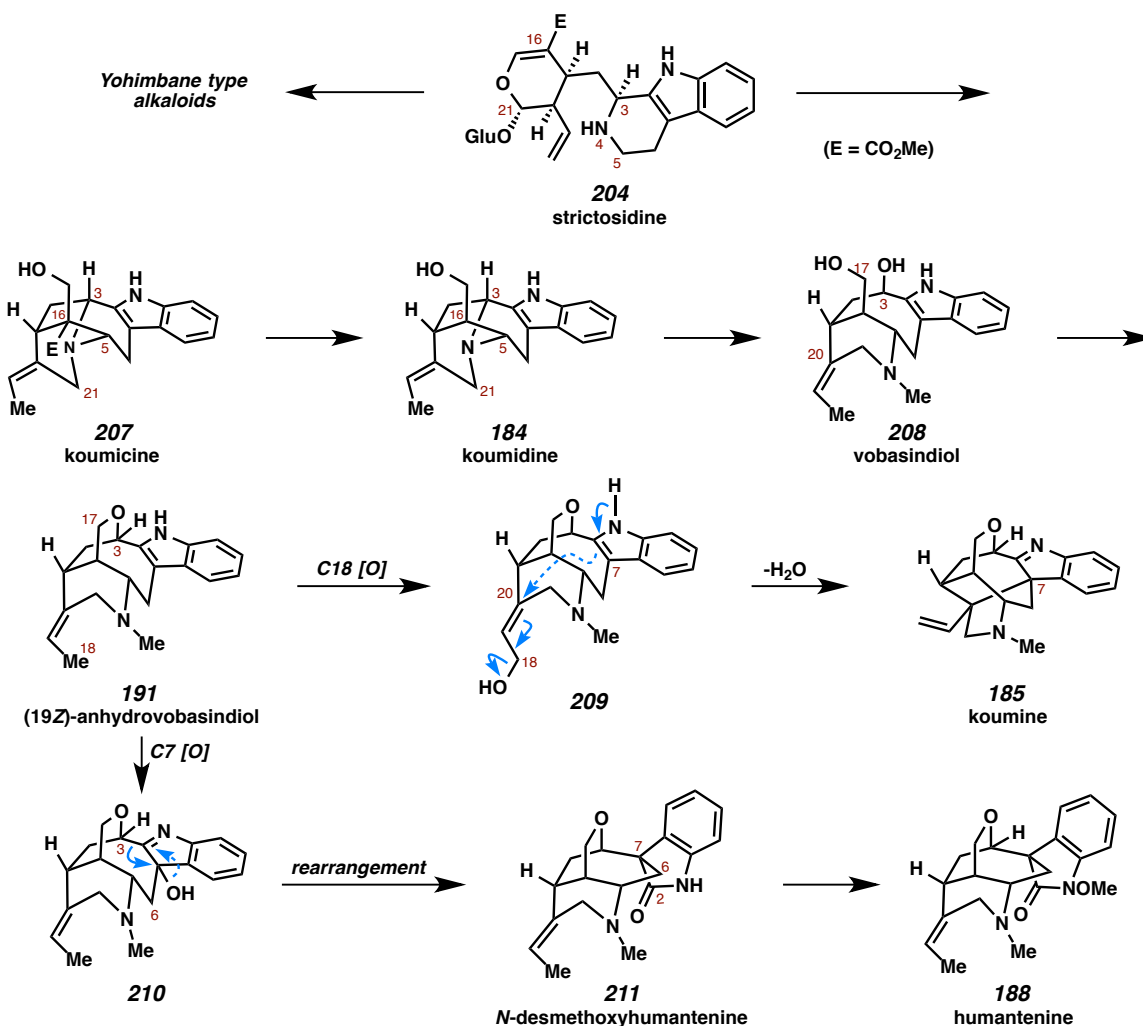
In 1977, Zenk and coworkers disclosed the incorporation of 0.47% of [6-¹⁴C]strictosidine (**204**) into gelsemine (**196**) in *G. sempervirens*.²³ Later, the enzyme that catalyzes the condensation of L-tryptophan (**205**) and secologanin (**206**) to provide strictosidine (**204**) was isolated (strictosidine synthase).²⁴ The *in vivo* transformations from strictosidine (**204**), however, are not well verified and sometimes rely merely on chemical corroboration.²⁵ Nonetheless, the proposed pathways offer a thoughtful examination of the underlying similarities between these alkaloid types.



Scheme 4.3.1. Studies Concerning Early Biosynthetic Precursors to the Gelsemium Alkaloids.

Through C5–C16 and N4–C21 bond assemblies from strictosidine (**204**), Sarpagine type alkaloid koumicine (**207**) is formed (Scheme 4.3.2). Removal of the ester at C16 via decarboxylation of koumicine

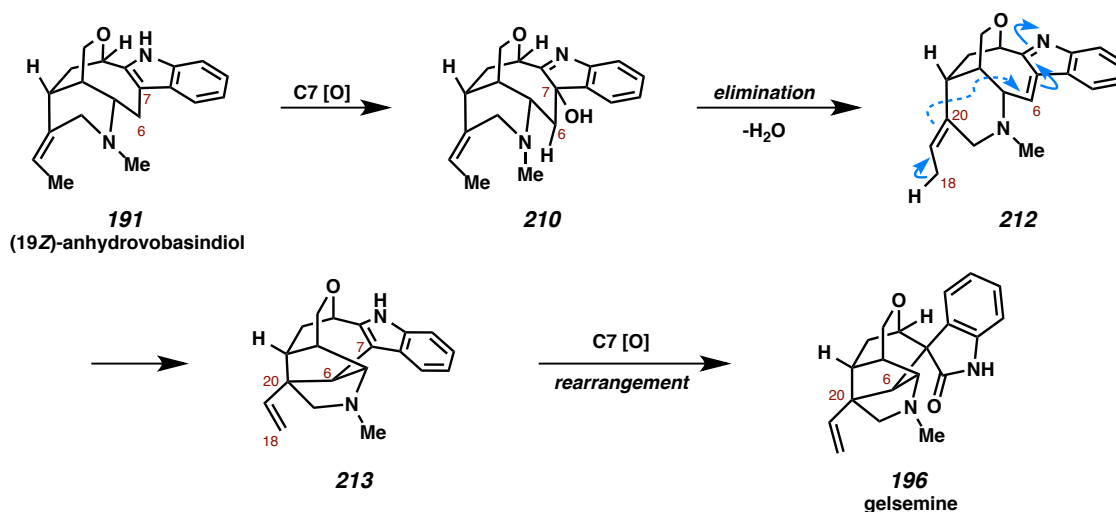
(207) produces koumidine (184). Following various possible redox steps as well as *N*-methylation, the ether linkage (O–C3) in (19*Z*)-anhydrovobasindiol (191) is made. It is plausible that vobasindiol (208) is a biosynthetic intermediate to (19*Z*)-anhydrovobasindiol (191). Moreover, this natural product (191) is a common ancestor and biogenetic branch point to the Koumine, Humantenine, and Gelsemine type alkaloids. Oxidation of (19*Z*)-anhydrovobasindiol (191) at C18 followed by S_N2' addition from C7 into C20 provides the Koumine type alkaloids, namely koumine (185). Moreover, oxidation at C7 is purported to deliver hypothetical intermediate 210. A pincaol-type rearrangement of this compound (210) then could afford known compound *N*-desmethoxyhumantenine (211), and thus entry into the Humantenine natural products.²⁶



Scheme 4.3.2. Proposed Biogenesis of Sarpagine, Koumine, and Humantenine Type Alkaloids.

4.3.2 Proposed Biogenesis of Gelsemine Type Alkaloids

The biosynthetic steps to produce the Gelsemine natural products are highly speculative but are believed to originate from (19Z)-anhydrovobasindiol (**191**). Oxidation of (19Z)-anhydrovobasindiol (**191**) at C7, followed by elimination, provides putative intermediate **212** (Scheme 4.3.3). A conjugate addition forms the key C6–C20 bond illustrated in hypothetical compound **213**.²⁷ The Gelsemine type alkaloids, such as gelsemine (**196**), are purported to arise via a similar oxidation/pinacol-type rearrangement process as described above. This generates the oxindole functionality and the observed stereochemistry at C7 as well as cleavage of the C2–C3 bond.

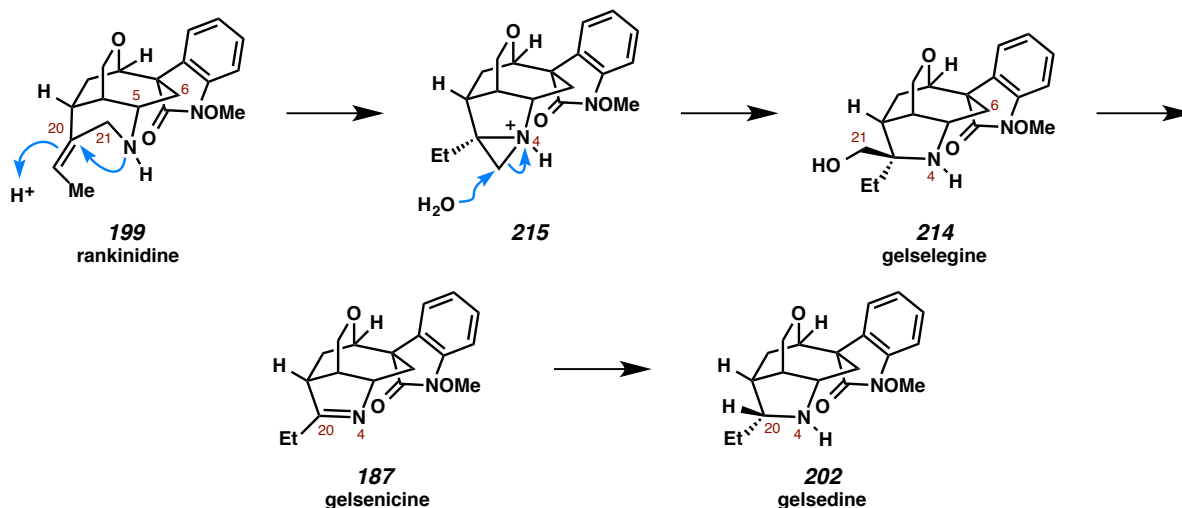


Scheme 4.3.3. Proposed Biosynthetic Pathway to Gelsemine Type Alkaloids from (19Z)-Anhydrovobasindiol (**191**).

4.3.3 Proposed Biogenesis of Gelsedine Type Alkaloids

Early biogenetic hypotheses concerning the Gelsedine structural class were based upon the loss of C21 early in the biogenesis (i.e., the Sarpagine stage).²⁸ The isolation of gelsegine (**214**),²⁹ however, prompted a revision of the biosynthetic precursors to the Gelsedine type alkaloids; and consequently, Humantenine type alkaloids were the new proposed ancestors (Scheme 4.3.4). Thus, from N⁴-desmethylhumantenine, or rankinidine (**199**), hypothetical aziridinium intermediate **215** is generated. Water then opens the aziridinium via S_N2 chemistry to provide Gelsedine type alkaloid gelsegine (**214**).

This natural product (**214**) is purported to be a precursor to major alkaloids gelsenicine (**187**) and gelsedine (**202**). While there is one synthetic study that reinforces this hypothesis,³⁰ the proposed pathway is still largely based on the existence of gelselegine (**214**).



Scheme 4.3.4. Proposed Biogenesis of Gelsedine Type Alkaloids from Rankinidine (**199**).

4.4 Pharmacological Effects

4.4.1 Effects of Consuming Plants of the Genus *Gelsemium*

As stated previously, all three species of flowering plants comprising the genus *Gelsemium* are poisonous. This toxicity has been recognized for hundreds of years; not surprising, the consumption of these plants has been linked to a number of suicides and homicides.³¹ Consumption of any portion (root, stem, leaves, etc.) can cause a number of symptoms: blurred vision, sweating, nausea, limb paralysis, convulsion, and respiratory depression so severe as to cause death.³² In spite of these reports, interesting medicinal properties are also well known. These purported uses range from the external treatment of eczema to healing of malarial fever. As both the toxic and medicinal properties are commonly attributed to the high concentration of alkaloids found in these plants, many more studies need to be completed in regards to the biological mechanisms.

4.4.2 Biological Properties of the Gelsemium Alkaloids

There are reports regarding the biological activity of specific Gelsemium alkaloids, including that of koumine (**185**), gelsenicine (**187**), and gelsemine (**196**, Figure 4.4.1). Koumine (**185**) has been shown *in vivo* to have positive effects of psoriasis, a skin disease, in mouse models.³³ Koumine (**185**) and gelsenicine (**187**) display antitumor activity; these natural products have cytotoxic effects on HepG2 cells, inhibit TE-11 cell proliferation, and inhibit MGC80-cell proliferation.³⁴ Koumine (**185**), gelsenicine (**187**), and gelsemine (**196**) have also displayed measurable analgesic effects *in vivo*.³⁵

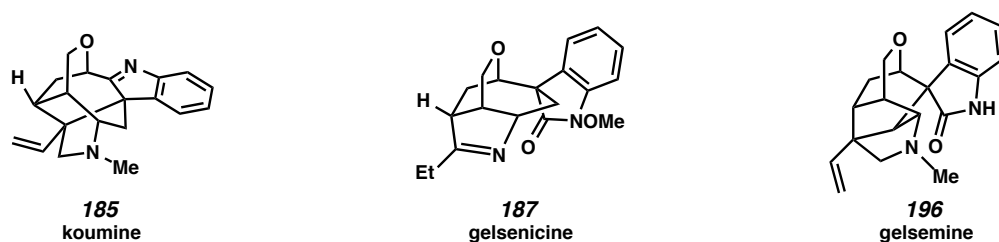


Figure 4.4.1. Examples of Gelsemium Alkaloids that Exhibit Specific Biological Properties.

In one notable study, Gelsemium alkaloids were tested for cytotoxicity against the A431 epidermoid carcinoma cell line.²¹ Gelsedine type alkaloids have cytotoxic effects (Figure 4.4.2). Specifically, gelsedine (**202**) and 14-acetoxygelsenicine (**203**) exhibit potent cytotoxic activity with EC_{50} values of 0.35 μ M and 0.25 μ M, respectively (cisplatin is the positive control, with an EC_{50} value of 3.5 μ M). Interestingly, non-Gelsedine type alkaloids have much lower levels of cytotoxicity. Natural products gelsemine, humantenine, and koumine are all inactive.

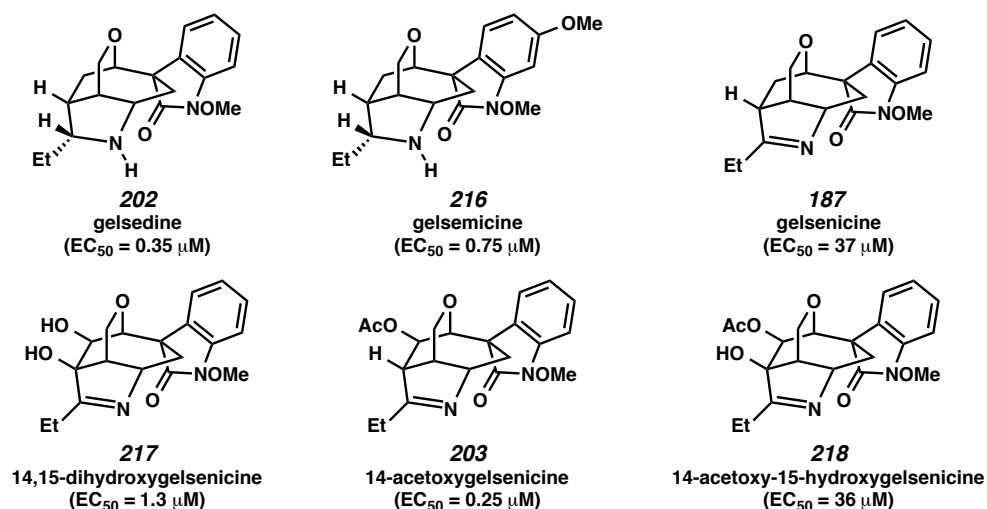


Figure 4.4.2. Kitajima and Coworkers' Observation of Cytotoxicity for Gelsedine Type Alkaloids.

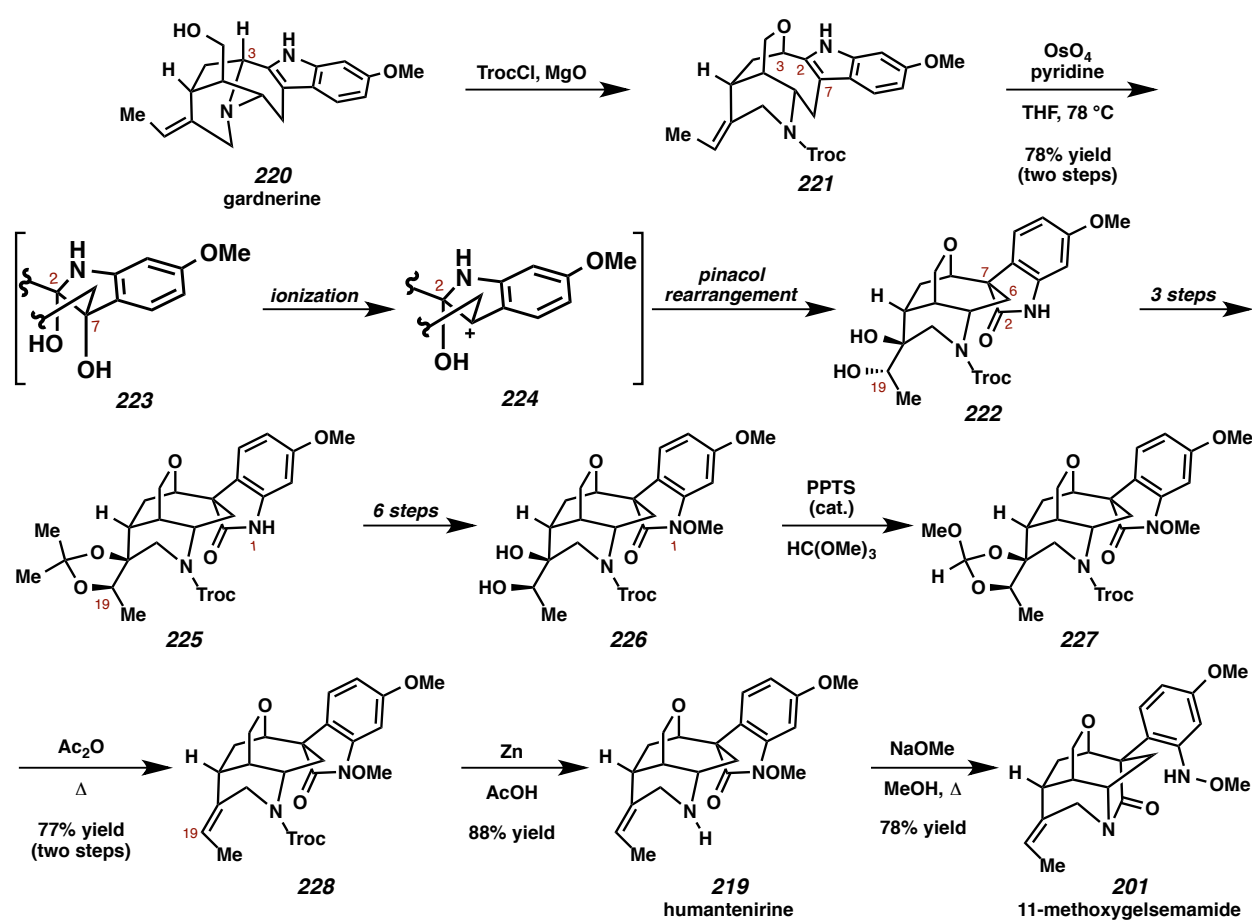
4.5 Synthetic Approaches to the Gelsemium Alkaloids

As a result of the somewhat contradictory reports of toxicity and medicinal benefits, more studies concerning biological applications of these alkaloids are needed. Efficient synthetic approaches to these molecules could enable investigations into structure-activity relationships and future biological applications. Here, syntheses of Humantenine, Gelsedine, and Gelsemine type alkaloids are highlighted. As a result of the large number of synthetic approaches to the Gelsemium alkaloids, the synthetic endeavors concerning the Yohimbane,³⁶ Sarpagine,³⁷ and Koumine³⁸ types will not be discussed herein.

4.5.1 Synthetic Approach to the Humantenine Type Alkaloids

To date, there have been no disclosed de novo syntheses of Humantenine type natural products. Many synthetic studies have focused on probing biosynthetic proposals and possibilities. These chemical studies culminated in Sakai and coworkers' semisynthesis of humantenirine (**219**) in 1994 (Scheme 4.5.1).³⁹ The authors chose gardnerine (**220**), a Sarpagine type alkaloid, as their starting point. Treatment of the natural product (**220**) with TrocCl and MgO provides ether **221**, constructing the desired C3–O bond and protection of the nitrogen atom. To test the proposed biosynthetic rearrangement of Sarpagine type alkaloids to produce oxindole-containing classes (Humantenine, Gelsemine, and Gelsedine),

oxidation of indole **221** with OsO₄ was attempted. This reaction in fact affords the desired oxindole (**222**) in 78% yield from gardnerine (**220**). The authors propose that initial dihydroxylation provides diol **223**, and after ionization to carbocation **224**, a pinacol rearrangement occurs. Inversion of the C19 stereochemistry of diol **222**, as well as acetonide formation to provide compound **225**, occurs in three steps. The authors found that this stereochemistry is essential to provide the correct olefin geometry in a later elimination step. In six additional steps, *N*-methoxyoxindole **226** is generated. Orthoformate construction, elimination, and subsequent amine deprotection with zinc in acetic acid provides humantenirine (**219**) with the correct *Z* olefin geometry. Conversion to Humantenine type alkaloid 11-methoxygelsemamide (**201**) is accomplished by treatment of humantenirine (**219**) with sodium methoxide.

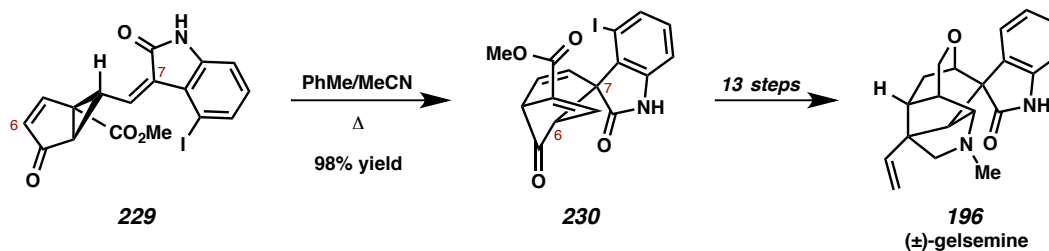


Scheme 4.5.1. Sakai and Coworkers' Semisynthesis of Humantenirine (**219**) and 11-Methoxygelsemamide (**201**).

4.5.2 Synthetic Approaches to the Gelsemine Type Alkaloids

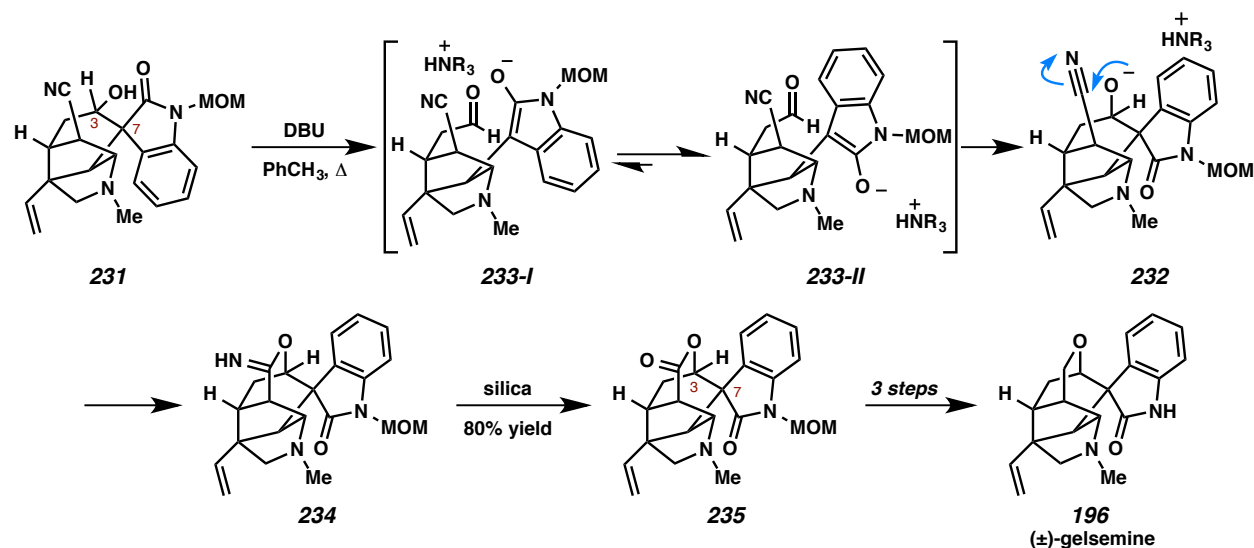
Gelsemine type alkaloids, in particular gelsemine (**196**), have attracted synthetic chemists' attention for decades. A staggering number of approaches toward, formal syntheses, and total syntheses have been disclosed to date.⁴⁰ Synthetic challenges commonly attributed to gelsemine (**196**) are the stereoselective construction of the quaternary C7 spirocenter and the facile synthesis of the fused ring systems. While these are a number of published syntheses, three successful approaches to gelsemine (**196**), highlighting various approaches to controlling the stereochemistry at C7, are described below.

In 1996, Fukuyama and coworkers completed the total synthesis of gelsemine (**196**, Scheme 4.5.2).⁴¹ Key to the researchers success was a highly selective [3,3]-sigmatropic rearrangement. Synthesis of divinylcyclopropane **229** occurs in 10 steps. Heat then effects the conversion of divinylcyclopropane **229** to bicycle **230** in 98% yield: this process provides the stereoselective formation of the C7 spirocenter. Thirteen additional steps are required to accomplish the total synthesis of gelsemine (**196**).⁴²



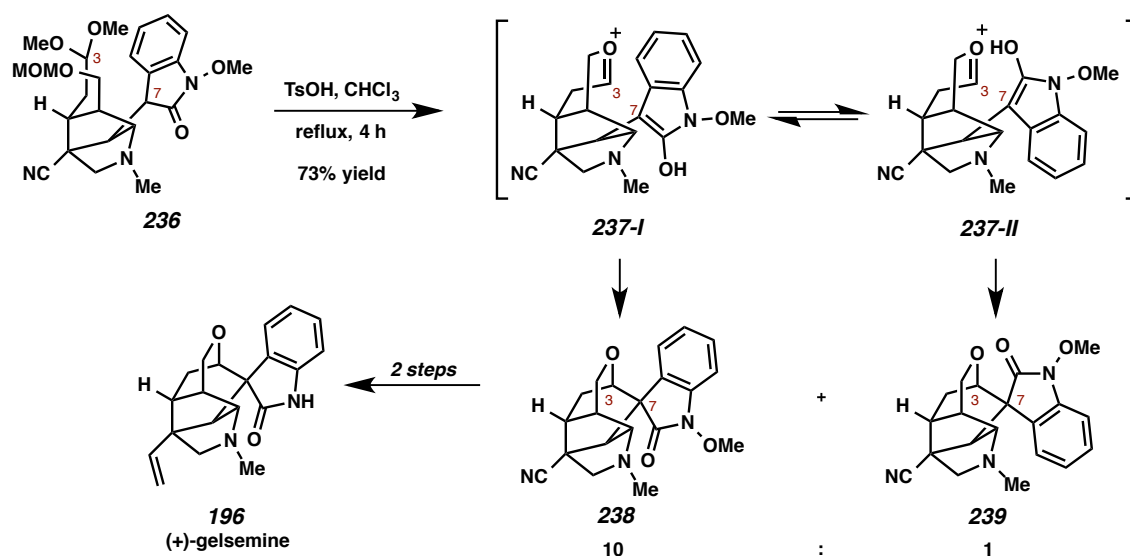
Scheme 4.5.2. A Racemic Synthesis of Gelsemine (**196**) by Fukuyama and Coworkers.

In 1999, Overman and coworkers also completed the synthesis of gelsemine (**196**, Scheme 4.5.3).⁴³ The synthesis showcases a fascinating cascade reaction, which forms two essential bonds in the natural product. The researchers utilized a Pd-catalyzed intramolecular Heck cyclization to generate oxindole **231** with the undesired C7 stereochemistry. Fortunately, base-mediated epimerization with DBU provides in situ formation of alkoxide **232**. The authors propose a conformational equilibrium, favoring enol **233-I**, to provide intermediate **232**. Following addition into the nitrile and purification on silica gel, lactone **235** is afforded. Three additional steps were necessary to finish the synthesis of gelsemine (**196**).⁴⁴



Scheme 4.5.3. A Racemic Synthesis of Gelsemine (**196**) by Overman and Coworkers.

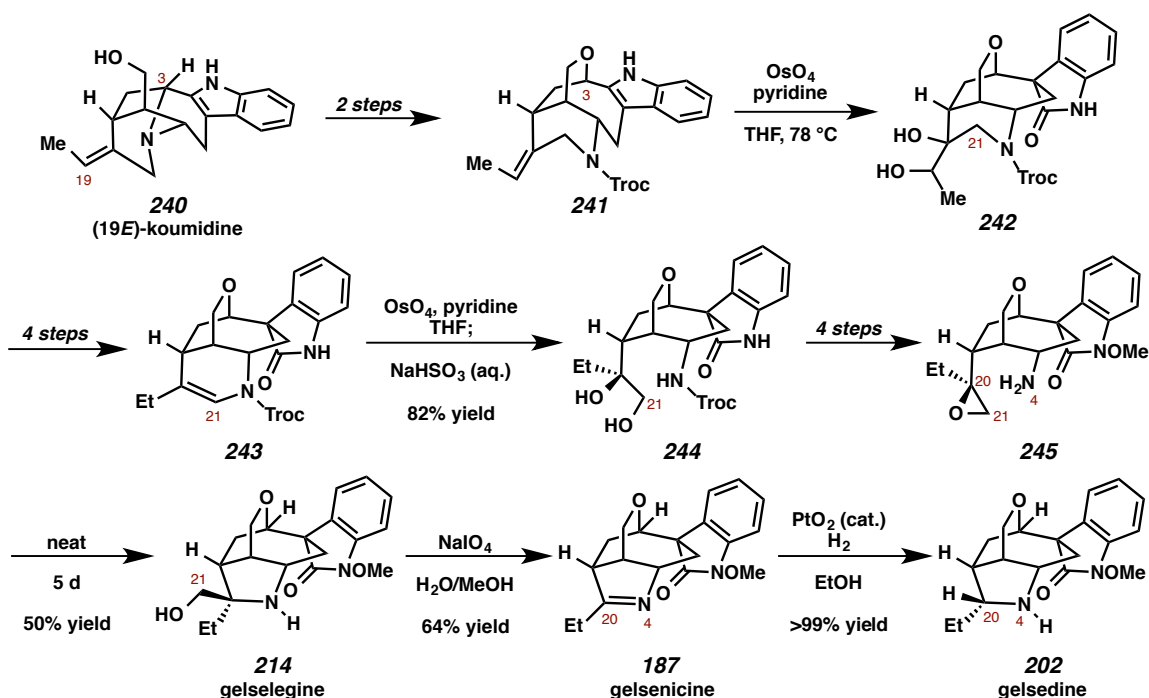
Qin and coworkers completed the asymmetric synthesis of (+)-gelsemine in 2012.⁴⁵ Their key step, shown in Scheme 4.5.4, makes use of oxindole-containing substrate **236**. Upon treatment of acid, MOM deprotection and subsequent oxonium formation provides oxocarbeniums **237-I** and **237-II**. Of these two conformations, the researchers suggest that enol **237-I** is favored. Thus, desired spirooxindole **238** is provided as the major product. Two steps are necessary to complete the asymmetric total synthesis of (+)-gelsemine (**196**). Interestingly, the authors note that removal of the methoxy group before the acid mediated cascade reaction results in a complex mixture upon exposure to acid; therefore, they speculate that gelsemine (**196**), as well as other alkaloids, may undergo N4 oxidation early in the biosynthesis.



Scheme 4.5.4. The Asymmetric Synthesis of Gelsemine (**196**) by Qin and Coworkers.

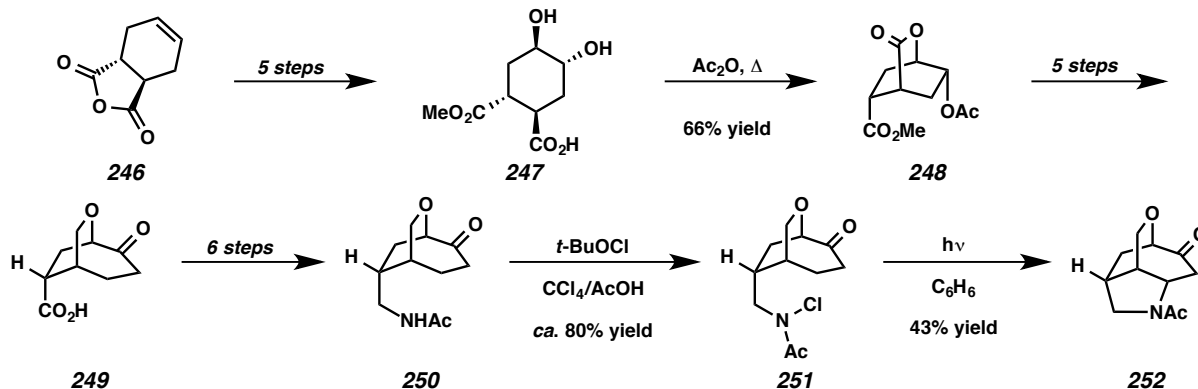
4.5.3 Synthetic Approaches to the Gelsedine Type Alkaloids

In 1990, Sakai and coworkers built on their previous work probing the possibility of biosynthetic intermediates with a semisynthesis of three Gelsedine type natural products: gelselegine (**214**), gelsenicine (**187**), and gelsedine (**202**, Scheme 4.5.5). Two steps are required to convert (19*E*)-koumidine (**240**) into indole **241**.⁴⁶ The authors again use OsO_4 to effect an oxidation/pinacol rearrangement to oxindole **242**. In four steps, diol **242** is converted into piperidine **243**. Oxidation and subsequent cleavage of the N4–C21 bond provides diol **244**. This diol (**244**) is then converted to epoxide **245** in four steps. Allowing the compound to sit neat for 5 days accomplishes the N4–C20 bond formation, providing gelselegine (**214**) in 50% yield. This natural product is converted to gelsenicine (**187**) via periodate-mediated oxidative cleavage in good yield. Finally, hydrogenation of gelsenicine (**187**) affords gelsedine (**202**) in quantitative yield.



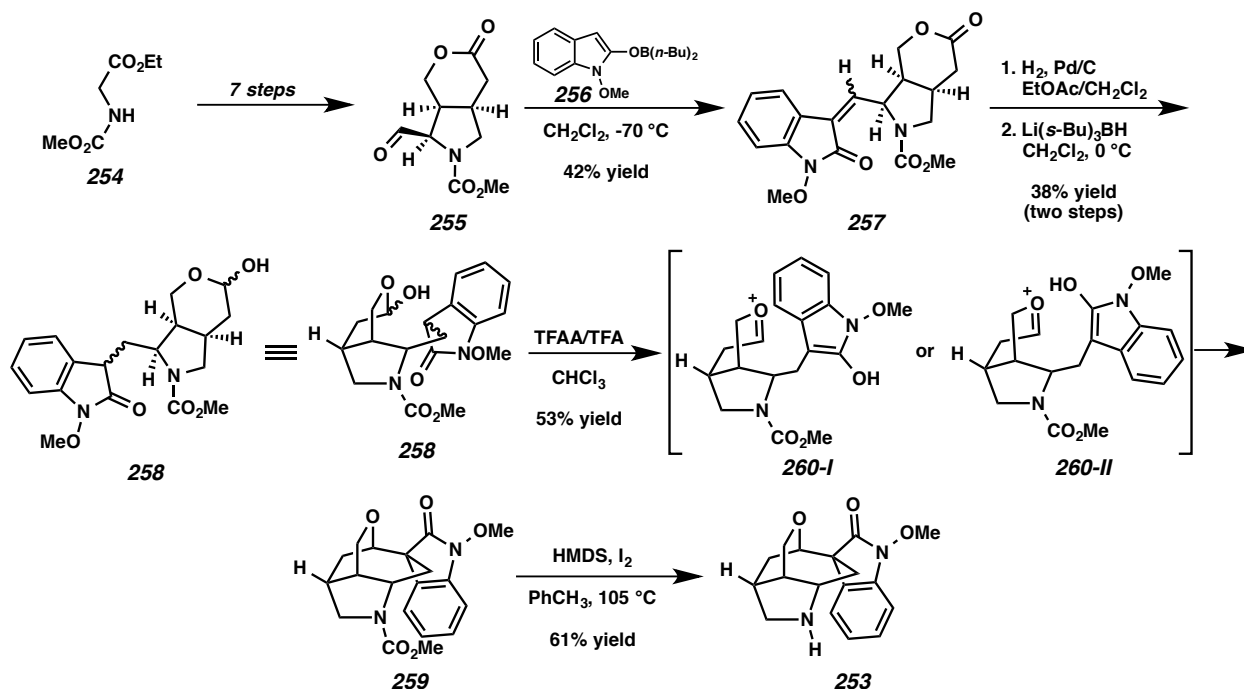
Scheme 4.5.5. Sakai and Coworkers' Semisynthesis of Gelsedine Type Alkaloids.

In 1979, Baldwin and Doll reported their approach to the core of gelsedine (Scheme 4.5.6).⁴⁷ In five steps, cyclic anhydride **246** is converted to cyclohexane **247**. Treatment of this diol with acetic anhydride at elevated temperatures furnishes the desired bicyclic framework (compound **248**) in 66% yield, and after five steps the ether-bridged ketone **249** is obtained. An additional six steps are necessary to convert acid **249** to acyl amine **250**. For their key sequence, amine **250** is converted to chloroamine **251** in good yield by oxidation with *tert*-butyl hypochlorite. Photo-induced radical cyclization affords the tricyclic core of the natural product, in the form of compound **252**, in 43% yield. This approach, while noteworthy for its time, is fairly lengthy. Additionally, one of the most challenging aspects to these molecules, stereoselective installation of the oxindole functionality, is unexplored.⁴⁸



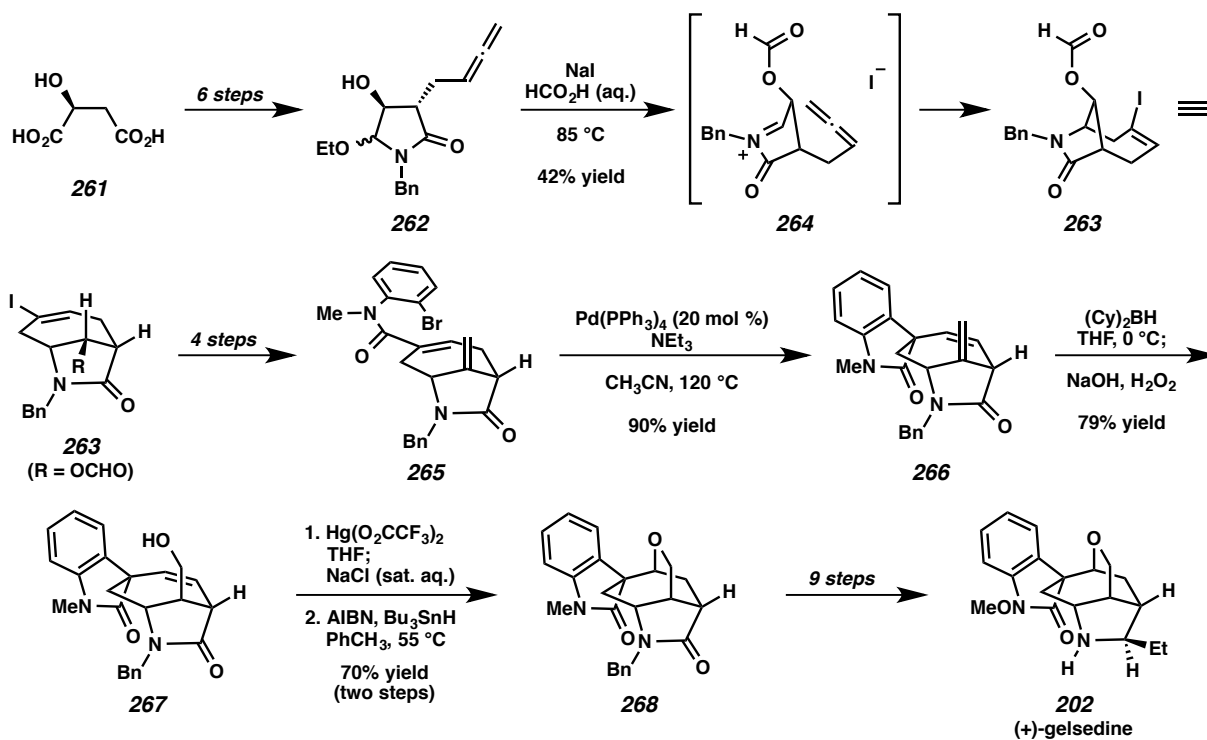
Scheme 4.5.6. Baldwin and Doll's Synthetic Approach to Gelsedine Type Alkaloids.

Eleven years after Baldwin and Doll's approach, Kende and coworkers disclosed their synthesis of (\pm)-7-*epi*-20-desethylgelsedine (**253**, Scheme 4.5.7).⁴⁹ Synthesis of aldehyde **255** is complete in seven steps from carbamate **254**. Aldol condensation of aldehyde **255** and boron enolate **256** provides alkene **257** in 42% yield. Reduction of the alkene followed by selective lactone reduction with $\text{Li}(s\text{-Bu})_3\text{BH}$ affords key step precursor **258** in moderate yield. The key step, an acid-mediated enol addition, provides ring-closed product **259**. Unfortunately, the stereochemistry at C7 did not match the stereochemistry found in the natural products. The authors propose kinetic closure of oxocarbenium **260-I** vs. oxocarbenium **260-II** (i.e., the ring does not reopen and close). After amine deprotection, (\pm)-7-*epi*-20-desethylgelsedine (**253**) is obtained.



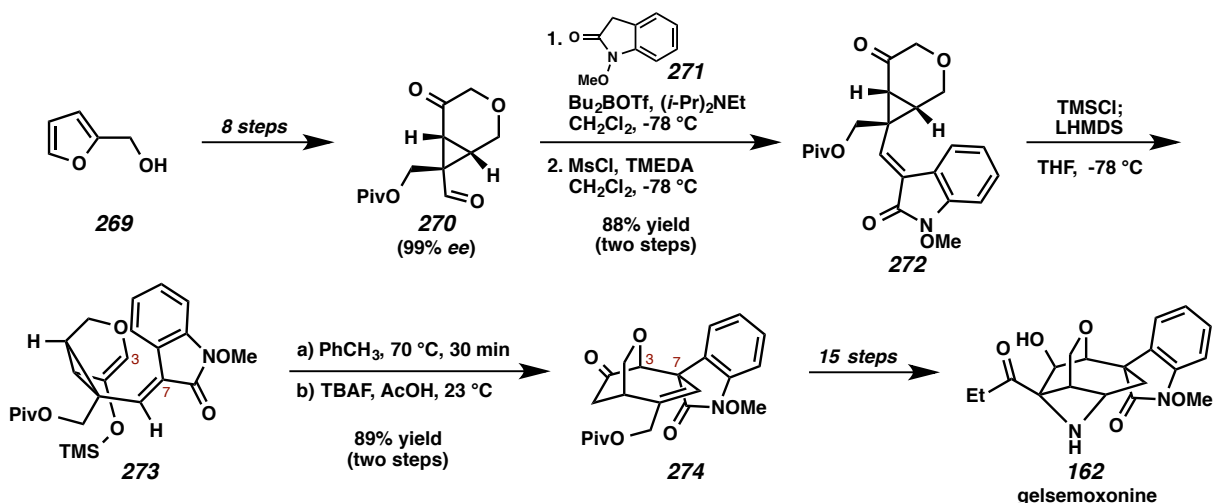
Scheme 4.5.7. The Synthesis of (±)-7-Epi-20-Desethylgelsedine (**253**) by Kende and Coworkers.

In 1999, Hiemstra and coworkers described the first total synthesis of a Gelsedine type alkaloid, (+)-gelsedine (**202**, Scheme 4.5.8).⁵⁰ First, (*S*)-maleic acid (**261**) is converted into allene **262** in six steps. Treatment of allene **262** with sodium iodide and formic acid provides vinyl iodide **263** in 42% yield. The authors propose the reaction occurs via iodide-mediated cyclization of the allene onto the acid-generated iminium (**264**). Vinyl iodide **263** is then converted into aryl bromide **265** in four steps. A Pd-catalyzed Heck cyclization is utilized to effect the formation of *N*-methyloxindole **266** in 90% yield as a single diastereomer. A chemoselective hydroboration/oxidation of the exocyclic olefin of diene **266** affords primary alcohol **267** in 79% yield. Oxymercuration of alkene **267** followed by reduction of the alkyl mercury compound provides ether **268** in 70% yield over two steps. Following a number of redox steps and functional group manipulations, (+)-gelsedine (**202**) is accessed.



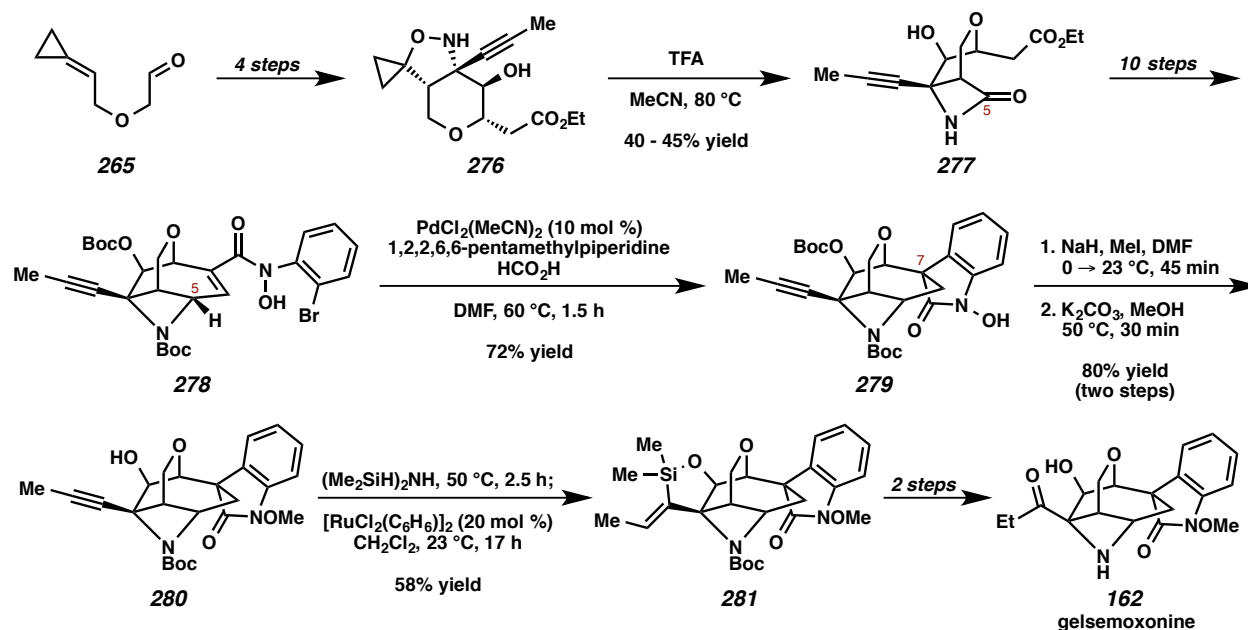
Scheme 4.5.8. The Synthesis of (+)-Gelsedine (**202**) by Hiemstra and Coworkers.

Recently, there has been increased interest in the synthesis of Gelsedine type alkaloids. Fukuyama and coworkers described the synthesis of gelsemoxonine (**162**) in 2011 (Scheme 4.5.9).⁵¹ In this synthesis, cyclopropane **270** is generated in eight steps and 99% *ee* from furfuryl alcohol (**269**). Boron-mediated aldol addition of *N*-methoxyoxindole (**271**) into aldehyde **270** and subsequent elimination provides vinylcyclopropane **272** in 88% yield over the two steps. Conversion of ketone **272** into silyl enol ether **273** is completed with trimethylsilyl chloride and lithium hexamethyldisilazide. Heating divinylcyclopropane **273** in toluene effects a thermal [3,3]-sigmatropic rearrangement, and ketone **274** is isolated after desilylation with tetrabutylammonium fluoride. It is noteworthy that the [3,3]-rearrangement is completely stereospecific; there is no other diastereomer formed in the reaction. In fifteen additional steps, the researchers complete the first synthesis of gelsemoxonine (**162**).



Scheme 4.5.9. The Asymmetric Total Synthesis of Gelsemoxonine (**162**) by Fukuyama and Coworkers.

Carreira and coworkers disclosed the synthesis of (\pm)-gelsemoxonine (**162**) in 2013 (Scheme 4.5.10).⁵² In four steps, starting material **275** is converted to isoxazolidine **276**. A ring contraction mediated by trifluoroacetic acid in acetonitrile provides β -lactam **277** in 40-45% yield;⁵³ this approach provides efficient access to the left portion of the molecule. After a number of functional group manipulations to afford aryl bromide **278**, reductive Heck cyclization gives hydroxyoxindole **279** in good yield as a single diastereomer. Subsequent methylation of *N*-hydroxyoxindole **279** with iodomethane followed by monodeprotection delivers homopropargylic alcohol **280** in 80% yield over two steps. A Ru-catalyzed regioselective hydrosilylation then affords vinylsilane **281**. Following Tamao-Fleming oxidation and removal of the remaining Boc protecting group, the total synthesis of gelsemoxonine (**162**) is complete.



Scheme 4.5.10. The Total Synthesis of Gelsemoxonine (**162**) by Carreira and Coworkers.

4.6 Conclusion

Alkaloids isolated from the genus *Gelsemium* offer both, a rich and interesting past as well as an intriguing future. Information concerning natural products within each structural type has been used to map out a logical biosynthetic pathway for the family. Additionally, the toxicity of these molecules and the potential medicinal applications warrant further studies. The syntheses highlighted herein are but a small sample of approaches to these natural products. That said, they offer many insights, including the evolution of approaches to these structurally similar molecules, the design of novel and creative annulation strategies, and the challenge of controlling the stereochemistry of C7. Perhaps most intriguing is the possibility of using the innate similarity of these alkaloids to synthesize a great deal of them with a single synthetic strategy. To date, however, this opportunity is yet to be realized.

CHAPTER FOUR NOTES AND REFERENCES

- ¹ URL: http://commons.wikimedia.org/wiki/File:Gelsemium_sempervirens3.jpg (Accessed on 11/19/2014)
- ² Struwe, L.; Albert, V. A.; Bremer, B. *Clandistics* **1994**, *10*, 175–206.
- ³ (a) Saxton, J. E. In *The Alkaloids*; Manske, R. H. F., Ed.; Academic Press: New York, 1965; Vol. 8, pp 93–117; (b) Liu, Z.-J.; Lu, R.-R. In *The Alkaloids*; Brossi, A., Ed.; Academic Press: San Diego, 1988; Vol. 33, pp 83–140; (c) Takayama, H.; Sakai, S.-I. In *The Alkaloids*; Cordell, G. A., Ed.; Academic Press: San Diego, 1997; Vol. 49, pp 1–78; (d) Jin, G.-L.; Su, Y.-P.; Liu, M.; Xu, Y.; Yang, J.; Liao, K.-J.; Yu, C.-X. *J. Ethnopharmacol.* **2014**, *152*, 33–52.
- ⁴ There are miscellaneous alkaloids that do not fit into these five types. See ref 3d for more details.
- ⁵ (a) Zhang, Z.; Wang, P.; Yuan, W.; Li, S. *Planta Med.* **2008**, *74*, 1818–1822; (b) Xu, Y.-K.; Yang, S.-P.; Liao, S.-G.; Zhang, H.; Lin, L.-P.; Ding, J.; Yue, J.-M. *J. Nat. Prod.* **2006**, *69*, 1347–1350.
- ⁶ Kogure, N.; Nishiya, C.; Kitajima, M.; Takayama, H. *Tetrahedron Lett.* **2005**, *46*, 5857–5861.
- ⁷ Kogure, N.; Someya, A.; Urano, A.; Kitajima, M.; Takayama, H. *J. Nat. Med.* **2007**, *61*, 208–212.
- ⁸ Initial isolation: Jin, H.; Xu, R. *Acta Chim. Sin.* **1982**, *40*, 1129–1135. Structural revision: (a) Schun, Y.; Cordell, G. A. *Phytochemistry* **1987**, *26*, 2875–2876; (b) Sakai, S.-I.; Wongseripipatana, S.; Ponglux, D.; Yokota, M.; Ogata, K.; Takayama, H.; Aimi, N. *Chem. Pharm. Bull.* **1987**, *35*, 4668–4671.
- ⁹ Ponglux, D.; Wongseripipatana, S.; Subhadhirasakul, S.; Takayama, H.; Yokota, M.; Ogata, K.; Phisalaphong, C.; Aimi, N.; Sakai, S.-I. *Tetrahedron* **1988**, *44*, 5075–5094.
- ¹⁰ Yamada, Y.; Kitajima, M.; Kogure, N.; Wongseripipatana, S.; Takayama, H. *Chem. Asian J.* **2011**, *6*, 166–173.
- ¹¹ (a) Chou, T. Q. *Chin. J. Physiol.* **1931**, *5*, 345–352; (b) Liu, C. T.; Wang, Q. W.; Wang, C. H. *J. Am. Chem. Soc.* **1981**, *103*, 4634–4635.
- ¹² Sun, M.; Hou, X.; Gao, H.; Guo, J.; Xiao, K. *Molecules* **2013**, *18*, 1819–1925.

- ¹³ (a) Sun, F.; Xing, Q. Y.; Liang, X. T. *J. Nat. Prod.* **1989**, *52*, 1180–1182; (b) Lin, L. Z.; Cordell, G. A.; Ni, C. Z.; Clardy, J. *Phytochemistry* **1990**, *29*, 965–968.
- ¹⁴ (a) Conroy, H.; Chakrabarti, J. K. *Tetrahedron Lett.* **1959**, *4*, 6–13; (b) Lovell, F. M.; Pepinsky, R.; Wilson, A. J. C. *Tetrahedron Lett.* **1959**, *4*, 1–5.
- ¹⁵ Ouyang, S.; Wang, L.; Zhang, Q.-W.; Wang, G.-C.; Wang, Y.; Huang, X.-J.; Zhang, X.-Q.; Jiang, R.-W.; Yao, X.-S.; Che, C.-T.; Ye, W.-C. *Tetrahedron* **2011**, *67*, 4807–4813.
- ¹⁶ Nikiforov, A.; Latzel, J.; Varmuza, K.; Wichtl, M. *Monatsh. Chem.* **1974**, *105*, 1292–1298.
- ¹⁷ Yang, J.; Chen, Y. *Acta Pharm. Sin.* **1984**, *19*, 686–690.
- ¹⁸ Yeh, S.; Cordell, G. A. *J. Nat. Prod.* **1986**, *49*, 806–808.
- ¹⁹ Zhang, Z.; Di, Y.-T.; Wang, Y.-H.; Zhang, Z.; Mu, S.-Z.; Fang, X.; Zhang, Y.; Tan, C.-J.; Zhang, Q.; Yan, X.-H.; Guo, J.; Li, C.-S.; Hao, X.-J. *Tetrahedron*, **2009**, *65*, 4551–4556.
- ²⁰ (a) Lin, L. Z.; Cordell, G. A.; Ni, C. Z.; Clardy, J. *Tetrahedron Lett.* **1989**, *30*, 1177–1180; (b) Lin, L. Z.; Cordell, G. A.; Ni, C. Z.; Clardy, J. *Tetrahedron Lett.* **1989**, *30*, 3354.
- ²¹ Kitajima, M.; Nakamura, T.; Kogure, N.; Ogawa, M.; Mitsuno, Y.; Ono, K.; Yano, S.; Aimi, N.; Takayama, H. *J. Nat. Prod.* **2006**, *69*, 715–718.
- ²² Initial isolation: Lin, L.-Z.; Cordell, G. A.; Ni, C.-Z.; Clardy, J. *Phytochemistry* **1991**, *30*, 1311–1315. Structural revision: Kitajima, M.; Kogure, N.; Yamaguchi, K.; Takayama, H.; Aimi, N. *Org. Lett.* **2003**, *5*, 2075–2078.
- ²³ Stöckigt, J.; Zenk, M. H. *J. Chem. Soc., Chem. Commun.*, **1977**, 646–648.
- ²⁴ Nagakura, N.; Rüffer, M.; Zenk, M. H. *J. Chem. Soc., Perkin Trans. 1* **1979**, 2308–2312.
- ²⁵ Biosynthetic studies have been completed concerning some of these pathways in other plants. For an overview, see: O'Connor, S. E.; Maresh, J. J. *Nat. Prod. Rep.* **2006**, *23*, 532–547.
- ²⁶ It is unclear when oxidation at N1 occurs along the biosynthetic pathway.
- ²⁷ This step could occur via a number of different pathways. Only one is shown for simplicity.
- ²⁸ Takayama, H.; Horigome, M.; Aimi, N.; Sakai, S.-I. *Tetrahedron Lett.* **1990**, *31*, 1287–1290.

- ²⁹ Lin, L. Z.; Cordell, G. A.; Ni, C. Z.; Clardy, J. *Phytochemistry* **1990**, *29*, 3013–3017.
- ³⁰ Takayama, H.; Odaka, H.; Aimi, N.; Sakai, S.-I. *Tetrahedron Lett.* **1990**, *31*, 5483–5486.
- ³¹ Zhang, Y. G.; Huang, G. Z. *Am. J. Forensic Med. Pathol.* **1988**, *9*, 313–319.
- ³² (a) Tan, J.; Qiu, C.; Zhen, L.; Li, S. *Pharmacol. Clin. Chin. Mater. Med.* **1988**, *4*, 24–28; (b) Rujjanawate, C.; Kanjanapothi, D.; Panthong, A. *J. Ethnopharmacol.* **2003**, *89*, 91–95.
- ³³ Zhang, L. L.; Huang, C. Q.; Zhang, Z. Y.; Wang, Z. R.; Lin, J. M. *Acad. J. First Med. Coll. PLA* **2013**, *25*, 547–549.
- ³⁴ Huang, J.; Su, Y. P.; Yu, C. X.; Xu, Y.; Yang, J. *Strait Pharm.* **2010**, *22*, 197–200.
- ³⁵ (a) Liu, M.; Shen, J.; Liu, H.; Xu, Y.; Su, Y.-P.; Yang, J.; Xu, C.-X. *Biol. Pharm. Bull.* **2011**, *34*, 1877–1880; (b) Xu, Y.; Qiu, H. Q.; Liu, H.; Liu, M.; Huang, Z. Y.; Yang, J. *Pharmacol. Biochem. Behav.* **2012**, *101*, 504–514; (c) Zhang, J. Y.; Gong, N.; Huang, J. L. Guo, L. C.; Wang, Y. X. *Pain* **2013**, *11*, 2452–2462.
- ³⁶ For a recent synthesis of Yohimbane type alkaloid ourouparine, see: Kogure, N.; Someya, A.; Urano, A.; Kitajima, M.; Takayama, H. *J. Nat. Med.* **2007**, *61*, 208–212.
- ³⁷ For recent syntheses of Sarpagine type alkaloids, see: (a) Krüger, S.; Gaich, T. *Angew. Chem., Int. Ed.* **2014**, *53*, Early View, DOI: 10.1002/anie.201407280; (b) Edwankar, C. R.; Edwankar, R. V.; Namjoshi, O. A.; Deschamps, J.; Liao, X.; Cook, J. M. *J. Org. Chem.* **2013**, *78*, 6471–6487.
- ³⁸ For a synthesis of koumine, see: (a) Magnus, P.; Mugrage, B.; DeLuca, M. R.; Cain, G. A. *J. Am. Chem. Soc.* **1990**, *112*, 5220–5230; (b) Magnus, P.; Mugrage, B.; DeLuca, M. R.; Cain, G. A. *J. Am. Chem. Soc.* **1989**, *111*, 786–789.
- ³⁹ Takayama, H.; Kitajima, M.; Sakai, S.-I. *Tetrahedron* **1994**, *50*, 8363–8370.
- ⁴⁰ For a review focusing on synthetic approaches to gelsemine, see: Lin, H.; Danishefsky, S. J. *Angew. Chem., Int. Ed.* **2003**, *42*, 36–51.
- ⁴¹ Fukuyama, T.; Liu, G. *J. Am. Chem. Soc.* **1996**, *118*, 7426–7427.

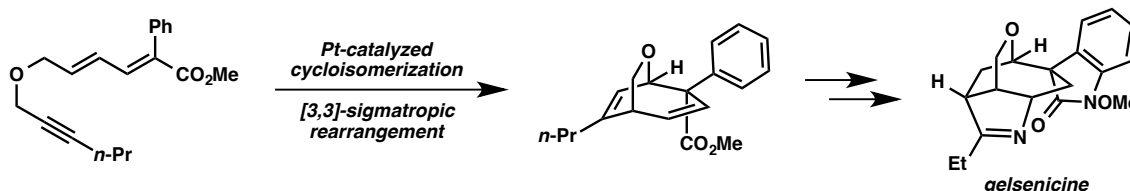
- ⁴² In 2000, Fukuyama and coworkers completed an asymmetric synthesis relying on similar chemistry. See: Yokoshima, S.; Tokuyama, H.; Fukuyama, T. *Angew. Chem., Int. Ed.* **2000**, *39*, 4073–4075.
- ⁴³ (a) Madin, A.; O'Donnell, C. J.; Oh, T.; Old, D. W.; Overman, L. E.; Sharp, M. *Angew. Chem., Int. Ed.* **1999**, *38*, 2934–2936; (b) Earley, W. G.; Jacobsen, J. E.; Madin, A.; Meier, P. G.; O'Donnell, C. J.; Oh, T.; Old, D. W.; Overman, L. E.; Sharp, M. *J. Am. Chem. Soc.* **2005**, *127*, 18046–18053; (c) Madin, A.; O'Donnell, C. J.; Oh, T.; Old, D. W.; Overman, L. E.; Sharp, M. *J. Am. Chem. Soc.* **2005**, *127*, 18054–18065; (d) Overman, L. E.; Sharp, M. *J. Org. Chem.* **1992**, *57*, 1035–1038.
- ⁴⁴ Overman and coworkers do explore another route in ref 43c, although the researchers still rely on the ability to epimerize C7.
- ⁴⁵ Zhou, X.; Xiao, T.; Iwama, Y.; Qin, Y. *Angew. Chem., Int. Ed.* **2012**, *51*, 4909–4912.
- ⁴⁶ Takayama, H.; Odaka, H.; Aimi, N.; Sakai, S.-I. *Tetrahedron Lett.* **1990**, *31*, 5483–5486.
- ⁴⁷ Baldwin, S. W.; Doll, R. J. *Tetrahedron Lett.* **1979**, *35*, 3275–3278.
- ⁴⁸ For another approach to these alkaloids, see: Hamer, N. K. *J. Chem. Soc., Chem. Commun.* **1990**, 102–103.
- ⁴⁹ Kende, A. S.; Luzzio, M. J.; Mendoza, J. S. *J. Org. Chem.* **1990**, *55*, 918–924.
- ⁵⁰ (a) Hiemstra, H.; Rutjes, F. P. J. T.; Fieseler, R. M.; Beyersbergen van Henegouwen, W. G. *Angew. Chem., Int. Ed.* **1999**, *38*, 2214–2217; (b) Beyersbergen van Henegouwen, W. G.; Fieseler, R. M.; Rutjes, F. P. J. T.; Hiemstra, H. *J. Org. Chem.* **2000**, *65*, 8317–8325.
- ⁵¹ Shimokawa, J.; Harada, T.; Yokoshima, S.; Fukuyama, T. *J. Am. Chem. Soc.* **2011**, *133*, 17634–17637.
- ⁵² Diethelm, S.; Carreira, E. M. *J. Am. Chem. Soc.* **2013**, *135*, 8500–8503.
- ⁵³ Diethelm, S.; Schoenebeck, F.; Carreira, E. M. *Org. Lett.* **2014**, *16*, 960–963.

CHAPTER FIVE

Towards a Unified Synthesis of Gelsemium Alkaloids: The Total Synthesis of (\pm)-Gelsenicine

5.1 Overview

As described in Chapter four, the Gelsemium alkaloids have a rich history. The complex structures and potential biological properties of these natural products are intriguing. Consequently, many total syntheses, semisyntheses, and approaches have been disclosed for various alkaloids isolated from the genus *Gelsemium*. Herein our use of transition metal-catalyzed alkyne activation to construct a core motif found throughout a large number of these natural products is detailed. In particular, we investigate a Pt-catalyzed cycloisomerization/[3,3]-sigmatropic rearrangement tandem process. Surprising results regarding this tandem process provide a deeper understanding of the transformation, and ultimately allow us to complete the first total synthesis of (\pm)-gelsenicine (Scheme 5.1.1).



Scheme 5.1.1. Use of Tandem Cycloisomerization/[3,3]-Sigmatropic Rearrangement in the Total Synthesis of Gelsenicine.

5.2 A Unified Synthetic Design of the Gelsemium Alkaloids

We envisage that the tandem cycloisomerization/[3,3]-rearrangement chemistry discussed in Section 3.5.8 may serve as a mode to quickly and efficiently access the core structure found in many of these natural products. Before this hypothesis is discussed in detail, however, it is important to recognize the common structure shared among many of these alkaloid natural products.

5.2.1 Structural Similarities in Alkaloids of the Gelsemine, Humantenine, and Gelsedine Types

As detailed in Chapter four, there are six structural types of alkaloids isolated from the genus *Gelsemium*: Yohimbane, Sarpagine, Koumine, Humantenine, Gelsedine, and Gelsemine. Three of these structural classes, while unique, share a common bicyclic core. Specifically, the Gelsemine, Humantenine, and Gelsedine types contain an embedded oxabicyclo[3.2.2]nonane (Figure 5.2.1). This motif is found in a staggering number of these alkaloids (>90); therefore, targeting this structure could prove very powerful in the synthesis of these natural products.

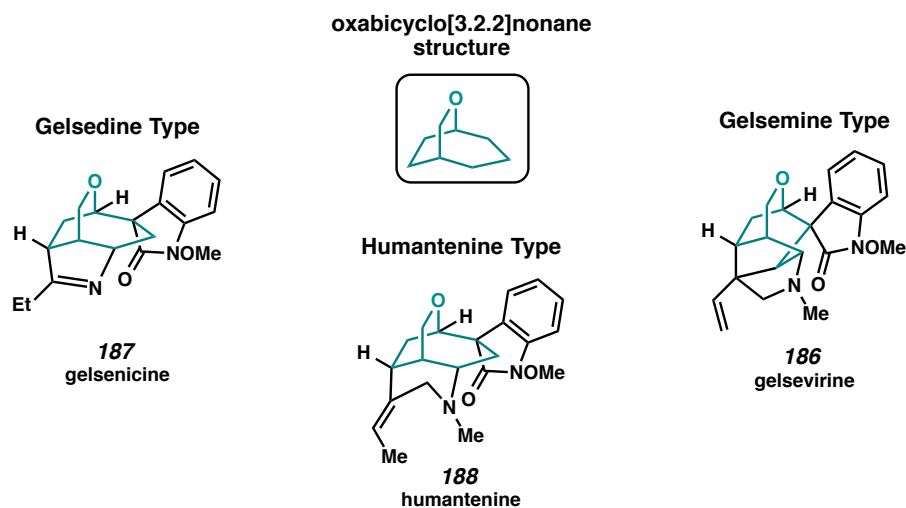


Figure 5.2.1. Oxabicyclo[3.2.2]nonane Structure Embedded in Gelsemine, Gelsedine, and Humantenine Type Alkaloids.

5.2.2 Retrosynthetic Analysis and Proposed Route to Core Structure

We initially identified oxabicyclo[3.2.2]nonadiene **282** as a suitable target, as it may provide divergent access to a large number of *Gelsemium* alkaloids (Figure 5.2.2). All three structural classes shown below contain the N4–C5 bond connectivity. As such, an approach that allows general access to the installation of N4 would be ideal. Gelsedine type natural products would be generated by installation of only one further bond connection, the N4–C20 bond. Similarly, introducing a bond between C20–C21, following N4–C5 formation to core structure **282**, would provide Humantenine type alkaloids. Finally, the most complex alkaloids within this family, the Gelsemine type, would arise from intermediate **282** via

N4–C5, C6–C20 and C20–C21 bond formations. We believe that a large number of these alkaloids can be synthesized from compound **282**. Moreover, we plan on efficiently accessing this intermediate using Pt-catalyzed enyne cycloisomerization chemistry.

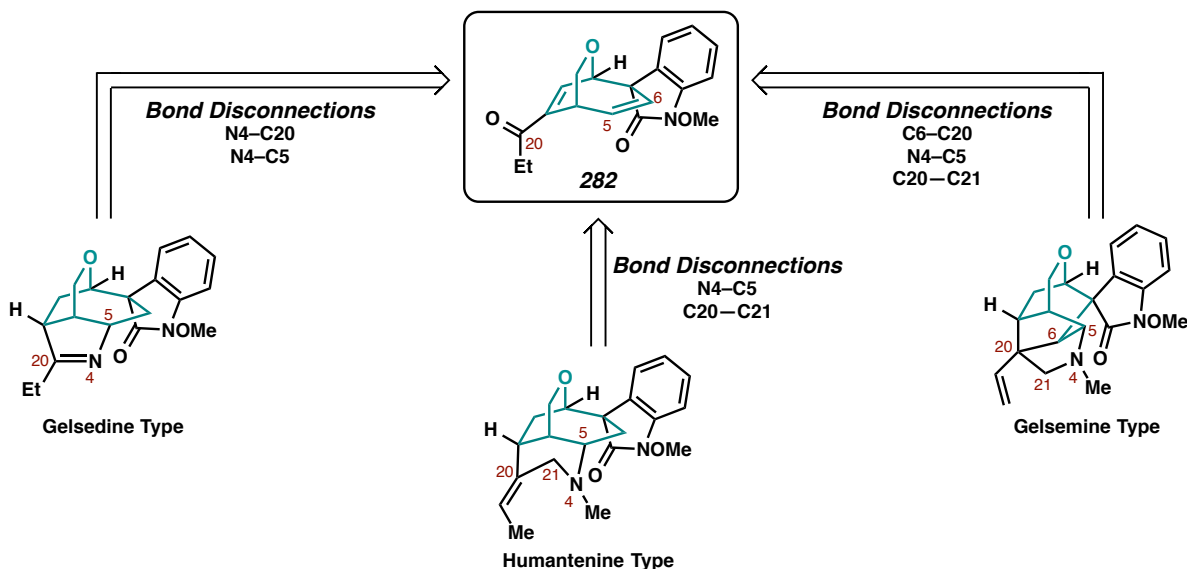
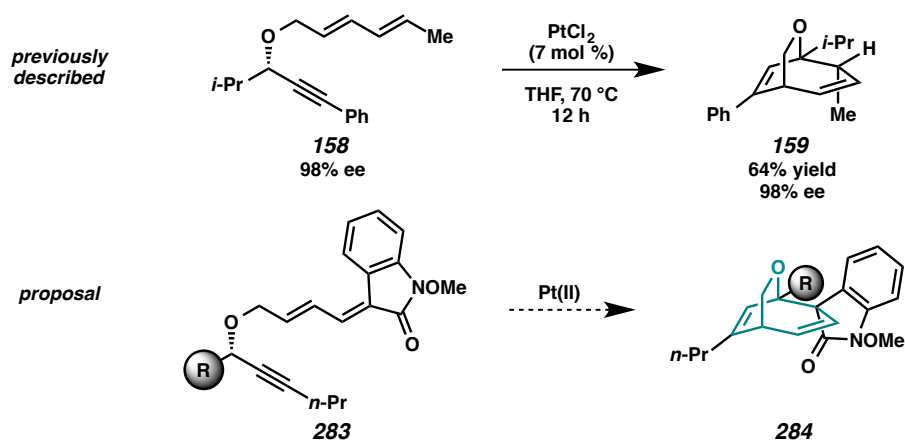


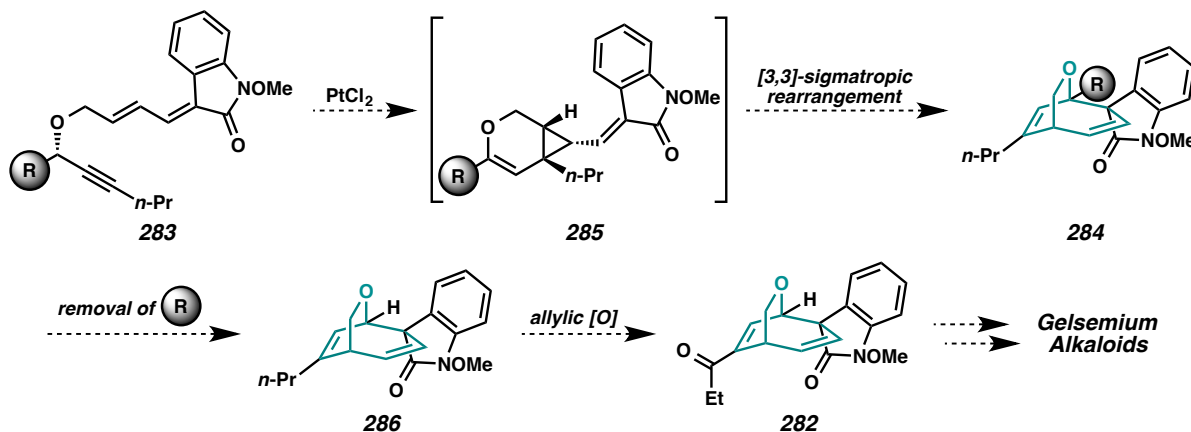
Figure 5.2.2. General Retrosynthesis of Different Structural Types to Common Intermediate **282**.

Our chirality transfer system described in Chapter three could provide an efficient method to construct common intermediate **282** enantioselectively. As previously described in 3.5.8, our chirality transfer protocol translates well to dienyne **158**. Upon treatment of compound **158** with catalytic PtCl_2 , the tandem cycloisomerization/[3,3]-sigmatropic rearrangement occurs, providing bridged bicycle **159** in 64% yield and excellent *ee* (reproduced in Scheme 5.2.1). Armed with this result, we were curious if we could effect the same transformation on an oxindole-containing substrate such as **283**. Under similar conditions, dienyne **283** should afford bicycle **284** with the illustrated stereochemistry. While we are optimistic that the proposed cycloisomerization/divinylcyclopropane rearrangement will succeed, there are concerns. First, we need to access the desired substrates efficiently. Once generated, we are unsure if there will be any unforeseeable complications with the cycloisomerization or the sigmatropic process. Lastly, if we can effect this overall transformation, are we then able to complete the synthesis of one of the alkaloids (i.e., is our product substrate suitable)?



Scheme 5.2.1. Previously Observed Tandem Process and Proposed Implementation on Substrate **283**.

Thus, we envisage that our chirality transfer cycloisomerization protocol will enable the expedient synthesis of common intermediate **282** (Scheme 5.2.2). In a more thorough proposed sequence, cycloisomerization of stereodefined dienyne **282** would provide divinylcyclopropane **285**. Poised for *in situ* [3,3]-sigmatropic rearrangement, divinylcyclopropane **285** would reorganize to enantioenriched oxabicyclo[3.2.2]nonadiene **284**. If successful, this would allow for the single-step generation of three stereocenters found in the natural products. Subsequent removal of the stereocontrolling R group and allylic oxidation would yield our desired common intermediate **282**. We favor the proposed allylic oxidation in preference to earlier incorporation of the carbonyl, as the ketone would not be tolerated in the cycloisomerization reaction.



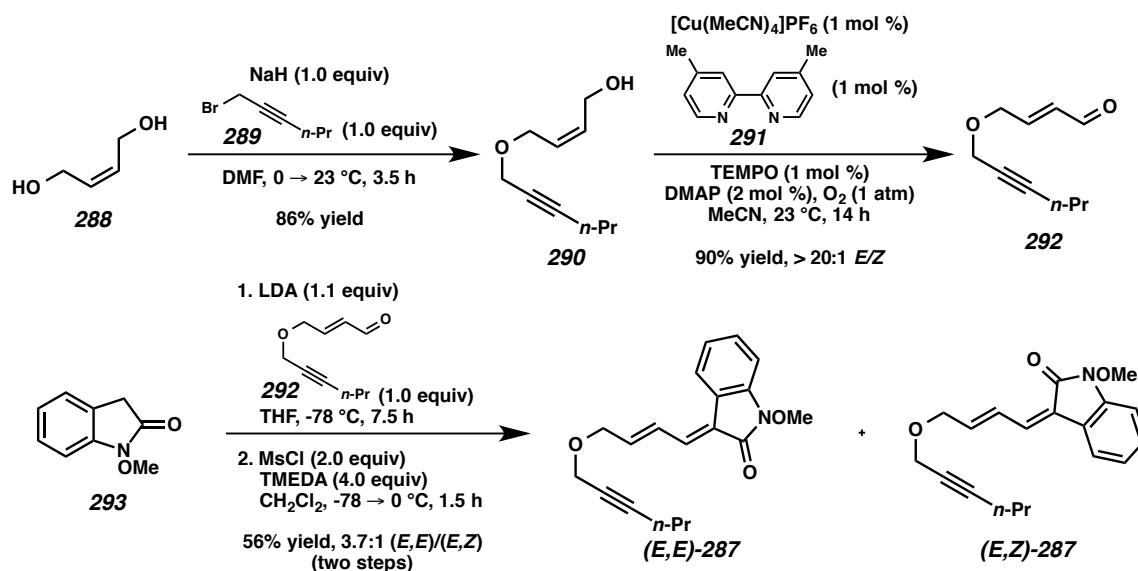
Scheme 5.2.2. Proposed Forward Route to Common Intermediate **282**.

5.3 First Generation Approach

We initially chose to attack the synthesis of common intermediate **282** in a racemic context. The choice to approach these molecules in a racemic system is twofold: (1) We need not worry about the nature of the stereocontrolling R group (e.g., functionality, attachment, and cleavage) and (2) We can quickly assess the feasibility of, and optimize proposed late stage transformations.

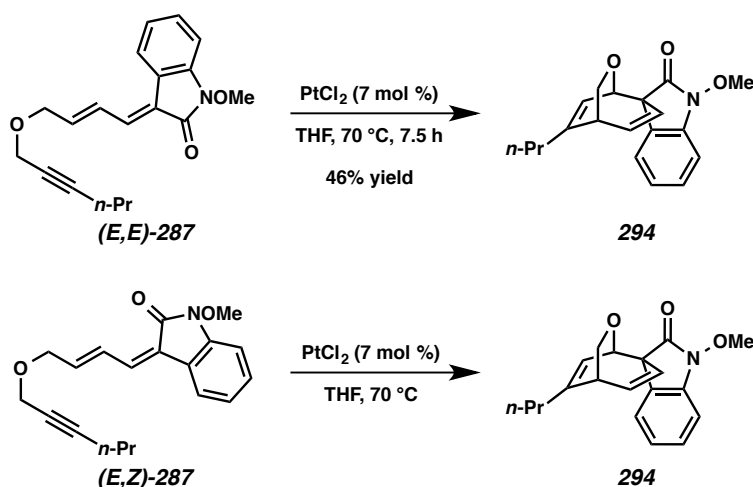
5.3.1 Initial Synthetic Studies

Thus, we first turned our attention to the synthesis of dienyne (*E,E*)-**287** (Scheme 5.3.1). Williamson ether synthesis of (*Z*)-but-2-ene-1,4-diol (**288**) with bromide **289** affords (*Z*)-allylic alcohol **290** in 86% yield.¹ Transformation of allylic alcohol **290** to enal **292** is complete in a single step utilizing a Cu-mediated oxidation followed by organocatalyzed alkene isomerization. These conditions are adapted from those disclosed by Christmann and coworkers in 2012.² Lithium diisopropylamine-promoted aldol reaction of *N*-methoxyoxindole (**293**) with enal **292** at -78 °C followed by elimination provides desired dienyne (*E,E*)-**287** in 44% yield over the two steps, plus dienyne (*E,Z*)-**287** in 12% yield.



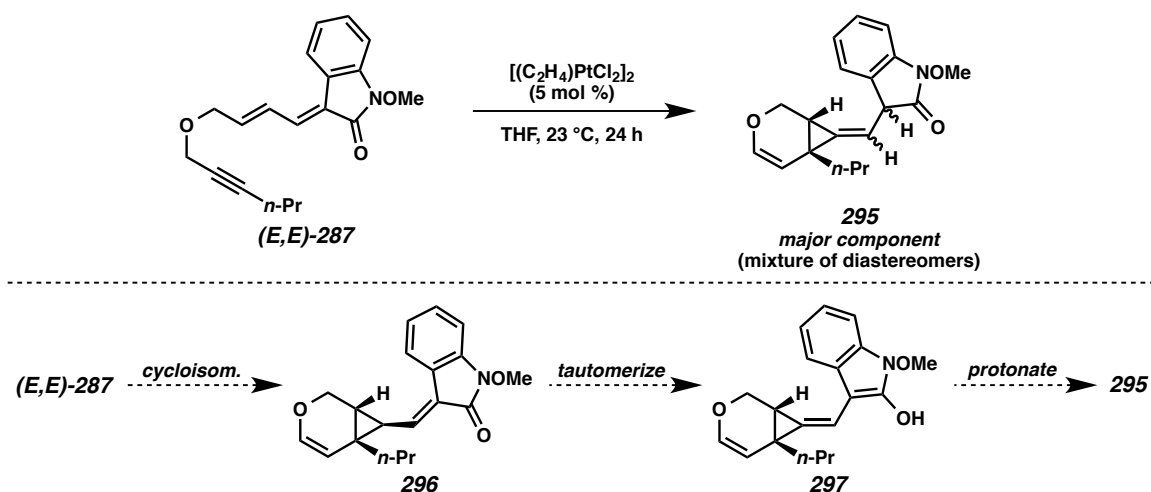
Scheme 5.3.1. Synthesis of Dienyne (*E,E*)-**287** and (*E,Z*)-**287**.

As stated prior, substrate (*E,E*)-**287** should generate our desired diastereomer after cycloisomerization and subsequent divinylcyclopropane rearrangement. To our surprise however, treatment of dienyne (*E,E*)-**287** to various isomerization conditions provides none of desired the oxabicyclic ether (**294**). Instead, oxabicyclic ether **294**, which is epimeric at the spirocenter, is formed as a single diastereomer in 46% yield.³ This result is quite unexpected, as high levels of stereospecificity are observed in the less functionalized system (**158** → **159**, Section 3.2.1). Furthermore, dienyne (*E,Z*)-**287** also produces undesired diastereomer **294**.⁴ This outcome is “expected” as bicyclic ether **294** is the result one would anticipate arising from dienyne (*E,Z*)-**287**. We were curious about the driving forces behind this surprising result. One possible explanation for the observed high level of stereoconvergency invokes thermodynamic isomerization of the olefin prior to the [3,3]-rearrangement.



Scheme 5.3.2. Cyclization Attempts on Dienes (*E,E*)-**287** and (*E,Z*)-**287**.

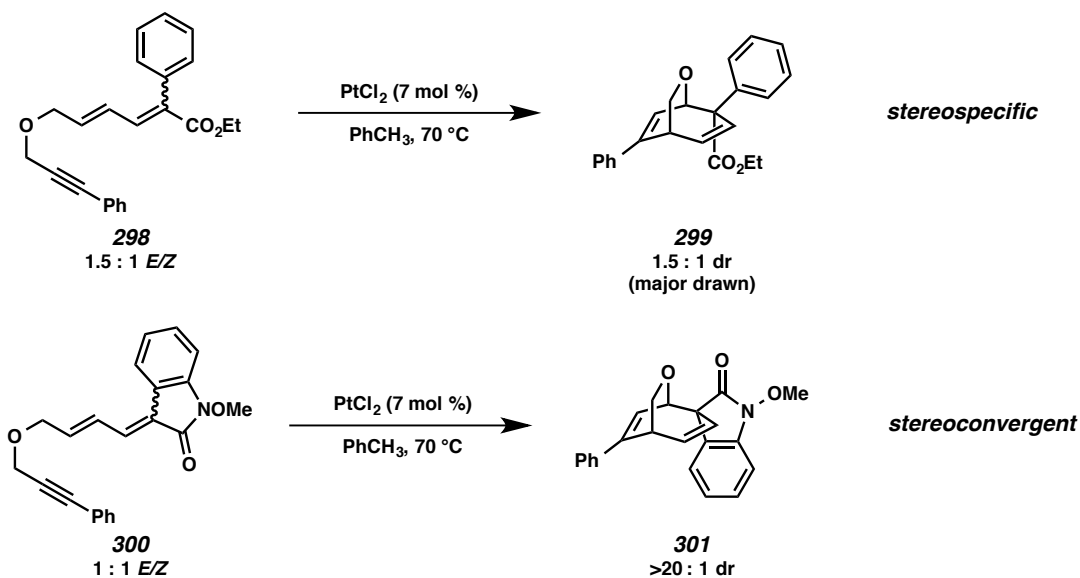
Isomerization may also be facilitated by formation of an aromatic intermediate. Evidence for this pathway is observed when using catalytic Zeise’s Dimer at 23 °C (Scheme 5.3.3). Under these milder conditions, the major product observed in ¹H NMR of the crude reaction mixture is methylene cyclopropane **295**. A driving force for the isomerization, which ultimately produces observed bicyclic ether **294** may be a favorable aromatic stabilization from presumed intermediate 2-hydroxyindole **297**.



Scheme 5.3.3. Observation of Methylene Cyclopropane **295**.

5.3.2 Two Different Stereochemical Outcomes

As the results discussed above indicate, one of the potential causes of the unexpected reaction outcome could be the presence of the oxindole. Thus, we explored the use of a substrate that would be unable to tautomerize via an aromatic intermediate, dienyne **298**. To our delight, treatment of dienyne **298** with catalytic $PtCl_2$ provides desired oxabicyclo **299** as a 1.5:1 mixture of diastereomers with complete stereospecificity (Scheme 5.3.4). In direct comparison, when oxindole-containing substrate **300** (as a 1:1 mixture of alkene isomers) is subjected to analogous conditions, a single diastereomer (**201**) is obtained. It is fascinating that subtle changes to diene substitution result in disparate reaction outcomes. Additionally, this result (**298** → **299**) provides new hope for our synthetic design.

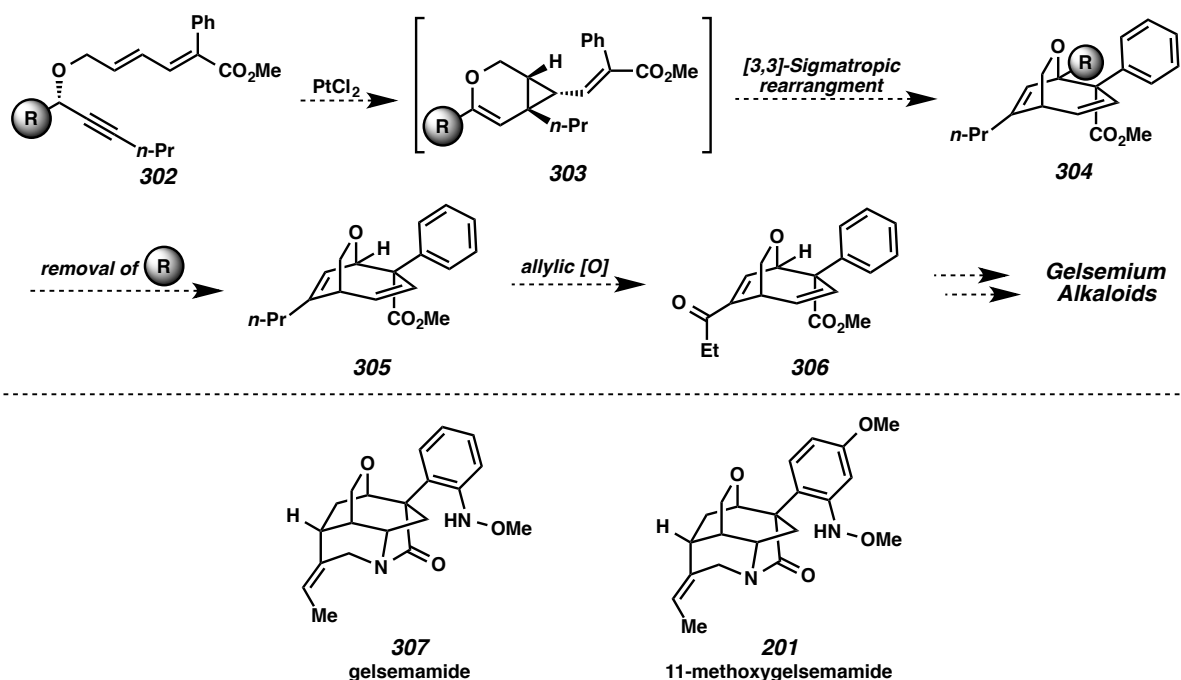


Scheme 5.3.4. Stereospecific and Stereoconvergent Processes.

5.4 Second Generation Approach

5.4.1 Revised Synthetic Strategy

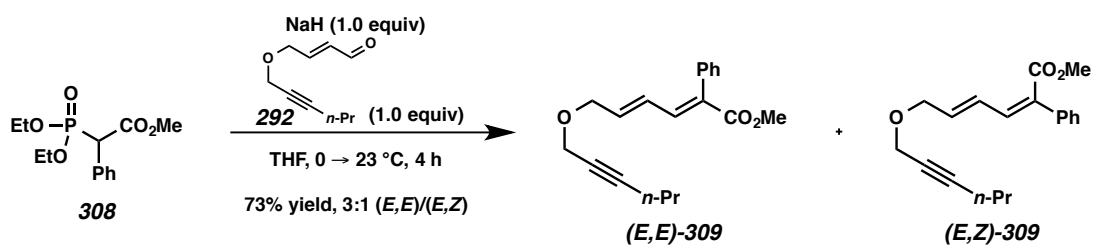
Informed by the insights gained in the described stereochemical studies, we revised our synthetic plan (Scheme 5.4.1). Tandem cycloisomerization/[3,3]-rearrangement of non-oxindole containing dienyne **302** followed by removal of the stereocontrolling R group would produce bridged bicycle **305**. Allylic oxidation would then afford enone **306**. This compound, enone **306**, represents our revised common intermediate. Conversion of enone **306** to diverse intermediates and late-stage oxindole formations would provide efficient access to a number of alkaloids. Additionally, our revised route could offer entry to non-oxindole containing natural products such as the gelsemiamides (**307** and **201**).



Scheme 5.4.1. Revised Synthetic Approach and the Structures of Gelsemamide (**307**) and 11-Methoxygelsemamide (**201**).

5.4.2 Second Generation Synthetic Studies

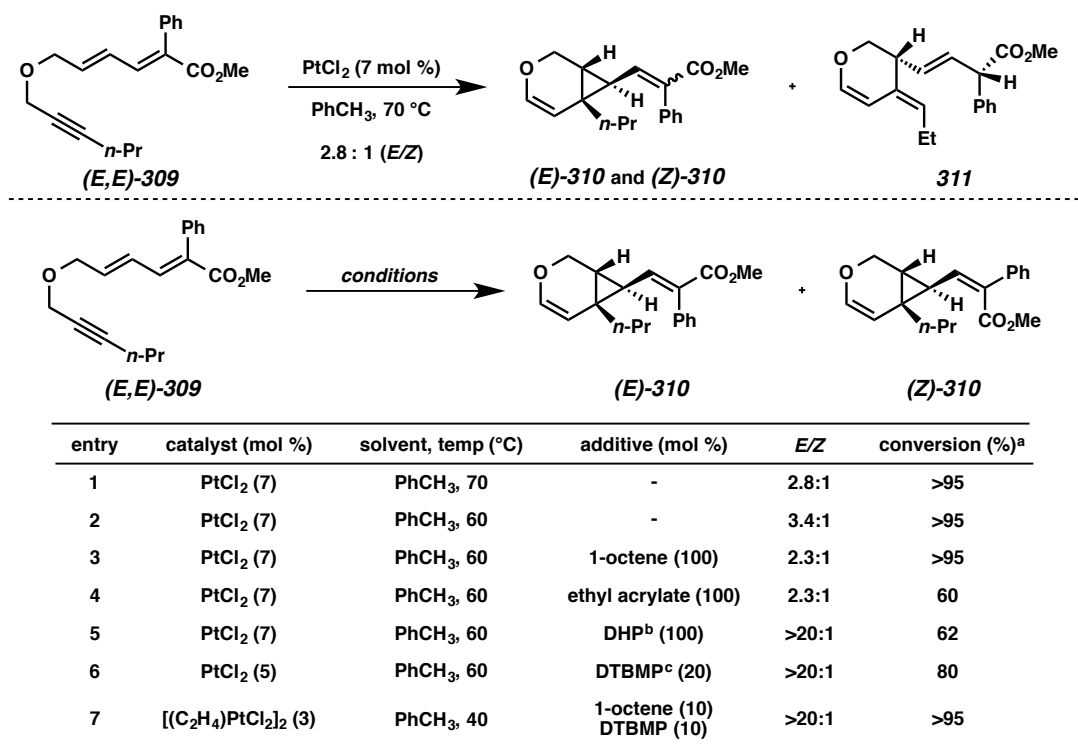
To begin our new sequence, Horner-Wadsworth-Emmons olefination of previously utilized enal **292** with phosphonate ester **308**⁵ affords a 3:1 mixture of alkene isomers, favoring our desired product ((*E,E*)-**309**, Scheme 5.4.2).⁶



Scheme 5.4.2. Synthesis of Dienyne (*E,E*)-**309**.

With (*E,E*)-**309** in hand, we were ready to attempt our proposed key step. On diene (*E,E*)-**309**, our standard cycloisomerization conditions (7 mol % PtCl_2 in toluene at 70 °C) provided none of our desired

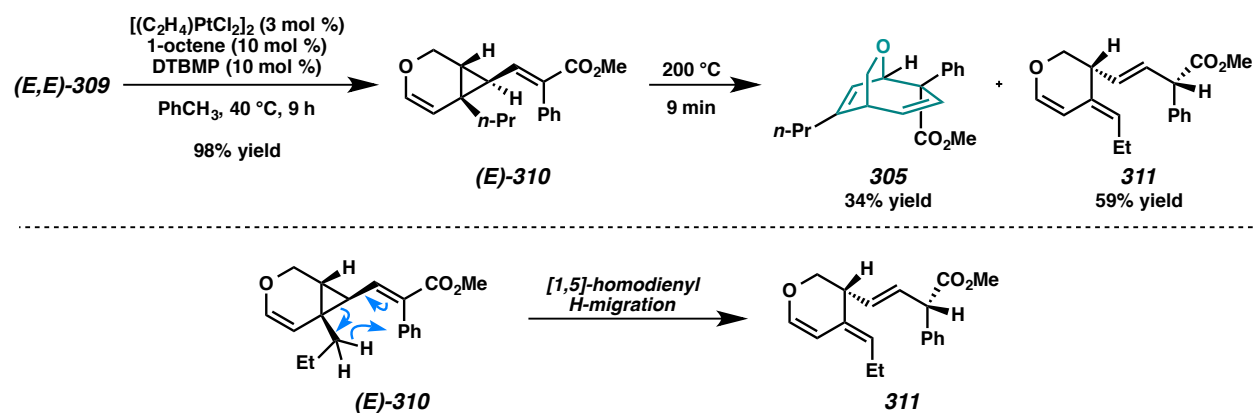
bicyclic product and a mixture of cycloisomerization isomers slightly favoring our desired product ((*E*)-**310**, Figure 5.4.1). Oddly, triene **311** was also isolated in *ca.* 15% yield.⁷ After this initial attempt, we decided to study each step—the cycloisomerization and the [3,3]-sigmatropic rearrangement—independently. First, we performed an optimization in order to see if the product *E/Z* ratio could be improved. Cooling the reaction down to 60 °C leads to a slight increase in *E/Z* selectivity as well as suppression of triene product **311** (entry 2).⁸ We next screened three electronically different alkene additives: 1-octene, ethyl acrylate, and 3,4-dihydropyran (DHP). Addition of the electronically neutral olefin, 1-octene, to the reaction mixture results in no change to the *E/Z* selectivity (entry 3) while addition of electron deficient ethyl acrylate leads to incomplete consumption of starting material (entry 4). Interestingly, addition of DHP (an electron rich olefin) provides excellent selectivity (entry 5); we reasoned that trace acid may be causing the alkene isomerization and that the enol ether is acting as a weak base. Indeed, addition of catalytic 2,6-di-*tert*-butyl-4-methylpyridine (DTBMP) confirms that base is necessary to eliminate alkene isomerization (entry 6). Thus, our optimized conditions, 3 mol % Zeise's Dimer in toluene at 40 °C with catalytic 1-octene and DTBMP, provides cycloisomerization product (*E*)-**310** in excellent conversion and *E/Z* ratio (>95%, >20:1, entry 7).⁹



a. Determined by ¹H NMR; b. 3,4-dihydropyran; c. 2,6-Di-*tert*-butyl-4-methylpyridine

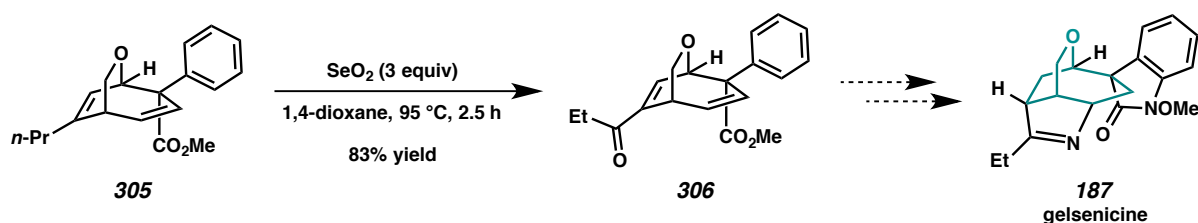
Figure 5.4.1. Initial Result and Optimization of Cycloisomerization on Dienyne (E,E) -309.

Thus, when dienyne (E,E) -309 is subjected to our optimized cycloisomerization conditions, cyclopropane precursor (E) -310 is isolated in 98% yield as a single diastereomer (Scheme 5.4.3). Unfortunately, when divinylcyclopropane (E) -310 is heated under a number of conditions, we again observe varying amounts of triene 311 along with our desired [3,3]-rearrangement product (305). Triene 311 likely arises from a [1,5]-homodienyl hydrogen migration, which can be a competing process in divinylcyclopropane rearrangements.¹⁰ Our optimal conditions (neat at 200 $^\circ\text{C}$ for 9 minutes) provide 34% yield of desired bicyclic diene 305 as a single diastereomer.



Scheme 5.4.3. Cycloisomerization/[3,3]-Sigmatropic Rearrangement and Potential [1,5]-Homodiényl Pathway.

Now, all that is necessary to provide our desired common precursor (**306**) is an oxidation of the trisubstituted alkene to the enone. This allylic oxidation is accomplished by the treatment of bicyclic **205** with excess selenium dioxide in 1,4-dioxane at 95 °C, providing enone **306** in 63% yield (Scheme 5.4.4). With enone **306** in hand, we have constructed our hypothesized common intermediate. We have initially targeted the total synthesis of a Gelsedine type alkaloid, gelsenicine (**187**).

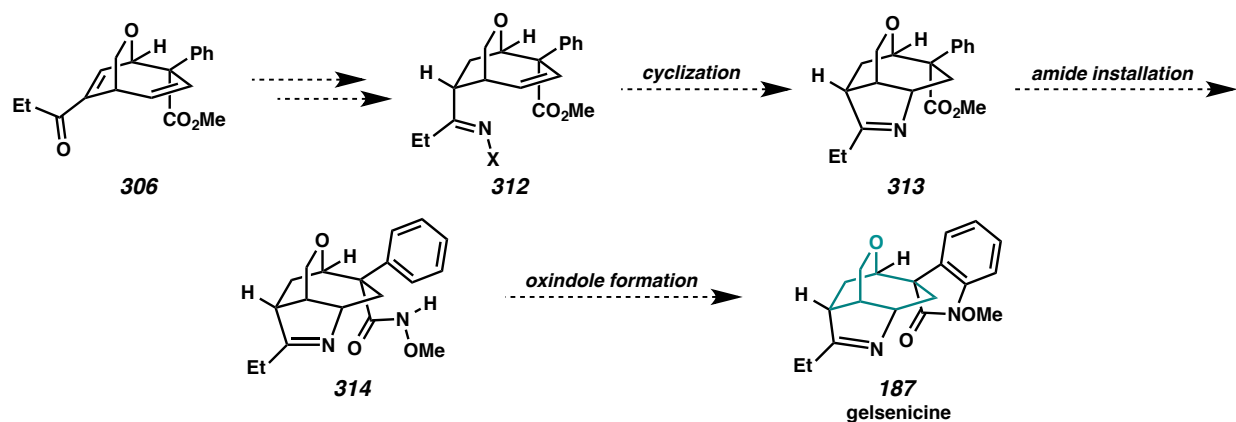


Scheme 5.4.4. Allylic Oxidation: Synthesis of the Hypothesized Common Intermediate (**306**).

5.4.3 Endgame Strategy

To construct gelsenicine (**187**), we propose the synthetic sequence shown below (Scheme 5.4.5). First, synthesis of activated iminyl **312** would be accomplished by a conjugate reduction of enone **303**, and conversion to an iminyl species. Cyclization of this activated iminyl compound (**212**) onto the

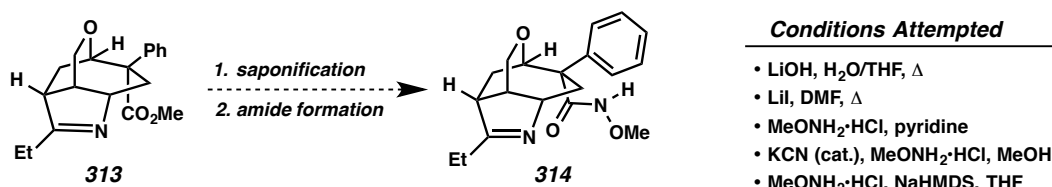
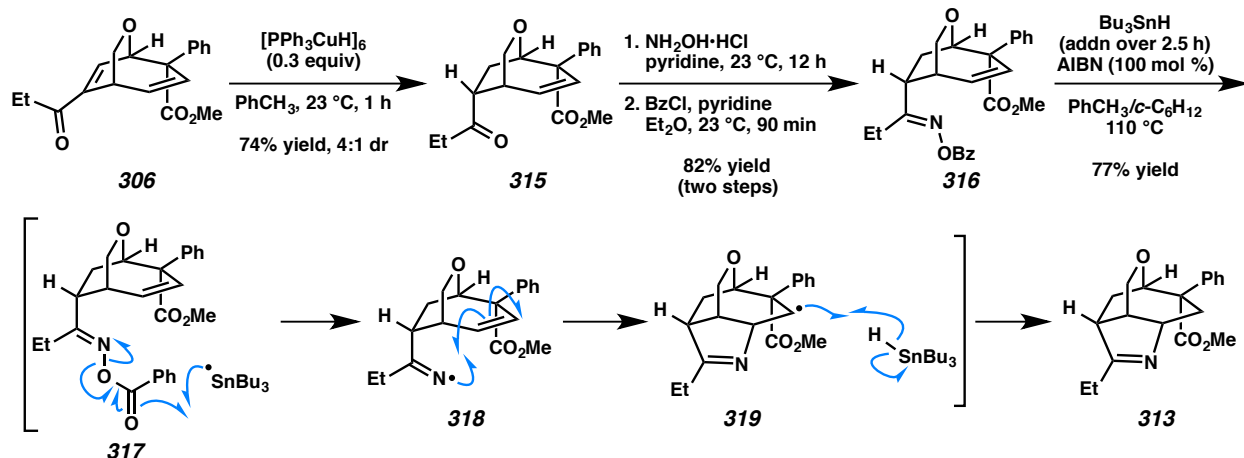
pendant alkene would provide pyrroline **313**.¹¹ Finally, conversion of ester **313** to *N*-methoxyamide **314** followed by cyclization would provide the oxindole ring¹² and gelsenicine (**187**) in efficient manner.



Scheme 5.4.5. Endgame Strategy to Gelsenicine (**187**).

5.4.4 Second Generation Endgame Synthetic Studies

This approach to gelsenicine showed initial promise. Chemoselective conjugate reduction of enone **306** with Stryker's Reagent ($[PPh_3CuH]_6$)¹³ provides desired ketone **315** in 74% yield and 4:1 dr (Scheme 5.4.6).¹⁴ Oxime formation and acylation with benzoyl chloride allows us to easily access radical cyclization precursor **316** in 82% yield over two steps. Slow addition of tributyltin hydride to benzoyl oxime **316** in the presence of 2,2'-azobis(2-methylpropionitrile) (AIBN) affords pyrroline intermediate **313** in 77% yield.¹⁵ This reaction is proposed to occur via tributyltin radical activation of the benzoyl group, generating iminyl radical **318**. Then, 5-*exo* cyclization produces 2' carbon radical intermediate **319**, and subsequent hydrogen radical abstraction from tributyltin hydride delivers our observed product (**313**). Unfortunately, all attempts to convert ester **313** to *N*-methoxyamide **314** have proven unsuccessful.

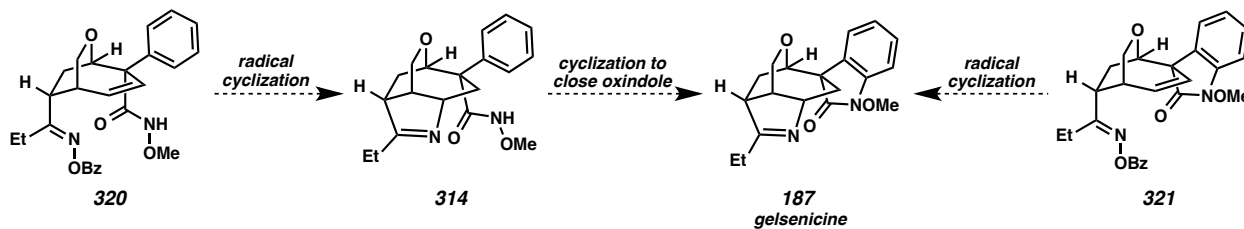


Scheme 5.4.6. Synthetic Route to Pyrrole **313** and Failed Attempts to Access Amide **314**.

5.5 Third Generation Approach

5.5.1 Revised Endgame Synthetic Strategy

The failure met with attempted saponification and amide formation on pyrrole **313** required us to further modify our synthetic plan. We trust that if the amide or oxindole are present before the radical cyclization, we can finish the synthesis. In this vein, benzoyl oxime **320** could provide cyclized product **314** via radical cyclization (Scheme 5.5.1), and subsequent oxindole closure would produce our target (**187**). Conversely, oxindole-containing substrate **321** could undergo radical cyclization and provide gelsenicine (**187**) in orthogonal manner.

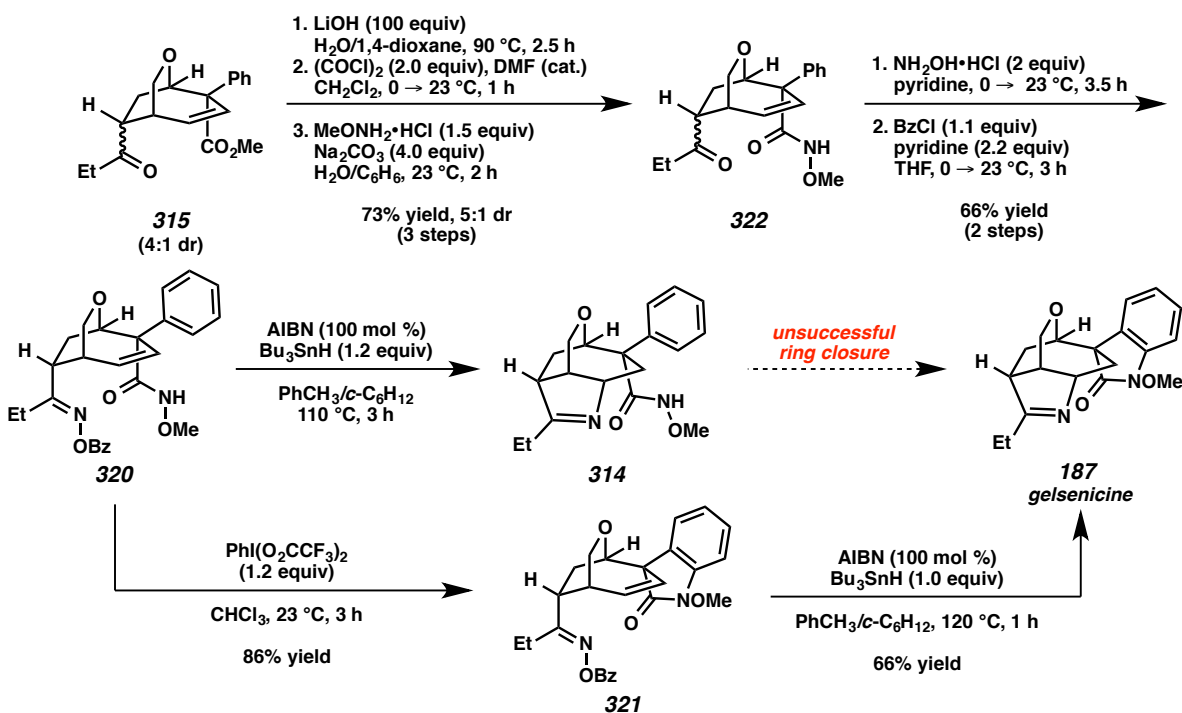


Scheme 5.5.1. Two Options for Finishing Gelsenicine (**187**).

5.5.2 Successful Endgame Strategy: The Total Synthesis of (\pm)-Gelsenicine

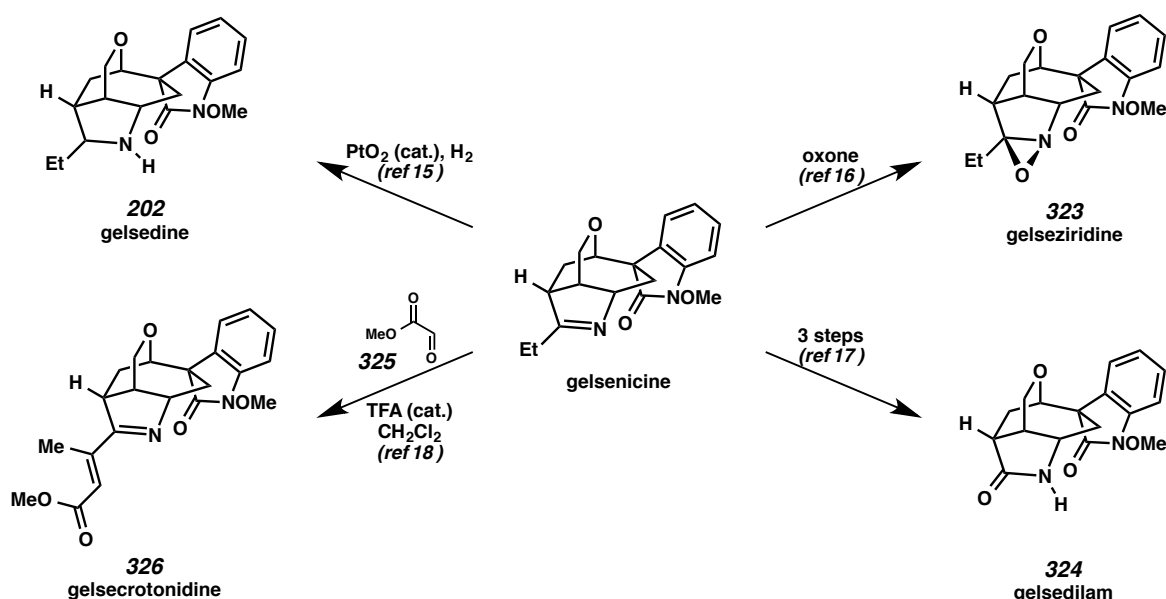
Following the new proposed endgame, ester **315** is efficiently converted into *N*-methoxyamide **322** in a three step sequence (Scheme 5.5.2). Then, treatment of amide **322** with hydroxylamine hydrochloride in pyridine followed by benzoylation affords cyclization precursor **320** in 66% yield over two steps. Radical cyclization of benzoyl oxime **320** provides pyrroline intermediate **314**. Sadly, we are unable to form the oxindole ring under a number of conditions. This is most likely a result of the labile nature of the pyrroline ring, much like the results with ester **313**.

We next attempted to end the synthesis by closing the oxindole ring first, as this would make the pyrroline closure the final step and hopefully eliminate complications. When amide **320** is treated with bis(trifluoroacetoxy)iodobenzene ($\text{PhI}(\text{O}_2\text{CCF}_3)_2$) in chloroform, oxindole **321** is obtained in 86% yield.^{12d} The target alkaloid, gelsenicine (**187**), is then obtained in 66% yield upon subjecting benzoyl oxime **321** to slow addition of AIBN and tributyltin hydride at 120 °C for 1 hour. This constitutes the first total synthesis of gelsenicine (**187**) in 14 steps. Importantly, the synthesis was completed without the use of protecting groups. This is additionally the shortest synthesis of a Gelsedine type alkaloid to date.



Scheme 5.5.2. Successful Endgame to Gelsenicine (**187**).

In completing this synthesis of gelsenicine (**187**), we have also achieved the formal synthesis of at least four other natural products of the Gelsedine type (Scheme 5.5.3). First, platinum oxide-catalyzed hydrogenation of gelsenicine (**187**) provides gelsedine (**202**).¹⁶ Conversely, oxidation of the pyrroline ring with oxone affords gelseziridine (**323**).¹⁷ In a three-step sequence, gelsedilam (**324**) is accessed from gelsenicine.¹⁸ Finally, an acid-mediated aldol reaction with methyl glyoxylate (**325**) provides gelsecrotonidine (**326**).^{19,20}



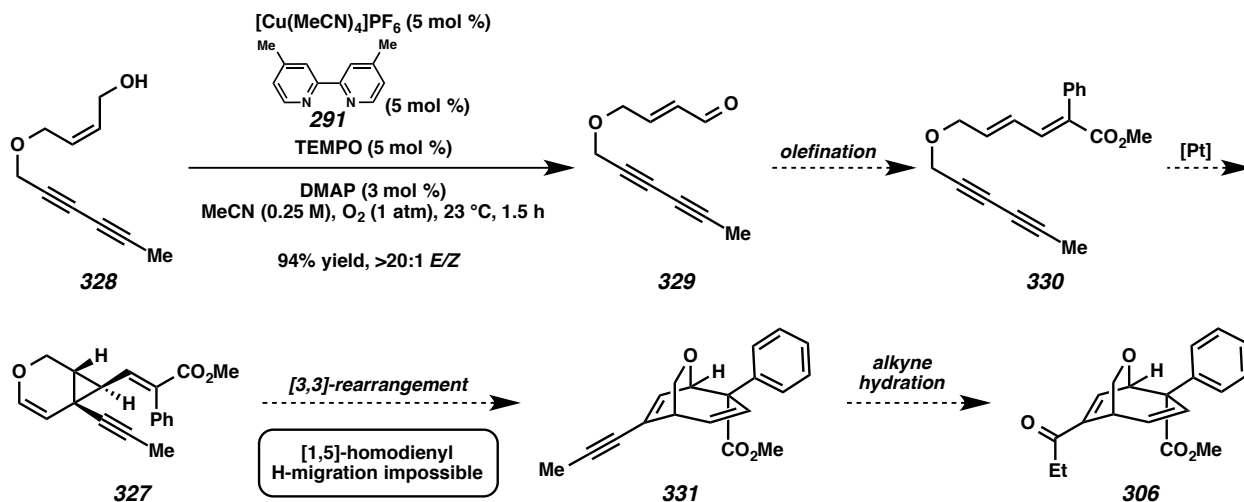
Scheme 5.5.3. Divergent Conversion of Gelsenicine to Additional Alkaloids.

5.6 Future Opportunities and Preliminary Results

5.6.1 Improving the Key Step Efficiency

One disappointing aspect to our efficient synthesis is the 34% yield in the [3,3]-sigmatropic rearrangement step. The likely culprit, as previously stated, is a facile [1,5]-homodienyl hydrogen migration. Currently, we are attempting to eliminate this pathway by removal of the hydrogen atoms alpha to the cyclopropane in the form of cyclopropane **327**. Our current efforts and proposed future steps are shown below in Scheme 5.6.1. Using a similar approach to our synthesis of gelsenicine, oxidation of allylic alcohol **328** occurs in 94% yield. Following olefination of aldehyde **329**, we will be ready to

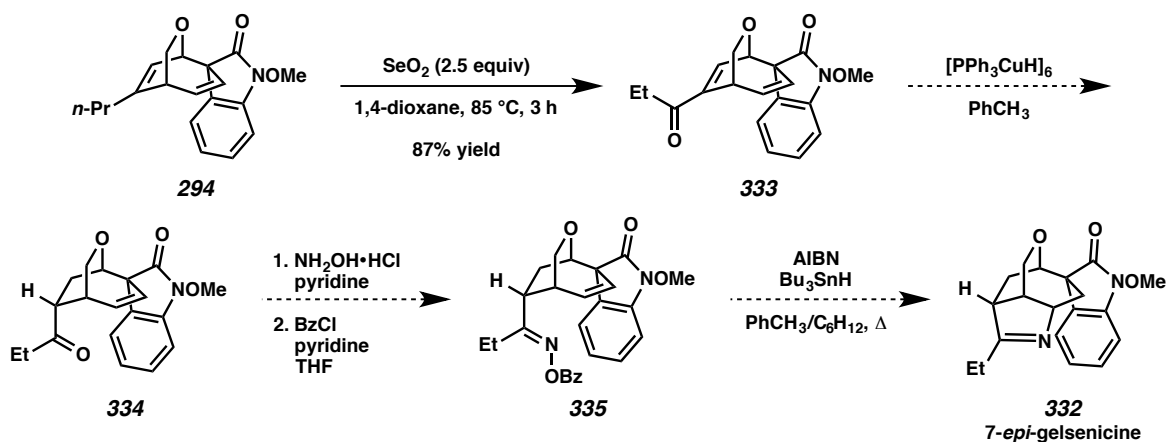
attempt cycloisomerization on compound **330**. If cycloisomerization occurs without complications, cyclopropane **327** can no longer undergo the undesired pathway. We are hopeful this will lead to increased yields of our desired bicycle **331**. We finally propose an alkyne hydration step to overlap with our previously synthesized intermediate **306**. If this modification of the synthesis is successful, more studies concerning additional targets can commence.



Scheme 5.6.1. Current Route to Overcome [1,5]-Homodienyl Hydrogen Migration Byproduct.

5.6.2 Synthetic Analogs: Towards a Synthesis of 7-Epi-Gelsenicine

Synthetic analogs of natural products sometimes have interesting biological properties.²¹ Thus, we are curious if the chemistry used in our synthesis of gelsenicine could be utilized in the synthesis of 7-*epi*-gelsenicine (**332**). While this work is preliminary, we are currently 4 steps from 7-*epi*-gelsenicine (Scheme 5.6.2). As previously described, we can access bicyclic diene **294** in 4 steps. Allylic oxidation with selenium dioxide provides enone **333** in good yield. Subsequent conjugate reduction with Stryker's Reagent would afford ketone **334**. We are hopeful that conversion to the benzoyl oxime (**335**) and radical cyclization to give 7-*epi*-gelsenicine (**332**) will be successful and completed in the near future. This would constitute a synthesis of 7-*epi*-gelsenicine (**332**) in nine steps, again without the use of protecting groups. Biological testing of this compound and others could prove fruitful.



Scheme 5.6.2. Progress Towards 7-*Epi*-Gelsenicine (**332**).

While our modular approach could lend itself to synthesizing analogs to gelsenicine, it may also be pertinent to see where we could utilize unsuccessful/dead end intermediates. This includes compounds we have already accessed, such as ester **313** or methoxyamide **314** (Figure 5.6.1). These intermediates, while not utilized in our synthesis, contain complex structures and their biological properties may be worth exploring.

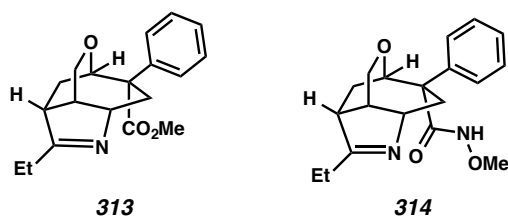
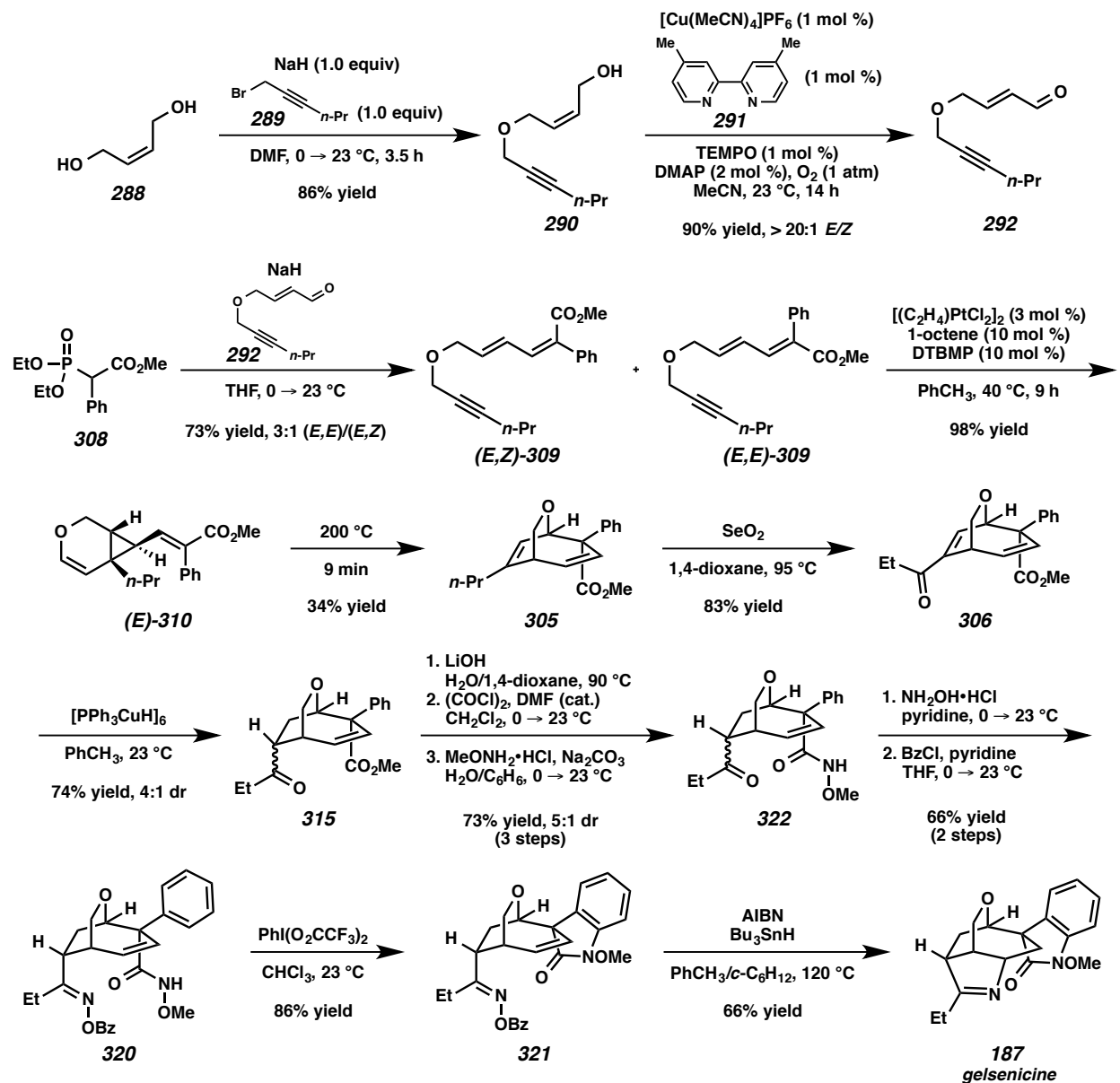


Figure 5.6.1. Advanced Intermediates **313** and **314** as Analogs.

5.7 Conclusion

Throughout this synthetic exploration, we have encountered many obstacles. In overcoming these roadblocks, we have gained insights that ultimately allowed for the successful racemic synthesis of gelsenicine. Our 14 step synthesis of gelsenicine is shown in Scheme 5.7.1. Key steps include the tandem cycloisomerization/[3,3]-sigmatropic rearrangement to provide bicycle **305**, hypervalent iodine-promoted oxindole cyclization (**320** \rightarrow **321**), and late stage radical cyclization of benzoyl oxime **321** to close the

pyrrolone ring and provide the natural product. The synthesis was completed without the need of protecting groups. Additionally, the synthesis of gelsenicine also constitutes the formal synthesis of four other natural products. We anticipate this synthesis will serve as a platform for the synthesis of a large number of Gelsemium alkaloids.



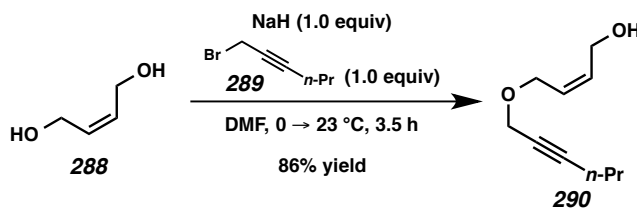
Scheme 5.7.1 Total Synthesis of Gelsenicine (**187**).²²

5.6 Experimental Section

5.6.1 Materials and Methods

Reactions were performed under an argon atmosphere unless otherwise noted. Tetrahydrofuran, diethyl ether, dichloromethane, acetonitrile, and toluene were purified by passing through activated alumina columns. All other solvents and reagents were used as received unless otherwise noted. Commercially available chemicals were purchased from Alfa Aesar (Ward Hill, MA), Sigma-Aldrich (St. Louis, MO), Oakwood Products (West Columbia, SC), Strem (Newburyport, MA), and TCI America (Portland, OR). Qualitative TLC analysis was performed on 250 mm thick, 60 Å, glass backed, F254 silica (Silicycle, Quebec City, Canada). Visualization was accomplished with UV light and exposure to iodine, exposure to *p*-anisaldehyde solution followed by heating, or exposure to KMnO₄ solution followed by heating. Flash chromatography was performed using Silicycle silica gel (230-400 mesh). ¹H NMR spectra were acquired on a Varian Mercury 300 (at 300 MHz), a Varian 400 (at 400 MHz), or an Agilent Inova 500 (at 500 MHz) and are reported relative to SiMe₄ (δ 0.00). ¹³C NMR spectra were acquired on a Varian 400 MR (at 100 MHz) or an Agilent Inova 500 (at 125 MHz) and are reported relative to SiMe₄ (δ 0.0). All IR spectra were obtained on an ATR-ZnSe as thin films with a Nicolet iS-50 FT-IR spectrometer and are reported in wavenumbers (ν). High resolution mass spectrometry (HRMS) data were acquired by the Colorado State University Central Instrument Facility on an Agilent 6210 TOF LC/MS.

5.6.2 Experimental Data Relevant to the Total Synthesis of Gelsenicine (187)



To a solution of *cis*-2-butene-1,4-diol (**288**, 6.30 mL, 76.7 mmol, 2.50 equiv) in anhydrous DMF (82.5 mL, 0.9 M) at 0 °C was added NaH (1.23 g, 60% dispersion in mineral oil, 30.7 mmol, 1.00 equiv) in two portions. The ice water bath was removed and the resulting mixture was stirred until the effervescence

ceased (*ca.* 30 min). To this mixture was added bromide **289**²³ (4.94 g, 30.7 mmol), as a solution in anhydrous THF (10 mL), dropwise over 10 min, and the reaction mixture was stirred at 23 °C for 2 h. The reaction was quenched with H₂O (100 mL) and poured into EtOAc (100 mL). The layers were separated and the aqueous layer was extracted with EtOAc (2 x 100 mL). The combined organic layers were washed successively with 10% aqueous LiCl solution (2 x 50 mL) and brine (50 mL). The organic layer was then dried over MgSO₄, filtered, and concentrated under reduced pressure. The resulting residue was purified via flash chromatography (2:1 hexanes/EtOAc), affording allylic alcohol **290** (4.44 g, 86% yield).

Alcohol 290:

Physical State: colorless oil.

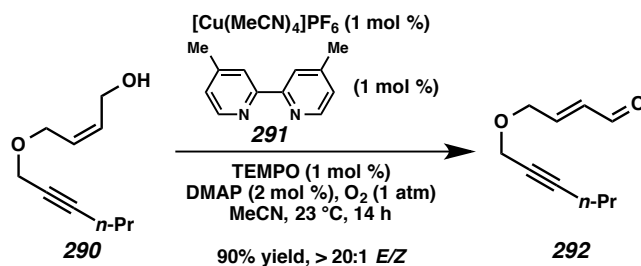
R_f: 0.32 (2:1 hexanes/EtOAc, KMnO₄).

IR (film): 3415 (br), 2965, 2224, 1243, 1069, 1032 cm⁻¹.

HRMS (APCI+): *m/z* calc. for (M + H)⁺ [C₁₀H₁₆O₂ + H]⁺: 169.1223, found 169.1228.

¹H NMR (400 MHz, CDCl₃): δ 5.84 (dtt, *J* = 11.3, 6.4, 1.4 Hz, 1H), 5.70 (dtt, *J* = 11.3, 6.4, 1.4 Hz, 1H), 4.23 (d, *J* = 6.1 Hz, 2H), 4.15-4.13 (comp m, 4H), 2.20 (tt, *J* = 7.1, 2.2 Hz, 2H), 1.78-1.68 (s, 1H), 1.54 (app. sextet, *J* = 7.2 Hz, 2H), 0.99 (t, *J* = 7.4 Hz, 3H).

¹³C NMR (100 MHz, CDCl₃): δ 132.9, 128.1, 87.5, 75.8, 64.8, 58.9, 58.0, 22.2, 20.9, 13.6.



To a solution of allylic alcohol **290** (2.00 g, 11.9 mmol) in MeCN (60.0 mL, 0.2 M) was added tetrakis(acetonitrile)copper (I) hexafluorophosphate (44.3 mg, 0.120 mmol, 1.00 mol %), 4,4'-dimethyl-2,2'-bipyridine (**291**, 21.9 mg, 0.120 mmol, 1.00 mol %), 2,2,6,6-tetramethyl-1-piperidinyloxy (18.6 mg, 0.210 mmol, 1.00 mol %) and 4-dimethylaminopyridine (30.0 mg, 0.240 mmol, 2.00 mol %). The

reaction vessel was then sparged with an O₂ balloon (bubbling through the solution) for 10 min and placed under 1 atm of O₂ via a balloon (replaced as needed through out the reaction). The resulting mixture was stirred at 23 °C for 15 h. The reaction mixture was then diluted with H₂O (400 mL) and poured into pentane (350 mL). The layers were separated and the aqueous layer was extracted with pentane (2 x 350 mL). The combined organic layers were washed with brine (150 mL), dried over MgSO₄, filtered, and concentrated under reduced pressure. The resulting residue was purified by flash chromatography (9:1 → 4:1 hexanes/EtOAc), affording enal **292** (1.77 g, 90% yield, >20:1 *E/Z*).

Enal 292:

Physical State: colorless oil.

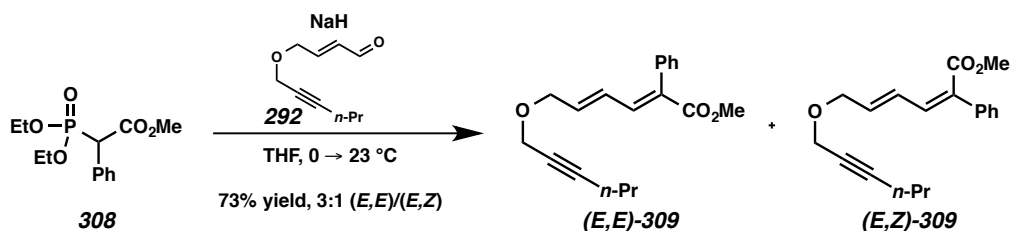
R_f: 0.38 (4:1 hexanes/EtOAc, KMnO₄).

IR (film): 2964, 2224, 1690, 1357, 1134, 1106 cm⁻¹.

HRMS (ESI+): *m/z* calc. for (M + H)⁺ [C₁₀H₁₄O₂ + H]⁺: 167.1067, found 167.1072.

¹H NMR (400 MHz, CDCl₃): δ 9.58 (d, *J* = 7.9 Hz, 1H), 6.84 (dt, *J* = 15.8, 4.3 Hz, 1H), 6.36 (ddt, *J* = 15.8, 7.9, 1.9 Hz, 1H), 4.33 (dd, *J* = 4.3, 1.9 Hz, 2H), 4.21 (t, *J* = 2.2 Hz, 2H), 2.20 (tt, *J* = 7.1, 2.2 Hz, 2H), 1.59-1.50 (m, 2H), 0.98 (t, *J* = 7.4 Hz, 3H).

¹³C NMR (100 MHz, CDCl₃): δ 193.0, 152.4, 131.8, 87.7, 75.0, 67.7, 58.6, 21.8, 20.6, 13.3.



To a solution of phosphonate ester **308**²⁴ (3.20 g, 11.2 mmol, 1.10 equiv) in anhydrous THF (12.5 mL, 0.9 M) under argon at 0 °C was added NaH (407 mg, 60% dispersion in mineral oil, 10.2 mmol, 1.00 equiv) in two portions. The ice water bath was removed and the resulting mixture was stirred until the effervescence ceased (*ca.* 25 min). The reaction mixture was then cooled back to 0 °C and enal **292** (1.69 g, 10.2 mmol) in THF (2.0 mL) was added dropwise over 2 min. After the addition, the ice water bath

was removed and the mixture was stirred at 23 °C for 4 h. The mixture was filtered through a long plug of silica (4:1 hexanes/EtOAc), and the solvent was removed under reduced pressure. The resulting residue was purified by repeated flash chromatography (15:1 → 9:1 hexanes/EtOAc), affording dienyne (*E,E*)-**309** (1.68 g, 55% yield) and (*E,Z*)-**309** (540 mg, 18% yield).

Dienyne (*E,E*)-309:

Physical State: colorless oil.

R_f: 0.36 (9:1 hexanes/EtOAc, anisaldehyde).

IR (film): 3056, 2961, 2223, 1710, 1639, 1592, 1433 cm⁻¹.

HRMS (ESI+): *m/z* calc. for (M + Na)⁺ [C₁₉H₂₂O₃ + Na]⁺: 321.1461, found 321.1473.

¹H NMR (400 MHz, CDCl₃): δ 7.46 (d, *J* = 10.9 Hz, 1H), 7.40-7.31 (comp m, 3H), 7.23-7.19 (m, 2H), 6.30 (ddt, *J* = 15.3, 10.8, 1.1 Hz, 1H), 6.21 (dt, *J* = 15.4, 5.5 Hz, 1H), 4.10-4.07 (comp m, 4H), 3.76 (s, 3H), 2.16 (tt, *J* = 7.1, 2.2 Hz, 2H), 1.50 (app. sextet, *J* = 7.2 Hz, 2H), 0.95 (t, *J* = 7.4 Hz, 3H).

¹³C NMR (100 MHz, CDCl₃): δ 168.2, 137.8, 136.9, 136.7, 133.5, 129.3, 128.5, 128.1, 127.7, 87.4, 75.9, 69.6, 58.2, 52.1, 22.2, 20.9, 13.7.

Dienyne (*E,Z*)-309:

Physical State: colorless oil.

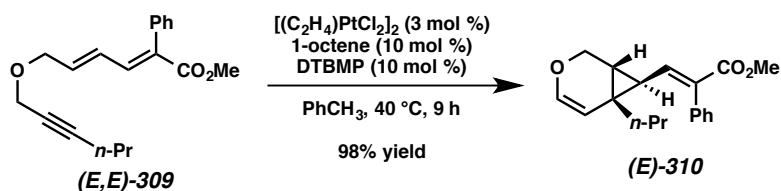
R_f: 0.38 (9:1 hexanes/EtOAc, anisaldehyde).

IR (film): 3057, 2961, 2282, 1710, 1638, 1594, 1433 cm⁻¹.

HRMS (ESI+): *m/z* calc. for (M + Na)⁺ [C₁₉H₂₂O₃ + Na]⁺: 321.1461, found 321.1467.

¹H NMR (400 MHz, CDCl₃): δ 7.35-7.29 (comp m, 5H), 7.01 (ddt, *J* = 15.2, 11.3, 1.5 Hz, 1H), 6.69 (d, *J* = 11.3 Hz, 1H), 6.10 (dtd, *J* = 15.3, 6.0, 0.8 Hz, 1H), 4.20 (dd, *J* = 6.0, 1.5 Hz, 2H), 4.17 (t, *J* = 2.2 Hz, 2H), 3.83 (s, 3H), 2.21 (tt, *J* = 7.1, 2.2 Hz, 2H), 1.60-1.51 (m, 2H), 1.00 (t, *J* = 7.4 Hz, 3H).

¹³C NMR (100 MHz, CDCl₃): δ 168.0, 139.8, 138.6, 135.0, 133.0, 130.3, 128.6, 128.1, 127.9, 87.5, 75.7, 69.4, 58.2, 52.4, 22.2, 20.9, 13.6.



To a solution of dienyne (*E,E*)-**309** (362 mg, 1.21 mmol) in anhydrous toluene (24.2 mL, 0.03 M) under argon was added 1-octene (18.9 μ L, 0.121 mmol, 10.0 mol %), DTBMP (24.8 mg, 0.121 mmol, 10.0 mol %), and Zeise's Dimer (21.0 mg, 0.0360 mmol, 3.00 mol %). This mixture was stirred at ambient temperature until all the solids were dissolved (*ca.* 20 min) then heated to 40 °C. After stirring for 9 h, the reaction mixture was cooled to 23 °C and triethylamine (150 μ L) was added. The mixture was concentrated under reduced pressure to *ca.* 5 mL and purified by flash chromatography (15:1 hexanes/EtOAc with 2% Et₃N), affording divinylcyclopropane (*E*)-**310** (354 mg, 98% yield).

Divinylcyclopropane (*E*)-**310**:

Physical State: colorless oil.

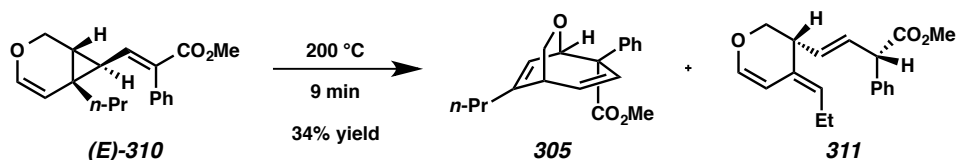
R_f: 0.38 (9:1 hexanes/EtOAc, KMnO₄).

IR (film): 2955, 1711, 1620, 1435, 1244, 1198 cm⁻¹.

HRMS (DART+): *m/z* calc. for (M + H)⁺ [C₁₉H₂₂O₃ + H]⁺: 299.1642, found 299.1645.

¹H NMR (400 MHz, CDCl₃): δ 7.39-7.28 (comp m, 3H), 7.25-7.23 (comp m, 2H), 6.78 (d, *J* = 10.8 Hz, 1H), 6.06 (d, *J* = 6.0 Hz, 1H), 5.02 (d, *J* = 6.0 Hz, 1H), 4.05 (d, *J* = 10.7 Hz, 1H), 3.81 (dd, *J* = 10.7, 2.3 Hz, 1H), 3.74 (s, 3H), 1.82 (dd, *J* = 10.8, 5.2 Hz, 1H), 1.67-1.40 (comp m, 6H), 0.96 (t, *J* = 7.1 Hz, 3H).

¹³C NMR (100 MHz, CDCl₃): δ 167.8, 144.0, 142.0, 135.2, 133.1, 130.3, 128.1, 127.6, 107.8, 61.4, 52.2, 35.7, 34.4, 32.7, 26.8, 20.7, 14.3.



To a flame dried vial under argon was charged divinylcyclopropane (*E*)-**310** (340 mg, 1.14 mmol) neat. The vessel was capped and placed on an aluminum heating block preheated to 200 °C and stirred at this temperature neat for 9 min, at which time the vial was cooled to 23 °C. The crude material was purified by flash chromatography (hexanes → 9:1 hexanes/EtOAc), affording desired bicycle **305** (114 mg, 34% yield) and triene **311** (200 mg, 59% yield).

Note: Extended reaction times reduced the yield of triene **311** but did not increase the conversion or yield of bicycle **305**.

Bicycle 305:

Physical State: colorless oil.

R_f: 0.39 (9:1 hexanes/EtOAc, KMnO₄).

IR (film): 2955, 1726, 1433, 1252, 1223, 955 cm⁻¹.

HRMS (APCI+): *m/z* calc. for (M + H)⁺ [C₁₉H₂₂O₃ + H]⁺: 299.1642, found 299.1649.

¹H NMR (400 MHz, CDCl₃): δ 7.46 (d, *J* = 7.3 Hz, 2H), 7.37-7.33 (m, 2H), 7.29 (d, *J* = 6.9 Hz, 1H), 6.37 (dd, *J* = 11.1, 8.6 Hz, 1H), 5.94 (dd, *J* = 6.1, 1.5 Hz, 1H), 5.81 (dd, *J* = 11.1, 2.3 Hz, 1H), 4.88 (dd, *J* = 6.1, 2.2 Hz, 1H), 4.06 (dd, *J* = 8.1, 1.1 Hz, 1H), 3.66 (s, 3H), 3.59 (dd, *J* = 8.1, 2.5 Hz, 1H), 2.65 (dd, *J* = 8.6, 1.5 Hz, 1H), 2.14 (t, *J* = 7.5 Hz, 2H), 1.53-1.46 (m, 2H), 0.91 (t, *J* = 7.3 Hz, 3H).

¹³C NMR (100 MHz, CDCl₃): δ 172.6, 151.0, 141.6, 132.6, 130.2, 128.5, 127.5, 126.9, 122.2, 69.4, 61.4, 52.2, 38.5, 37.9, 20.3, 13.7.

Triene 311:

Note: ¹H NMR contains 5-10% of **305**

Physical State: yellow oil.

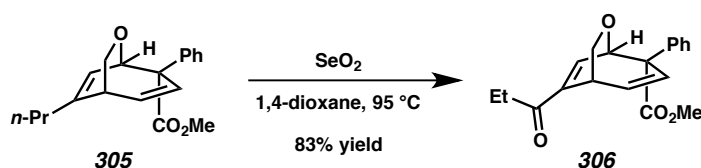
R_f: 0.48 (9:1 hexanes/EtOAc, KMnO₄).

IR (film): 2960, 1811, 1736, 1488, 1225, 1048, 926 cm⁻¹.

HRMS (DART+): *m/z* calc. for (M + NH₄)⁺ [C₁₉H₂₂O₃ + NH₄]⁺: 316.1907, found 316.1913.

¹H NMR (400 MHz, CDCl₃): δ 7.37-7.31 (comp m, 4H), 7.30-7.24 (m, 1H), 6.47 (dd, *J* = 6.2, 1.3 Hz, 1H), 6.16 (t, *J* = 10.3 Hz, 1H), 5.56 (dd, *J* = 6.2, 0.7 Hz, 1H), 5.45 (t, *J* = 10.3 Hz, 1H), 5.00 (td, *J* = 7.3, 0.8 Hz, 1H), 4.63 (d, *J* = 9.8 Hz, 1H), 3.80 (dd, *J* = 10.3, 4.1 Hz, 1H), 3.68 (s, 3H), 3.59 (t, *J* = 9.8 Hz, 1H), 3.44-3.37 (m, 1H), 2.19-2.04 (m, 2H), 0.98 (t, *J* = 7.5 Hz, 3H).

¹³C NMR (100 MHz, CDCl₃): δ 173.0, 145.3, 139.1, 129.6, 129.5, 129.0, 128.7, 127.8, 127.5, 124.7, 101.2, 69.8, 52.4, 50.0, 38.3, 20.5, 14.4.



To a solution of bicyclic **305** (231 mg, 0.772 mmol) in 1,4-dioxane (7.74 mL, 0.1 M) under argon was added selenium dioxide (258 mg, 2.32 mmol, 3.00 equiv). The resulting mixture was sealed and heated to 95 °C. After stirring for 2.5 h at 95 °C, the reaction mixture was allowed to cool to 23 °C, diluted with hexanes and filtered through a short plug of silica (2:1 hexanes/EtOAc). The solvent was removed under reduced pressure and the crude material was purified by flash chromatography (10:1 hexanes/EtOAc), affording enone **306** (201 mg, 83% yield).

Note: If the reaction is stopped short of completion, the allylic alcohol intermediate is observed in varying quantities in ¹H NMR of the crude reaction mixture. Alcohol *R_f*: 0.15 (4:1 hexanes/EtOAc, KMnO₄).

Enone 306:

Physical State: colorless oil.

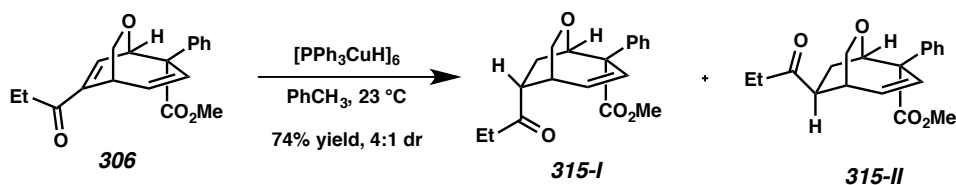
R_f: 0.40 (4:1 hexanes/EtOAc, KMnO₄).

IR (film): 2953, 1723, 1672, 1377, 1254, 1224, 1195 cm⁻¹.

HRMS (ESI⁺): *m/z* calc. for (M + H)⁺ [C₁₉H₂₀O₄ + H]⁺: 313.1434, found 313.1433.

¹H NMR (400 MHz, CDCl₃): δ 7.43-7.30 (comp m, 5H), 6.45 (dd, *J* = 11.1, 8.7 Hz, 1H), 5.80 (dd, *J* = 11.1, 2.1 Hz, 1H), 5.06 (dd, *J* = 6.3, 2.1 Hz, 1H), 4.17 (dd, *J* = 8.4, 1.0 Hz, 1H), 3.67 (s, 3H), 3.66-3.63 (m, 1H), 3.58 (dd, *J* = 8.4, 2.8 Hz, 1H), 2.84-2.68 (m, 2H), 1.15 (t, *J* = 7.3 Hz, 3H).

¹³C NMR (100 MHz, CDCl₃): δ 165.5, 147.4, 138.8, 133.9, 129.3, 128.6, 127.7, 126.5, 76.4, 69.7, 61.2, 52.3, 30.9, 29.9, 8.3.



In an N₂-filled glovebox, enone **306** (189 mg, 0.605 mmol) and Stryker's Reagent (356 mg, 0.182 mmol, 0.300 equiv) were taken up in toluene (6.72 mL, 0.09 M), sealed with a rubber septum and electrical tape, and removed from the glovebox. The resulting mixture was stirred sealed for 1 h. The septum was removed, and after stirring open to air for *ca.* 30 min, the mixture was filtered through silica (2:1 hexanes/EtOAc). The solvent removed under reduced pressure and the crude material was purified by flash chromatography (9:1 → 4:1 hexanes/EtOAc), affording ketones **315-I** (115.8 mg, 61% yield) and **315-II** (24.4 mg, 13% yield) as separable diastereomers.

Enone 315-I:

Note: The ¹H and ¹³C NMR spectra have a minor impurity of triphenylphosphine. ¹H NMR: δ 7.36 (s, 15 H); ¹³C NMR: δ 137.4, 133.7, 128.6, 128.5.

Physical State: colorless oil.

R_f: 0.47 (2:1 hexanes/EtOAc, KMnO₄).

IR (film): 3054, 2936, 1725, 1434, 1223 cm⁻¹.

HRMS (APCI+): *m/z* calc. for (M + H)⁺ [C₁₉H₂₂O₄ + H]⁺: 315.1591, found 315.1595.

¹H NMR (300 MHz, CDCl₃): δ 7.45-7.39 (comp m, 2H), 7.34-7.26 (comp m, 3H), 6.30 (dd, *J* = 10.9, 7.8 Hz, 1H), 6.24-6.18 (m, 1H), 4.91 (dd, *J* = 8.4, 1.7 Hz, 1H), 3.77-3.67 (m, 2H), 3.64 (s, 3H), 2.63-2.52 (m, 1H), 2.51-2.43 (m, 2H), 2.11-2.03 (m, 1H), 1.07 (t, *J* = 7.3 Hz, 3H).

¹³C NMR (100 MHz, CDCl₃): δ 210.9, 173.1, 134.0, 129.7, 129.1, 127.6, 126.5, 74.1, 70.0, 64.7, 52.7, 47.6, 33.4, 33.2, 27.1, 7.9.

Enone 315-II:

Note: The ¹H and ¹³C NMR spectra have a minor impurity of triphenylphosphine. ¹H NMR: δ 7.36 (s, 15 H); ¹³C NMR: δ 137.4, 133.7, 128.6, 128.5.

Physical State: colorless oil.

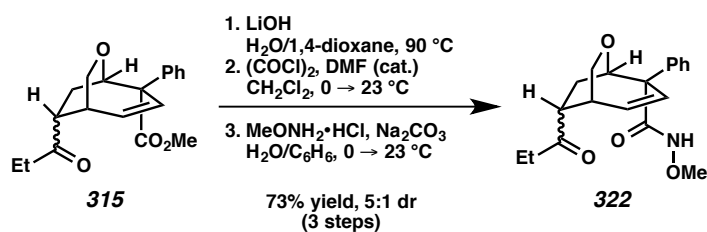
R_f: 0.57 (2:1 hexanes/EtOAc, KMnO₄).

IR (film): 3053, 2935, 2874, 1724, 1434, 1222 cm⁻¹.

HRMS (DART+): *m/z* calc. for (M + NH₄)⁺ [C₁₉H₂₂O₄ + NH₄]⁺: 332.1856, found 332.1865.

¹H NMR (300 MHz, CDCl₃): δ 7.44-7.40 (m, 2H), 7.34-7.28 (comp m, 3H), 6.40 (dd, *J* = 10.8, 8.8 Hz, 1H), 6.11 (dd, *J* = 10.9, 1.9 Hz, 1H), 4.67 (app. d, *J* = 6.2 Hz, 1H), 3.84 (dd, *J* = 10.0, 2.8 Hz, 1H), 3.74-3.71 (m, 1H), 3.70 (s, 3H), 2.98-2.93 (m, 1H), 2.72-2.69 (m, 1H), 2.63-2.43 (comp m, 3H), 2.34 (dd, *J* = 13.4, 10.4 Hz, 1H), 1.08 (t, *J* = 7.3 Hz, 3H).

¹³C NMR (100 MHz, CDCl₃): δ 211.0, 173.3, 141.8, 134.0, 131.7, 127.4, 126.8, 74.2, 65.2, 64.2, 52.5, 47.1, 33.8, 32.8, 25.9, 8.2.



To a solution of enone **315** (80.1 mg, 0.255 mmol) in 1,4-dioxane (2.55 mL, 0.1 M) and H₂O (2.00 mL, 0.128 M) at 23 °C was added lithium hydroxide (611 mg, 25.5 mmol, 100 equiv). This mixture was heated to 90 °C and stirred at this temperature for 2.5 h. The mixture was cooled with an ice water bath and 1 M HCl_(aq) was added dropwise until the pH was *ca.* 3. This mixture was then poured into EtOAc (20 mL) and the layers were separated. The aqueous layer was extracted with EtOAc (2 x 30 mL). The combined organic layers were washed with brine (20 mL). The organic layer was then dried over MgSO₄, filtered, and concentrated under reduced pressure. The resulting residue was azeotroped with toluene (3 x 1 mL) and taken on crude (100 mg).

Crude acid R_f: 0.09 (1:1 hexanes/Et₂O, KMnO₄).

A solution of crude carboxylic acid in anhydrous CH₂Cl₂ (3.19 mL, 0.0800 M to **315**) under argon was cooled to 0 °C and oxalyl chloride (43.7 μL, 0.510 mmol, 2.00 equiv to **315**) was added. Dimethylformamide (*ca.* 2 μL, catalytic) was then added to the solution and the resulting mixture was stirred at 0 °C for 15 min, at which time the ice water bath was removed. After stirring at 23 °C for 2 h, the volatile materials were removed under reduced pressure. The resultant residue was azeotroped with toluene (3 x 1.5 mL) to provide crude acid chloride (112 mg).

Crude acid chlorides R_f: 0.38 (major) and 0.56 (minor) (1:1 hexanes/Et₂O, KMnO₄).

To a solution of *O*-methylhydroxylamine hydrochloride (31.9 mg, 0.383 mmol, 1.50 equiv to **315**) in benzene (1.19 mL, 0.21 M to **315**) and H₂O (2.00 mL, 0.13 M to **315**) stirring vigorously at *ca.* 0 °C was added sodium carbonate (108 mg, 1.02 mmol, 4.00 equiv to **315**). This was stirred for 10 min at 23 °C, and then crude acid chloride **315** in benzene (2.00 mL, 0.13 M to **315**) was added. The resulting biphasic mixture was stirred at 23 °C for 40 min, poured into aqueous HCl (25 mL, 0.05 M) and extracted with EtOAc (3 x 30 mL). The combined organic layers were washed with brine (1 x 20 mL), dried over

MgSO₄, and filtered. After removal of the solvent under reduced pressure, the crude material was purified by flash chromatography (4:1 → 1:1 hexanes/EtOAc), affording amide **322** (61.1 mg, 73% yield).

Amide 322:

Physical State: colorless film.

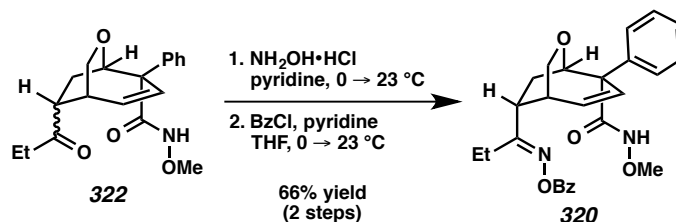
R_f: 0.33 (1:1 hexanes/EtOAc, KMnO₄).

IR (film): 3159 (br), 2926, 1708, 1670, 1438, 1118 cm⁻¹.

HRMS (DART+): *m/z* calc. for (M + H)⁺ [C₁₉H₂₃NO₄ + H]⁺: 330.1700, found 330.1703.

¹H NMR (400 MHz, CDCl₃) major reported: δ 8.12 (br s, 1H), 7.52 (d, *J* = 7.4 Hz, 2H), 7.36 (app. t, *J* = 7.5 Hz, 2H), 7.31-7.28 (m, 1H), 6.32 (dd, *J* = 10.8, 8.4 Hz, 1H), 5.86 (d, *J* = 10.6 Hz, 1H), 4.83 (dd, *J* = 8.2, 2.0 Hz, 1H), 3.77-3.72 (comp m, 3H), 3.68 (br s, 3H), 2.95 (td, *J* = 9.2, 3.1 Hz, 1H), 2.80-2.75 (m, 1H), 2.63-2.43 (comp m, 4H), 2.33 (dd, *J* = 14.5, 8.7 Hz, 1H), 1.08 (t, *J* = 7.3 Hz, 3H).

¹³C NMR (100 MHz, CDCl₃) major reported: δ 211.5, 141.0, 134.8, 128.9, 128.8, 127.7, 127.1, 74.4, 69.5, 64.2, 63.5, 47.9, 33.53, 33.45, 27.0, 7.9.



To a solution of amide **322** (42.5 mg, 0.129 mmol) in pyridine (1.29 mL, 0.1 M) at 0 °C was added hydroxylamine hydrochloride (17.9 mg, 0.258 mmol, 2.00 equiv). The reaction mixture was stirred at 23 °C for 3.5 h, at which time it was poured into 1 M aqueous HCl saturated with NaCl (10 mL) and EtOAc (20 mL). The layers were separated and the aqueous layer was extracted with EtOAc (2 x 20 mL). The combined organic layers were washed with brine (10 mL), dried over MgSO₄, and filtered. The crude material (59.2 mg) was taken on immediately.

To a solution of crude oxime and pyridine (22.9 μL , 0.248 mmol, 2.2 equiv) in THF (1.29 mL, 0.1 M) at 0 $^{\circ}\text{C}$ was added benzoyl chloride (16.5 μL , 0.142 mmol, 1.1 equiv). After stirring for 3 h at 23 $^{\circ}\text{C}$, 1 M HCl (aq) (5.0 mL) was added. This was diluted with EtOAc (15 mL). The layers were separated and the aqueous layer was extracted with EtOAc (2 x 15 mL). The combined organic layers were washed with brine (10 mL), dried over MgSO_4 , and filtered. The crude material was purified by flash chromatography (4:1 \rightarrow 1:1 hexanes/EtOAc), affording benzoate **320** (38.1 mg, 66% yield over two steps).

Benzoate 320:

Physical State: white powder.

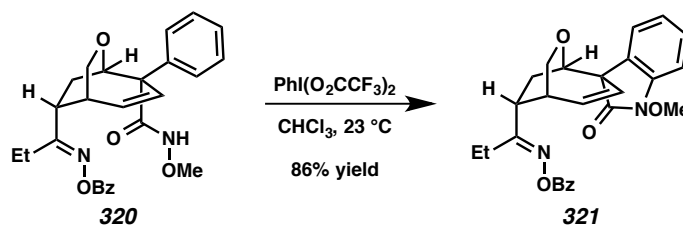
R_f: 0.33 (1:1 hexanes/EtOAc, KMnO_4).

IR (film): 3254 (br), 2936, 2876, 1741, 1662, 1246 cm^{-1} .

HRMS (APCI+): m/z calc. for $(\text{M} + \text{Na})^+ [\text{C}_{26}\text{H}_{28}\text{N}_2\text{O}_5 + \text{Na}]^+$: 471.1890, found 471.1882.

^1H NMR (400 MHz, CDCl_3): δ 8.96 (s, 1H), 8.07 (d, $J = 7.2$ Hz, 2H), 7.63-7.58 (comp m, 3H), 7.50 (t, $J = 7.7$ Hz, 2H), 7.36 (t, $J = 7.6$ Hz, 2H), 7.29 (d, $J = 7.3$ Hz, 1H), 6.38 (dd, $J = 10.8, 8.5$ Hz, 1H), 6.03 (dd, $J = 10.9, 1.8$ Hz, 1H), 4.86 (dd, $J = 8.0, 1.7$ Hz, 1H), 3.86 (d, $J = 9.4$ Hz, 1H), 3.82 (dd, $J = 9.7, 3.9$ Hz, 1H), 3.67 (s, 3H), 3.05 (ddd, $J = 9.6, 8.1, 3.0$ Hz, 1H), 2.82-2.78 (m, 1H), 2.68-2.59 (m, 1H), 2.51 (q, $J = 7.5$ Hz, 2H), 2.37 (dd, $J = 14.7, 8.1$ Hz, 1H), 1.25 (t, $J = 7.6$ Hz, 3H).

^{13}C NMR (100 MHz, CDCl_3): δ 172.3, 171.9, 164.4, 141.2, 134.8, 133.5, 129.7, 129.2, 128.9, 128.8, 128.6, 127.5, 127.4, 74.8, 69.9, 63.9, 63.7, 41.1, 34.3, 28.3, 23.0, 11.1.



To a solution of oxime **320** (5.0 mg, 0.011 mmol) in chloroform (140 μL , 0.08 M) under argon was added bis(trifluoroacetoxy)iodobenzene (5.8 mg, 0.013 mmol, 1.2 equiv). After stirring at ambient temperature

for 3 h, solid NaHCO₃ (ca. 50 mg, excess) was added. This mixture was stirred for 5 min and filtered through a short silica plug (eluent = 1:1 hexanes/EtOAc). The solvent was removed under reduced pressure and the resulting residue was purified by flash chromatography (3:1 → 2:1 hexanes/EtOAc), affording oxindole **321** (4.2 mg, 86% yield).

Oxindole 321:

Physical State: white solid.

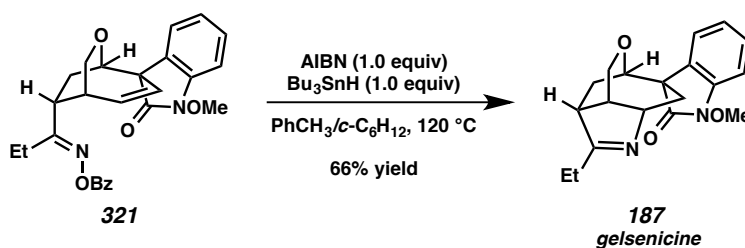
R_f: 0.24 (2:1 hexanes/EtOAc, KMnO₄).

IR (film): 2939, 2877, 1724, 1616, 1464, 1246, 1064 cm⁻¹.

HRMS (DART+): *m/z* calc. for (M + H)⁺ [C₂₆H₂₆N₂O₅ + H]⁺: 447.1914, found 447.1917.

¹H NMR (400 MHz, CDCl₃): δ 8.08 (d, *J* = 7.1 Hz, 2H), 7.60 (t, *J* = 7.4 Hz, 1H), 7.49 (t, *J* = 7.6 Hz, 2H), 7.36-7.31 (m, 2H), 7.13 (t, *J* = 7.6 Hz, 1H), 7.01 (d, *J* = 7.6 Hz, 1H), 6.49 (dd, *J* = 10.6, 8.4 Hz, 1H), 5.33 (dd, *J* = 10.6, 2.0 Hz, 1H), 4.34 (d, *J* = 9.4 Hz, 1H), 4.17 (dd, *J* = 9.5, 4.3 Hz, 1H), 4.01 (s, 3H), 3.83 (dd, *J* = 8.5, 2.0 Hz, 1H), 3.25 (td, *J* = 9.6, 2.7 Hz, 1H), 3.07 (dd, *J* = 14.1, 9.6 Hz, 1H), 3.00 (dt, *J* = 8.0, 3.8 Hz, 1H), 2.77 (dq, *J* = 13.6, 7.1 Hz, 1H), 2.57 (dq, *J* = 13.6, 7.1 Hz, 1H), 2.44 (dt, *J* = 14.1, 9.1 Hz, 1H), 1.30 (t, *J* = 7.6 Hz, 3H).

¹³C NMR (100 MHz, CDCl₃): δ 172.1, 171.7, 164.0, 138.9, 136.3, 133.3, 129.7, 129.5, 128.9, 128.7, 127.2, 126.5, 123.6, 107.4, 73.5, 72.4, 63.6, 60.7, 40.7, 34.2, 25.0, 21.8, 11.2.



To a degassed solution of benzoyl oxime **321** (2.5 mg, 0.0056 mmol) in toluene (400 μL, 0.014 M) under argon at 120 °C was added a degassed solution of azobisisobutyronitrile (1.0 mg, 0.0056 mmol, 1.0 equiv) and tributyltin hydride (1.5 μL, 0.0056 mmol, 1.0 equiv) in cyclohexane (100 μL) via syringe

pump over 45 min. The reaction mixture was stirred for an additional 15 min at 120 °C, removed from the heat, and allowed to cool to ambient temperature. The solvent was removed under reduced pressure and the crude residue was purified by flash chromatography (6:4:3 petroleum ether/Et₂O/MeOH → 6:4:4 petroleum ether/Et₂O/MeOH), affording gelsenicine (**187**, 1.2 mg, 66% yield).

Gelsenicine (187):

Physical State: white solid.

R_f: 0.10 (3:1:1 petroleum ether/Et₂O/MeOH, I₂ → KMnO₄).

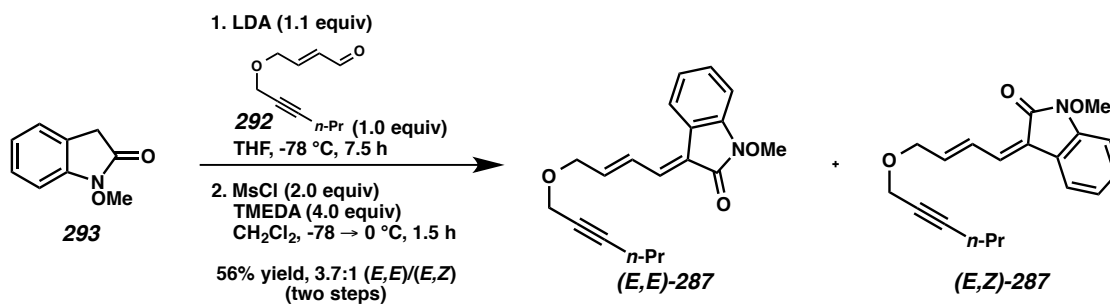
IR (film): 2922, 2852, 1726, 1645, 1616, 1465, 1111 cm⁻¹.

HRMS (APCI⁺): *m/z* calc. for (M + H)⁺ [C₁₉H₂₂N₂O₃ + H]⁺: 327.1703, found 327.1695.

¹H NMR (500 MHz, CDCl₃): δ 7.54 (d, *J* = 7.2 Hz, 1H), 7.07 (td, *J* = 7.6, 1.0 Hz, 1H), 6.88 (d, *J* = 7.9 Hz, 1H), 4.44-4.39 (m, 1H), 4.28 (dd, *J* = 4.7, 2.3 Hz, 2H), 3.94 (s, 3H), 3.73 (dd, *J* = 4.5, 1.8 Hz, 1H), 2.86 (t, *J* = 9.3 Hz, 1H), 2.72 (dq, *J* = 16.5, 8.0 Hz, 1H), 2.59-2.55 (m, 1H), 2.37 (dd, *J* = 11.4, 3.4 Hz, 2H), 2.29 (dd, *J* = 15.3, 1.8 Hz, 1H), 2.13 (ddd, *J* = 14.9, 10.1, 4.8 Hz, 1H), 1.29 (t, *J* = 7.4 Hz, 3H).

¹³C NMR (125 MHz, CDCl₃): 128.0, 124.7, 123.3, 106.5, 74.9, 72.6, 63.3, 62.1, 42.5, 39.8, 37.7, 27.0, 25.7, 10.0.

5.6.3 Experimental Data Relevant to the First Generation Approach



To a solution of diisopropylamine (300 μL, 2.17 mmol, 1.20 equiv) in THF (6.16 mL, 0.35 M to DIPA) at -78 °C was added *n*-butyllithium (790 μL, 2.5 M in hexanes, 1.99 mmol, 1.10 equiv) dropwise over *ca.* 1 min. The resulting solution was stirred at -78 °C for 30 min and then oxindole **293**²⁵ (295 mg, 1.81 mmol,

1.00 equiv) in THF (1.38 mL, 1.3 M to **293**) was added dropwise over 5 min. The resulting solution was stirred at $-78\text{ }^{\circ}\text{C}$ for 2 h, at which time enal **292** (300 mg, 1.81 mmol) in THF (1.80 mL, 1.0 M to **292**) was added dropwise over 5 min. The resulting mixture was stirred at $-78\text{ }^{\circ}\text{C}$ for 5.5 h, at which time a dilute solution of AcOH in THF (*ca.* 0.5 M) was added. The solution was then allowed to warm to ambient temperature and poured into brine (50 mL). The layers were separated and the aqueous layer was extracted with EtOAc (3 x 30 mL). The combined organic layers were washed with brine (50 mL), dried over MgSO_4 , and filtered. The solvent was removed under reduced pressure and the resulting residue was taken on crude.

To a solution of crude alcohol in CH_2Cl_2 (25.5 mL, 0.06 M) at $-78\text{ }^{\circ}\text{C}$ was added MsCl (237 μL , 3.06 mmol) followed by TMEDA (918 μL , 6.12 mmol). The resulting mixture was stirred at $-78\text{ }^{\circ}\text{C}$ for 2 h then $0\text{ }^{\circ}\text{C}$ for 1.5 h, at which time H_2O (10 mL) was added. The layers were separated and the aqueous was extracted with EtOAc (3 x 55 mL). The combined organic layers were washed with 1 M HCl (15 mL), brine (20 mL), dried over MgSO_4 , and filtered. The solvent was removed under reduced pressure and the resulting residue was purified by flash chromatography (9:1 \rightarrow 3:1 hexanes/EtOAc), affording (*E,E*)-**287** (230 mg, 41% yield over two steps) and (*E,Z*)-**287** (66.7 mg, 12% yield over two steps) as separable olefin isomers.

Dienyne (*E,E*)-287:

Physical State: yellow oil.

R_f: 0.48 (2:1 hexanes/EtOAc, UV and KMnO_4).

IR (film): 2935, 2223, 1714, 1609, 1459, 1321, 1070 cm^{-1} .

HRMS (ESI+): *m/z* calc. for $(\text{M} + \text{H})^+$ [$\text{C}_{19}\text{H}_{21}\text{NO}_3 + \text{H}$] $^+$: 312.1594, found 312.1599.

^1H NMR (400 MHz, CDCl_3): δ 7.64 (d, $J = 7.6\text{ Hz}$, 1H), 7.35 (d, $J = 12.2\text{ Hz}$, 1H), 7.29 (td, $J = 7.7, 0.9\text{ Hz}$, 1H), 7.21-7.13 (m, 1H), 7.06 (td, $J = 7.7, 1.0\text{ Hz}$, 1H), 6.98 (d, $J = 7.8\text{ Hz}$, 1H), 6.47 (dt, $J = 14.9, 5.0\text{ Hz}$, 1H), 4.32 (dd, $J = 5.0, 1.7\text{ Hz}$, 2H), 4.25 (t, $J = 2.2\text{ Hz}$, 2H), 4.04 (s, 3H), 2.22 (tt, $J = 7.1, 2.2\text{ Hz}$, 2H), 1.56 (app. sextet, $J = 7.2\text{ Hz}$, 2H), 1.00 (t, $J = 7.4\text{ Hz}$, 3H).

^{13}C NMR (100 MHz, CDCl_3): δ 163.9, 143.5, 139.6, 135.8, 129.2, 126.0, 123.9, 123.2, 122.8, 119.1, 107.4, 87.8, 75.7, 69.1, 63.9, 58.7, 22.2, 20.9, 13.6.

Dienyne (*E,Z*)-287:

Physical State: orange oil.

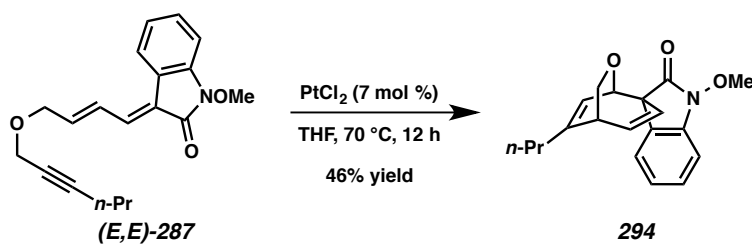
R_f: 0.62 (2:1 hexanes/EtOAc, UV and KMnO_4).

IR (film): 2935, 2218, 1706, 1612, 1463, 1046 cm^{-1} .

HRMS (ESI+): m/z calc. for $(\text{M} + \text{Na})^+ [\text{C}_{19}\text{H}_{21}\text{NO}_3 + \text{Na}]^+$: 334.1414, found 334.1421.

^1H NMR (400 MHz, CDCl_3): δ 7.96 (ddt, $J = 15.5, 11.5, 1.5$ Hz, 1H), 7.41 (d, $J = 7.4$ Hz, 1H), 7.27 (td, $J = 7.7, 1.0$ Hz, 1H), 7.13 (d, $J = 11.5$ Hz, 1H), 7.03 (td, $J = 7.6, 1.0$ Hz, 1H), 6.94 (d, $J = 7.7$ Hz, 1H), 6.33 (dtd, $J = 15.5, 6.1, 0.8$ Hz, 1H), 4.28 (dd, $J = 6.1, 1.5$ Hz, 2H), 4.19 (t, $J = 2.2$ Hz, 2H), 4.04 (s, 3H), 2.21 (tt, $J = 7.1, 2.2$ Hz, 2H), 1.55 (app. sextet, $J = 7.2$ Hz, 2H), 0.99 (t, $J = 7.4$ Hz, 3H).

^{13}C NMR (100 MHz, CDCl_3): δ 162.6, 142.0, 138.6, 136.0, 129.3, 127.7, 122.9, 122.6, 119.9, 119.6, 107.2, 87.6, 75.8, 69.6, 63.9, 58.4, 22.2, 20.9, 13.7.



To a solution of diene (*E,E*)-**287** (115.1 mg, 0.338 mmol) in anhydrous THF (4.83 mL, 0.07 M) under argon was added PtCl_2 (6.29 mg, 23.7 μmol , 7.0 mol %), and then the reaction was sealed. The resulting mixture was heated at 70 °C for 12 h, at which time it was removed from the heat and allowed to cool to ambient temperature. The solvent was removed under reduced pressure and the resulting residue was purified by flash chromatography (4:1 \rightarrow 2:1 hexanes/EtOAc), affording bicycle **294** (48.3 mg, 46% yield).

Bicycle 294:

Physical State: white solid.

R_f: 0.61 (1:1 hexanes/EtOAc, UV and KMnO₄).

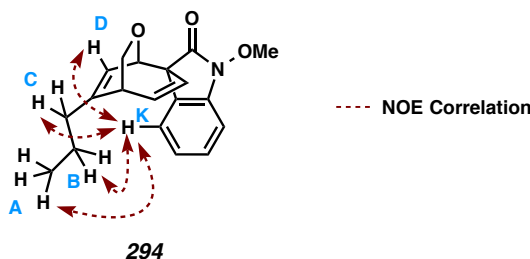
IR (film): 2925, 2853, 1727, 1613, 1463 cm⁻¹.

HRMS (DART+): *m/z* calc. for (M + H)⁺ [C₁₉H₂₁NO₃ + H]⁺: 312.1594, found 312.1599.

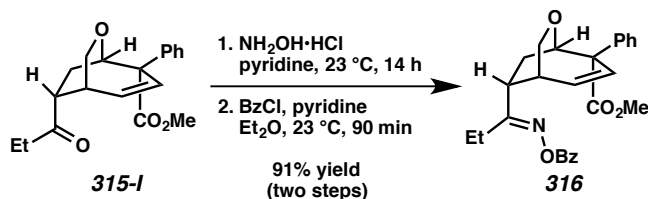
¹H NMR (500 MHz, CDCl₃): δ 7.29 (td, *J* = 7.7, 0.8 Hz, 1H), 7.08 (d, *J* = 7.2 Hz, 1H), 7.01-6.95 (comp m, 2H), 6.50 (dd, *J* = 10.5, 8.7 Hz, 1H), 5.75 (d, *J* = 6.3 Hz, 1H), 5.11 (dd, *J* = 10.5, 1.8 Hz, 1H), 4.40 (d, *J* = 8.2 Hz, 1H), 4.24 (dd, *J* = 6.3, 1.8 Hz, 1H), 4.05 (s, 3H), 3.74 (dd, *J* = 8.2, 3.0 Hz, 1H), 2.80 (app. d, *J* = 8.7 Hz, 1H), 2.25 (t, *J* = 7.5 Hz, 2H), 1.63-1.53 (m, 2H), 1.03 (t, *J* = 7.3 Hz, 3H).

¹³C NMR (125 MHz, CDCl₃): δ 173.4, 151.9, 140.0, 135.7, 129.0, 126.6, 126.0, 124.7, 122.7, 121.0, 107.6, 74.7, 69.4, 63.8, 57.9, 38.3, 38.0, 20.7, 14.2.

NOE Correlation Spectra: See Appendix three.



5.6.4 Additional Reactions



To a solution of amide **315-I** (115.0 mg, 0.366 mmol) in pyridine (3.66 mL, 0.1 M) at 23 °C was added hydroxylamine hydrochloride (28.0 mg, 0.402 mmol, 1.10 equiv). The reaction mixture was stirred at 23 °C for 14 h, at which time it was poured into 1 M aqueous HCl saturated with NaCl (10 mL) and EtOAc (20 mL). The layers were separated and the aqueous layer was extracted with EtOAc (2 x 20 mL). The

combined organic layers were washed with brine (10 mL), dried over MgSO₄, and filtered. After removal of the volatile materials, the resulting crude material (155 mg) was taken on immediately.

To a solution of crude oxime and pyridine (35.2 μL, 0.437 mmol, 1.2 equiv) in Et₂O (1.21 mL, 0.3 M) at 23 °C was added benzoyl chloride (46.6 μL, 0.400 mmol, 1.1 equiv). After stirring for 1.5 h at 23 °C, 1 M HCl (aq) (5.0 mL) was added. This was diluted with EtOAc (15 mL). The layers were separated and the aqueous layer was extracted with EtOAc (2 x 15 mL). The combined organic layers were washed with brine (10 mL), dried over MgSO₄, and filtered. The solvent was removed under reduced pressure and the crude material was purified by flash chromatography (4:1 hexanes/EtOAc), affording benzoate **316** (145.0 mg, 91% yield over two steps).

Benzoate 316:

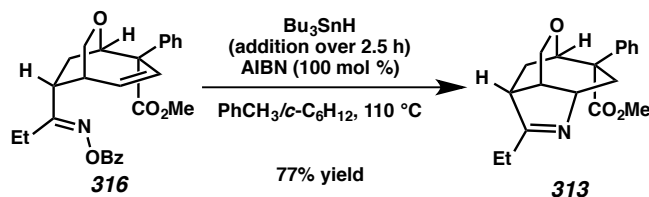
Physical State: white solid.

R_f: 0.33 (2:1 hexanes/EtOAc, KMnO₄).

IR (film): 2926, 1728, 1655, 1082, 1063 cm⁻¹.

HRMS (ESI⁺): *m/z* calc. for (M + H)⁺ [C₂₆H₂₇NO₅ + H]⁺: 434.1962, found 434.1966.

¹H NMR (300 MHz, CDCl₃): δ 8.09-8.02 (m, 2H), 7.60 (ddt, *J* = 8.5, 6.3, 1.8 Hz, 1H), 7.51-7.45 (comp m, 5H), 7.39-7.27 (comp m, 3H), 6.53 (dd, *J* = 10.9, 8.2 Hz, 1H), 6.31 (dd, *J* = 10.9, 2.0 Hz, 1H), 4.99 (dd, *J* = 8.5, 1.9 Hz, 1H), 3.80-3.73 (m, 2H), 3.63 (s, 3H), 3.04 (ddd, *J* = 10.5, 8.5, 2.1 Hz, 1H), 2.92-2.88 (m, 1H), 2.75-2.60 (m, 2H), 2.38 (dq, *J* = 13.6, 7.1 Hz, 1H), 1.95 (dd, *J* = 13.6, 10.3 Hz, 1H), 1.23 (t, *J* = 7.7 Hz, 3H).



To a solution of oxime **316** (30.0 mg, 69.2 μmol) in toluene (692 μL, 0.1 M) at 110 °C was added a solution of azobisisobutyronitrile (11.4 mg, 69.2 μmol, 100 mol %) and tributyltin hydride (22.3 μL, 83.0

μmol , 1.2 equiv) in cyclohexane (692 μL , 0.1 M) via syringe pump over 2.5 h. The reaction mixture was stirred for an additional 30 min at 110 $^{\circ}\text{C}$ then removed from the heat. The solvent was removed under reduced pressure and the crude residue purified by flash chromatography (6:2 petroleum ether/ Et_2O \rightarrow 6:2:1 petroleum ether/ Et_2O /MeOH), affording pyrroline **313** (17.6 mg, 77% yield).

Pyrroline **313**:

Note: The ^1H -NMR spectrum contains a small amount of a Bu_3Sn -containing impurity.

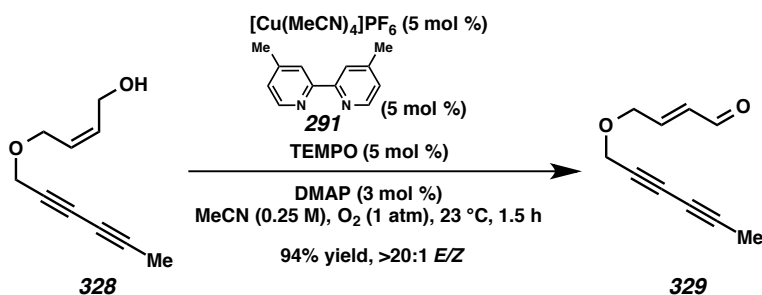
Physical State: white solid.

R_f: 0.23 (6:2:1 petroleum ether/ Et_2O /MeOH, I_2 then KMnO_4).

IR (film): 2926, 1719, 1639, 1445, 1212 cm^{-1} .

HRMS (ESI⁺): m/z calc. for $(\text{M} + \text{H})^+$ [$\text{C}_{19}\text{H}_{24}\text{NO}_3 + \text{H}$]⁺: 314.1751, found 314.1761.

^1H NMR (400 MHz, CDCl_3): δ 7.44 (d, $J = 7.8$ Hz, 2H), 7.30 (t, $J = 7.7$ Hz, 2H), 7.21 (t, $J = 7.2$ Hz, 1H), 4.55 (t, $J = 3.2$ Hz, 1H), 4.48-4.46 (m, 1H), 4.09 (app. qd, $J = 11.8, 2.2$ Hz, 2H), 3.59 (s, 3H), 3.07 (dd, $J = 14.6, 3.1$ Hz, 1H), 2.80 (t, $J = 9.1$ Hz, 1H), 2.59-2.49 (comp m, 2H), 2.43-2.35 (m, 2H), 2.30-2.21 (m, 2H), 1.18 (t, $J = 7.4$ Hz, 3H).



To a solution of allylic alcohol **328** (450 mg, 2.74 mmol) in MeCN (10.9 mL, 0.25 M) was added tetrakis(acetonitrile)copper (I) hexafluorophosphate (10.2 mg, 0.0274 mmol, 1.00 mol %), 4,4'-dimethyl-2,2'-bipyridine (**291**, 5.0 mg, 0.0274 mmol, 1.00 mol %), 2,2,6,6-tetramethyl-1-piperidinyloxy (4.28 mg, 0.0274 mmol, 1.00 mol %) and 4-dimethylaminopyridine (6.70 mg, 0.0548 mmol, 2.00 mol %). The reaction vessel was then sparged with an O_2 balloon (bubbling through the solution) for 10 min and placed under 1 atm of O_2 via a balloon (replaced as needed through out the reaction). The resulting

mixture was stirred at 23 °C for 21 h. The reaction mixture was then diluted with H₂O (40 mL) and poured into pentane (55 mL). The layers were separated and the aqueous layer was extracted with pentane (2 x 55 mL). The combined organic layers were washed with brine (40 mL), dried over MgSO₄, filtered, and concentrated under reduced pressure. The resulting residue was purified by flash chromatography (9:1 → 3:1 hexanes/EtOAc), affording enal **329** (350 mg, 79% yield, >20:1 *E/Z*).

Enal 329:

Physical State: slight yellow oil.

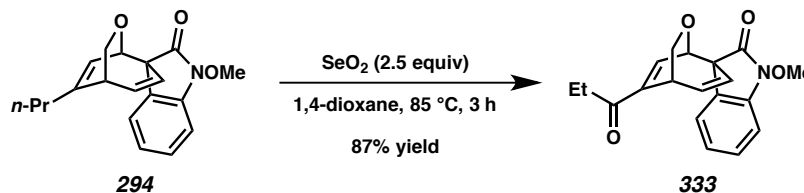
R_f: 0.25 (4:1 hexanes/EtOAc, anisaldehyde).

IR (film): 2845, 2258, 1688, 1352, 1108, 1029 cm⁻¹.

HRMS (ESI⁺): *m/z* calc. for (M + H)⁺ [C₁₀H₁₀O₂ + H]⁺: 163.0754, found 163.0750.

¹H NMR (400 MHz, CDCl₃): δ 9.58 (d, *J* = 7.9 Hz, 1H), 6.82 (dt, *J* = 15.8, 4.3 Hz, 1H), 6.34 (ddt, *J* = 15.8, 7.9, 1.9 Hz, 1H), 4.34 (dd, *J* = 4.3, 1.9 Hz, 2H), 4.28 (s, 2H), 1.95 (s, 3H).

¹³C NMR (100 MHz, CDCl₃): δ 193.2, 152.0, 132.2, 77.6, 72.4, 70.2, 68.3, 63.7, 58.9, 4.4.



To a solution of bicyclic enone **294** (25.4 mg, 0.0816 mmol) in 1,4-dioxane (1.17 mL, 0.07 M) under argon was added selenium dioxide (22.7 mg, 0.204 mmol, 2.50 equiv). The resulting mixture was sealed and heated to 85 °C. After stirring for 3 h at 85 °C, the reaction mixture was allowed to cool to 23 °C, diluted with hexanes, and immediately purified by flash chromatography (4:1 → 1:1 hexanes/EtOAc), affording enone **333** (23.0 mg, 87% yield).

Enone 333:

Physical State: white solid.

R_f: 0.44 (1:1 hexanes/EtOAc, KMnO₄).

HRMS (ESI+): m/z calc. for $(M + Na)^+ [C_{19}H_{19}NO_4 + Na]^+$: 348.1206, found 348.1199.

1H NMR (400 MHz, $CDCl_3$): δ 7.37-7.33 (m, 1H), 7.05-6.96 (comp m, 4H), 6.54 (dd, $J = 10.6, 8.8$ Hz, 1H), 5.13 (dd, $J = 10.6, 2.0$ Hz, 1H), 4.52-4.48 (m, 2H), 4.08 (s, 3H), 3.78-3.73 (comp m, 2H), 2.79 (q, $J = 7.3$ Hz, 2H), 1.21 (t, $J = 7.3$ Hz, 3H).

^{13}C NMR (100 MHz, $CDCl_3$): δ 197.5, 172.2, 148.2, 139.9, 136.1, 135.0, 129.4, 126.1, 125.2, 123.7, 122.9, 107.9, 74.1, 69.8, 63.7, 56.6, 31.0, 30.2, 29.7, 8.2.

CHAPTER FIVE NOTES AND REFERENCES

¹ Yield based on bromide **289**.

² Könning, D.; Hiller, W.; Christmann, M. *Org. Lett.* **2012**, *14*, 5258–5261.

³ The stereochemistry of the spirocenter was confirmed by ROESY ¹H-¹H NMR data.

⁴ Determined by ¹H NMR of the crude reaction mixture.

⁵ Geirsson, J. K. F.; Njardarson, J. T. *Tetrahedron Lett.* **1994**, *35*, 9071–9072.

⁶ Isomerization of our undesired dienyne ((*E,Z*)-**309**) can be completed with tributylphosphine at 55 °C, thus affording enrichment to our desired substrate ((*E,E*)-**309**).

⁷ The stereochemistry of triene **311** is unconfirmed.

⁸ The pathway responsible for the formation of triene **311** seems to be operable at temperatures greater than 60 °C.

⁹ It is our working hypothesis that 1-octene allows the catalyst to stay active and that DTBMP removes trace acid from the reaction mixture.

¹⁰ (a) Vshyvenko, J.W. Reed, T. Hudlicky and E. Piers, 5.22 Rearrangements of Vinylcyclopropanes, Divinylcyclopropanes, and Related Systems, In *Comprehensive Organic Synthesis II* (Second Edition), edited by Paul Knochel, Elsevier, Amsterdam, **2014**, pp. 999–1076; (b) Glass, D. S.; Boikess, R. S.; Winstein, S. *Tetrahedron Lett.* **1966**, *10*, 999–1008.

¹¹ The cyclization of activated oximes to provide pyrrolines is precedented. For two reviews, see: (a) Kitamura, M.; Narasaka, K. *Bull. Chem. Soc. Jpn.* **2008**, *81*, 539–547; (b) Zard, S. Z. *Synlett* **1996**, 1148–1154.

¹² There are reported methods for the conversion of *N*-methoxyamides to oxindoles. See: (a) Fleming, I.; Loreto, M. A.; Wallace, I. H. M.; Michael, J. P. *J. Chem. Soc., Perkin Trans. 1*, **1986**, 349–359; (b) Fleming, I.; Moses, R. C.; Tercel, M.; Ziv, J. *J. Chem. Soc., Perkin Trans. 1*, **1991**, 617–626; (c) Wasa, M.; Yu, J.-Q. *J. Am. Chem. Soc.* **2008**, *130*, 14058–14059; (d) Kikugawa, Y.; Kawase, M. *Chem. Lett.* **1990**, *4*, 581–582.

- ¹³ (a) Mahoney, W. S.; Brestensky, D. M.; Stryker, J. M. *J. Am. Chem. Soc.* **1988**, *110*, 291–293; (b) Lee, D.-w.; Yun, J. *Tetrahedron Lett.* **2005**, *46*, 2037–2039.
- ¹⁴ Epimerization of the undesired diastereomer can be accomplished in the presence of sodium methoxide in methanol to provide a thermodynamic mixture of ketones **315-I** (desired) and **315-II**.
- ¹⁵ Boivin, J.; Callier-Dublanchet, A.-C.; Quiclet-Sire, B.; Schiano, A.-M.; Zard, S. Z. *Tetrahedron* **1995**, *51*, 6517–6528.
- ¹⁶ Takayama, H.; Tominaga, Y.; Kitajima, M.; Aimi, N.; Sakai, S.-I. *J. Org. Chem.* **1994**, *59*, 4381–4385.
- ¹⁷ Qu, J.; Fang, L.; Ren, X.-D.; Liu, Y.; Yu, S.-S.; Li, L.; Bao, X.-Q.; Zhang, D.; Li, Y.; Ma, S.-G. *J. Nat. Prod.* **2013**, *76*, 2203–2209.
- ¹⁸ Kogure, N.; Ishii, N.; Kitajima, M.; Wongseripipatana, S.; Takayama, H. *Org. Lett.* **2006**, *8*, 3085–3088.
- ¹⁹ Yamada, Y.; Kitajima, M.; Kogure, N.; Takayama, H. *Tetrahedron* **2008**, *64*, 7690–7694.
- ²⁰ In similar fashion, gelsevanillidine has been synthesized from gelsenicine. See: Yamada, Y.; Kitajima, M.; Kogure, N.; Wongseripipatana, S.; Takayama, H. *Tetrahedron Lett.* **2009**, *50*, 3341–3344.
- ²¹ Wender, P. A.; Donnelly, A. C.; Loy, B. A.; Near, K. E.; Staveness, D. *Natural Products in Medicinal Chemistry* (Ed: S. Hanessian) Wiley-VCH, **2014**, Ch. 14, 475–544; (b) Wender, P. A.; Verma, V. A.; Paxton, T. J.; Pillow, T. H. *Acc. Chem. Res.* **2008**, 40–49.
- ²² This figure is reproduced from others throughout this chapter.
- ²³ Zhao, L.; Lu, X.; Xu, W. *J. Org. Chem.* **2005**, *70*, 4059–4063.
- ²⁴ Geirsson, J. K. F.; Njardarson, J. T. *Tetrahedron Lett.* **1994**, *35*, 9071–9072.
- ²⁵ Kawase, M.; Kitamura, T.; Kikugawa, Y. *J. Org. Chem.* **1989**, *54*, 3394–3403.

APPENDIX ONE

Spectra Relevant to Chapter Three

Cycloisomerization of Enynes as a Platform to Study Catalytic Reactivity

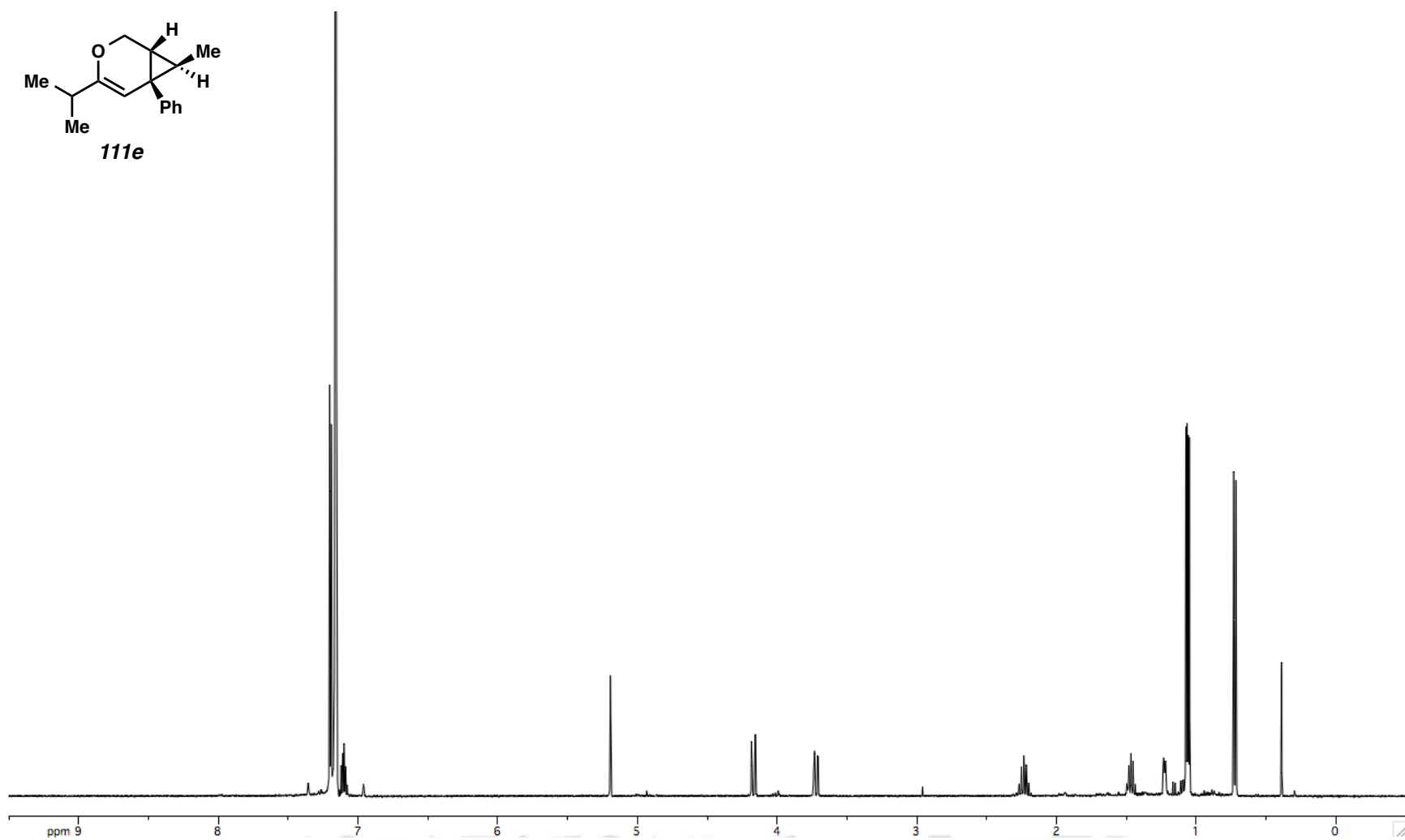
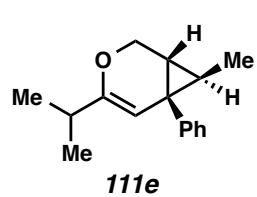
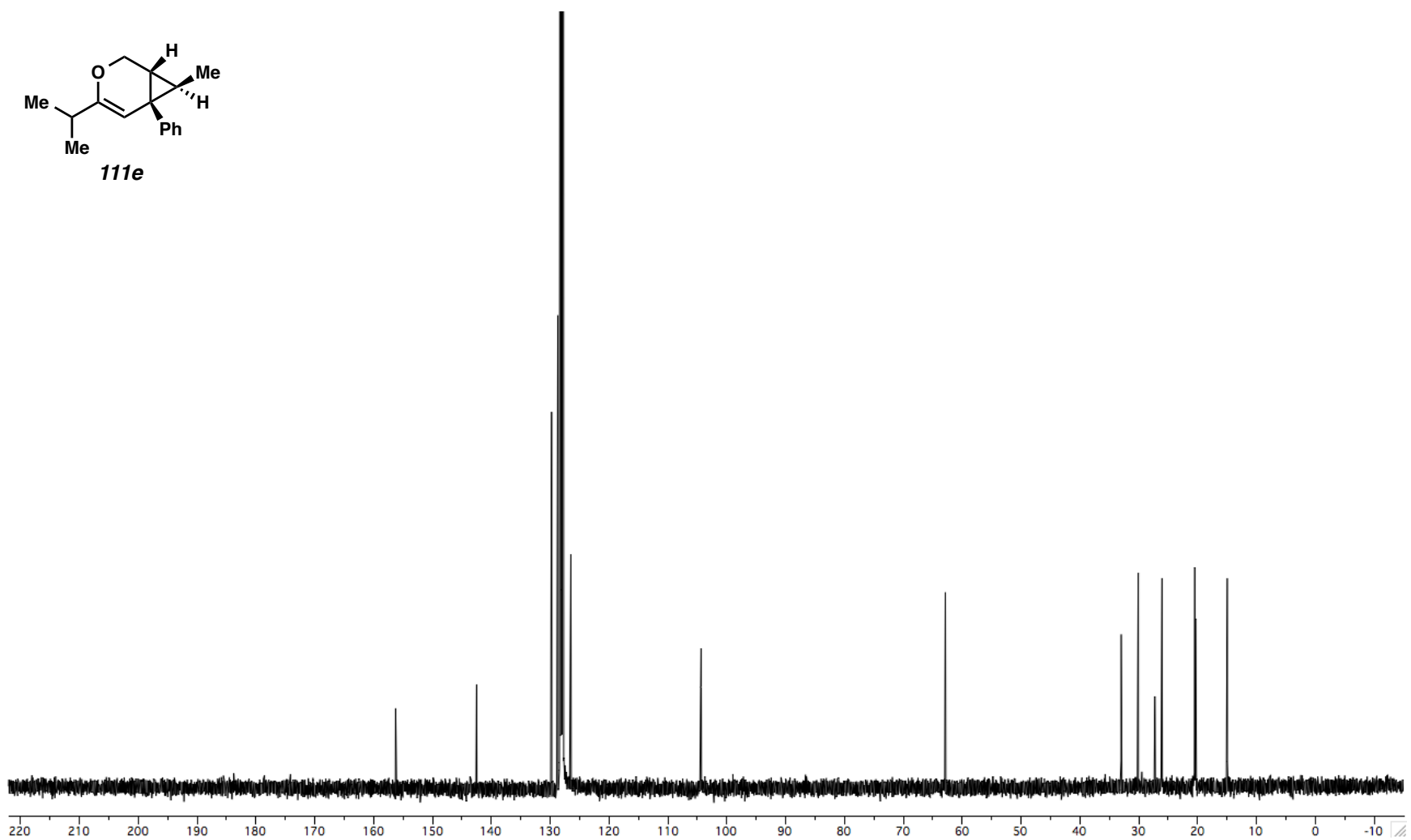


Figure A1.1. ^1H NMR (400 MHz, C_6D_6) of Compound **111e**.



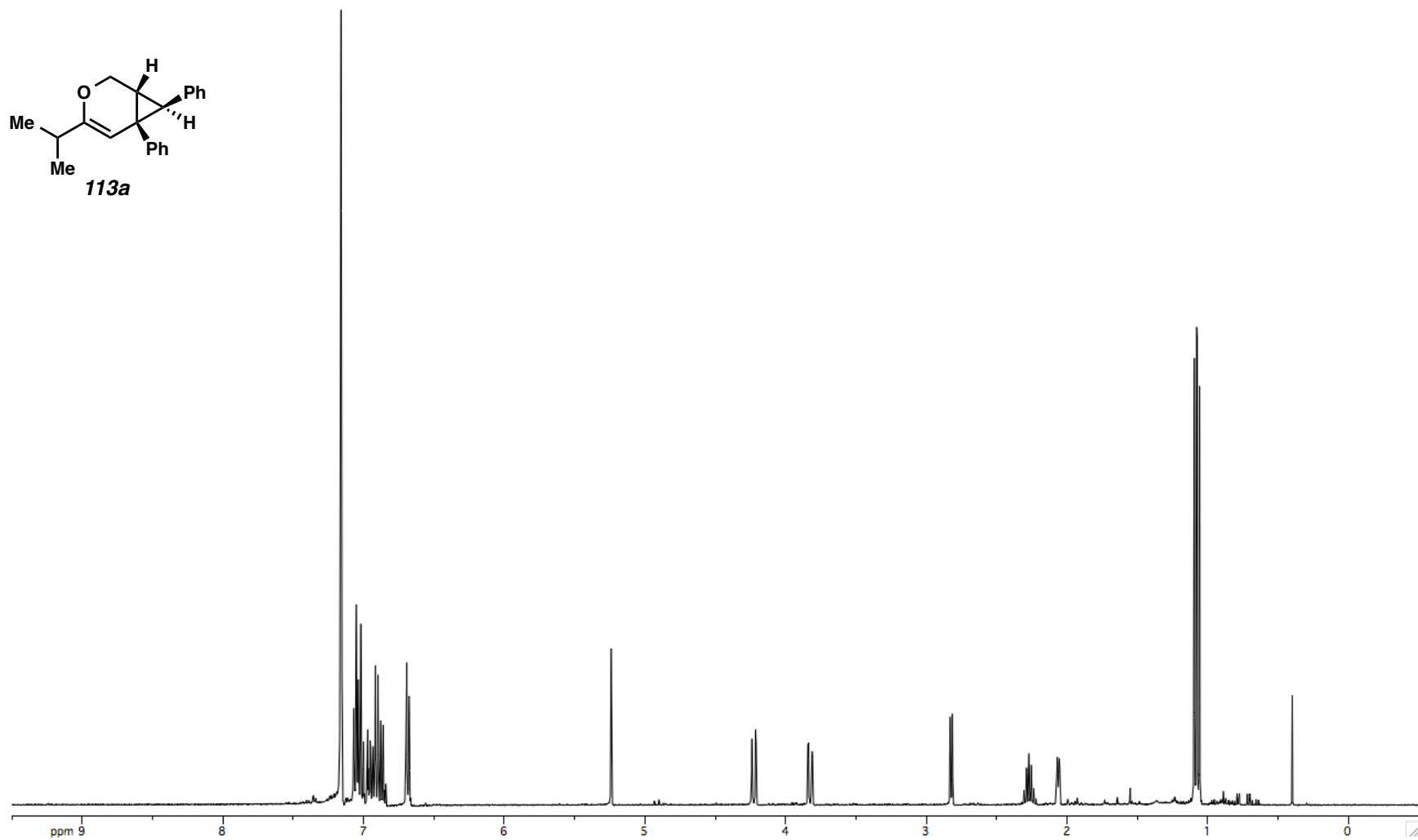


Figure A1.3. ^1H NMR (400 MHz, C_6D_6) of Compound **113a**.

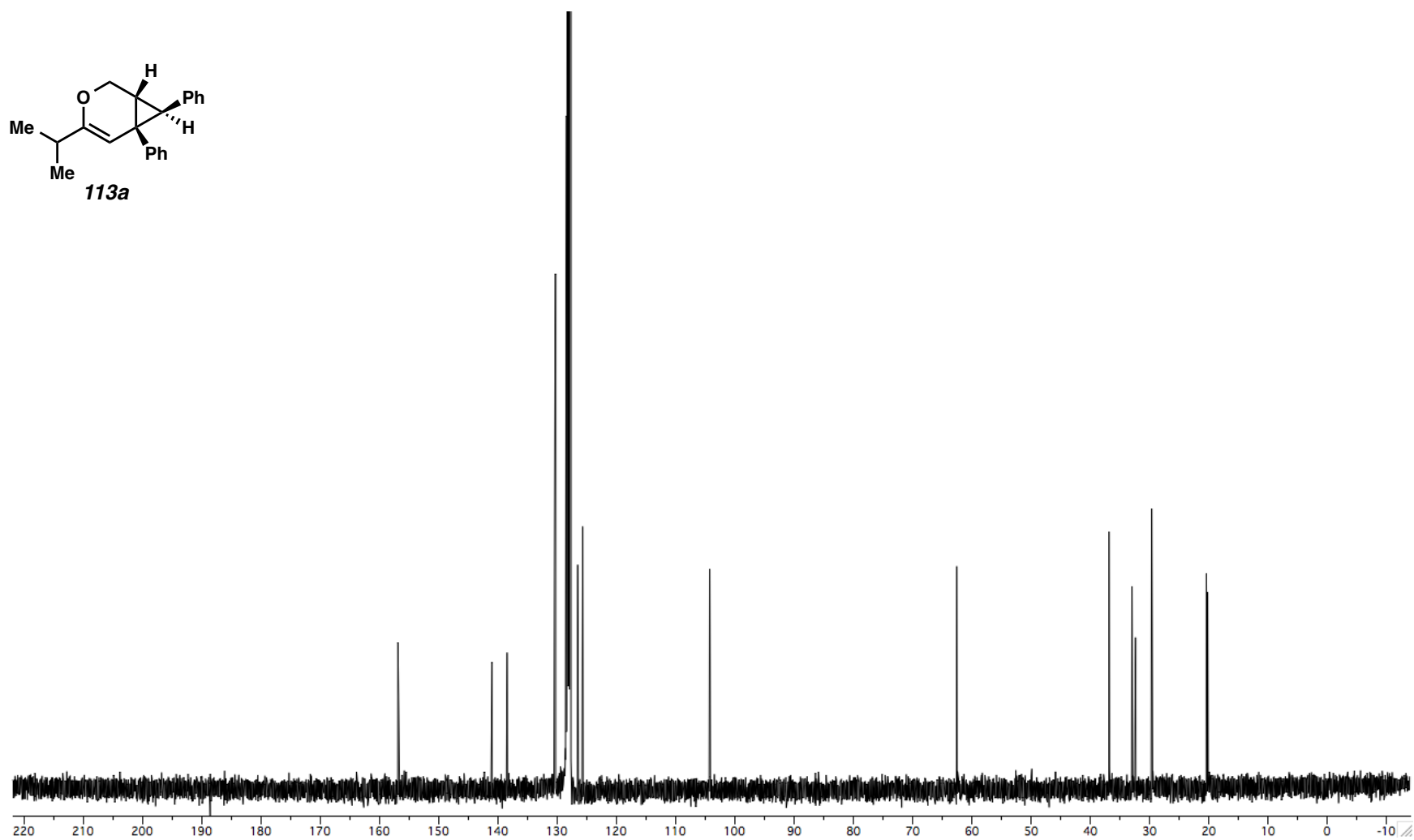


Figure A1.4. ^{13}C NMR (100 MHz, C_6D_6) of Compound **113a**.

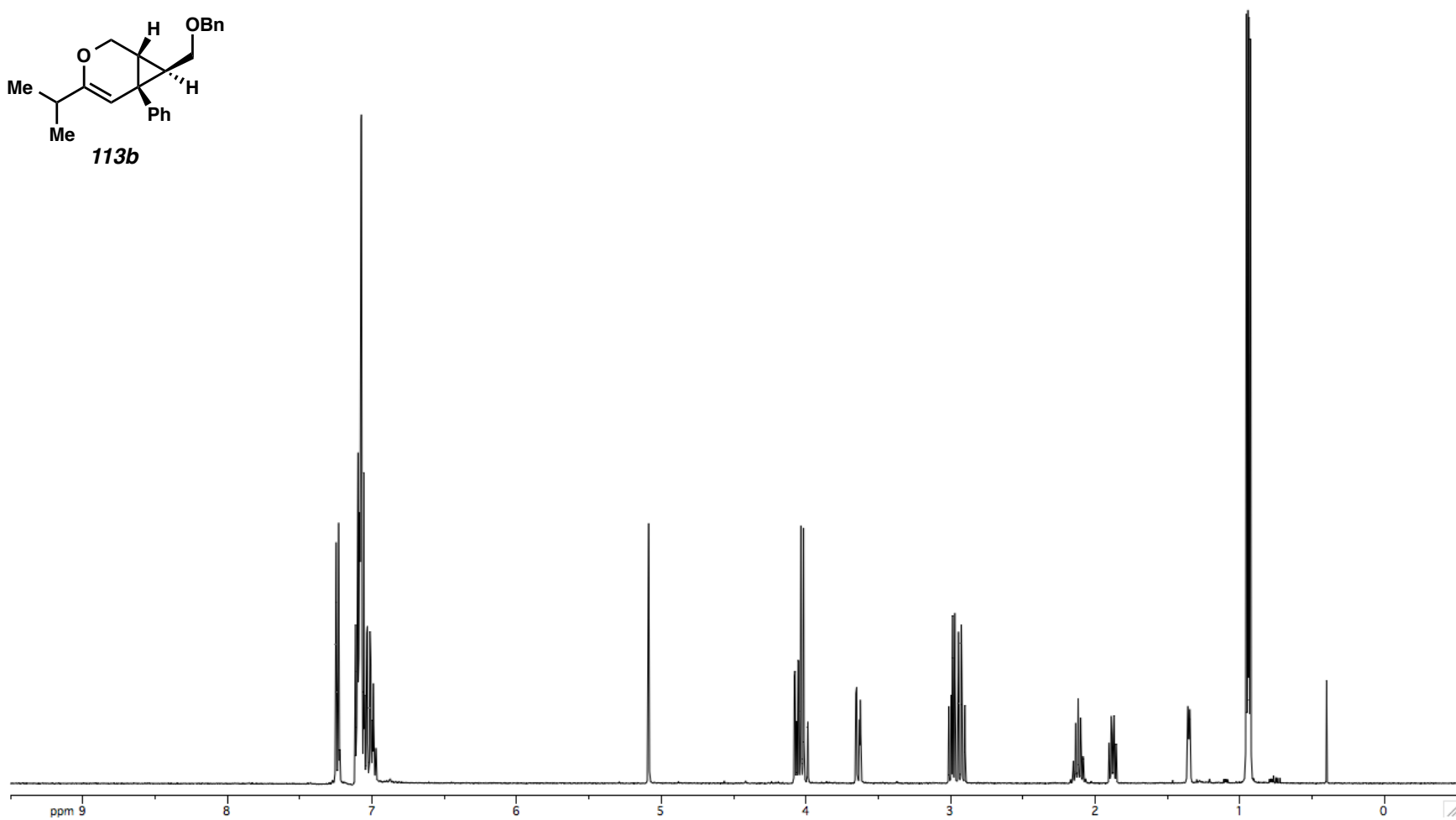
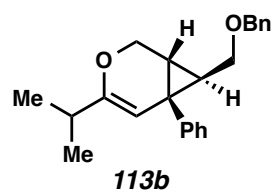


Figure A1.5. ^1H NMR (400 MHz, C_6D_6) of Compound **113b**.

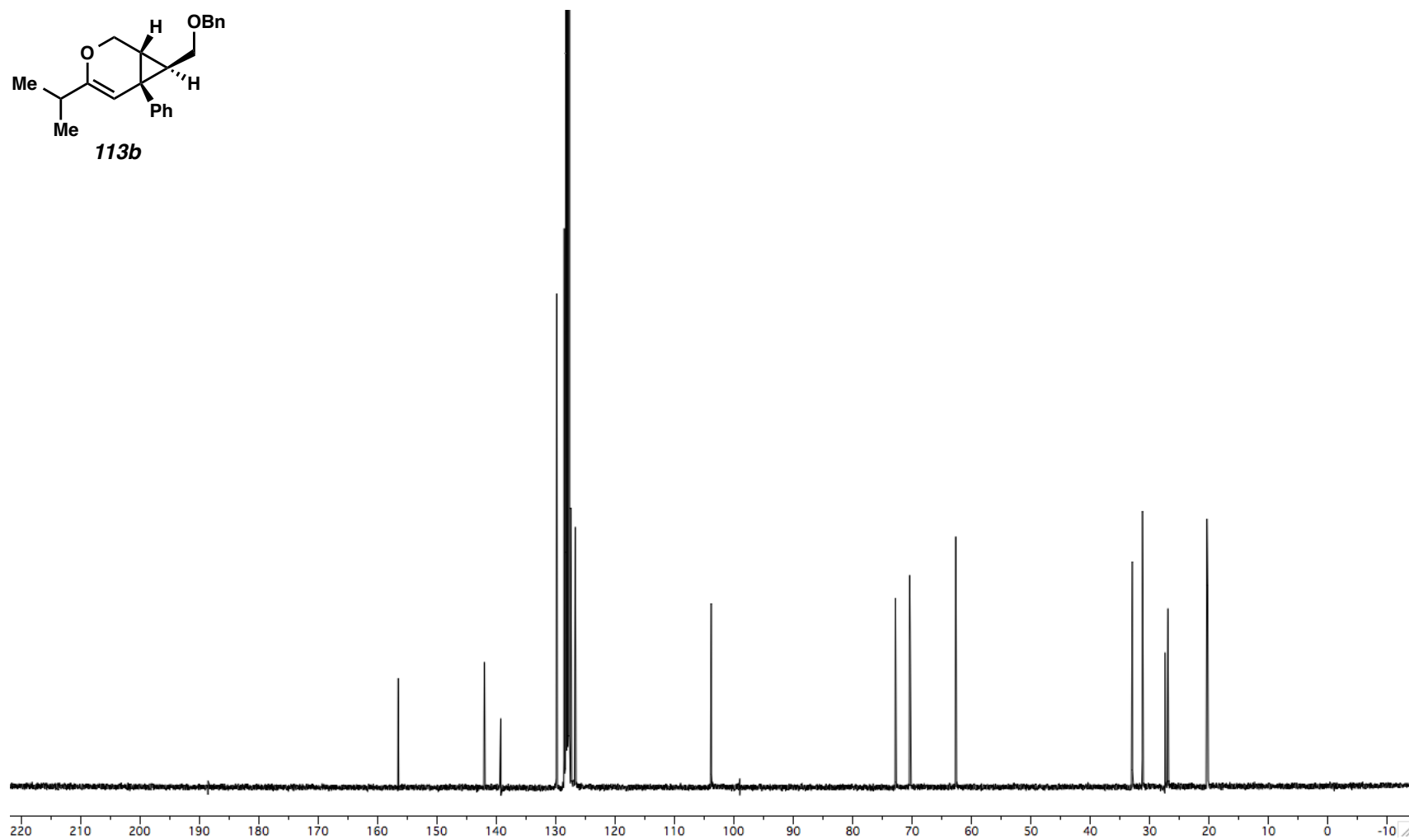
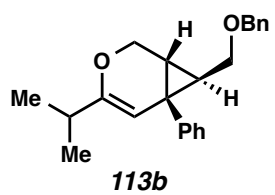


Figure A1.6. ^{13}C NMR (100 MHz, C_6D_6) of Compound **113b**.

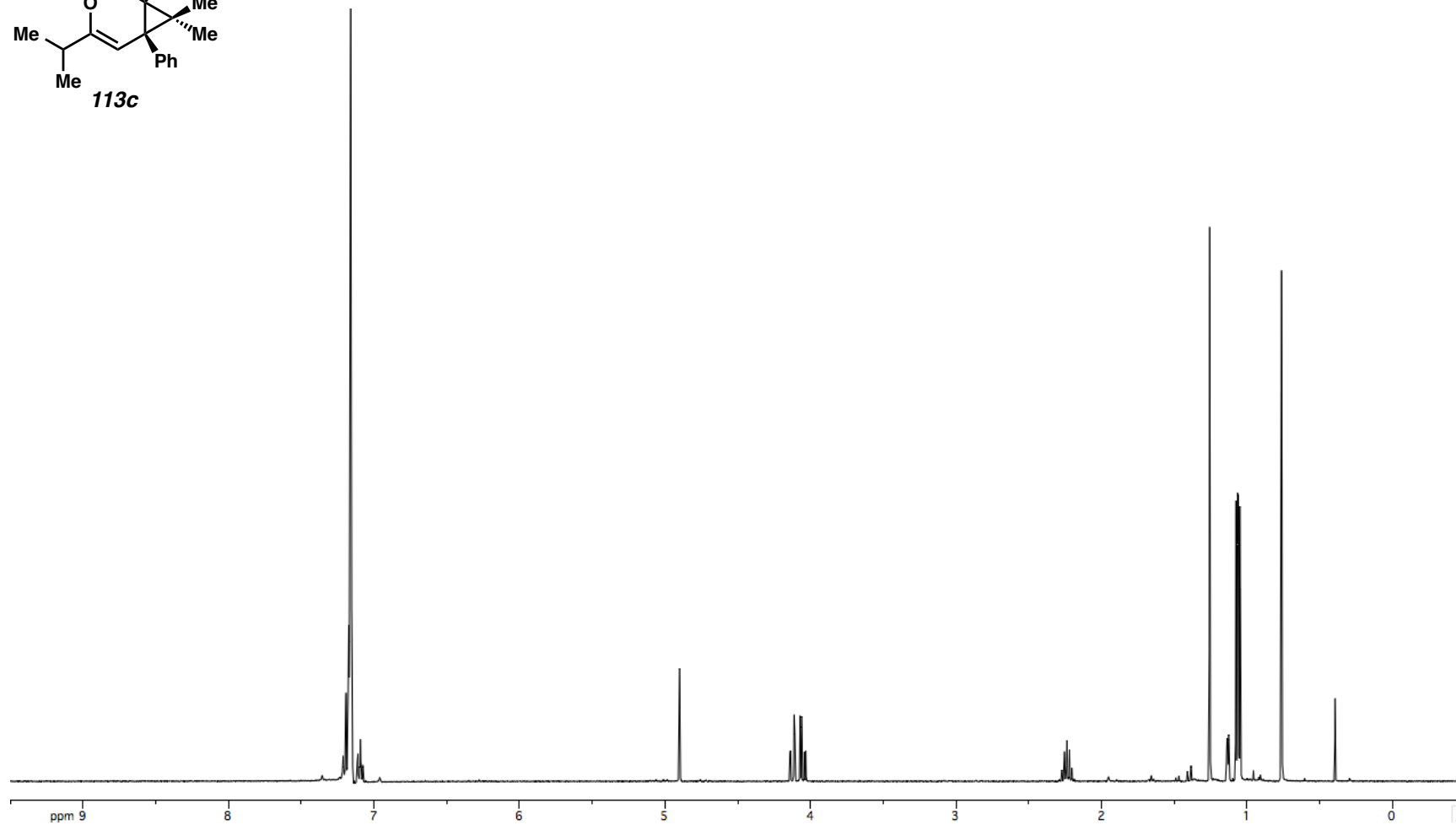
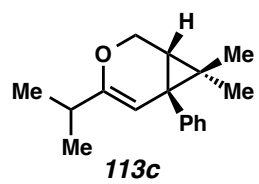


Figure A1.7. ^1H NMR (400 MHz, C_6D_6) of Compound **113c**.

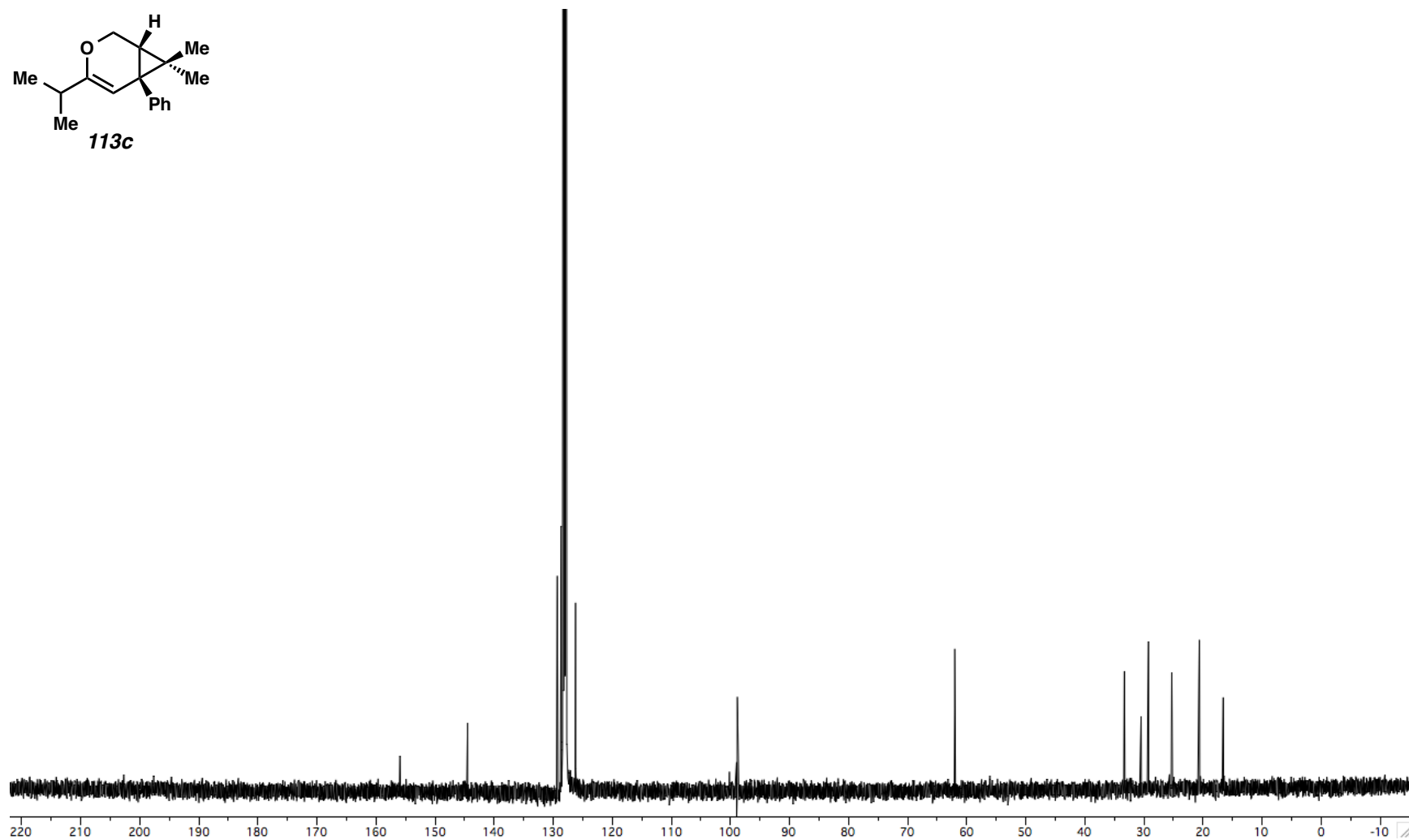
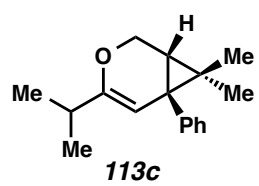


Figure A1.8. ^{13}C NMR (100 MHz, C_6D_6) of Compound **113c**.

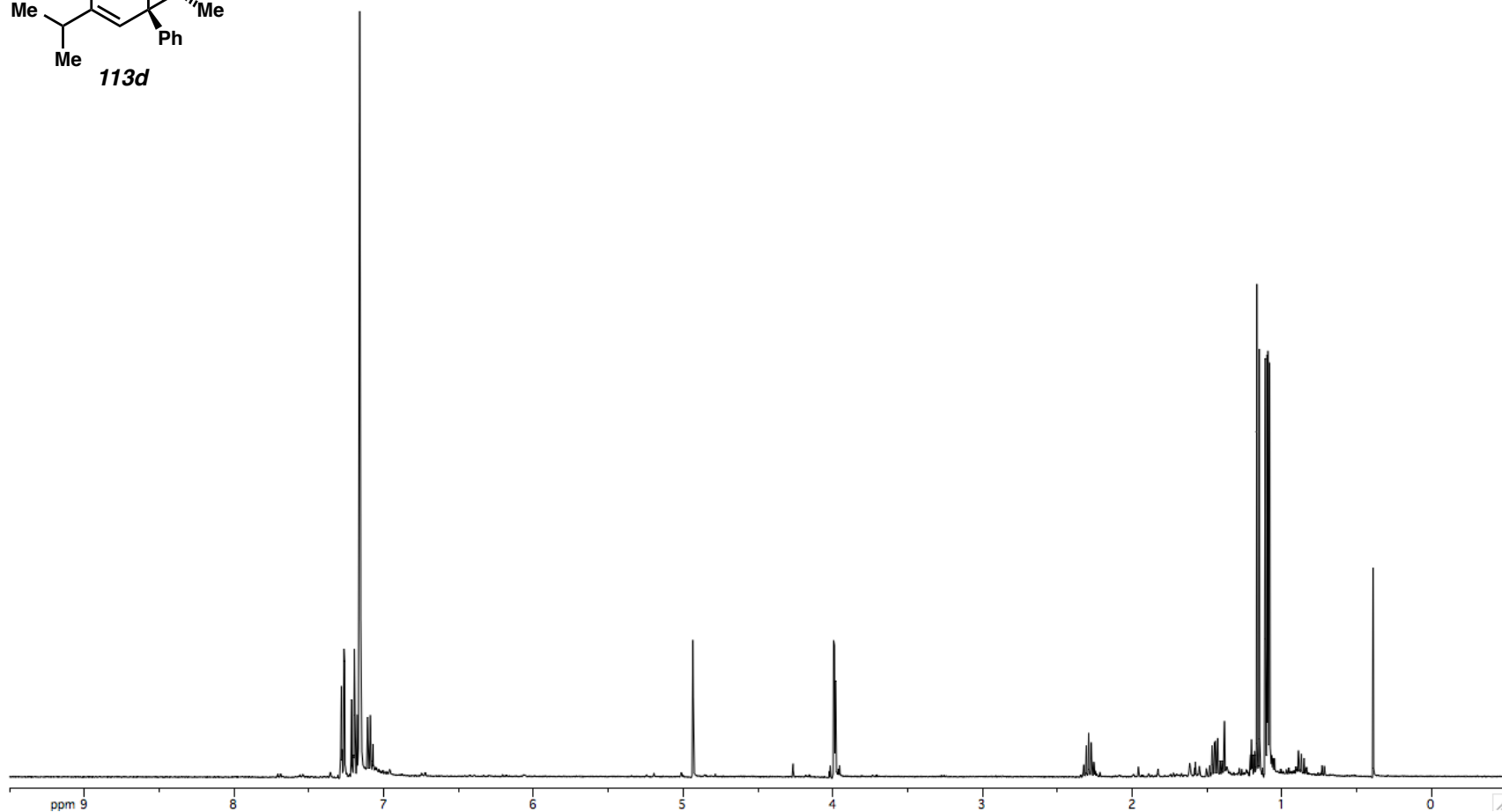
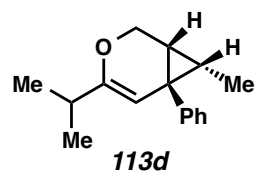


Figure A1.9. ¹H NMR (400 MHz, C₆D₆) of Compound **113d**.

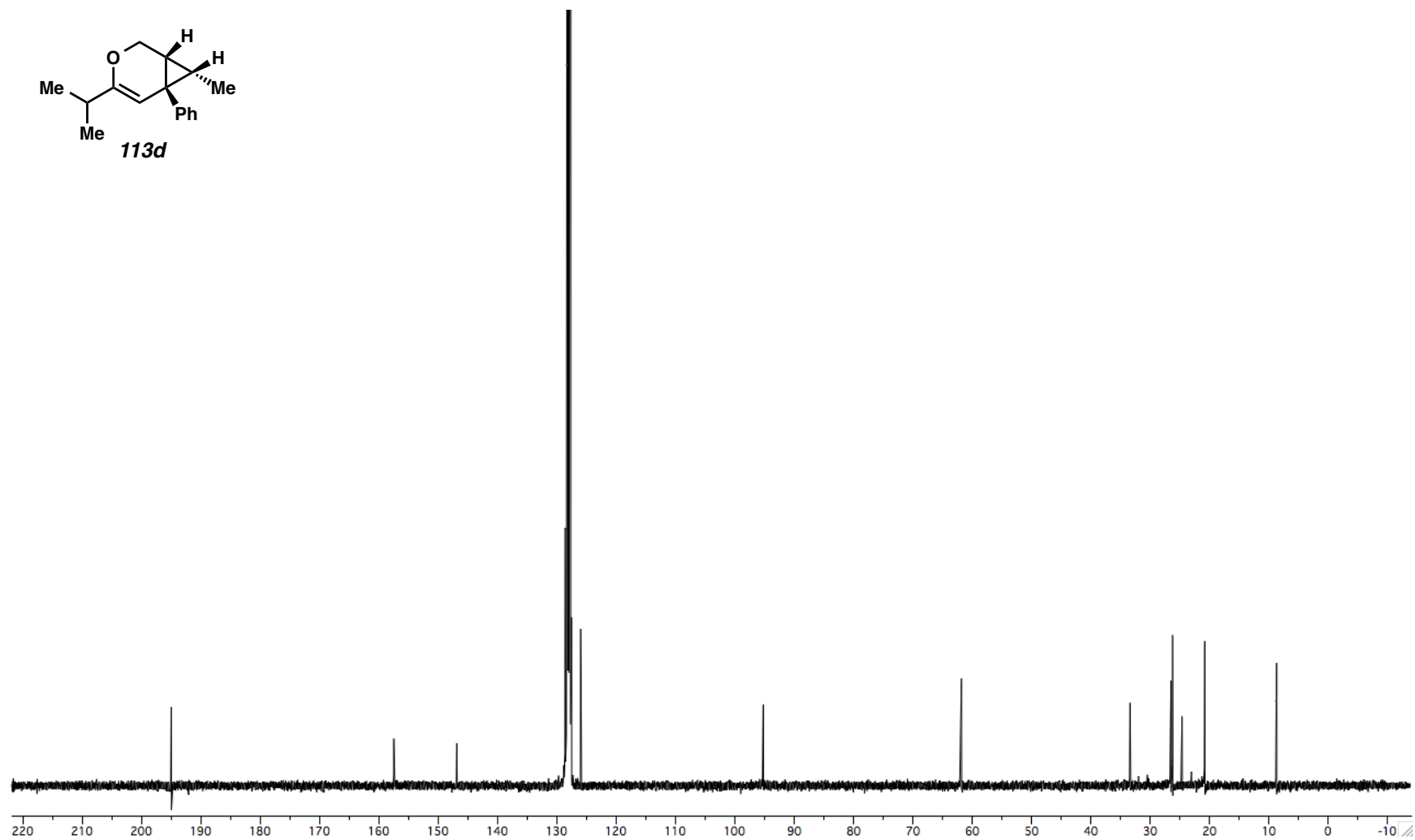
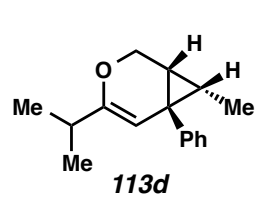


Figure A1.10. ^{13}C NMR (100 MHz, C_6D_6) of Compound **113d**.

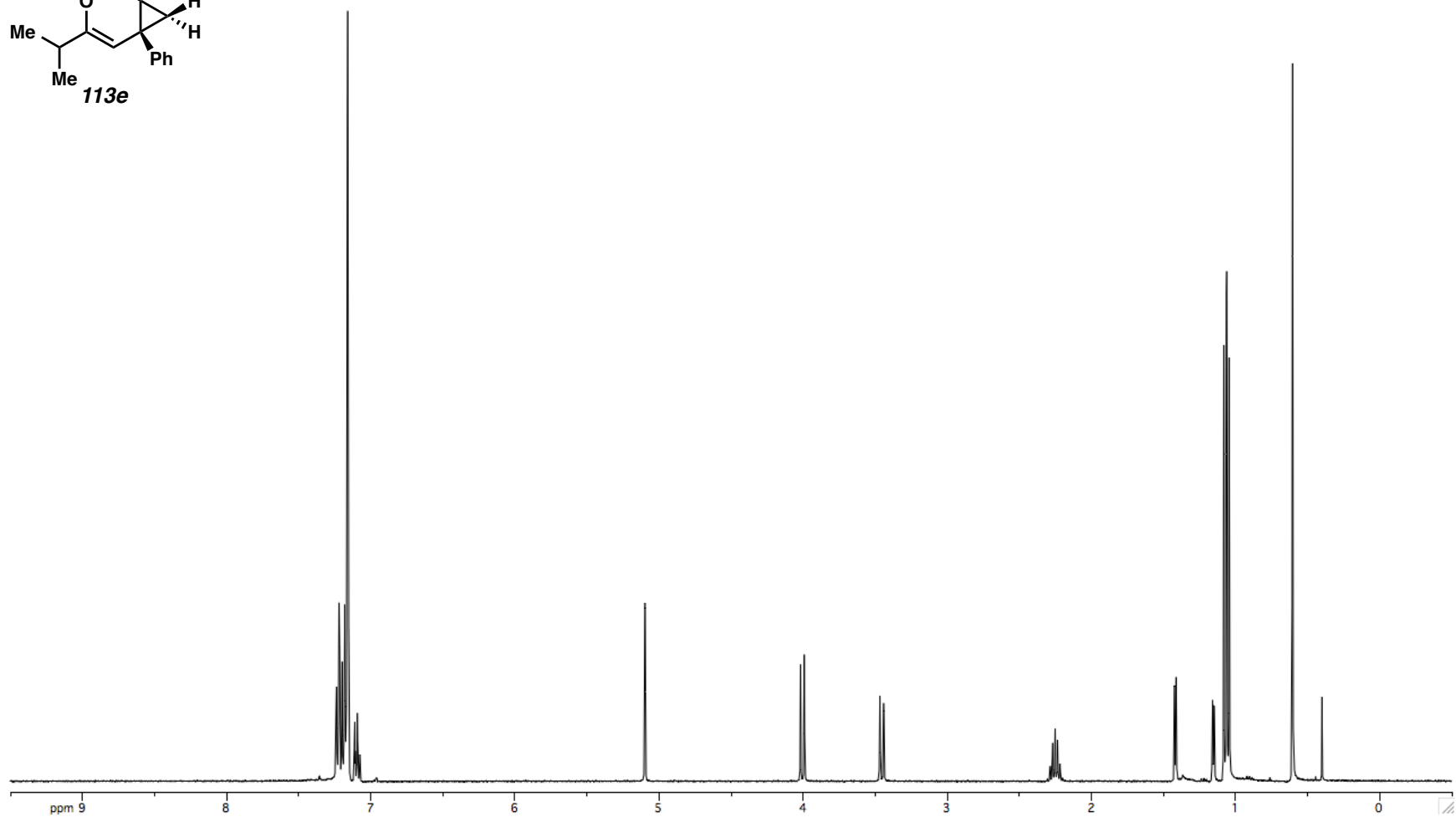
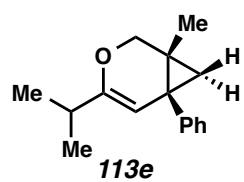


Figure A1.11. ^1H NMR (400 MHz, C_6D_6) of Compound **113e**.

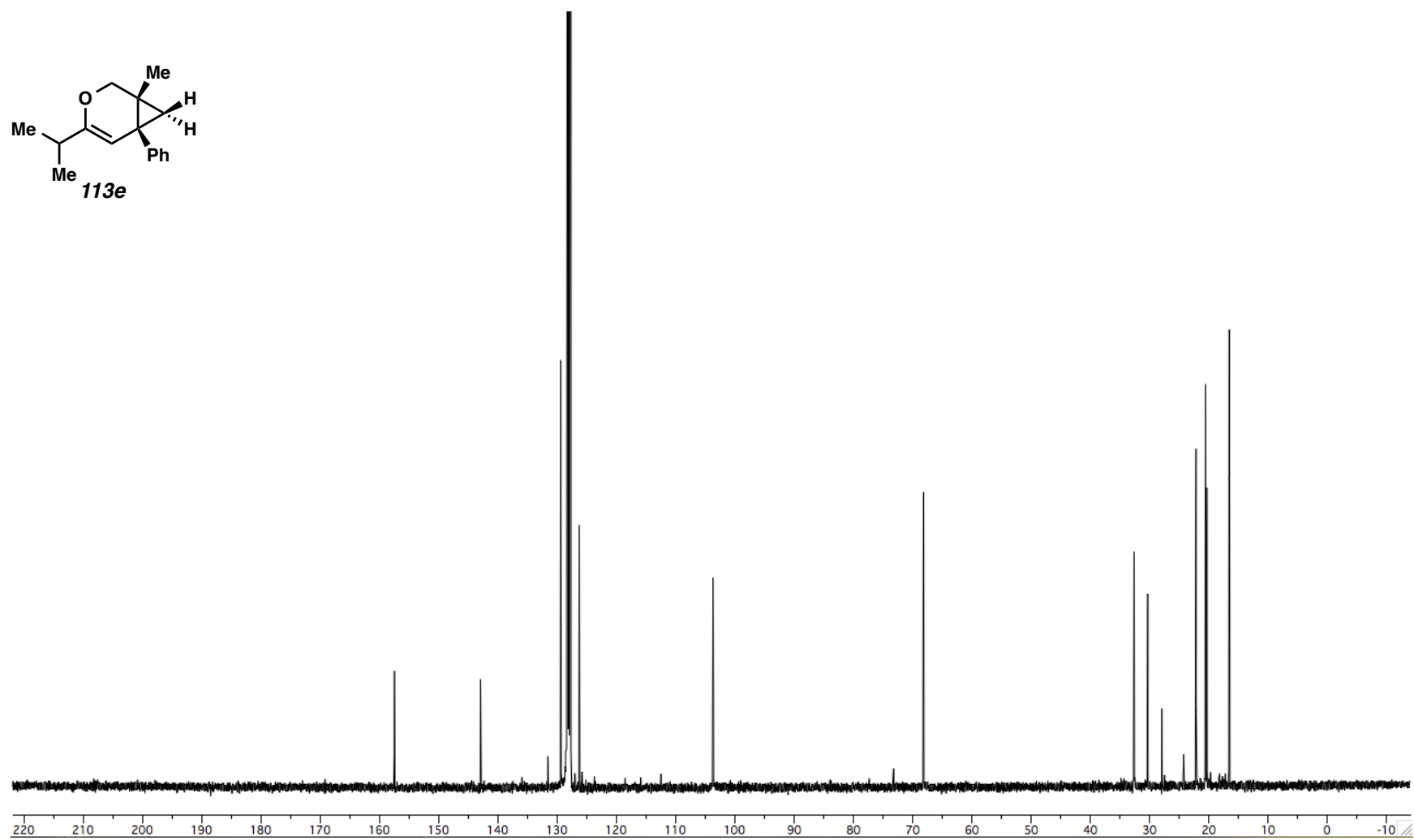


Figure A1.12. ^{13}C NMR (100 MHz, C_6D_6) of Compound **113e**.

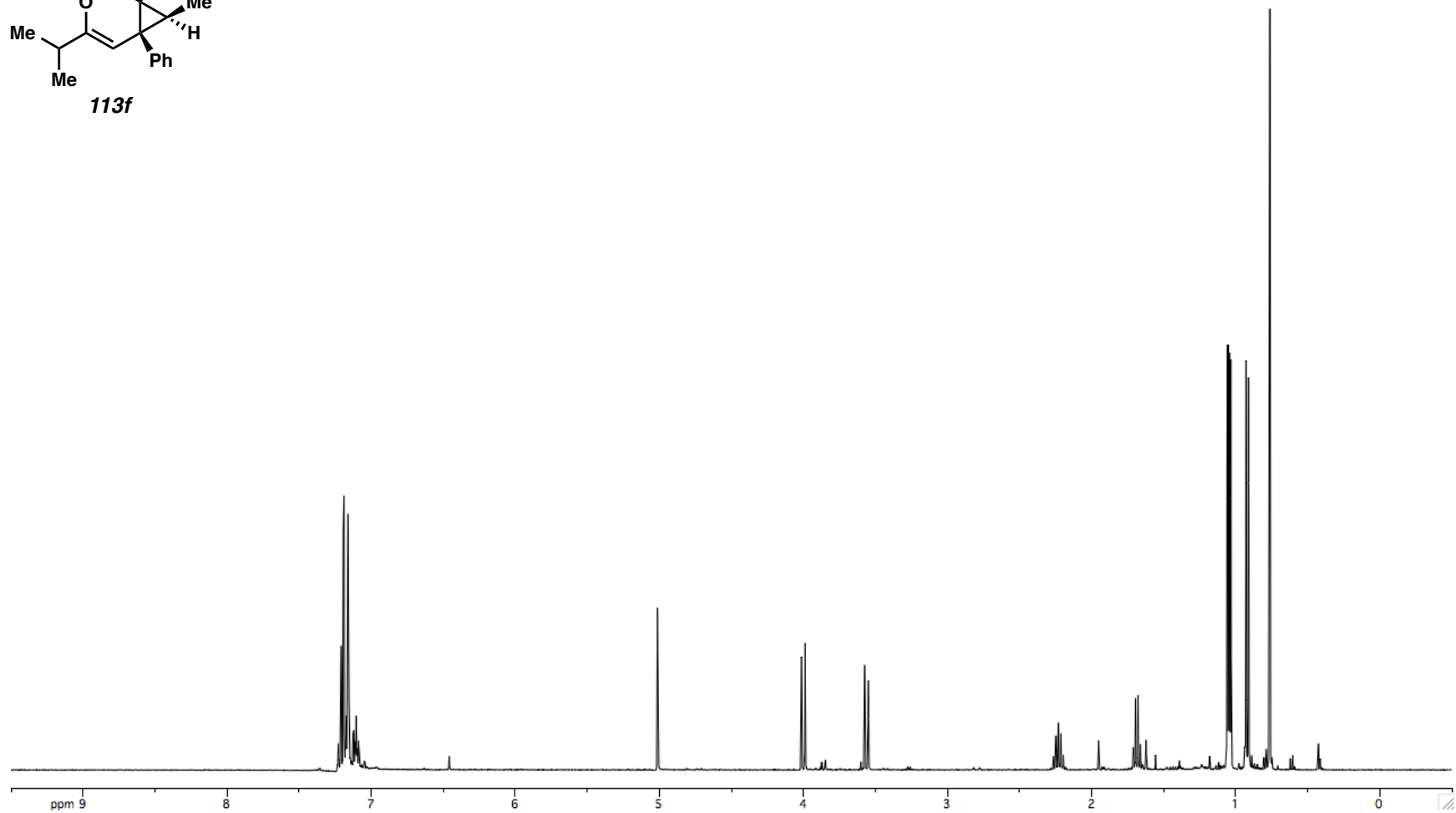
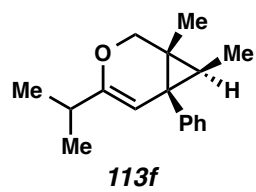


Figure A1.13. ^1H NMR (400 MHz, C_6D_6) of Compound **113f**.

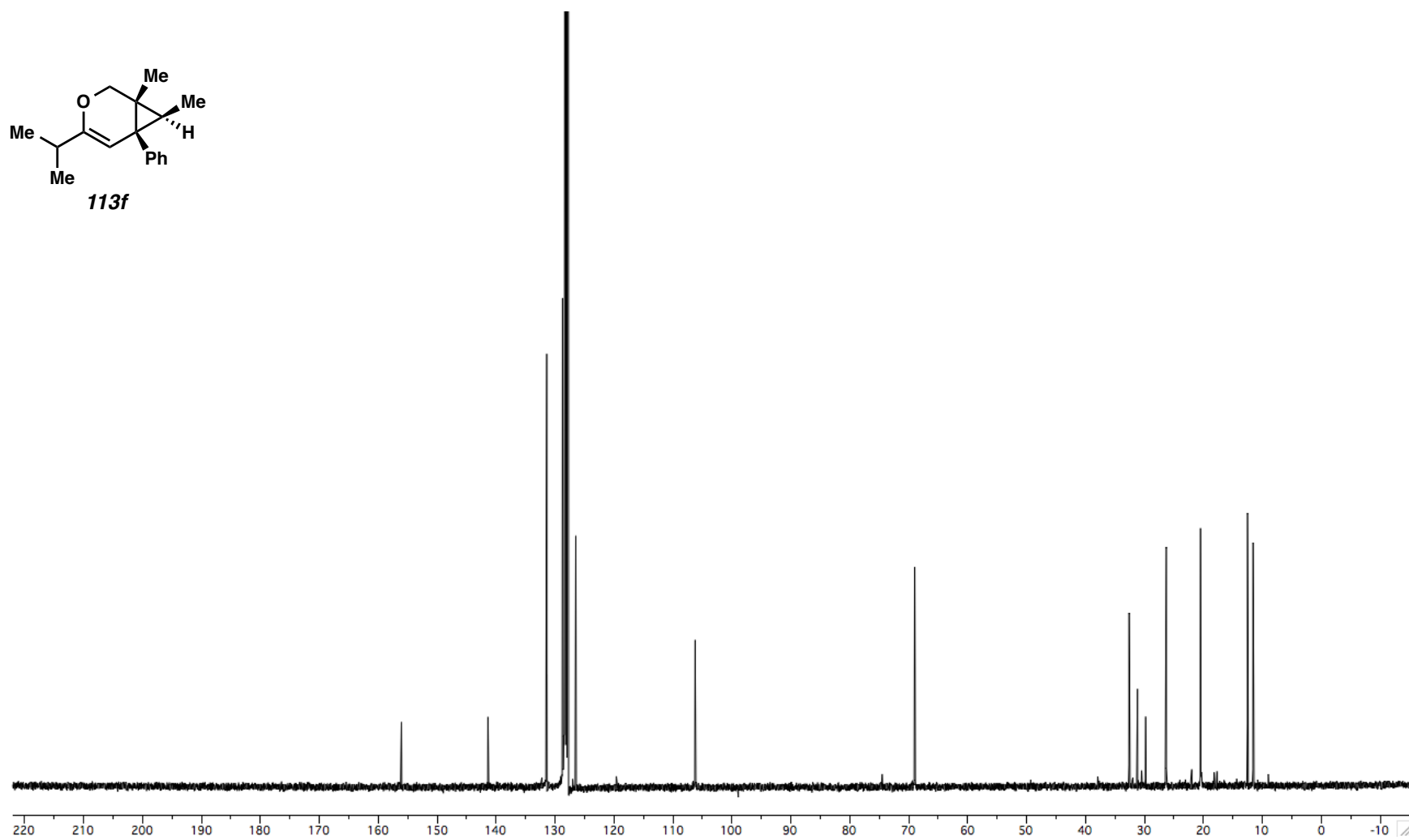


Figure A1.14. ¹³C NMR (100 MHz, C₆D₆) of Compound **113f**.

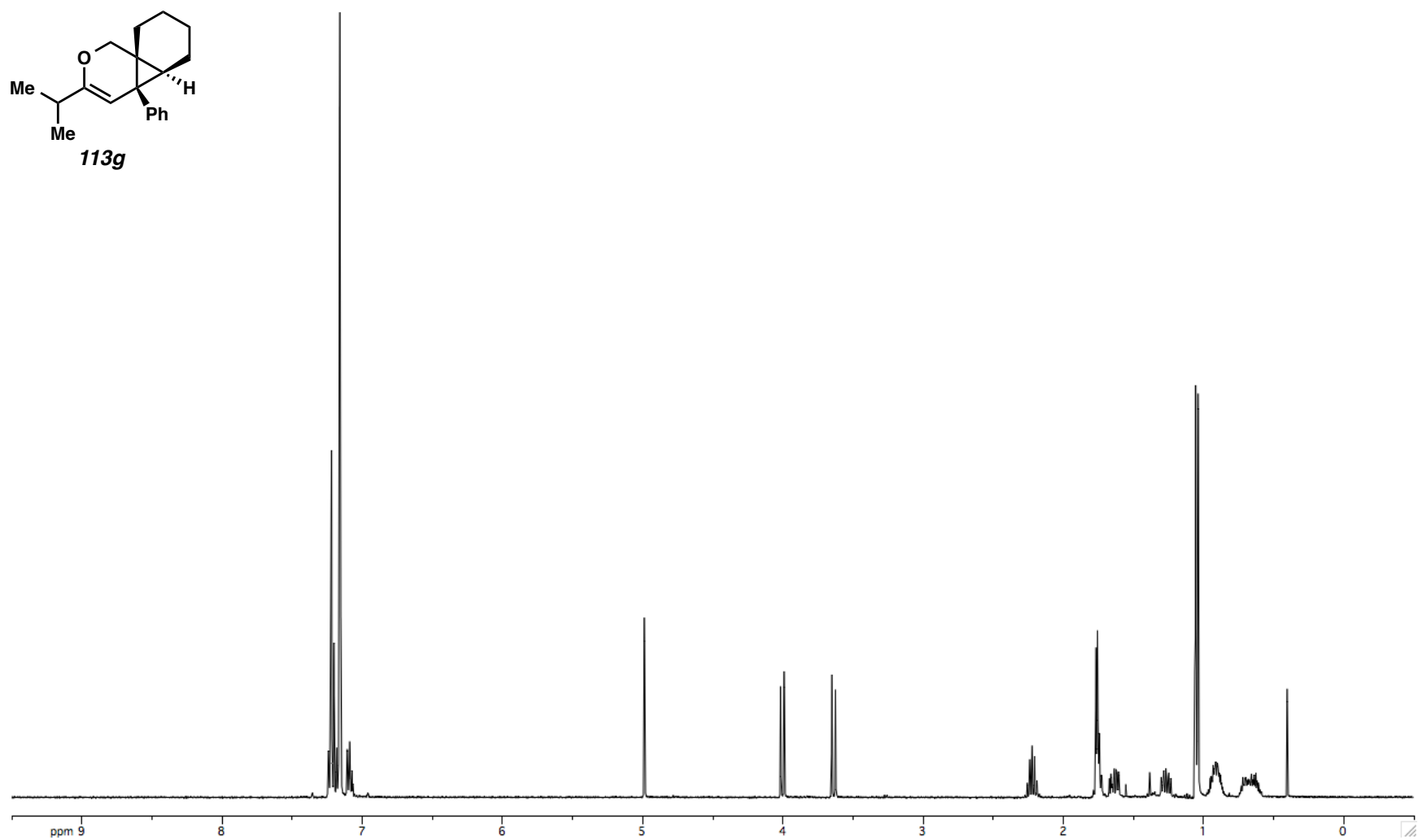
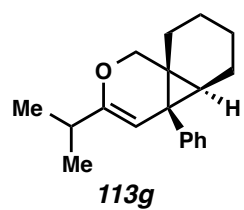


Figure A1.15. ^1H NMR (400 MHz, C_6D_6) of Compound **113g**.

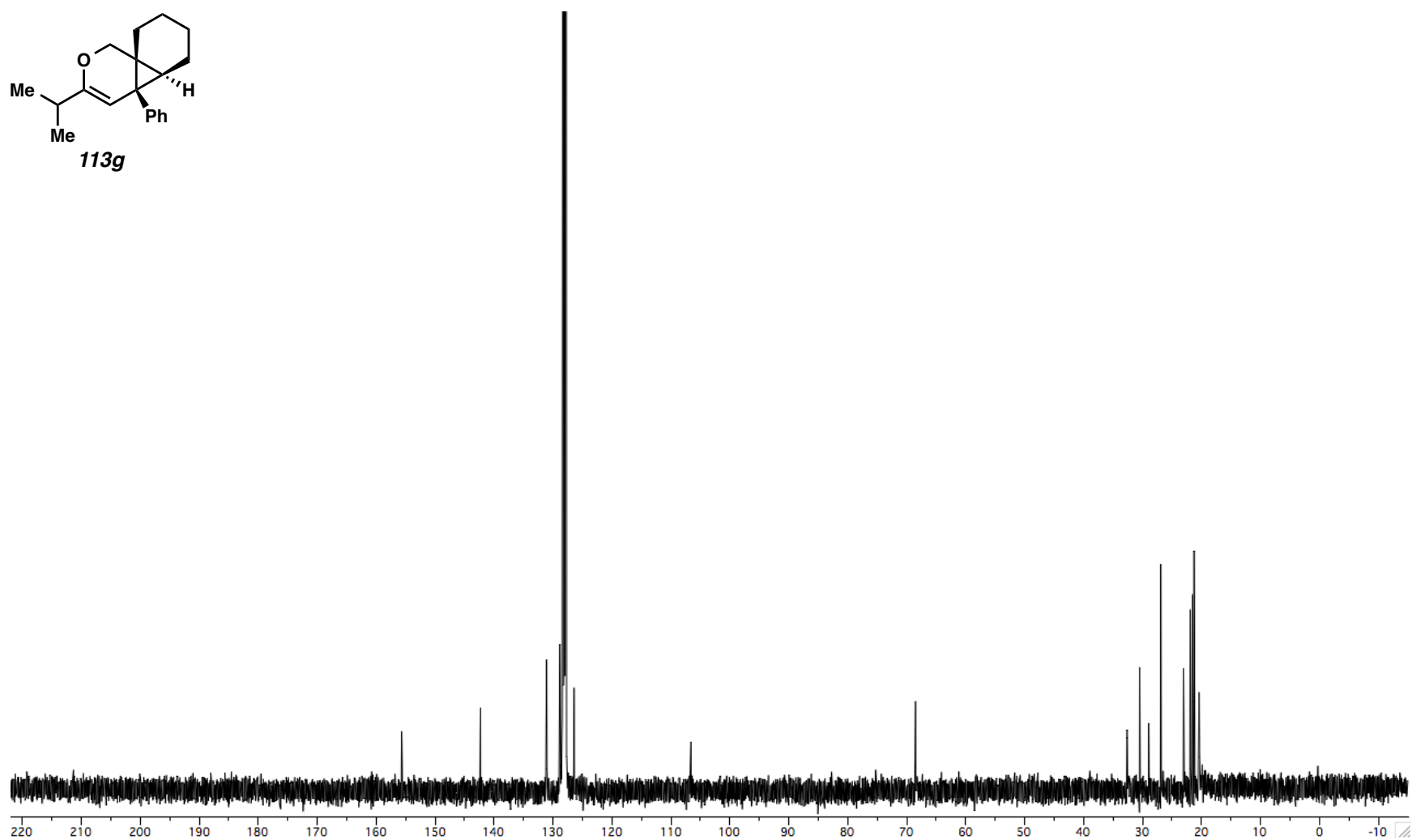
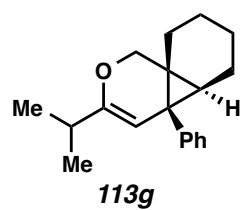


Figure A1.16. ^{13}C NMR (100 MHz, C_6D_6) of Compound **113g**.

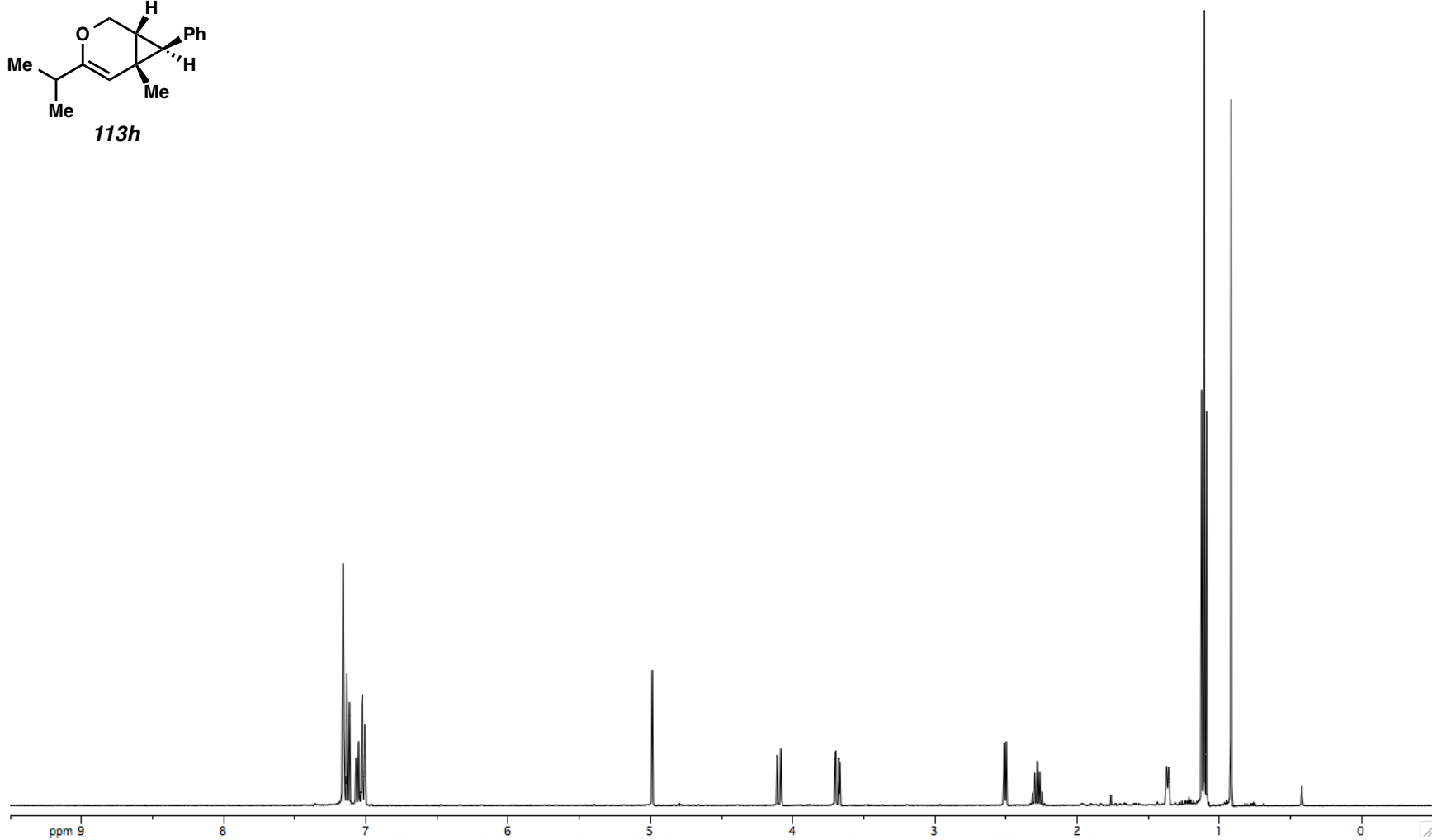
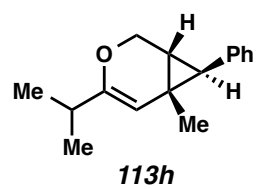


Figure A1.17. ^1H NMR (400 MHz, C_6D_6) of Compound **113h**.

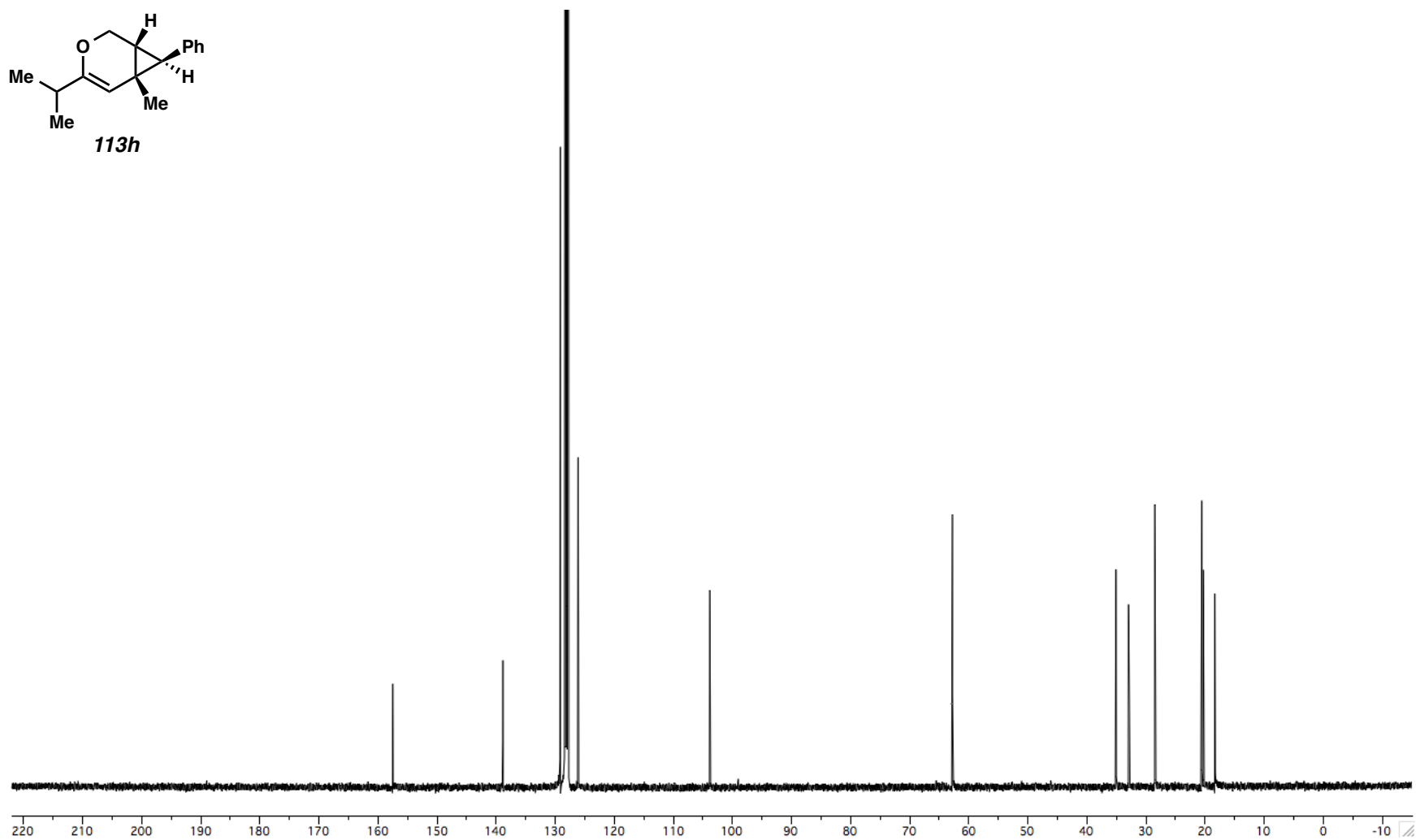
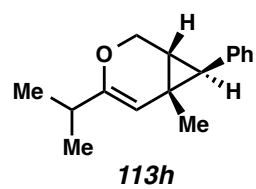


Figure A1.18. ^{13}C NMR (100 MHz, C_6D_6) of Compound **113h**.

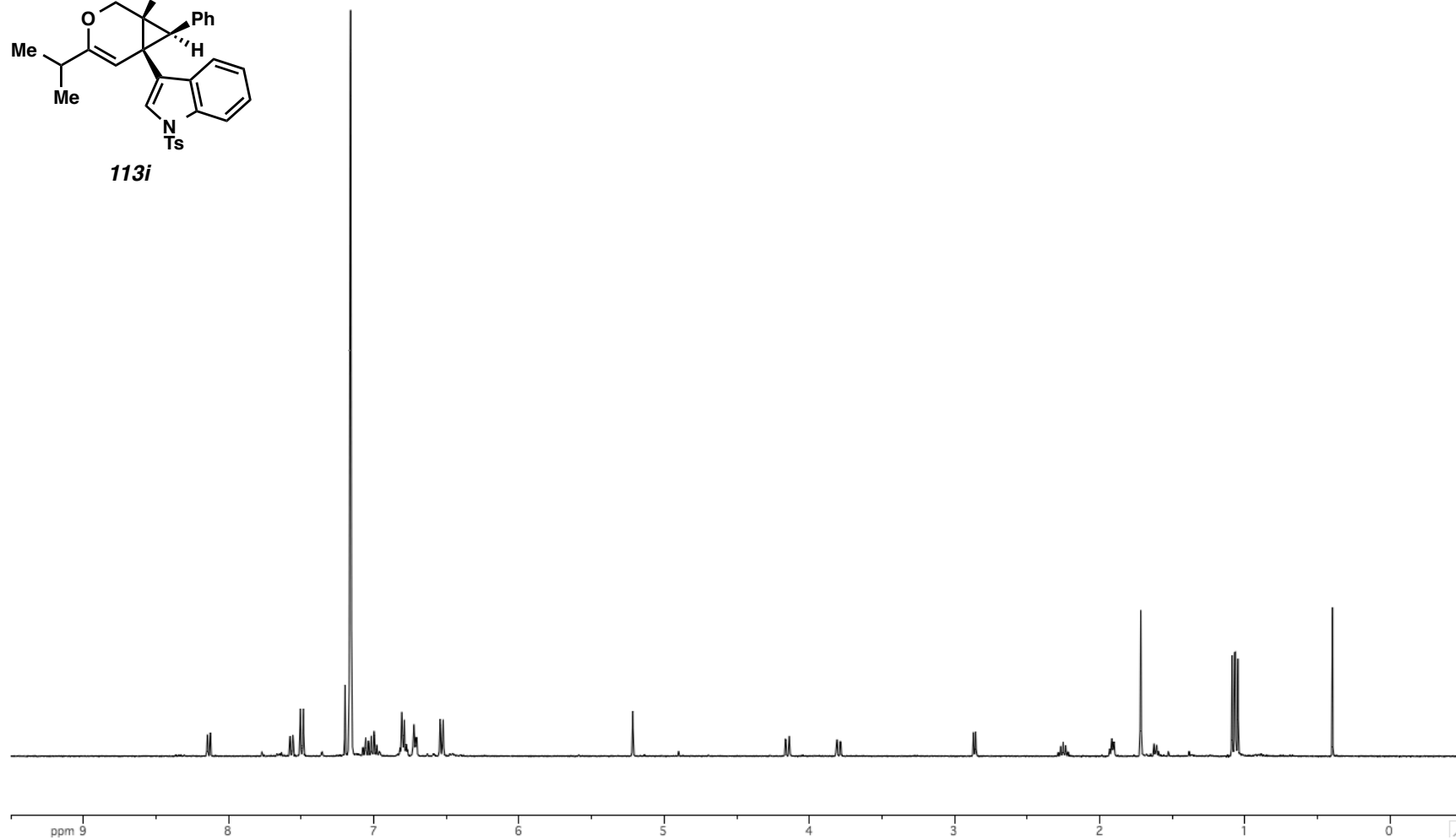
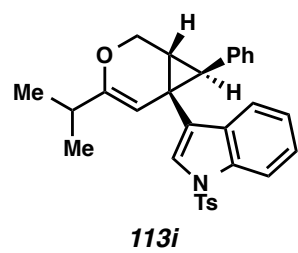


Figure A1.19. ^1H NMR (400 MHz, C_6D_6) of Compound **113i**.

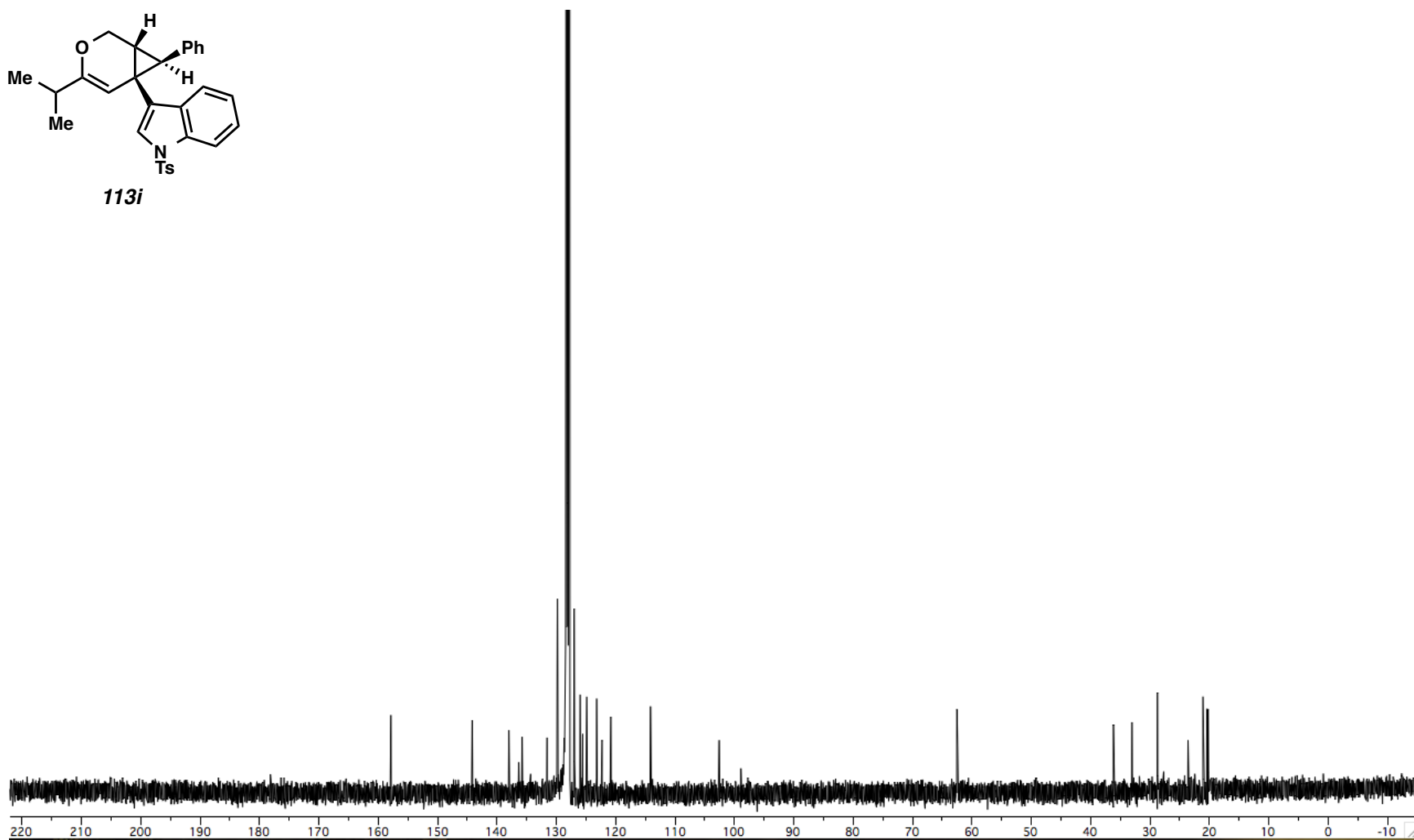
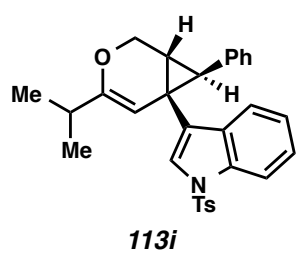


Figure A1.20. ^{13}C NMR (100 MHz, C_6D_6) of Compound **113i**.

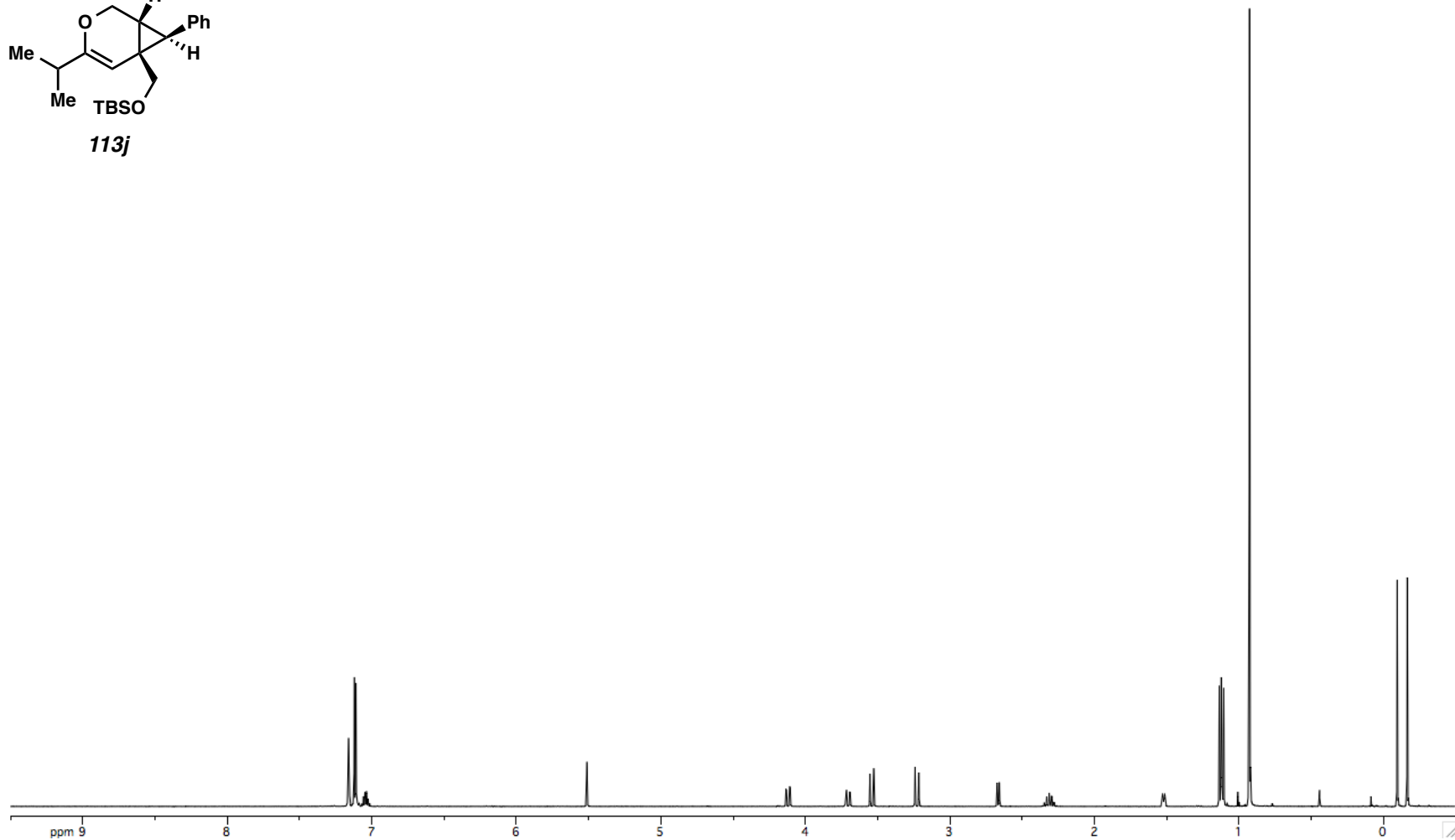
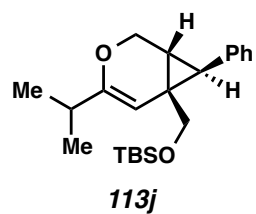


Figure A1.21. ^1H NMR (400 MHz, C_6D_6) of Compound **113j**.

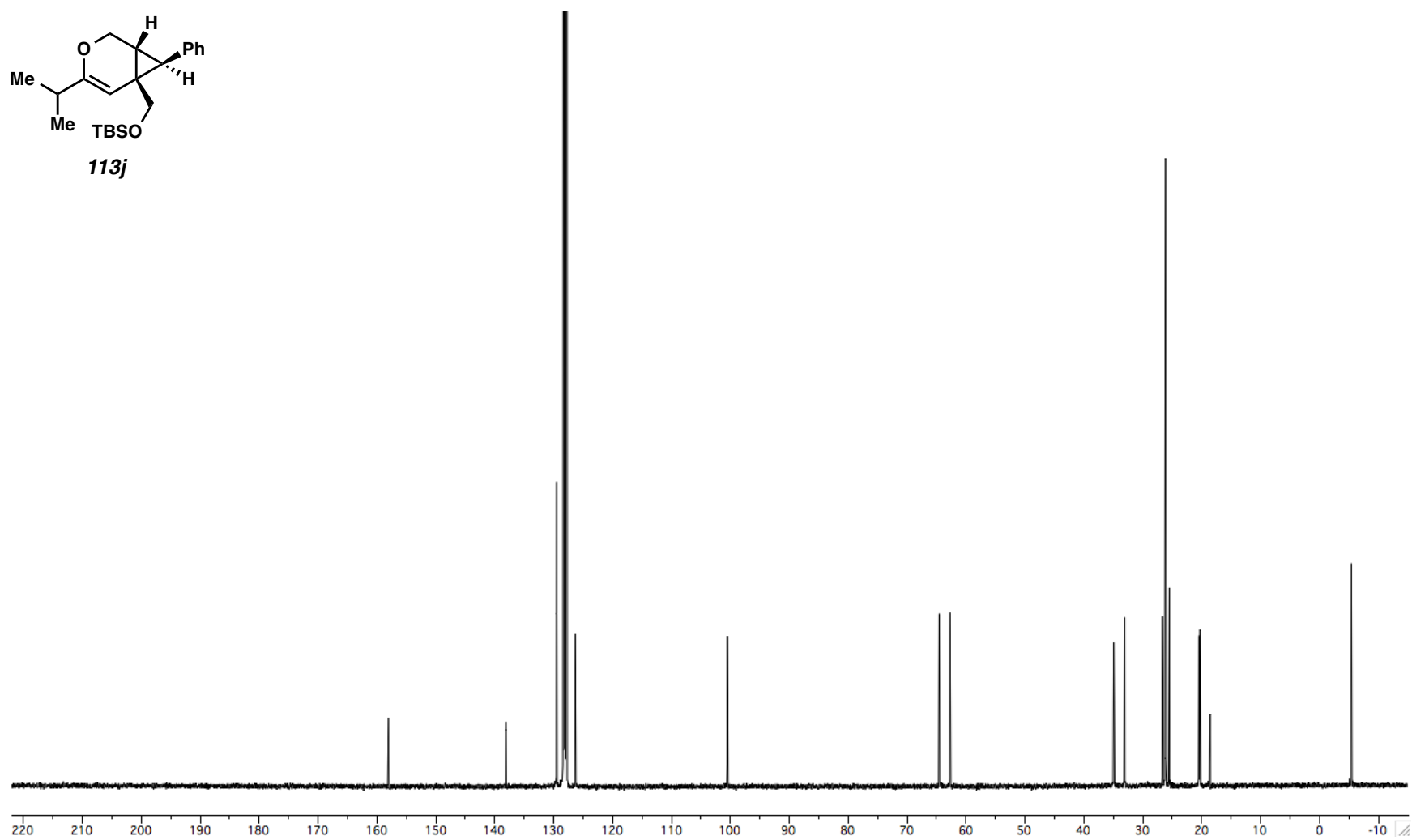
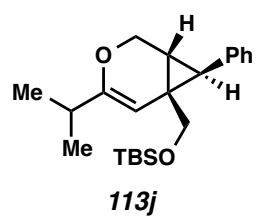


Figure A1.22. ^{13}C NMR (100 MHz, C_6D_6) of Compound **113j**.

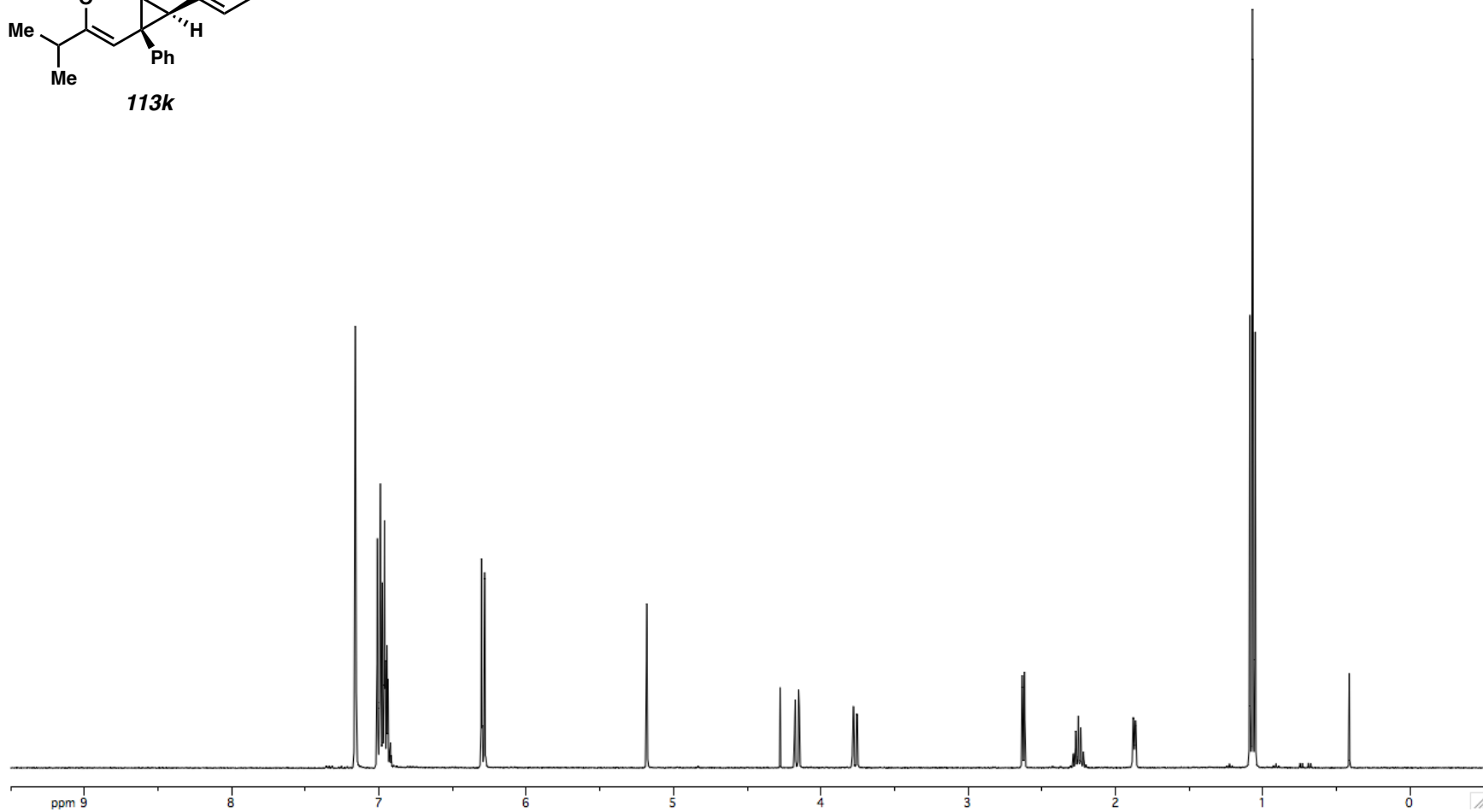
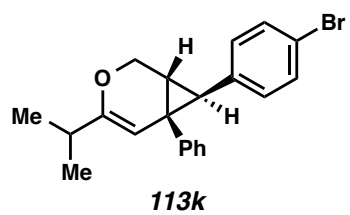


Figure A1.23. ^1H NMR (400 MHz, C_6D_6) of Compound **113k**.

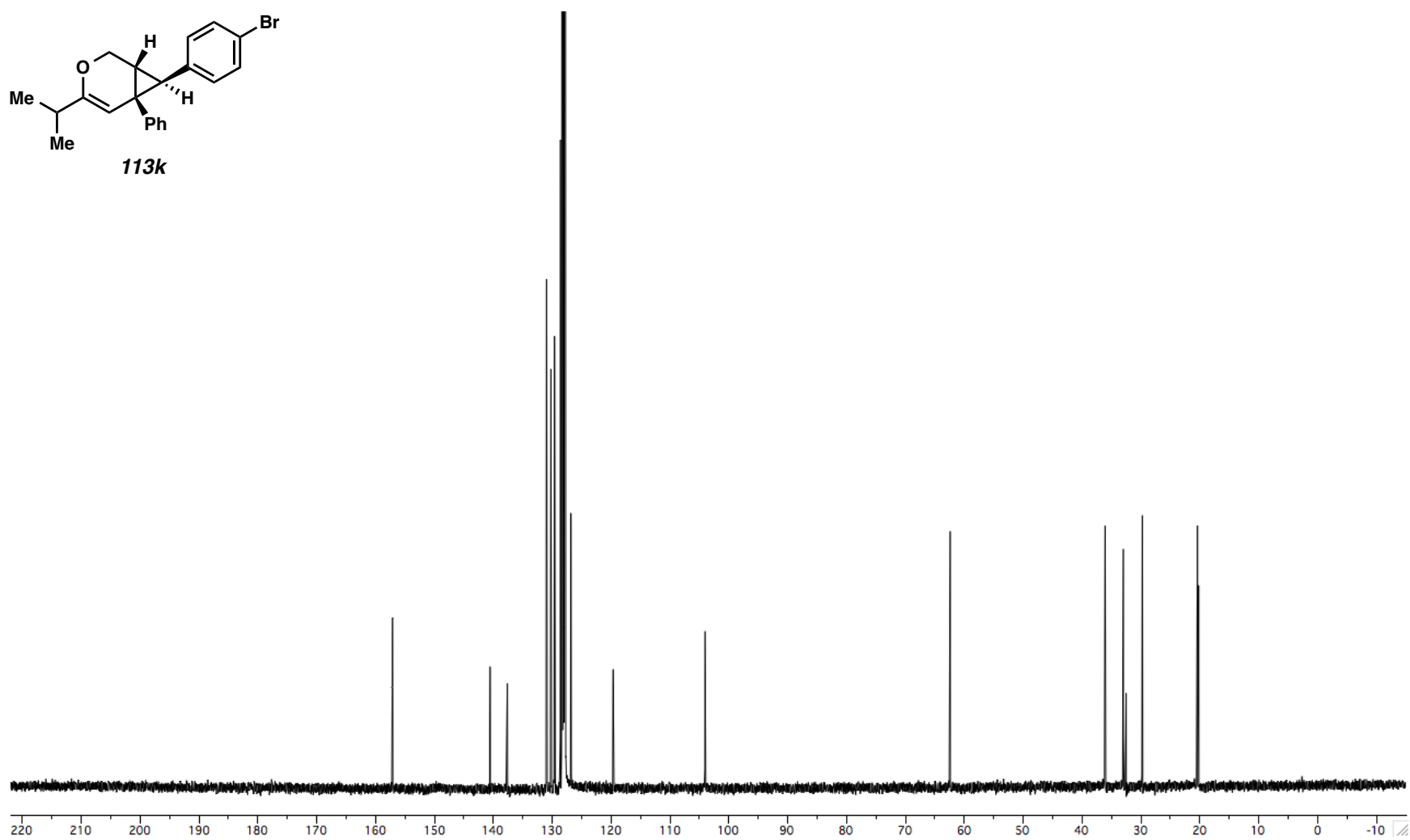
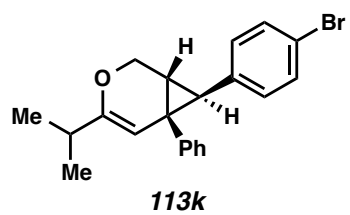


Figure A1.24. ^{13}C NMR (100 MHz, C_6D_6) of Compound **113k**.

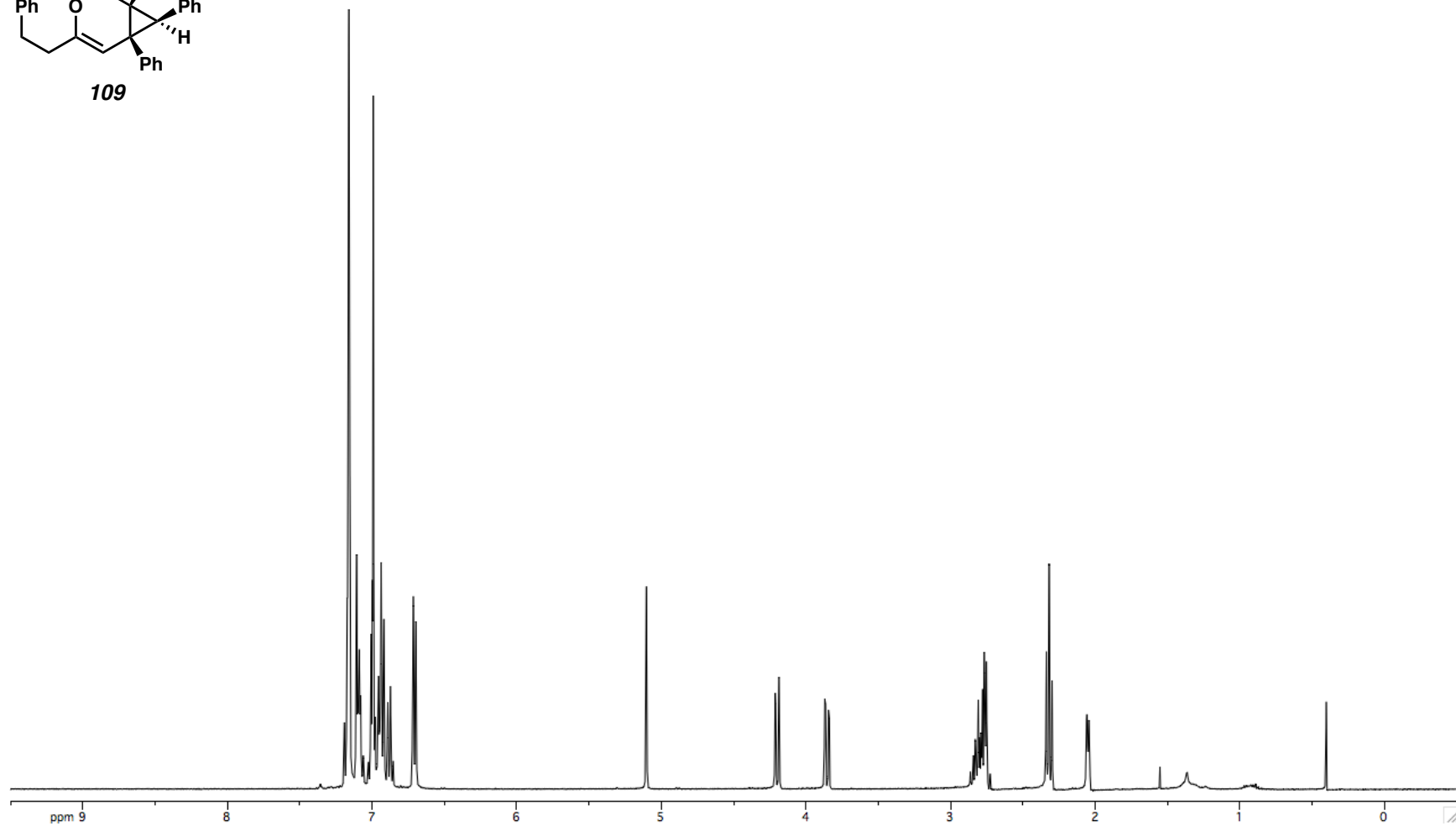
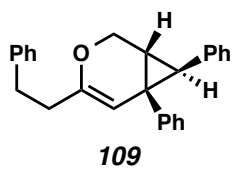


Figure A1.25. ¹H NMR (400 MHz, C₆D₆) of Compound **109**.

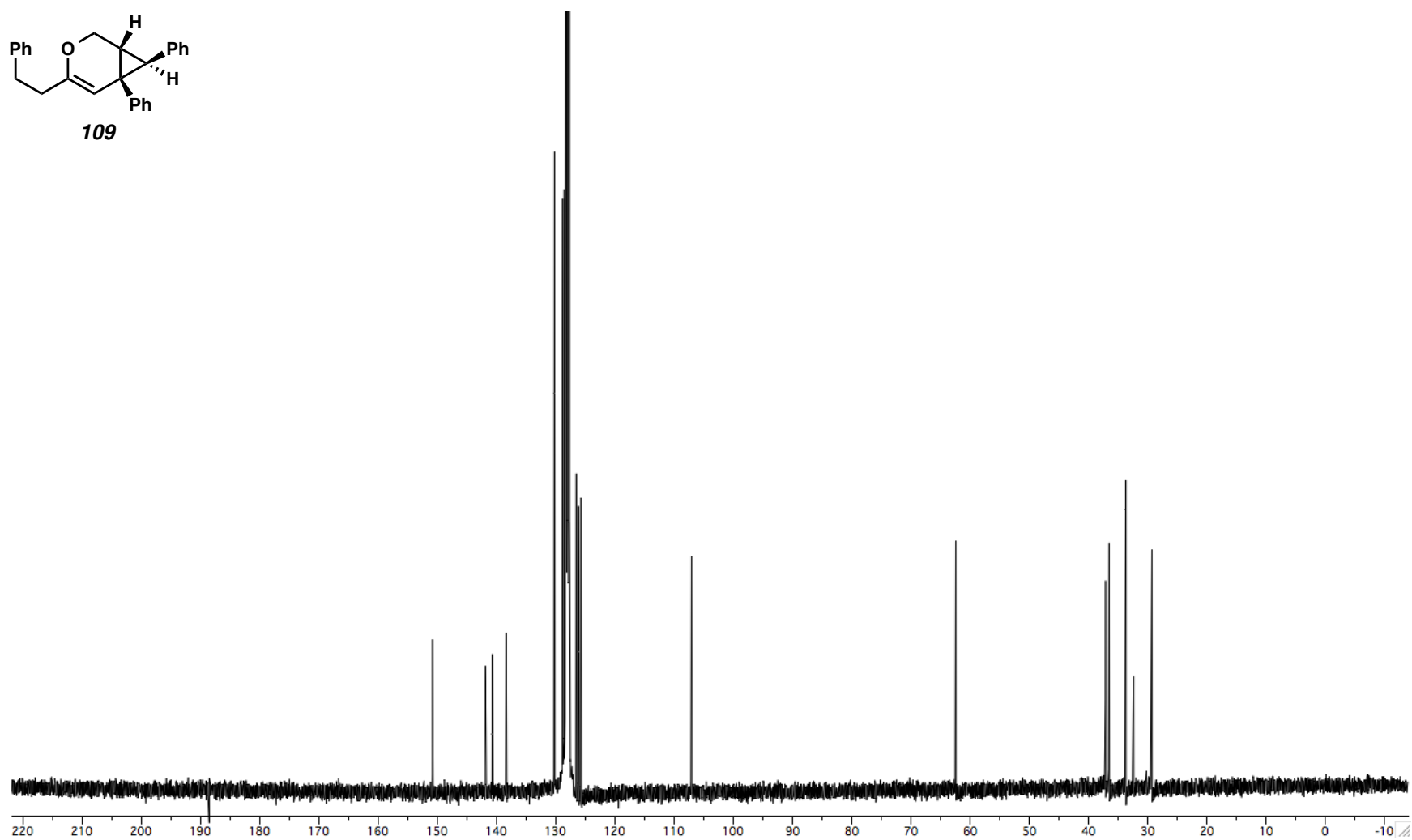
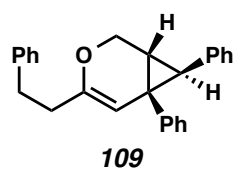


Figure A1.26. ^{13}C NMR (100 MHz, C_6D_6) of Compound **109**.

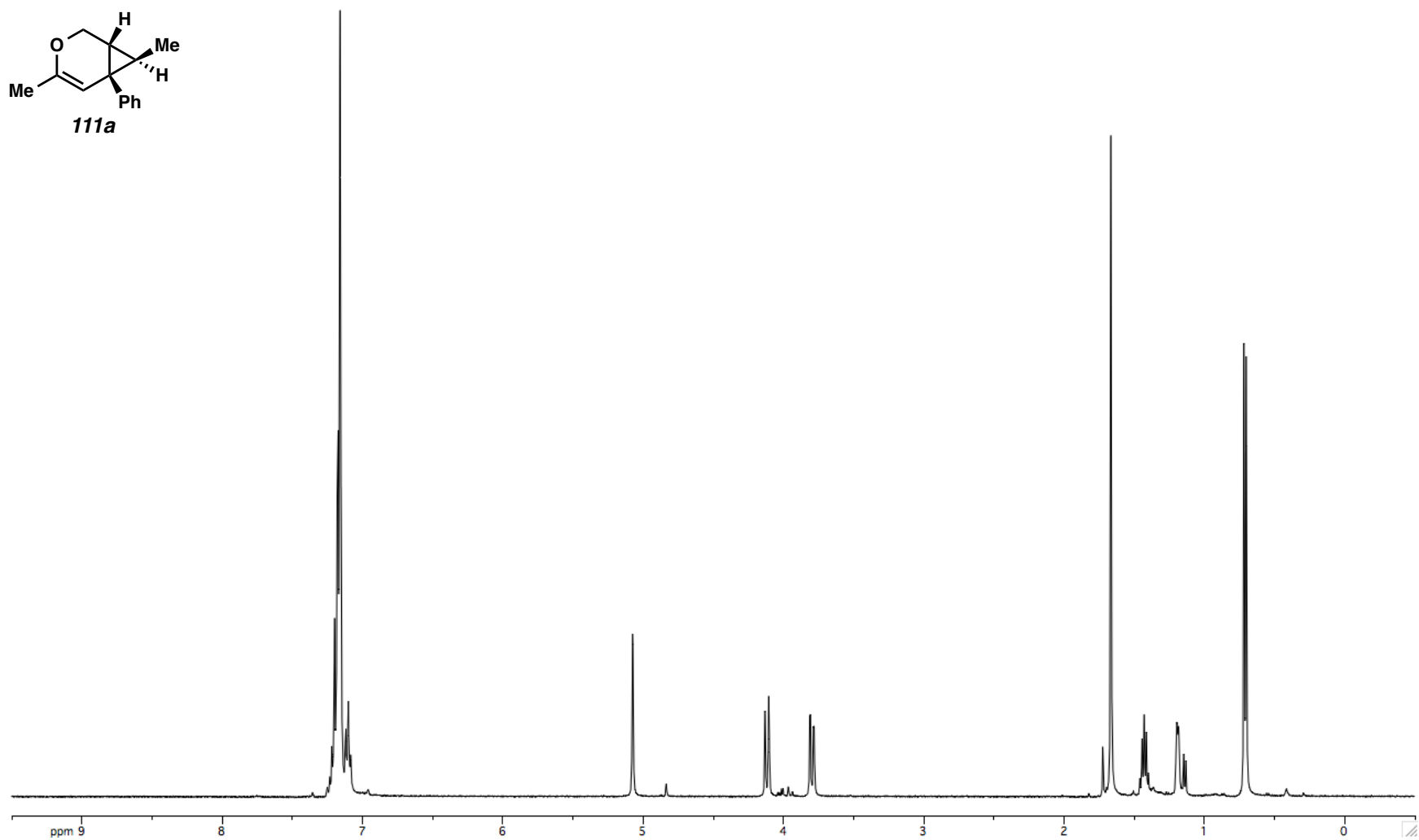
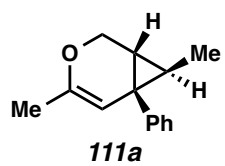


Figure A1.27. ^1H NMR (400 MHz, C_6D_6) of Compound **111a**.

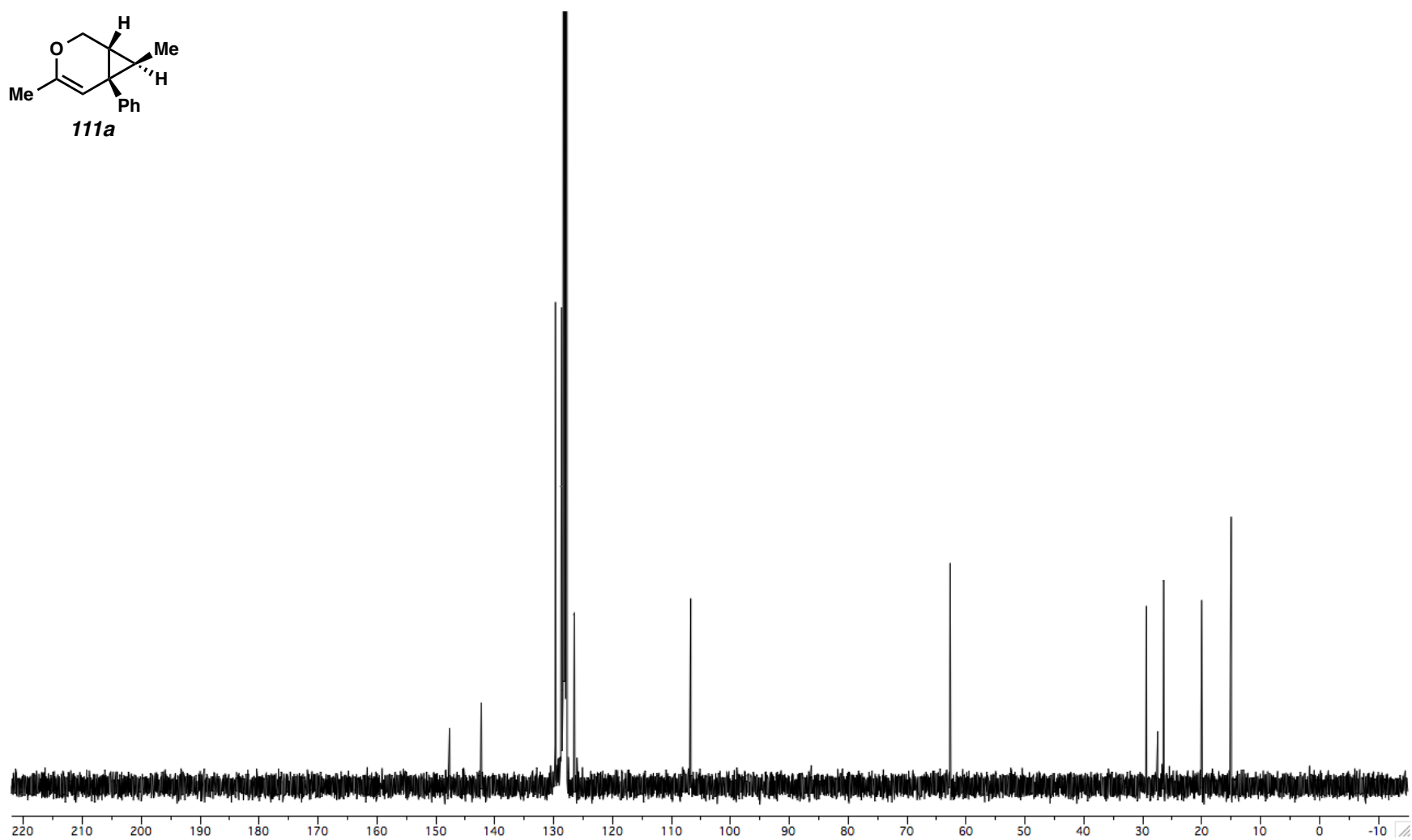
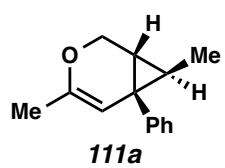


Figure A1.28. ^{13}C NMR (100 MHz, C_6D_6) of Compound **111a**.

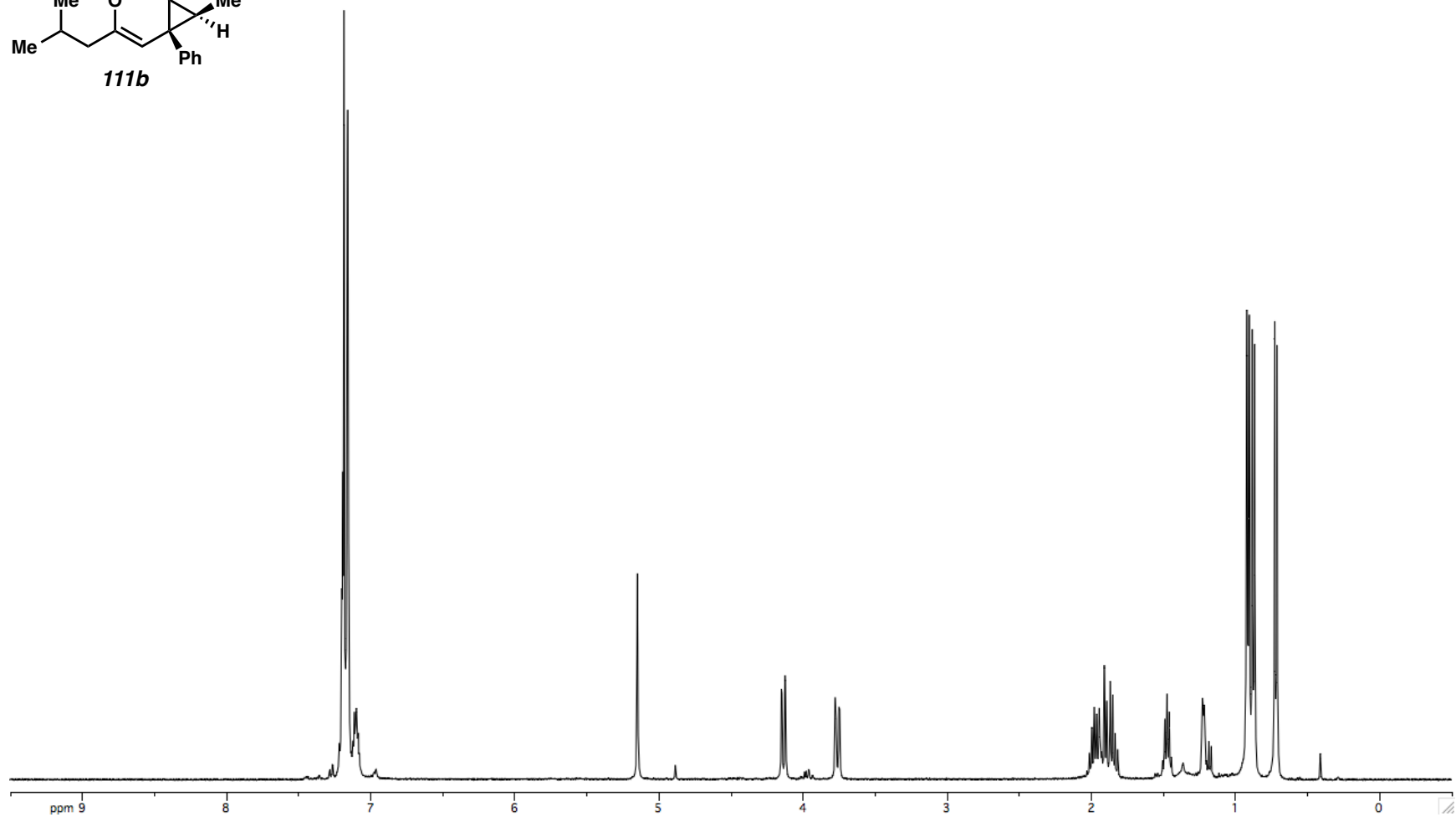
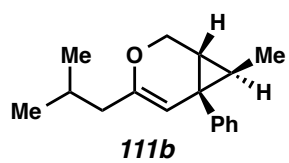


Figure A1.29. ^1H NMR (400 MHz, C_6D_6) of Compound **111b**.

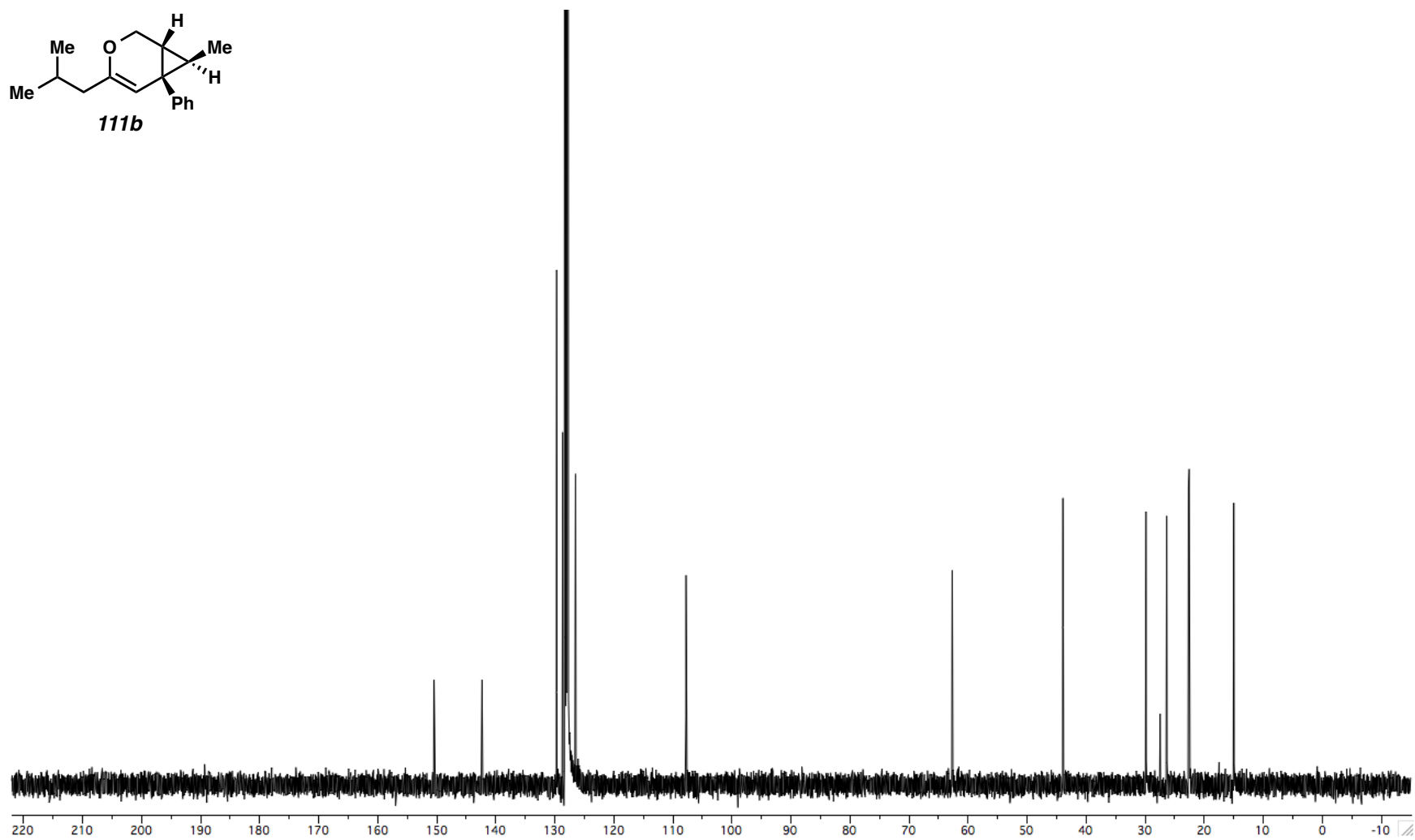
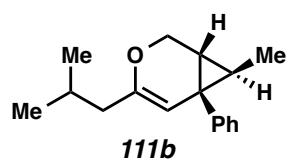


Figure A1.30. ^{13}C NMR (100 MHz, C_6D_6) of Compound **111b**.

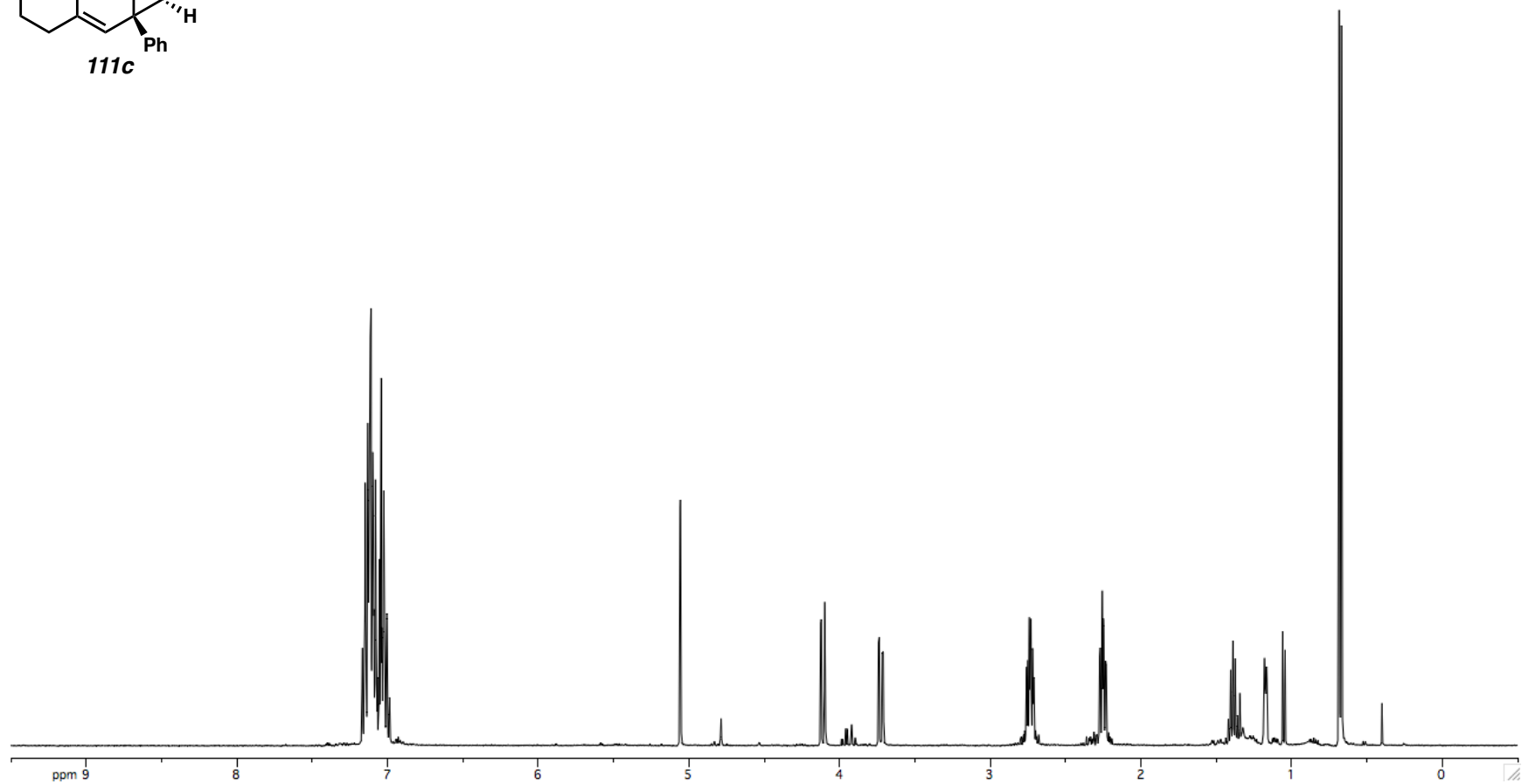
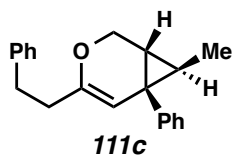


Figure A1.31. ^1H NMR (400 MHz, C_6D_6) of Compound **111c**.

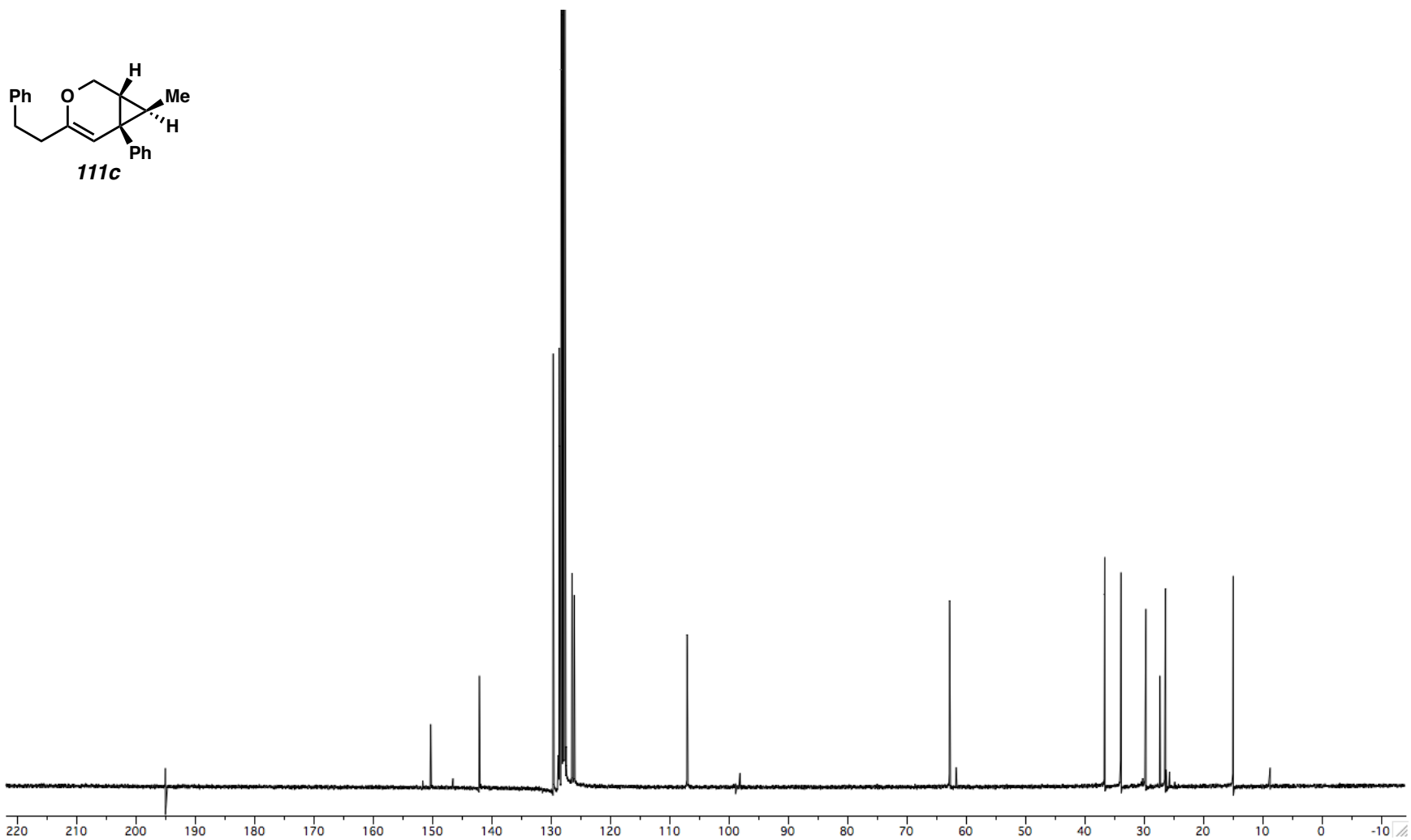


Figure A1.32. ^{13}C NMR (100 MHz, C_6D_6) of Compound **111c**.

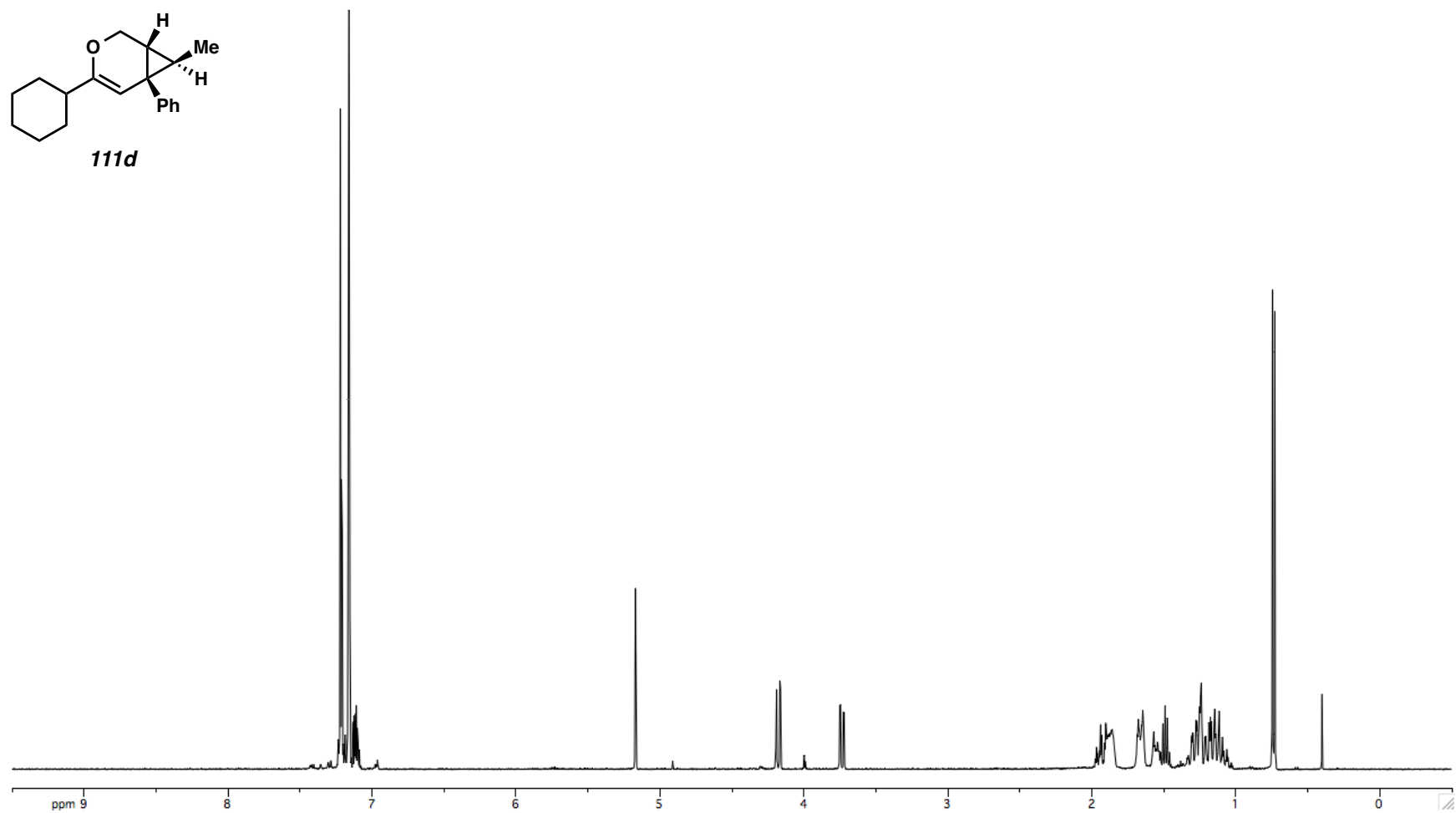
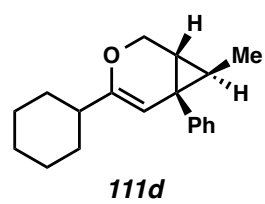


Figure A1.33. ^1H NMR (400 MHz, C_6D_6) of Compound **111d**.

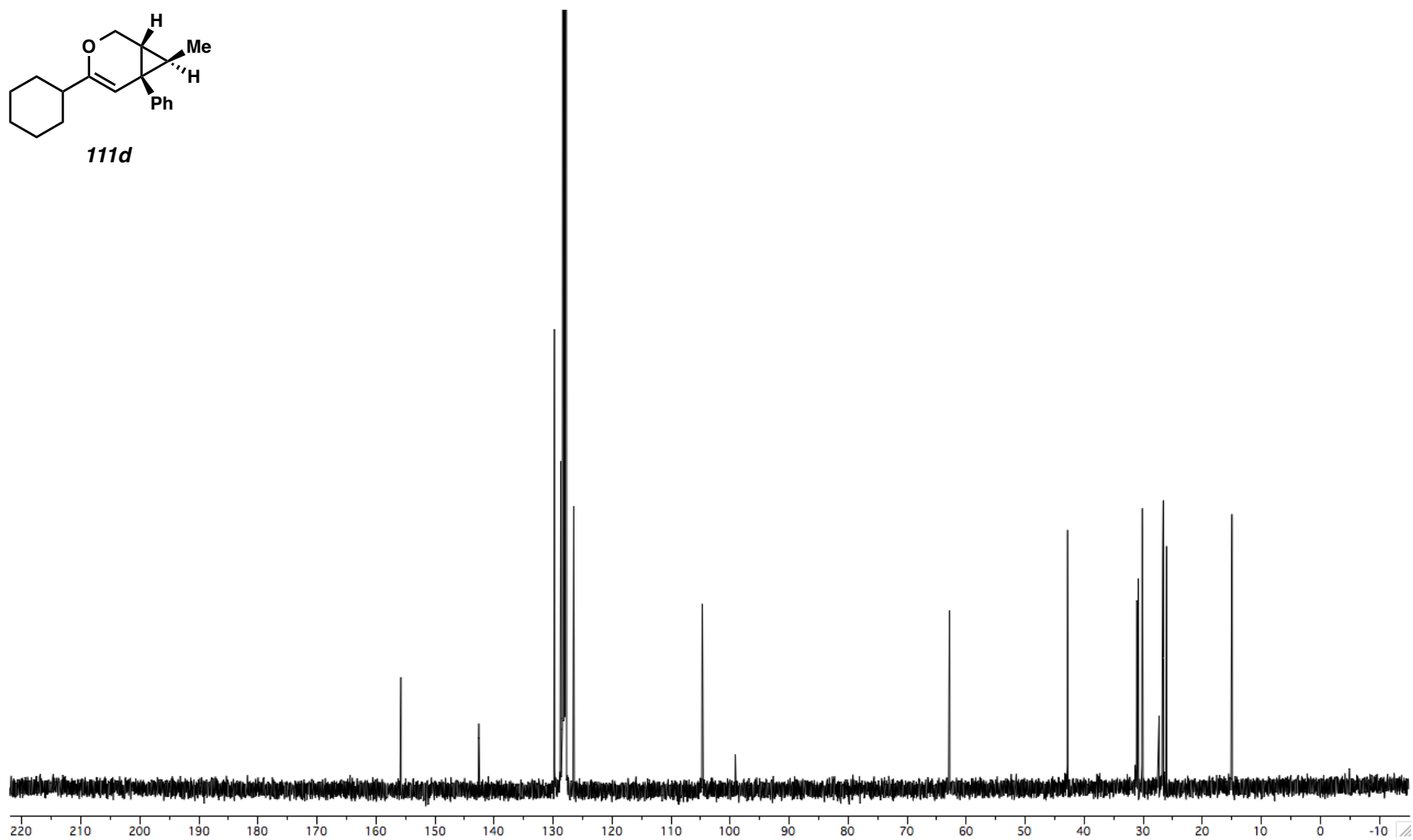
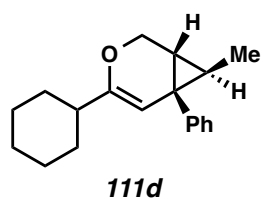


Figure A1.34. ^{13}C NMR (100 MHz, C_6D_6) of Compound **111d**.

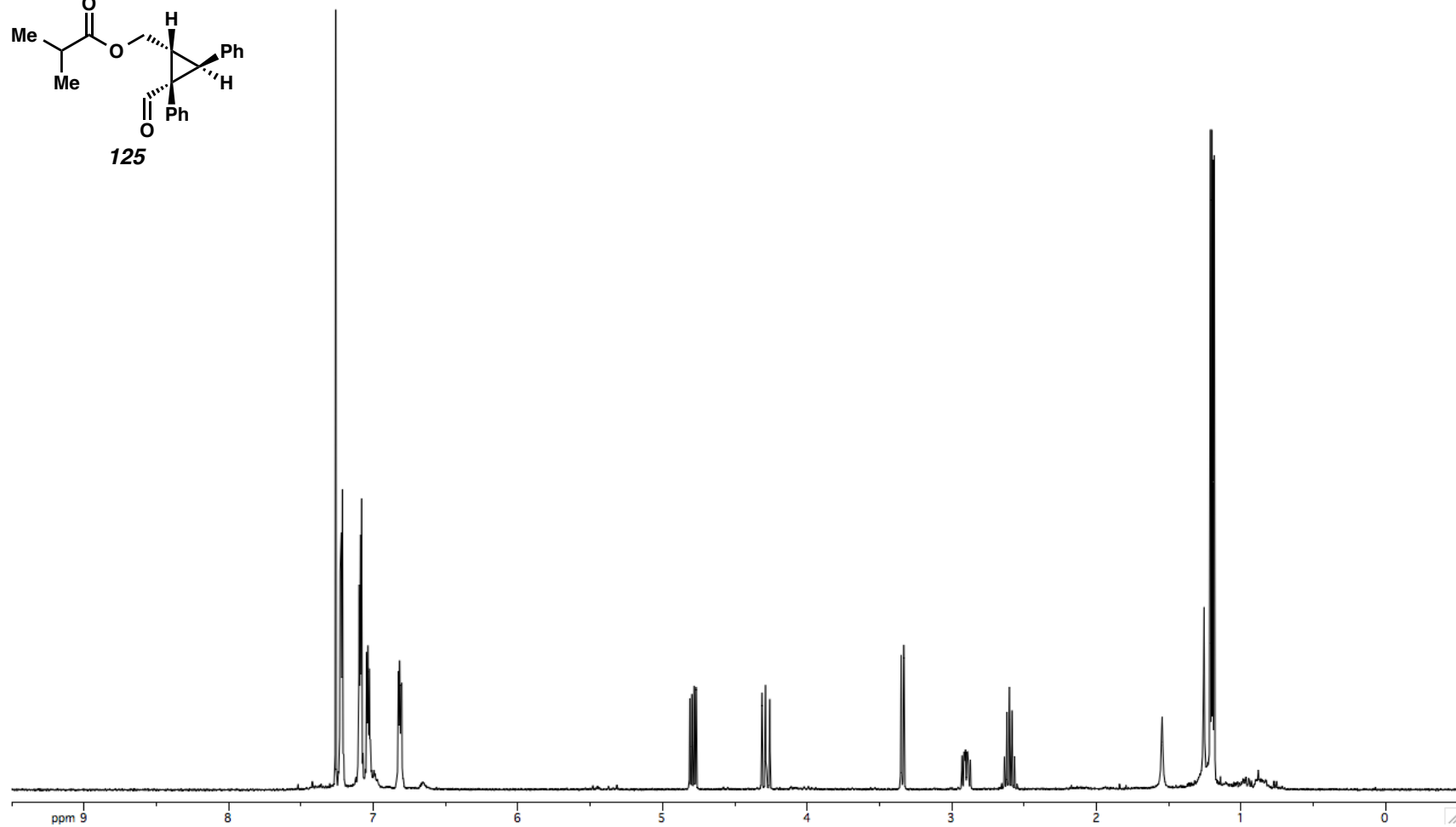
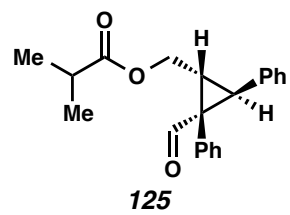


Figure A1.35. ¹H NMR (400 MHz, CDCl₃) of Compound 125.

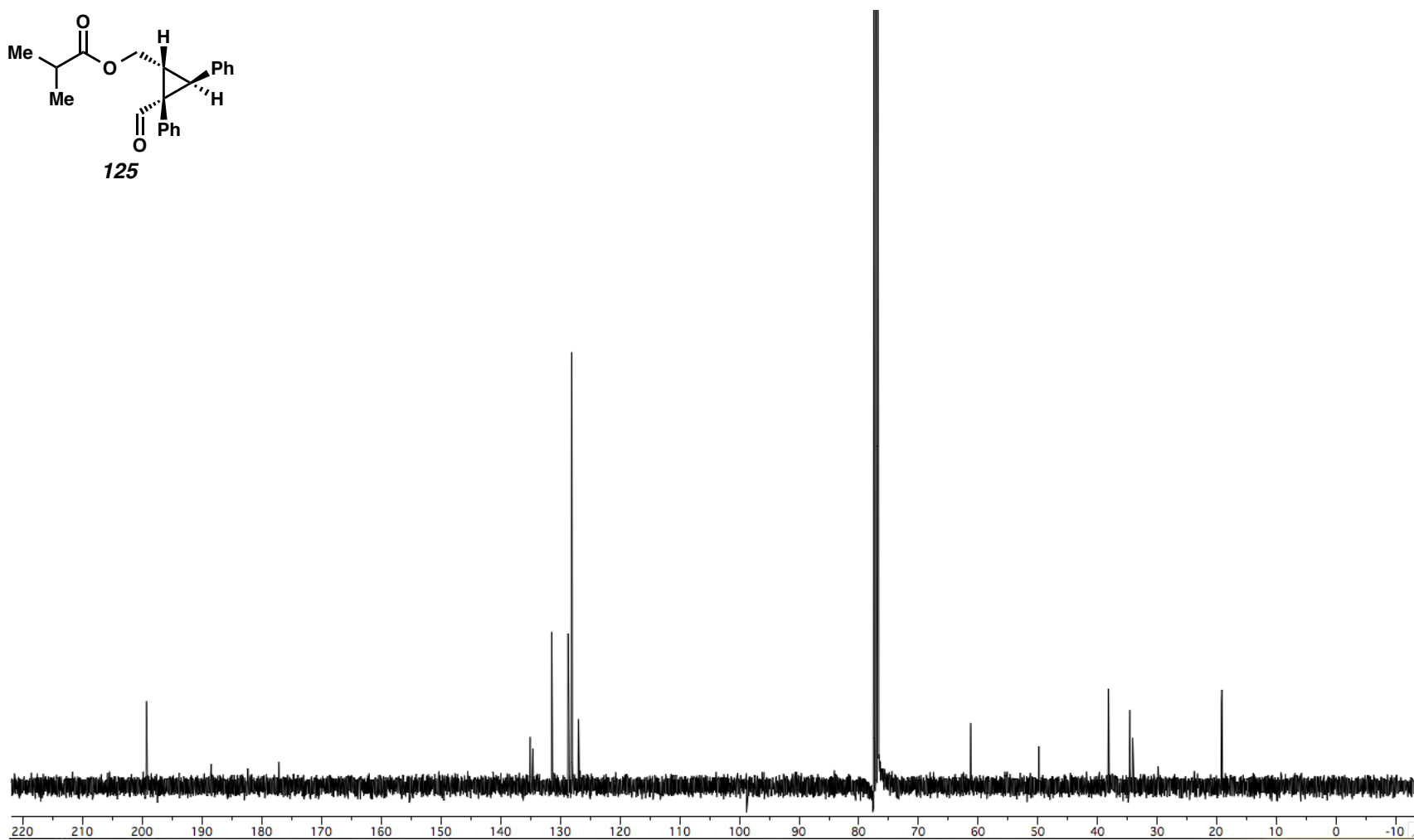
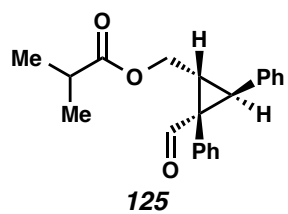


Figure A1.36. ^{13}C NMR (100 MHz, CDCl₃) of Compound 125.

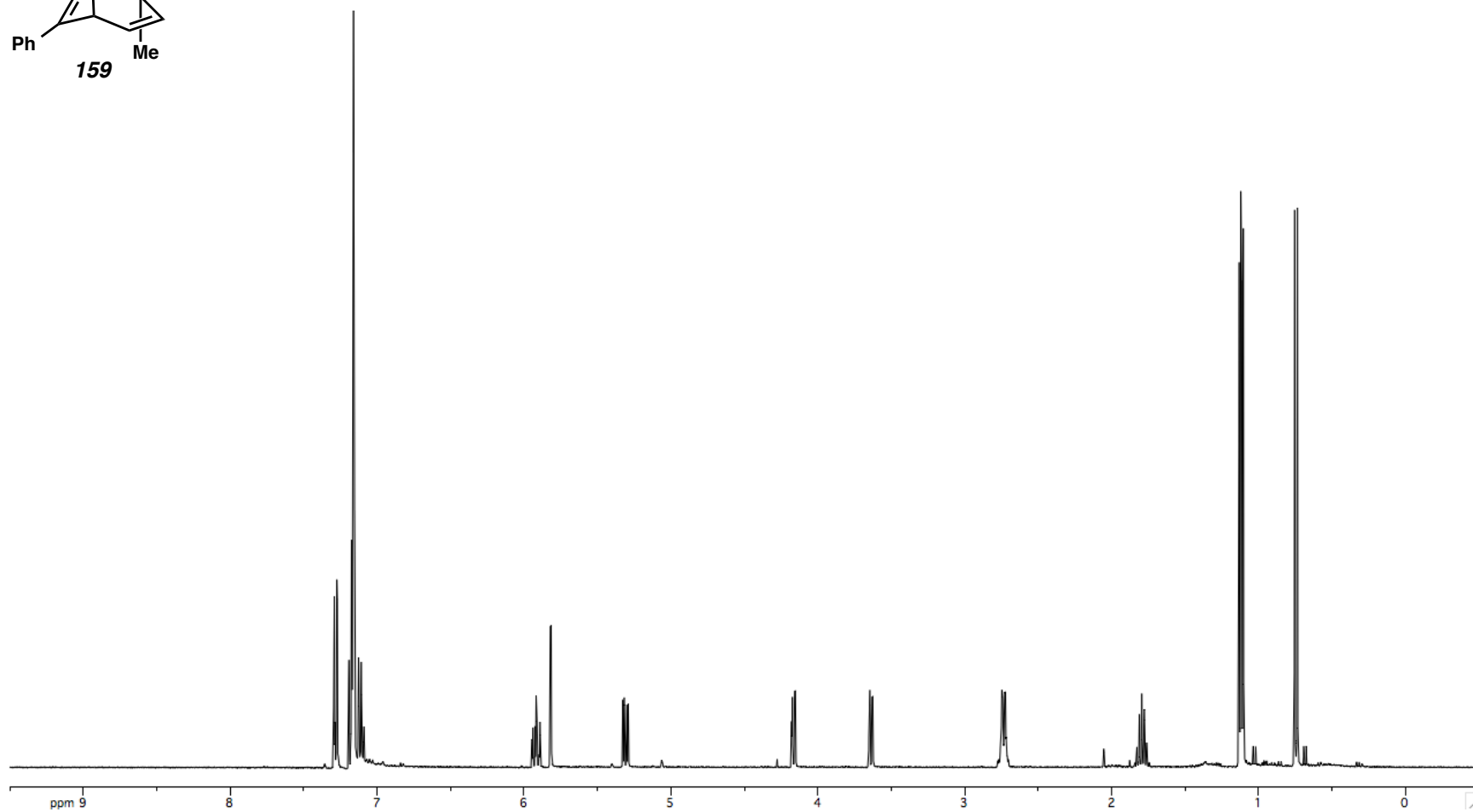
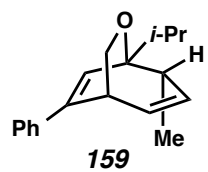


Figure A1.37. ^1H NMR (400 MHz, C_6D_6) of Compound **159**.

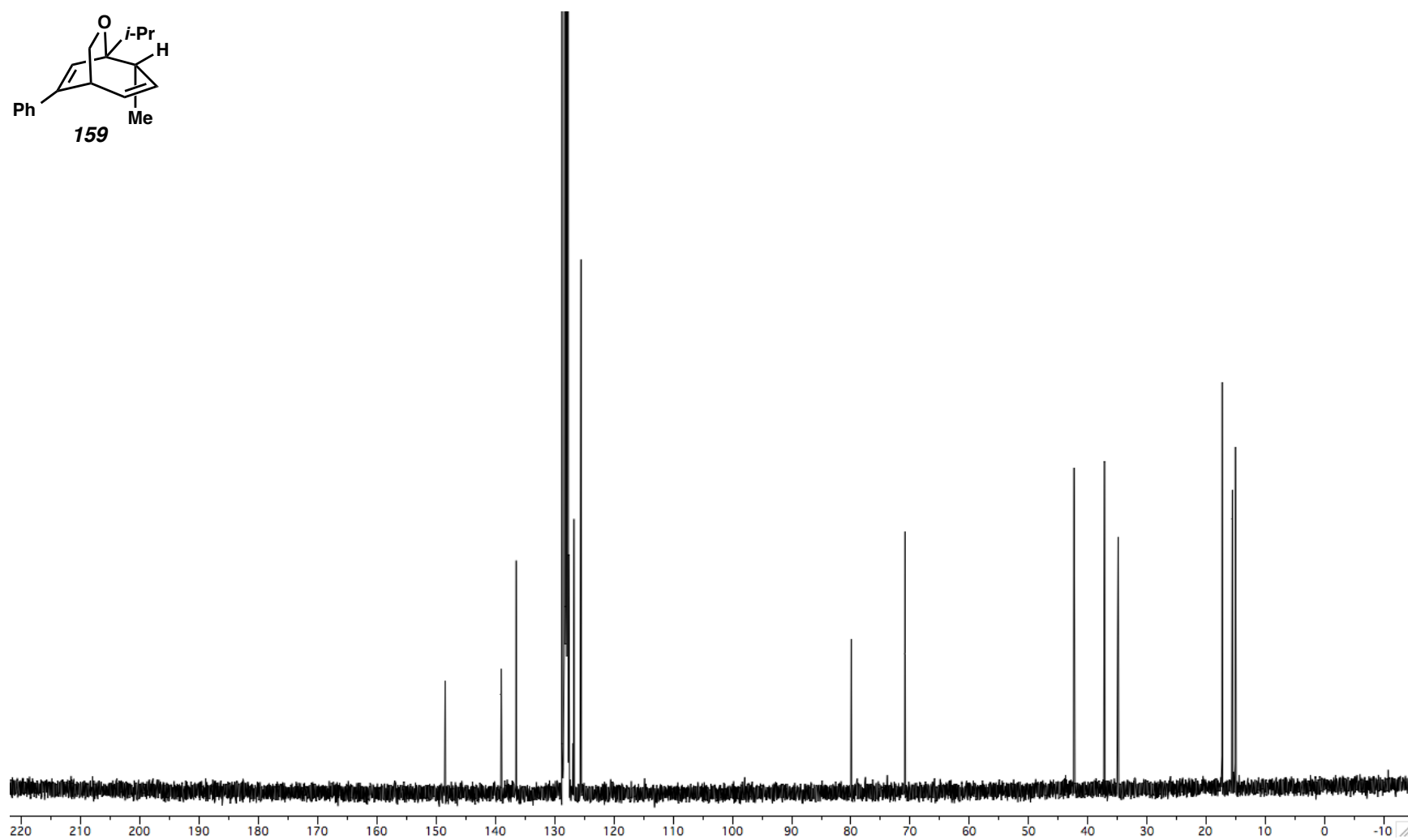
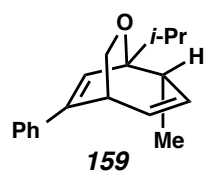


Figure A1.38. ^{13}C NMR (100 MHz, C_6D_6) of Compound 159.

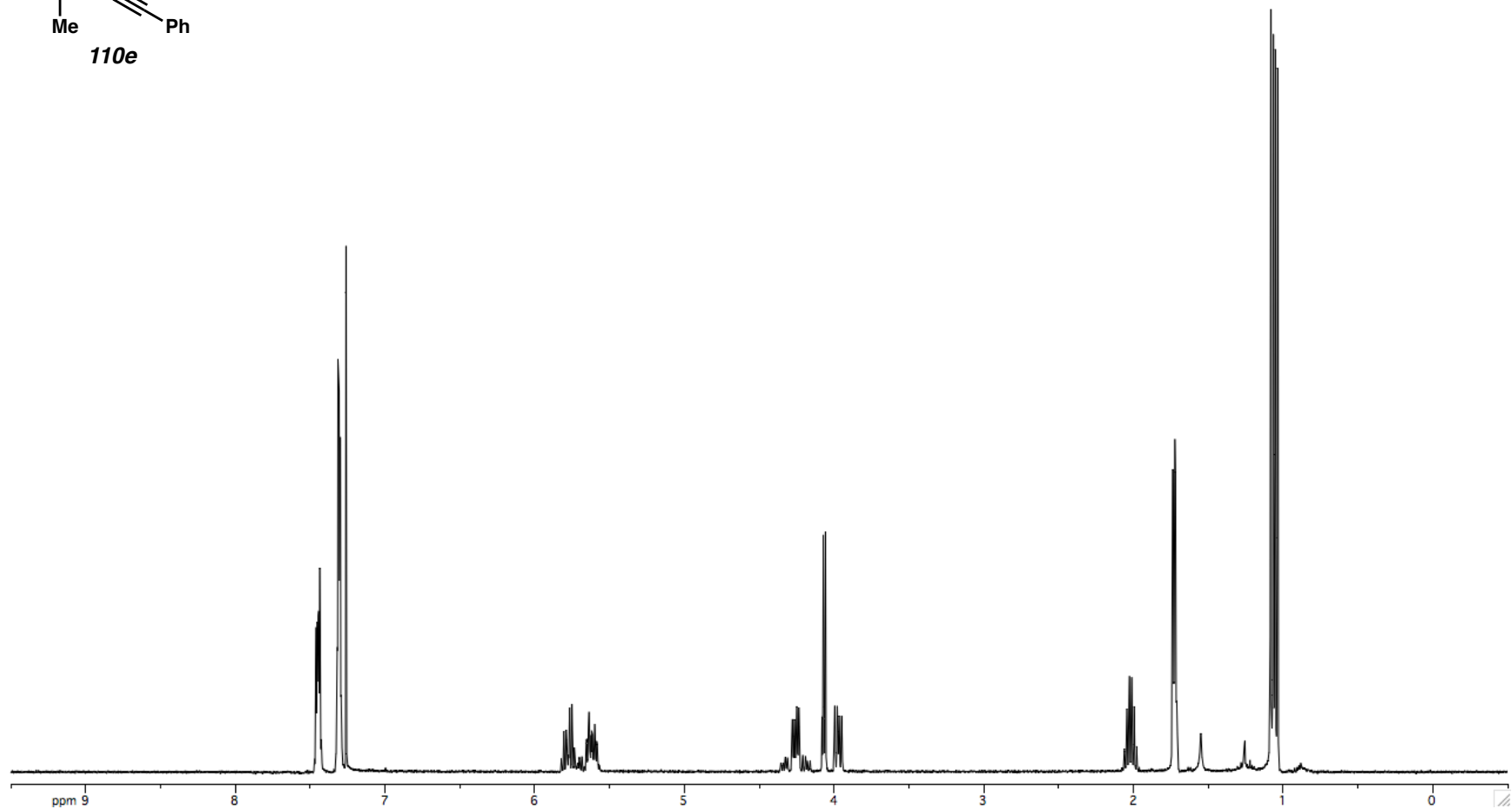
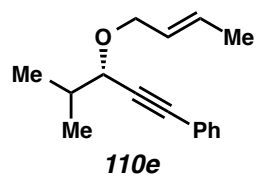


Figure A1.39. ^1H NMR (400 MHz, CDCl_3) of Compound **110e**.

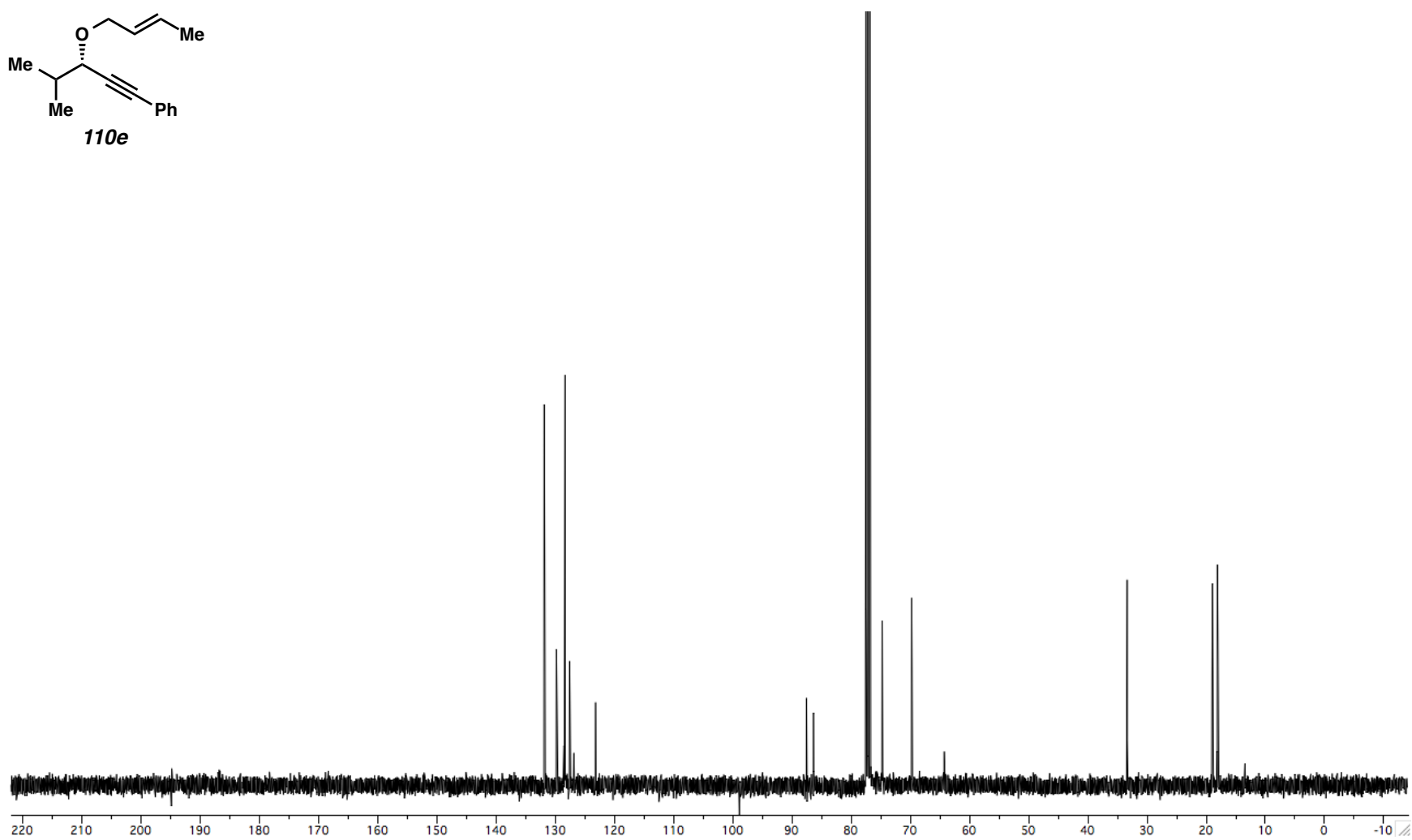
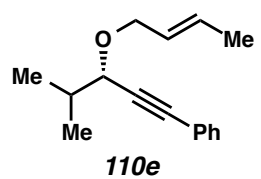


Figure A1.40. ^{13}C NMR (100 MHz, CDCl_3) of Compound **110e**.

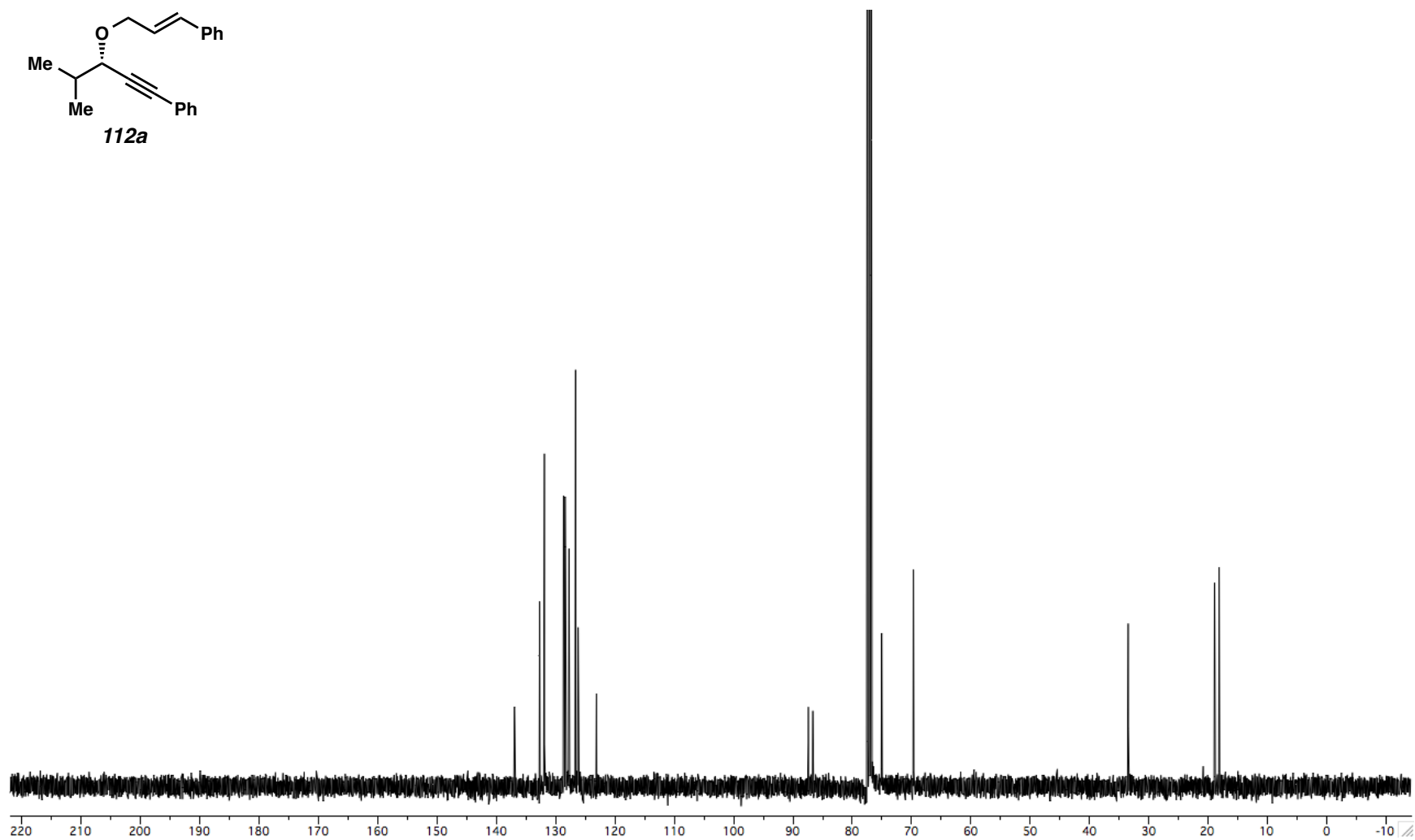
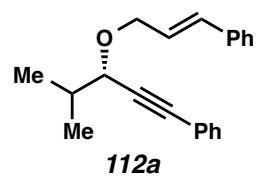


Figure A1.42. ^{13}C NMR (100 MHz, CDCl_3) of Compound **112a**.

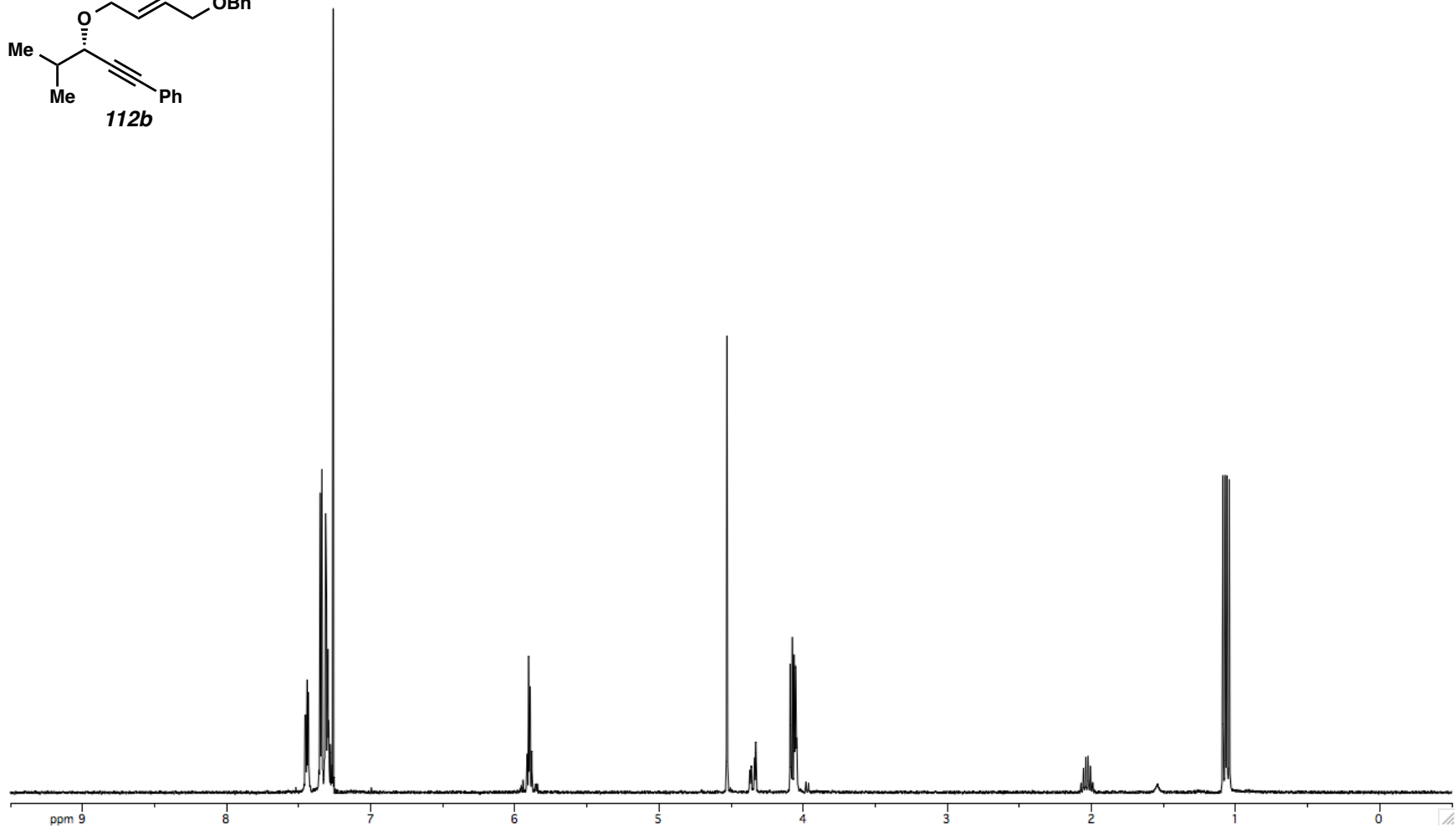
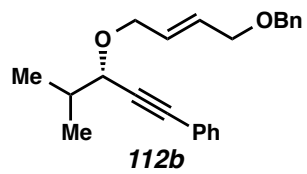


Figure A1.43. ^1H NMR (400 MHz, CDCl_3) of Compound **112b**.

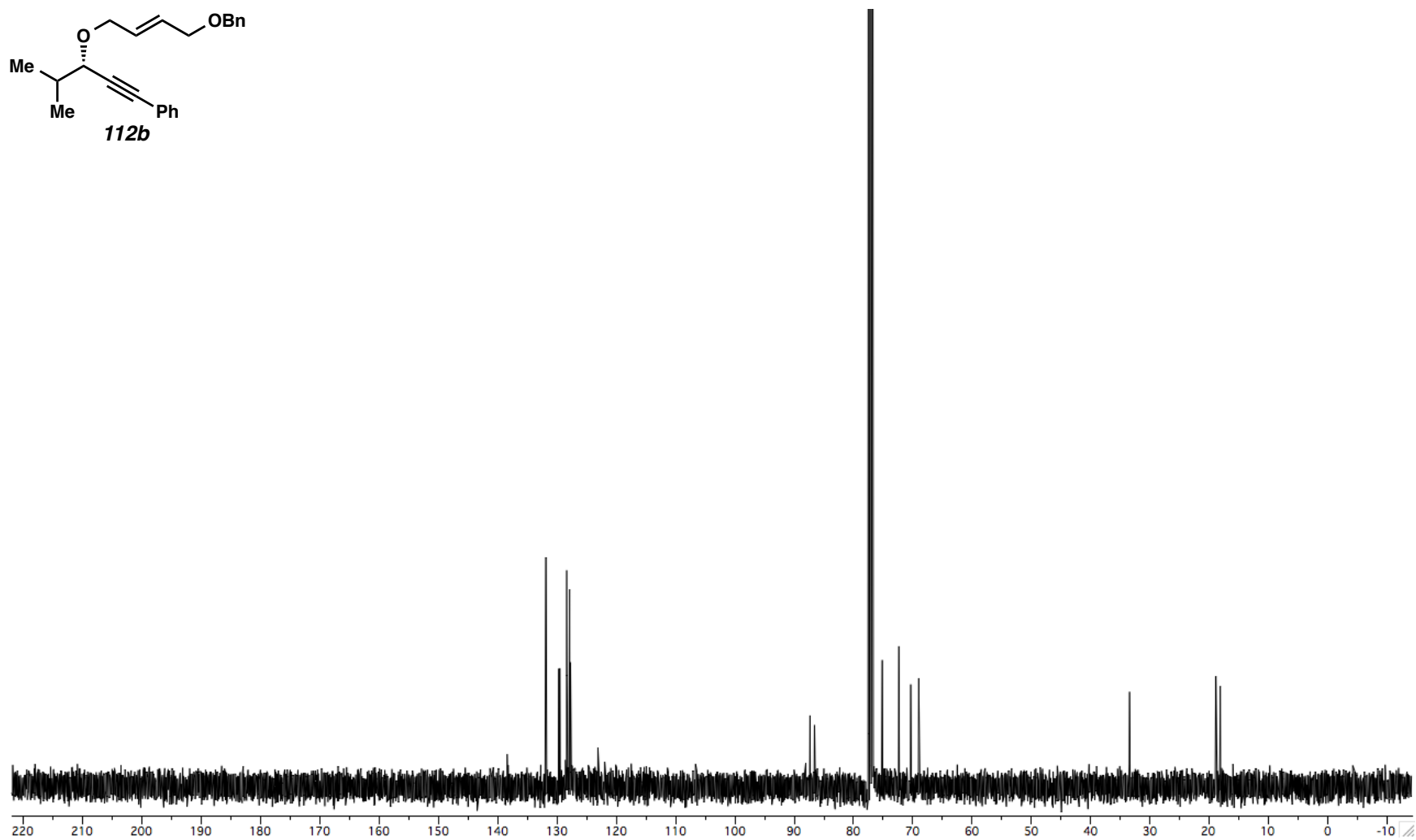
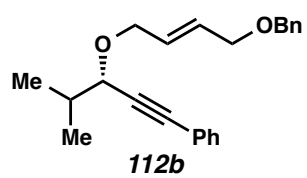


Figure A1.44. ¹³C NMR (100 MHz, CDCl₃) of Compound **112b**.

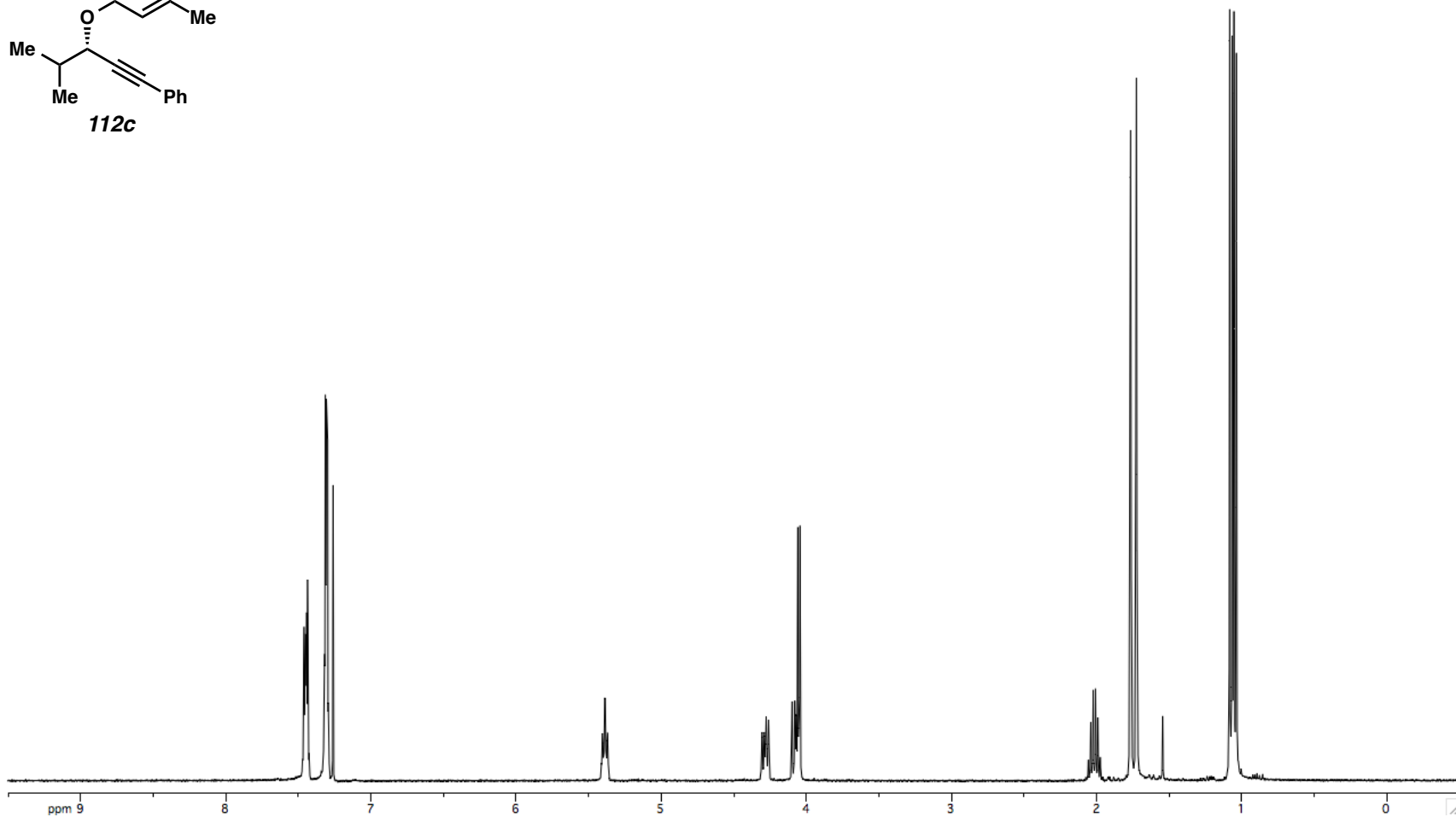
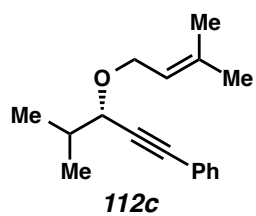


Figure A1.45. ^1H NMR (400 MHz, CDCl_3) of Compound **112c**.

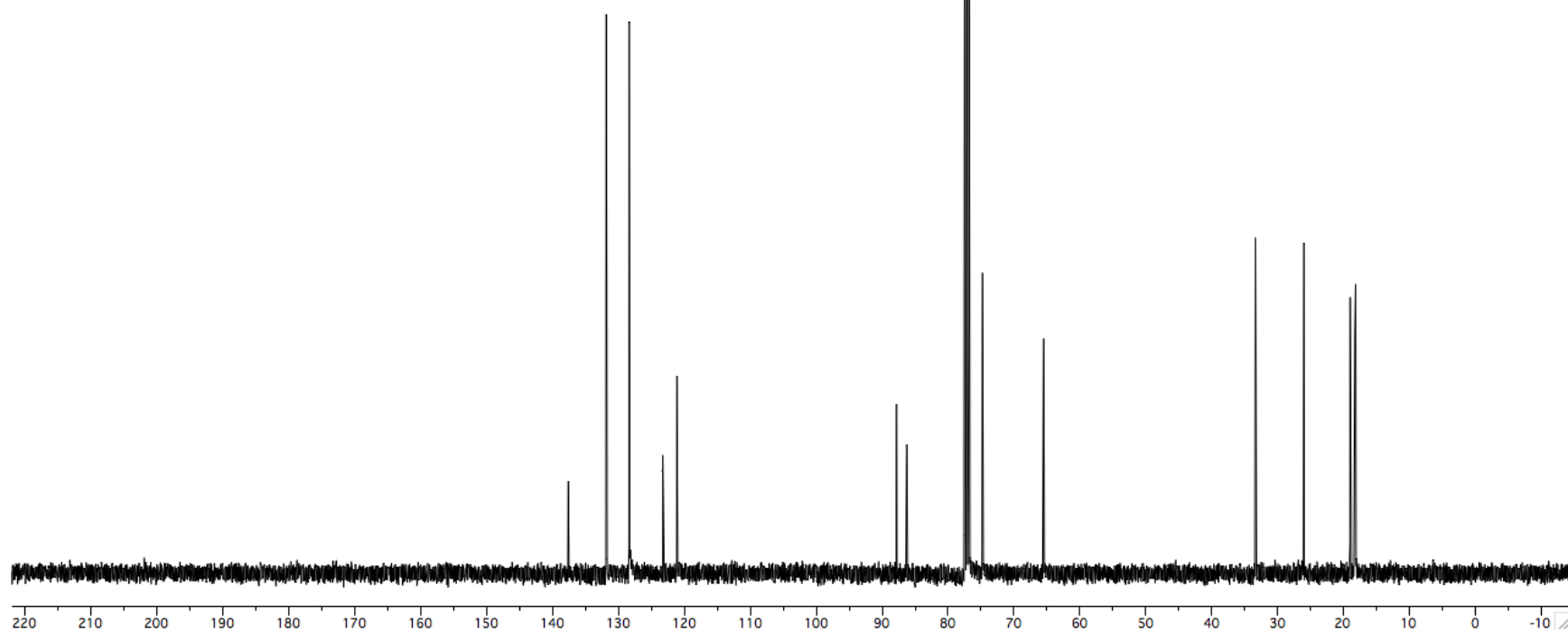
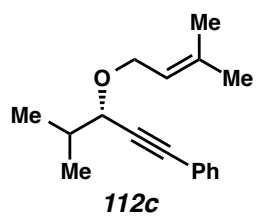


Figure A1.46. ^{13}C NMR (100 MHz, CDCl_3) of Compound **112c**.

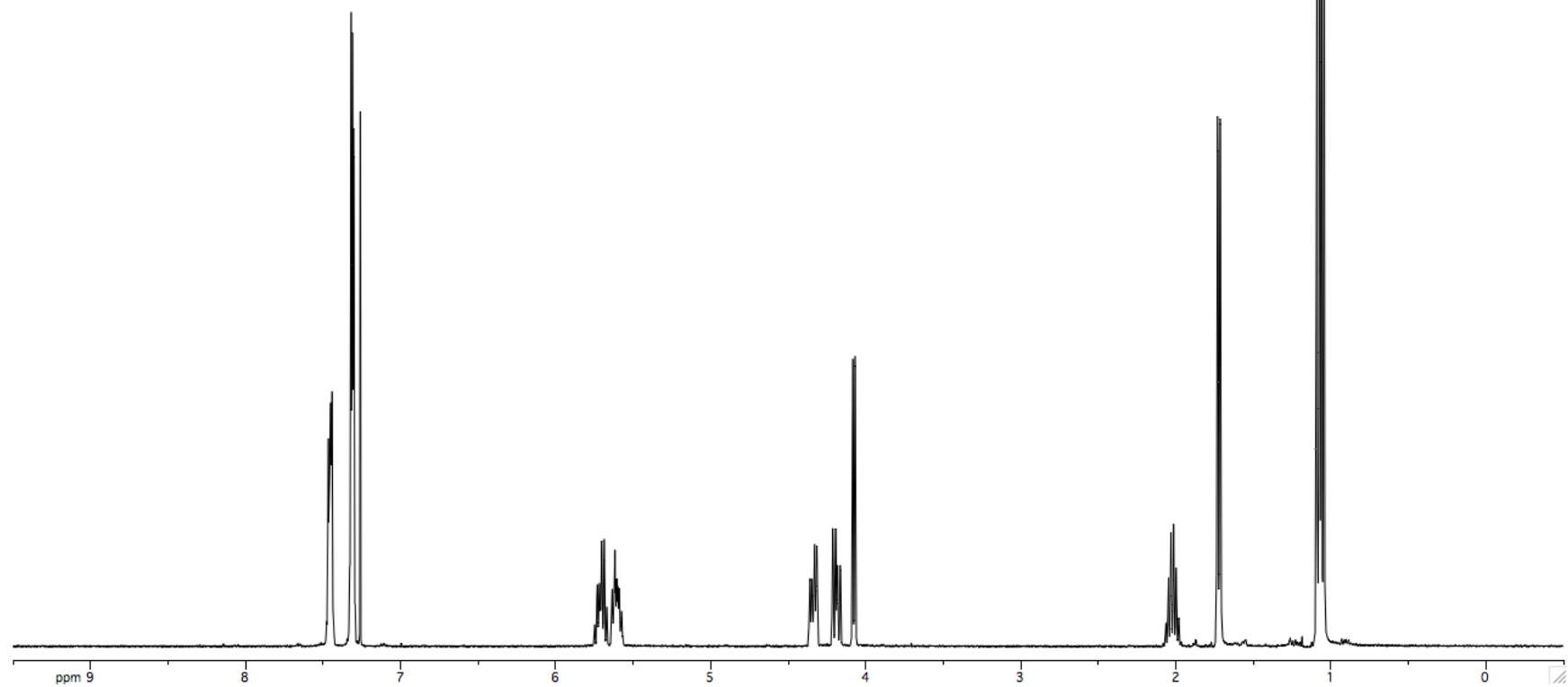
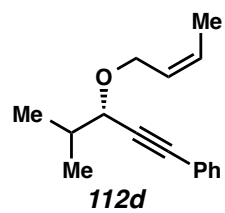


Figure A1.47. ^1H NMR (400 MHz, CDCl_3) of Compound **112d**.

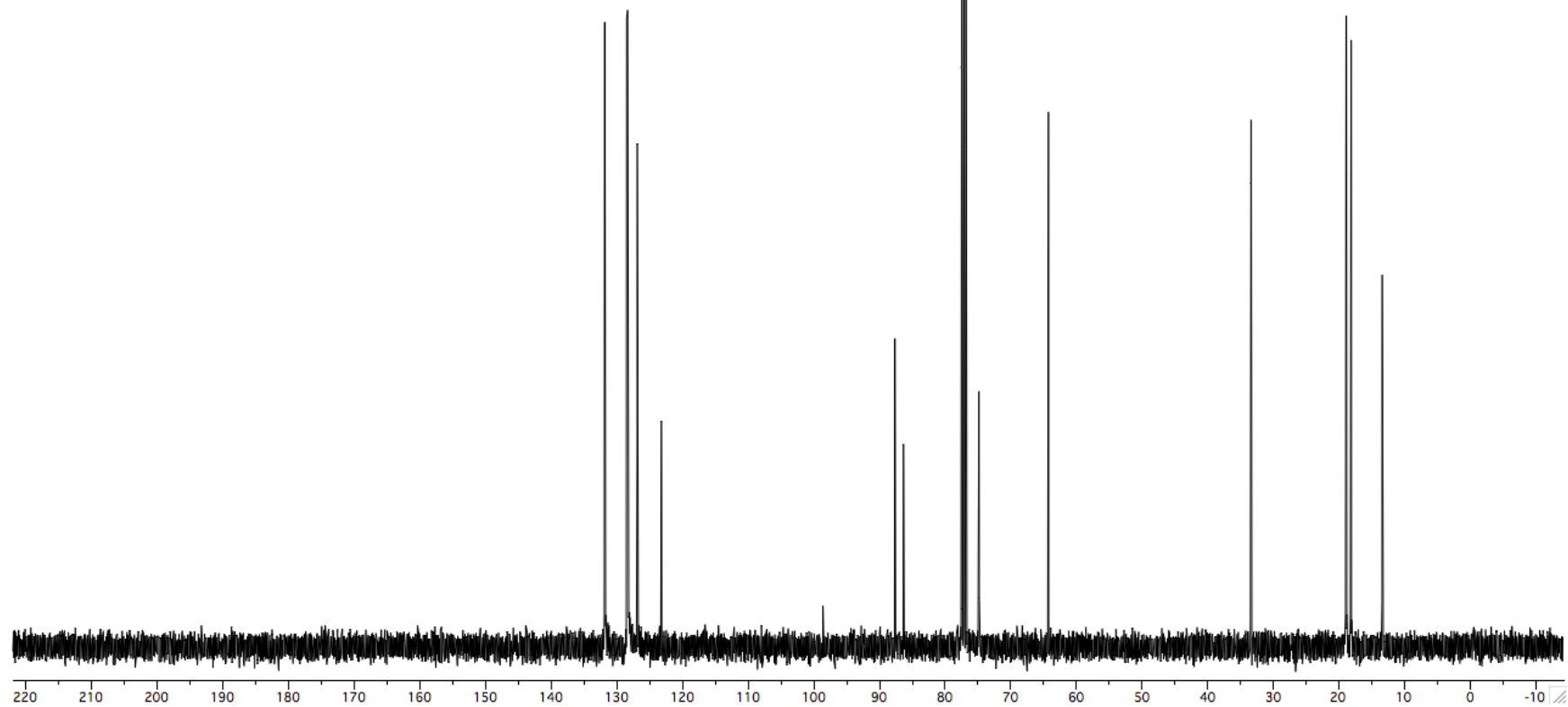
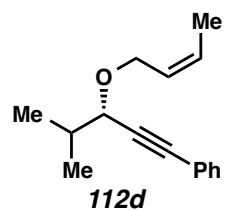


Figure A1.48. ^{13}C NMR (100 MHz, CDCl_3) of Compound **112d**.

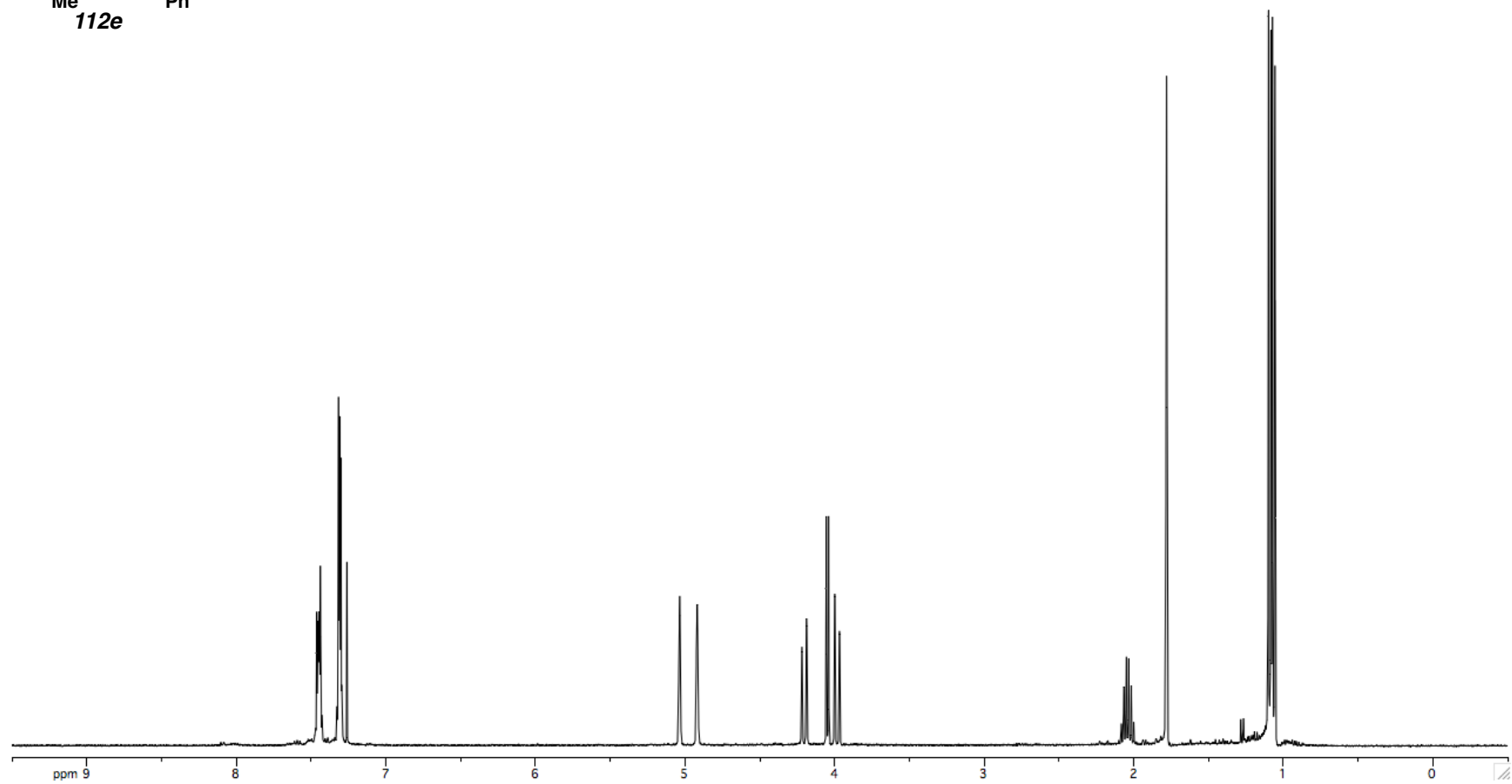
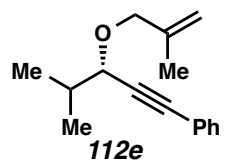


Figure A1.49. ^1H NMR (400 MHz, CDCl_3) of Compound **112e**.

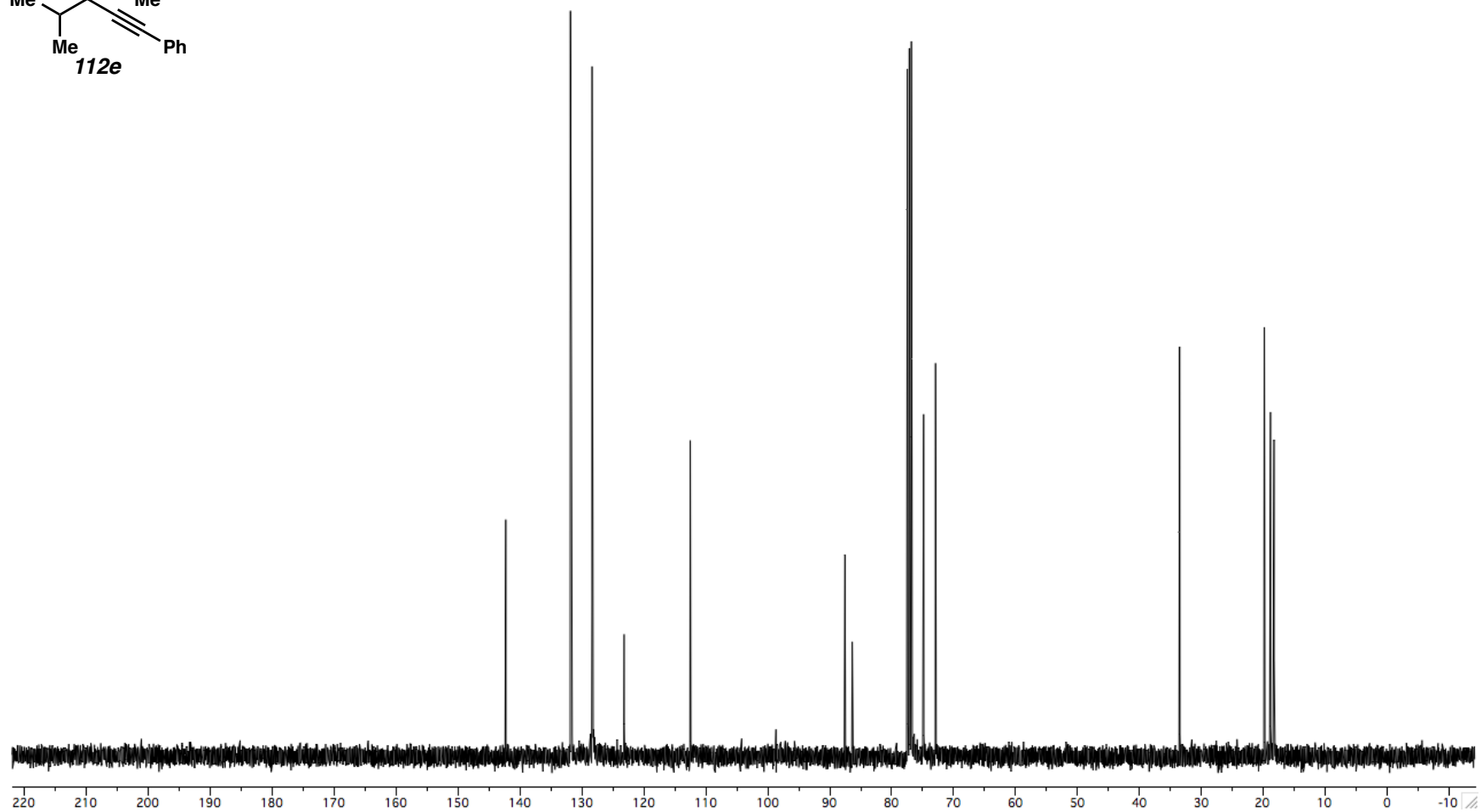
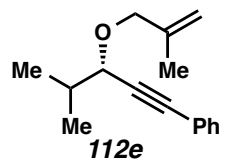


Figure A1.50. ^{13}C NMR (100 MHz, CDCl_3) of Compound **112e**.

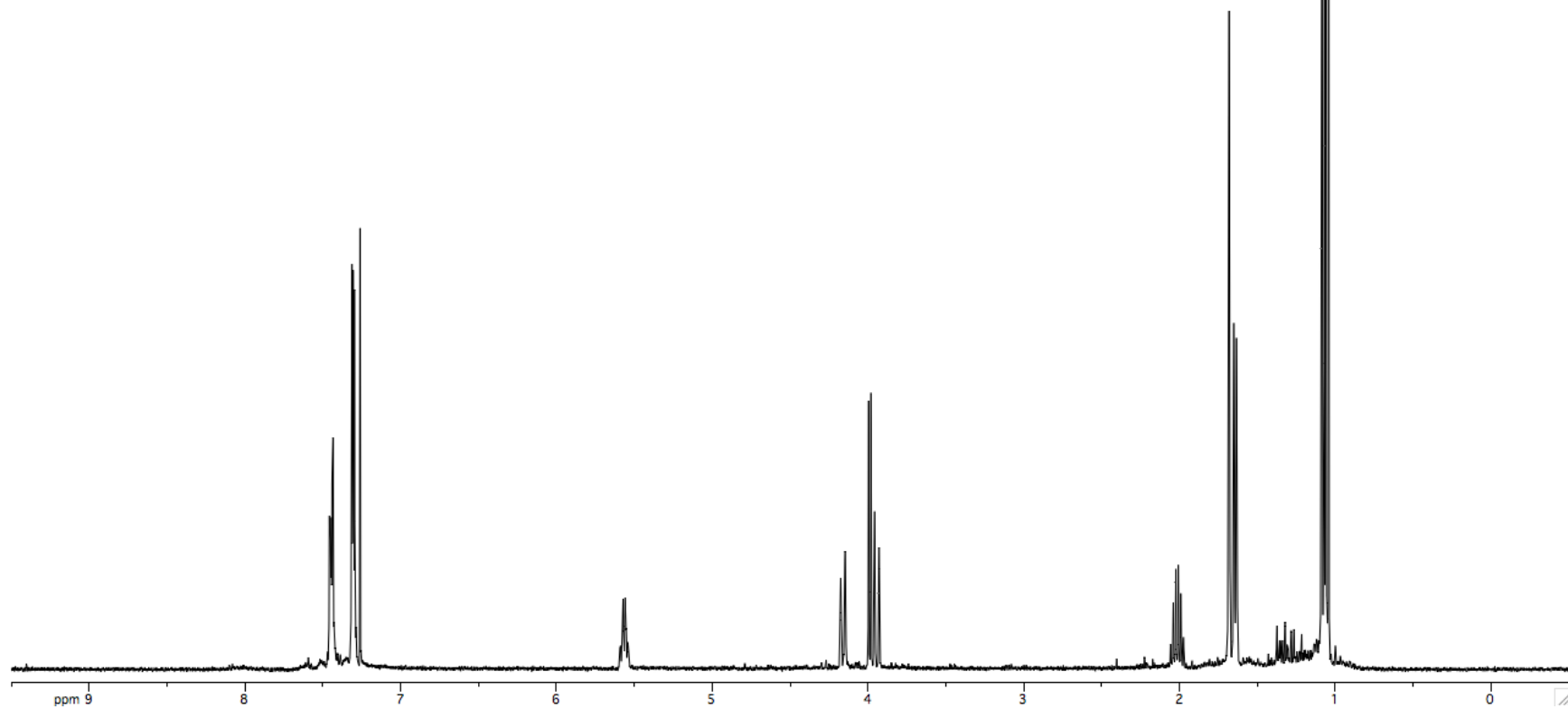
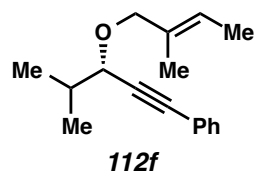


Figure A1.51. ^1H NMR (400 MHz, CDCl_3) of Compound **112f**.

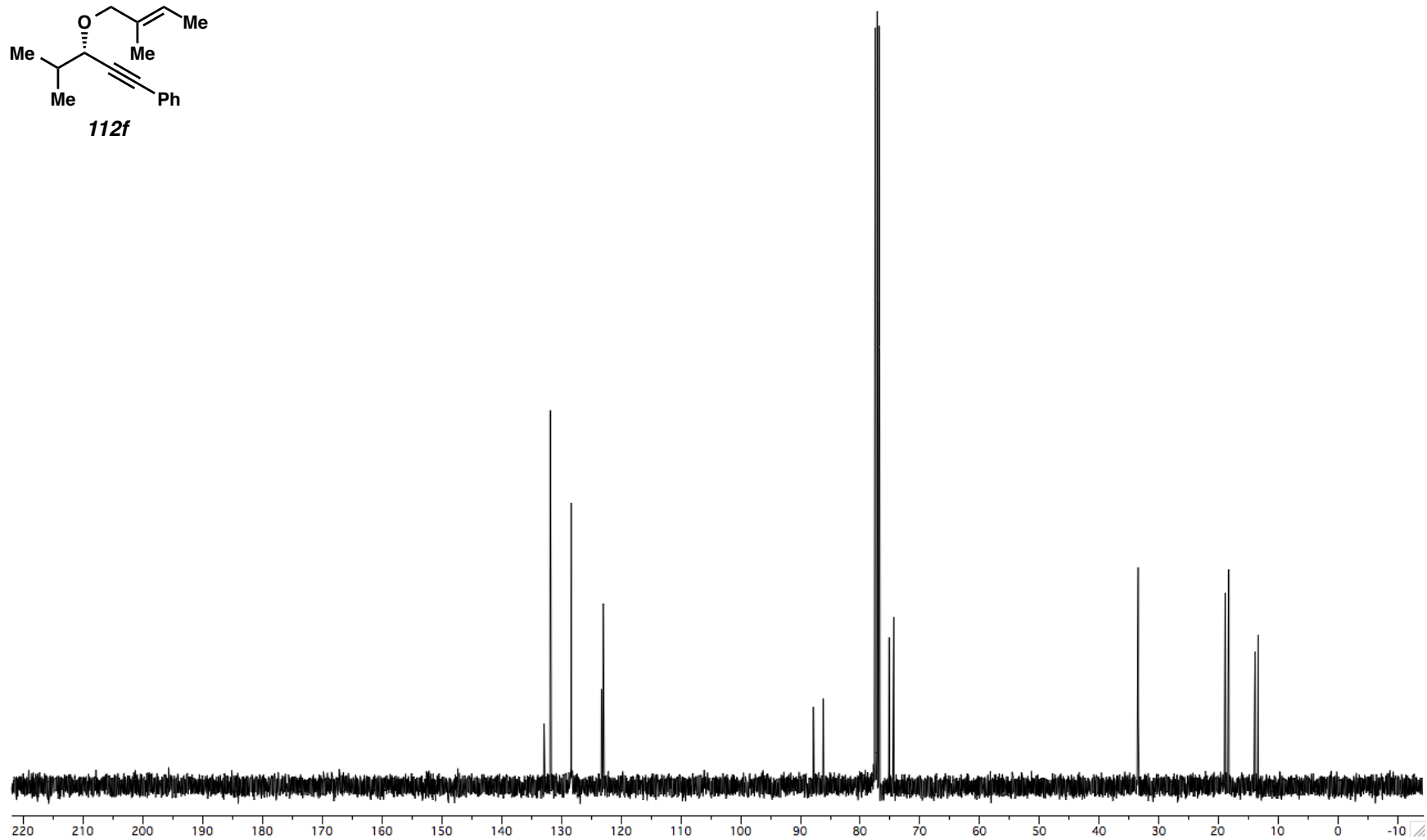
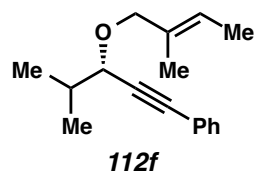


Figure A1.52. ^{13}C NMR (100 MHz, CDCl_3) of Compound **112f**.

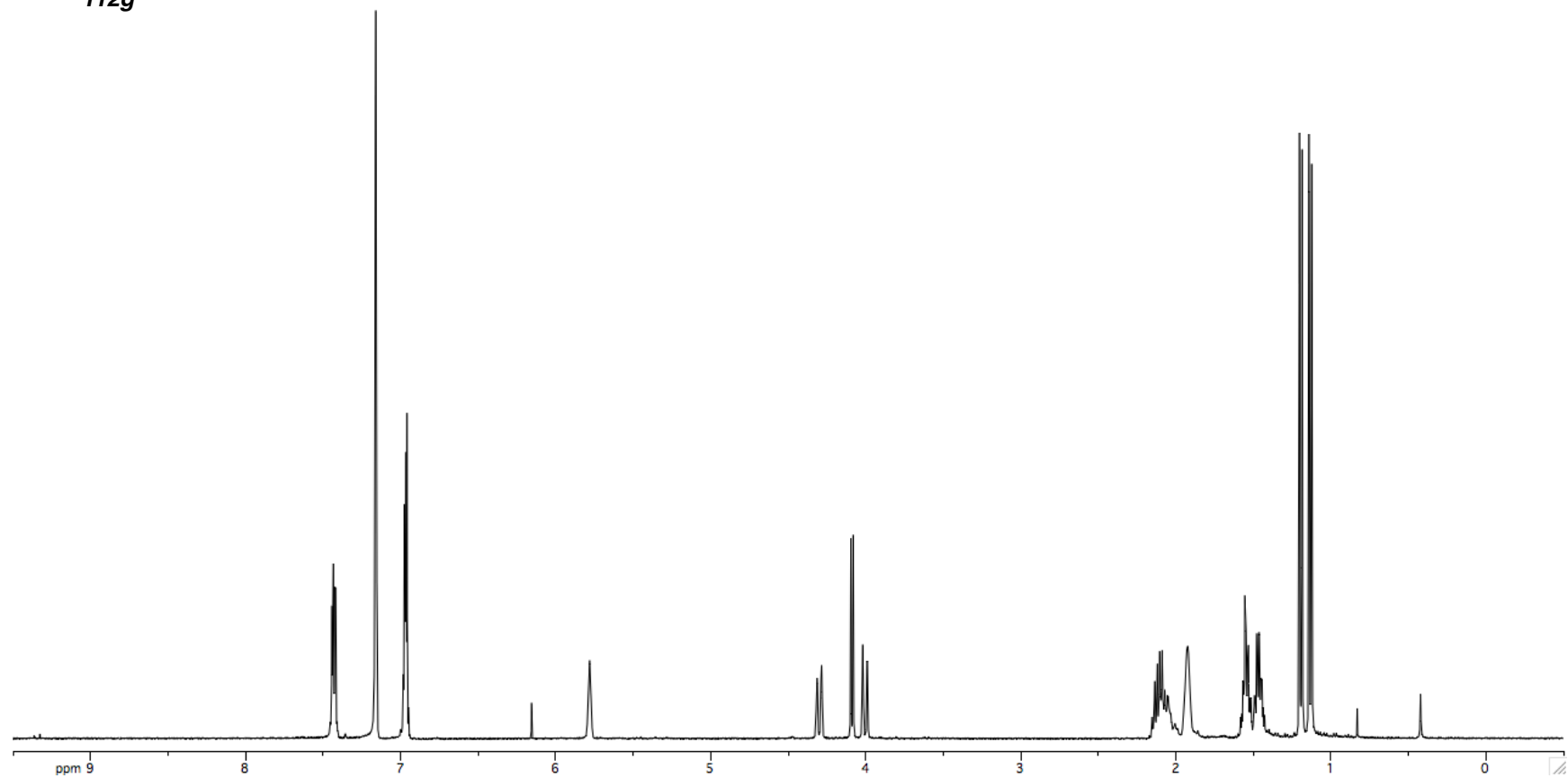
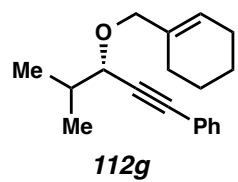


Figure A1.53. ^{13}C NMR (100 MHz, C_6D_6) of Compound **112g**.

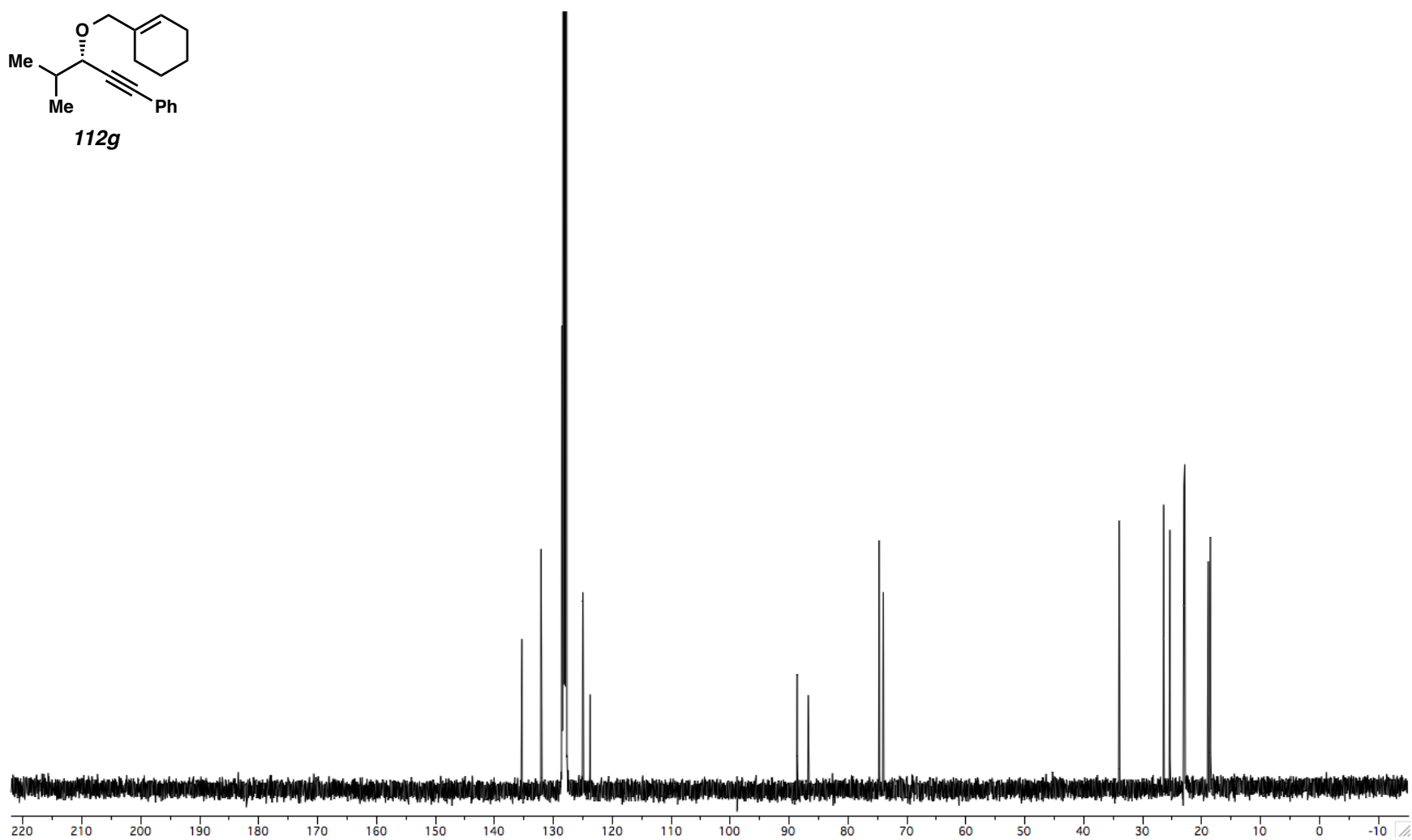
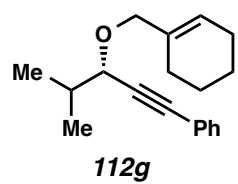


Figure A1.54. ^{13}C NMR (100 MHz, C_6D_6) of Compound **112g**.

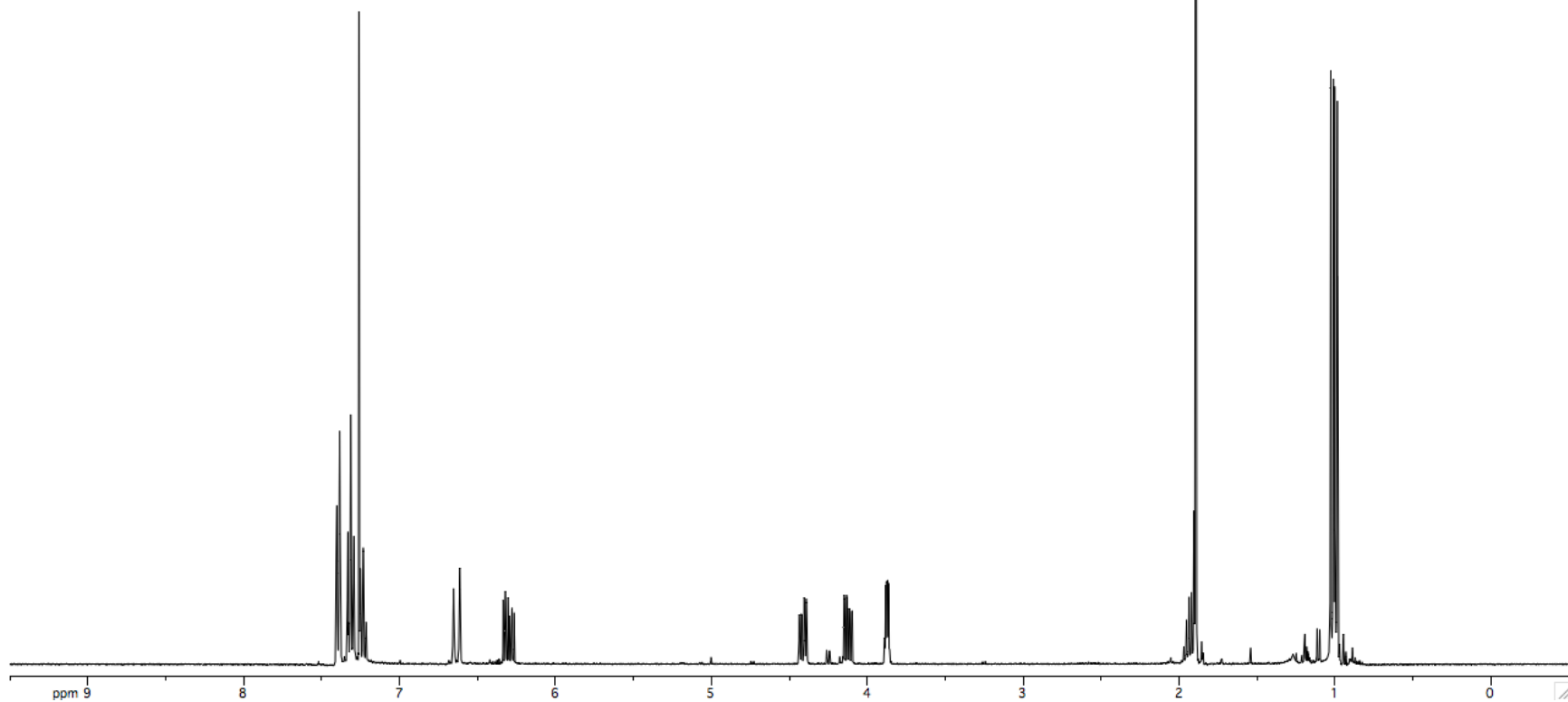
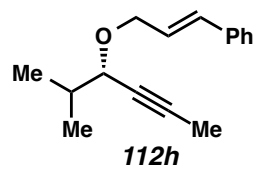


Figure A1.55. ^1H NMR (400 MHz, CDCl_3) of Compound **112h**.

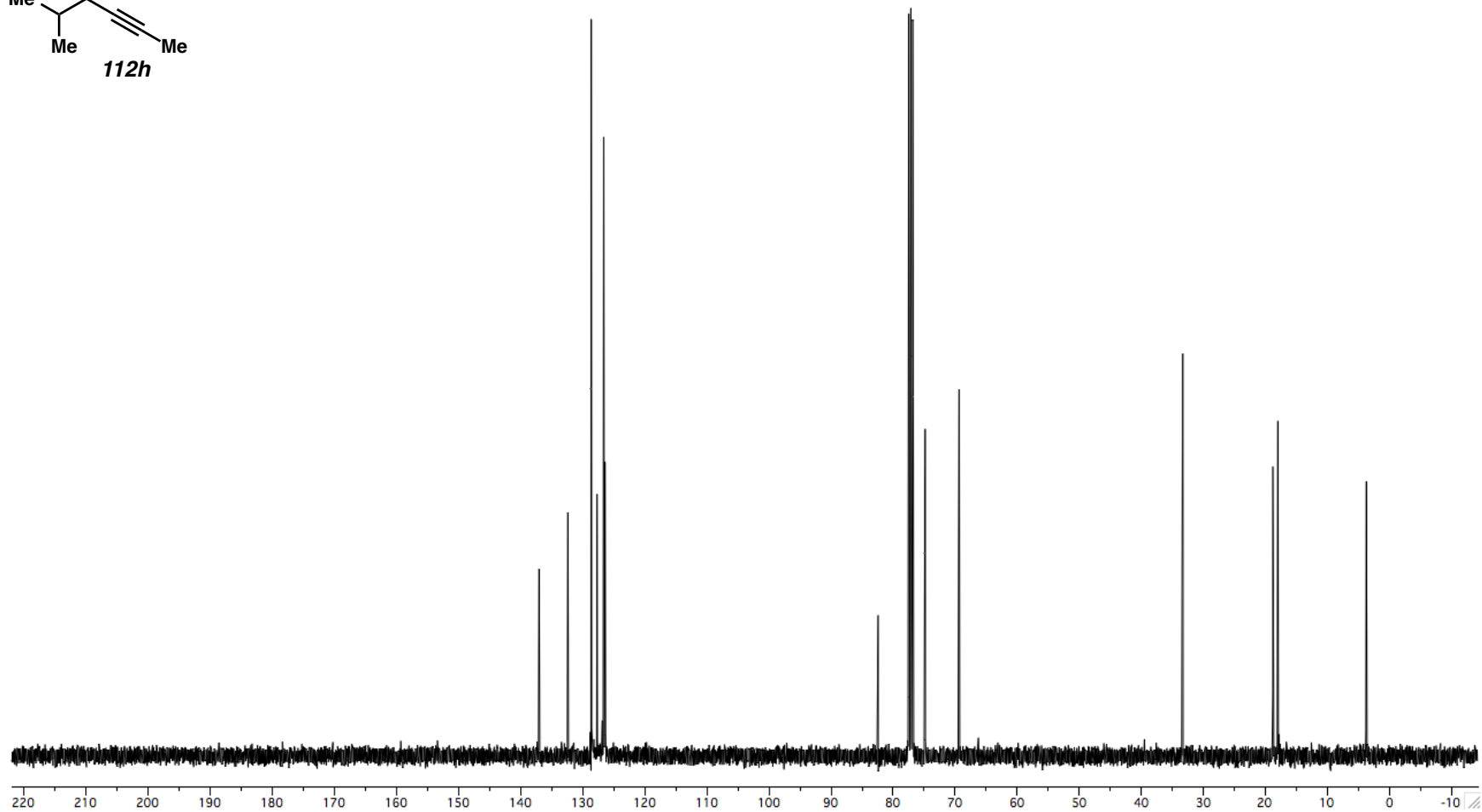
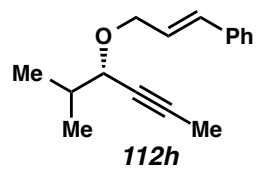


Figure A1.56. ^{13}C NMR (100 MHz, CDCl_3) of Compound **112h**.

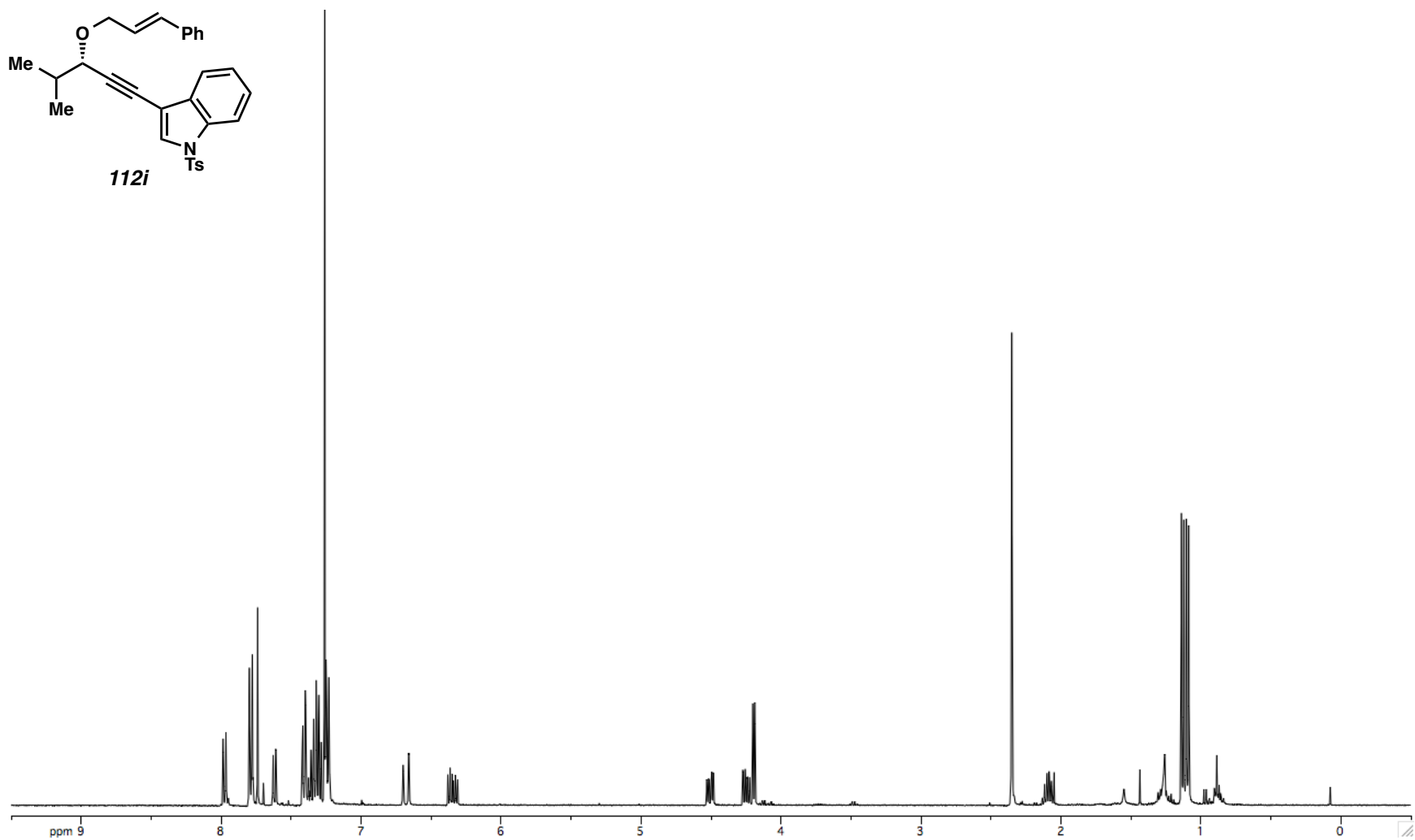
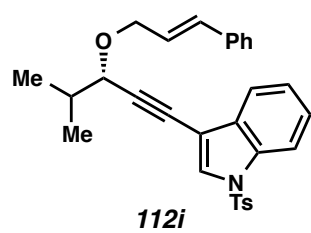


Figure A1.57. ^1H NMR (400 MHz, CDCl_3) of Compound **112i**.

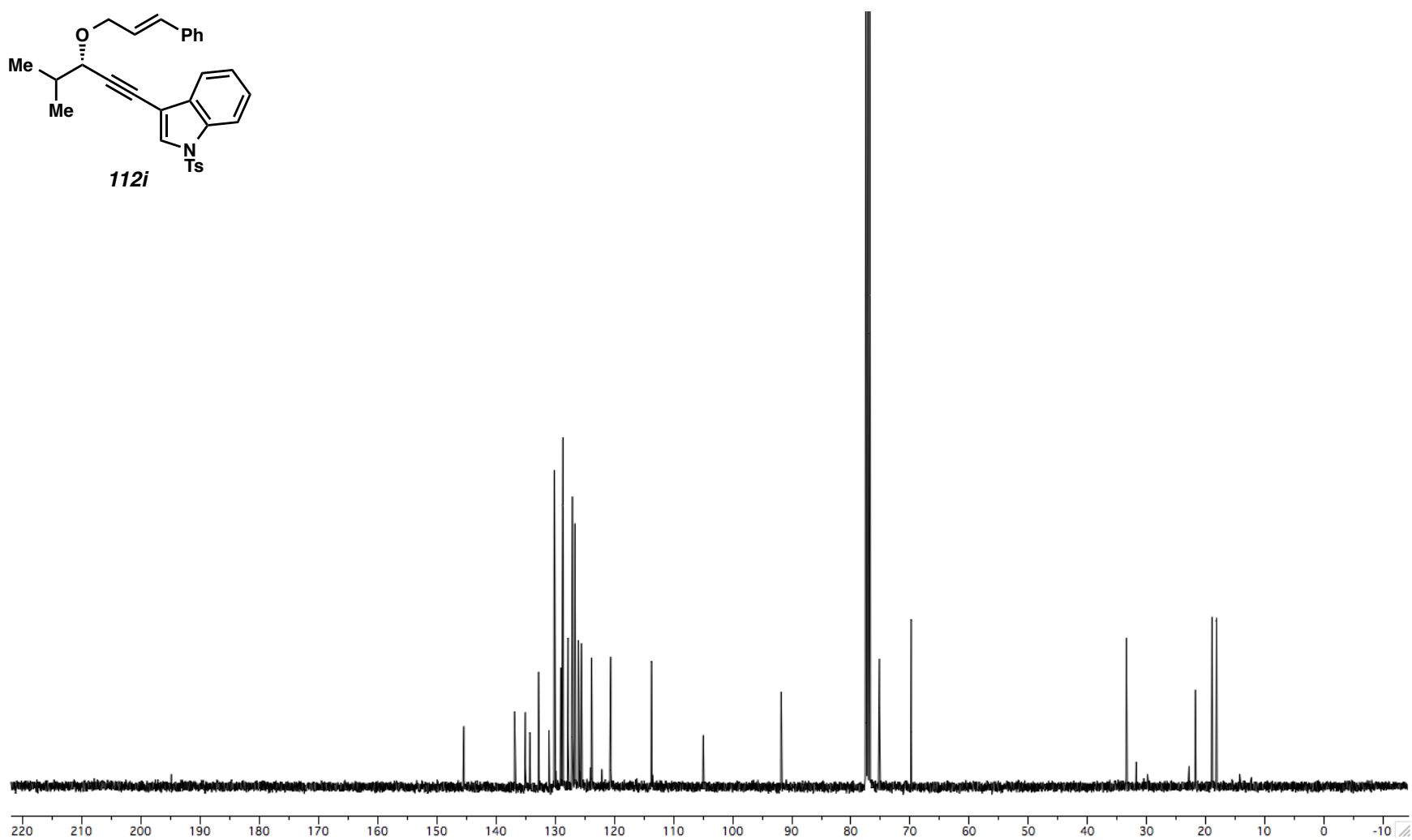
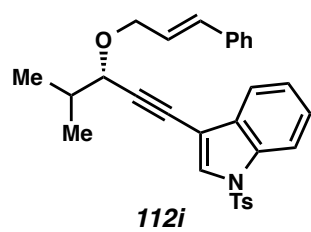


Figure A1.58. ¹³C NMR (100 MHz, CDCl₃) of Compound **112i**.

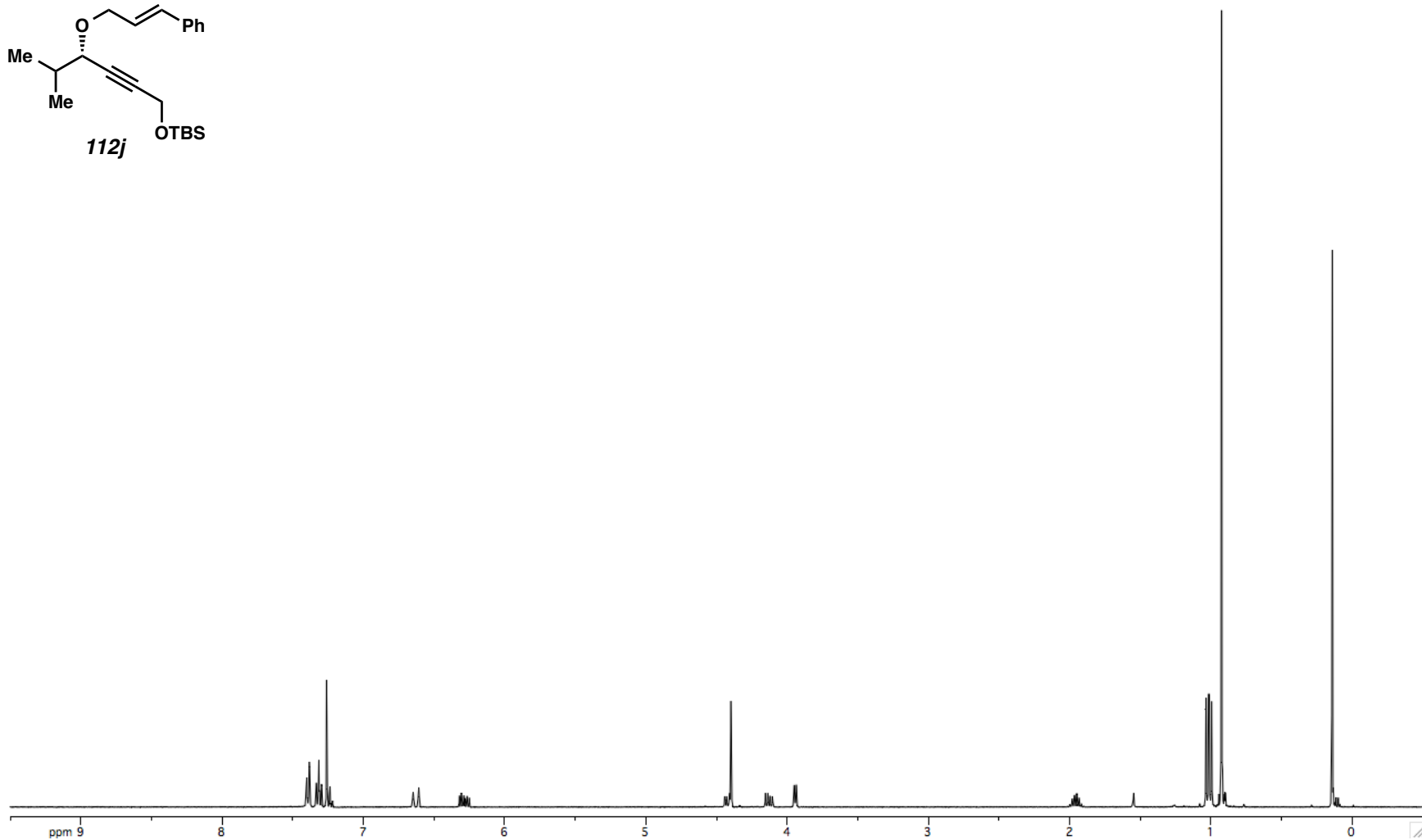
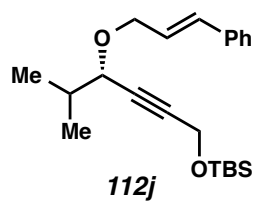


Figure A1.59. ¹H NMR (400 MHz, CDCl₃) of Compound **112j**.

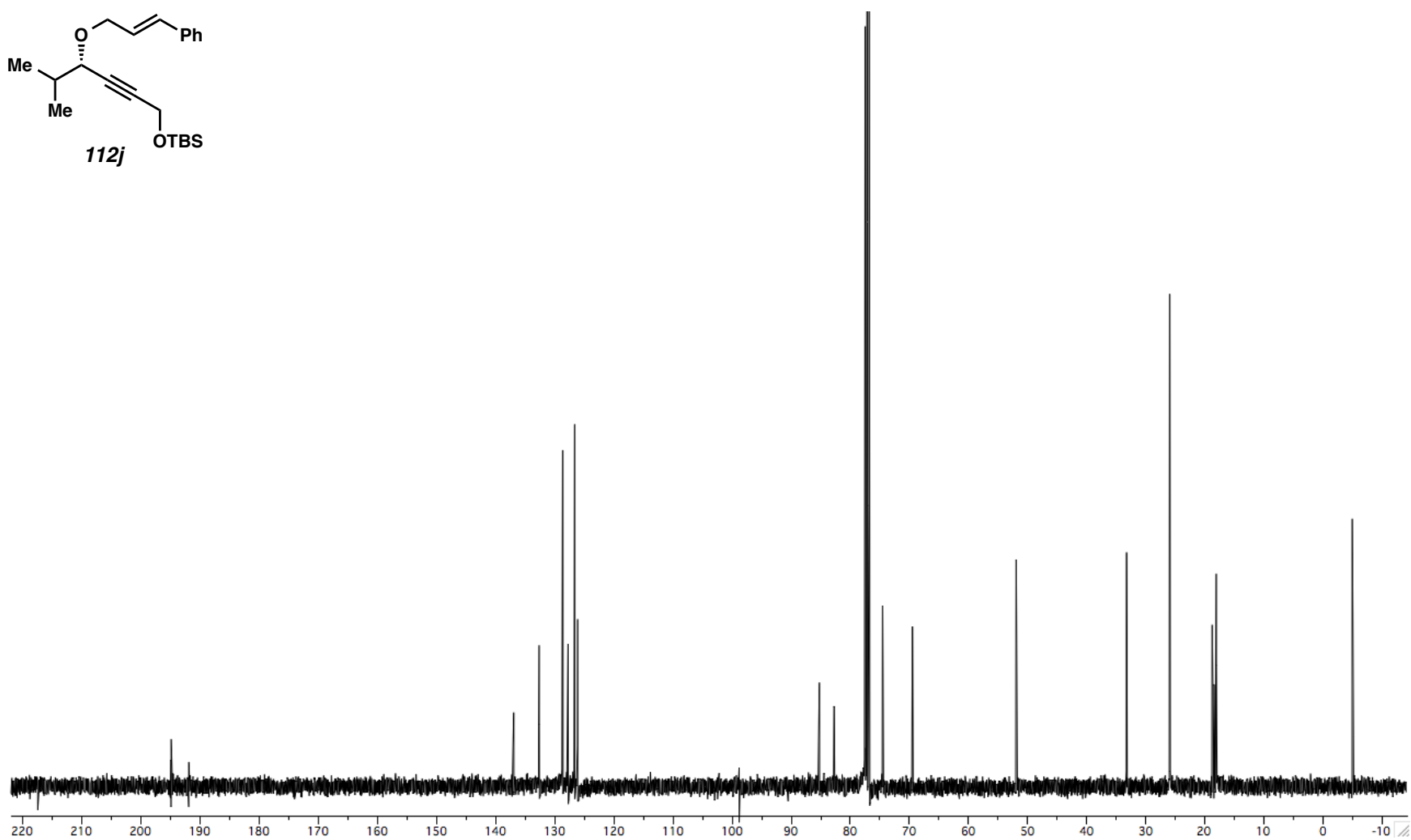
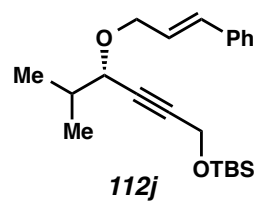


Figure A1.60. ^{13}C NMR (100 MHz, CDCl_3) of Compound **112j**.

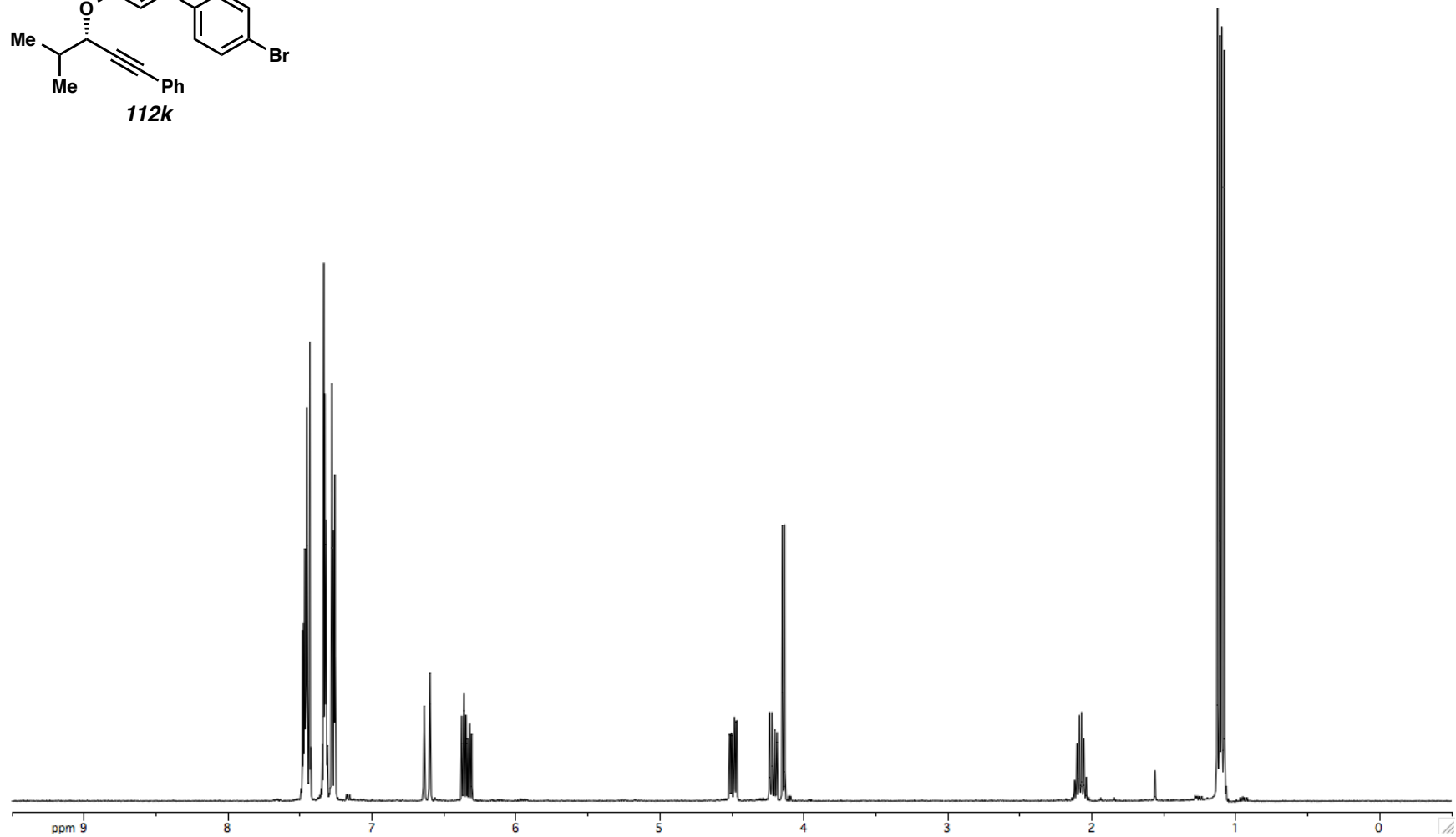
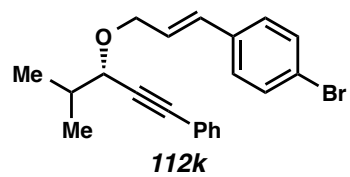


Figure A1.61. ^1H NMR (400 MHz, CDCl_3) of Compound **112k**.

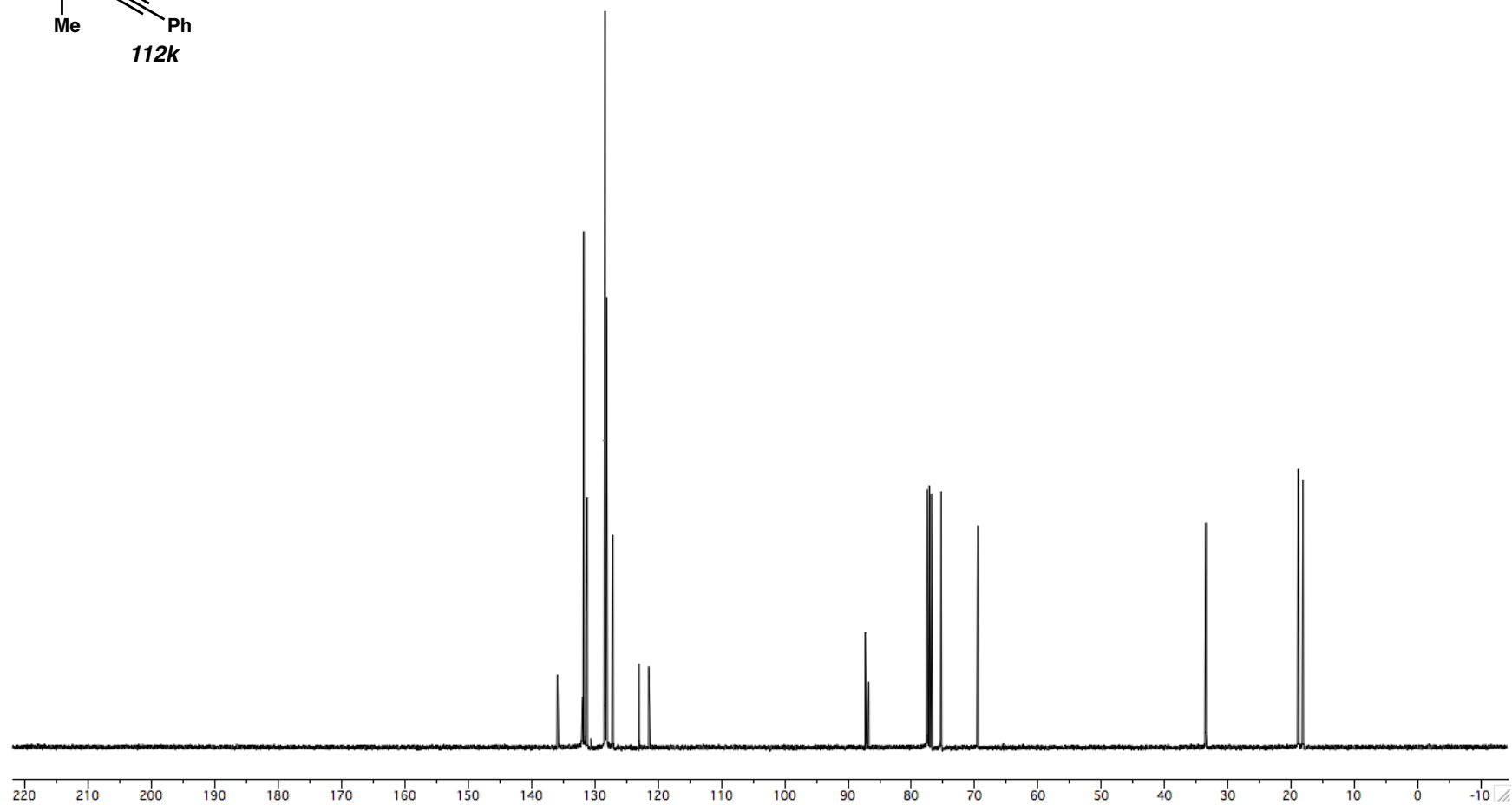
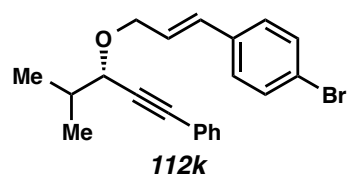


Figure A1.62. ^{13}C NMR (100 MHz, CDCl_3) of Compound **112k**.

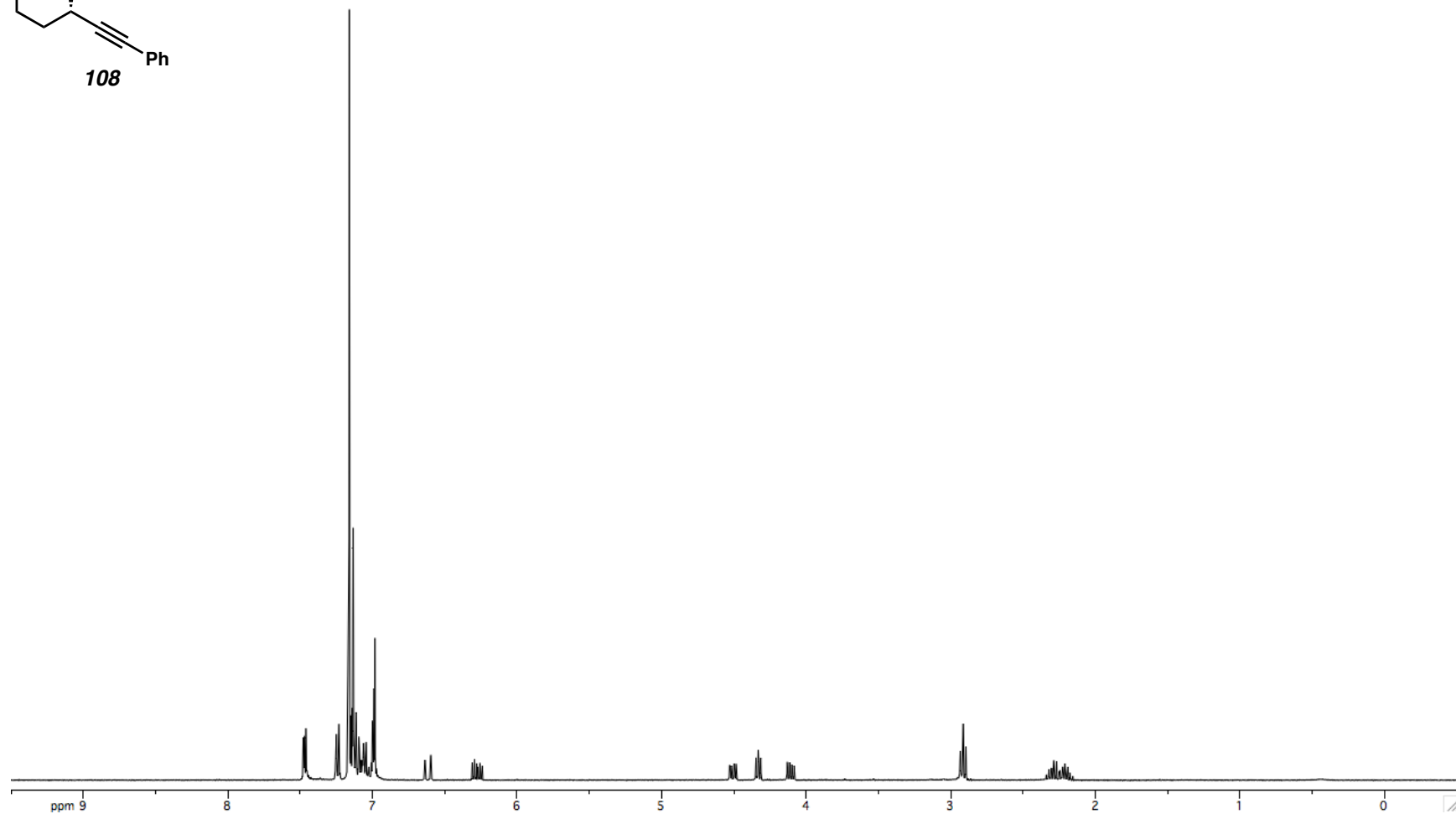
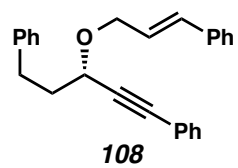


Figure A1.63. ^1H NMR (400 MHz, C_6D_6) of Compound **108**.

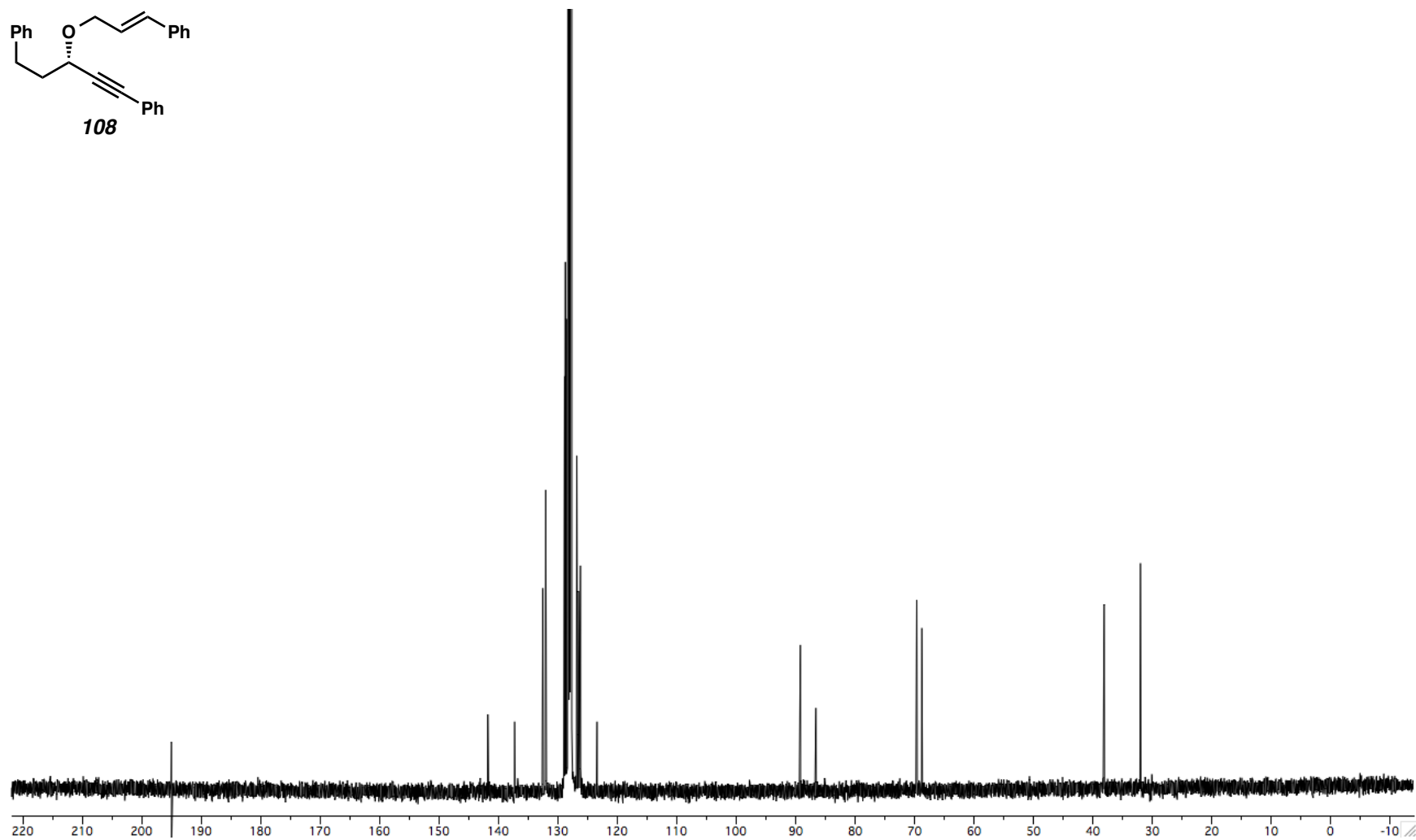
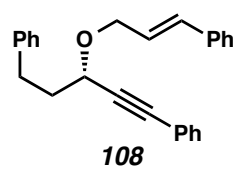


Figure A1.64. ^{13}C NMR (100 MHz, C_6D_6) of Compound **108**.

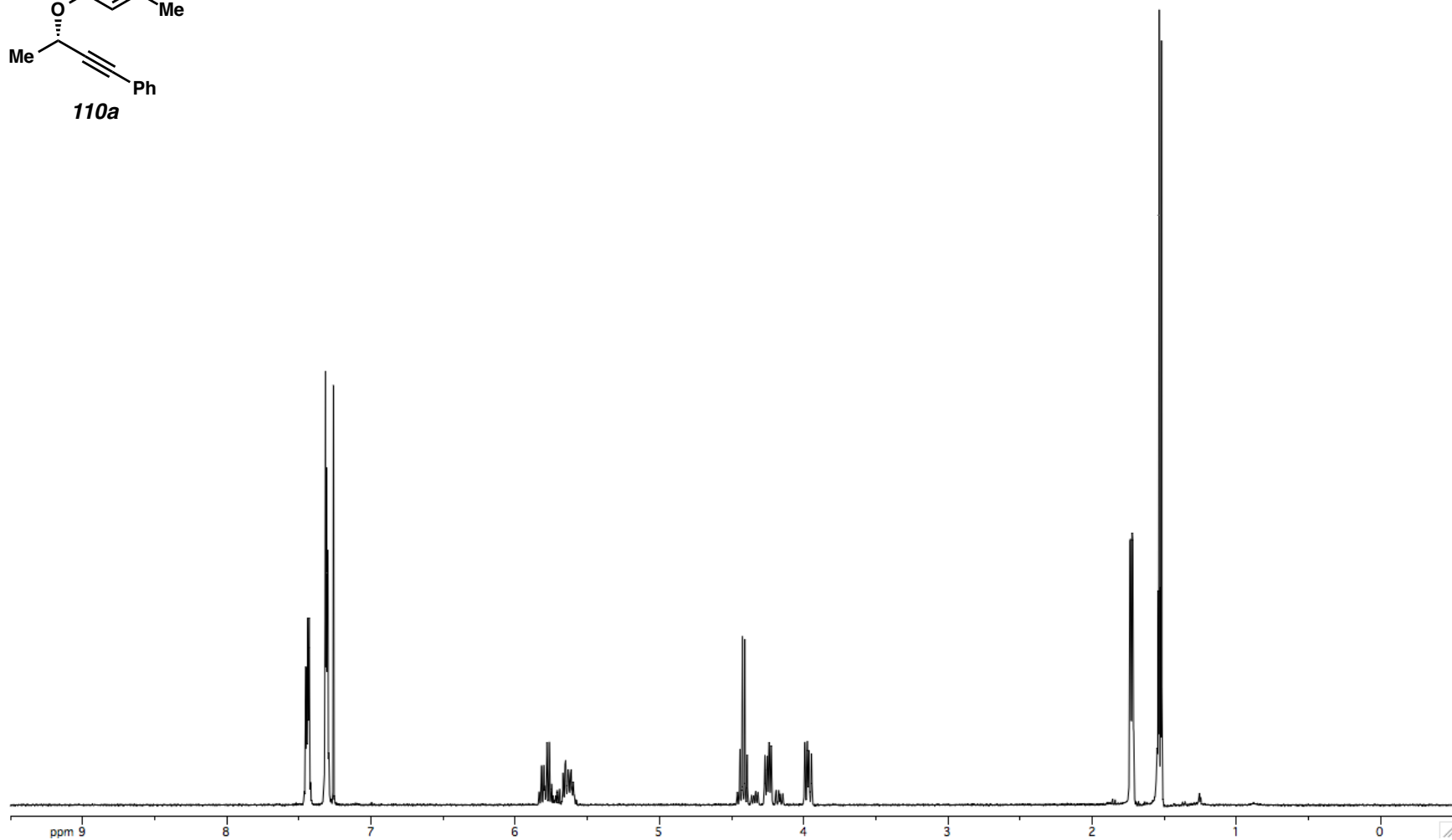
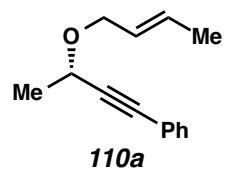


Figure A1.65. ^1H NMR (400 MHz, CDCl_3) of Compound **110a**.

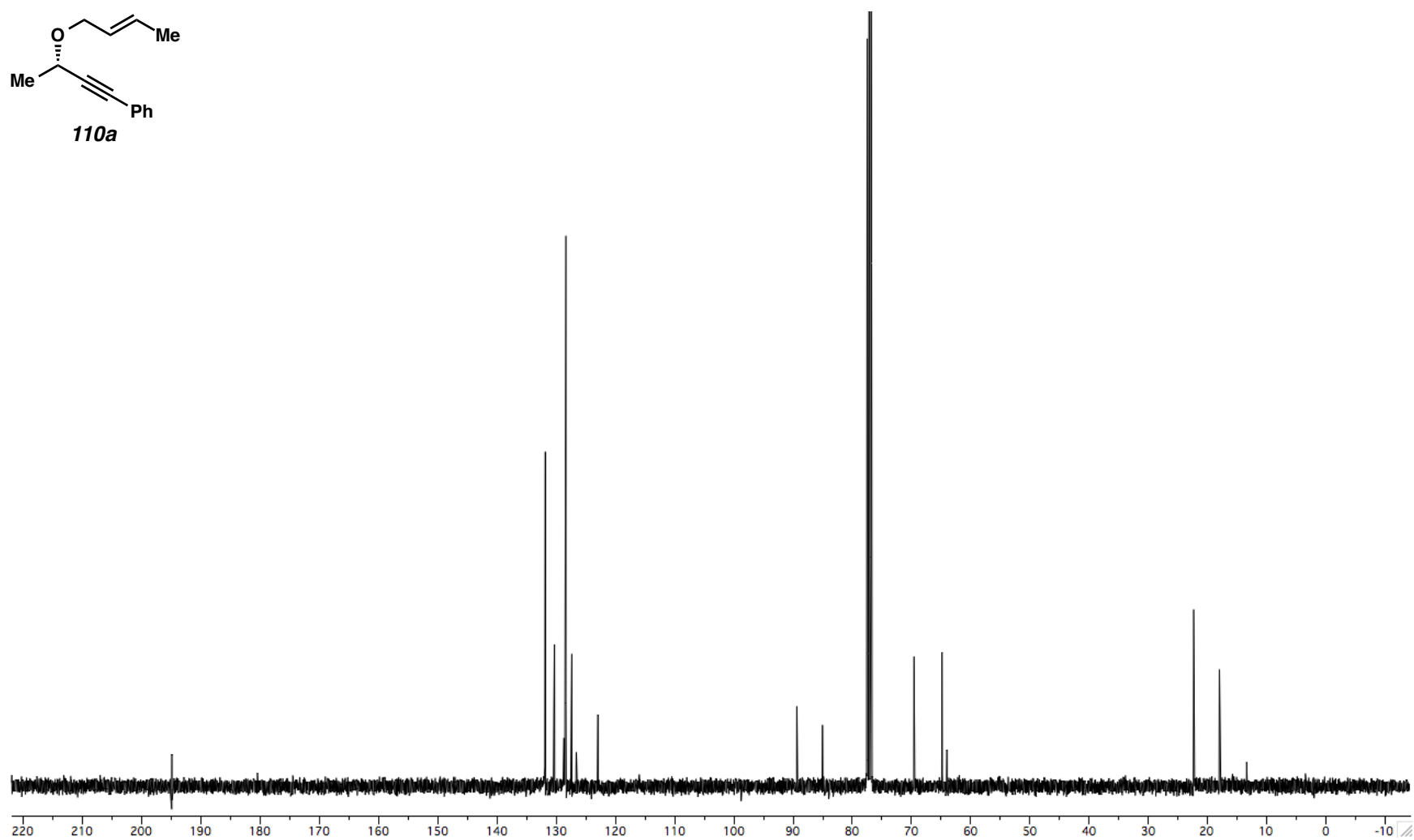
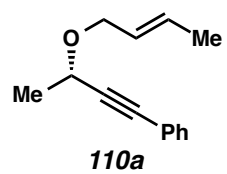


Figure A1.66. ^{13}C NMR (100 MHz, CDCl_3) of Compound **110a**.

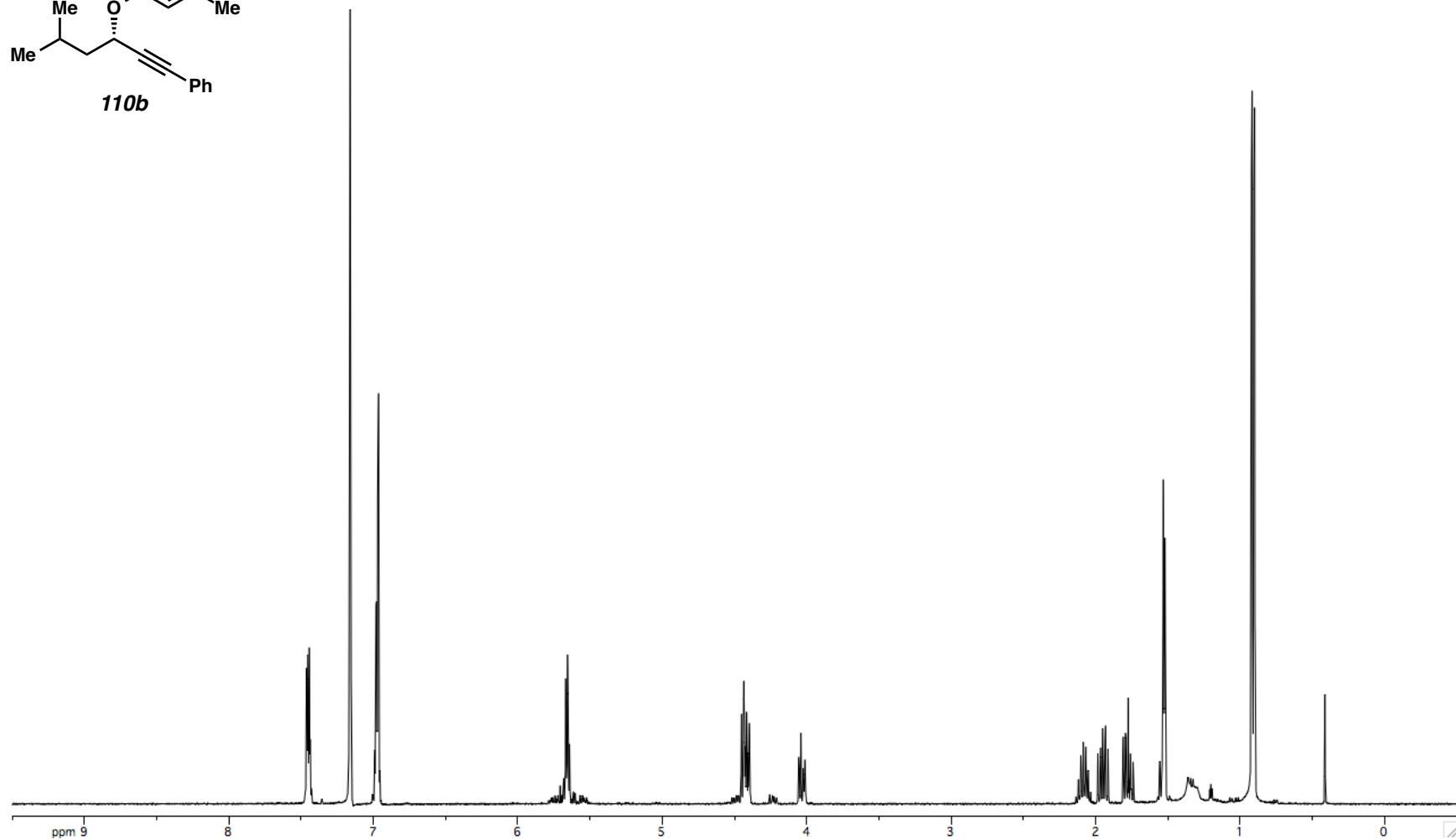
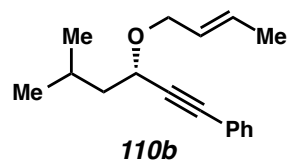


Figure A1.67. ^1H NMR (400 MHz, C_6D_6) of Compound **110b**.

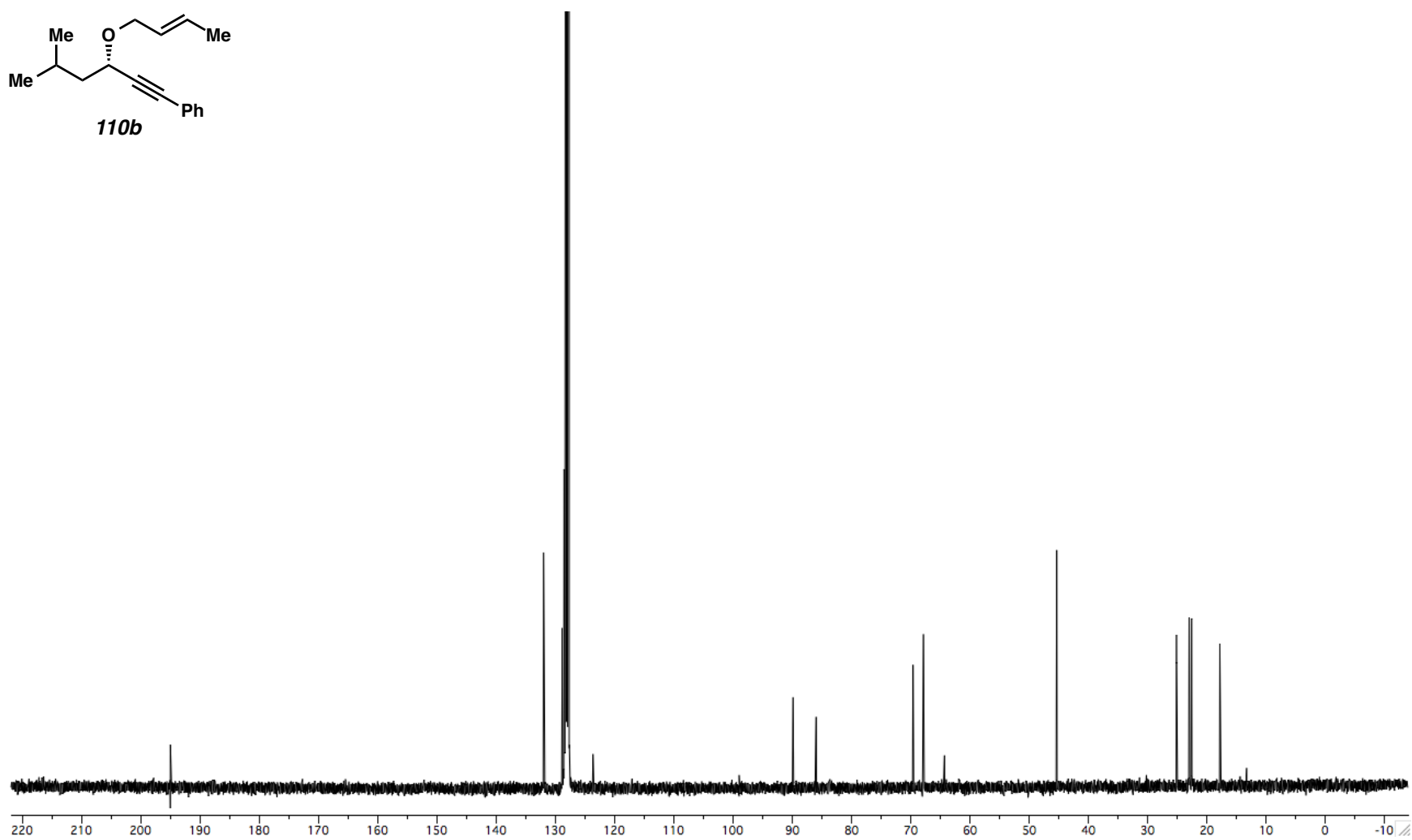
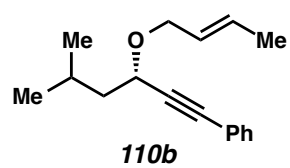


Figure A1.68. ^{13}C NMR (100 MHz, C_6D_6) of Compound **110b**.

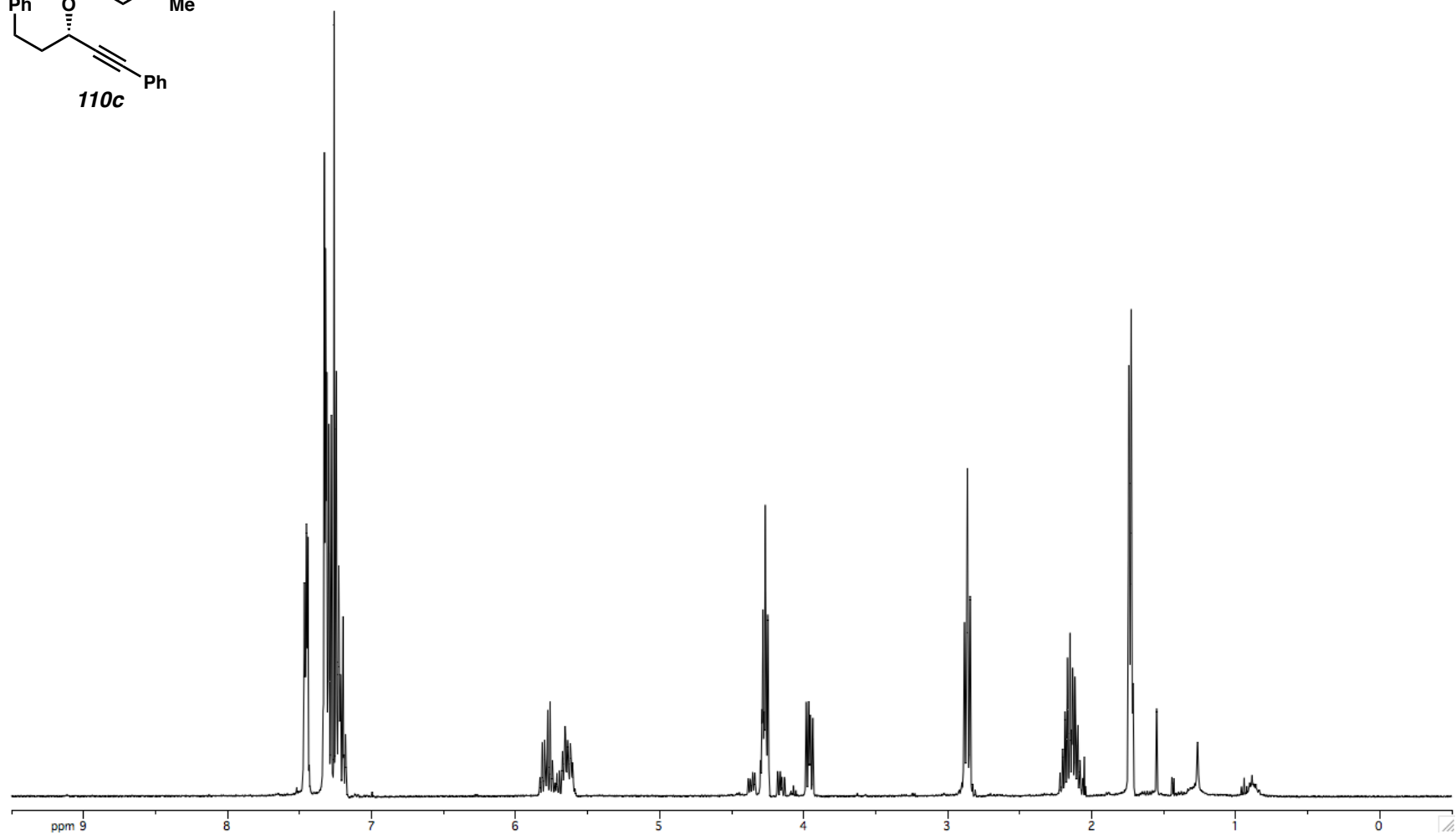
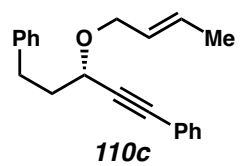


Figure A1.69. ^1H NMR (400 MHz, CDCl_3) of Compound **110c**.

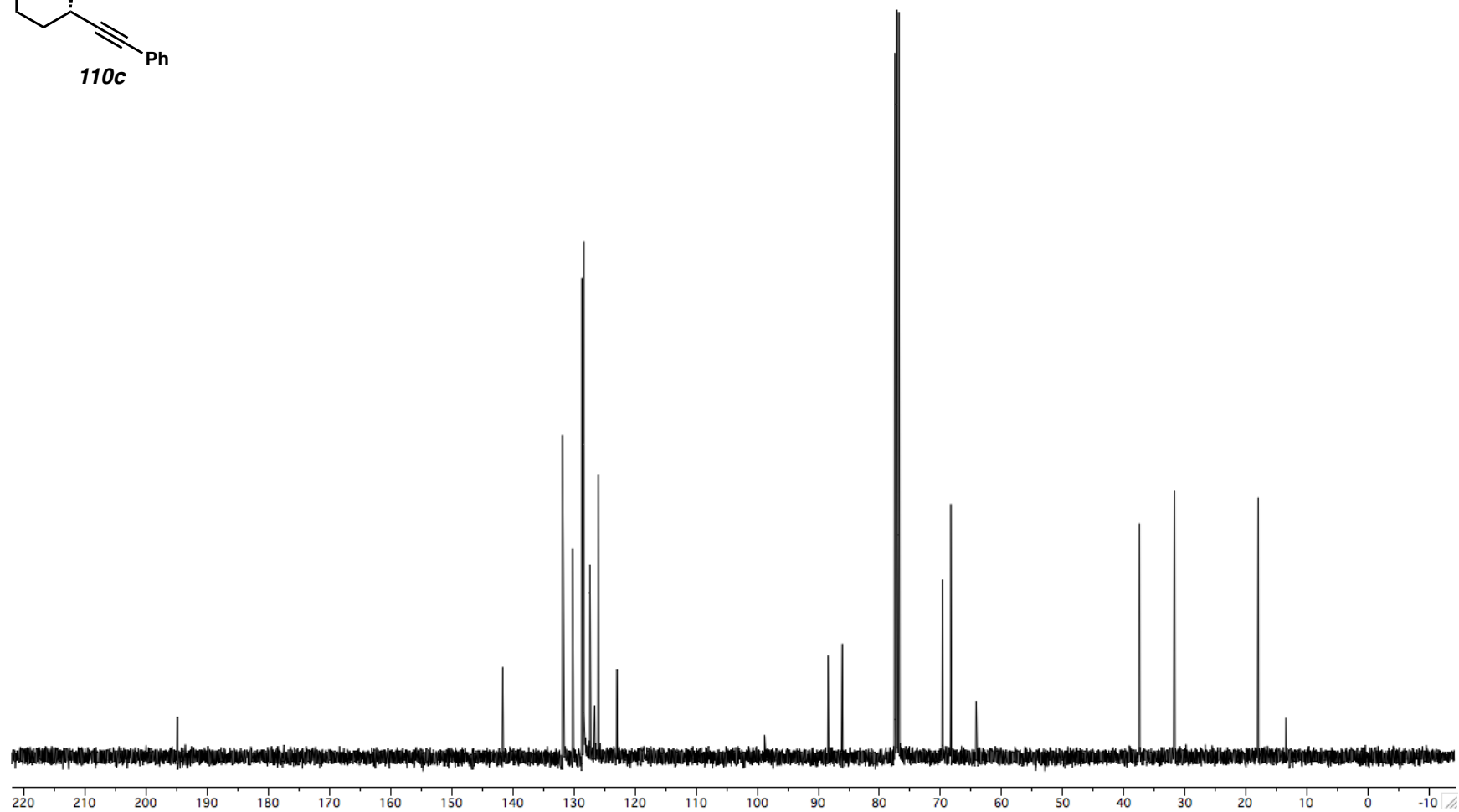
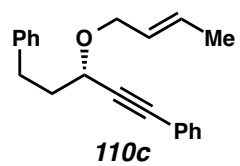


Figure A1.70. ^{13}C NMR (100 MHz, CDCl_3) of Compound **110c**.

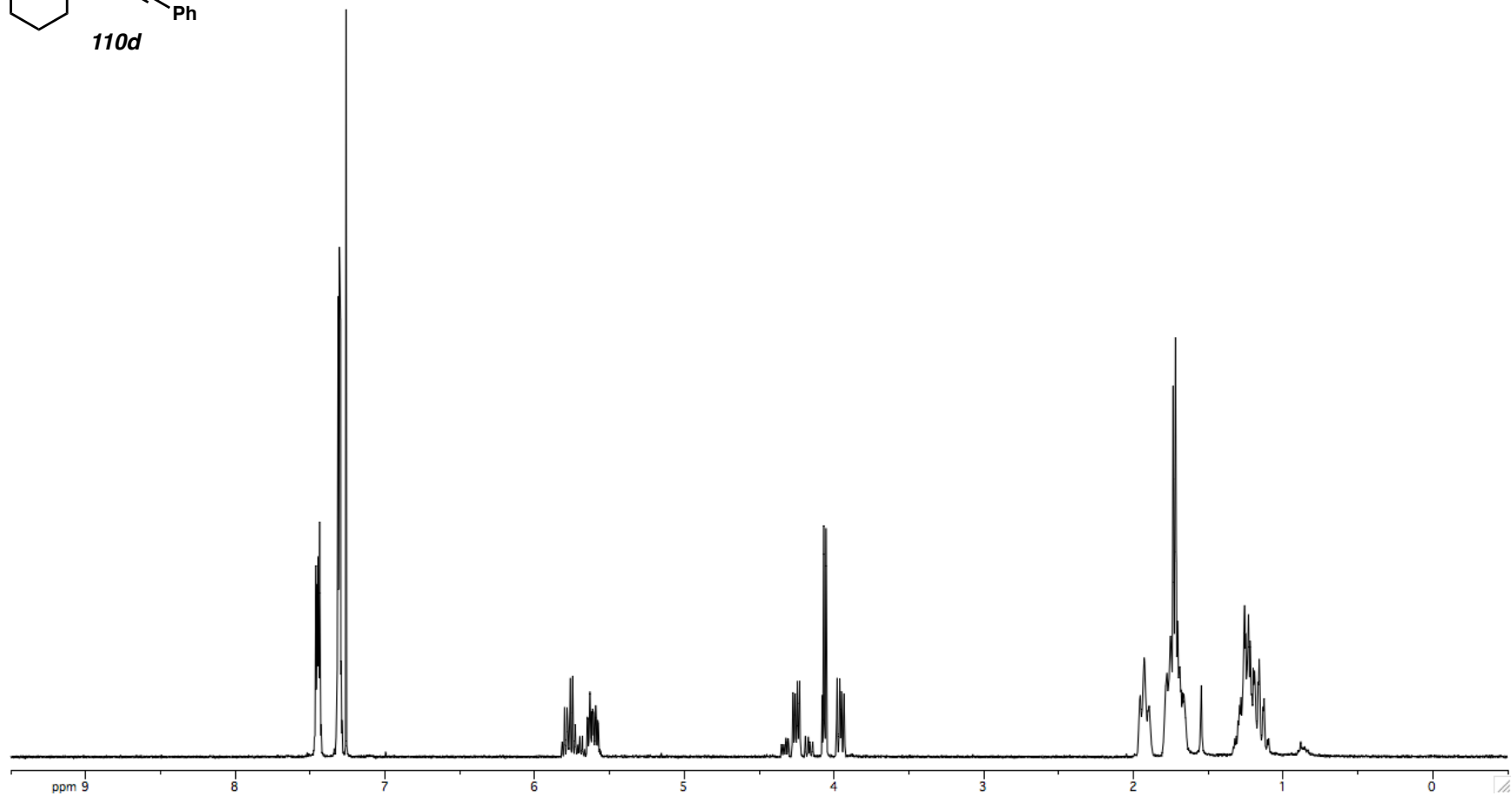
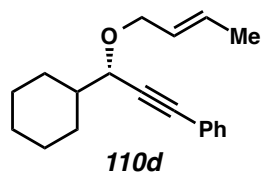


Figure A1.71. ¹H NMR (400 MHz, CDCl₃) of Compound **110d**.

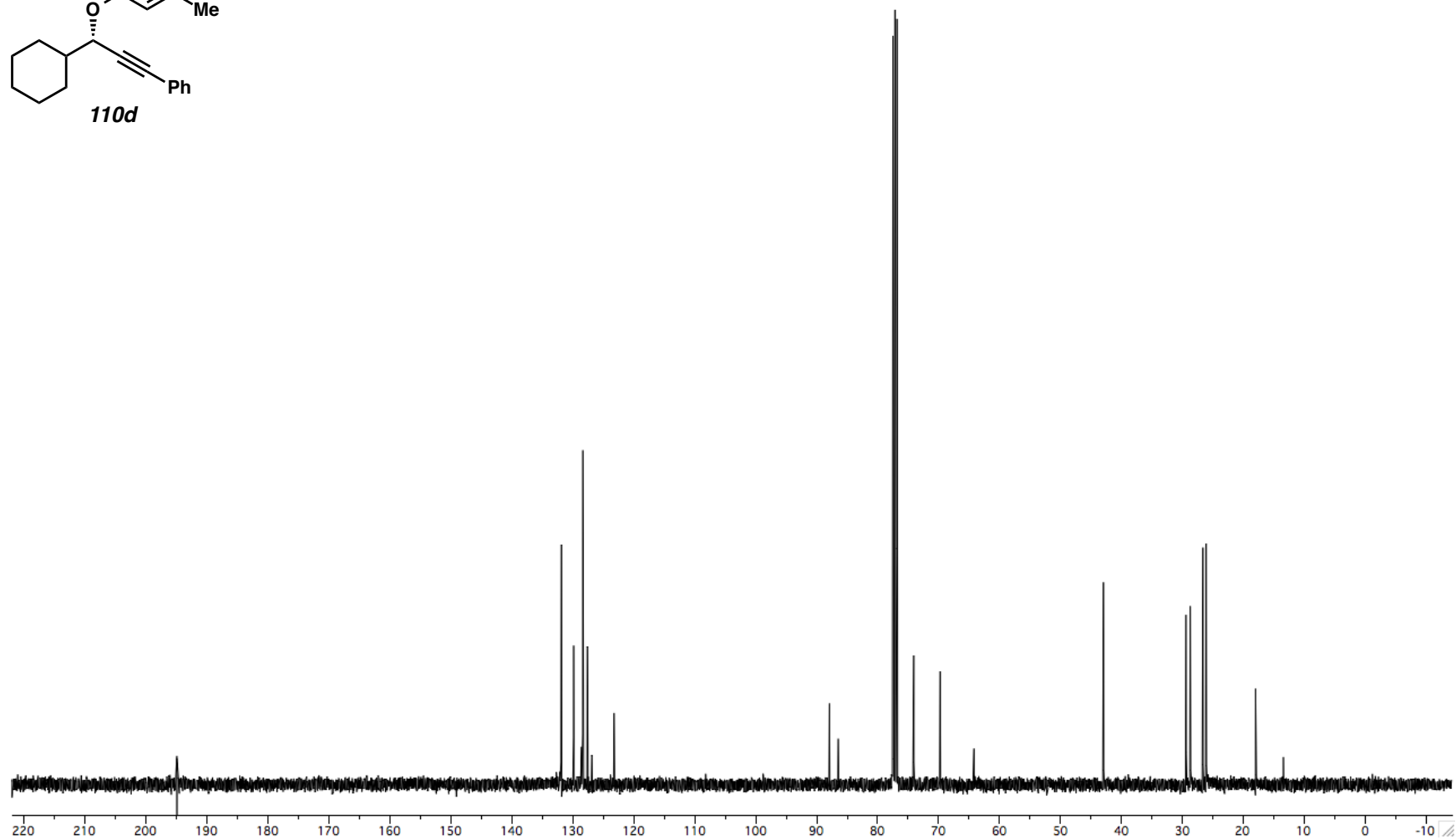
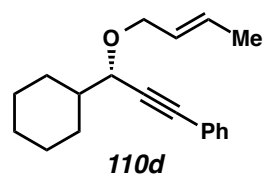


Figure A1.72. ^{13}C NMR (100 MHz, CDCl_3) of Compound **110d**.

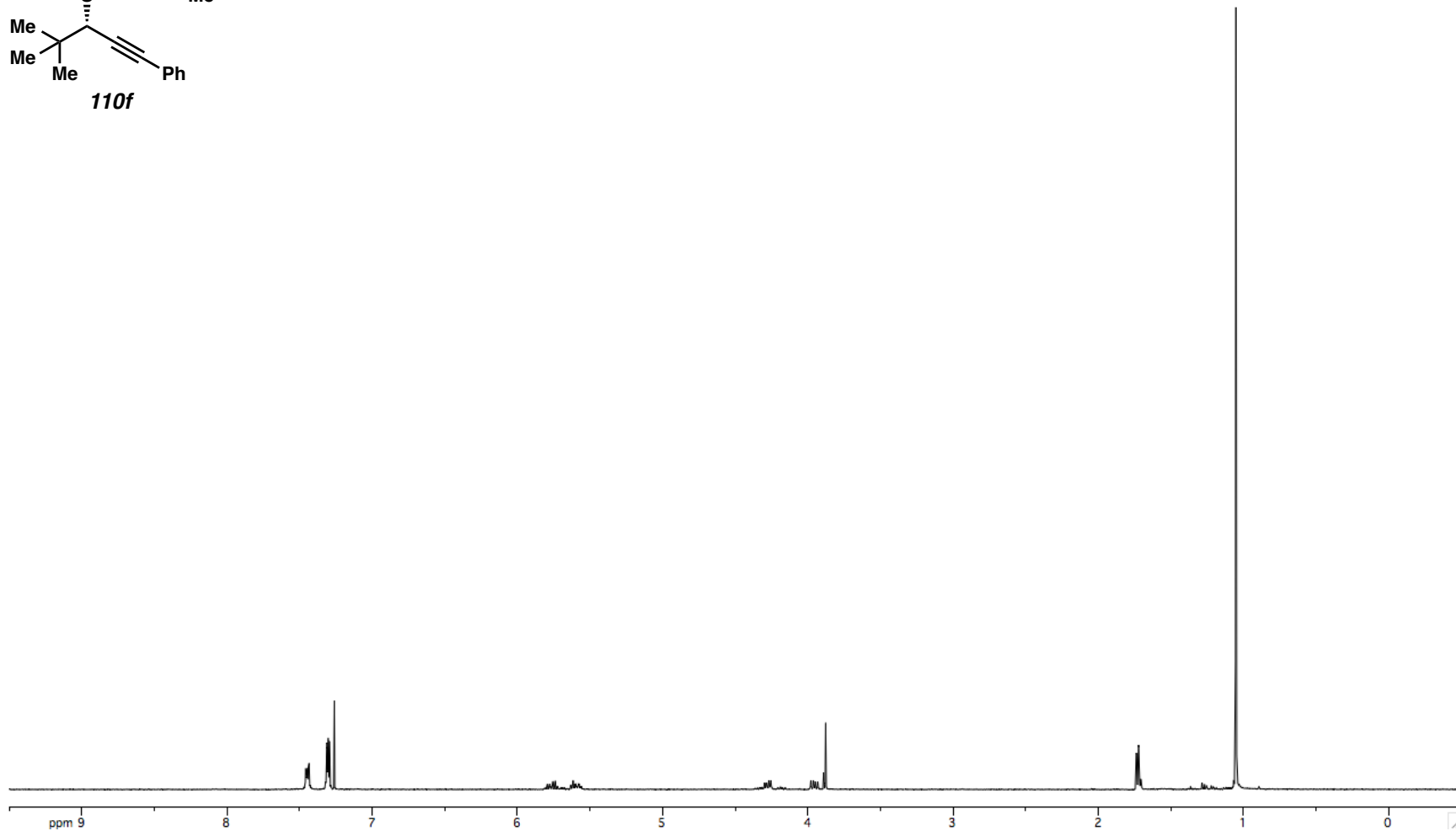
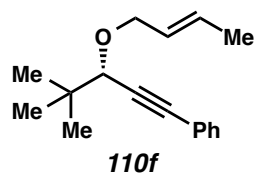


Figure A1.73. ^1H NMR (400 MHz, CDCl_3) of Compound **110f**.

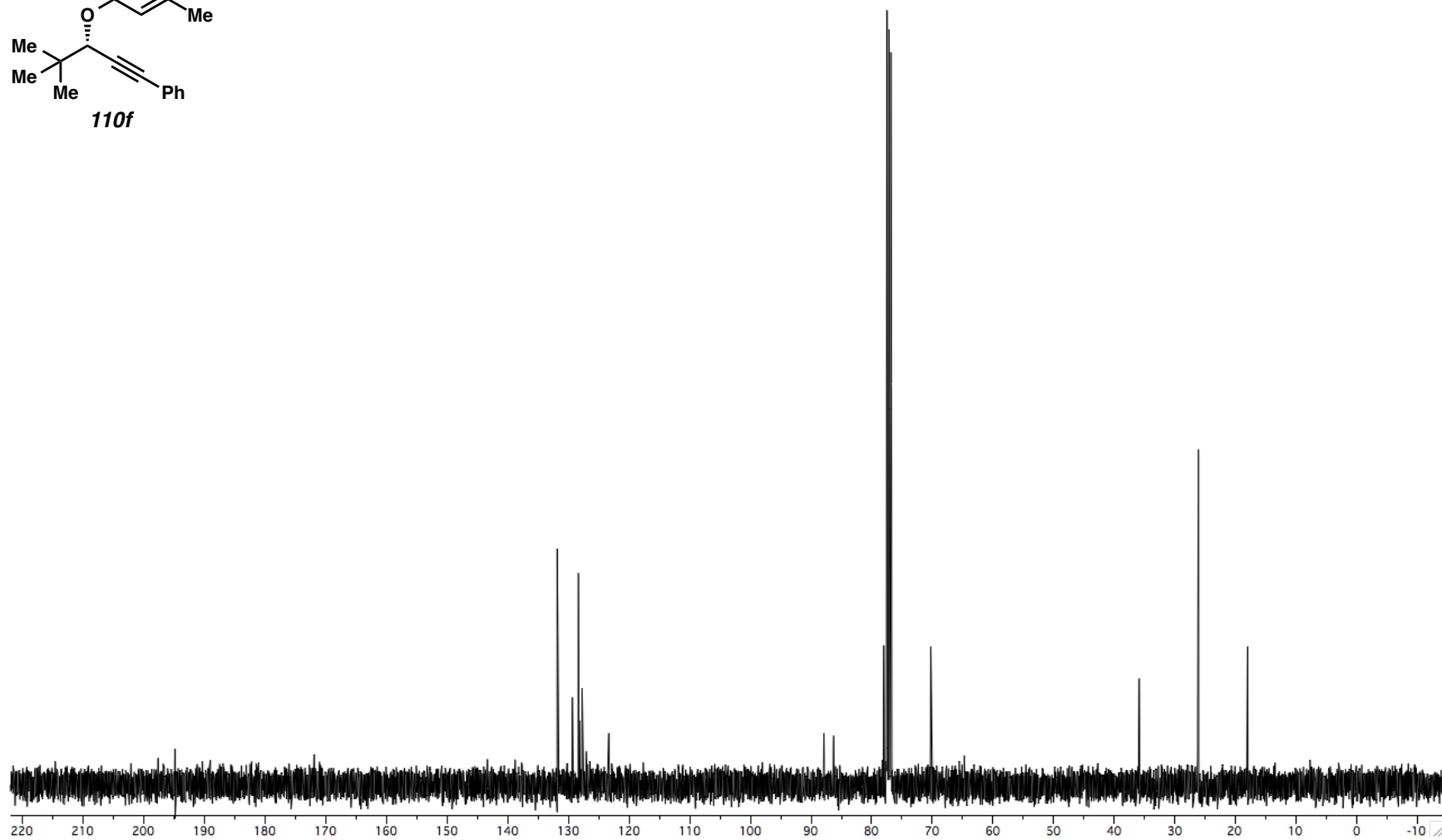
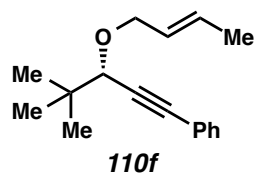


Figure A1.74. ^{13}C NMR (100 MHz, CDCl_3) of Compound **110f**.

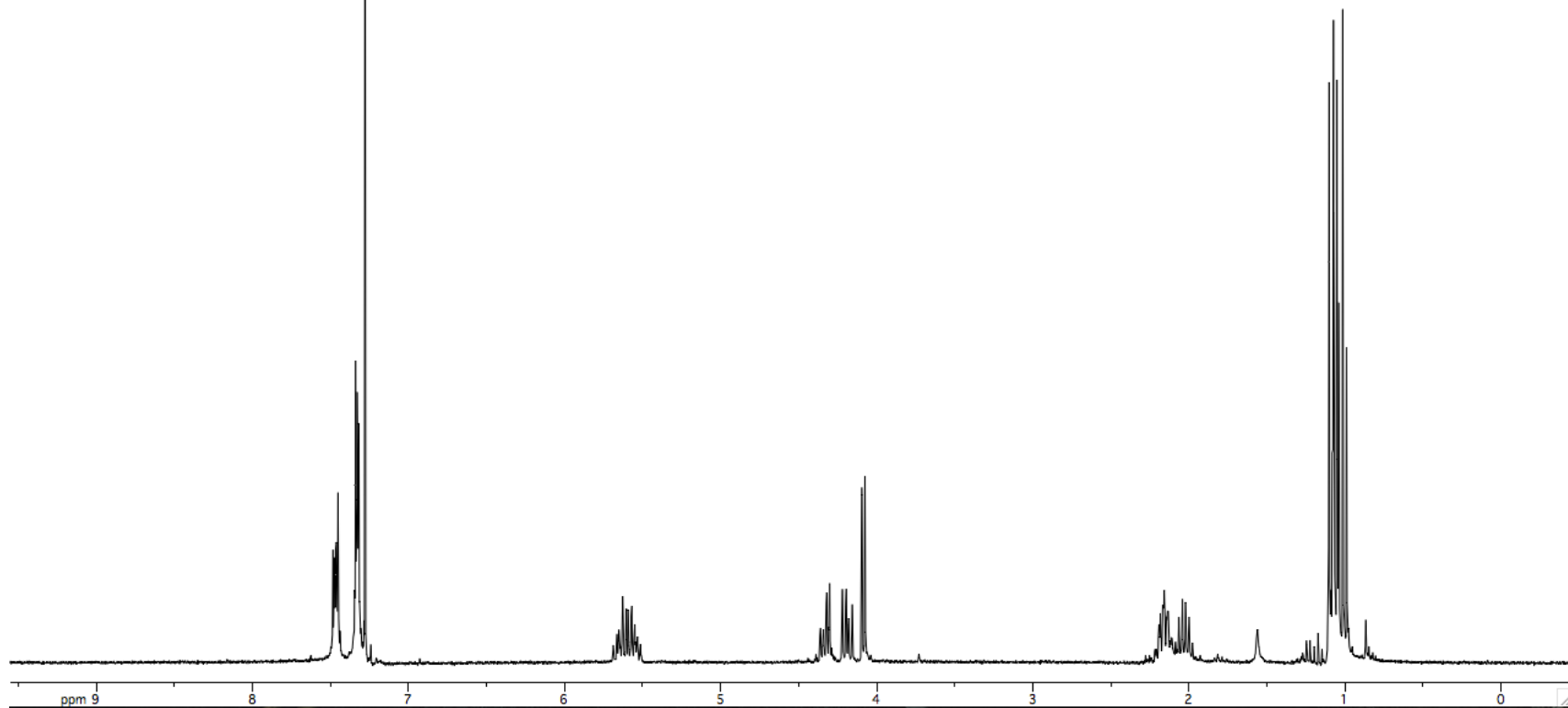
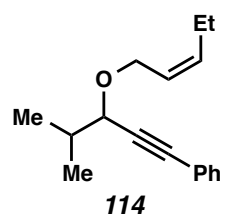


Figure A1.75. ^1H NMR (300 MHz, CDCl_3) of Compound **114**.

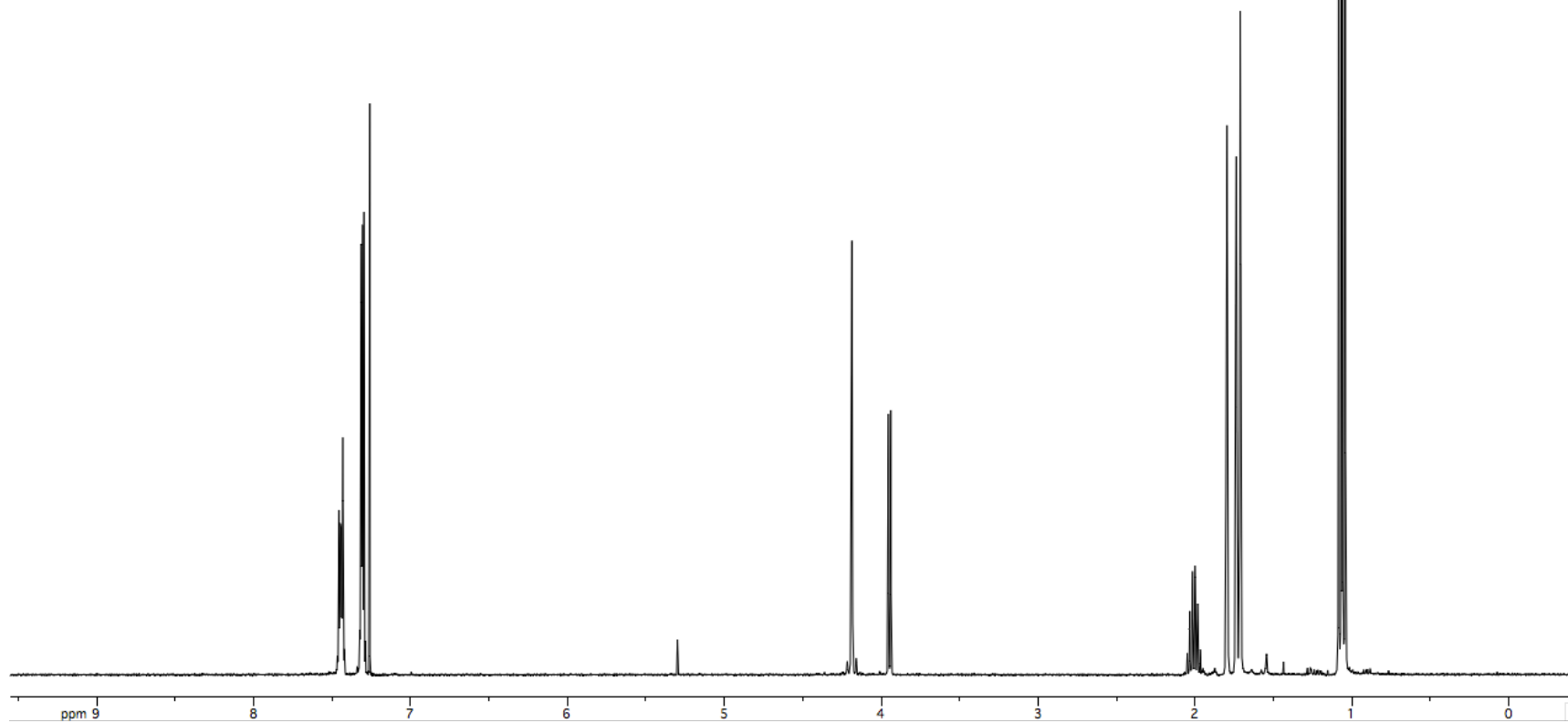
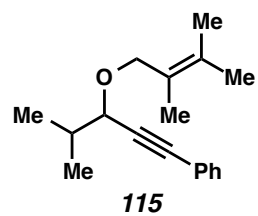


Figure A1.76. ^1H NMR (400 MHz, CDCl_3) of Compound **115**.

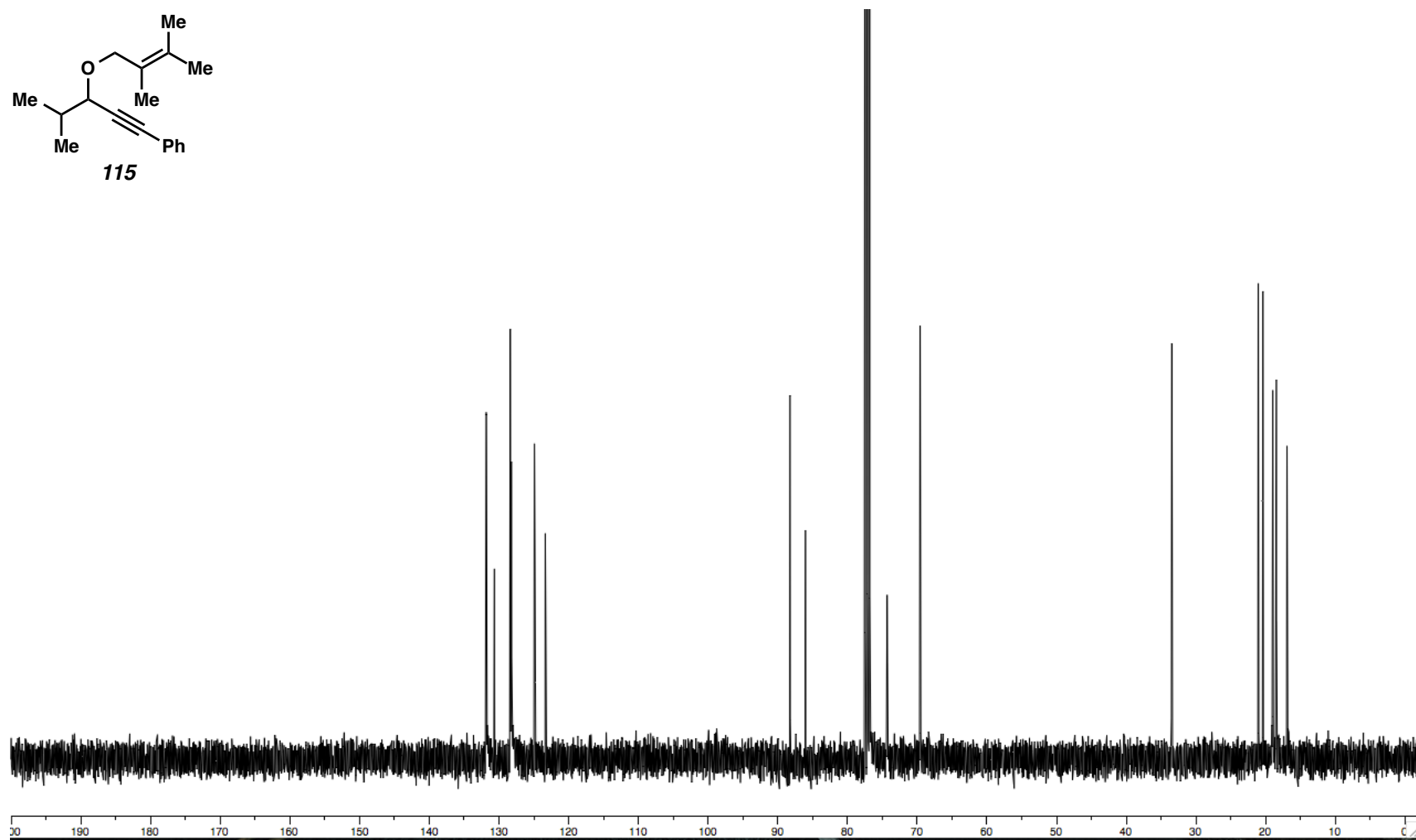
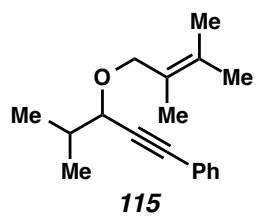


Figure A1.77. ^{13}C NMR (100 MHz, CDCl_3) of Compound **115**.

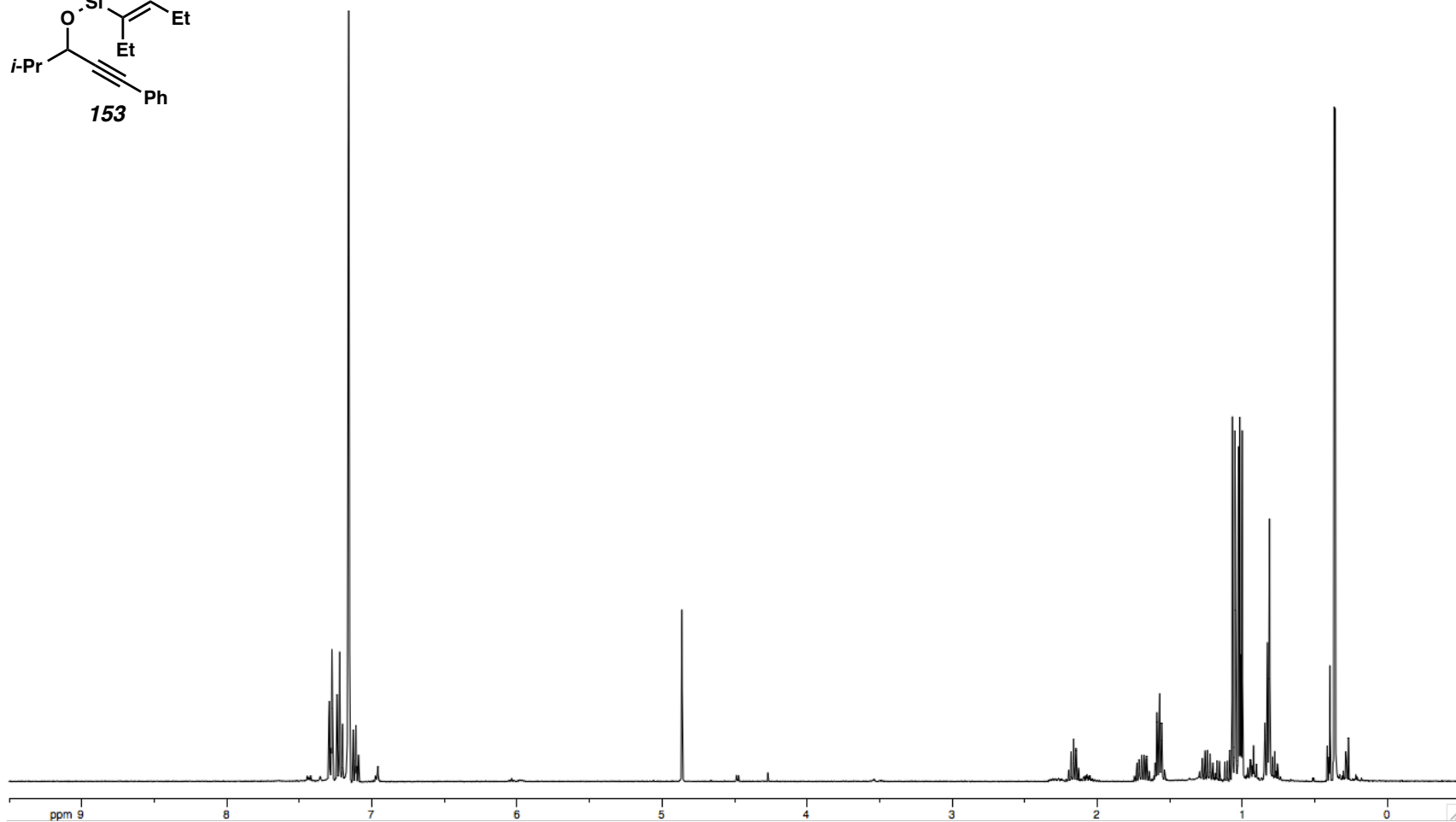
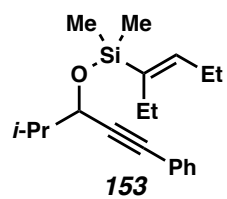


Figure A1.78. ^1H NMR (400 MHz, C_6D_6) of Compound **153**.

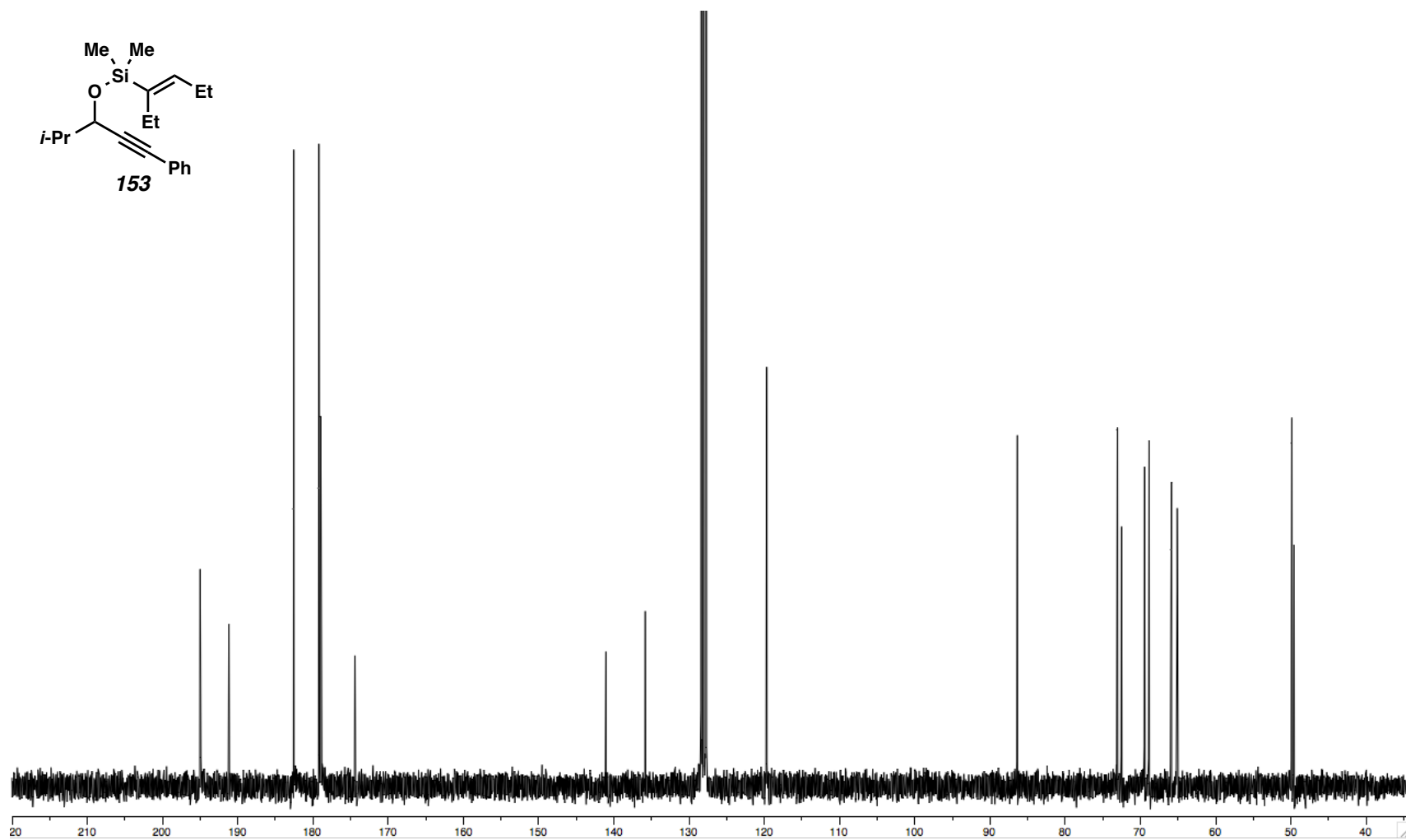


Figure A1.79. ^{13}C NMR (100 MHz, C_6D_6) of Compound 153.

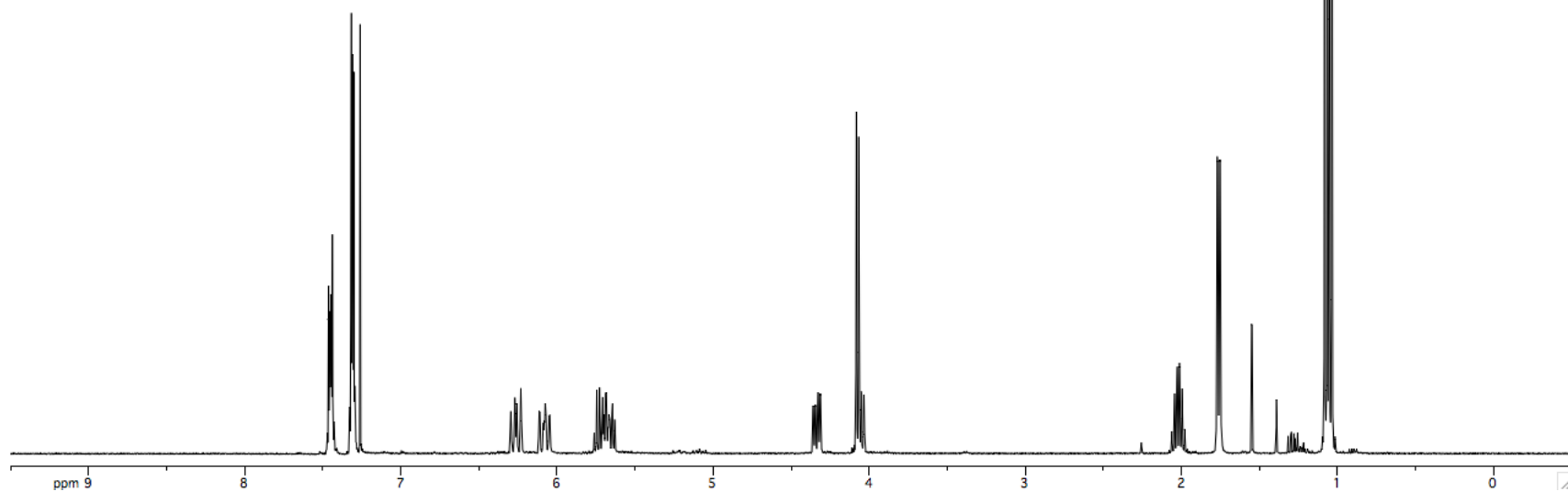
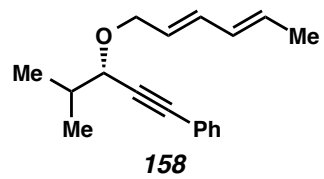


Figure A1.80. ^1H NMR (400 MHz, CDCl_3) of Compound **158**.

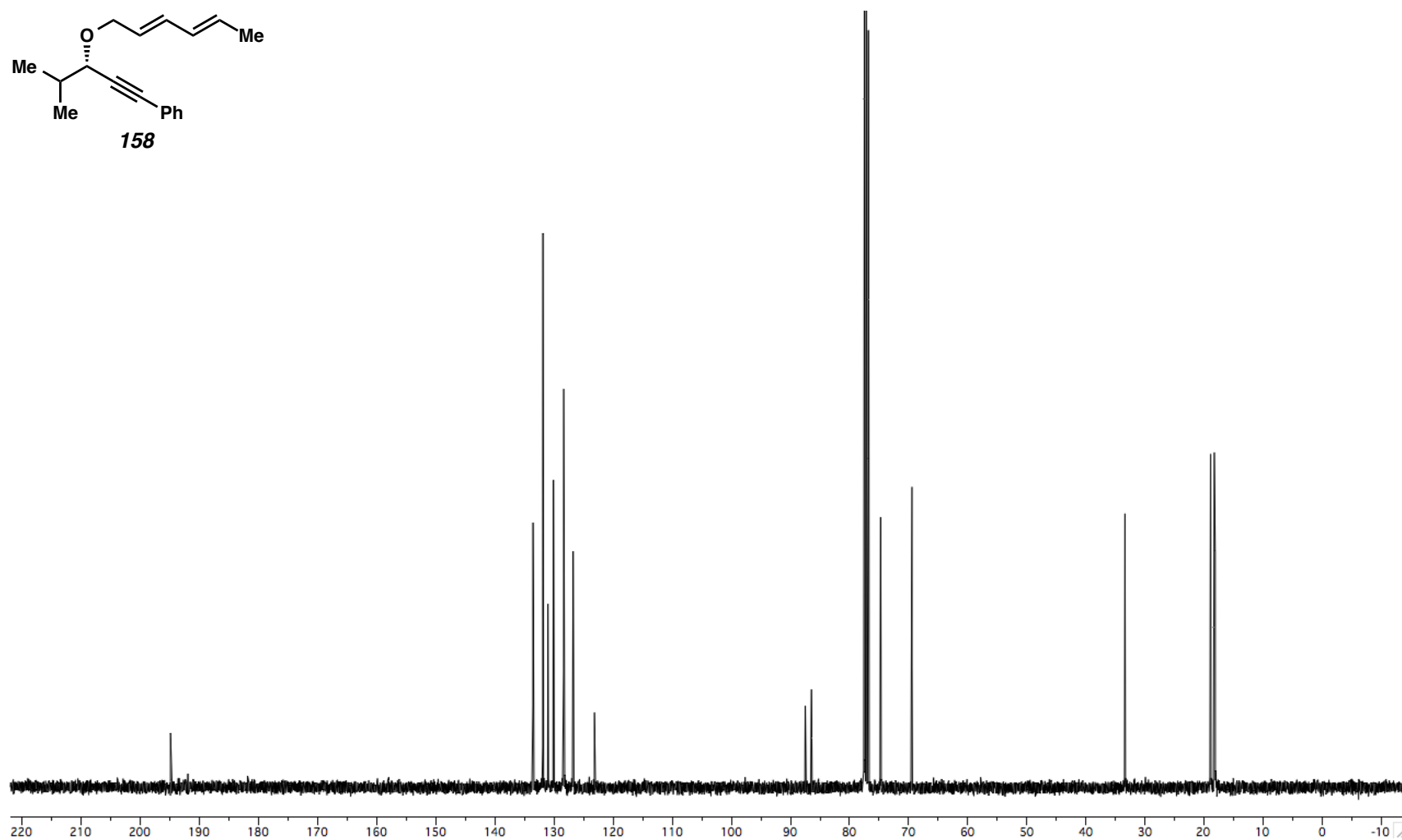
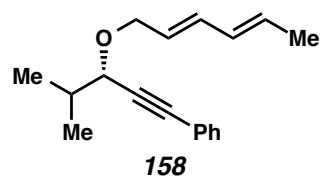


Figure A1.81. ^{13}C NMR (100 MHz, CDCl_3) of Compound **158**.

APPENDIX TWO

Crystallographic Data Relevant to Compound **113k**

Table 1. Crystal data and structure refinement for **113k**.

Identification code	ef09_0m	
Empirical formula	C ₂₁ H ₂₁ BrO	
Formula weight	369.29	
Temperature	100(2) K	
Wavelength	0.71073 Å	
Crystal system	Monoclinic	
Space group	P2 ₁	
Unit cell dimensions	<i>a</i> = 8.7086(4) Å	<i>a</i> = 90°.
	<i>b</i> = 10.3343(5) Å	<i>b</i> = 113.168(2)°.
	<i>c</i> = 10.3919(5) Å	<i>c</i> = 90°.
Volume	859.82(7) Å ³	
Z	2	
Density (calculated)	1.426 Mg/m ³	
Absorption coefficient	2.393 mm ⁻¹	
F(000)	380	
Crystal size	0.66 x 0.49 x 0.29 mm ³	
Theta range for data collection	2.13 to 33.29°.	
Index ranges	-13 ≤ <i>h</i> ≤ 12, -15 ≤ <i>k</i> ≤ 14, -16 ≤ <i>l</i> ≤ 15	
Reflections collected	22316	
Independent reflections	5869 [R(int) = 0.0255]	
Completeness to theta = 33.29°	99.7 %	
Absorption correction	Semi-empirical from equivalents	
Max. and min. transmission	0.5447 and 0.3011	
Refinement method	Full-matrix least-squares on F ²	
Data / restraints / parameters	5869 / 1 / 211	
Goodness-of-fit on F ²	1.041	
Final R indices [I > 2σ(I)]	R1 = 0.0281, wR2 = 0.0692	
R indices (all data)	R1 = 0.0306, wR2 = 0.0700	
Absolute structure parameter	0.022(6)	
Largest diff. peak and hole	1.630 and -0.749 e.Å ⁻³	

Table 2. Atomic coordinates ($\times 10^4$) and equivalent isotropic displacement parameters ($\text{\AA}^2 \times 10^3$) for **113k**. $U(\text{eq})$ is defined as one third of the trace of the orthogonalized U_{ij} tensor.

	x	y	z	$U(\text{eq})$
Br(1)	-533(1)	1540(1)	-3037(1)	23(1)
C(1)	597(2)	1364(2)	-1061(2)	14(1)
C(2)	469(2)	202(2)	-452(2)	17(1)
C(3)	1339(2)	48(2)	983(2)	16(1)
C(4)	2330(2)	1043(2)	1812(2)	12(1)
C(5)	2407(2)	2208(2)	1166(2)	14(1)
C(6)	1546(2)	2378(2)	-275(2)	15(1)
C(7)	3336(2)	883(2)	3338(2)	12(1)
C(8)	3157(2)	-277(2)	4146(2)	15(1)
C(9)	4739(3)	-793(2)	5282(2)	24(1)
C(10)	4666(2)	849(2)	6844(2)	17(1)
C(11)	3559(2)	1554(2)	5836(1)	13(1)
C(12)	2550(2)	1011(2)	4433(2)	12(1)
C(13)	717(2)	1321(2)	3890(2)	12(1)
C(14)	-497(2)	385(2)	3694(2)	16(1)
C(15)	-2173(2)	741(2)	3225(2)	21(1)
C(16)	-2639(2)	2029(2)	2947(2)	24(1)
C(17)	-1432(2)	2972(2)	3143(2)	22(1)
C(18)	236(2)	2613(2)	3607(2)	18(1)
C(19)	5627(2)	1234(2)	8346(2)	21(1)
C(20)	5145(3)	357(2)	9319(2)	29(1)
C(21)	5395(3)	2663(2)	8623(2)	24(1)
O(1)	4980(2)	-439(2)	6665(2)	27(1)

Table 3. Bond lengths [\AA] and angles [$^\circ$] for **113k**.

Br(1)-C(1)	1.9045(15)	C(3)-C(4)-C(7)	122.39(15)
C(1)-C(2)	1.382(3)	C(4)-C(5)-C(6)	121.22(15)
C(1)-C(6)	1.385(2)	C(1)-C(6)-C(5)	118.74(16)
C(2)-C(3)	1.392(2)	C(4)-C(7)-C(8)	122.36(14)
C(3)-C(4)	1.400(2)	C(4)-C(7)-C(12)	121.89(13)
C(4)-C(5)	1.393(2)	C(8)-C(7)-C(12)	59.02(10)
C(4)-C(7)	1.489(2)	C(12)-C(8)-C(7)	61.85(11)
C(5)-C(6)	1.397(2)	C(12)-C(8)-C(9)	116.05(14)
C(7)-C(8)	1.506(2)	C(7)-C(8)-C(9)	116.87(15)
C(7)-C(12)	1.547(2)	O(1)-C(9)-C(8)	115.23(15)
C(8)-C(12)	1.505(2)	C(11)-C(10)-O(1)	122.75(17)
C(8)-C(9)	1.515(2)	C(11)-C(10)-C(19)	127.44(17)
C(9)-O(1)	1.416(2)	O(1)-C(10)-C(19)	109.56(14)
C(10)-C(11)	1.328(2)	C(10)-C(11)-C(12)	122.2(2)
C(10)-O(1)	1.385(2)	C(11)-C(12)-C(13)	114.74(13)
C(10)-C(19)	1.506(2)	C(11)-C(12)-C(8)	114.23(14)
C(11)-C(12)	1.485(2)	C(13)-C(12)-C(8)	121.24(14)
C(12)-C(13)	1.504(2)	C(11)-C(12)-C(7)	119.46(13)
C(13)-C(14)	1.387(2)	C(13)-C(12)-C(7)	117.03(13)
C(13)-C(18)	1.396(2)	C(8)-C(12)-C(7)	59.13(11)
C(14)-C(15)	1.394(3)	C(14)-C(13)-C(18)	119.21(15)
C(15)-C(16)	1.389(3)	C(14)-C(13)-C(12)	122.76(15)
C(16)-C(17)	1.388(3)	C(18)-C(13)-C(12)	118.01(14)
C(17)-C(18)	1.389(2)	C(13)-C(14)-C(15)	119.99(17)
C(19)-C(21)	1.533(3)	C(16)-C(15)-C(14)	120.35(18)
C(19)-C(20)	1.534(3)	C(17)-C(16)-C(15)	120.03(18)
		C(16)-C(17)-C(18)	119.44(19)
C(2)-C(1)-C(6)	121.64(14)	C(17)-C(18)-C(13)	120.98(17)
C(2)-C(1)-Br(1)	118.42(13)	C(10)-C(19)-C(21)	112.88(15)
C(6)-C(1)-Br(1)	119.93(13)	C(10)-C(19)-C(20)	110.01(16)
C(1)-C(2)-C(3)	118.83(15)	C(21)-C(19)-C(20)	110.81(16)
C(2)-C(3)-C(4)	121.29(16)	C(10)-O(1)-C(9)	115.23(15)
C(5)-C(4)-C(3)	118.27(14)		
C(5)-C(4)-C(7)	119.31(14)		

Table 4. Anisotropic displacement parameters ($\text{\AA}^2 \times 10^3$) for **113k**. The anisotropic displacement factor exponent takes the form: $-2p^2[h^2 a^*2U^{11} + \dots + 2 h k a^* b^* U^{12}]$

	U ¹¹	U ²²	U ³³	U ²³	U ¹³	U ¹²
Br(1)	36(1)	20(1)	11(1)	2(1)	6(1)	6(1)
C(1)	17(1)	16(1)	11(1)	0(1)	7(1)	3(1)
C(2)	22(1)	15(1)	12(1)	-1(1)	4(1)	-2(1)
C(3)	21(1)	13(1)	12(1)	0(1)	5(1)	-3(1)
C(4)	13(1)	12(1)	12(1)	-1(1)	6(1)	0(1)
C(5)	14(1)	12(1)	16(1)	0(1)	5(1)	-1(1)
C(6)	18(1)	12(1)	16(1)	3(1)	8(1)	3(1)
C(7)	13(1)	12(1)	12(1)	0(1)	5(1)	1(1)
C(8)	21(1)	11(1)	12(1)	0(1)	5(1)	2(1)
C(9)	34(1)	20(1)	15(1)	0(1)	5(1)	13(1)
C(10)	15(1)	18(1)	15(1)	-2(1)	4(1)	3(1)
C(11)	17(1)	11(1)	12(1)	0(1)	5(1)	2(1)
C(12)	16(1)	10(1)	10(1)	1(1)	3(1)	1(1)
C(13)	14(1)	14(1)	10(1)	0(1)	5(1)	0(1)
C(14)	20(1)	14(1)	15(1)	-1(1)	9(1)	-3(1)
C(15)	17(1)	28(1)	17(1)	-1(1)	6(1)	-7(1)
C(16)	13(1)	36(1)	22(1)	4(1)	6(1)	1(1)
C(17)	16(1)	24(1)	27(1)	6(1)	8(1)	5(1)
C(18)	15(1)	16(1)	21(1)	3(1)	7(1)	1(1)
C(19)	18(1)	25(1)	13(1)	-3(1)	-1(1)	5(1)
C(20)	43(1)	24(1)	15(1)	2(1)	6(1)	6(1)
C(21)	30(1)	22(1)	17(1)	-8(1)	6(1)	-4(1)
O(1)	34(1)	24(1)	17(1)	-1(1)	5(1)	11(1)

Table 5. Hydrogen coordinates ($\times 10^4$) and isotropic displacement parameters ($\text{\AA}^2 \times 10^3$) for **113k**.

	x	y	z	U(eq)
H(2)	-202	-480	-1005	20
H(3)	1259	-749	1410	19
H(5)	3057	2899	1715	17
H(6)	1611	3175	-707	18
H(7)	4502	1225	3658	15
H(8)	2285	-927	3619	18
H(9A)	4726	-1749	5220	29
H(9B)	5707	-481	5096	29
H(11)	3409	2435	6018	16
H(14)	-186	-498	3880	19
H(15)	-3002	98	3094	25
H(16)	-3783	2266	2623	29
H(17)	-1745	3855	2961	27
H(18)	1061	3257	3732	21
H(19)	6840	1093	8564	25
H(20A)	3975	509	9164	43
H(20B)	5860	552	10295	43
H(20C)	5293	-551	9120	43
H(21A)	5686	3205	7978	36
H(21B)	6123	2880	9590	36
H(21C)	4228	2818	8479	36

APPENDIX THREE

Spectra Relevant to Chapter Five

Towards a Unified Synthesis of Gelsemium Alkaloids: The Total Synthesis of (±)-Gelsenicine

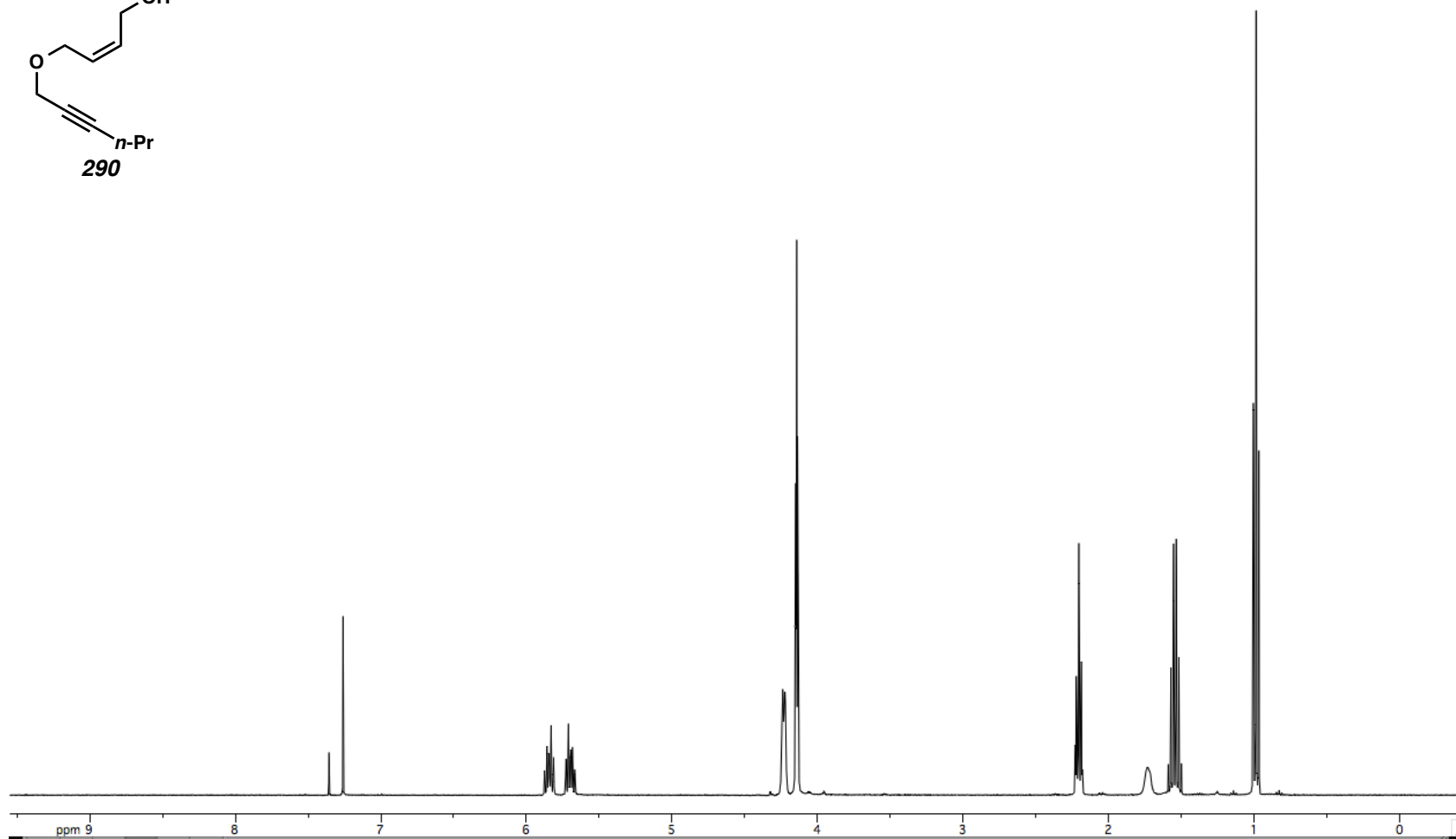
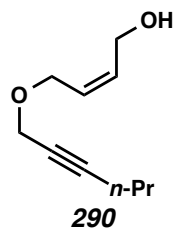


Figure A3.1. ¹H NMR (400 MHz, CDCl₃) of Compound **290**.

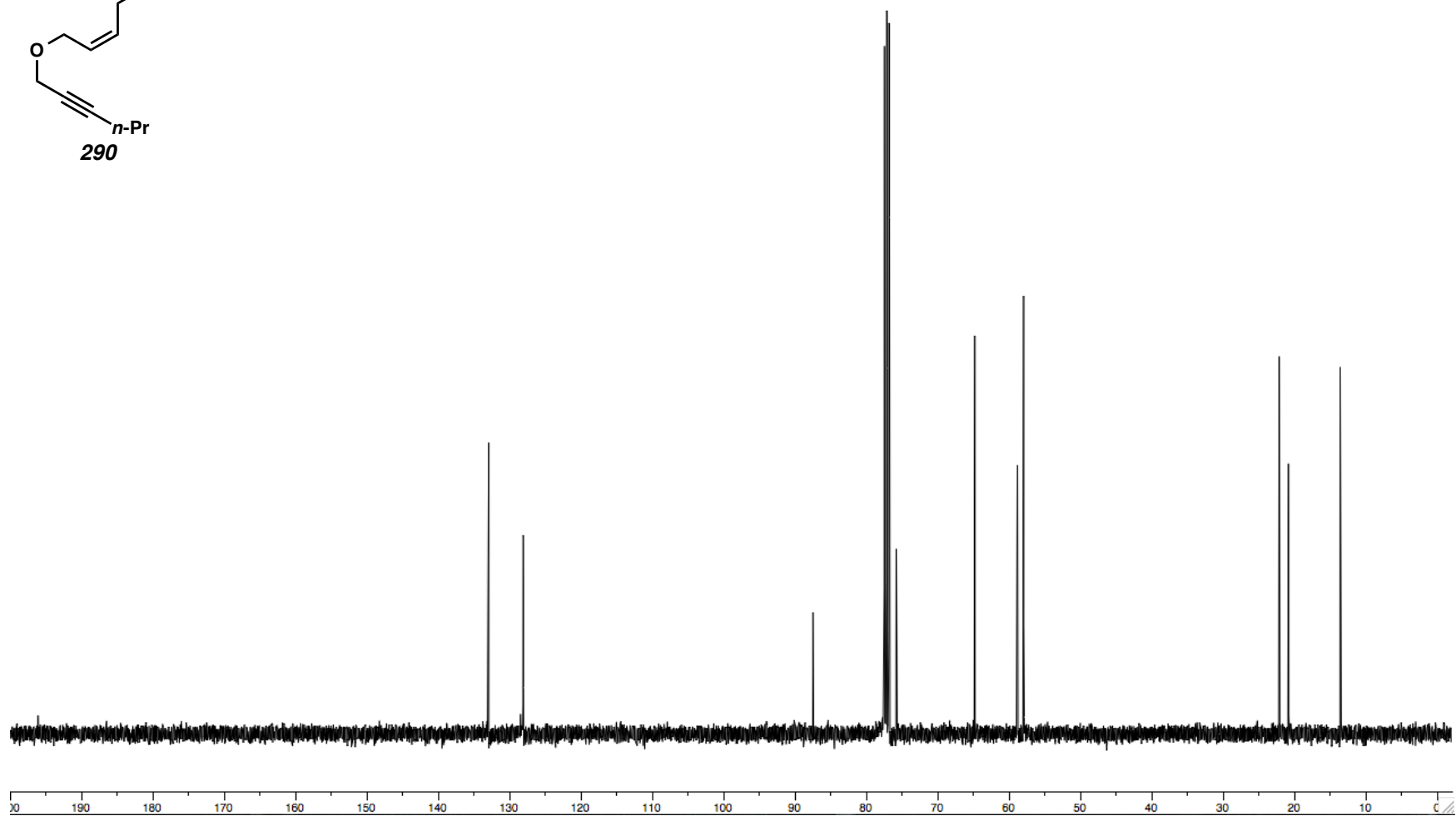
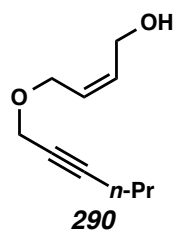


Figure A3.2. ^{13}C NMR (100 MHz, CDCl_3) of Compound **290**.

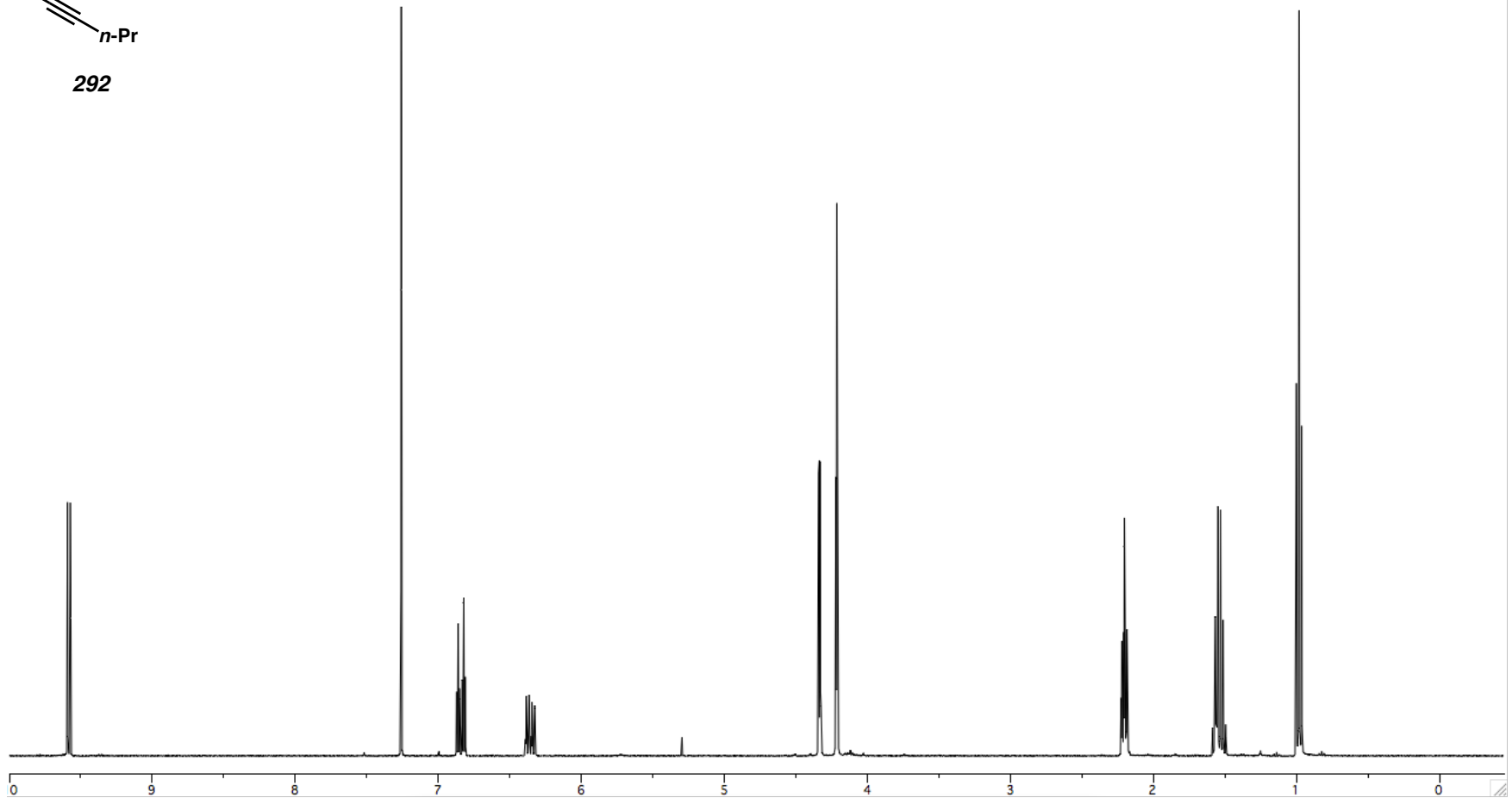
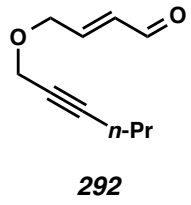
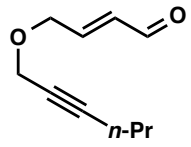


Figure A3.3. ^1H NMR (400 MHz, CDCl_3) of Compound **292**.



292

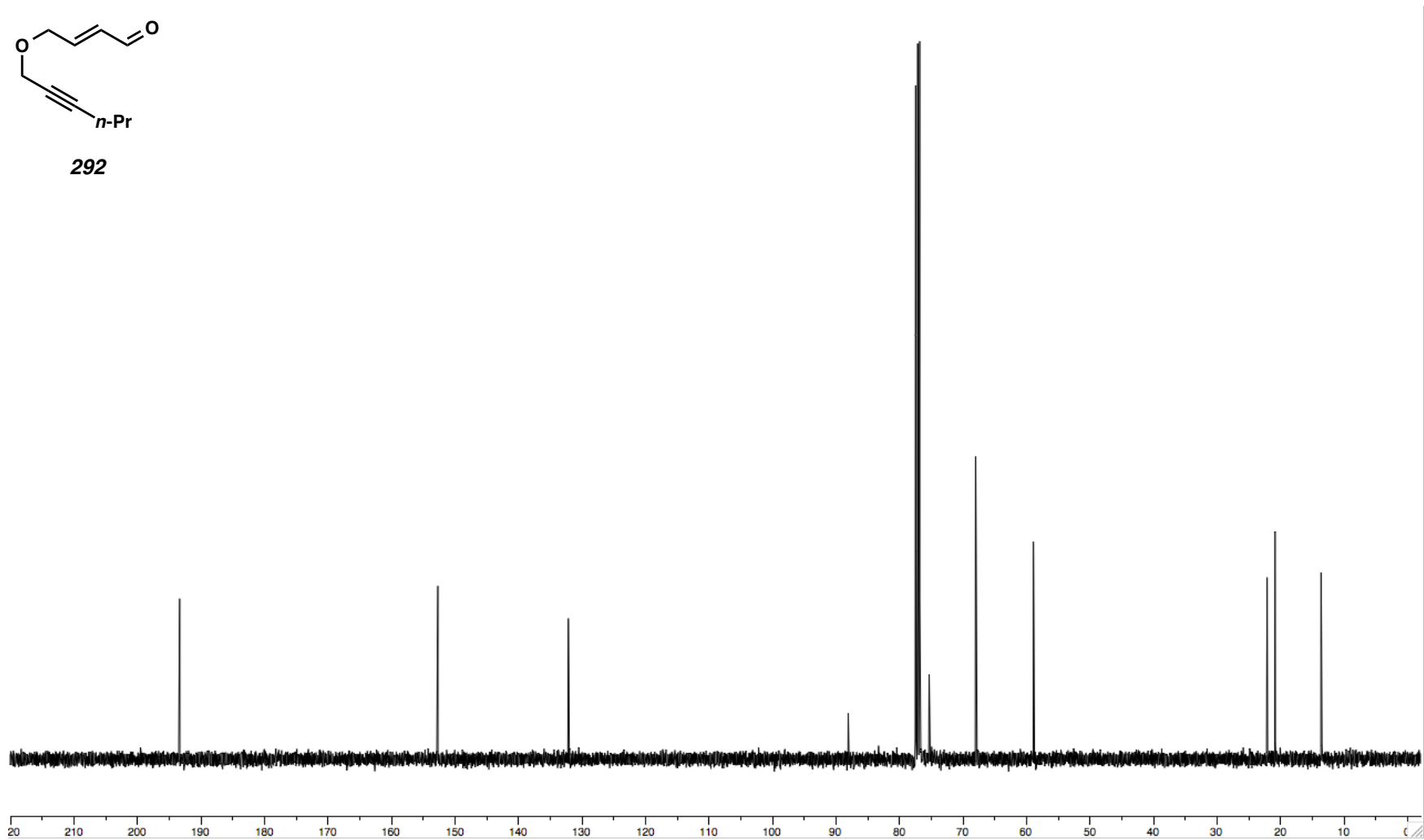


Figure A3.4. ^{13}C NMR (100 MHz, CDCl_3) of Compound **292**.

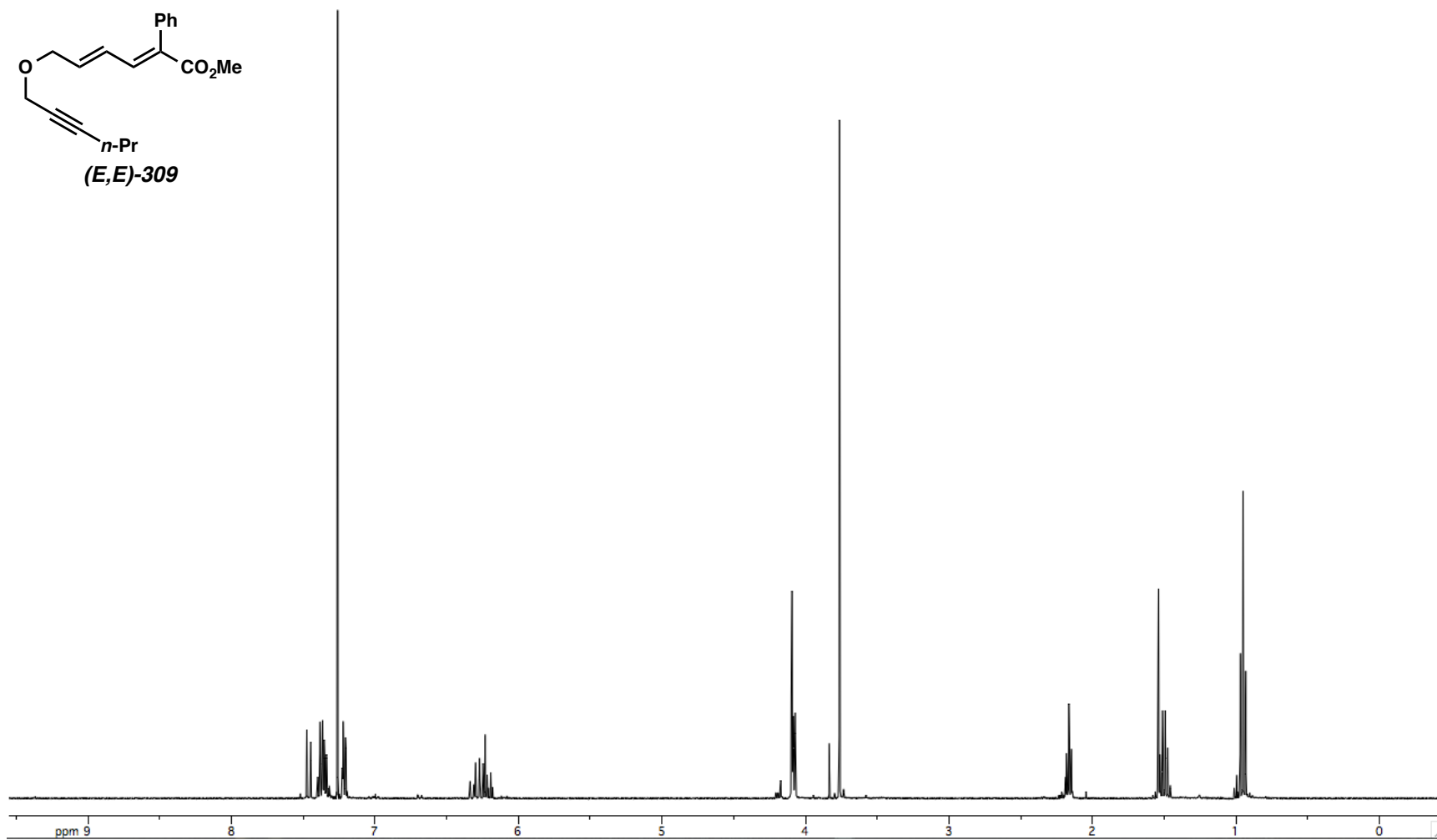
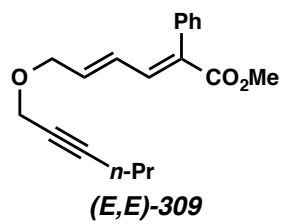


Figure A3.5. ^1H NMR (400 MHz, CDCl_3) of Compound (*E,E*)-309.

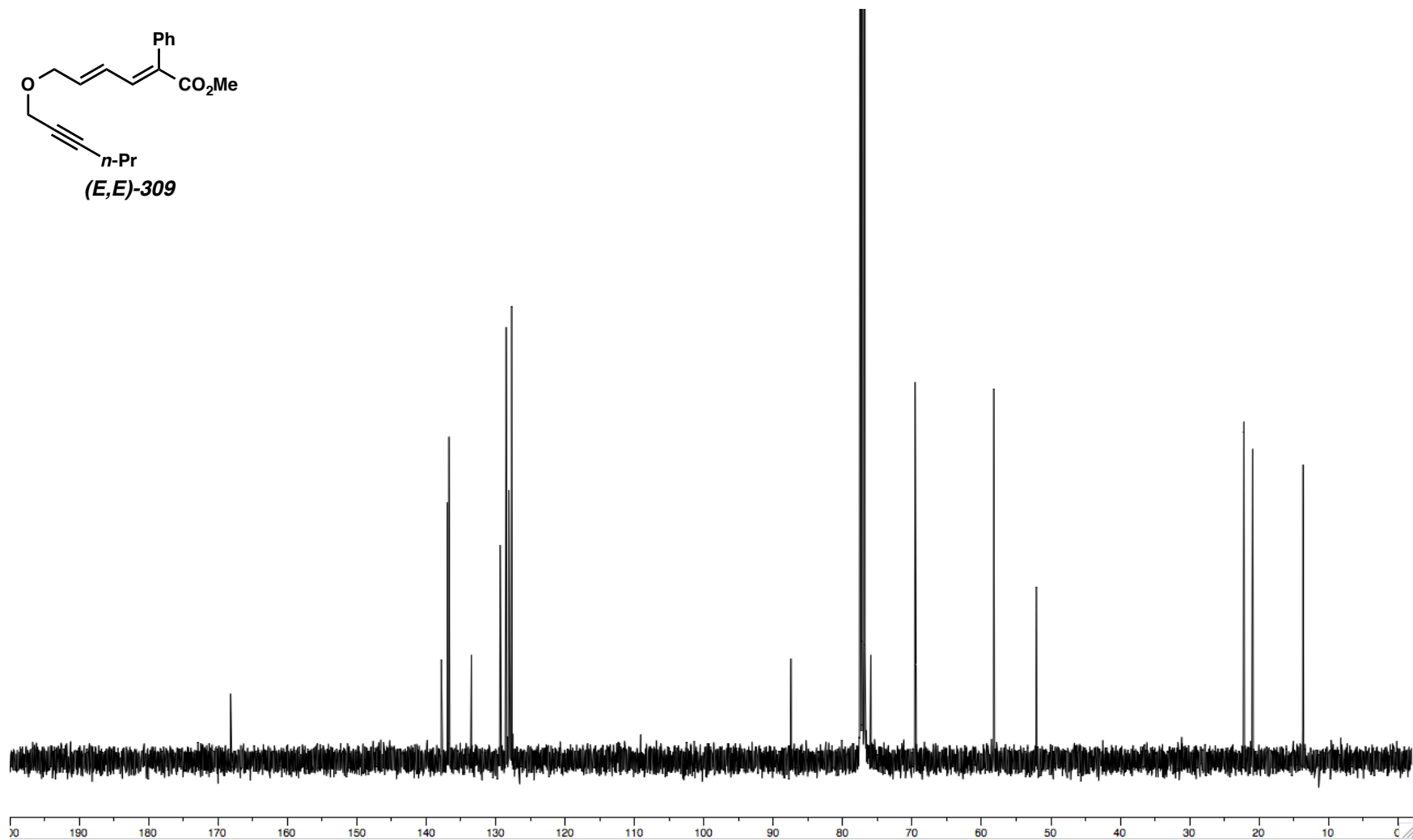
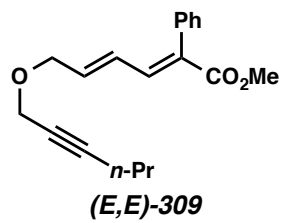


Figure A3.6. ^{13}C NMR (100 MHz, CDCl_3) of Compound *(E,E)*-309.

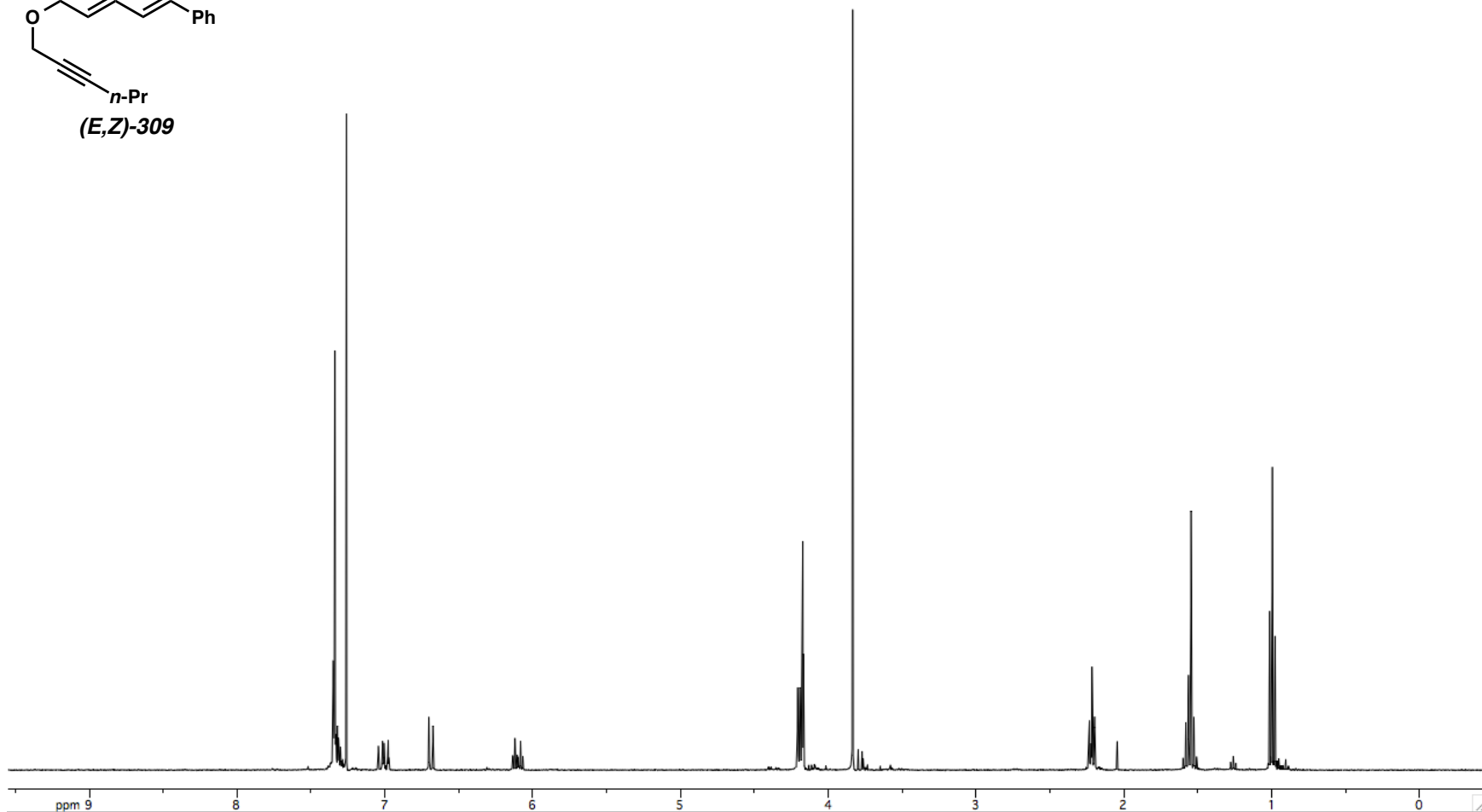
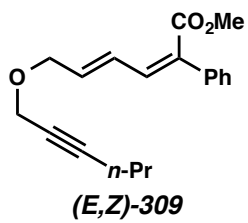


Figure A3.7. ^1H NMR (400 MHz, CDCl_3) of Compound *(E,Z)*-309.

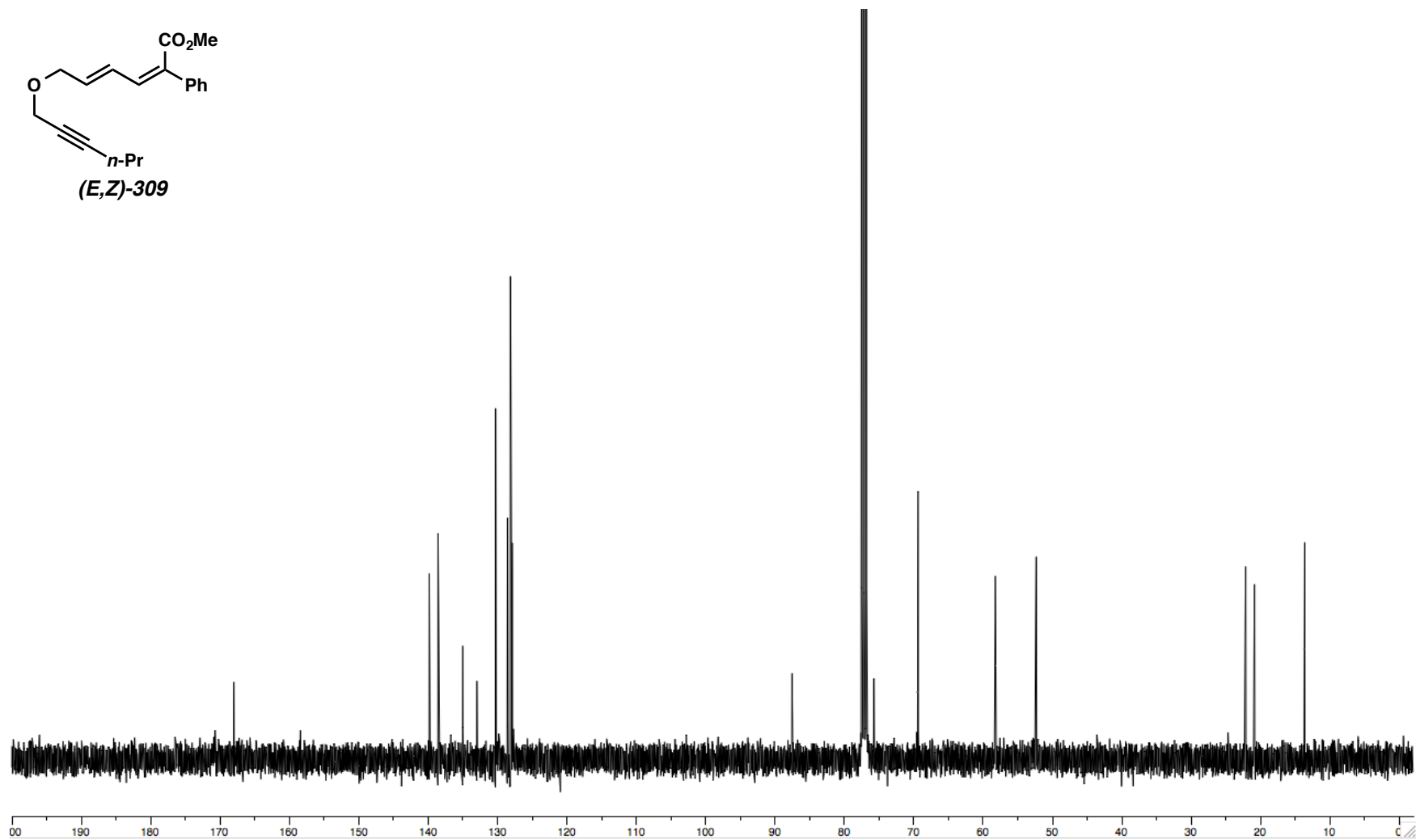


Figure A3.8. ^{13}C NMR (100 MHz, CDCl_3) of Compound **(E,Z)-309**.

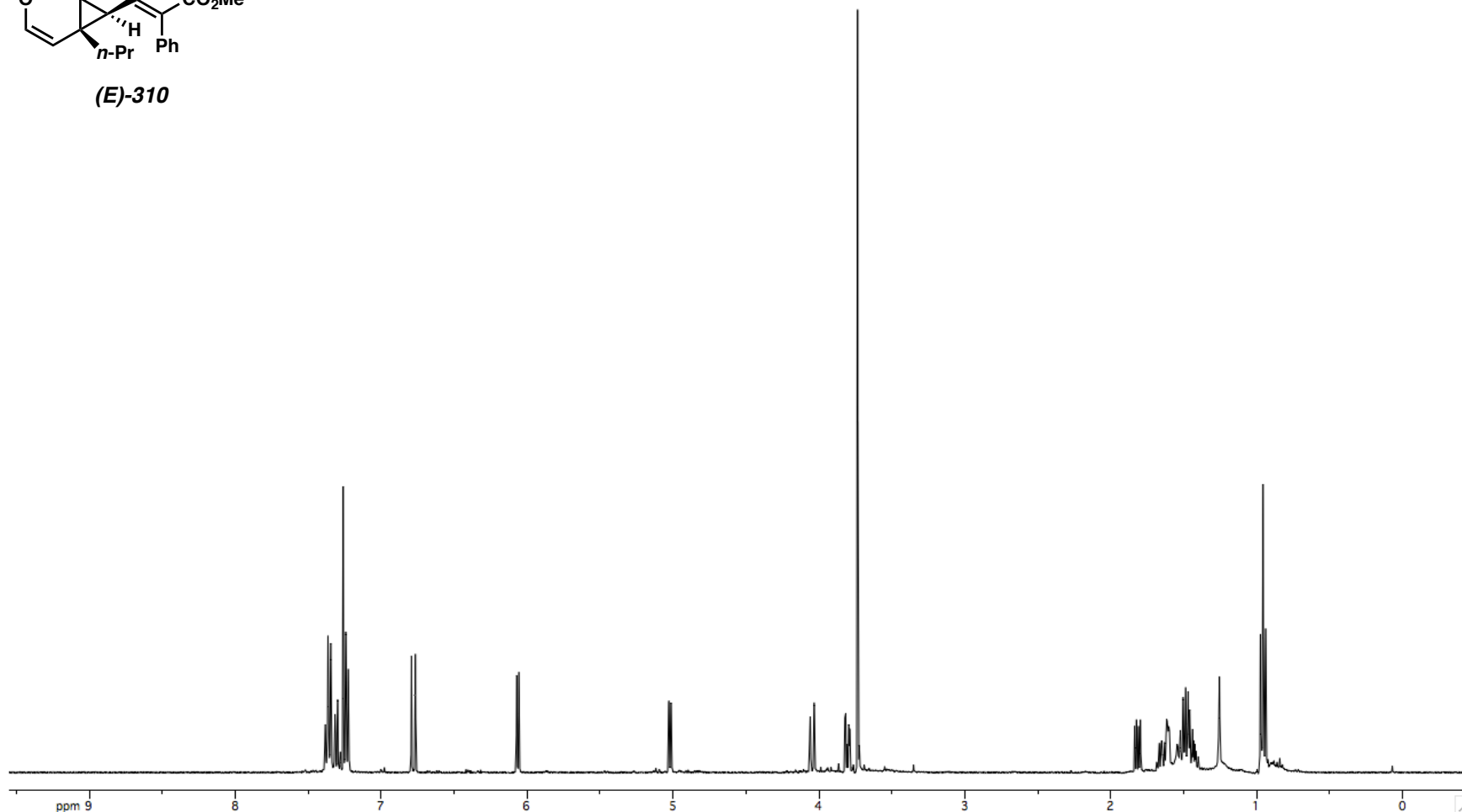
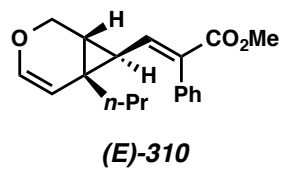


Figure A3.9. ^1H NMR (400 MHz, CDCl_3) of Compound (E)-310.

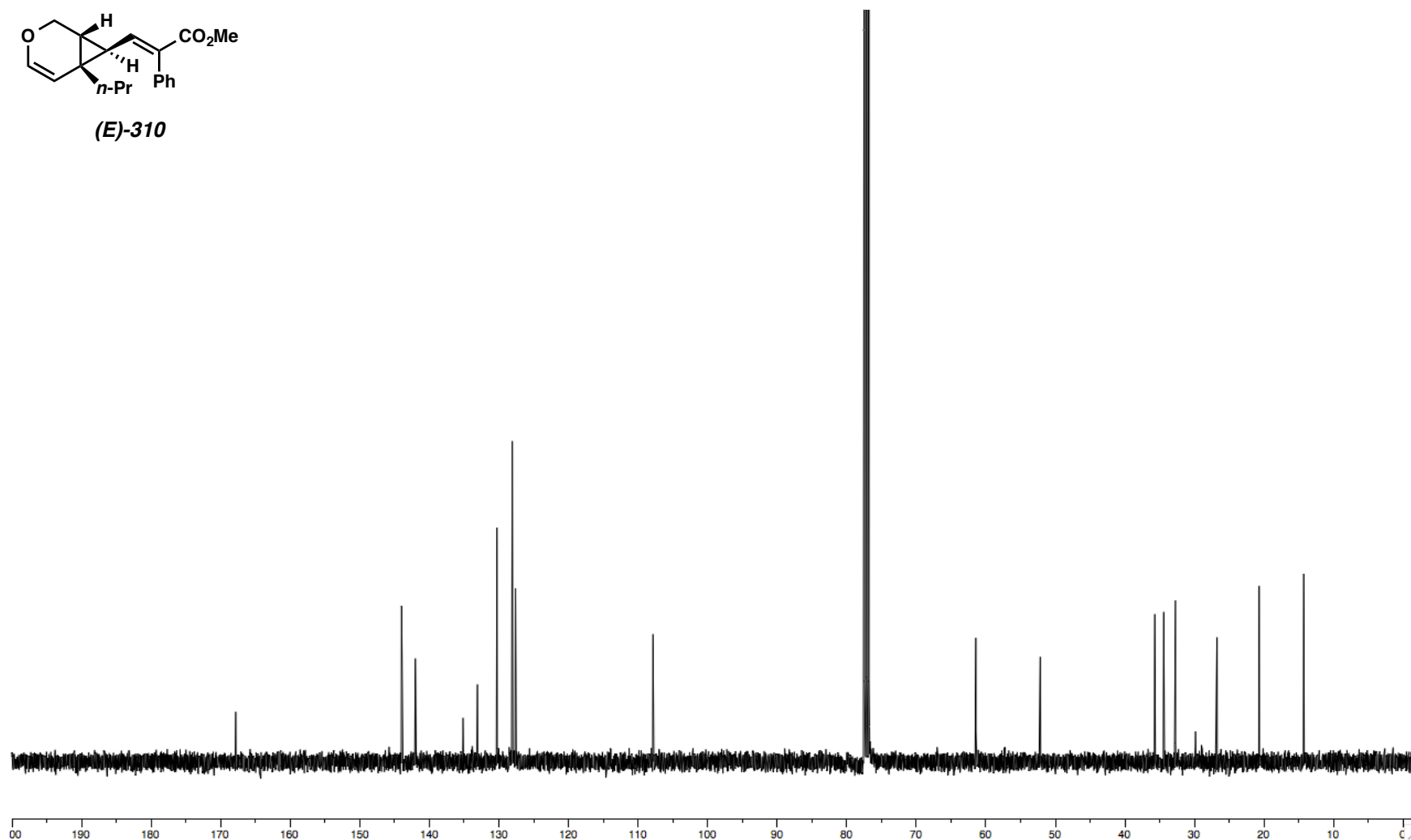
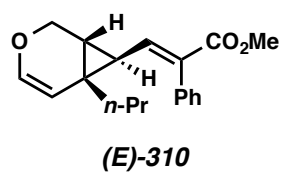


Figure A3.10. ¹³C NMR (100 MHz, CDCl₃) of Compound (E)-310.

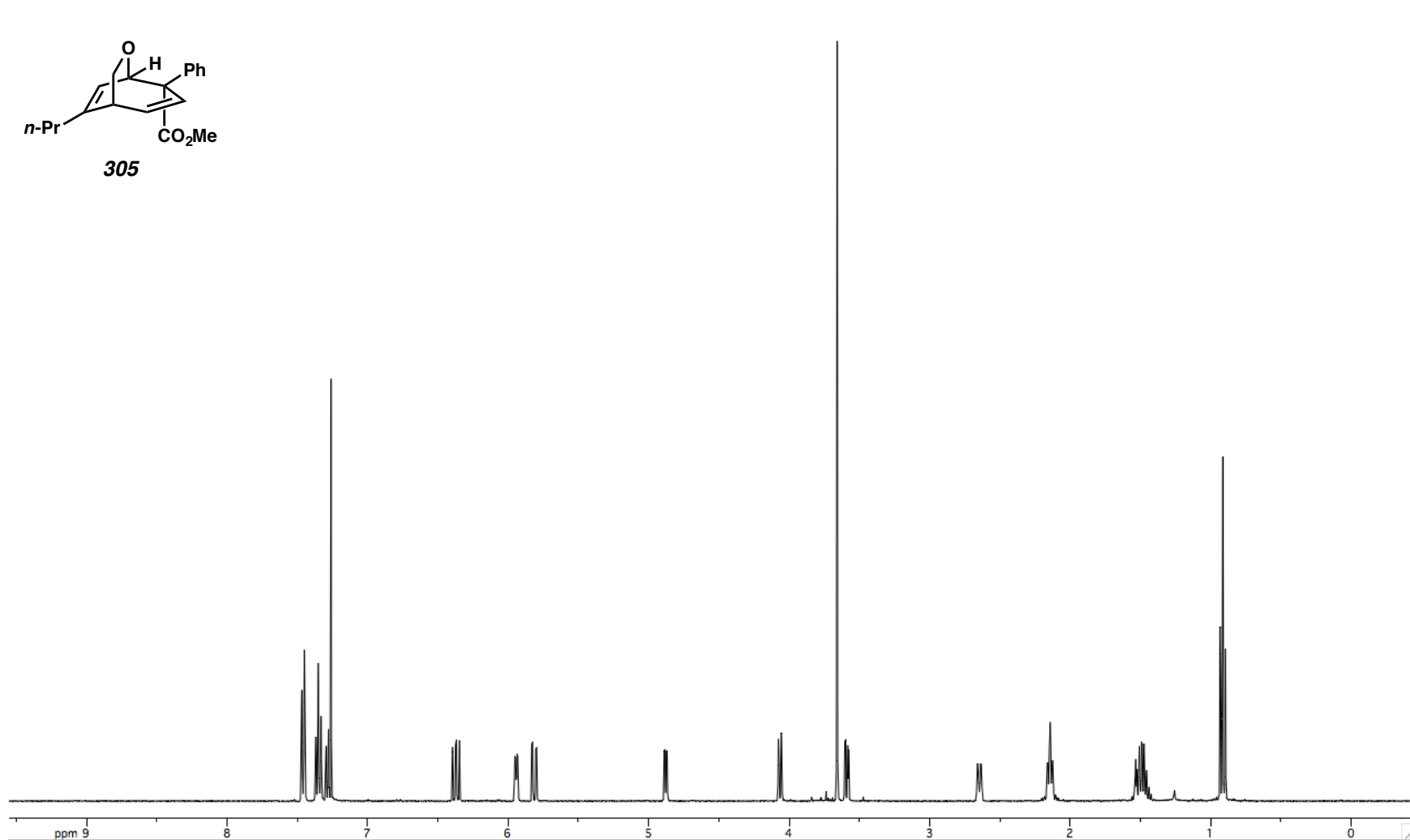
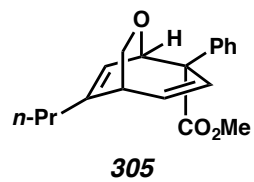


Figure A3.11. ^1H NMR (400 MHz, CDCl_3) of Compound **305**.

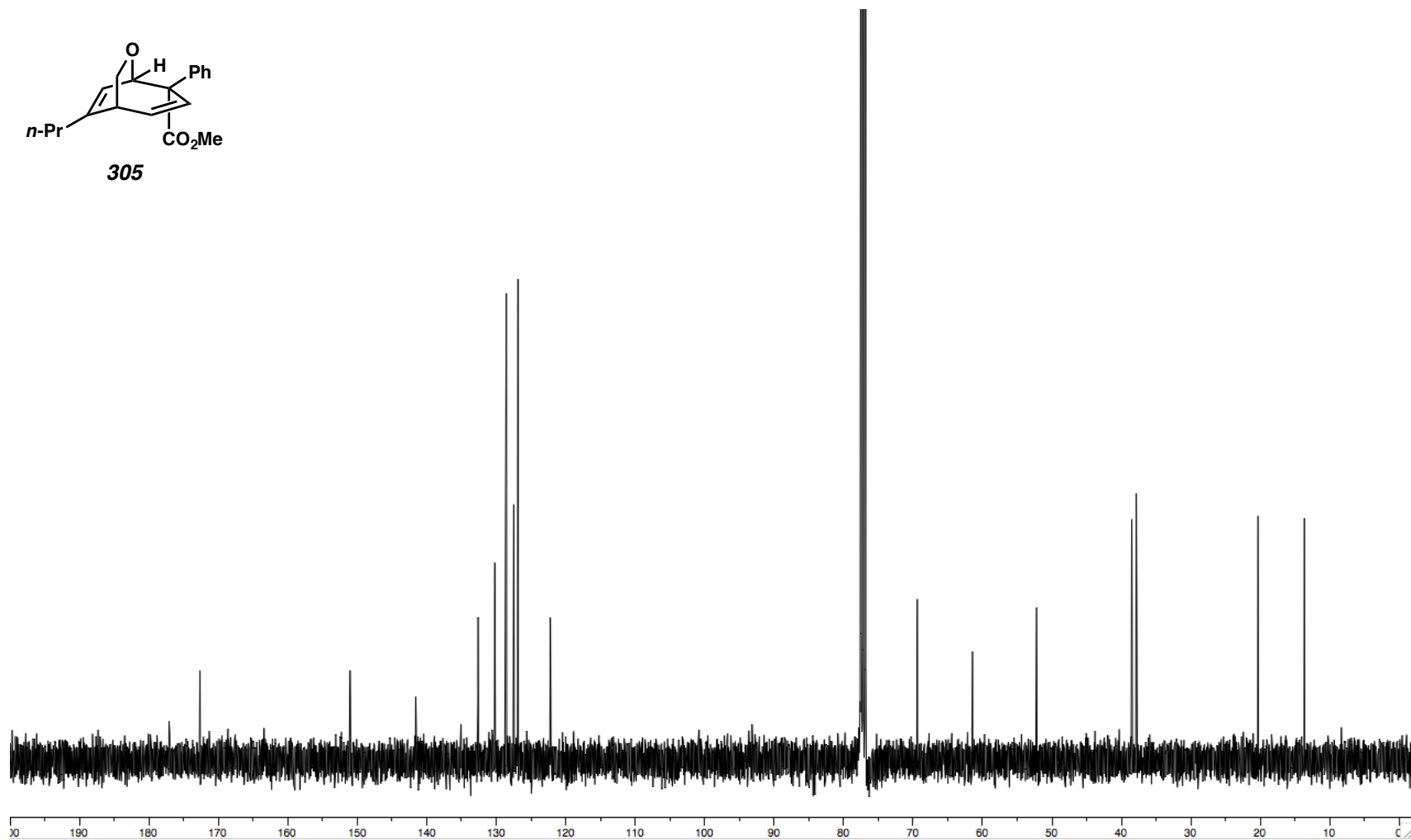
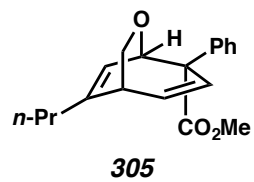


Figure A3.12. ^{13}C NMR (100 MHz, CDCl_3) of Compound **305**.

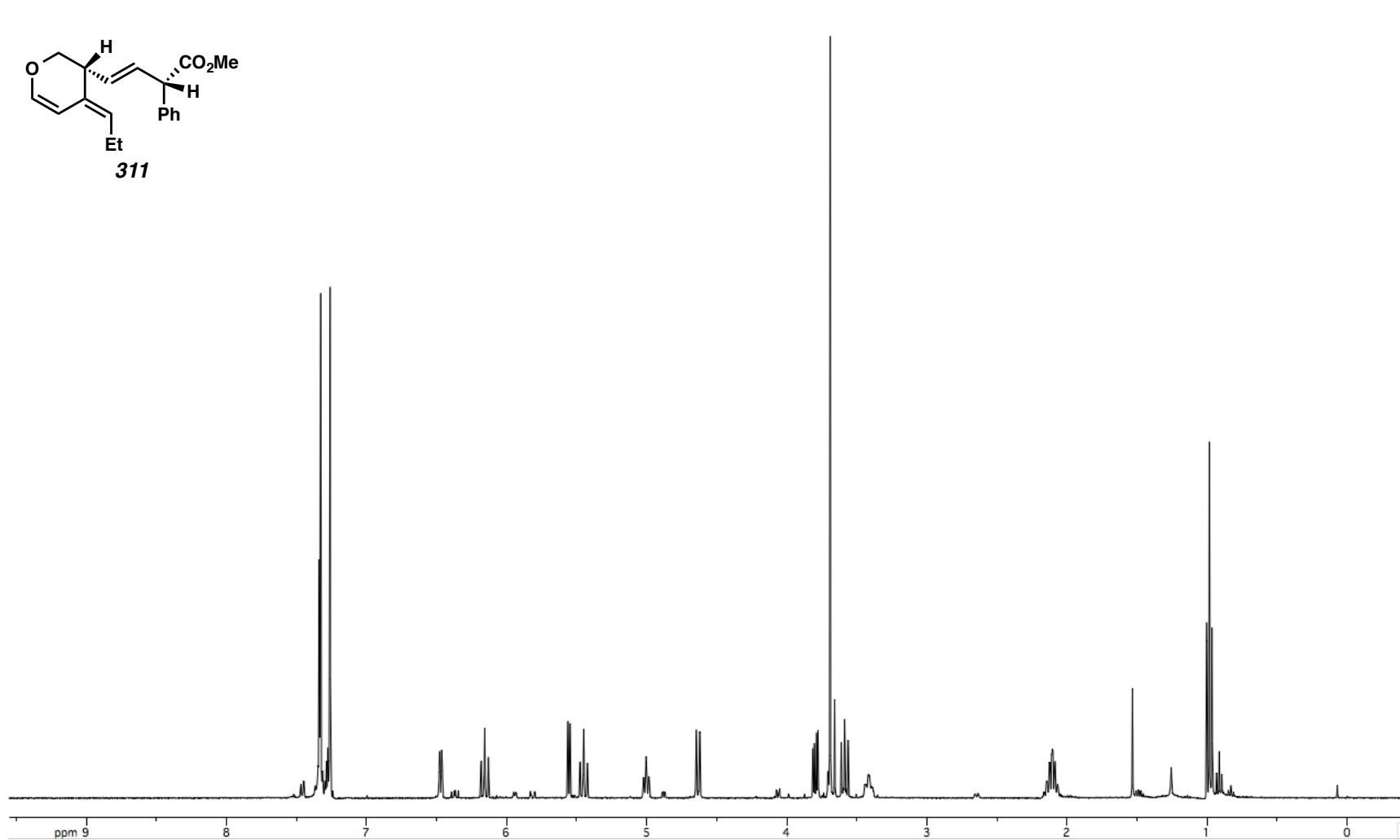
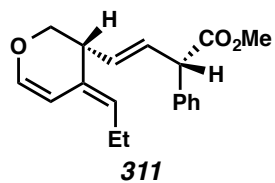


Figure A3.13. ^1H NMR (400 MHz, CDCl_3) of Compound **311**.

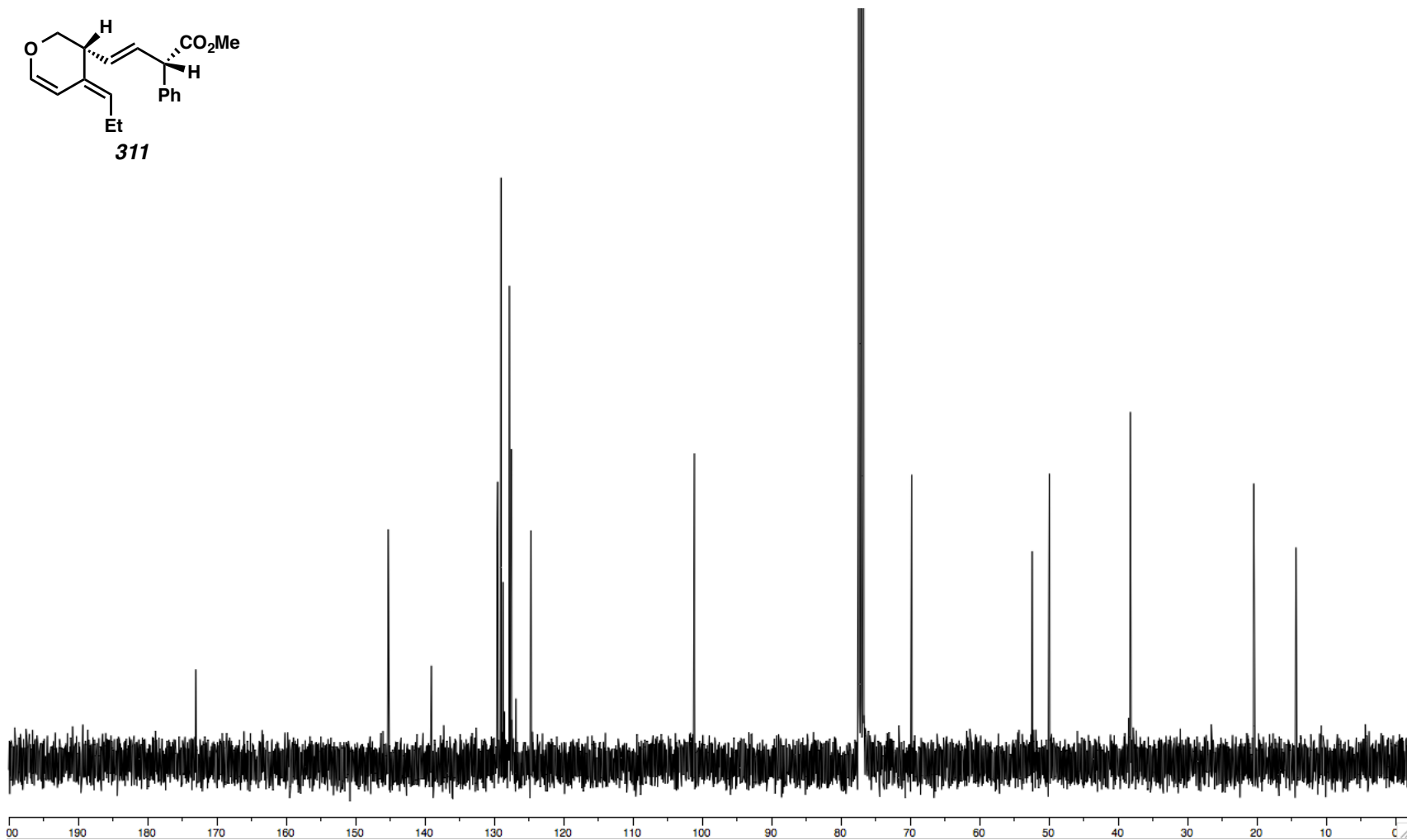
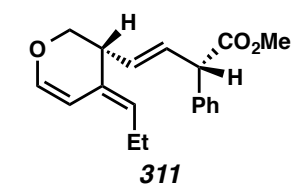


Figure A3.14. ¹³C NMR (100 MHz, CDCl₃) of Compound **311**.

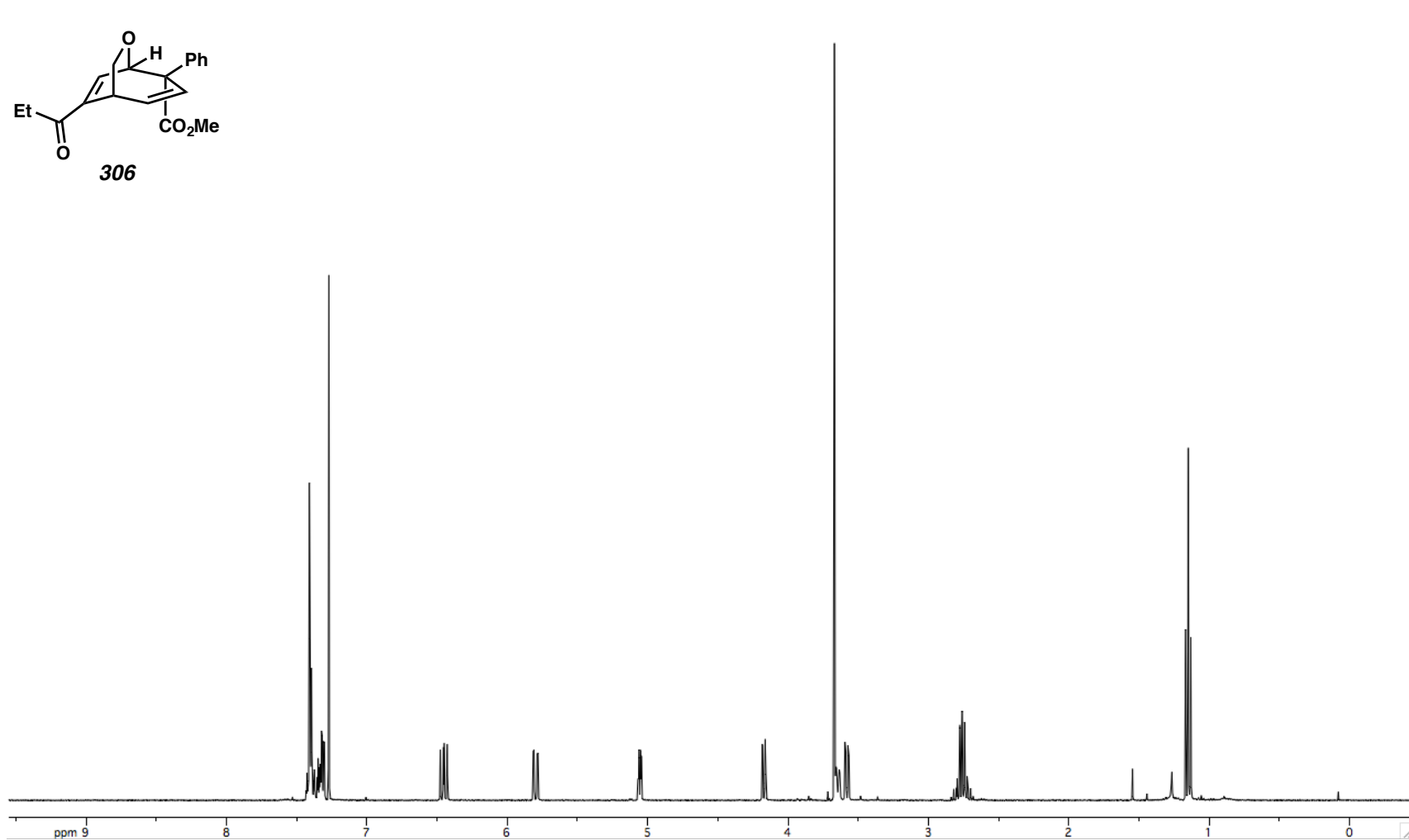
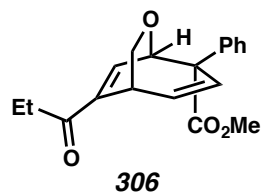


Figure A3.15. ^1H NMR (400 MHz, CDCl_3) of Compound **306**.

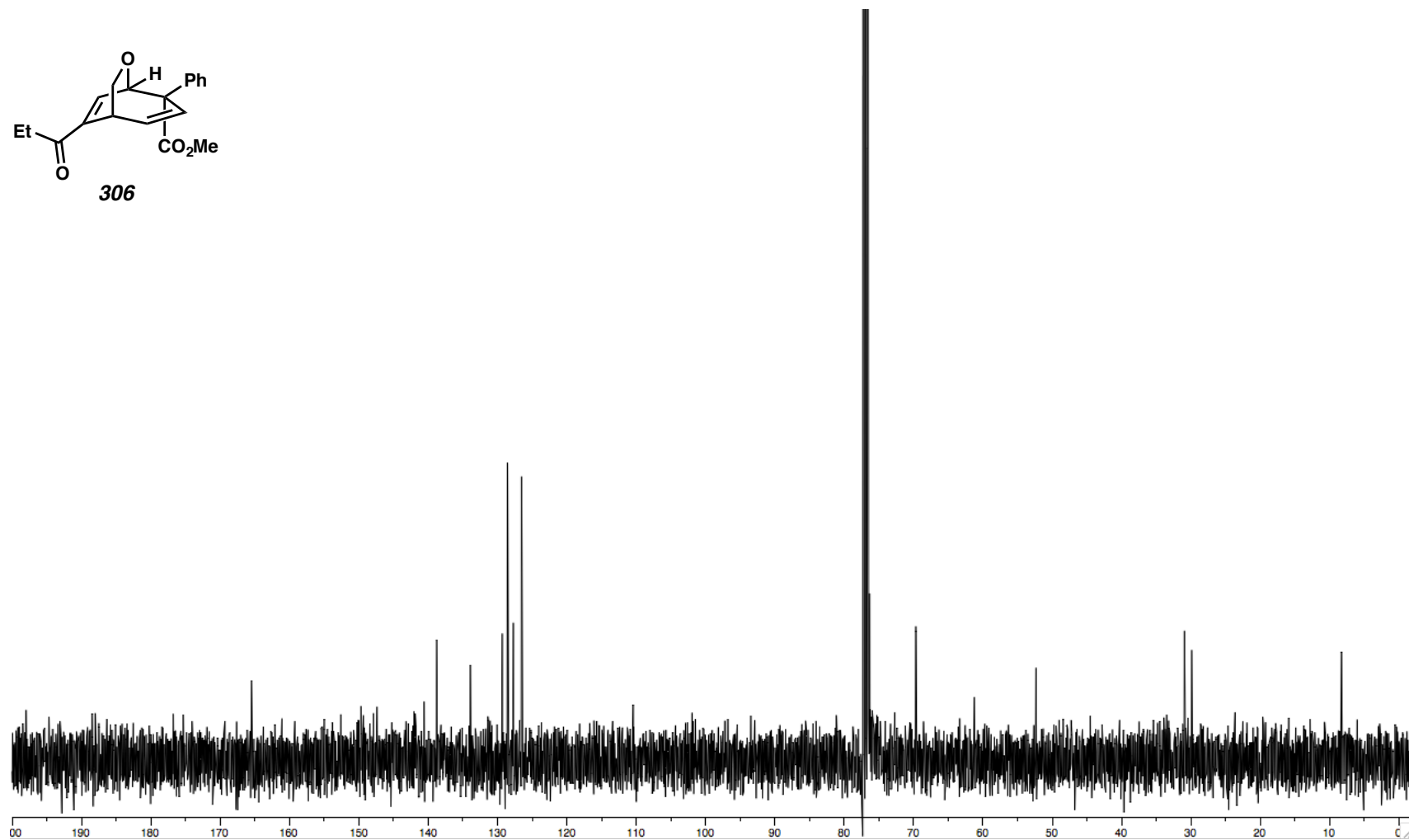
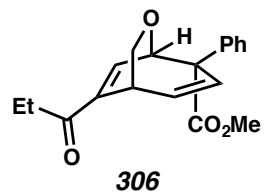


Figure A3.16. ^{13}C NMR (100 MHz, CDCl_3) of Compound **306**.

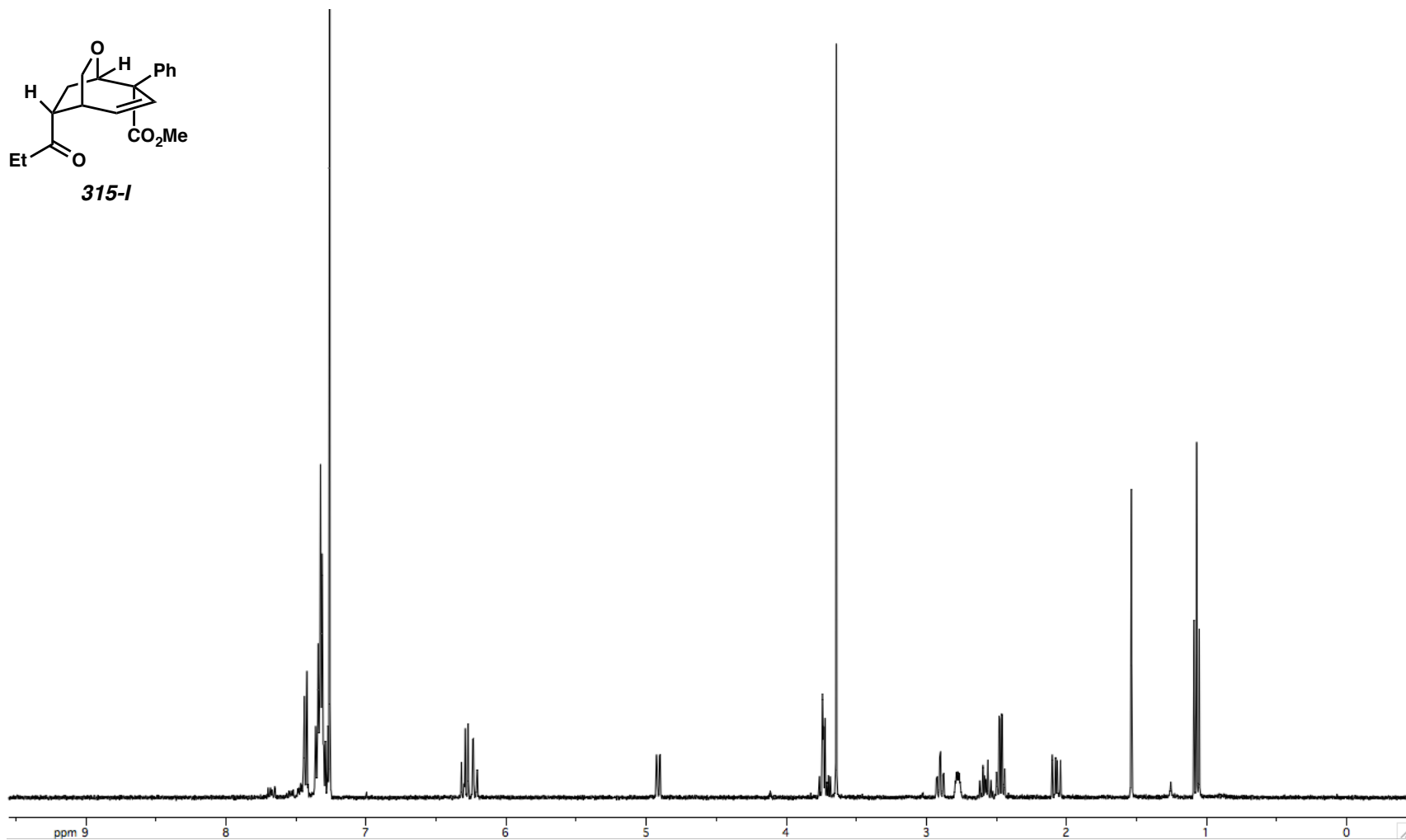


Figure A3.17. ¹H NMR (400 MHz, CDCl₃) of Compound **315-I**.

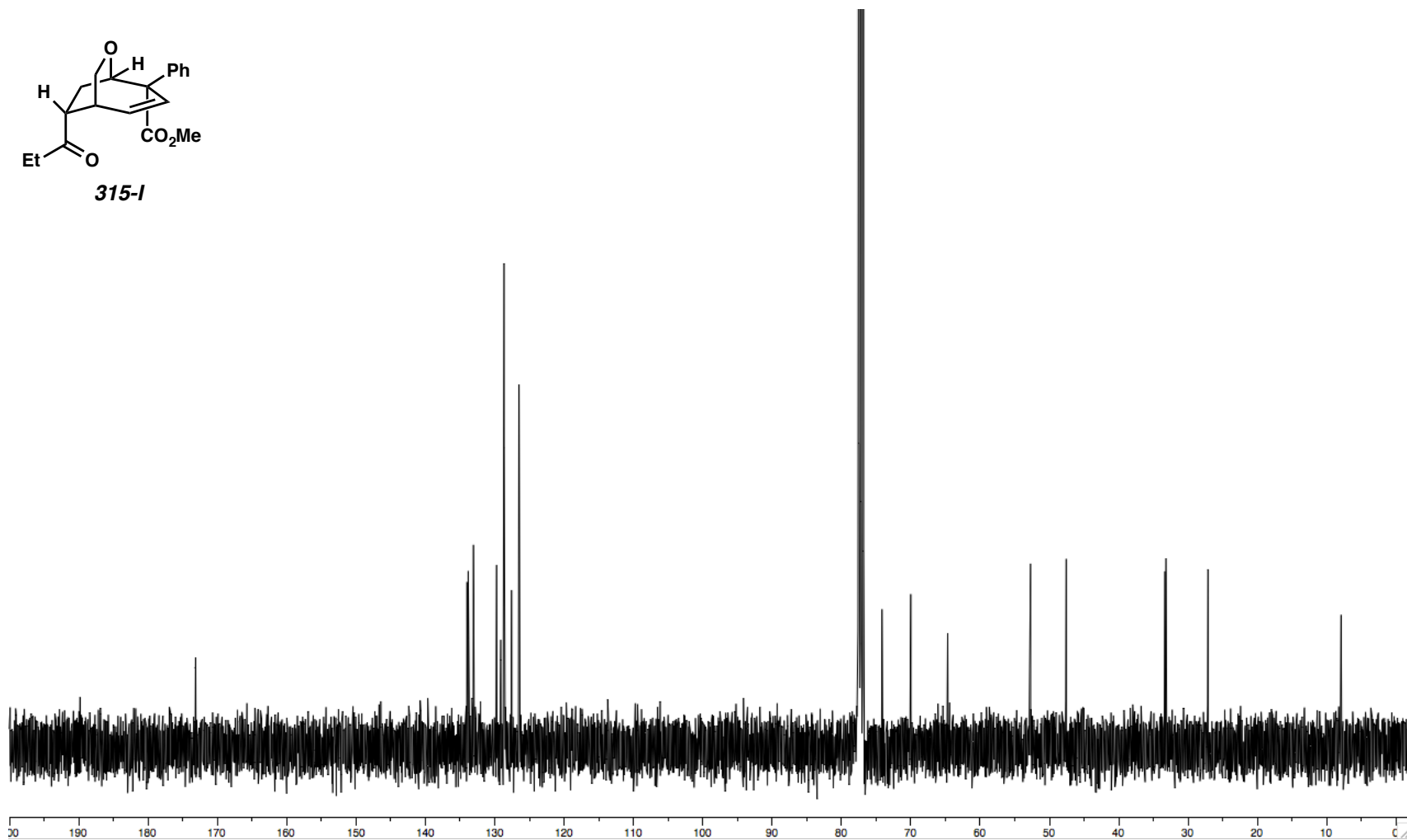
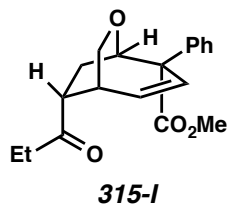
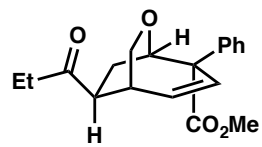


Figure A3.18. ^{13}C NMR (100 MHz, CDCl_3) of Compound **315-I**.



315-II

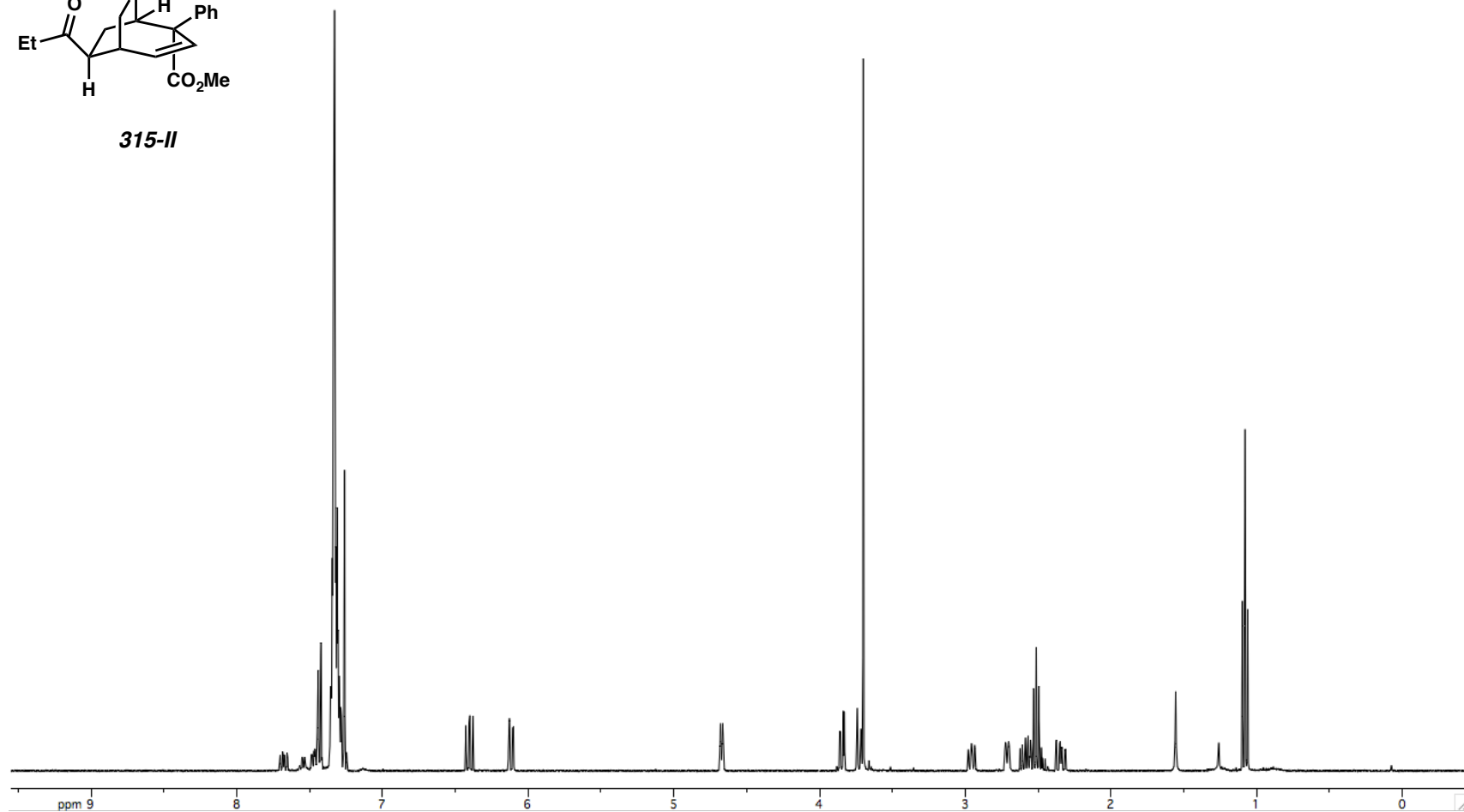
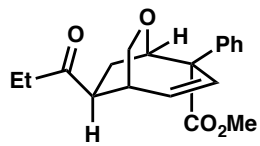


Figure A3.19. ¹H NMR (400 MHz, CDCl₃) of Compound **315-II**.



315-II

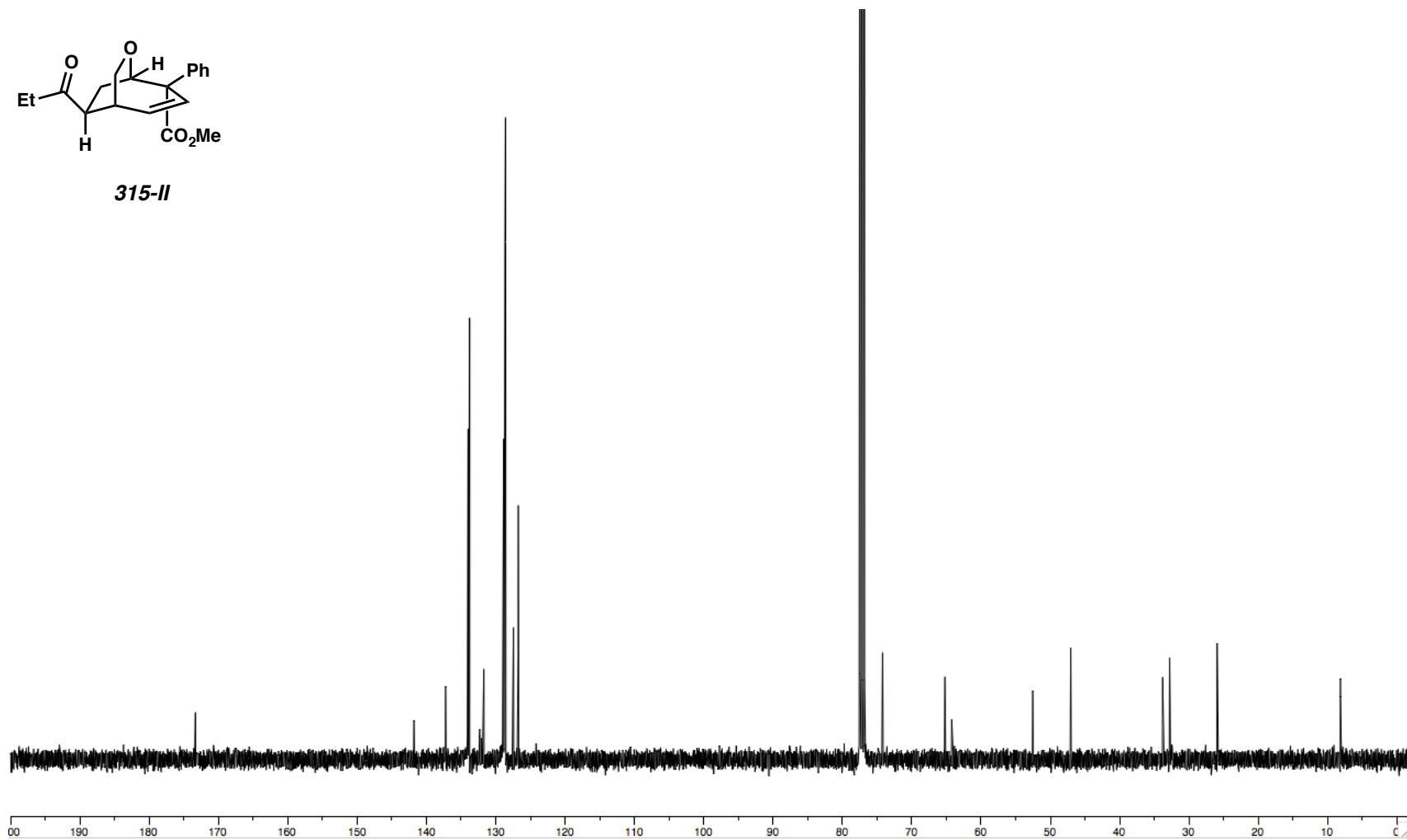


Figure A3.20. ¹³C NMR (100 MHz, CDCl₃) of Compound 315-II.

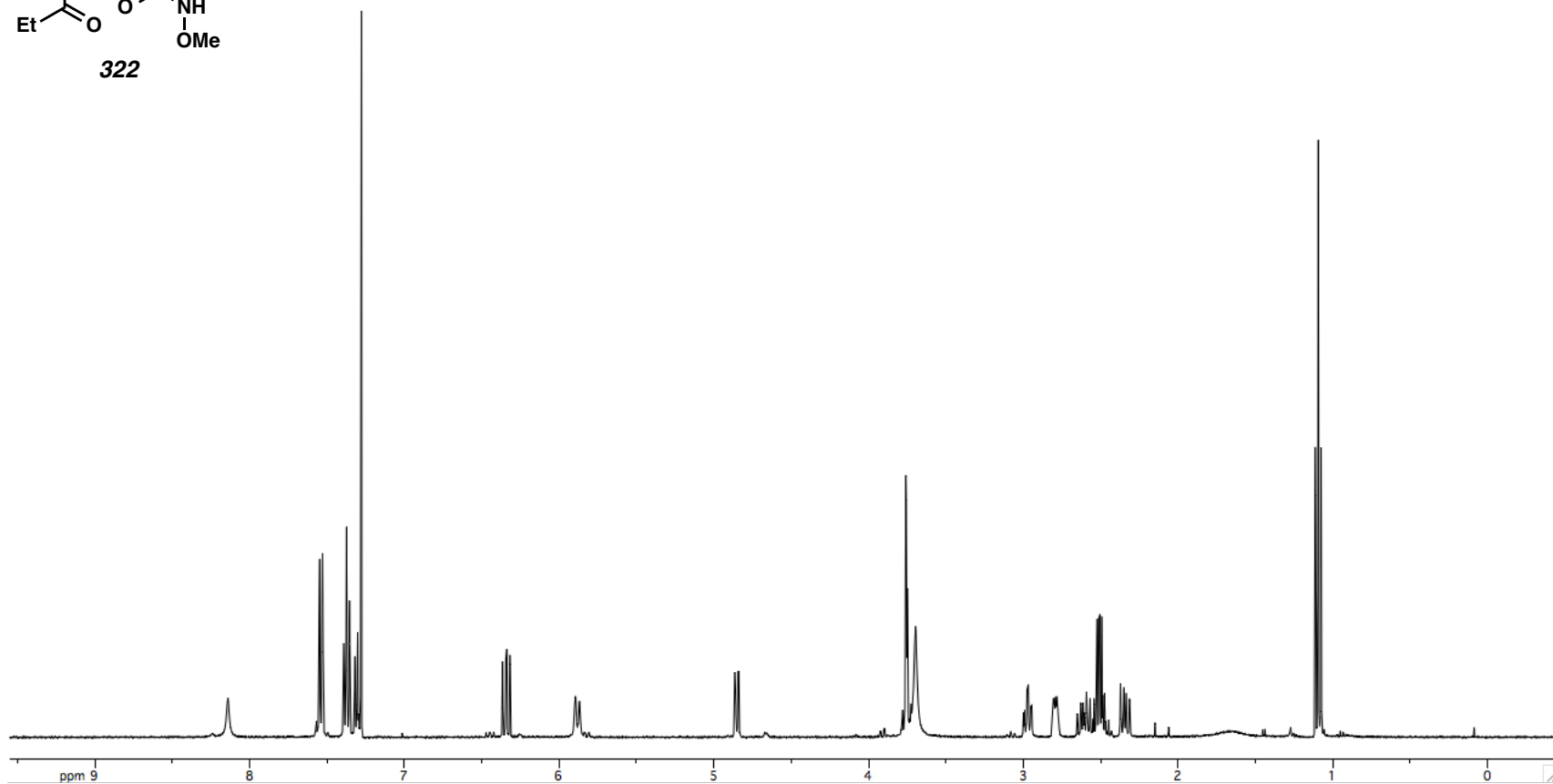
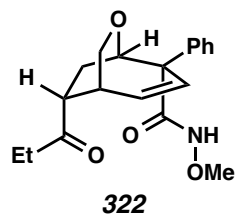


Figure A3.21. ^1H NMR (400 MHz, CDCl_3) of Compound **322**.

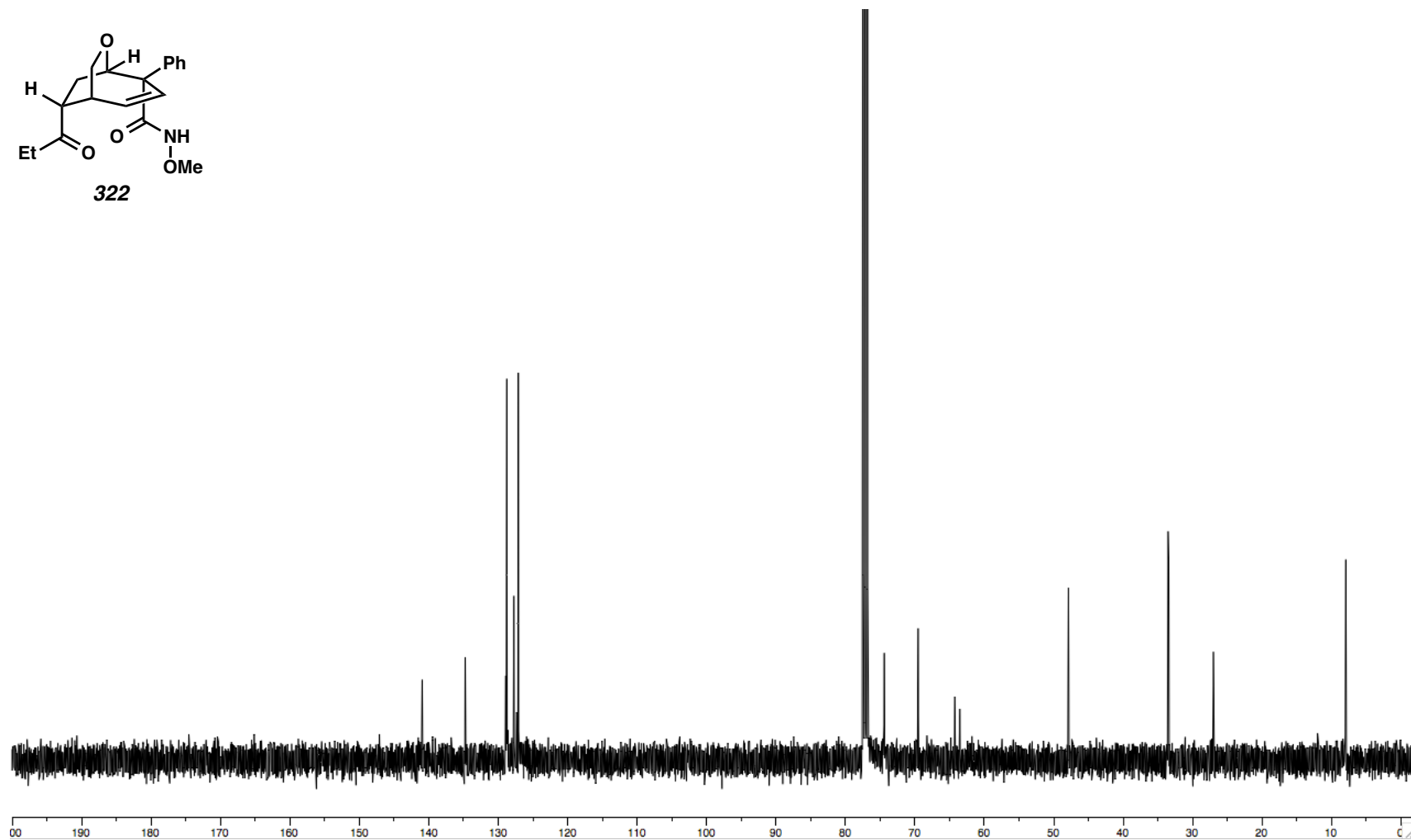
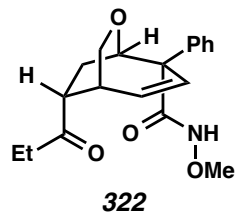


Figure A3.22. ^{13}C NMR (100 MHz, CDCl_3) of Compound **322**.

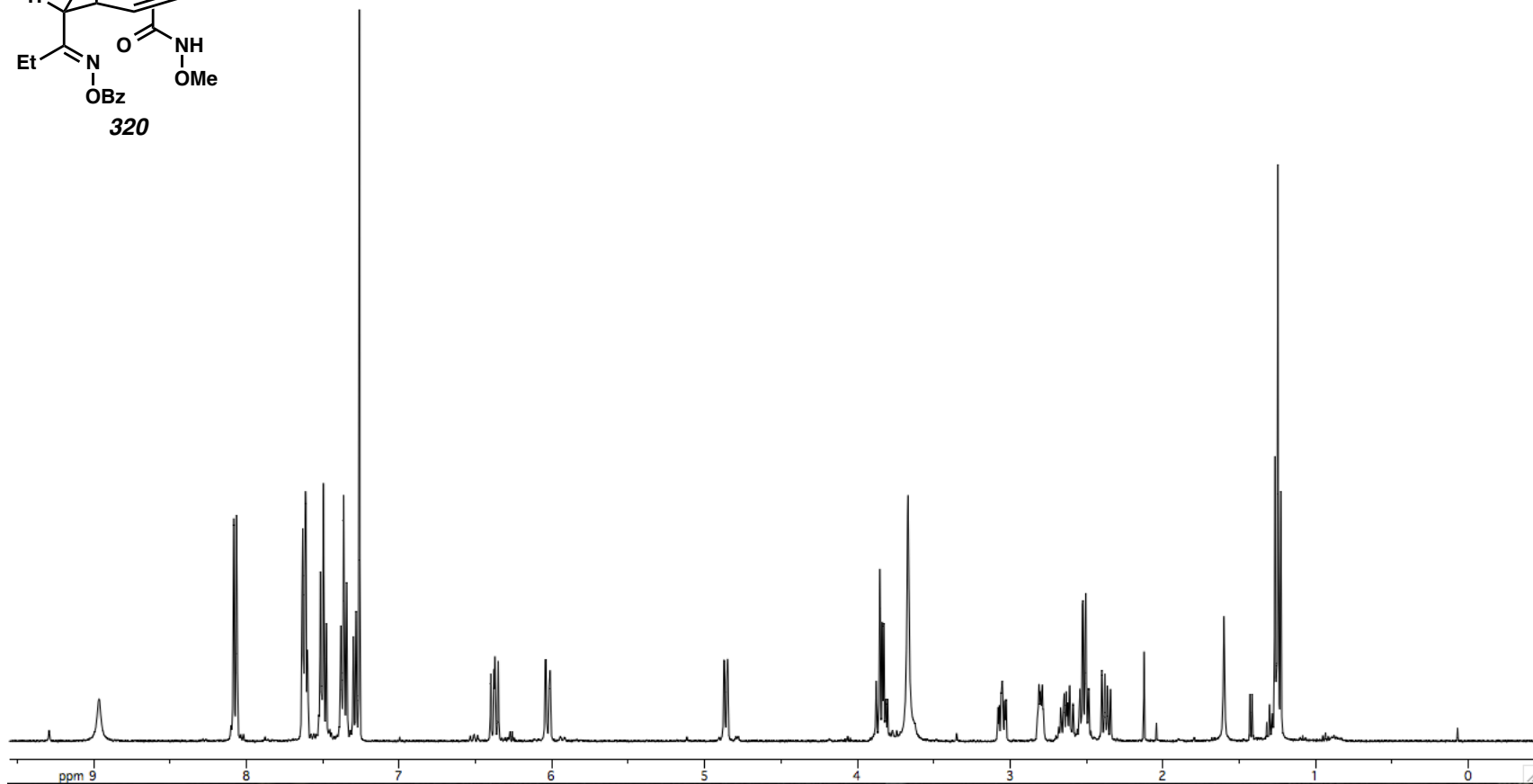
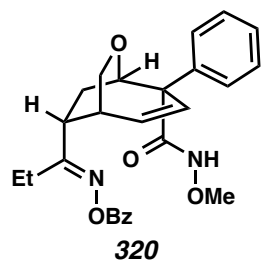


Figure A3.23. ^1H NMR (400 MHz, CDCl_3) of Compound **320**.

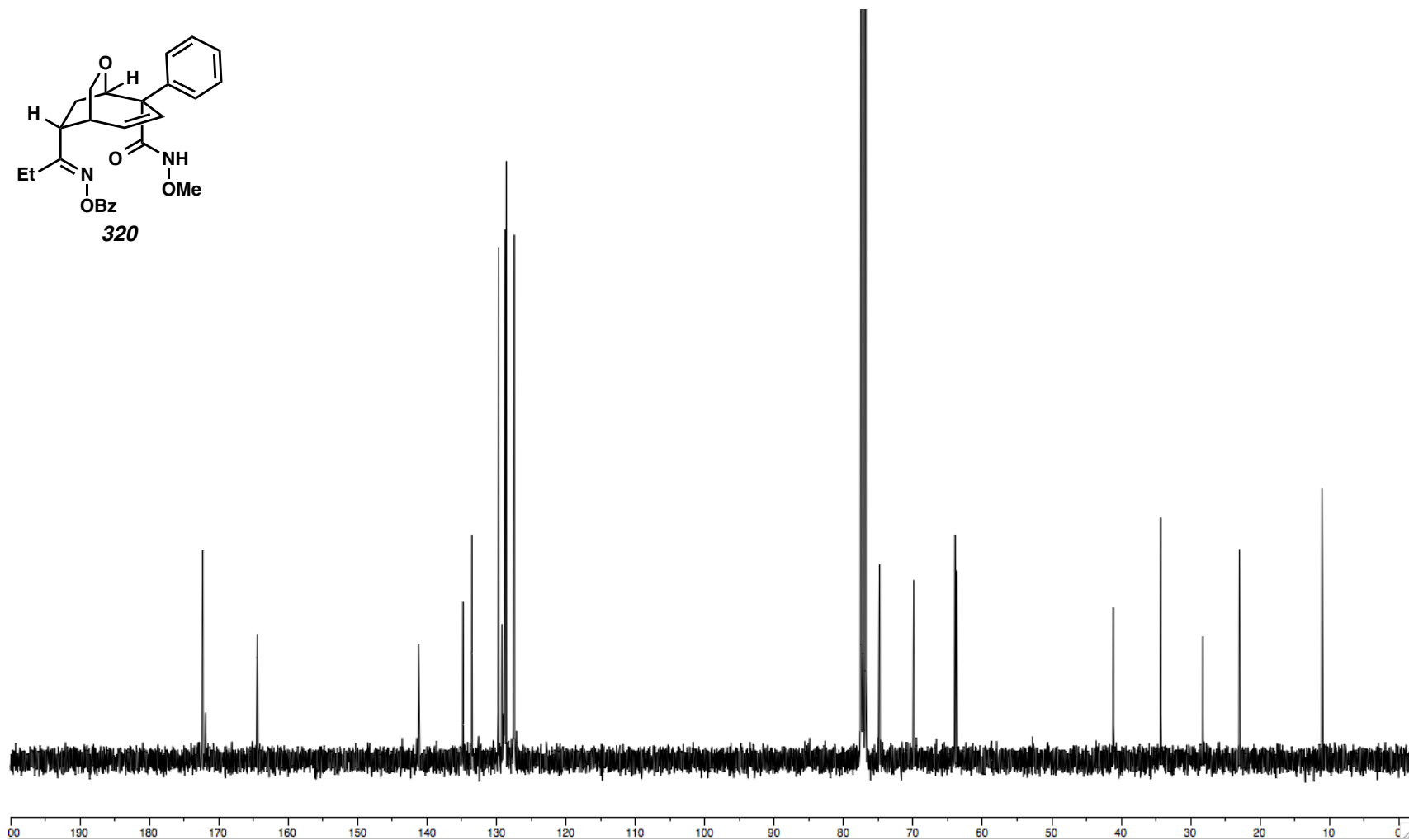
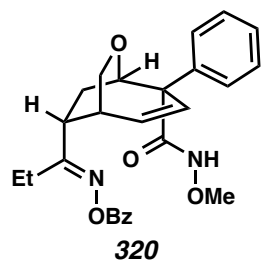


Figure A3.24. ^{13}C NMR (100 MHz, CDCl_3) of Compound **320**.

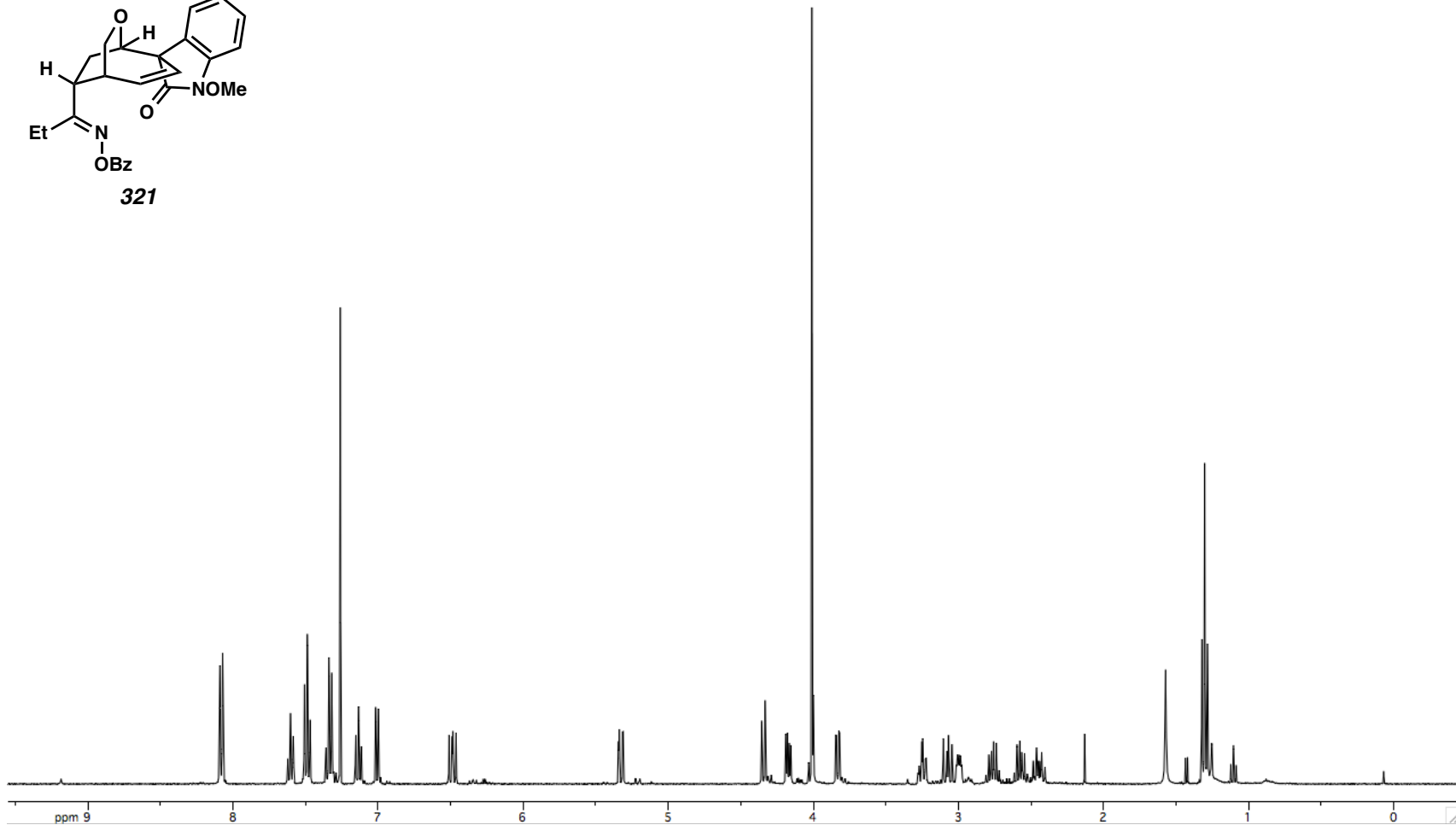
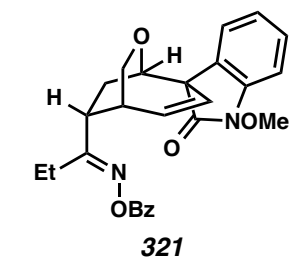


Figure A3.25. ^1H NMR (400 MHz, CDCl_3) of Compound **321**.

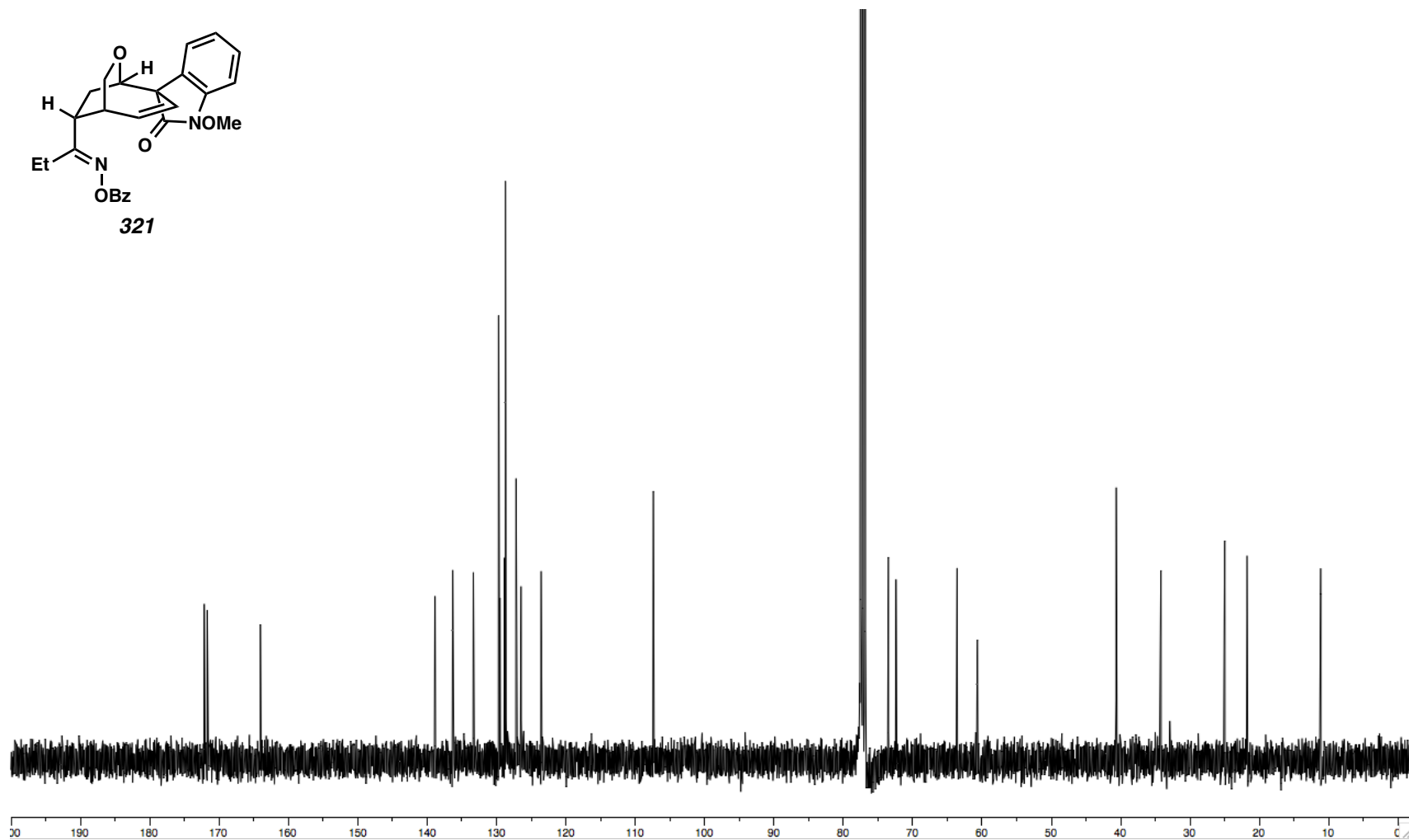


Figure A3.26. ^{13}C NMR (100 MHz, CDCl_3) of Compound 321.

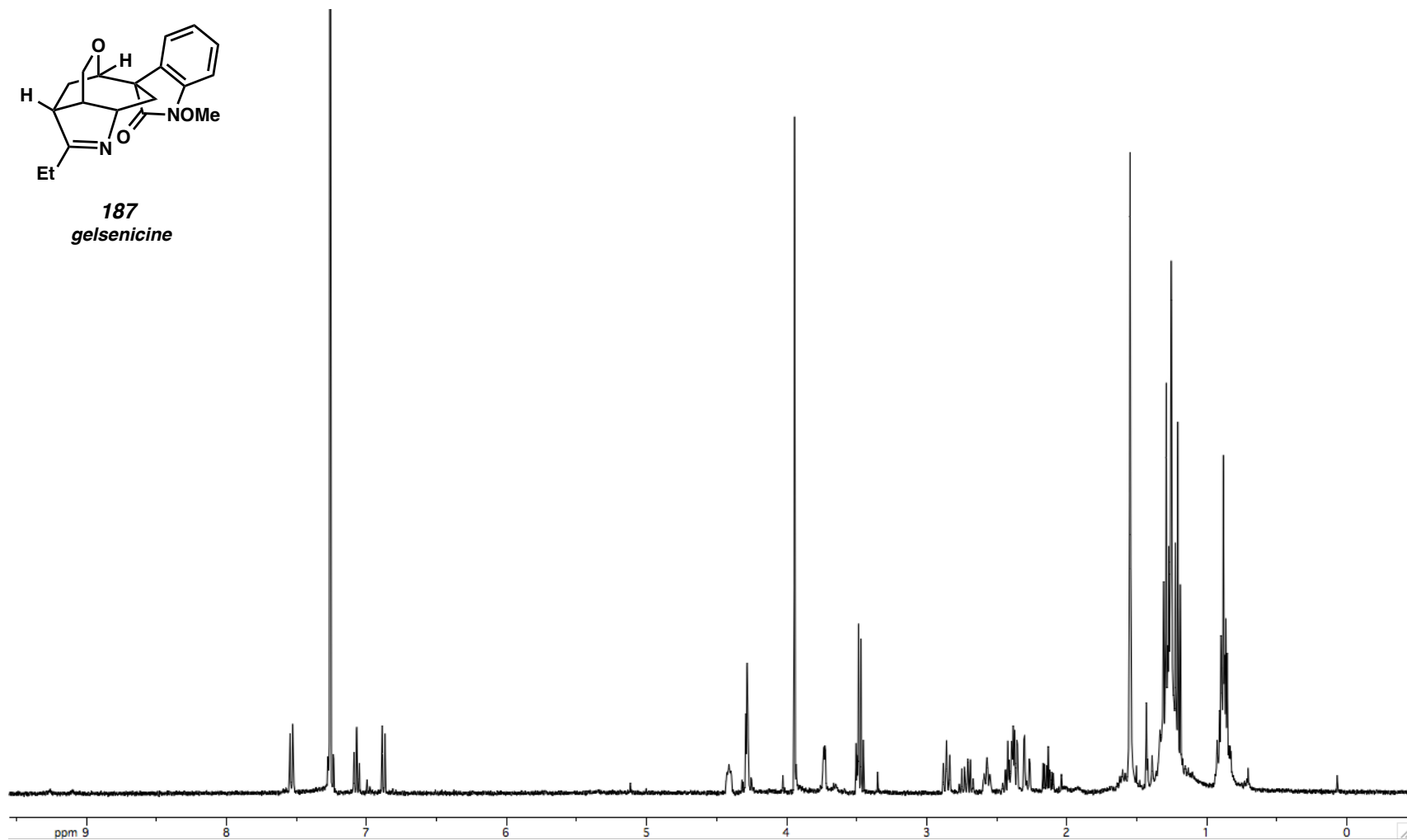
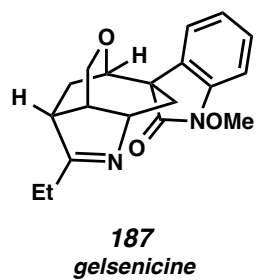
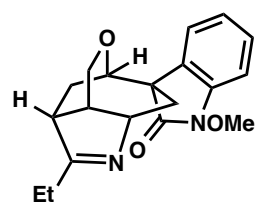


Figure A3.27. ^1H NMR (500 MHz, CDCl_3) of Compound **187**.



187
gelsenicine

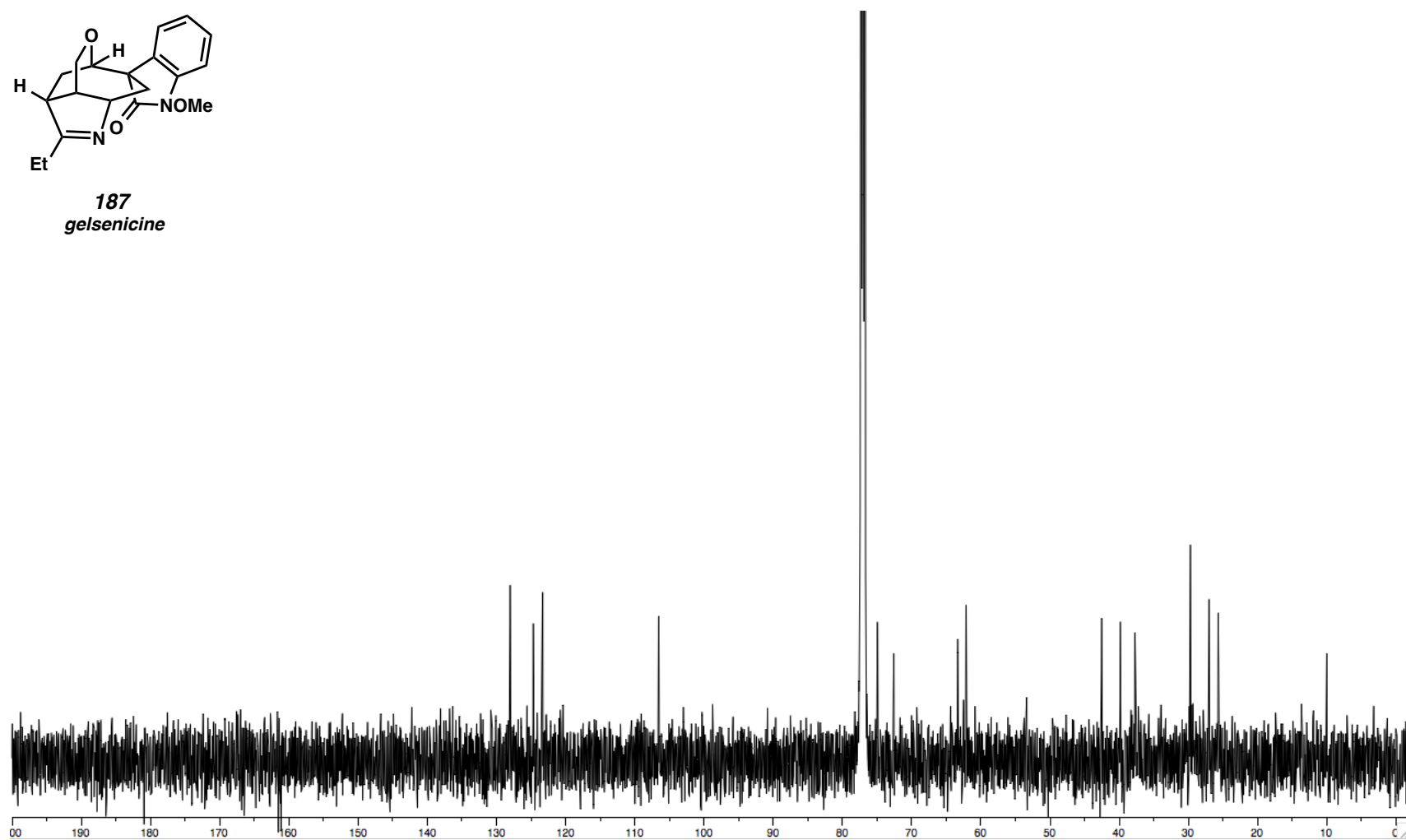
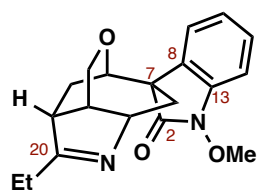


Figure A3.28.A ¹³C NMR (125 MHz, CDCl₃) of Compound **187**.



187
gelsenicine

Missing Assignments

C20	184.4
C2	171.2
C13	138.1
C8	132.3
C7	55.8

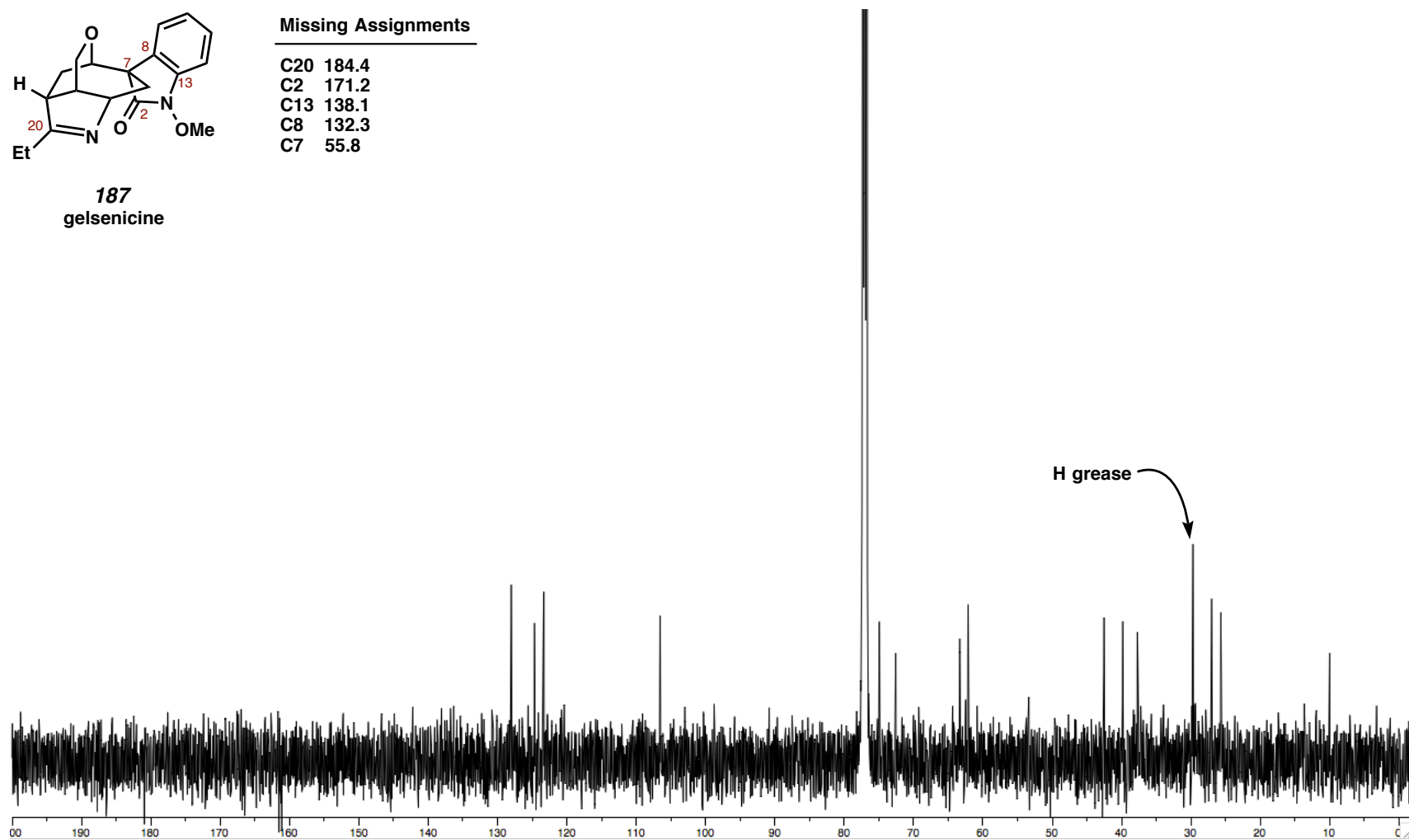


Figure A3.28.B ^{13}C NMR (125 MHz, CDCl_3) of Compound **187** with missing peaks indicated.

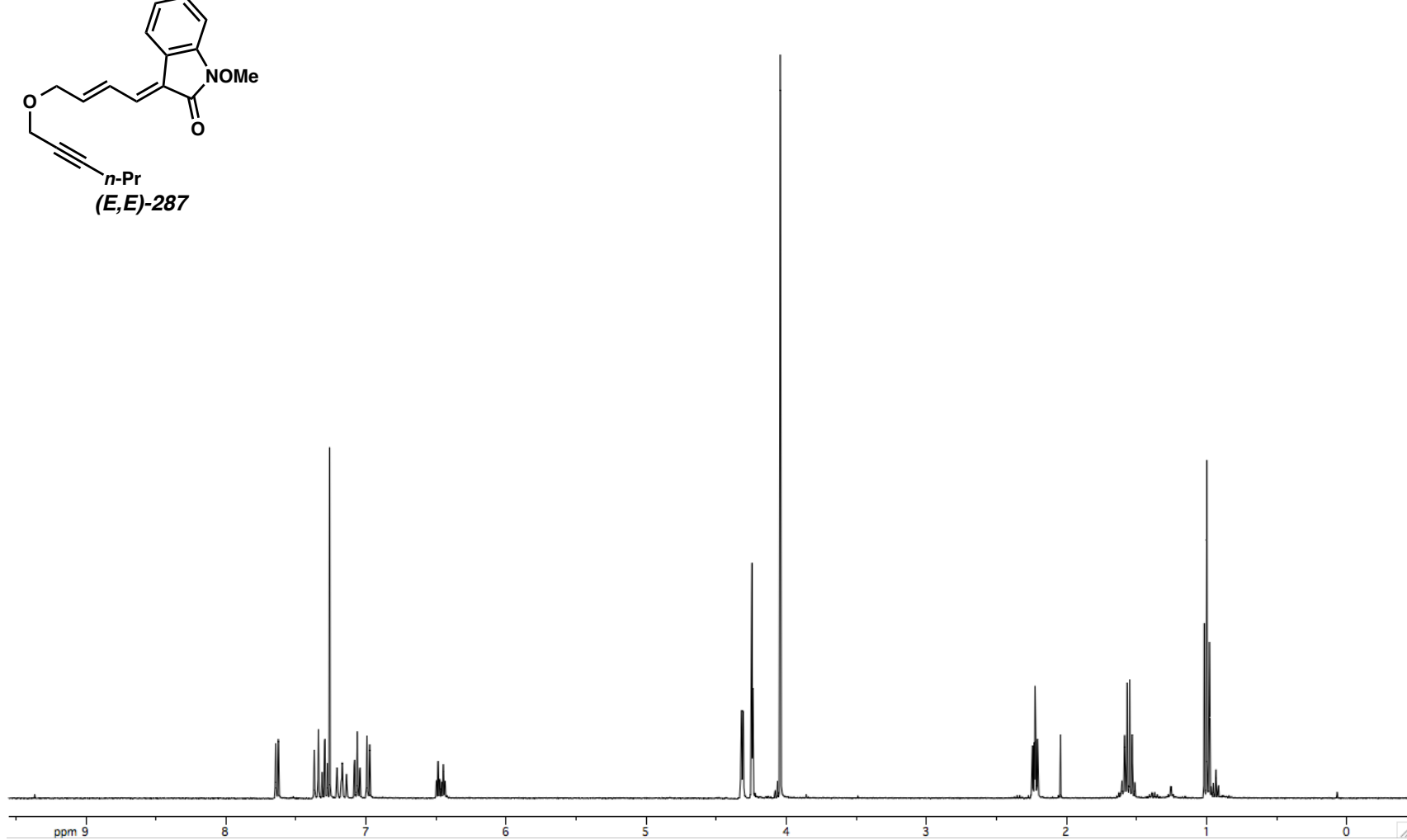
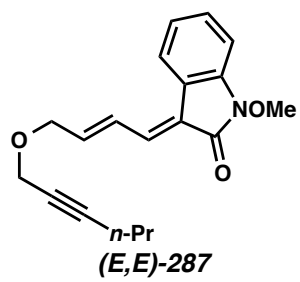


Figure A3.29. ^1H NMR (400 MHz, CDCl_3) of Compound (*E,E*)-287.

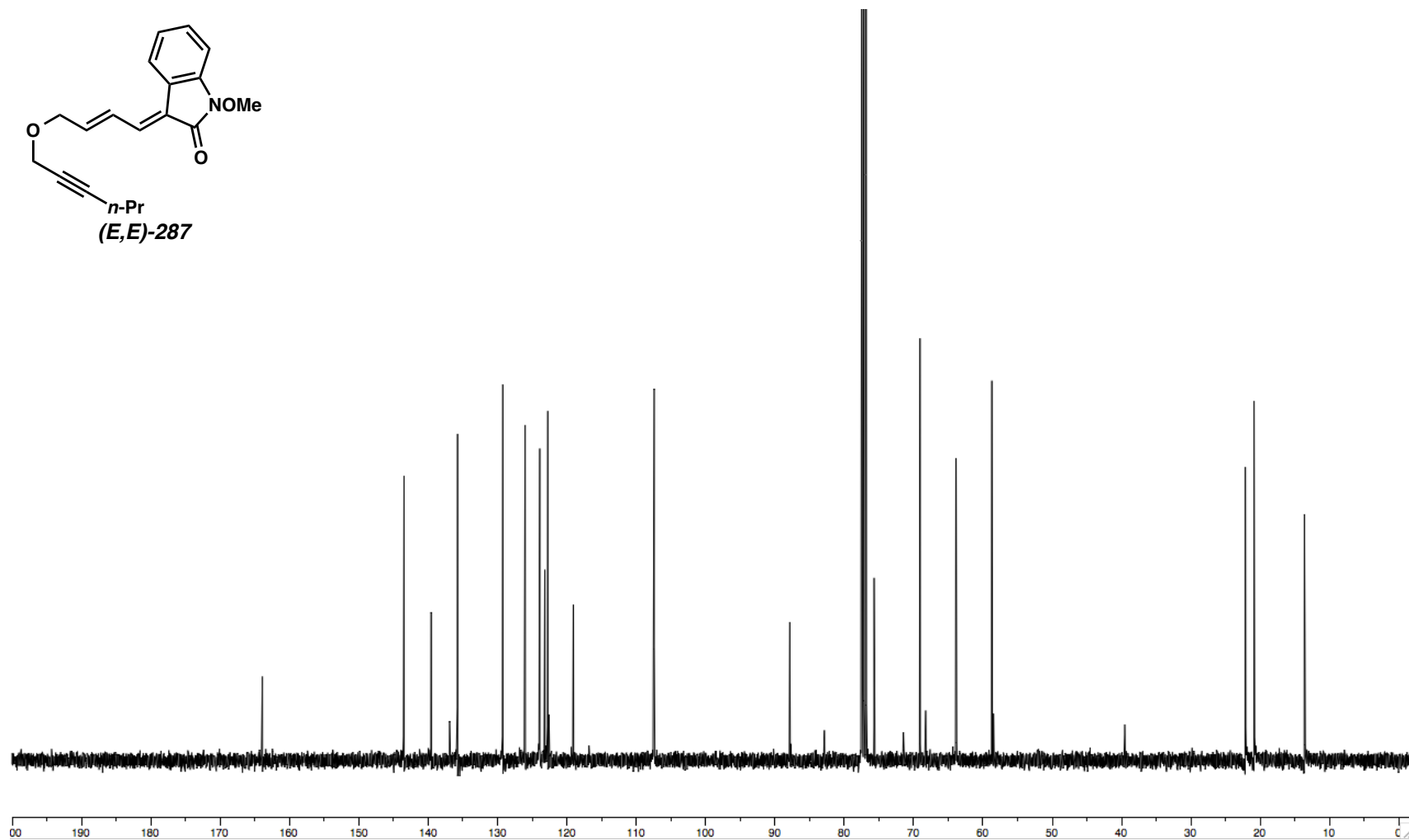
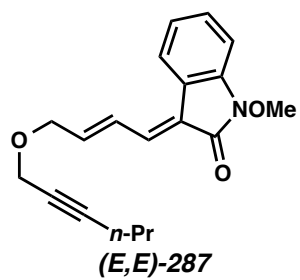


Figure A3.30. ¹³C NMR (100 MHz, CDCl₃) of Compound (*E,E*)-287.

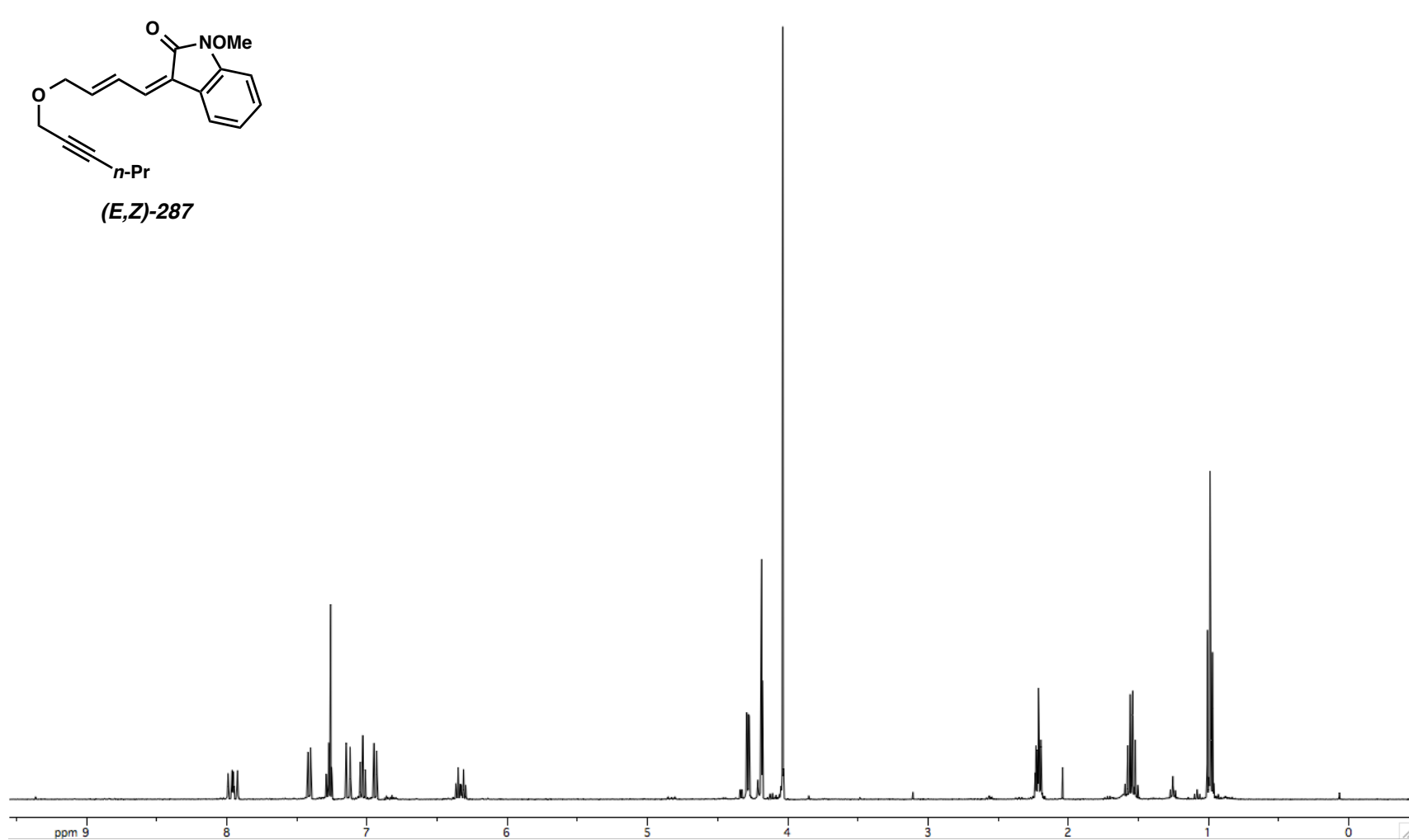
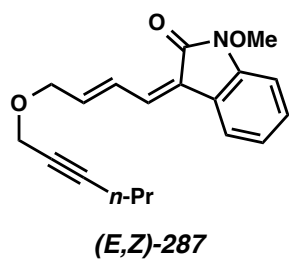


Figure A3.31. ^1H NMR (400 MHz, CDCl_3) of Compound *(E,Z)*-287.

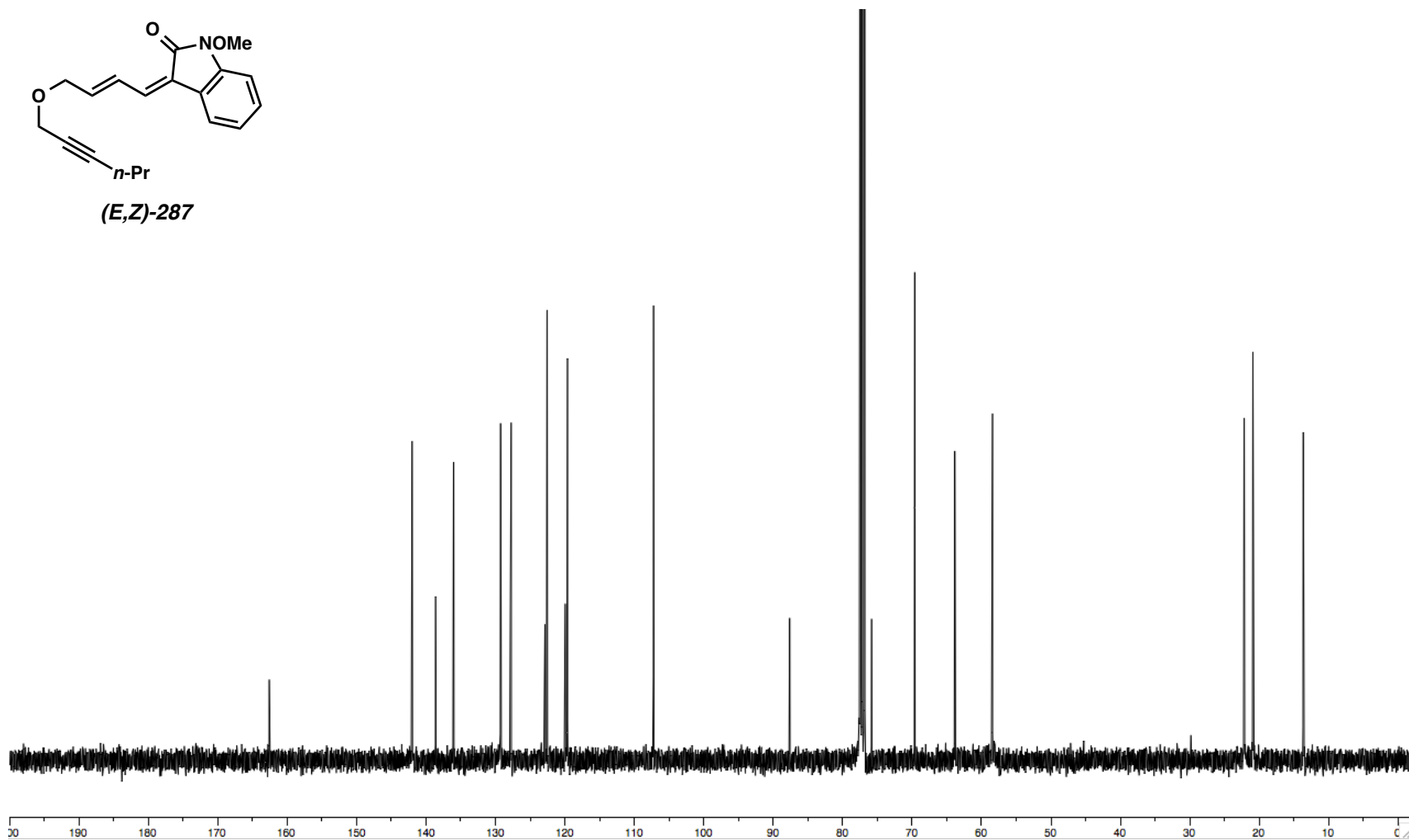
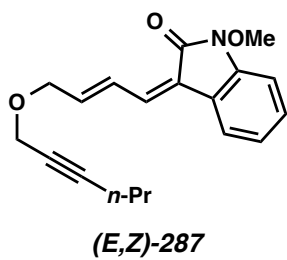
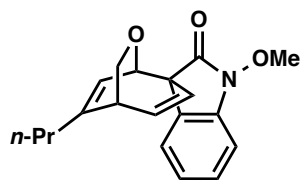


Figure A3.32. ^{13}C NMR (100 MHz, CDCl_3) of Compound *(E,Z)*-287.



294

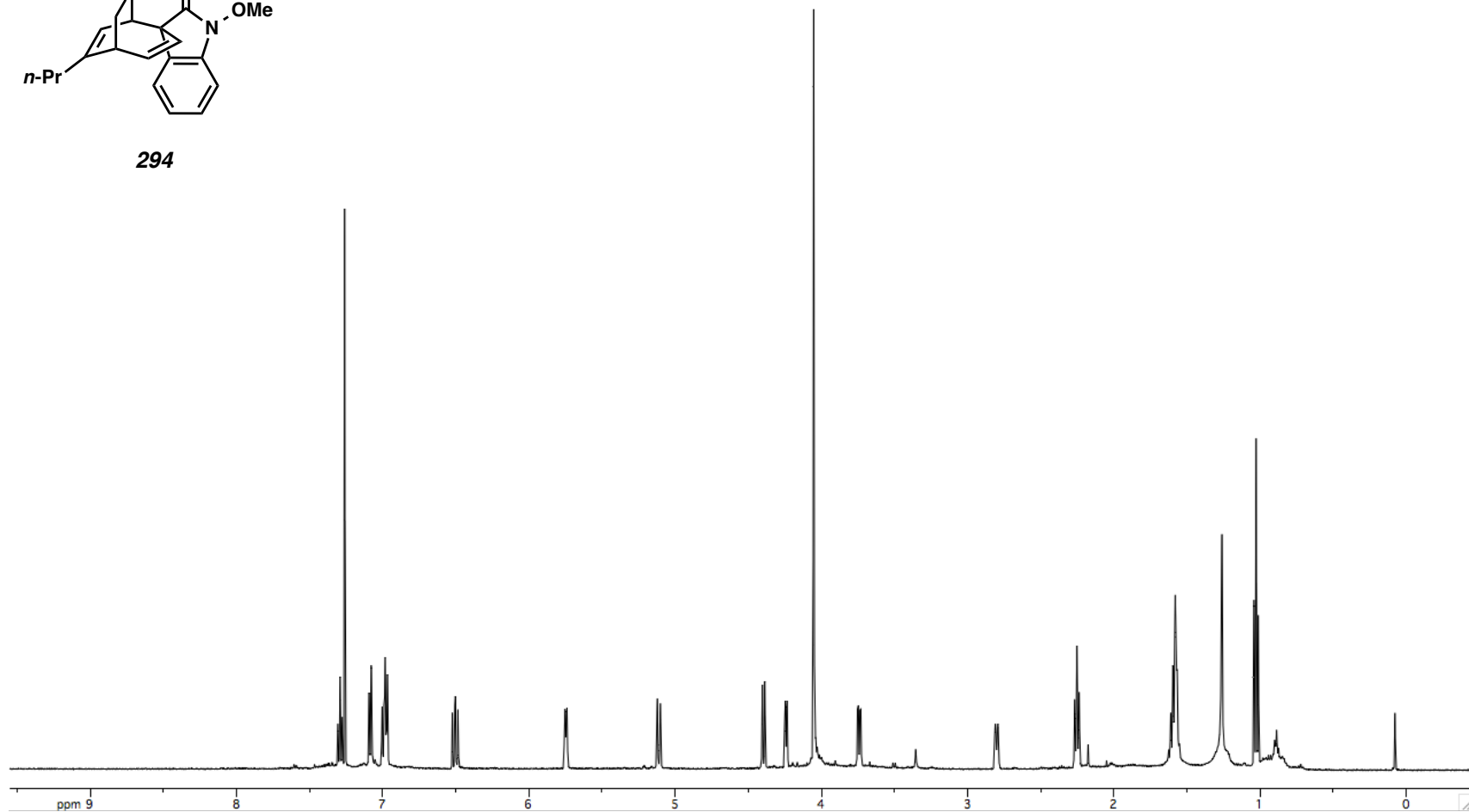
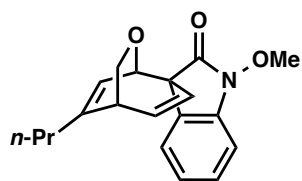


Figure A3.33. ¹H NMR (500 MHz, CDCl₃) of Compound 294.



294

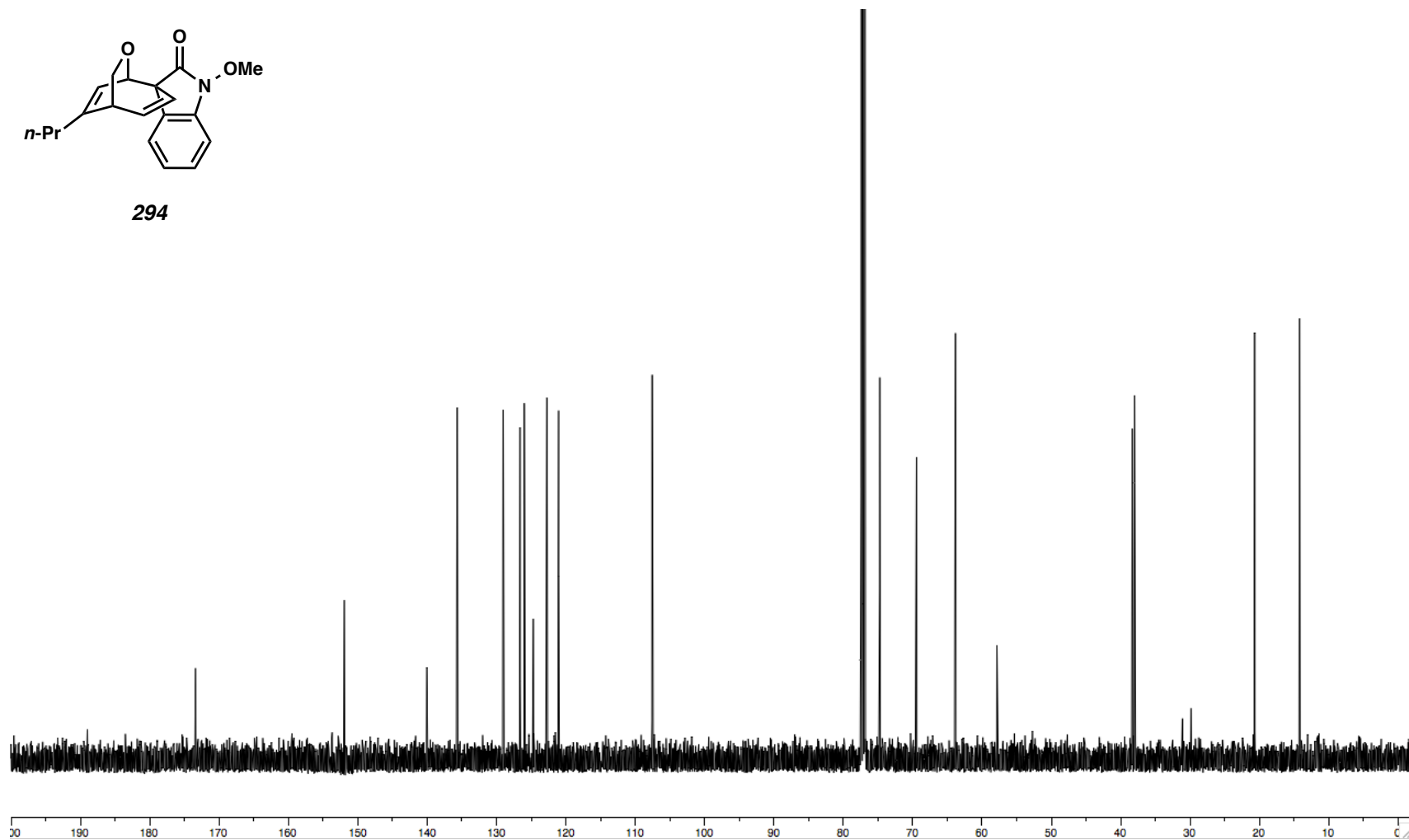


Figure A3.34. ^{13}C NMR (125 MHz, CDCl_3) of Compound 294.

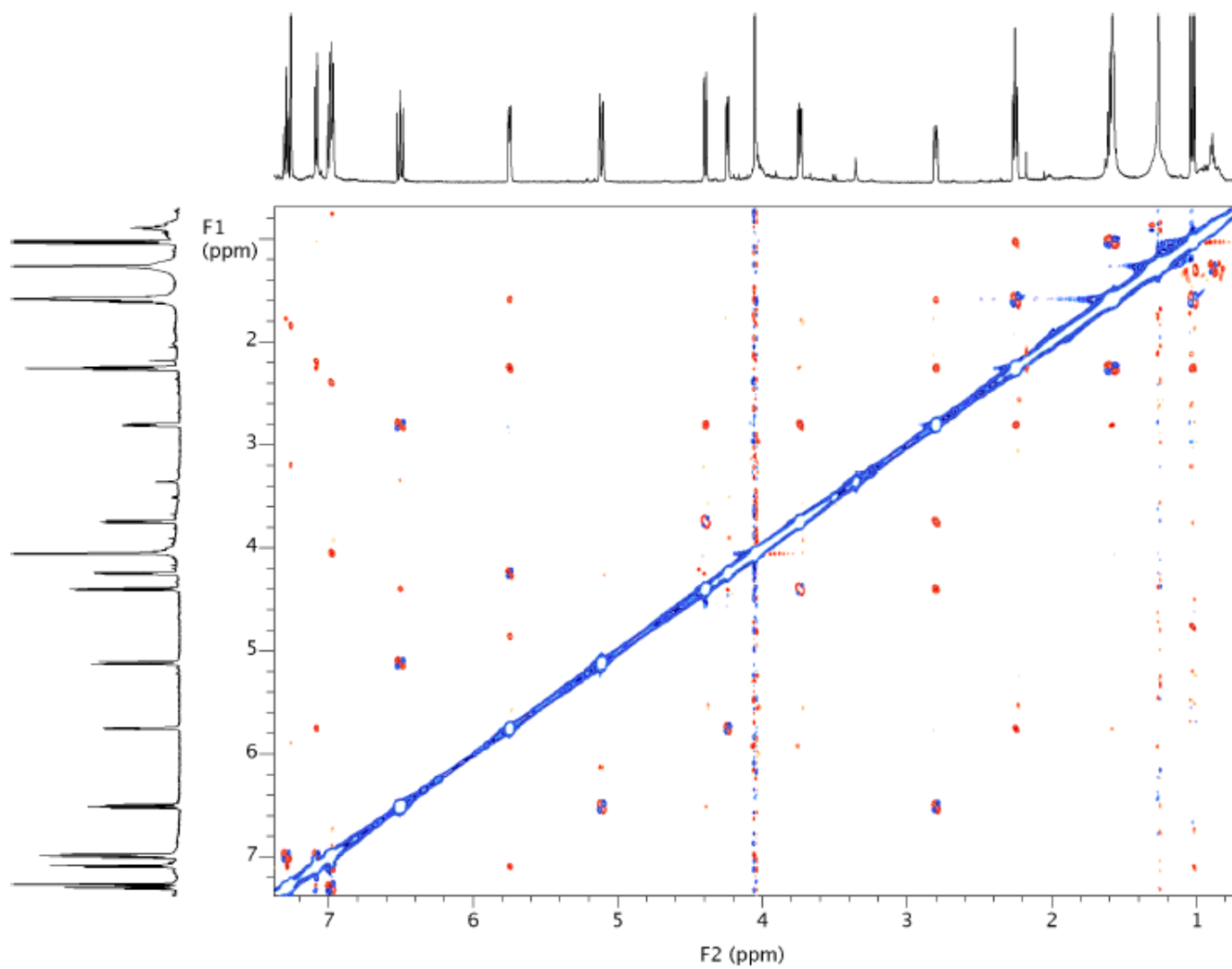


Figure A3.35. ^1H - ^1H ROESY Spectra of Compound 294.

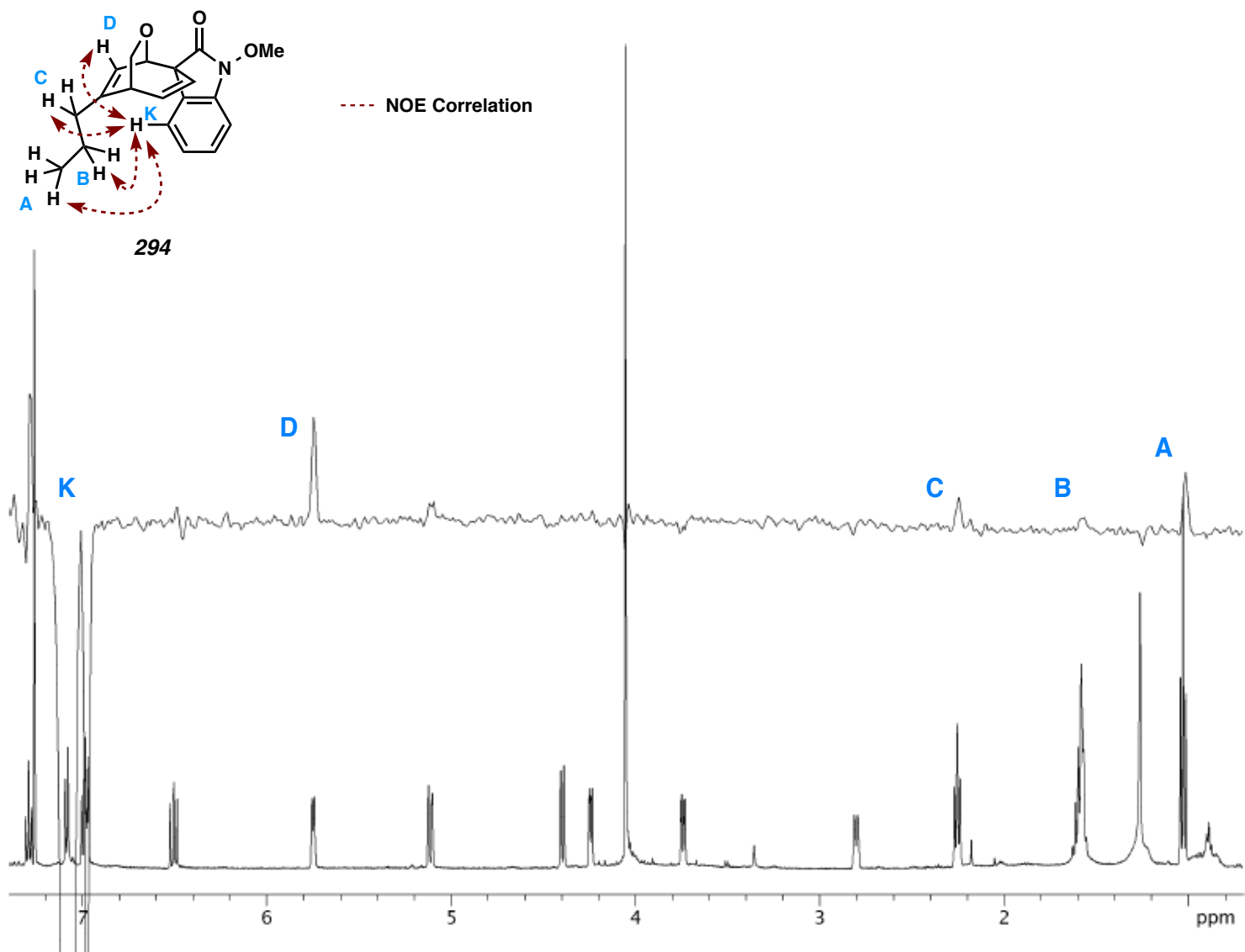


Figure A3.36. Isolated ^1H - ^1H ROESY Data of Compound **294**.

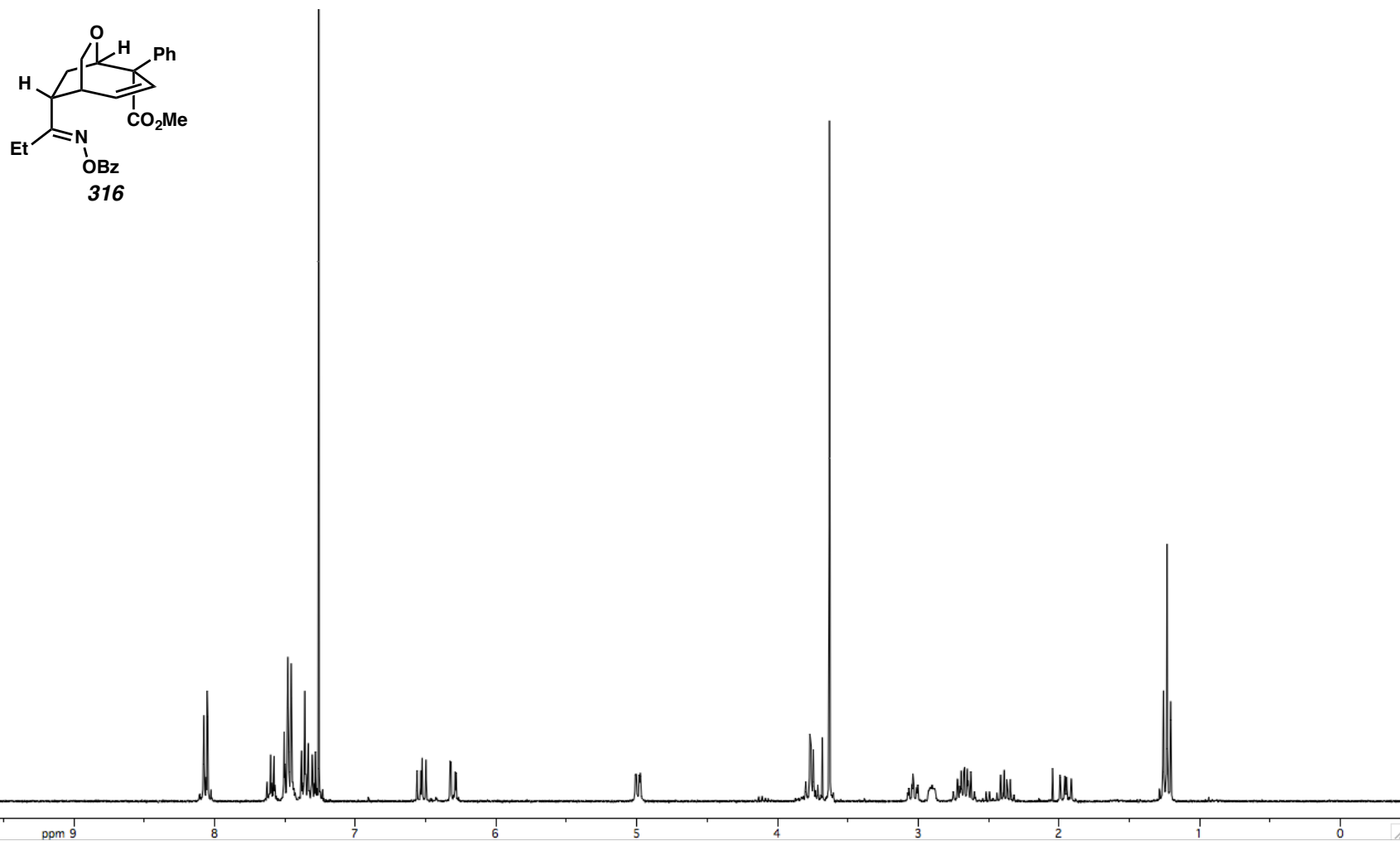


Figure A3.37. ¹H NMR (300 MHz, CDCl₃) of Compound 316.

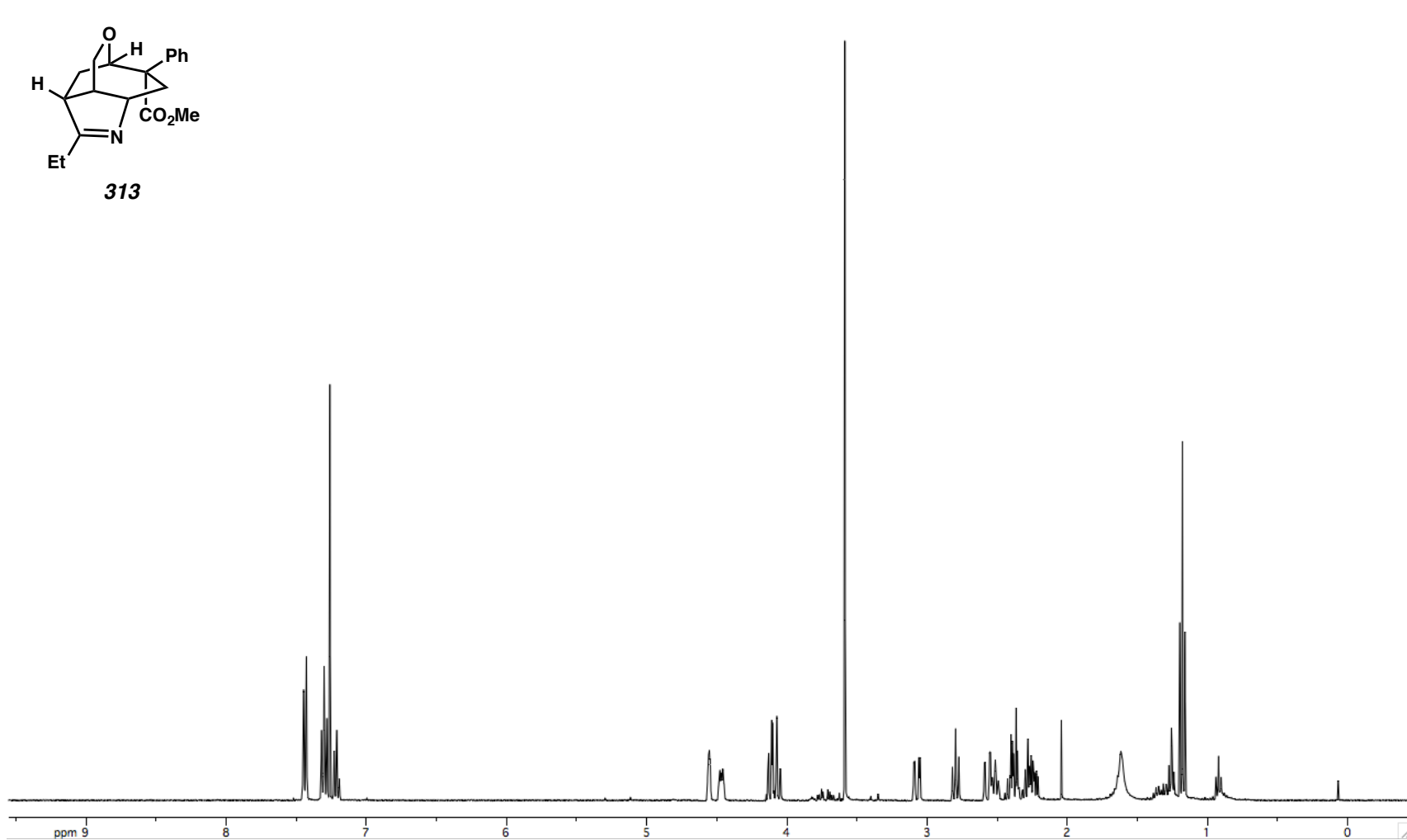
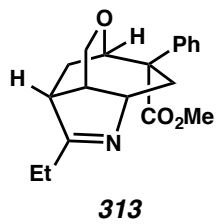
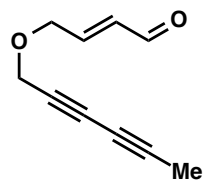


Figure A3.38. ^1H NMR (400 MHz, CDCl_3) of Compound **313**.



329

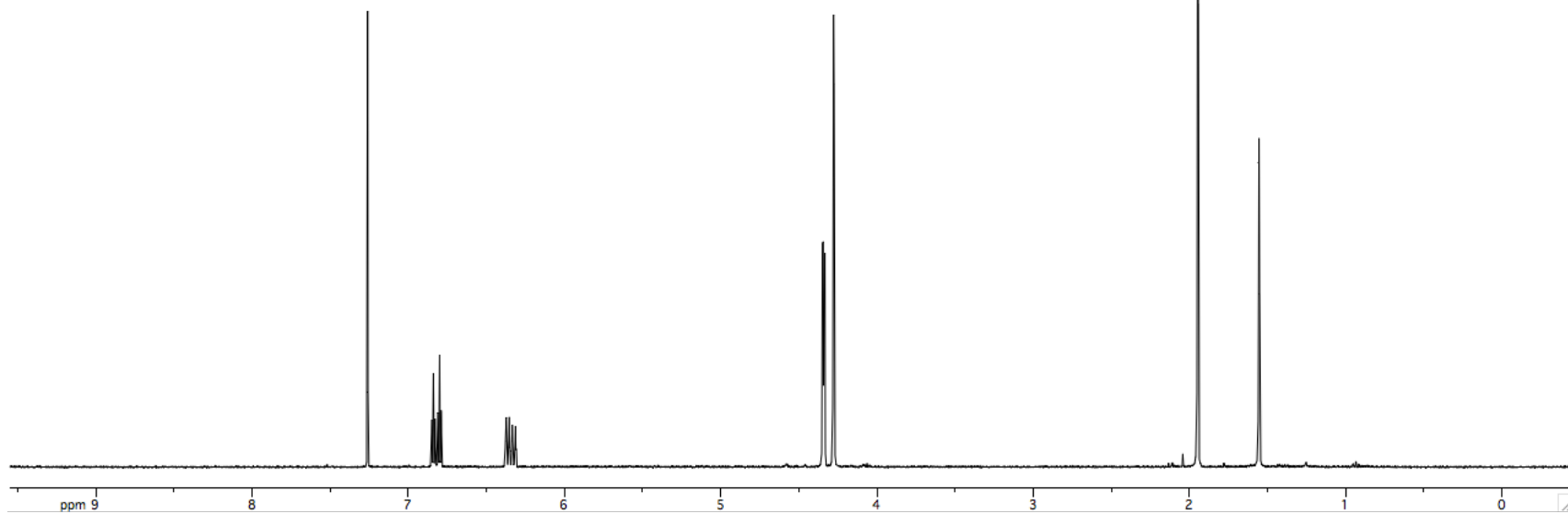
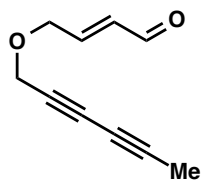


Figure A3.39. ¹H NMR (400 MHz, CDCl₃) of Compound 329.



329

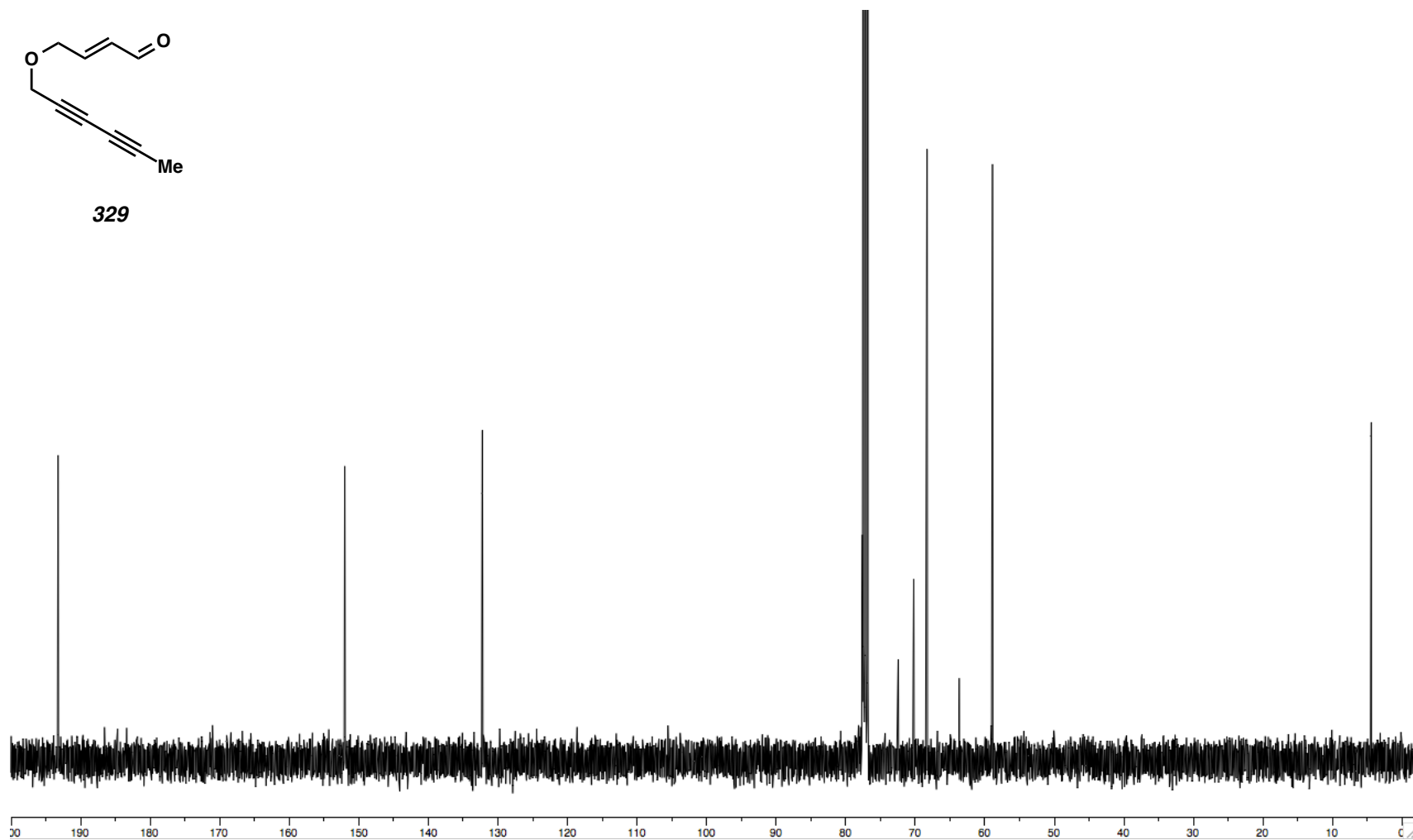


Figure A3.40. ^{13}C NMR (100 MHz, CDCl_3) of Compound **329**.

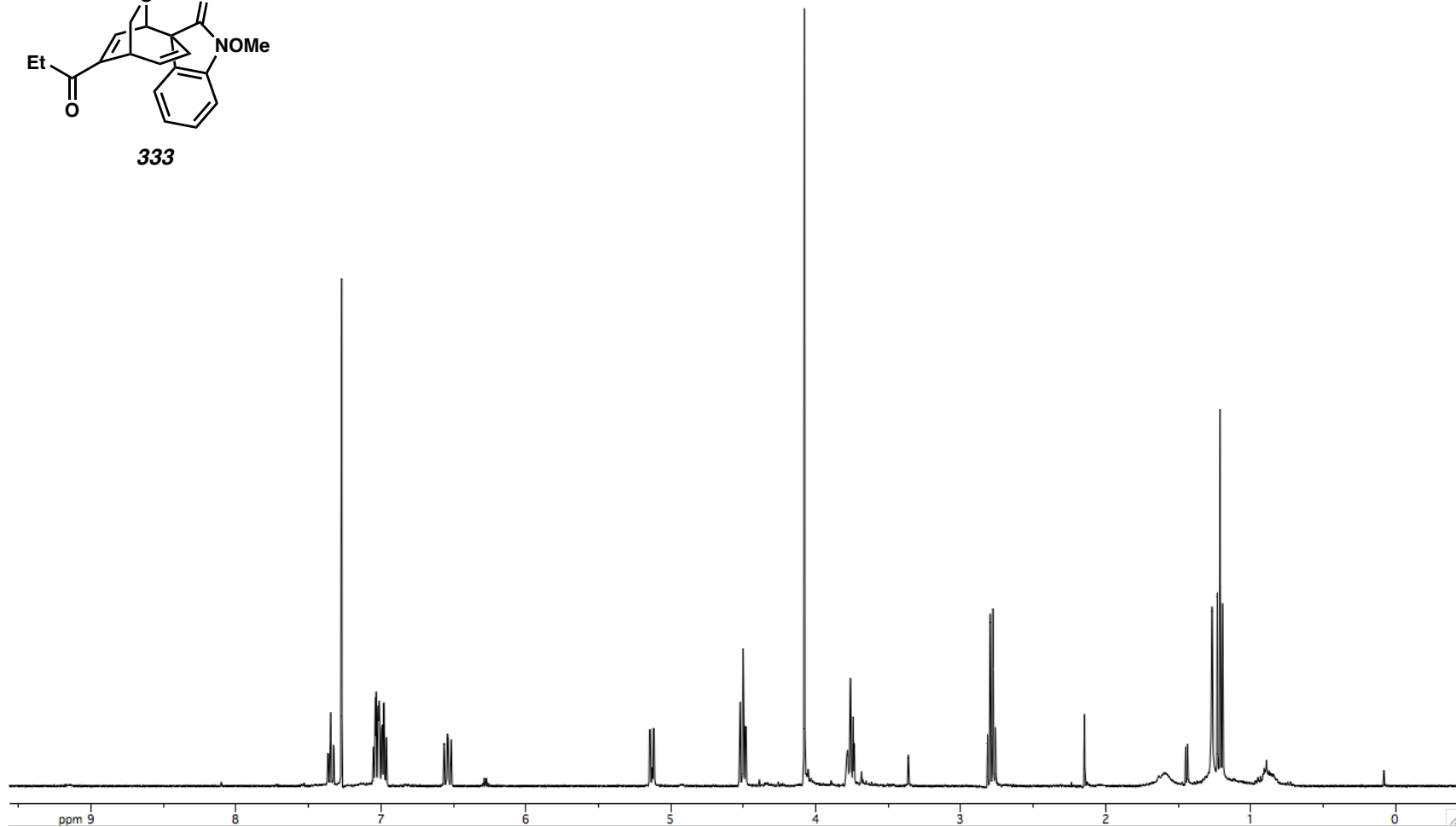
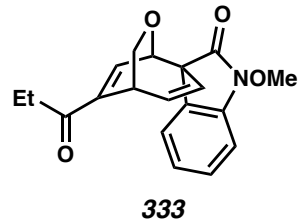


Figure A3.41. ^1H NMR (400 MHz, CDCl_3) of Compound **333**.

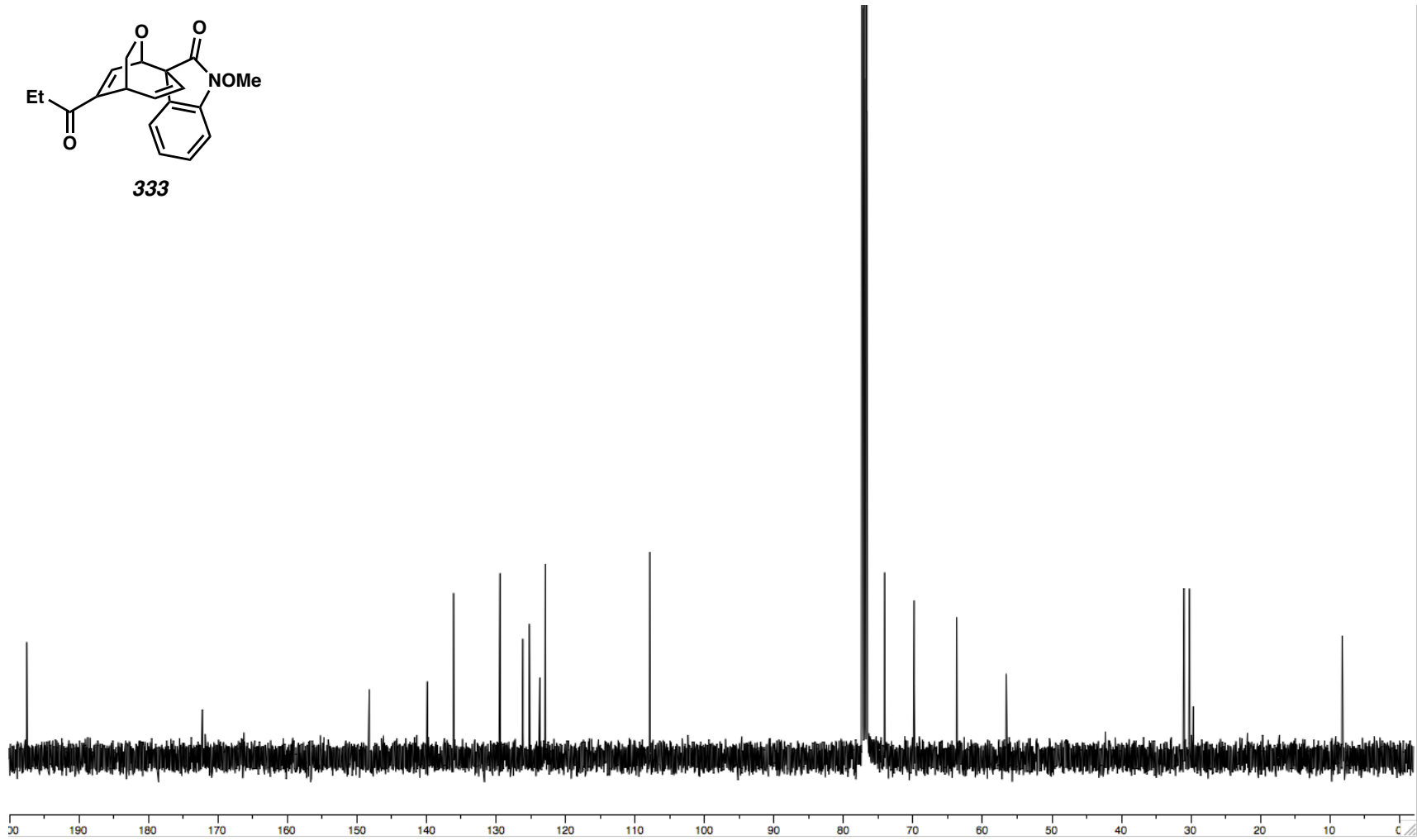
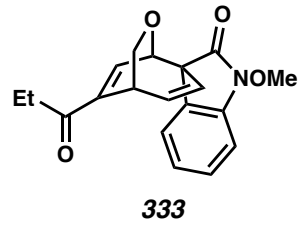


Figure A3.42. ^{13}C NMR (100 MHz, CDCl_3) of Compound **333**.